

Master's thesis

Hussain Shakeel Butt

Novel dual imidazolium-based ionic liquids for extractive desulfurization of fuel oil

Master's thesis in Organic Chemistry

Supervisor: Professor Anne Fiksdahl

Co-supervisor: Dr. Lethesh Kallidianhiyil Chellappan

May 2019

NTNU
Norwegian University of Science and Technology
Faculty of Natural Sciences
Department of Chemistry



Norwegian University of
Science and Technology

Hussain Shakeel Butt

Novel dual imidazolium-based ionic liquids for extractive desulfurization of fuel oil

Master's thesis in Organic Chemistry
Supervisor: Professor Anne Fiksdahl
Co-supervisor: Dr. Lethesh Kallidianthiyil Chellappan
May 2019

Norwegian University of Science and Technology
Faculty of Natural Sciences
Department of Chemistry



Norwegian University of
Science and Technology

Declaration

I hereby declare that I wrote this thesis independently and that I have not used any other sources of information than those given in the list of references. The study was conducted in accordance with the rules and regulations at the Department of Chemistry at the Norwegian University of Science and Technology (NTNU). The work was conducted from August 2018 to May 2019 as a member of the Fiksdahl group.

Trondheim, May 23rd 2019

Hussain Shakeel Butt

Acknowledgements

First, I would like to thank my supervisor Prof. Anne Fiksdahl for giving me the opportunity to join her group. I appreciate all help and guidance during my time in her lab, and that she gave me the opportunity to grow as a scientist and to challenge myself as a chemist.

I also want to thank my co-supervisor Dr. Lethesh Kallidianthiyil Chellappan for always answering my many questions and for guiding me whenever I needed help in the lab. I appreciate that you always gave good feedback and helped me to improve in the lab.

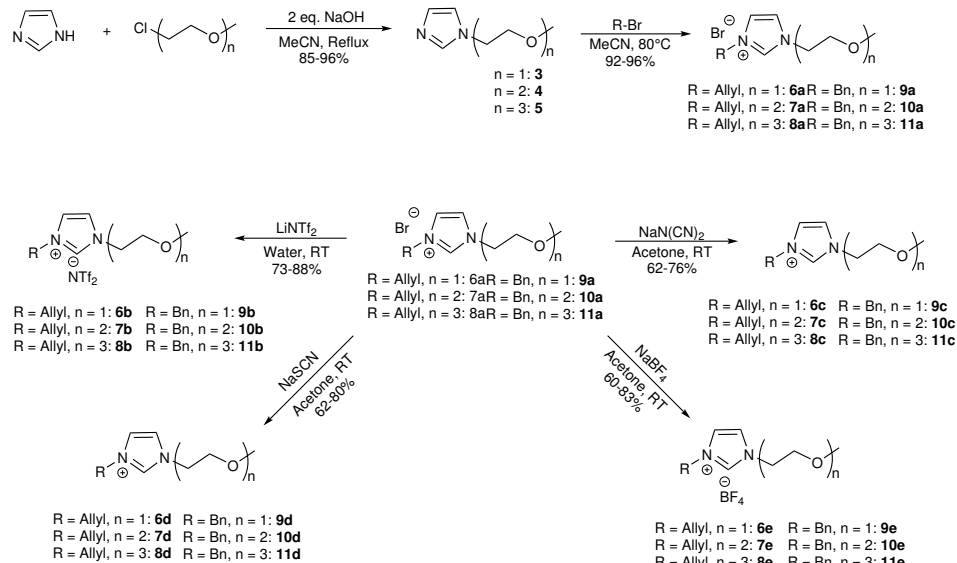
In addition, I want to thank the other members of the Fiksdahl group - it has been a pleasure to work with you and learn from you. I would also like to thank Dr. Susana Villa Gonzalez for helping me with the MS analyses, and others at the Department of Chemistry for all provided help during my thesis.

Finally, a special thanks to my friends and my family for always having my back and for encouraging me during my time at NTNU and during my master thesis. I would not have been here today without your love and support.

Abstract

The aim of this master's project was to synthesize a series of dual functionalized imidazolium-based ionic liquids (ILs) for the desulfurization of dibenzothiophene (DBT) and 4,6-dimethylbibenzothiophene (4,6-DMDBT) from *n*-dodecane. The effect on the desulfurization efficiency by increasing the length of diethylene glycol chains and the presence of π -electron containing substituents (allyl and benzyl) on imidazole was investigated.

The bromide salts were synthesized through S_N2 -reactions with diethylene glycol chains, followed by alkylation with bromide substituents. The ILs were obtained by anion exchange between the bromide salts formed and the desired anion ($[NTf_2]$, $[N(CN)_2]$, $[SCN]$ and $[BF_4]$). Synthetic procedure for allyl and benzyl bearing ILs is presented:

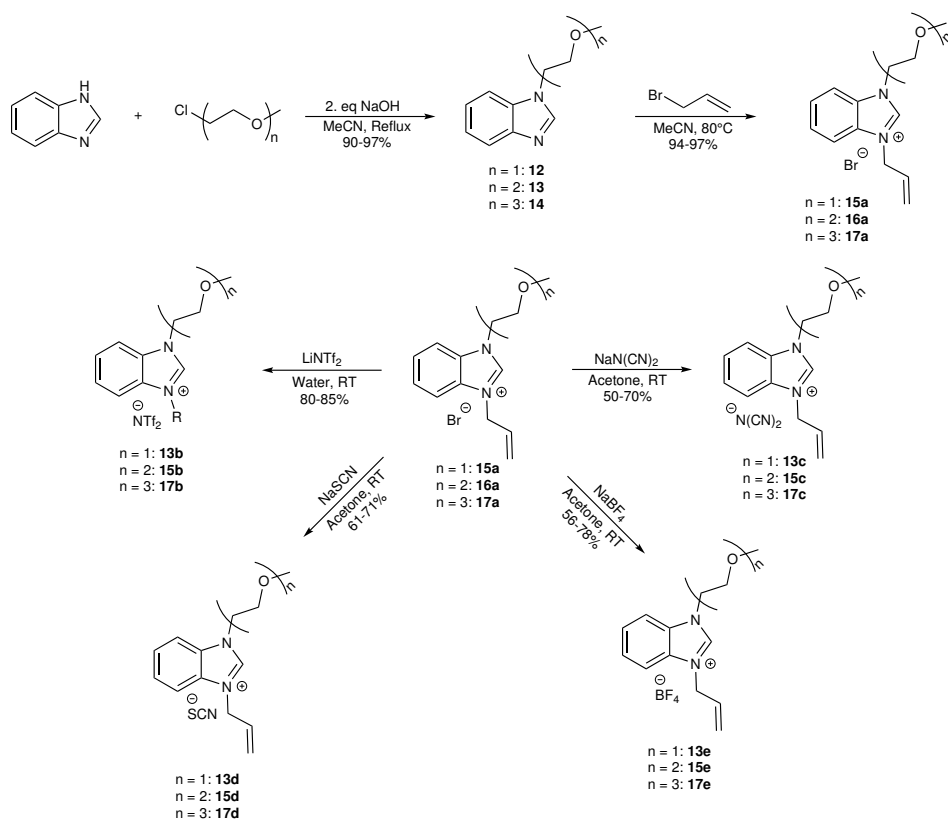


The desulfurization was performed on a model oil (MO) with 500 ppm sulfur content consisting of DBT and 4,6-DMDBT in *n*-dodecane. For the imidazolium based ILs, increasing the ether chain enhanced the extraction efficiency. Among the allyl bearing ILs (**6-8**), IL **8b** exhibited highest desulfurization efficiency for 4,6-DMDBT, while **8c** exhibited highest desulfurization efficiency for DBT, presumably due to the hydrophobic nature of the [NTf₂] anion in **8b**. However, due to environmental and toxicity issues of the [NTf₂] anion IL, **8c** was chosen for optimization studies, in which the effect of mass ratio of IL:MO, temperature and extraction time were investigated. The optimized conditions were found to be 2:1 ratio of IL:MO at 25°C and 15 min. In a single stage extraction, the desulfurization efficiencies were 69% and 33% of DBT and 4,6-DMDBT, respectively. Furthermore, ¹H-NMR study of IL **8c** revealed that the acidic C2-proton on the imidazolium core, previously reported to contribute significantly in desulfurization of sulfur compounds, had little impact in this study due to intramolecular interaction between the proton and the oxygen in the ether chain.

Changing the functional group from allyl to benzyl (ILs **9-11**) had negligible effect on the removal of DBT, while having a positive effect on the extraction of 4,6-DMDBT. The enhancement of desulfurization 4,6-DMDBT may arise from the increase of π -electrons, thus enhancing the $\pi-\pi$ interactions. As for ILs **6-8**, extending the ether chain also lead to higher desulfurization. In addition, the [N(CN)₂] and [NTf₂] anion showed similar desulfurization pattern for DBT and 4,6-DMDBT as observed for the allyl bearing ILs. The extraction efficiencies of DBT and 4,6-DMDBT for the [NTf₂] based IL (**11b**) were 53% and 29%,

respectively. The $[N(CN)_2]$ based IL (**11c**) extracted 56% and 24% of DBT and 4,6-DMDBT, respectively.

In addition, benzoimidazolium-based ILs bearing allyl group and increasing diethylene chains were also investigated. The synthetic procedure for benzoimidazolium-based ILs is presented:



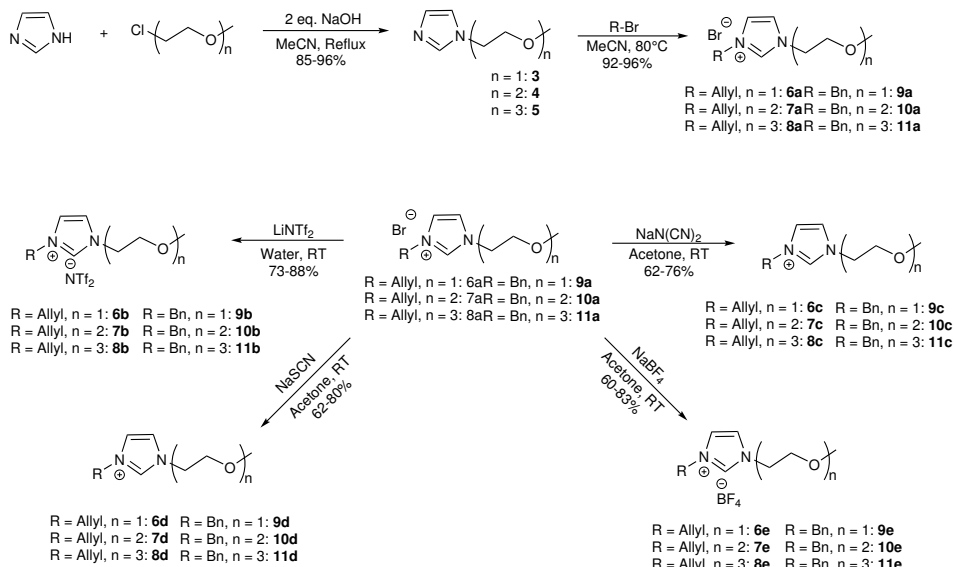
The desulfurization study of benzoimidazolium-based ILs exhibited higher extraction efficiency than the imidazolium-based ILs. However, prolonging of the ether chain resulted in lower S-removal for the benzoimidazolium-based ILs. An ¹H-NMR study of the benzoimidazolium-based IL **15b** revealed that the acidic C2-proton interacts more strongly

in the desulfurization through hydrogen bonding with the sulfur in DBT and an increase in the ether chain shields the proton by intramolecular hydrogen bonding. The highest desulfurization efficiency was observed for IL **15b**, extracting 69% of DBT and 51% of 4,6-DMDBT.

Sammendrag

Formålet med dette masterprosjektet var å syntetisere en serie av dobbelfunksjonaliserte imidazolium-baserte ioniske væsker (ILs) for desulfurisering av dibenzothiophene (DBT) og 4,6-dimetylbenzothiophene (4,6-DMDBT) fra *n*-dodekan. Effekten på desulfuriseringseffektiviteten ved å øke lengden til dietylenglykol-kjeden og substituenter som innehar π -elektoner (allyl og benzyl) på imidazole ble undersøkt.

Bromidsaltene ble syntetisert gjennom S_N2 -reaksjoner med dietylenglykol kjeder og alkylbromidsubstituenter. ILs ble syntetisert gjennom anionbytte mellom det dannede bromidsaltet og det ønskede anionet ($[NTf_2]$, $[N(CN)_2]$, $[SCN]$ and $[BF_4]$). Den syntetiske prosedyren for allyl- og benzylbærende ILs er presentert:



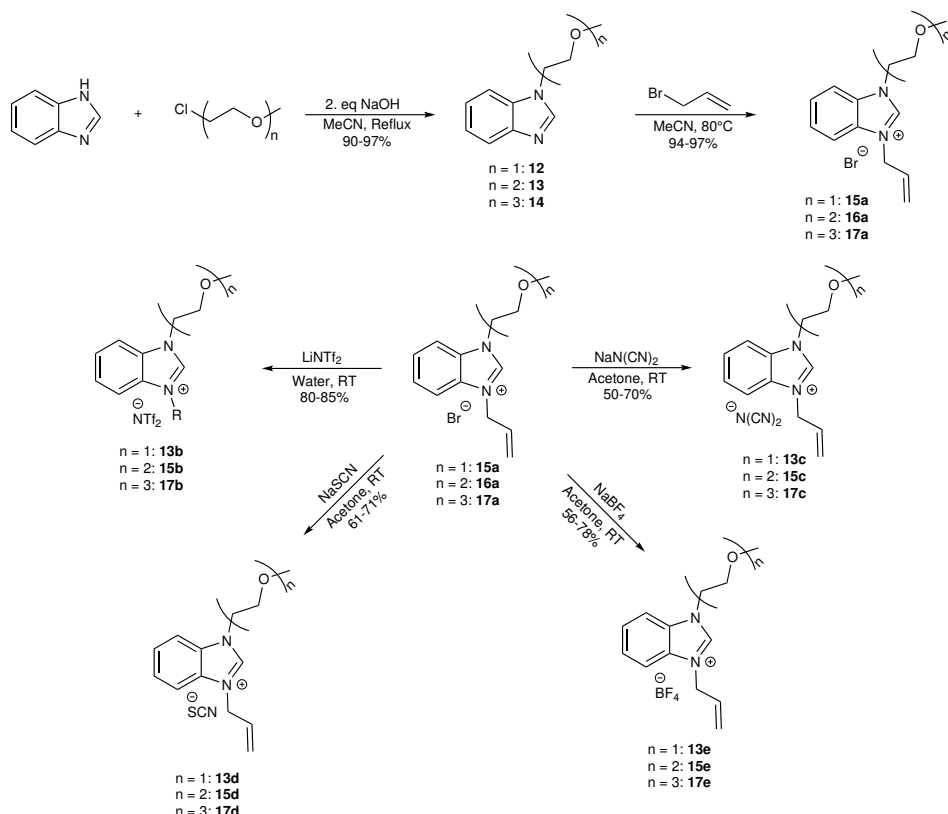
Desulfuriseringen ble gjennomført med en modellolje (MO) med et

innhold av 500 ppm svovel bestående av DBT og 4,6-DMDBT i *n*-dodekan. For de imidazoliumbaserte ILs, førte en økning av eterkjedene til en økt ekstraksjonseffektivitet. Blant de allylbærende ILs (**6-8**), utviste IL **8b** and **8c** de høyeste desulfuriseringseffektivitetene for 4,6-DMDBT of DBT, respektivt, trolig på grunn av den hydrofobiske naturen til [NTf₂] anionet. Med tanke på miljø, og toksiteten til [NTf₂] anion ILs, ble **8c** valgt for videre optimiseringsstudier, der effekten av masseforhold for IL:MO, temperatur og ekstrasjonstid ble undersøkt. De optimaliserte forholdene ble funnet til å være 2:1 masseforhold av IL:MO ved 25°C og 15 min. I en ett-trinnsekstraksjon var ekstraheringseffektiviteten 69% and 33% for DBT og 4,6-DMDBT, respektivt. Videre viste et ¹H-NMR studie av IL **8c** at det sure C2-protonet på imidazol, tidligere rapportert til å signifikannt bidra i desulfurisering av svovelforbindelser, hadde liten innvirkning i dette studiet, trolig på grunn av intramolekylære interaksjoner mellom protonet og oksygenet i eterkjeden.

Endring av den funksjonelle gruppen fra allyl til benzyl (ILs **9-11**) hadde ingen nevneverdig effekt på fjerningen av DPT, men det hadde en positiv effekt på ekstraksjonen av 4,6-DMDBT. Økningen av desulfuriseringen av 4,6-DMDBT kan komme av det økte antallet av π -elektroner, som dermed øker π -interaksjonene. Som for ILs **6-8**, vil en økning av eterkjedene også føre til ytterligere desulfurisering. I tillegg viste [N(CN)₂] og [NTf₂] anionene lignende desulfuriseringsmønster for DBT og 4,6-DMDBT som observert for de allylbærende ILs. Ekstraksjonseffektiviteten av DBT og 4,6-DMDBT for den [NTf₂]-baserte IL (**11b**) var respektivt 53% and 29%. Den [N(CN)₂]-baserte IL (**11c**)

ekstraherte respektive 56% and 24% av DBT og 4,6-DMDBT.

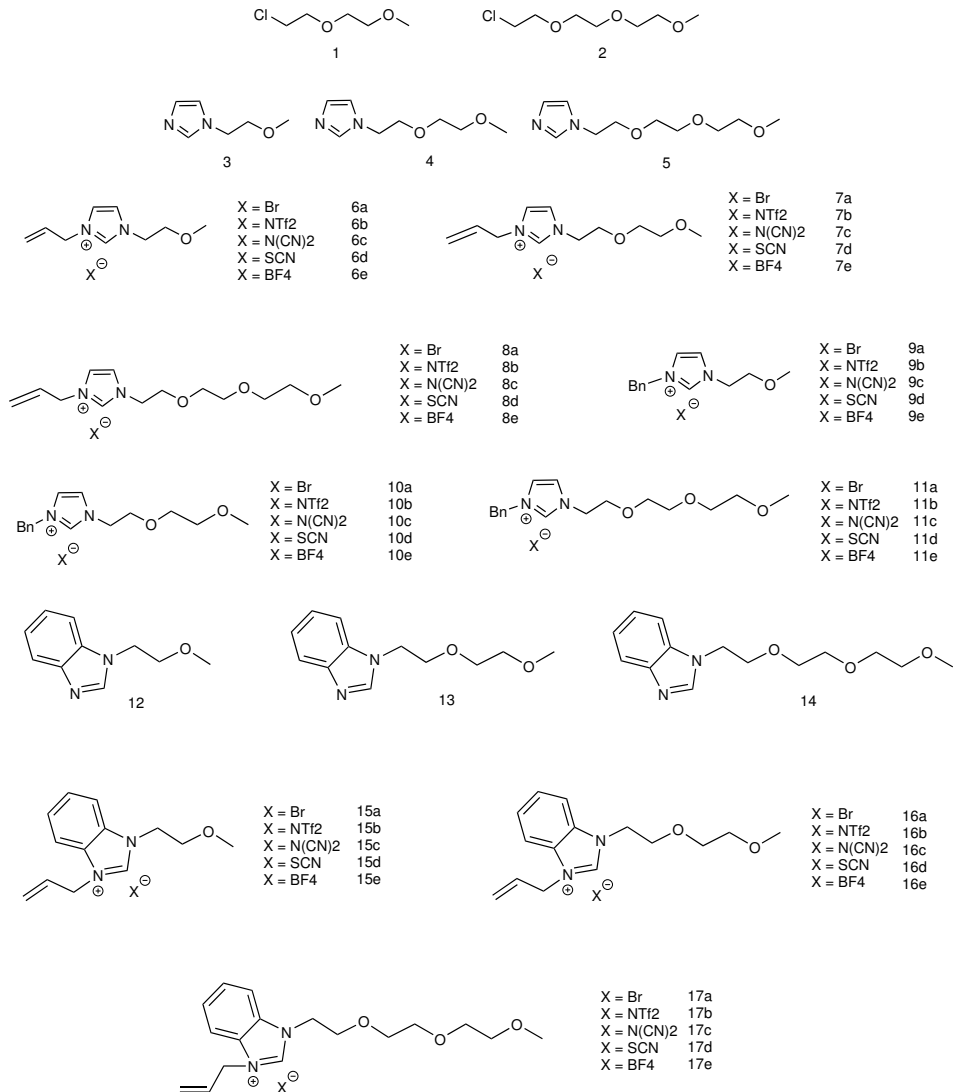
I tillegg ble benzoimidazolium baserte ILs med en allylgruppe og forlenget dietylenkjede undersøkt. Den syntetiske prosedyren for benzoimidazoliumbaserte ILs er presentert:



Desulfuriseringssstudiet av benzoimidazoliumbaserte ILs utviste høyere ekstraksjonseffektivitet. Forlengelse av eterkjeden resulterte i mindre S-fjerning. Et $^1\text{H-NMR}$ studie viste at det sure C2-protonet interagerer sterkere i desulfuriseringen gjennom hydrogenbindinger, og ved en økning av eterkjedene beskyttes protonet av intramolekulære hydrogenbindinger. Den høyeste desulfuriseringseffektiviteten ble observert

for IL **15b**, som ekstraherte 69% av DBT og 51% av 4,6-DMDBT.

List of compounds



Abbreviations

2MBP	2-methoxybiphenyl
4,6-DMDBT	4,6-dimethyldiobenzothiophene
BDS	Biodesulfurization
BF_4^-	Tetrafluoroborate
[BMIM][BF ₄]	1-butyl-3-methylimidazolium tetrafluoroborate
[BMIM][Cl]	1-butyl-3-methylimidazolium chloride
[BMIM][FeCl ₃]	1-butyl-3-methylimidazolium trichloroferrate
[BMIM][N(CN) ₂]	1-butyl-3-methylimidazolium dicyanamide
[BMIM][PF ₆]	1-butyl-3-methylimidazolium hexafluorophosphate
C ₀	Inital concentration
C _f	Final concentration
[C ₂ C ₁ im][BF ₄]	3-methyl-imidazolium tetrafluoroborate
[C ₄ mim]	1-butyl-3-methylimidazolium
CDCl ₃	Deuterated chloroform
Cys	Cysteine
δ	Chemical shift
d	Doublet

DBT	Dibenzothiophene
[DBU][Pr]	1,8-diazobi-cyclo[5.4.0]undec-7-ene propionate
DCM	Dichloromethane
Dox	DBT oxidation genes
<i>dszC</i>	Desulfurization gene C
EDS	Extractive desulfurization
[EtNH ₃][NO ₃]	Ethylammoniumnitrate
HBPS	2-hydroxybiphenyl-2-sulfinate
[HC ₄ im][HSO ₄]	1-butylimidazolium hydrogensulfate
HDS	Hydrodesulfurization
[HMIm][(CH ₂) ₄ SO ₃]	3-(3-methyl-1 <i>H</i> -imidazolium)propane-1-sulfonic acid
IL	Ionic liquid
IR	Infrared spectroscopy
K _N	Nernst partition coefficient
LG	Leaving group
m	Multiplet
MeOD	Deuterated methanol

MO	Model oil
$\text{N}(\text{CN})_2$	Dicyanamide
NO_X	Nitrogen oxide
NTf_2	Bistriflimide
Nu	Nucleophile
ODS	Oxidative desulfurization
Omim	1-octyl-3-methylimidazolium nitrate
PEG	Polyethylene glycol
PIL	Polyionic IL
R	Percentage of sulfur removal
RP-HPLC	Reverse phase high performance liquid chromatography
RTIL	Room-temperature IL
s	Singlet
SO_X	Sulfur oxide
S-content	Sulfur content
S-removal	Sulfur removal
SCN	Thiocyanate
SMIL	Supported membrane IL

%S-removal	Percent sulfur removal
t	Triplet
[TBHEP][Br]	tri- <i>n</i> -butyl-(2hydroxyethyl)phosphonium bromide
[THTDP][BF ₄]	Trihexyl(tetradecyl) phosphonium tetrafluoroborate
TMS	Tetramethylsilane
TSIL	Task-specific IL

Contents

1	Introduction	1
1.1	Fossil fuels	1
1.2	Hydrodesulfurization (HDS)	2
1.3	Alternative methods for desulfurization	3
1.4	Aim of the project	7
2	Theory	10
2.1	Ionic Liquids	10
2.1.1	Synthesis of ILs	12
2.1.2	Purification of ILs	12
2.2	Extractive desulfurization (EDS)	14
2.2.1	Parameters in desulfurization	16
2.3	Oxidative desulfurization (ODS)	17
2.4	Biodesulfurization	20
2.5	The S _N 2 reaction	22
2.6	Conversion of alcohol to R-X	23
3	Results and discussion	26
3.1	Synthesis of imidazolium-based ILs	27
3.1.1	Synthesis of 1-chloro-2-(2-methoxyethoxy)ethane (1) and 1-chloro-2-(2-(2-methoxyethoxy)ethoxy)ethane (2)	27
3.1.2	Synthesis of imidazole ether precursors	27
3.1.3	N-alkylation of imidazole ether precursors	29

3.2	Synthesis of benzimidazole ethers	30
3.3	Anion metathesis	30
3.4	Desulfurization of MO using allyl functionalized ILs	35
3.4.1	Effect of the anion	35
3.4.2	Effect of the cation	38
3.5	Optimization studies for IL 8c	40
3.5.1	Effect of mass ratio	41
3.5.2	Effect of time on the desulfurization	42
3.5.3	Effect of the temperature	45
3.5.4	Recyclability of IL 8c	46
3.5.5	^1H -NMR-studies	49
3.6	Desulfurization of MO using benzyl functionalized ILs .	55
3.6.1	Effect of the anion	55
3.6.2	Effect of the cation	57
3.7	Desulfurization of MO with benzoimidazolium based ILs	57
3.7.1	Effect of the anion	58
3.7.2	Effect of the cation	60
4	Conclusion	64
5	Further work	67
6	Experimental	69
6.1	Synthesis of 1-(2-methoxyethyl)-1 <i>H</i> -imidazole (3) . . .	71
6.2	Synthesis of 1-allyl-3-(2-methoxyethyl)-1 <i>H</i> -imidazolium bromide (6a)	71

6.3	Synthesis of 1-allyl-3-(2-methoxyethyl)-1 <i>H</i> -imidazolium bis(trifluoromethylsulfonyl)imide (6b)	72
6.4	Synthesis of 1-allyl-3-(2-methoxyethyl)-1 <i>H</i> -imidazolium dicyanamide (6c)	73
6.5	Synthesis of 1-allyl-3-(2-methoxyethyl)-1 <i>H</i> -imidazolium thiocyanate (6d)	74
6.6	Synthesis of 1-allyl-3-(2-methoxyethyl)-1 <i>H</i> -imidazolium tetrafluoroborate (6e)	75
6.7	Synthesis of 1-chloro-2-(2-methoxyethoxy)ethane (1)	76
6.8	Synthesis of 1-(2-(2-methoxyethoxy)ethyl)-1 <i>H</i> -imidazole (4)	77
6.9	Synthesis of 3-allyl-1-(2-(2-methoxyethoxy)ethyl)-1 <i>H</i> -imidazolium bromide (7a)	77
6.10	Synthesis of 3-allyl-1-(2-(2-methoxyethoxy)ethyl)-1 <i>H</i> -imidazolium bis(trifluoromethylsulfonyl)imide (7b)	78
6.11	Synthesis of 3-allyl-1-(2-(2-methoxyethoxy)ethyl)-1 <i>H</i> -imidazolium dicyanamide (7c)	79
6.12	Synthesis of 3-allyl-1-(2-(2-methoxyethoxy)ethyl)-1 <i>H</i> -imidazolium thiocyanate (7d)	80
6.13	Synthesis of 3-allyl-1-(2-(2-methoxyethoxy)ethyl)-1 <i>H</i> -imidazolium tetrafluoroborate (7e)	81
6.14	Synthesis of 1-chloro-2-(2-(2-methoxyethoxy)ethoxy)ethane (2)	82

6.15 Synthesis of 1-(2-(2-methoxyethoxy)ethoxyethyl)-1 <i>H</i> -imidazole (5)	82
6.16 Synthesis of 3-allyl-1-(2-(2-methoxyethoxy)ethoxyethyl)-1 <i>H</i> -imidazolium bromide (8a)	83
6.17 Synthesis of 3-allyl-1-(2-(2-methoxyethoxy)ethoxyethyl)-1 <i>H</i> -imidazolium bis(trifluoromethylsulfonyl)imide (8b)	83
6.18 Synthesis of 3-allyl-1-(2-(2-methoxyethoxy)ethoxyethyl)-1 <i>H</i> -imidazolium dicyanamide (8c)	85
6.19 Synthesis of 3-allyl-1-(2-(2-methoxyethoxy)ethoxyethyl)-1 <i>H</i> -imidazolium thiocyanate (8d)	86
6.20 Synthesis of 3-allyl-1-(2-(2-methoxyethoxy)ethoxyethyl)-1 <i>H</i> -imidazolium tetrafluoroborate (8e)	87
6.21 Synthesis of 3-benzyl-1-(2-methoxyethyl)-1 <i>H</i> -imidazolium bromide (9a)	88
6.22 Synthesis of 3-benzyl-1-(2-methoxyethyl)-1 <i>H</i> -imidazolium bis(trifluoromethylsulfonyl)imide (9b)	89
6.23 Synthesis of 3-benzyl-1-(2-methoxyethyl)-1 <i>H</i> -imidazolium dicyanamide (9c)	90
6.24 Synthesis of 3-benzyl-1-(2-methoxyethyl)-1 <i>H</i> -imidazolium thiocyanate (9d)	91

6.25 Synthesis of 3-benzyl-1-(2-methoxyethyl)-1 <i>H</i> -imidazolium tetrafluoroborate (9e)	92
6.26 Synthesis of 3-benzyl-1-(2-(2-methoxyethoxy)ethyl)-1 <i>H</i> -imidazolium bromide (10a)	93
6.27 Synthesis of 3-benzyl-1-(2-(2-methoxyethoxy)ethyl)-1 <i>H</i> -imidazolium bis(trifluoromethylsulfonyl)imide (10b)	93
6.28 Synthesis of 3-benzyl-1-(2-(2-methoxyethoxy)ethyl)-1 <i>H</i> -imidazolium dicyanamide (10c)	94
6.29 Synthesis of 3-benzyl-1-(2-(2-methoxyethoxy)ethyl)-1 <i>H</i> -imidazolium thiocyanate (10d)	95
6.30 Synthesis of 3-benzyl-1-(2-(2-methoxyethoxy)ethyl)-1 <i>H</i> -imidazolium tetrafluoroborate (10e)	97
6.31 Synthesis of 3-benzyl-1-(2-(2-methoxyethoxy)ethoxyethyl)-1 <i>H</i> -imidazolium bromide (11a)	98
6.32 Synthesis of 3-benzyl-1-(2-(2-methoxyethoxy)ethoxyethyl)-1 <i>H</i> -imidazolium bis(trifluoromethylsulfonyl)imide (11b)	98
6.33 Synthesis of 3-benzyl-1-(2-(2-methoxyethoxy)ethoxyethyl)-1 <i>H</i> -imidazolium dicyanamide (11c)	99

6.34 Synthesis of 3-benzyl-1-(2-(2-methoxyethoxy)ethoxyethyl)-1 <i>H</i> -imidazolium thiocyanate (11d)	100
6.35 Synthesis of 3-benzyl-1-(2-(2-methoxyethoxy)ethoxyethyl)-1 <i>H</i> -imidazolium tetrafluoroborate (11e)	101
6.36 Synthesis of 1-(2-methoxyethyl)-1 <i>H</i> -benzoimidazole (12)	102
6.37 1-(2-(2-methoxyethoxyethyl)-1 <i>H</i> -benzoimidazole(13)	103
6.38 Synthesis of 1-(2-(2-methoxyethoxy)ethoxyethyl)-1 <i>H</i> -benzoimidazole (14)	103
6.39 Synthesis of 3-allyl-1-(2-methoxyethyl)-1 <i>H</i> -benzoimidazolium bromide (15a)	104
6.40 Synthesis of 3-allyl-1-(2-methoxyethyl)-1 <i>H</i> -benzoimidazolium bis(trifluoromethylsulfonyl)imide (15b)	104
6.41 Synthesis of 3-allyl-1-(2-methoxyethyl)-1 <i>H</i> -benzoimidazolium dicyanamide (15c)	105
6.42 Synthesis of 3-allyl-1-(2-methoxyethyl)-1 <i>H</i> -benzoimidazolium thiocyanate (15d)	106
6.43 Synthesis of 3-allyl-1-(2-methoxyethyl)-1 <i>H</i> -benzoimidazolium tetrafluoroborate (15e)	107
6.44 Synthesis of 3-allyl-1-(2-(2-methoxyethoxyethyl)-1 <i>H</i> -benzoimidazolium bromide (16a)	108

6.45 Synthesis of 3-allyl-1-(2-(2-methoxyethoxy)-ethyl)-1 <i>H</i> -benzoimidazolium bis(trifluoromethylsulfonyl)imide (16b)	109
6.46 Synthesis of 3-allyl-1-(2-(2-methoxyethoxy)-ethyl)-1 <i>H</i> -benzoimidazolium dicyanamide (16c)	110
6.47 Synthesis of 3-allyl-1-(2-(2-methoxyethoxy)-ethyl)-1 <i>H</i> -benzoimidazolium thiocyanate (16d)	111
6.48 Synthesis of 3-allyl-1-(2-(2-methoxyethoxy)-ethyl)-1 <i>H</i> -benzoimidazolium tetrafluoroborate (16e)	112
6.49 Synthesis of 3-allyl-1-(2-(2-methoxyethoxy)-ethyl)-1 <i>H</i> -benzoimidazolium bromide (17a)	113
6.50 Synthesis of 3-allyl-1-(2-(2-methoxyethoxy)-ethyl)-1 <i>H</i> -benzoimidazolium bis(trifluoromethylsulfonyl)imide (17b)	114
6.51 Synthesis of 3-allyl-1-(2-(2-methoxyethoxy)-ethyl)-1 <i>H</i> -benzoimidazolium dicyanamide (17c)	115
6.52 Synthesis of 3-allyl-1-(2-(2-methoxyethoxy)-ethyl)-1 <i>H</i> -benzoimidazolium thiocyanate (17d)	116
6.53 Synthesis of 3-allyl-1-(2-(2-methoxyethoxy)-ethyl)-1 <i>H</i> -benzoimidazolium tetrafluoroborate (17e)	118

1 Introduction

1.1 Fossil fuels

Nowadays, automobiles have become a major part of daily life, and the production of vehicles fueled by gasoline or diesel is increasing exponentially. As the technology has developed throughout the years, the world has relied more on fuel based inventions. It is an essential part of life, with more than 80% of global energy being satisfied by fossil fuels. However, the extensive use of fuel, has had severe consequences on the environment in the form of air pollution, ozone depletion and acid rain. These consequences are mostly due to feed contaminants in the crude oil. The number of contaminants may vary, but they usually consist of pollutants such as sulfurated, nitrogenated and aromatic compounds, naphthenic acids and asphaltenes, in addition to gases such as H₂S, CO₂ and N₂.[1] As a result of this, oil refineries are required by governmental organizations, such as the EU, to keep the sulfur content in the fuel oil below 10 ppm.[2] There are many methods to reduce the sulfur content below the required level. However, major challenges arise when satisfying the legal requirements at the same time as using environmental friendly and economical methods, thus highlighting the need for new, improved methods for desulfurization.

1.2 Hydrodesulfurization (HDS)

One of the main contributors to air pollution is the formation of sulfur oxides (SO_X) and nitrogen oxides (NO_X) gases, derived from their respective sulfurated- and nitrogenated compounds upon combustion in automobiles. Over time, inactivity of the catalyst in vehicles used to reduce CO and NO_x emission can occur.[3] In petroleum, organic sulfur (Figure 1) constitutes the main source of sulfur compounds.

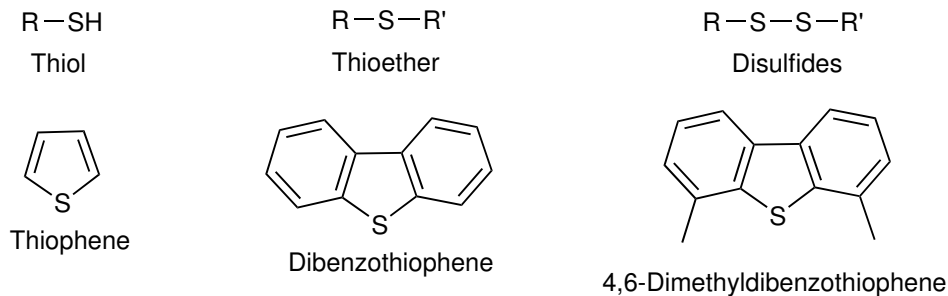


Figure 1: Structure of common sulfur compounds found in fuel oils.

The most common industrial method for removal of sulfur compounds from crude oil is hydrodesulfurization (HDS). In this method, desulfurization is achieved by the catalytic conversion of sulfur compounds to H_2S using $\text{Co-Mo}/\text{Al}_2\text{O}_3$ or $\text{Ni-Mo}/\text{Al}_2\text{O}_3$ as catalyst in a trickle bed reactor. The oxidation of produced H_2S to elemental sulfur is achieved through the Claus process, which is based on a catalytic reaction with O_2 .[4][5] HDS has proven to be successful in the removal of sulfides, disulfides and thiols, but it suffers from various drawbacks, including the requirement of harsh operating conditions such as high temperature (300-400°C) and high pressure (20-100 atm of H_2). In addition, HDS is not effective for the removal of heterocyclic sulfur compounds such

as thiophene, dibenzothiophene (DBT), 4,6-dimethyldibenzothiophene (4,6-DMDBT) and their derivatives.

In HDS, the reactivity of the sterically hindered sulfur compounds (DMDBT) is very low owing to the shielding of catalyst surface from the sulfur atom by the methyl groups. Due to the aromaticity of the benzothiophenic core, the molecule is planar, thus, it can not rotate to facilitate the interactions between the sulfur and the catalyst.[6] Hence, the reactivity order of the aromatic sulfur compounds in the HDS process is 4,6-DMDBT < DBT < Thiophene. To carry out the removal of these compounds, more harsh conditions and expensive catalysts are required, which will lead to saturation of the aromatic compound, hence allowing free rotation. However, this severely affects the economical feasibility of the process. In addition, it will reduce the octane number, which is an important parameter in determining the quality of the fuel oil.[7]

1.3 Alternative methods for desulfurization

In order to find effective methods for desulfurization of fuel oils, other processes have been explored, including methods such as extractive desulfurization (EDS), oxidative desulfurization (ODS) and biodesulfurization (BDS). However, all these methods suffer from several disadvantages. Despite the fact that ODS has resulted in high desulfurization efficiency, the long extraction time, high cost and difficulty in regeneration of the catalyst are still major challenges. BDS lacks an efficient biocatalyst for the desulfurization process, which has prevented

the development of ODS from the laboratory to industrial scale. The shortcomings of EDS are the requirement of high solvent to fuel oil ratio and the lack of efficient non-toxic extracting solvents.

Studies on organic solvents as extracting media in EDS have been conducted. However, due to high volatility, poor selectivity towards sulfur compounds and high toxicity, it is necessary to develop environmental friendly solvents (non-volatile, non-toxic and readily biodegradable). Furthermore, the solvent must yield high extraction efficiency and be economical to synthesize.

Ionic liquids (ILs) are a class of compounds that have recently been employed in desulfurization.[8] ILs are organic salt with a melting point below 100 °C. Owing to their negligible vapour pressure, high thermal stability, recyclability and high affinity towards sulfur, ILs are usually preferred over traditional organic solvents as an extraction medium in EDS.[9] Several studies have reported the use of ILs in EDS with promising results. For instance, Safa *et al.* reported nitrate based pyridinium and imidazolium ILs for the extraction of DBT. The superior IL was found to be

1-octyl-3-methylimidazolium nitrate ([Omim][NO₃]), which had an extraction efficiency of 95% in a single stage extraction.[10] However, the nitrate anion has shown to be explosive and toxic to aquatic life.[11][12]

Ko *et al.* reported the desulfurization of DBT from fuel oil using 1-butyl-3-methylimidazolium chloride ([BMIM][Cl]) and 1-butyl-3-methylimidazolium trichloroferrate [BMIM][FeCl₃] ILs. [BMIM][Cl] and [BMIM][FeCl₃] showed an extraction efficiency 17% and 34% re-

spectively. However, a complete removal of DBT was observed at a 2:1 molar ratio of FeCl_3 and $[\text{BMIM}][\text{Cl}]$. The increase could be explained by a Lewis acid-base interaction between the Fe^{3+} ion and DBT.[13] Despite the promising results, ILs containing metal halide anions increase the toxicity against marine organisms.[14]

Dharaskar *et al.* investigated trihexyl(tetradecyl) phosphonium tetrafluoroborate ($[\text{THTDP}][\text{BF}_4]$) as an extracting reagent for the removal of sulfur contaminants. The EDS was performed in an ultrasonic bath, which gave a 93% extraction efficiency in a single step. The high sulfur removal (S-removal) was explained by the increase of reaction rates in view of the formation of radicals, cleavage of bonds and mass transfer.[15] It has been observed to provide useful effects during desulfurization.[16] Nonetheless, BF_4 and other fluoride containing anions have ecotoxicological issues that arise upon disposal due to their tendency to form hydrogen fluoride.[17]

In order to implement EDS in industrial desulfurization, non-toxic and biodegradable ILs with high sulfur desulfurization performance is necessary, considering environmental problems upon waste disposal. Raj *et al.* presented relatively non-toxic and biodegradable ILs by introducing an ester moiety. Several ILs containing methyl propionate attached to an imidazolium cationic core were studied. However, the extraction efficiency was not sufficient (less than 80%), which might be due to the presence of only one functional group on the cation.[18]

Another approach may be the introduction of diethylene glycol groups on the cationic core of ILs, which may reduce the toxicity and increase

the biodegradability of the IL.[19] Furthermore, promising results have been obtained using polyethylene glycol containing (PEG) ILs, which lead to higher desulfurization as the glycol chain increased.[20, 21] The observation could be explained by the presence of the electronegative oxygen atoms which increases the electrostatic n- π interactions between ILs and sulfur compounds.[22] In addition, it is well known that π - π interactions between ILs and the aromatic sulfur compounds plays an important role in the desulfurization.[23] Based on this, the current project investigates the removal of aromatic sulfur compounds, such as DBT and 4,6-DMDBT, from n-dodecane. The EDS will be performed by dual functionalized imidazolium based ILs, containing PEG and aromatic groups. Imidazolium is chosen as the cationic core due to its low toxicity, possibility of attaching two functional groups, its ability to have π - π interactions with the aromatic sulfur compounds and its biodegradability.[24] Table 1 shows some of the results obtained by imidazole based ILs in literature.

Table 1: An overview of reported extraction efficiencies obtained by EDS using imidazole based ILs. The mass-ratio between the IL and the model oil (MO) is 1:1.[9][25][18][10][26][5][27][28]

IL	Compound	Model Oil(MO)	% Removal
[BMI][N(CN) ₂]	DBT	Gasoline	49
[MMIM][MeSO ₄]	DBT	Hexane	40
[BMIM][HSO ₄]	DBT/BT/TS	<i>n</i> -Dodecane	69
[OMIM][NO ₃]	DBT	<i>n</i> -Decane	95
[C ₄ MIM][SCN]	DBT	<i>n</i> -Dodecane	66
[C ₄ C ₁ Im][BF ₄]	DBT	<i>n</i> -Decane/Toluene ^a	20
[C ₁₀ C ₁ mim][NTf ₂]	DBT	<i>n</i> Octane/Toluene ^b	58
[C ₂ C _N Im(EtO) ₃ Me] [NTf ₂]	DBT	<i>n</i> -Dodecane	74
[Bmim][dcnm]	DBT	Hexane/Toluene ^c	66
[C ₄ mim][dcnm]	DBT	Hexane/Toluene ^c	52

a: MO: 85 wt% *n*-Decane and 15 wt% toluene

b: MO: 85 wt% *n*-Octane and 15 wt% toluene

c: MO: 85 wt% *n*-Hexane and 15 wt% toluene

1.4 Aim of the project

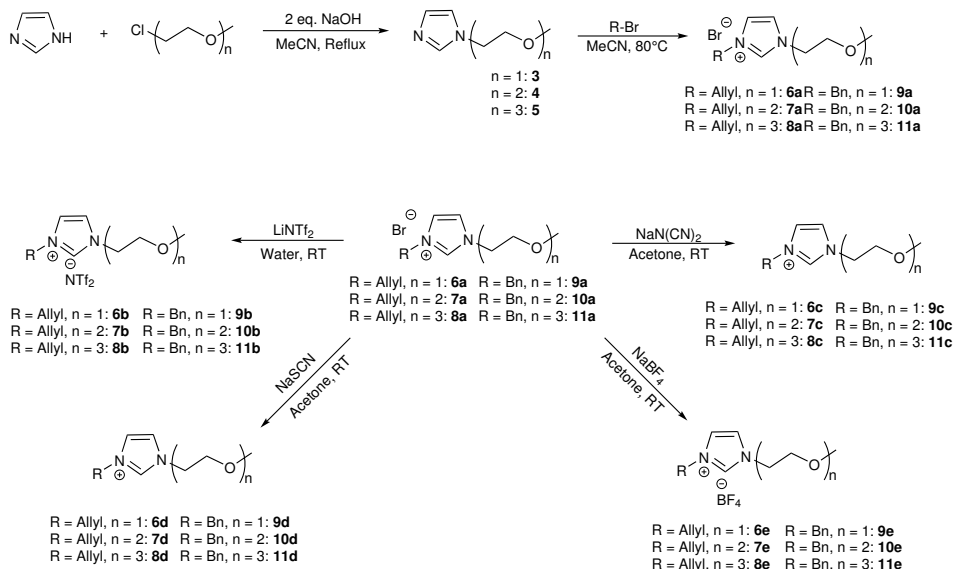
The overall aim of this project is to synthesize dual functionalized imidazolium-based ILs and study their desulfurization efficiency. The ILs are designed in order to achieve the following criteria:

- High desulfurization efficiency
- Low toxicity
- High biodegradability
- Easy and economical synthesis

The ILs will be prepared by S_N2-reactions between the imidazole and

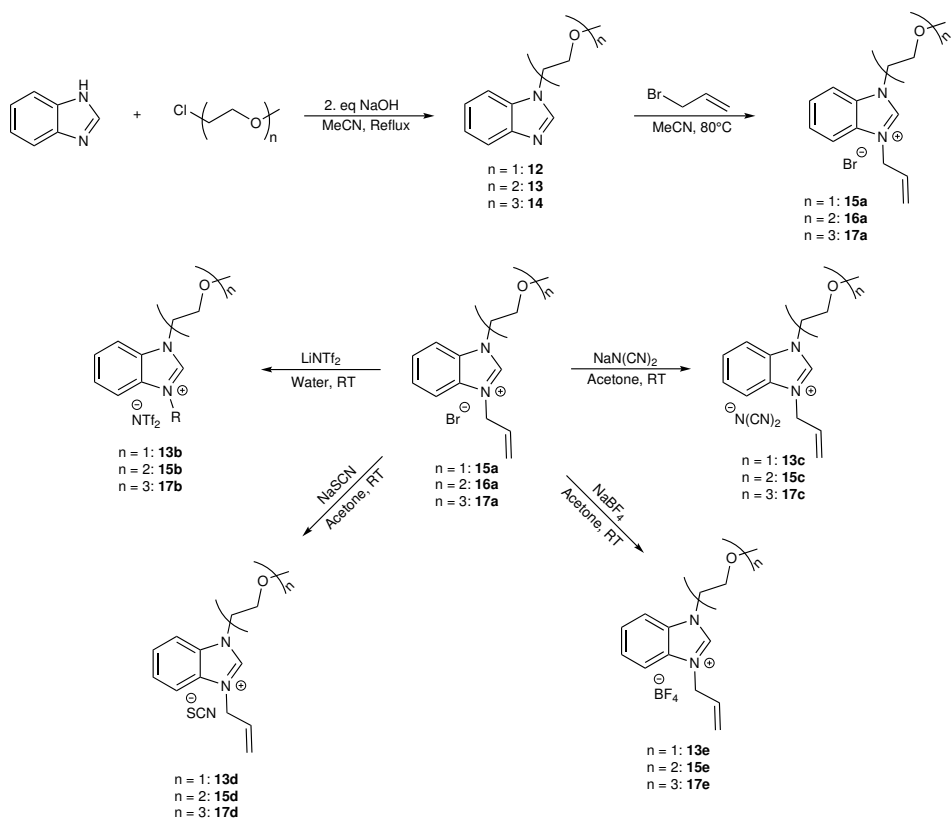
the appropriate halide alkyl (Scheme 1), such as diethylene glycol chain and aromatic substituents (benzyl and allyl group). This gives a series of bromide salts (**6a-10a** and **15a-17a**). Finally, anion exchange with the desired anions (NTf_2 , $\text{N}(\text{CN})_2$, SCN and BF_4^-) yields the target ILs.

The presence of aromatic substituents and increasing number of ether groups on the imidazolium cation will be used to study the effect on the desulfurization efficiency.



Scheme 1: Synthesis of dual functionalized imidazolium based ILs containing diethylene glycol chain ($n=1-3$), allyl and benzyl groups.

Furthermore, corresponding investigation will also be performed with benzimidazolium ILs bearing increasing diethylene glycol chain length and an allyl group. A schematic procedure for the synthesis of benzimidazolium ILs (**15-17**) is shown in Scheme 2.



Scheme 2: Synthesis of benzimidazolium based dual functionalized ILs containing varying number of diethylene glycol chain ($n=1-3$) and allyl group.

2 Theory

2.1 Ionic Liquids

Many definitions have been formulated for ionic liquids (ILs). The most common definition is that ILs are liquid salts with a melting point below 100°C.[29] The cation is usually an organic compound, while the anions are usually inorganic, but can in some cases be organic, in nature. The structure of the cation hinders the resulting salt from forming a compact crystal lattice. This prevents crystallization, thus the ILs remain in liquid state at a wide range of temperatures.[30]

The first synthesized IL was ethylammoniumnitrate ($[\text{EtNH}_3][\text{NO}_3]$) reported by Paul Walden as early as 1914.[31] The properties of ILs were not thoroughly studied at the time, but a few decades later, the number of articles regarding synthesis and applications of ILs has vastly increased. As a result, researchers have discovered broad applications for ILs, such as CO₂-capture[32][33], catalysts[34][35], solvent for organic synthesis[36][37] and electrolytes for various (magnesium and lithium) ion batteries[38][39]. High thermal stability, tuneable polarity, low volatility, and intrinsic ionic conductivity, are some of the reason for their growing application fields.[38][29] Owing to the tuneability of physicochemical properties, easy synthesis and special set of unique properties (low vapor pressure, wide liquid range, etc), ILs are named "designer solvents".[40] Due to the endless possibilities in the selection of cations and anions, different classes of ILs have been de-

veloped, such as room-temperature ILs(RTILs)[41], task-specific ILs (TSILs)[42], polyionic ILs (PILs)[43] and supported membrane ILs (SMILs)[44]. Some common cations and anions used in ILs are shown in Figure 2 and Figure 3.[29]

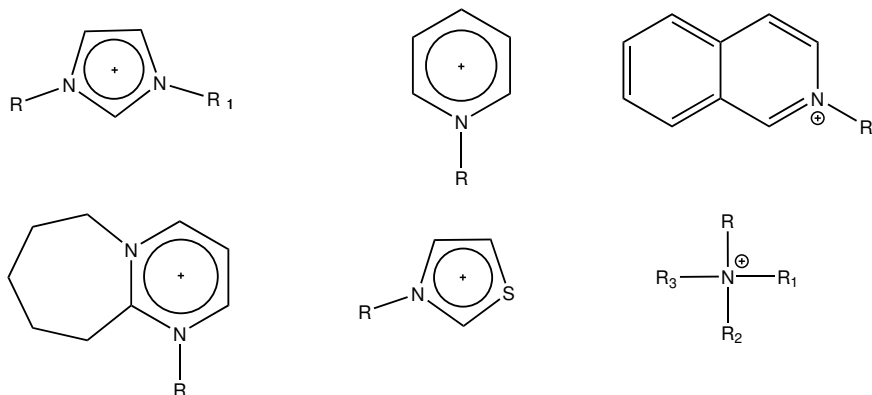


Figure 2: Common cations for ionic liquids.

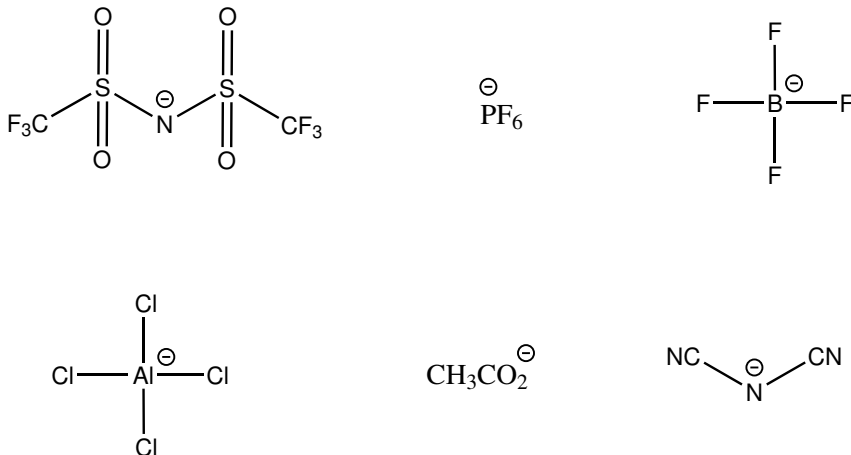


Figure 3: Common anions for ionic liquids.

2.1.1 Synthesis of ILs

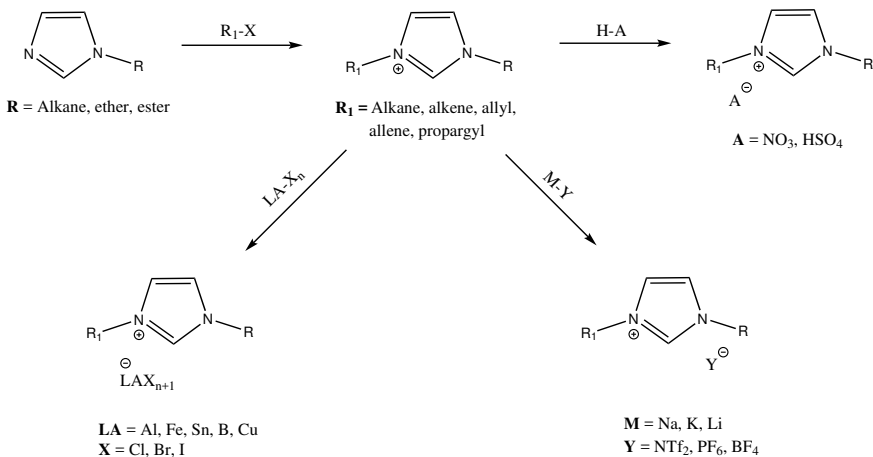
Two benefits of ILs are their easy synthesis and their accessibility through several reaction pathways. One of the possible reaction pathways include protonation of an amine or a phosphine with acids (phosphoric acid, sulfuric acid), resulting in the formation of the PILs. These type of ILs can be achieved through the transfer of a proton from a Brønsted acid to a Brønsted base.[45] Another way to synthesize ILs is the quaternization reaction of an amine or a phosphine through a S_N2 -reaction, usually with a haloalkane, followed by the anion exchange reaction of the resulting halide salt with a metal salt of the desired anions.[29]

Alkylation reactions have various advantages, such as the availability of cheap alkyl halides, mild reaction conditions, high yields, etc. Furthermore, the halide salts of the ILs can easily undergo an anion exchange to give the desired IL.

The anion-exchange reactions can be performed through several pathways: treatment of halide salts with Lewis acids, anion metathesis with metal salt of the desired anion and the reaction with protic acids.[29] A general synthesis of ILs is shown in Scheme 3.

2.1.2 Purification of ILs

The importance of the purity of the synthesized ILs depends on their field of application. However, researchers usually aim to obtain "ultra pure" ILs in order to prevent impurities affecting the physico-



Scheme 3: A general synthesis of ILs through anion exchange using Lewis acid and anion methathesis.[29]

chemical properties of the ILs. For instance, a considerable difference in melting point (10 °C) for 3-methyl-imidazolium tetrafluoroborate ([C₂C₁im][BF₄]) has been reported by two different studies.[46][47] Furthermore, discoloration due to halide impurities is common, but usually does not affect the results. However, negative effects of discoloration have been reported in an acidity study of 1-butylimidazolium hydrogensulfate ([HC₄im][HSO₄]) using UV-vis spectroscopy. The IL had a unnoticeable green tinted colour, which blocked out the lower wavelengths, thus preventing the measurement from being performed.[48]

The impurities in ILs can broadly be divided into three categories: contamination from the starting material, contamination from the undertaken reactions, and unwanted solvents. To eliminate contamination from the starting material, they should be purified, *e.g.* by distillation. The starting material should then be stored under inert atmosphere to prevent water contamination.[29]

Contamination from undertaken reactions usually arise from either unreacted starting materials or side-reactions. In alkylation reactions, haloalkanes should be used in a small molar excess to ensure complete reaction with amines, phosphines or sulfides. The unreacted haloalkanes can be readily evaporated, due to their low boiling point. Alkali metal halide salts (NaCl, NaBr, etc.) formed in the anion exchange reactions are usually removed by several washing steps in solvents where the ILs and the halide salts have significant difference in solubility.[48] To ensure complete removal of solvents, it is recommended to dry the IL at a temperature between 60-70°C.[48]

2.2 Extractive desulfurization (EDS)

Among the existing desulfurization methods, extractive desulfurization (EDS) is the easiest to implement in the petroleum industry. This method offers very mild conditions, selective removal of S-compounds, no requirement of catalyst or hydrogen, an easy process and no side reaction with the fuel oil.[7] EDS is based on simple extraction with polar organic solvents, *e.g.* acetonitrile, DMSO or DMF, in order to extract sulfur compounds from the fuel oil. Owing to the difference in polarity, two immiscible layers will be formed. Separating the layers will result in fuel oil with lower sulfur content (S-content) and organic solvent containing the extracted sulfur compounds.[2] However, organic solvents have major drawbacks that lead to safety and environmental problems. This includes high volatility, contamination of the fuel oil and difficult solvent recovery. Thus, other extracting reagent

alternatives have been explored.

The application of ILs in EDS has shown promising results. Higher extraction efficiency has been reported in a shorter period of time and under mild conditions. EDS using ILs was first reported by Bösmann *et al.*[49] They investigated the effect of the cations and anions on the desulfurization efficiency of ILs. This was achieved by studying various imidazolium-based chloroaluminate ILs. The results indicated that the higher desulfurization was obtained by increasing the size of the cations. In addition, a significant effect of the anion size had an influence upon equal molar ratio of IL:MO. Furthermore, changing the anion can also alter the %S-removal. Chen *et al.* investigated EDS and ODS with 3-(3-methyl-1*H*-imidazolium)propane-1-sulfonic acid ($[\text{HMIm}][\text{(CH}_2)_4\text{SO}_3]$) with several anions. Using dihydrogen phosphate ($[\text{H}_2\text{PO}_4]$) as the anion, resulted in 10% desulfurization efficiency. However, changing the anion from $[\text{H}_2\text{PO}_4]$ to zinc(III) chloride ($[\text{ZnCl}_3]$), resulted in an enhancement of the extraction efficiency to 28%.[50]

The viscosity of the IL plays an important a role in EDS. A study conducted by Asumana *et al.* investigated dicyanamide-based ILs with different cationic cores. The results showed that the highest desulfurization was obtained by 1-butyl-3-methylimidazolium dicyanamide ($[\text{BMIM}][\text{N}(\text{CN})_2]$), which had the lowest viscosity. Furthermore, they observed that as the viscosity increased, the desulfurization efficiency decreased. This might be due to the slower mass transfer of the S-compound from the oil phase to the IL phase, and thus may give

poorer dispersion of the IL in the oil.[27]

As mentioned in the introduction, π - π interactions plays an important role in EDS. A theoretical study by Nie *et.al* indicated that several interactions between ILs and sulfur compounds occurs during desulfurization. According to the study, the most dominant interactions are π - π interactions and hydrogen bonding. Hence, to increase sulfur extraction, ILs should contain functional groups that enhance these interaction.[51] A theoretical study reported by Holbrey *et al.*, suggested that the π - π interactions take place in a "sandwich"-like structure where the aromatic compound is in the middle of two IL-molecules.[52]

Although ILs in EDS are showing promising results, they still suffer from several drawbacks. As of today, the single stage extraction efficiency of environmental-friendly ILs is not yet sufficient enough (less than 80%). Multiple extractions are often required in order to yield a fuel oil with low S-content. Other drawbacks are requirement of high IL:fuel ratio and the cost of ILs.

2.2.1 Parameters in desulfurization

The percentage removal of sulfur compounds from MO, can be calculated using Equation 1:[15]

$$R = \frac{C_0 - C_f}{C_0} * 100\% \quad (1)$$

where R is the percentage sulfur removal and C_0 and C_f are the initial and final concentrations of sulfur compounds in the MO. Another

important parameter is the Nernst partition coefficient (K_N), which is useful to evaluate the EDS performance. It gives information about the ratio between concentration of sulfur compounds in the IL and MO. In other words, K_N is the ILs affinity towards the sulfur molecules, which can be expressed by Equation 2:

$$K_N = \frac{C_0 - C_f}{C_f} * \frac{m_{IL}}{m_{MO}} \quad (2)$$

where C_0 and C_f are the initial and final concentrations and m_{IL}/m_{MO} is the mass ratio between the IL and MO.[15][9]

2.3 Oxidative desulfurization (ODS)

Another promising method for the desulfurization of fuel oil is oxidative desulfurization (ODS). ODS is of interest mainly due to its reactivity towards sterically hindered sulfur compounds. It is the reverse of the reactivity observed in the HDS process, *i.e.* 4,6-DMDBT > DBT > BT. This may be due to an increase of electron density owing to the electron donating groups.[53] Considering that DBT and its derivatives constitute the majority of the sulfur compounds in fuel oils, researchers have found this method very promising.

The ODS process consists of two main steps. The first step is the oxidation of the sulfur compound to sulfones, which can be achieved through the use of an oxidizing agent. The oxidation of the sulfur atom changes the physical and chemical properties of the sulfur compound significantly, thus making it more polar. The second step is the

removal of the oxidized sulfur compounds, which is usually achieved by extraction with a polar solvent, such as DMSO, DMF, methanol or acetonitrile.

One of the first reported studies used NO_2 as an oxidising agent. However, other oxidants have also been explored due to the environmental and health issues related to NO_2 .^{[4][54]} Taking economic factors and ecological constraints into account, H_2O_2 has been found a promising candidate as an oxidising agent.^[55] H_2O_2 is promising due to its attractive properties such as being non-polluting, less corrosive and it generates water as the byproduct during ODS, in addition to the low cost and commercial availability. Owing to their slow oxidation in the absence of acid catalysts, various combinations of H_2O_2 and several transition metal salts with high oxidation number and Lewis acidity were explored as catalysts for oxidation of aromatic sulfur compounds.^{[56][57]} However, one of the main problems with these catalysts is the long reaction time. This is due to the presence of two reaction phases, in which the oxidizing reagent is present in the polar phase while the sulfur compounds are in the non-polar phase.^[58] Another alternative for the transition metal catalyst is phase transfer catalysts, which leads increased mass-transfer across the polar-apolar interphase.^{[59][60][61]}

When a catalyst is employed, the observed reactivity order for the sulfur compounds is: DBT>4,6-DMDBT>BT. The reactivity appears to be affected by the steric hindrance of the sulfur compounds. This might be due to the aromatic rings which elicit an increase in the

electron charge density of the S-atom, thus making oxidation with H₂O₂ easier.[59]

The most studied catalyst in literature is the Mo/Al₂O₃, which provided excellent S-removal.[62][63] However, the Mo/Al₂O₃ has a tendency to leach into the reaction medium and result in the loss of the catalyst.[64] This problem can be solved by the synthesis of Al₂O₃ supported Mo catalysts.[65][66][67]

The mechanism in ODS begins with the oxidiation of a phase transfer catalyst by the oxidizing agent in the polar phase. This leads to formation of a peroxy compound, which migrates to the apolar phase. Hence, the catalyst can interact with the sulfur compound by first oxidizing it to a sulfoxide through an oxygen atom transfer reaction. Furthermore, an oxidation of the sulfoxide occurs in the same manner resulting in the formation of sulfone. The sulfone migrates to the polar phase due to the drastic change in polarity. The catalyst can be regenerated either at the polar-apolar interphase or in the polar phase upon reaction with H₂O₂.[58][4]

The organic solvent used in ODS can be recovered by distillation and can be reused.[2] However, organic solvents have many disadvantages such as difficulty in solvent recovery due to high volatility and contamination of fuel oil.[4] Therefore, ILs have been suggested as an alternative to traditional solvents. In addition to act as a solvent, ILs have also shown to work as an oxidizing reagent. Lo *et al.* used a combination of oxidative and extractive desulfurization, in which they used 1-butyl-3-methylimidazolium hexafluorophosphate ([BMIM][PF₆]) and

1-butyl-3-methylimidazolium tetrafluoroborate ($[\text{BMIM}][\text{BF}_4]$) ILs as the extracting agent. Comparing to EDS, the results obtained in this study indicated a significant increase in the extraction efficiency (from 7% to 55% for $[\text{BMIM}][\text{BF}_4]$ and from 8% to 85% for $[\text{BMIM}][\text{PF}_6]$). However, the extraction time was unacceptably long (10 h). Furthermore, the water-immiscible $[\text{BMIM}][\text{PF}_6]$ gave better results than the water soluble $[\text{BMIM}][\text{BF}_4]$, owing to better dispersion of the less polar IL.[68]

Even though high S-removal has been obtained through extraction-oxidation desulfurization using ILs, this method has many disadvantages. For instance, problems may arise upon regeneration of the catalyst. An ideal ODS would be a method in which a catalyst is not required. Nonetheless, earlier studies have reported lower yields or the necessity of a high $\text{H}_2\text{O}_2/\text{S}$ ratio in the absence of a catalyst. The field of IL application in ODS is relatively new, thus several possibilities are still not investigated. Other issues concerning ODS are the cost of the ILs, waste treatment of sulfone formed in the reaction and possible side reactions under high temperatures.[4][58]

2.4 Biodesulfurization

Bacteria in natural systems assimilate sulfur in small amounts for maintenance and growth.[69] Cysteine (Cys) production in plants usually undergoes a microbial-catalyzed sulfur cycling in order to obtain sufficient amounts of inorganic sulfates needed. This leads to a series of reactions and intermediates, which ends up reducing the sulfur com-

pound to sulfide needed in the biosynthesis of Cys.[70] Researchers have looked for a way to exploit the properties of the bacteria in desulfurization through a process called biodesulfurization (BDS). Promising results have been obtained because bacteria can degrade DBT and its derivatives.[69]

The two most common pathways in BDS are the Kodama pathway and the 4S-pathway.[71] The Kodama pathway involves the cleavage of carbon-carbon bonds of DBT. The first step of this pathway is the lateral dioxygenation of one of the phenyl rings catalyzed by DBT oxidation genes (Dox) ABDE. This is followed by a cleavage of the ring by DoxG genes and hydrolysis by DoxJI genes to form the water soluble hydroxyl-formyl-benzothiophene and pyruvate as the end products.[72] The DBT degradation is usually plasmid encoded in different *Pseudomonas* strains.[73]

The most common pathway however, is the 4S-pathway and it is the most studied pathway due to removal of the sulfur from the DBT-skeleton. The first step is the activation of the thiophene ring for cleavage by oxidation of the sulfur to sulfoxide, catalyzed by the desulfurization gene C (*dszC*). The sulfoxide undergoes a second oxidation in the same manner, leading to the formation of DBT-sulfone. Cleavage of the thiophene ring is achieved by *dszA*, leading to the formation of 2-hydroxybiphenyl-2-sulfinate (HBPS). Using *dszB*, the sulfinate group can be removed, resulting in 2-hydroxybiphenyl (2HBP).[74] Further studies have also shown that 2HBP can further be methoxylated by the use of *Microbacterium* sp. strain ZD-M2, which resulted not only

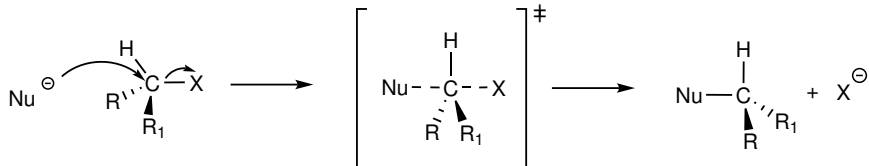
in 2-methoxybiphenyl (2MBP), but also biphenyl.[75]

Studies of BDS-processes have gained an increasing interest, but as of today, BDS-processes struggle to yield fuel oils with low S-content. The desulfurization process is still unclear and a deeper understanding is needed in order to apply it in the industrial level. The solution to improve the desulfurization efficiency of BDS is the genetic modification of the current bacterias or discovery of new biocatalysts.[76] The requirements for a novel biocatalyst would be higher specific desulfurization activity, broader substrate range, higher substrate affinity in biphasic reaction systems containing toxic solvents, activity for a long period of time and higher thermal tolerance.[69]

2.5 The S_N2 reaction

The S_N2 reaction is one of the most fundamental reactions in organic chemistry and consists of a nucleophile (Nu) replacing a leaving group (LG) in a molecule. The Nu is always a Lewis base and it may be neutral or negatively charged. The LG is a stable functional group or an atom that accepts a lone pair as the bond between the carbon it is attached to and itself breaks. The Nu attacks the molecule from the opposite side with respect to the LG, *i.e.* the angle between the LG and Nu is 180° (Scheme 4). This leads to the transition state where the Nu is connecting to the carbon of interest while LG is departing at the same time. In the final product, the Nu is attached to the carbon and the LG is detached. The LGs are usually halogens and follow the reactivity order: I > Br > Cl > F due to increasing C-halogen

bond strength, polarizability and size. If there is a chiral center at the carbon that is attacked, an inversion of configuration will occur.[77]



Scheme 4: A general S_N2 mechanism showing the inversion of the configuration.[77]

In S_N2 reactions, the reactivity order is: methyl > 1° > 2° in order of increasing steric hindrance, which means a decrease in accessibility of the relevant carbon atom. The Nu is usually a strong Lewis base and S_N2 -reactions are usually performed in polar aprotic solvents, such as acetonitrile. However, substitution reactions often compete with elimination reactions if the Nu can act as a Brønsted base.

Since both the nucleophile and the substrate are involved in the rate-determining step, the overall order should be secondary and can be expressed by Equation 3.

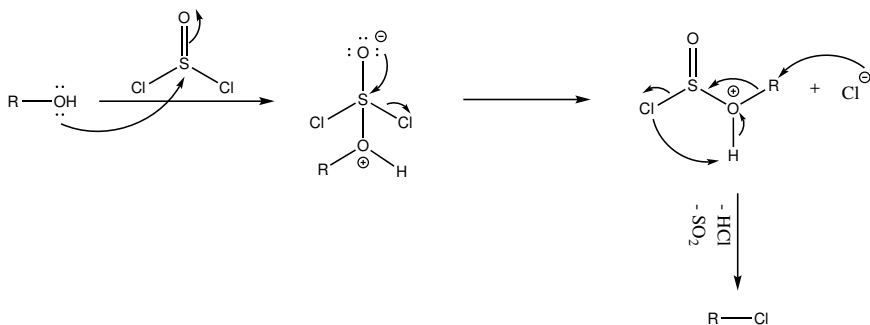
$$\text{Rate} = [\text{Nu}][\text{HCR}_1\text{R}_2\text{X}] \quad (3)$$

2.6 Conversion of alcohol to R-X

Alcohols are interesting compounds in organic synthesis, but it is well known that they are poor LGs. Hence, the conversion of the OH-group into a better LG is usually needed. The choice of an appropri-

ate reagent usually depends on the stability of the alcohol and other functional groups in the molecule. For instance, unsubstituted primary alcohols can readily be converted by the use of hydrogen halides through an easy S_N2 -reaction.[78]

However, most organic compounds of interest tend to not tolerate the conditions required to undergo a simple hydrogen halide reaction. In such cases, other alternatives are needed. The most common conversion reagents to transform alcohols into alkyl halides are thionyl chloride, phosphorus trichloride and phosphorus tribromide. These reactions offer milder conditions and are suitable for alcohols that are neither acid sensitive nor prone to structural rearrangement. A reaction mechanism using thionyl chloride is shown in Scheme 5.[79]



Scheme 5: Reaction mechanism for converting alcohols to halides using thionyl chloride.

The first step of the reaction is the attack of the alcohol on the sulfur in thionyl chloride, leading to the formation of chlorosulfite ester. The sulfoxide is regenerated upon the release of one of the chlorides. The final step is the nucleophilic attack of the chloride ion on the R-group, and through several subsequent steps, R-Cl is formed with HCl and

SO_2 as side products. A base, such as pyridine or triethylamine, can be used to deprotonate the alcohol, which promotes the reaction.[77]

3 Results and discussion

In this section, the synthesis of the ionic liquids and precursors performed in the thesis will be discussed along with the desulfurization performance of the synthesized ILs. In addition, the optimization studies on the extraction of sulfur contaminants from the model oil and the interaction between the ionic liquids and DBT/4,6-DMDBT will be discussed.

All target IL precursors were fully characterized by NMR spectroscopy, FT-IR spectroscopy and HR-MS (in positive and negative mode) for confirmation of the respective cations and anions. The chemical shifts were assigned by 2D-NMR spectroscopy.

A calibration curve was made by plotting known concentrations of the sulfur compounds against the area under their respective peak obtained by reverse phase high performance liquid chromatography (RP-HPLC) and UV-vis detection. The extraction efficiency was calculated by analyzing the model oil after EDS.

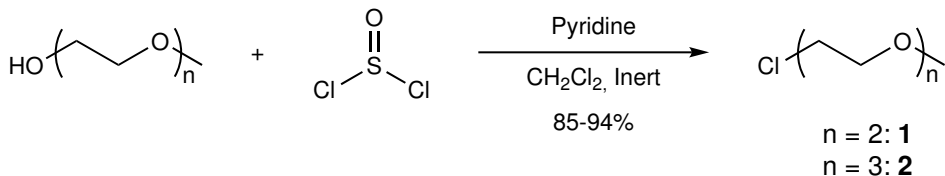
The EDS was performed by stirring a 1:1 mass ratio of the ILs and the MO containing DBT and 4,6-DMDBT dissolved in *n*-dodecane for 2 h, unless stated otherwise. The oil layer (upper layer) was extracted and analyzed by HPLC to calculate the extraction efficiency. The analysis were carried out in triplicate and the average value of the area under the peak was used in the calculation of desulfurization efficiency, which can be found in the Appendix.

3.1 Synthesis of imidazolium-based ILs

In this section, the synthetic procedures for all synthesized ILs are presented and discussed.

3.1.1 Synthesis of 1-chloro-2-(2-methoxyethoxy)ethane (**1**) and 1-chloro-2-(2-(2-methoxyethoxy)ethoxy)ethane (**2**)

Fiksdahl *et al.* suggested the transformation of the alcohols on diethylene glycol to chloride by reaction with thionyl chloride and pyridine, to yield 1-chloro-2-(2-methoxyethoxy)ethane (**1**) and 1-chloro-2-(2-(2-methoxyethoxy)ethoxy)ethane (**2**). However, in this project, compound **1** and **2** (Scheme 6) were synthesized under inert atmosphere. This led to increased yield of compound **1** (from 69% to 85%) and compound **2** (from 60% to 94%).



Scheme 6: Synthetic procedure of compound **1** and **2**.

3.1.2 Synthesis of imidazole ether precursors

Previous work in the Fiksdahl group proposed the formation of compound 1-(2-methoxyethyl)-1*H*-imidazole ether (**3**) through a S_N2-reaction

of imidazole with commercially available 2-chloroethyl methyl ether and an excess (2 eq.) of sodium ethoxide. In this project, the reaction yielded the desired product **3** when performed in small scale. However, during a scale-up of the reaction, unexpected precipitation occurred upon removal of solvent under reduced pressure. In addition, ¹H-NMR spectra of the compound showed traces of unreacted imidazole and several unknown peaks, assumed to be sodium ethoxide. Despite increasing the reaction time to 48 h and 72 h, traces of imidazole could still be observed. To purify the compound, the solution was dissolved in dichloromethane (DCM) and left in the freezer over night to allow the precipitation of excess sodium ethoxide. The solution was filtered and DCM was evaporated under reduced pressure. However, precipitation still occurred. Although same procedure was repeated in chloroform, the complete removal of sodium ethoxide was not successful.

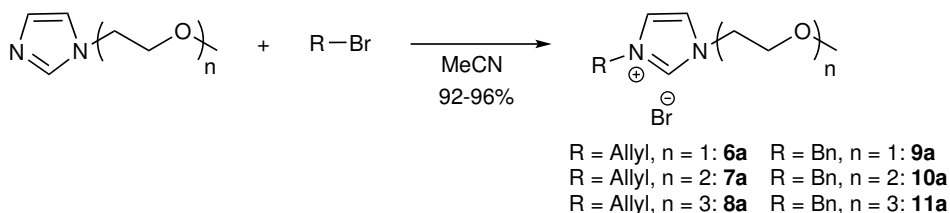
Additional methods, including DCM and chloroform extraction and filtering through a layer of four filter papers, were tested to remove the observed precipitation, without success. Another attempt was to change the base from sodium ethoxide to sodium hydroxide, which yielded pure product without precipitation. Furthermore, a scale-up of the reaction was performed and resulted in excellent yield. Hence, the remaining imidazole ethers were synthesized according to Scheme 7, affording compound **3**, 1-(2-(2-methoxyethoxy)ethyl)-1*H*-imidazole (**4**) and 1-(2-(2-(2-methoxyethoxy)ethoxy)ethyl)-1*H*-imidazole (**5**) in 96%, 94% and 86% yield, respectively.



Scheme 7: Synthetic procedure of compound **3**, **4** and **5**.

3.1.3 *N*-alkylation of imidazole ether precursors

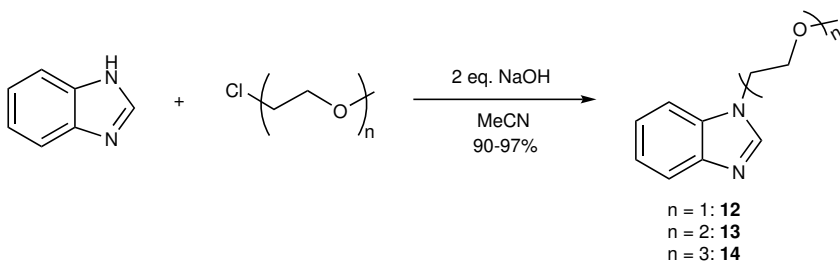
N-alkylation of imidazole ethers was achieved through an S_N2 reaction with allyl bromide or benzyl bromide, resulting in the formation of bromide salts (Scheme 8). 1-Allyl-3-(2-methoxyethyl)-1*H*-imidazolium-bromide (**6a**), 3-allyl-1-(2-(2-methoxyethoxy)ethyl)-1*H*-imidazolium bromide (**7a**) and 3-allyl-1-(2-(2-methoxyethoxy)ethyl)-1*H*-imidazolium bromide (**8a**) were achieved with allyl bromide in 94%, 95% and 94% yield, respectively. 3-Benzyl-3-(2-methoxyethyl)-1*H*-imidazolium bromide (**9a**), 3-benzyl-1-(2-(2-methoxyethoxy)ethyl)-1*H*-imidazolium bromide (**10a**) and 3-benzyl-1-(2-(2-methoxyethoxy)ethyl)-1*H*-imidazolium bromide (**11a**) were achieved with benzyl bromide in 92%, 95%, 96% yield, respectively (Scheme 8).



Scheme 8: Synthetic procedure of compound **6a**, **7a**, **8a**, **9a**, **10a** and **11a**.

3.2 Synthesis of benzimidazole ethers

Following similar procedure as for the synthesis of imidazole ethers, 1-(2-methoxyethyl)-1*H*-benzimidazole (**12**), 1-(2-(2-methoxyethoxy)ethyl)-1*H*-benzimidazole (**13**) and 1-(2-(2-methoxyethoxy)ethoxyethyl)-1*H*-benzimidazole (**14**) were achieved in 97%, 94%, and 90% yield, respectively. A schematic procedure for the synthesis of the benzimidazole ethers is shown in Scheme 9.

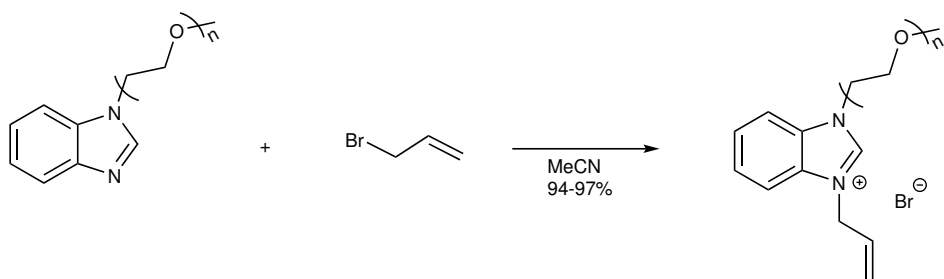


Scheme 9: Synthetic procedure of compound **12**, **13** and **14**.

Following the similar procedure as for the *N*-alkylation of imidazole ethers, 3-allyl-1-(2-methoxyethyl)-1*H*-benzoimidazolium bromide (**15a**), 3-allyl-1-(2-(2-methoxyethoxy)ethyl)-1*H*-benzimidazolium bromide (**16a**) and 3-allyl-1-(2-(2-methoxyethoxy)ethoxyethyl)-1*H*-benzoimidazolium (**17a**) were obtained in 96%, 94% and 97% yield, respectively (Scheme 10).

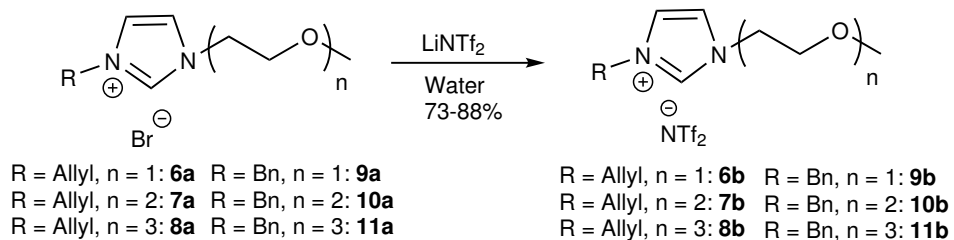
3.3 Anion metathesis

The target ILs were obtained by anion exchange of imidazolium bromide precursors (**6a-11a** and **15a-17a**). In order to introduce the NTf_2

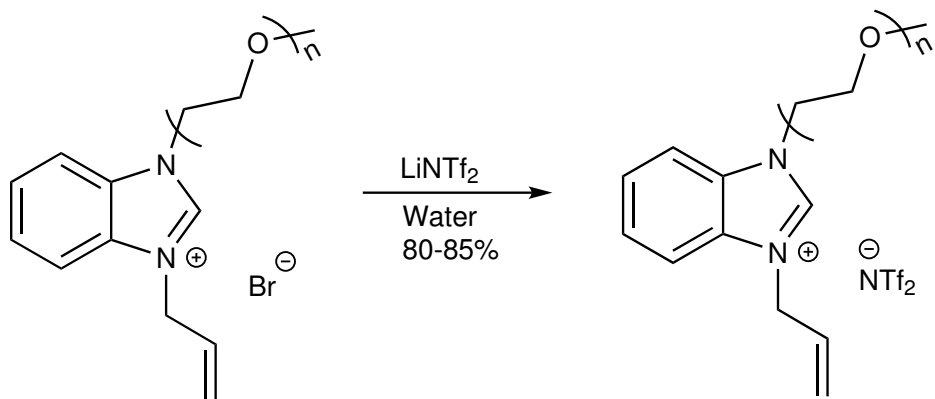


Scheme 10: Synthetic procedure of compound **15a**, **16a** and **17a**

as anion, commercially available bis(trifluoromethane)sulfonimide lithium salt was mixed with the appropriate bromide salt (**6a-11a** and **15a-17a**) of the IL and the mixture was stirred for 2 h in water at room temperature. Finally, the IL was washed several times with water until no precipitation of AgBr in the water phase was observed upon addition of an aqueous solution of AgNO₃. The synthetic procedure of the synthesis of NTf₂ based ILs (**9b-11b** and **15b-17b**) is shown in Scheme 11 and Scheme 12.



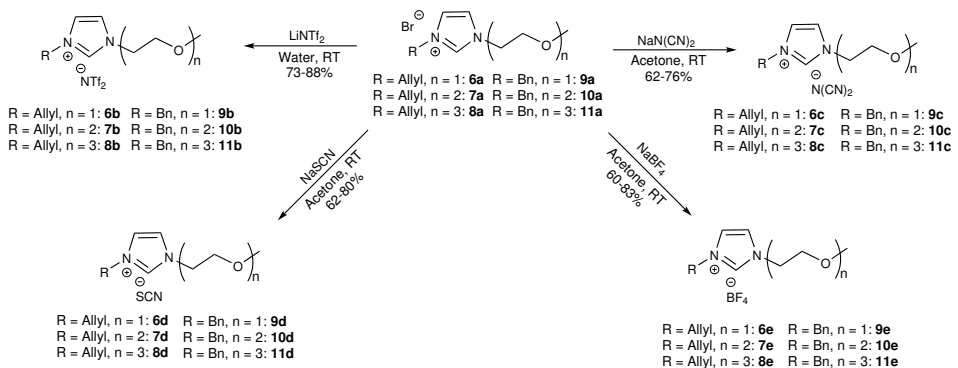
Scheme 11: Synthetic procedure of ILs **6b-11b**.



Scheme 12: Synthetic procedure of ILs **15b-17b**

The ILs with counter ions $[\text{N}(\text{CN})_2^-]$, $[\text{SCN}^-]$ and $[\text{BF}_4^-]$ were prepared by stirring the ILs and sodium salt of the respective anions (1.1 equivalent) in acetone. The same procedure was also attempted in DCM, but complete anion exchange did not occur according to NMR. This may be due to the poor solubility of the sodium salt of the anions in DCM. The synthetic procedure for obtaining the ILs with the desired anion is shown in Scheme 13 for the imidazolium based ILs (**6-11**) and Scheme 14 for the benzoimidazolium based ILs (**15-17**).

All anions, except the $[\text{NTf}_2^-]$ anion, could not be confirmed by negative mode HR-MS without high ppm error due to low molar mass. However, the presence of the $[\text{SCN}]$ and $[\text{N}(\text{CN})_2]$ anions was confirmed by the observation of an additional peak in ^{13}C -NMR with low intensity (approximately 119 ppm and 130 ppm, respectively). Furthermore, the presence of the $[\text{SCN}]$ and $[\text{N}(\text{CN})_2]$ anions were also observed by



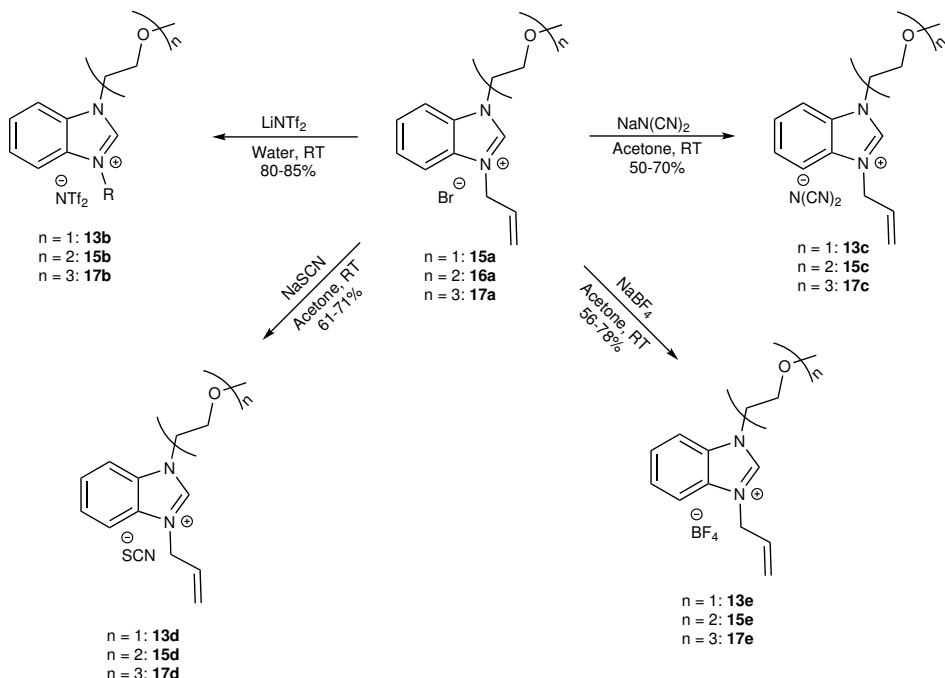
Scheme 13: Synthetic procedure for ILs **6c-11c**, **6d-11d** and **6e-11e**.

FT-IR, which showed the characteristic strong peak of triple bonds (approximately at 2000 cm^{-1}). The presence of $[\text{BF}_4^-]$ anions were confirmed by $^{19}\text{F-NMR}$.

The chemical structure and shift for the imidazolium protons for different ILs are shown in Scheme 15.

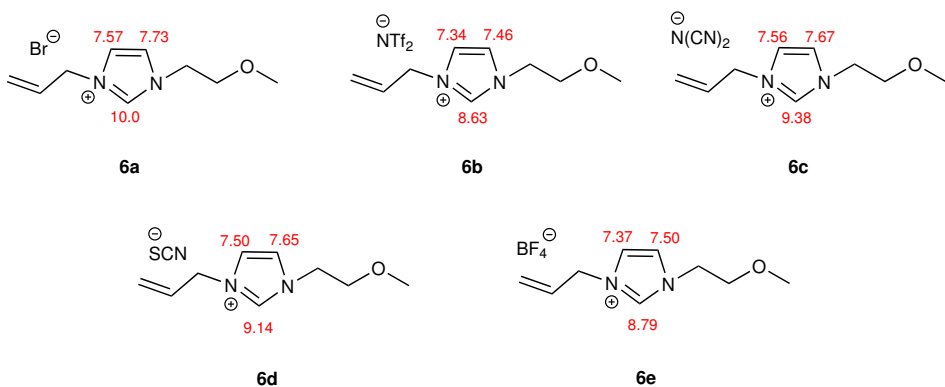
The order of the anion with the highest chemical shifts was: $[\text{Br}] > [\text{N}(\text{CN})_2] > [\text{SCN}] > [\text{BF}_4^-] > [\text{NTf}_2]$. It is evident that the change of anion affects the $^1\text{H-NMR}$ shift values for the imidazolium protons. However, the effect of the anions on the protons of the functional groups was insignificant and therefore not included in the scheme.

Upon anion exchange, all ILs experienced a significant decrease in $^1\text{H-NMR}$ shift values. For instance, comparing IL **6a** and **6b**, the shift values decreased from 10.0, 7.73 and 7.57 to 8.63, 7.46 and 7.34, upon changing from the bromide anion to the NTf_2^- . This may be due to the bromide anion coordinating stronger with the imidazolium cation than the other weakly coordinating anions.[80] Furthermore, the shift for the acidic C2-proton decreased significantly for IL **6b** compared



Scheme 14: Synthetic procedure for ILs **15-17**

to the other anions, possibly due to the hydrogen bonding between the proton and the sulfate group in $[\text{NTf}_2]$.^[81] Similar behaviour was also observed for the benzyl-based ILs (Scheme 16). However, the shift values for the imidazolium protons were less affected upon anion exchange when the substituent was changed from allyl to the larger benzyl group, presumably because of increased steric hindrance of the protons.



Scheme 15: The chemical structure and shift for the imidazolium protons of compounds **6a-6e**.

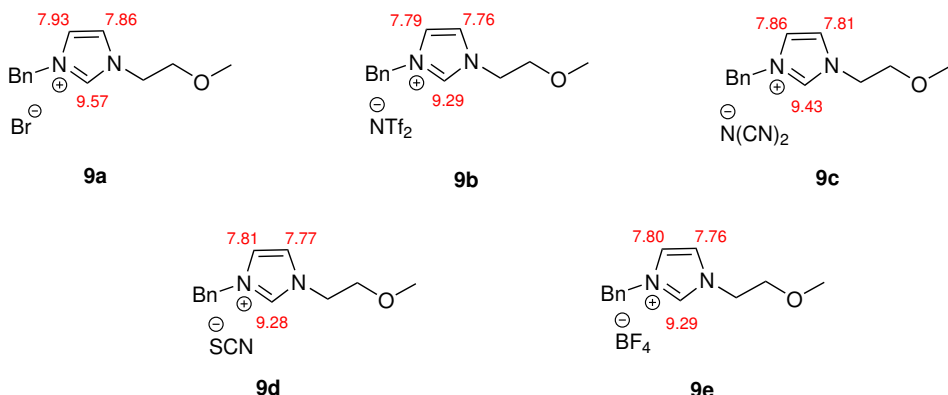
3.4 Desulfurization of MO using allyl functionalized ILs

In this section, the results from the desulfurization of DBT and 4,6-DMDBT by allyl functionalized ILs with increasing ether chain presented and the effect of the cation and anion on the extraction efficiency is discussed.

3.4.1 Effect of the anion

The percentage sulfur removal (%S-removal) of DBT and 4,6-DMDBT by the imidazolium ILs bearing the allylic group and increasing number of ether groups is shown in Table 2.

The desulfurization efficiency of DBT with ILs containing one diethylene group (**6b-6e**), decreased (40%, 45%, 40% and 27%, respectively) in the following order of anion: $[\text{N}(\text{CN})_2] > [\text{NTf}_2] \approx [\text{SCN}] > [\text{BF}_4]$.



Scheme 16: The chemical structure and shift for the imidazolium protons of compounds **9a-9e**

This observation is contradictory to results obtained by Raj *et al.*, who reported that the $[\text{NTf}_2]$ anion showed higher extraction efficiency compared to other anions used in their study.[9]. However, desulfurization studies conducted by Gao *et al.*, using butylpyridinium ILs, indicated that the dicyanamide anion performed better than the $[\text{NTf}_2]$.[82] Wilfred *et al.* investigated EDS of DBT with 1-butyl-3-methylimidazolium [C_4mim] based ILs. They observed that the extraction efficiency followed the anion order: $[\text{SCN}] \approx [\text{N}(\text{CN})_2] > [\text{NTf}_2]$. Hence, it can be concluded that the order of the anion on desulfurization efficiency mainly depend on the cation.

As for 4,6-DMDBT, the efficiency reduces significantly compared to DBT, in accordance with previous studies.[83]. For instance, while compound **6c** could extract 40% of DBT, the IL only extracted 19% 4,6-DMDBT. Owing to the steric hindrance experienced by the sulfur due to the presence of the methyl groups, a decrease of the interac-

Table 2: Desulfurization efficiency of ILs **6b-6e**, **7b-7e** and **8b-8e**. Experimental conditions: 25°C, extraction time: 2h, mass ratio IL:Model oil, 1:1. MO: 500 ppm total of DBT and 4,6-DMDBT in *n*-dodecane.

IL	DBT-Removal [%]	4-6-DMDBT-Removal [%]
6b	40	19
6c	45	14
6d	40	12
6e	27	8
7b	49	28
7c	53	19
7d	40	13
7e	39	14
8b	50	26
8c	59	24
8d	44	14
8e	40	12

tions between the IL and the sulfur in the refractory sulfur compounds was observed.[84] The IL with the $[\text{N}(\text{CN})_2]$ anion showed superior desulfurization efficiency for DBT, while the highest desulfurization of 4,6-DMDBT was obtained with the $[\text{NTf}_2]$ anion. Thus the order for removal of 4,6-DMDBT was $[\text{NTf}_2] > [\text{N}(\text{CN})_2] > [\text{SCN}] > [\text{BF}_4]$ with the respective values 19%, 14%, 12% and 8%. The $[\text{NTf}_2]$ anion is known to substantially increase the hydrophobicity of ILs, thus increasing the hydrophobic interactions.[7] These hydrophobic interactions appear to have a greater influence on the removal of 4,6-DMDBT than DBT, probably due to DBT being slightly more polar than its derivative.

Considering the S-removal efficiency obtained with different anions,

it is evident that the anions has an impact on the desulfurization of sulfur compounds. The results also indicates that all anions, besides $[N(CN)_2]$, does not show a significant increase when the alkoxy chain increases from diethylene glycol to triethylene glycol.

3.4.2 Effect of the cation

The effect of the cation was also investigated as part of this project. By comparing the extraction performances of the different cations with their respective anions (Table 2), it is evident that the increase in size of the cation also increases the extraction efficiency of the sulfur compounds, as shown by the desulfurization efficiency of *e.g.* **6b** < **7b** < **8b**. For all the anions studied, the extraction efficiency increased with the size of the cationic core, consistent with studies on pyridinium based PILS.[85] The enhanced performance is due to the prolonged alkyl chain length, thus increasing the van der Waals volume. As a result, the hydrogen bonding between the acidic C₂-proton in imidazole and the anion is weakened.[86] The weakened interactions promote the S-H hydrogen bonding between the sulfur in DBT/4,6-DMDBT and the C₂-proton, leading to enhancement of the ILs affinity towards the sulfur compounds.[51]

The cationic core of ILs lacks the ability to pack closely, thus giving rise to cavities between the ions. Alkoxy chains have been reported to increase the number of cavities due to high rotational flexibility. An increased number of cavities have shown to decrease the viscosity and increase the mass-transport.[87] Consequently, a longer alkoxy chain

will lead to enhancement of the extraction efficiency. Similar observations have been made with polyether based ammonium ILs.[3]

Other interactions that enhanced the desulfurization performance were the electrostatic interactions ($n-\pi$) between the oxygen in the glycol chain on the ILs and the sulfur in DBT/4,6-DMDBT, which is in accordance with observations made with morpholinium-based ILs.[20] Zhang *et al.* studied the sulfur-oxygen intermolecular interactions between thiophene, thiazole and thiadiazole and several oxygen containing biological compounds. The results revealed strong interactions between the sulfur and oxygen, thus increasing affinity towards each other.[88]

As previously mentioned, the $[\text{NTf}_2]$ -based ILs gave higher extraction efficiency of 4,6-DMDBT while those with the $[\text{N}(\text{CN})_2]$ anion extracted more DBT. The result of increasing the number of ether groups from monoethylene glycol to diethylene glycol (from **6b** to **7b** for the $[\text{NTf}_2]$ anion and from **6c** to **7c** for $[\text{N}(\text{CN})_2]$ anion) led to an increase in the desulfurization of 4,6-DMDBT. The difference between the two anions increased from 5% to 9%. For the removal of DBT, however, the efficiency difference is not affected significantly. This might be due to an decrease in viscosity, thus allowing stronger interactions with 4,6-DMDBT.

3.5 Optimization studies for IL 8c

In this section, optimization studies will be discussed for the superior IL, bearing allylic substituent. As mentioned above, the $[NTf_2]$ and $[N(CN)_2]$ anions exhibited higher efficiency for 4,6-DMDBT and DBT, respectively. Taking the toxicity of the $[NTf_2]$ anion into account, the optimization studies will therefore be performed on the $[N(CN)_2]$ bearing IL **8c**.

3.5.1 Effect of mass ratio

The effect of the IL:MO ratio (1:1, 2:1, 3:1, 4:1, 5:1) on the extraction efficiency of DBT and 4,6-DMDBT using IL **8c** is shown in Figure 4.

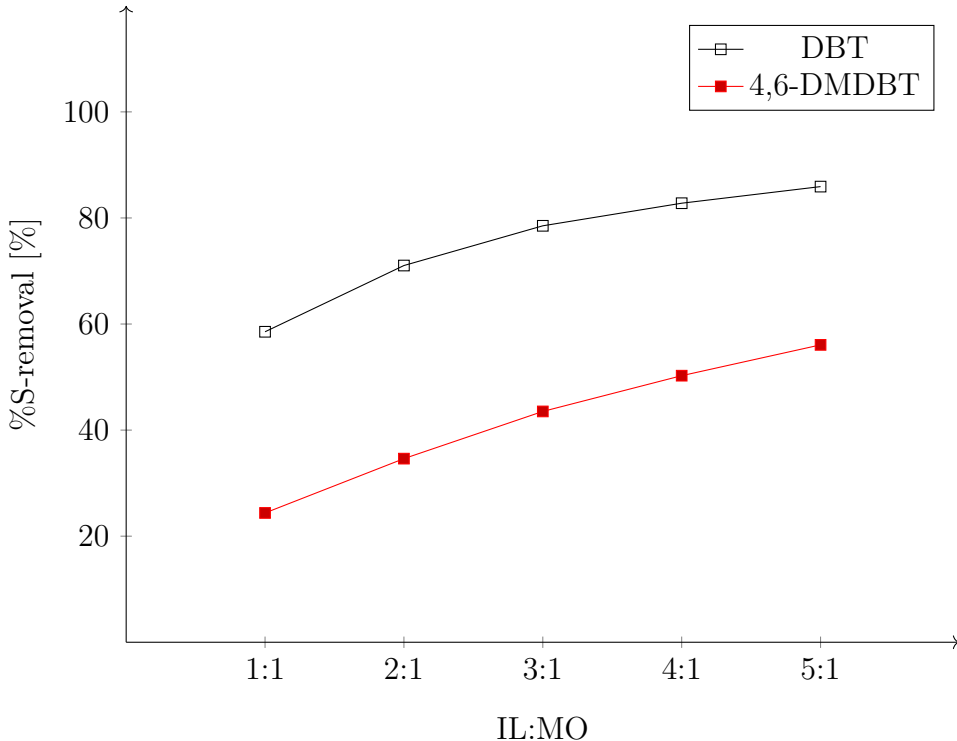


Figure 4: The effect of IL:MO ratio on the desulfurization efficiency of IL **8c** towards DBT and 4,6-DMDBT. Experimental conditions: Temperature: 25°C, stirring time: 2 h.

The influence of mass ratio is an important factor when evaluating the application of ILs in EDS. In order to compensate for the high cost of ILs, low mass ratio is preferred. The results indicate that the desulfurization efficiency of DBT and 4,6-DMDBT is enhanced as the mass ratio increases. The values of desulfurization efficiency for the mass ratios 1:1, 2:1, 3:1, 4:1 and 5:1 were calculated to be

59%, 71%, 79%, 83% and 85% for DBT and 24%, 35%, 44%, 50% and 56% for 4,6-DMDBT. The extraction efficiency of DBT increased 1.2 times when the mass ratio increased from 1:1 to 2:1 of the IL, whereas it increased 1.4 times for 4,6-DMDBT. This may arise from the increase of hydrophobic interactions due to the methyl groups on 4,6-DMDBT. For the remaining ratios, the desulfurization efficiency increased approximately 1.1 times for each ratio, while for the 4,6-DMDBT it decreased (1.3, 1.2 and 1.1). The decreasing effect for 4,6-DMDBT may indicate saturation of the hydrophobic interactions, thus experiencing similar interactions as DBT.

Comparing the effect of mass ratio on the increase of extraction efficiency, several reports suggest negligible increase approximately around a 2:1 ratio of the IL.[89][90][91] The increase of extraction efficiency might be due to an increase of mass transfer, thus allowing stronger interactions between the IL and the sulfur compounds. In order to keep the EDS as economically viable, it was decided to proceed with 2:1 mass ratio of the IL in the further optimization studies.

3.5.2 Effect of time on the desulfurization

The effect of extraction time on the desulfurization of DBT and 4,6-DMDBT using IL **8c** is shown in Figure 5. The results are based on five samples measured at 15, 30, 45, 60 and 120 min.

The extraction studies revealed that the time had minor influence on the desulfurization efficiency of DBT. Between 15 min and 60 min, the extraction efficiency remained 69%. Upon stirring for 120 min, the

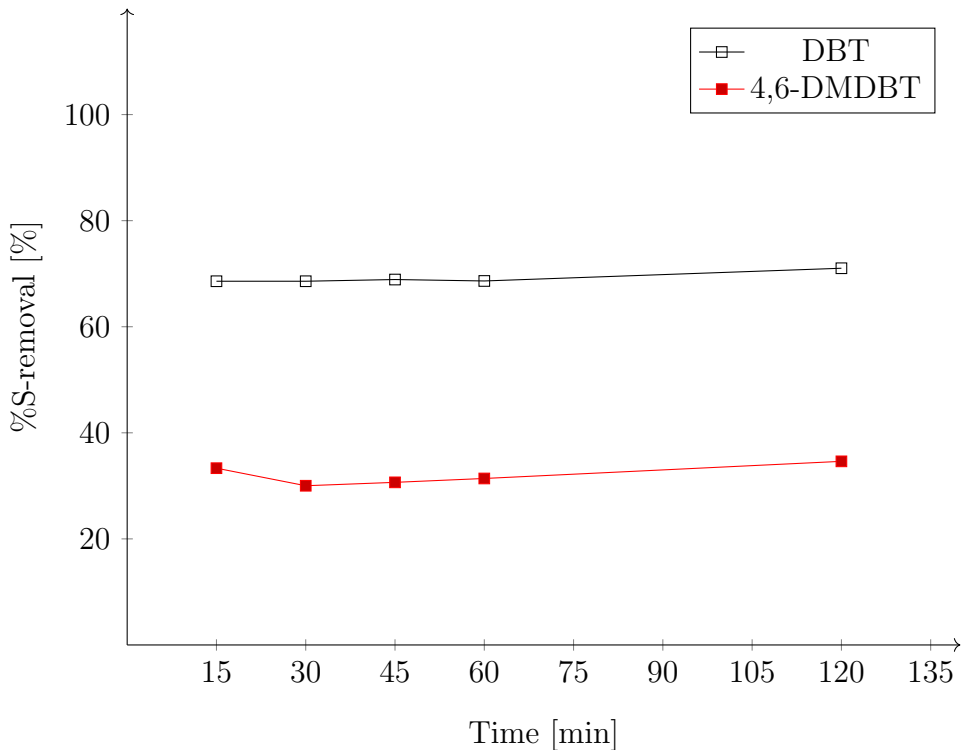


Figure 5: The effect of time on the EDS of DBT and 4,6-DMDBT using IL **8c**. Experimental conditions: Temperature: 25 °C, mass ratio: 2:1 (IL:MO).

extraction efficiency was only enhanced by 3%. Thus, it may appear that the EDS reaches thermodynamic equilibrium between the IL and DBT within 15 min.

The extraction time had a slightly more positive effect on the removal of 4,6-DMDBT than DBT. After 15 min, 33% of 4,6-DMDBT was extracted. However, the desulfurization efficiency decreased to 30% when stirred for 30 min. Furthermore, the extraction efficiency slowly increased between 30 min and 120 min to 35%. The %S-removal appears to vary little after 15 min, thus indicating that the thermody-

namic equilibrium between the IL and 4,6-DMDBT settles after 15 min. Therefore, 15 min was selected as the optimum time for the further extraction studies.

The short extraction time observed in this study may be due the presence of several functional groups and their respective interactions. For instance, the allyl group can contribute to the π - π interactions between the imidazolium cation and the aromatic sulfur compounds. Furthermore, the oxygen atom on the ether group can interact with the sulfur on the DBT and 4,6-DMDBT through n- π interactions.

The viscosity has a major impact on the extraction time. To illustrate the influence of the viscosity on extraction efficiency, two studies conducted by Ren *et al.* and Dharaskar *et al.* will be used as examples. Ren *et al.* studied low viscous PILs of 1,8-diazobicyclo[5.4.0]undec-7-ene combined with different acidic anions, such as formate and acetate, for the desulfurization of DBT, BT and 4,6-DMDBT. After an extraction study, the most promising IL was found to be 1,8-diazobi-cyclo[5.4.0]undec-7-ene propionate ([DBU][Pr]) and the measured viscosity was found to be 133.8 mPa*s. The thermodynamic equilibrium was reached after 5 min due to faster mass transfer.[84] In contrast, Dharaskar *et al.* investigated [BMIM][BF₄] for the desulfurization of DBT and the reported a higher viscosity value (173.5 mPa*s). Upon optimization of the extraction time, the optimal performance was obtained after 30 min at 30°C.[92]

3.5.3 Effect of the temperature

The effect of the temperature on the desulfurization efficiency of DBT and 4,6-DMDBT is shown in Figure 6.

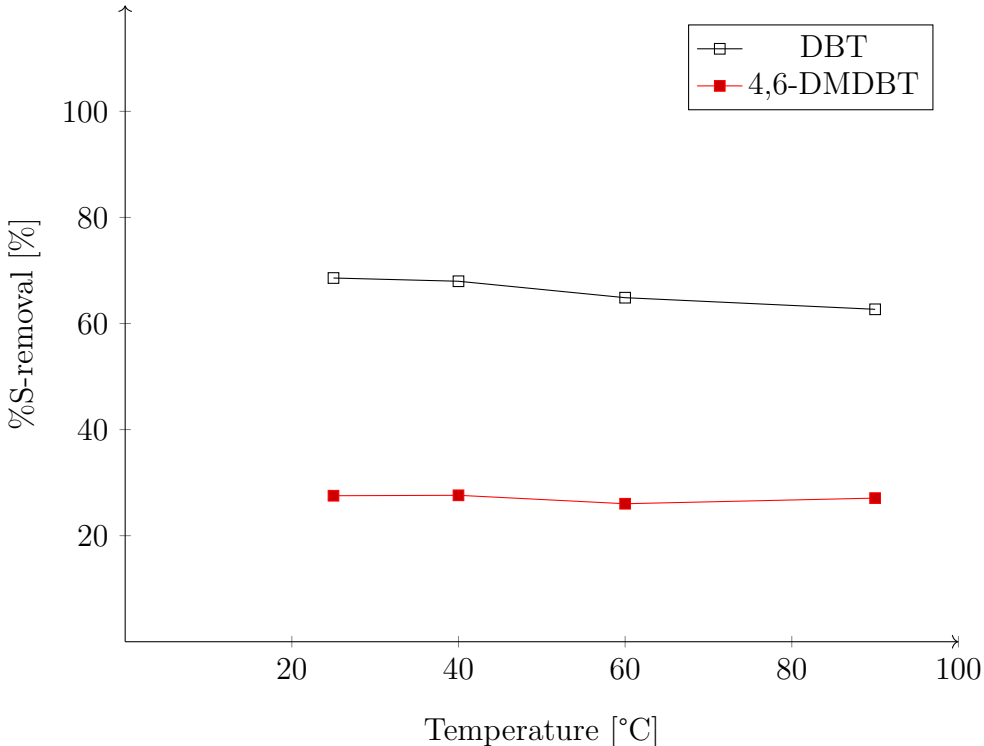


Figure 6: The effect of temperature during EDS of DBT and 4,6-DMDBT using IL **8c**. Experimental conditions: Extraction time: 15 min, mass ratio: 2:1 (IL:MO).

The investigated temperatures were 25°C, 40°C, 60°C and 90°C. For the removal of DBT, the efficiency slightly decreased as the temperature increased with the respective values 69%, 68%, 65% and 63%, indicating that the extraction efficiency maximum is reached at 25 °C. These results are in agreement with the earlier study reported by Ren *et al.* using DBU-based ILs.[5]

The increase in temperature has no significant influence on the extraction efficiency of 4,6-DMDBT. A slight decrease in extraction efficiency from 28% to 26% was observed upon heating from 40 °C to 60 °C. However, increase in temperature from 60°C to 90°C resulted in a small increase in the extraction efficiency (27%). Nevertheless, the effect of temperature is negligible and, based on the results achieved, the optimized temperature was determined to be 25 °C.

3.5.4 Recyclability of IL **8c**

In addition to achieve high desulfurization efficiency, another important aspect is the recyclability of ILs. In order to be economical and environmentally friendly, the desulfurization efficiency of the ILs should remain constant over several cycles. To explore this property, the desulfurization was performed under the optimized conditions for IL **8c** and the oil phase was extracted. Subsequently, a new batch of MO was added and the same procedure was repeated. The results are depicted in Figure 7.

The recyclability study revealed a significant reduction in the extraction efficiency of DBT after 5 cycles (18%). The extraction efficiency was reduced from 69% and, in the 9th cycle, the %S-removal decreased to 6%. The drastic reduction is due to rapid saturation of active sites in the IL-molecule, hence preventing the remaining DBT molecules from interacting with the IL. Similar trends in the recyclability have been reported with tri-*n*-butyl-(2hydroxyethyl)phosphonium bromide ([TBHEP][Br]) and [Bmim]Cl/FeCl₃.[93][94] Nevertheless, Raj *et al.*

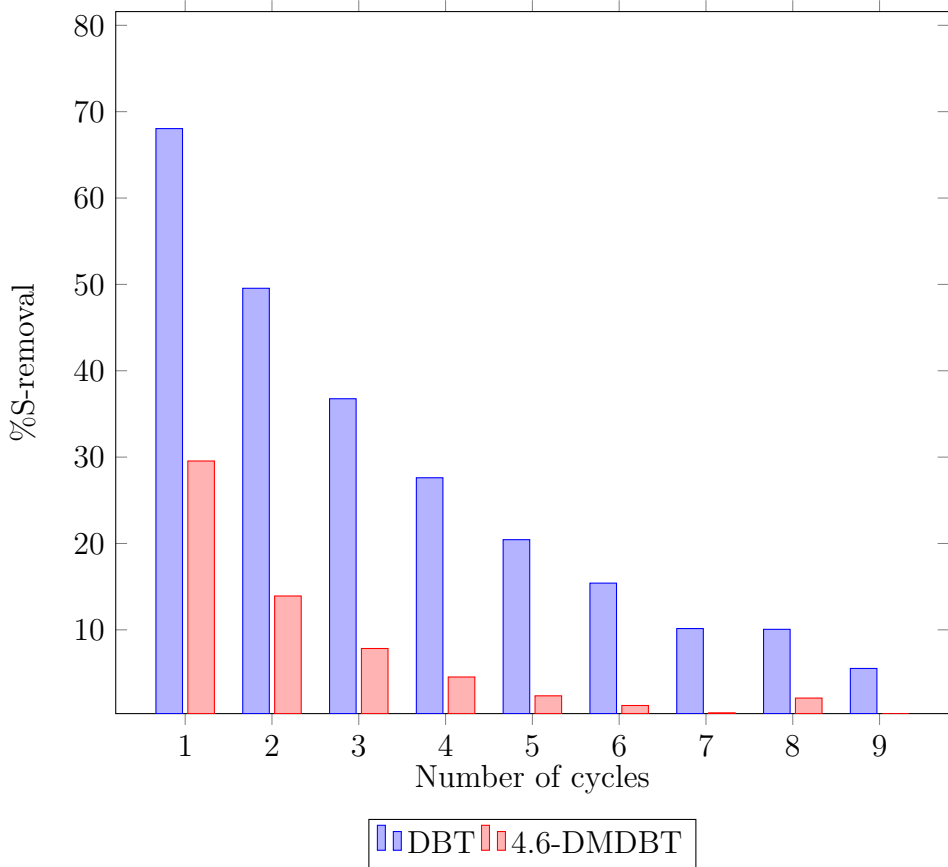


Figure 7: Recyclability test for IL **8c** using 500 ppm of DBT and 4,6-DMDBT in *n*-dodecane.

reported a recyclability test of a similar IL with an acrylonitrile group instead of an allyl group and NTf_2 as the anion instead of $\text{N}(\text{CN})_2$. In their study, the decrease in desulfurization was negligible for 8 cycles.[9] The contradictory results obtained in this project was suspected to arise from the presence of 4,6-DMDBT. Hence, a recyclability test was performed for IL **8c** with a MO solely containing DBT dissolved in *n*-dodecan. The results are depicted in Figure 8.

In the absence 4,6-DMDBT, the decreasing trend of the desulfurization

efficiency could still be observed, indicating that the presence of 4,6-DMDBT does not affect the recyclability.

Evaluating the results obtained considering IL **8c** and its desulfurization efficiencies, it can be concluded that the IL **8c** gives similar performance as compared to the ILs reported in the literature for the removal of refractory sulfur compounds. It is interesting to note that the ILs developed in this work have significantly higher extraction efficiency for the more sterically hindered sulfur compounds (4,6-DMDBT) compared to the ILs reported in the literature.

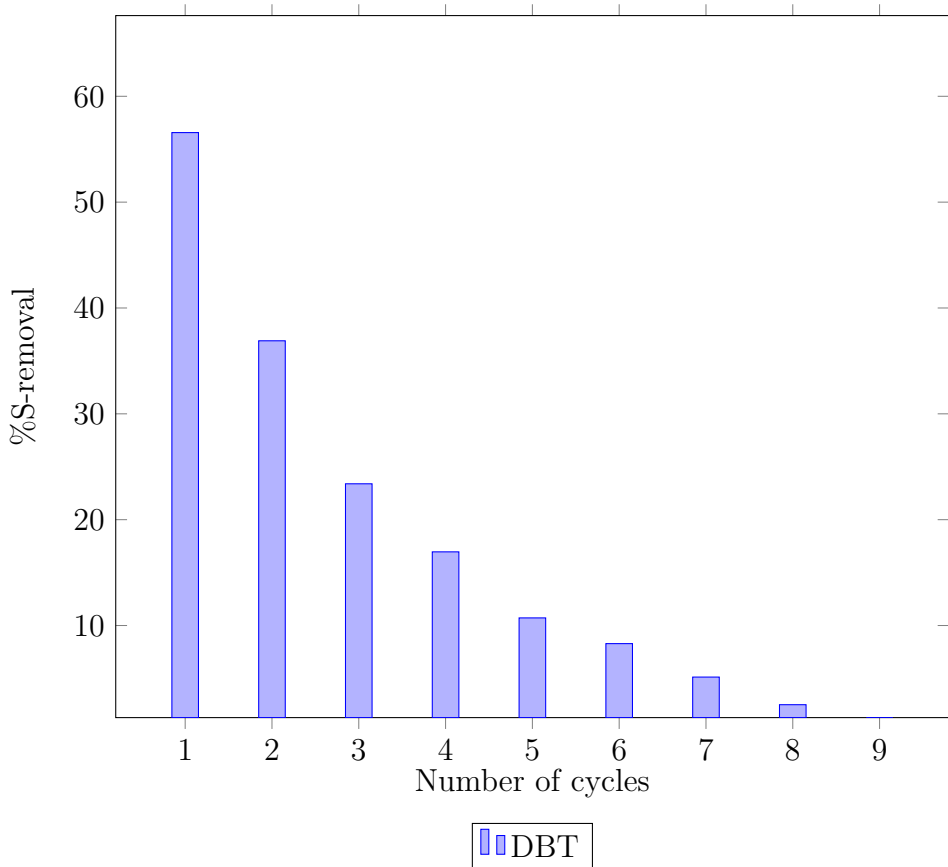


Figure 8: Recyclability test for IL **8c** using 100 ppm of DBT in *n*-dodecane.

3.5.5 $^1\text{H-NMR}$ -studies

In order to understand the extractive mechanism, a $^1\text{H-NMR}$ study was performed with different IL:DBT ratios of IL **8c**. Figure 9 shows the structure of IL **8c** marked with letters which correspond to the assigned $^1\text{H-NMR}$ peaks in Figure 10.

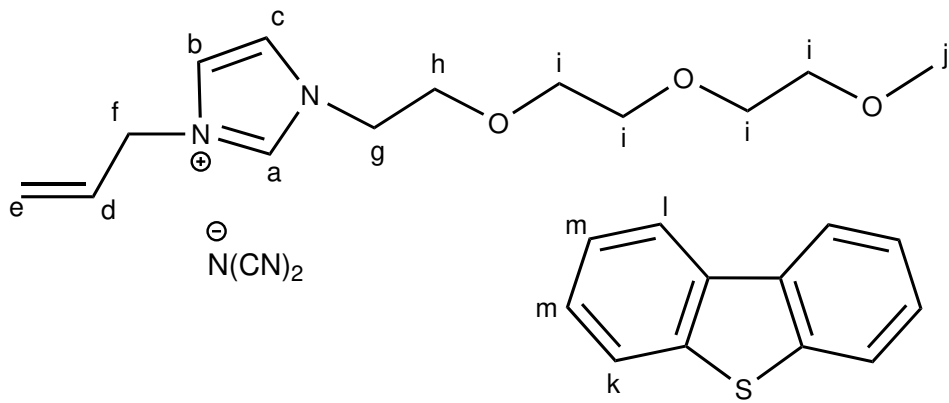


Figure 9: Structure of IL **8c** and DBT marked with letters corresponding to their chemical shift obtained by $^1\text{H-NMR}$ in Figure 10.

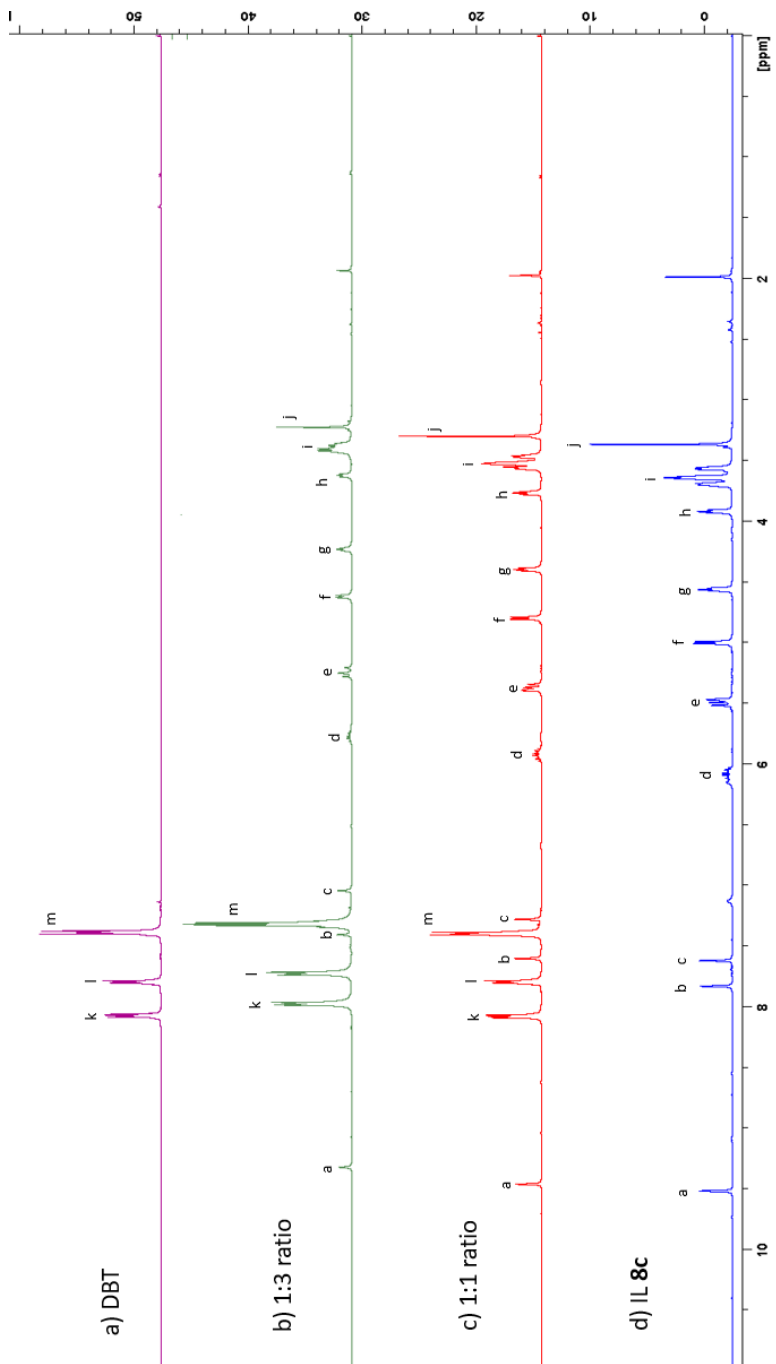


Figure 10: ¹H-NMR spectra of IL **8c** and DBT with different IL:DBT ratios. a) Pure DBT b) 1:3 ratio c) 1:1 ratio d) Pure IL **8c**.

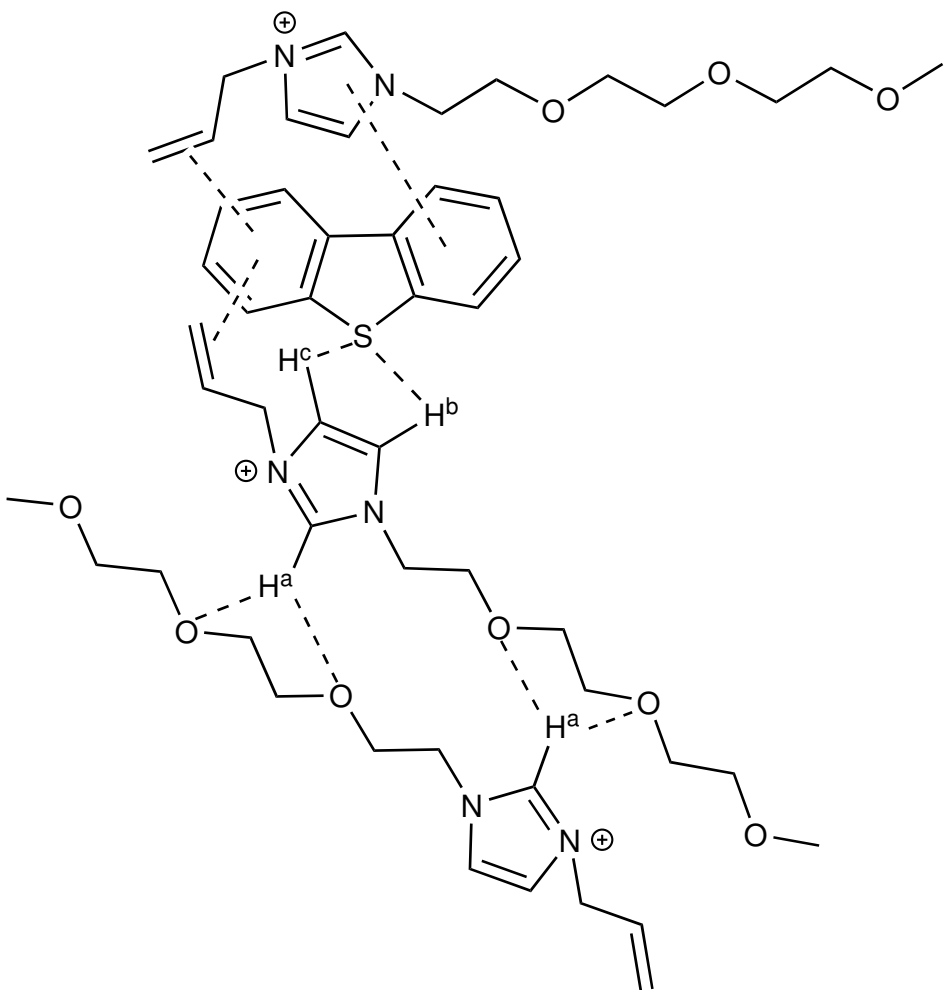
The ^1H -NMR shift values from various IL:DBT ratios are shown in Table 3.

Table 3: ^1H shift values obtained from the different mass ratio of IL:DBT given in ppm.

Proton	IL	1:1	1:3
a	9.52	9.46	9.32
b	7.83	7.60	7.41
c	7.62	7.28	7.04
d	6.08	5.92	5.78
e	5.49	5.37	5.25
f	5.00	4.80	4.62
g	4.56	4.40	4.23
h	3.92	3.77	3.62
i	3.64	3.53	3.40
j	3.37	3.30	3.22
k	8.07	8.08	7.97
l	7.80	7.80	7.73
m	7.39	7.40	7.32

During the EDS, all the IL protons experienced an upfield shift as the DBT composition increased. The protons that were affected to the greatest extent by the presence of DBT, were proton H^b and H^c on the imidazolium core. The difference in shift values for the allyl group (H^d, H^e and H^f) on the IL decreased as the spatial distance between the protons and the imidazolium core increased. Nevertheless, similar movements were also observed for the ether protons (H^g, H^h, Hⁱ and H^j) and the upfield shift is similar for both functional groups. This indicates that the allyl group and the ether group contributed almost equally to the interactions between the aromatic sulfur compounds and the ILs.

A similar experiment was performed by Su *et al.*, where they investigated the interactions between thiophene and alkyl based imidazolium ILs. However, a contradictory result was obtained regarding the chemical shift of the acidic proton H^a. The ¹H-NMR study with different IL:thiophene ratios, showed that the proton H^a was affected most.[95] However, in this study proton H^a experienced a smaller chemical shift, presumably due to the inter-molecular hydrogen bonding between the oxygen atom of the ether chain and the acidic C-2 proton H^a. This shields the H^a proton, thus prohibiting the interaction with the sulfur in DBT. As a result, the sulfur can readily form hydrogen bonds with the other protons (H^b and H^c) on the imidazolium ring and resulted in the formation of a liquid clathrate, as proposed by Holbrey *et al.* (Scheme 17).[52][12]



Scheme 17: A proposed interaction mechanism between the IL and DBT in a liquid clathrate formation.[52][12]

3.6 Desulfurization of MO using benzyl functionalized ILs

It has been reported that the π - π interactions between the aromatic sulfur compounds and the aromatic groups on the cationic core of ILs play a major role in the extraction efficiency of EDS. In order to unravel the effect of π - π interactions, a benzyl group was incorporated into the ILs to enhance the π - π interactions and thus increase the extraction of the sulfur compounds.

3.6.1 Effect of the anion

The %S-removal of DBT and 4,6-DMDBT by the imidazolium IL bearing the allylic group and increasing number of ether groups is shown in Table 4.

The desulfurization efficiency toward both DBT and 4,6-DMDBT with ILs containing one ether group (**9b-9e**), decreased in the order of anion: $[\text{NTf}_2] > [\text{N}(\text{CN})_2] > [\text{BF}_4] > [\text{SCN}]$. The order of the $[\text{NTf}_2]$ anion and $[\text{N}(\text{CN})_2]$ changed compared to the order observed with the allyl-based ILs (**6b-6e**). As mentioned previously, the $[\text{NTf}_2]$ is known to increase the hydrophobicity of the IL. In combination with the hydrophobic benzyl group, the hydrophobicity of IL **9b** may have increased to an even greater extent, allowing stronger interactions with DBT than the more polar ($[\text{N}(\text{CN})_2]$) IL (**9c**). This may also explain the observed enhancement on the extraction performance of 4,6-DMDBT for all anions besides $[\text{SCN}]$ (**9d**) which was observed to be very viscous. However,

Table 4: Desulfurization efficiency of ILs **6b-6e**, **7b-7e** and **8b-8e**. Experimental conditions: 25°C, extraction time: 2h, mass ratio IL:Model oil, 1:1. MO: 500 ppm total of DBT and 4,6-DMDBT in *n*-dodecane.

IL	DBT-Removal [%]	4-6-DMDBT-Removal [%]
9b	48	26
9c	44	15
9d	12	5
9e	36	18
10b	50	29
10c	50	26
10d	44	22
10e	40	20
11b	53	29
11c	56	24
11d	40	19
11e	47	19

the extraction efficiency of all anions, besides [SCN], increased slightly upon extension of the ether chain from monoethylene to diethylene. The efficiency of the [SCN] anion on the other hand, enhanced drastically upon the increase of the ether chain, which appeared to be less viscous than IL **9d**.

By increasing the ether chain length further from diethylene glycol, the anion appears to have negligible effect in the desulfurization studies. This may indicate that the anions play a less important role when the size of the cation is increased.

3.6.2 Effect of the cation

The change of the aromatic substituent resulted in an increase of desulfurization efficiency for DBT and 4,6-DMDBT. The improved %S-removal might be due to the presence of the larger benzyl group, which reduces the polarity. This facilitates a more efficient dispersion of the ILs (**9-11** in Table 4) in the oil phase. As a result, the π - π interactions between the ILs and the aromatic sulfur compounds are enhanced. In addition, the change of the aromatic substituent to a more π -electron-rich system could also have contributed to the π - π interactions. Similar increase of desulfurization efficiency has also been investigated by Yu *et al.* upon change to benzyl-based IL.[3] These results confirm that an increase in π - π electrons can yield higher extraction of aromatic sulfur compounds. Furthermore, the extraction efficiency improves upon enlarging the cationic core by increasing the ether chain, in accordance with results obtained with the allyl based ILs. However, the %S-removal does still not satisfy the requirements aimed for in this project. Thus, new ILs were explored in order to comprehend and advance in the field of EDS.

3.7 Desulfurization of MO with benzoimidazolium based ILs

DBU has been reported as a promising extractive reagent for EDS. However, the cost and toxicity of DBU make it unfavourable. Based on the results demonstrated in the literature, a search for similar structure

and lower toxicity led to benzoimidazolium-based ILs. Several aspects were taken into consideration upon deciding to study benzimidazole, including low toxicity, a cheaper alternative to DBU and the fused aromatic system. The last property was of great interest to study in order to observe the effect of a benzo-fused imidazole. Therefore, this section describes the effect of the anion and cation during EDS with benzoimidazolium-based ILs.

3.7.1 Effect of the anion

The desulfurization efficiency of benzoimidazolium based ILs bearing the allylic group and increasing number of ether groups is shown in Table 5.

Table 5: Desulfurization efficiency of ILs **6b-6e**, **7b-7e** and **8b-8e**. Experimental conditions: 25°C, extraction time: 2h, mass ratio IL:Model oil, 1:1. MO: 500 ppm total of DBT and 4,6-DMDBT in *n*-dodecane.

IL	DBT-Removal [%]	4-6-DMDBT-Removal [%]
15b	69	51
15c	-*	-*
15d	-*	-*
15e	-*	-*
16b	68	52
16c	60	39
16d	46	18
16e	57	32
17b	56	52
17c	46	41
17d	35	30
17e	37	32

*The IL was obtained as a solid.

The order of the anions for desulfurization of DBT and 4,6-DMDBT decreased in the order $[NTf_2] > [N(CN)_2] > [BF_4] > [SCN]$. Desulfurization studies could not be performed for compound **15c-15e** due to the formation of solid ILs. However, IL **15b** extracted 69% of DBT in a single extraction step, which is a higher extraction efficiency than IL **8c** under optimized conditions. Simultaneously, 51% extraction was achieved for the desulfurization of 4,6-DMDBT. The same amount was achieved at a 4:1 mass ratio of IL:MO of IL **8c**.

For the ILs bearing the diethylene chain, it is evident that the anion has a significant impact on the desulfurization efficiency. For instance, with the IL **16c**, the desulfurization of DBT and 4,6-DMDBT was found to be 60% and 39%, respectively. Meanwhile, the extractive desulfurization of DBT and 4,6-DMDBT with IL **16d** resulted in 46% and 18% S-removal, respectively. The difference in desulfurization efficiency is mainly due to the formation of low-viscosity $[N(CN)_2]$ based ILs, as observed previously. Furthermore, the use of benzoimidazolium-based ILs has resulted in the largest efficiency gap between the $[NTf_2]$ anion and $[N(CN)_2]$ when compared to the previously mentioned ILs. Thus, it appears that larger difference in the extraction efficiency can be achieved by making the cationic core less polar. However, high hydrophobicity may also lead to increased solubility of the IL in the oil phase, and the possibility of contaminating the fuel oil.

3.7.2 Effect of the cation

According to previous observations in this project, increasing the size of the cation tends to enhance the extraction efficiency. However, the enlargement of the benzoimidazolium core appears to have a decreasing effect on the desulfurization efficiency. For instance, increasing the ether chain from diether to triether for the $[\text{BF}_4^-]$ anion (from IL **16e** to IL **17e**), the desulfurization efficiency decreased considerably (from 57% to 37% S-removal). In order to explain the significant reduction, an ^1H -NMR study of DBT and IL **15b** (Figure 11) was performed under similar conditions as for the ^1H -NMR study of IL **8c** (Figure 10). The ^1H -NMR spectra at various IL:DBT ratios are shown in Figure 12 and the shift values for each proton are presented in Table 6.

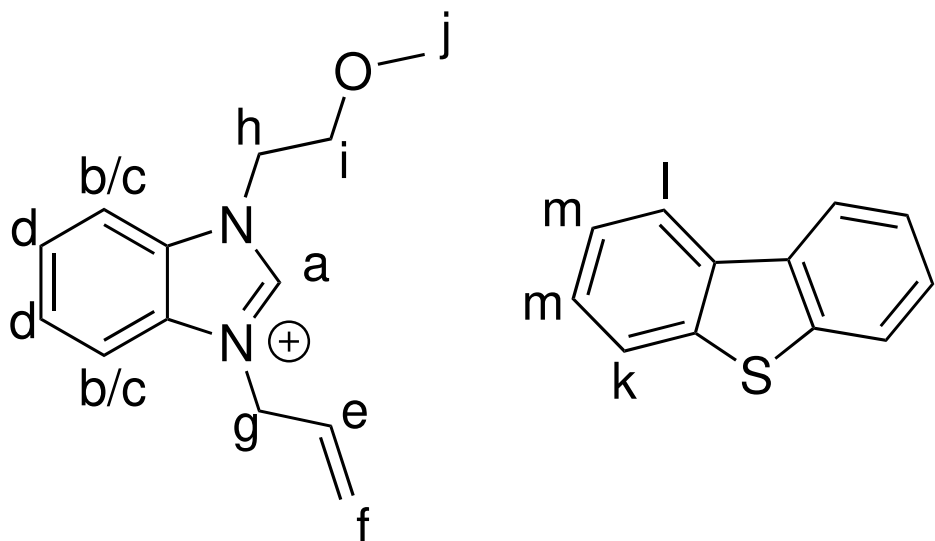


Figure 11: Structure of IL **15b** and DBT marked with letters corresponding to their chemical shift obtained by ^1H -NMR in Figure 12

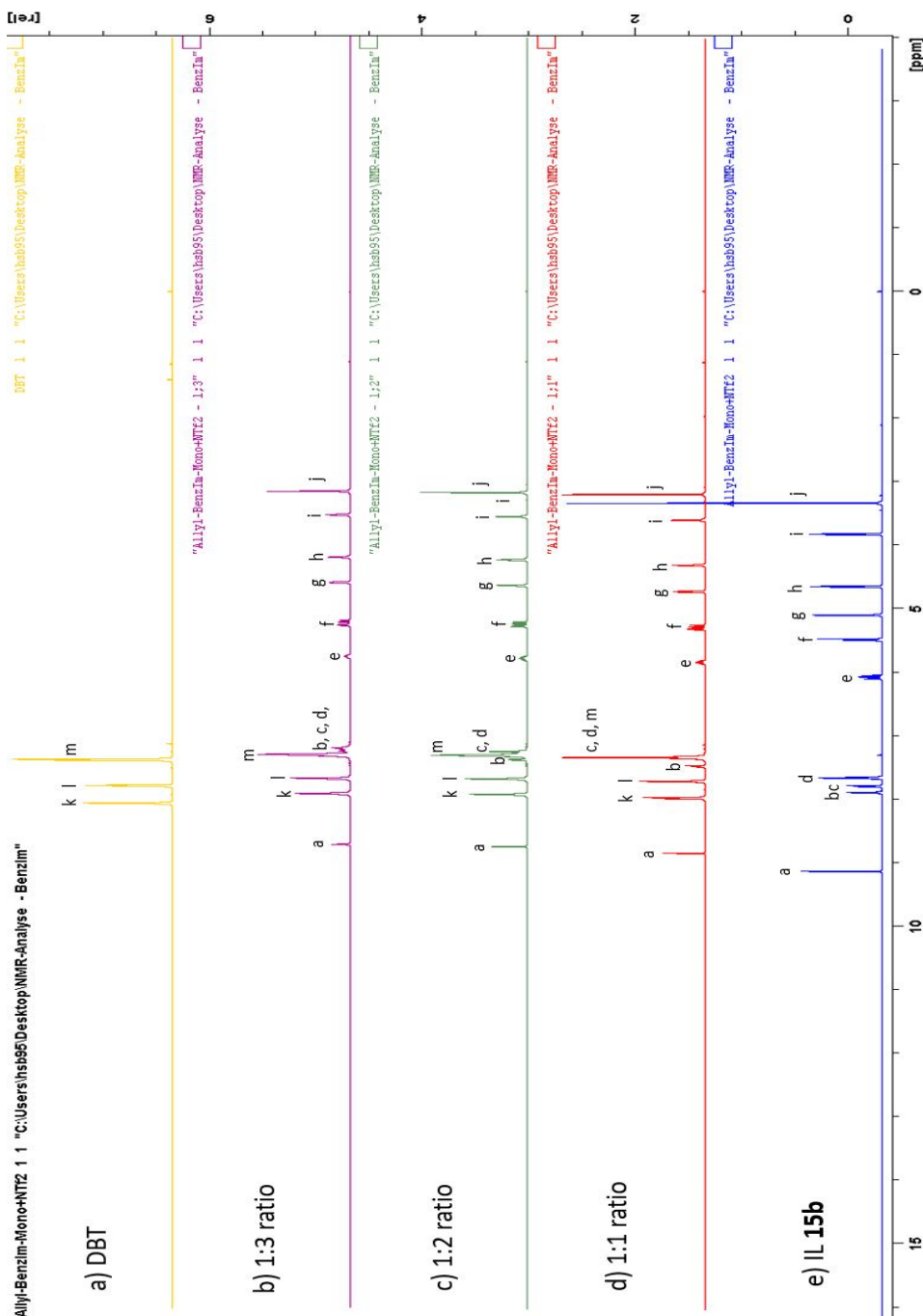


Figure 12: ^1H -NMR of IL **15b** and DBT with different IL:DBT ratios.
a) Pure DBT b) 1:3 ratio c) 1:2 ratio d) 1:1 ratio e) Pure IL **15b**.

Table 6: ^1H -NMR spectra of IL **8c** and DBT with different IL:DBT ratios. a) Neat DBT b) 1:3 ratio c) 1:2 ratio d) 1:1 ratio e) Neat IL **15b**.

Proton	IL	1:1	1:2	1:3
a	9.13	8.85	8.74	8.71
b	7.89	7.48	7.37	_-*
c	7.79	7.37	7.27	_-*
d	7.66	7.34	7.24	_-*
e	6.08	5.84	5.78	5.75
f	5.49	5.29	5.24	5.22
g	5.10	4.73	4.63	4.58
h	4.65	4.31	4.23	4.18
i	3.83	3.60	3.55	3.52
j	3.33	3.20	3.17	3.15
k	8.07	7.98	7.92	7.90
l	7.80	7.72	7.68	7.66
m	7.39	7.34	7.31	7.29

*The shift could not be assigned due to overlapping of peaks.

Upon undergoing the EDS, all protons shifted upfield. However, in contrast to the ^1H -NMR study performed for IL **8c**, the acidic proton H^a of IL **15b** shifted notably upon addition of DBT. This may indicate that the sulfur in DBT interacted more with the proton H^a in IL **15b** than in IL **8c**. Extension of the ether chain, increases the intramolecular hydrogen bonding between the oxygen atoms in the ether moiety and the acidic H^a proton, as observed earlier. This shields the proton H^a from the sulfur in DBT, thus preventing the sulphur compound from interacting with the proton. The hydrogen bonding between the H^a and sulfur appears to play a vital role in the desulfurization of DBT. However, the removal of 4,6-DMDBT was not significantly affected by the increase of the ether chain length, which might be due to

the steric hindrance of the sulfur atom by the methyl groups, therefore preventing it from interacting with proton H^a. In other words, the hydrogen bonding between the sulfur in 4,6-DMDBT and hydrogen H^a is negligible upon EDS.

By comparing the imidazolium-based ILs bearing the benzyl group (**9-11**) with corresponding benzoimidazolium-based ILs, the desulfurization efficiency increases considerably. This might be due to enhancement of delocalized π -electrons, which increase π - π interactions. Furthermore, the phenyl ring in the benzyl is not directly attached to the imidazolium core and can therefore rotate freely around the CH₂-group. As a result of this, the phenyl group in benzyl may not be in the same plane as the imidazolium core during EDS, thus contributing partially to the π - π interactions. However, the benzimidazole is a condensed ring system consisting of a phenyl ring and an imidazolium core, hence forcing the phenyl group to be in the same plane.[96]

4 Conclusion

The objective of this study was to synthesize novel dual functionalized imidazolium and benzoimidazolium based ILs for the desulfurization of DBT and 4,6-DMDBT. The desulfurization was performed by dual functionalized imidazolium-based ILs containing diethylene glycol chains and π -electron containing substituents (allyl and benzyl).

For the allyl group bearing imidazolium-based ILs (**6-8**), increasing the length of the ether chains on the imidazolium cation resulted in higher desulfurization due to the increase in the electrostatic interaction between the oxygen atoms and the sulfur atom in DBT and 4,6-DMDBT. The $[\text{N}(\text{CN})_2]$ and $[\text{NTf}_2]$ anion based-ILs exhibited higher extraction efficiency for DBT and 4,6-DMDBT, respectively. This may be due to increased hydrophobicity by the presence of $[\text{NTf}_2]$, thus increasing the hydrophobic interactions. DBT appears to not be affected by the increase of the aforementioned interactions, presumably because 4,6-DMDBT is slightly more non-polar than DBT.

Optimization of the desulfurization studies using $[\text{N}(\text{CN})_2]$ anion-based ILs **8c** was performed, in which the effect of mass ratio of IL:MO, temperature and extraction time was studied. The results revealed that extraction equilibrium could be reached within 15 min at 25°C at a 2:1 ratio of ILs to model oil. An extraction efficiency of 69% and 33% was obtained for DBT and 4,6-DMDBT, respectively. An $^1\text{H-NMR}$ study was performed under the optimized conditions for IL **8c** with DBT. The results indicated that the acidic C2-proton had negligible

interactions with DBT due to intramolecular hydrogen bonding with the oxygen atoms in the ether chain. The most affected protons by the presence of DBT was the C4 and C5 protons on the imidazolium ring, which is an indication of the hydrogen bond formation between the C4- and C5-protons and sulfur atoms in BDT and DMBDT.

The change of the substituent from allyl to benzyl led to enhancement of the desulfurization efficiency. As observed for IL **6-8**, increasing the cationic core size resulted in enhancement of the extraction efficiency. For the allylic ILs (**6-8**), the $[N(CN)_2]$ showed higher affinity towards DBT, while the $[NTf_2]$ showed higher affinity towards 4,6-DMDBT, similar to what was observed with benzylic ILs (**9-11**). The extraction efficiencies of DBT and 4,6-DMDBT was 56% and 24% for IL **11c** and 53% and 29% for IL **11b**, respectively.

In addition, benzoimidazolium-based ILs (**15-17**) were studied for the desulfurization DBT and 4,6-DMDBT. The results revealed that higher sulfur extraction efficiency was obtained for benimidazolium-based ILs compared to the imidazolium-based ILs. The significant difference between benzoimidazolium and benzyl bearing imidazolium ILs may be due to the free rotation of the benzylic group. This allows the phenyl ring to not be in the same plane as the imidazolium core during EDS. Benzoimidazolium based ILs on the other hand, consist of condensed phenyl and imidazole rings, thus forcing the phenyl ring to be in the same plane as the imidazolium core.

In contrast to the imidazolium-based ILs, increasing the ether chain resulted in lower extraction efficiency for the benzoimidazolium-based

ILs. A ^1H -NMR study with IL **8b** and DBT revealed that the acidic C2 proton of benzoimidazolium-based ILs interacts stronger than the acidic C2-proton of imidazolium based ILs. By extending the ether chain, the intramolecular hydrogen bonding observed in IL **8c** increases and shields the proton from the sulfur in DBT. Therefore, the highest desulfurization efficiency was obtained by the IL with shortest ether chain, *i.e.* the $[\text{NTf}_2]$ based IL **15b** (69% and 51% of DBT and 4,6-DMDBT, respectively).

5 Further work

This project revealed that the benzyl bearing imidazolium and benzoimidazolium based ILs provided higher extraction efficiency than allyl bearing imidazolium based ILs. Therefore, promising result may be obtained upon optimization of the extraction conditions. In addition, the toxicity of all synthesized ILs should be measured in the interest of industrial application.

As a part of this project, the effect of π - π -interaction was shown to play a significant role in EDS. Furthermore, the more rigid benzoimidazolium-based ILs showed significant increase in extraction efficiency compared to the allyl and benzyl bearing ILs, possibly indicating the importance of having the aromatic substituent in the same plane as the cationic core. Based on this, an interesting approach would be to study the effect of the phenyl group in 1 or 3 position of the imidazole, which can be attained through *N*-arylation. Investigation of the effect of different substituents on the phenyl ring from electron donating groups to electron withdrawing group is another possibility.

¹H-NMR study of IL **8c** indicated that the acidic C2-proton on the imidazolium core interacted poorly due to intramolecular hydrogen bonding. Thus, replacing the proton with a functional group may enhance the desulfurization efficiency. The commercially available 2-phenylimidazole, where the IL can consist of up to three functional groups, is a possible alternative to the proton.

¹H-NMR study of IL **15b** revealed that the extension of the ether

chain leads to decrease in the desulfurization efficiency. Thus, the effect of replacing the ether chain with an aromatic substituent would be interesting to study.

6 Experimental

General Methods

All commercially available chemicals were used without further purification. ^1H -NMR and ^{13}C -NMR spectra were recorded either on a Bruker Advance DPX 400 MHz spectrometer or a Bruker Advance III 600 MHz spectrometer. Spectra are presented with acquisition parameters (shown in Appendix). Chemical shifts (δ) are given in parts per million (ppm) and the shifts are assigned with respect to tetramethylsilane (TMS). Coupling constants are given in Hertz. The multiplicities are assigned as singlet (s), doublet (d), triplet (t), multiplet (m) or a combination of these. The solvents used for NMR were deuterated chloroform (CDCl_3) with residual shift $\delta(\text{ppm}) = 7.26$ (s) for ^1H -NMR and $\delta(\text{ppm}) = 77.36$ for ^{13}C -NMR. Deuterated dimethylsulfoxide (DMSO) $\delta(\text{ppm}) = 2.50$ for ^1H -NMR and $\delta(\text{ppm}) = 39.52$ for ^{13}C -NMR. Deuterated methanol (MD_3OD) with shifts $\delta(\text{ppm})$: 3.31 (s) for ^1H -NMR and $\delta(\text{ppm}) = 49$ for ^{13}C -NMR. Water content were measured using Coloumetric Karl Fischer titrator (Mettler Toledo, DL39).

Infrared spectroscopy (IR) was performed with a Nicolet 20SXC FT-IR spectrometer using EZ OMNIC software and a Bruker Alpha FTIR spectrometer using OPUS V7 softare to analyes the IR-spectra. Accurate mass determination in positive and negative mode was performed on a "Synapt G2-S" Q-TOF instrument from Water TM. Samples were ionized by the use of ASAP probe (APCI) or ESI probe. No chromato-

graphic separation was used previous to the mass analysis. Calculated exact mass and spectra processing was done by Waters TM Software Masslynx V4.1 SCN871. High Performance Liquid Chromatography was performed using Agilent 1260 TCC with autosampler and a 1260 Diode Array Detector (DAD). A Zorbax Eclipse XDB-C18 4.6 x 150 mm reverse phase column was used as the stationary phase. All spectra can be seen in Appendix.

6.1 Synthesis of 1-(2-methoxyethyl)-1*H*-imidazole (3)

Imidazole (7.35g, 107.9 mmol) and NaOH (8.63g, 215.8 mmol) were mixed for 30 min at room temperature in acetonitrile (60 mL). 2-chloroethyl methyl ether (10.20g, 107.9 mmol) was added and the solution was refluxed for 24h. The precipitate formed was filtered off and the solvent was removed under reduced pressure, resulting in 96% yield (18.1 g, 143.8 mmol) of compound **3** as an orange liquid.

¹H-NMR (400 MHz, MeOD): δ (ppm): 7.65 (s, 1H, N=CH-N), 7.15 (s, 1H, CH=CH-N), 6.96 (s, 1H, N-CH=CH), 4.19 (t, 2H, J = 5.0 Hz, N-CH₂-CH₂, 3.66 (t, 2H, J = 5.0 Hz, CH₂-CH₂-O), 3.34 (s, 3H, O-CH₃)

6.2 Synthesis of 1-allyl-3-(2-methoxyethyl)-1*H*-imidazolium bromide (**6a**)

Compound **3** (15.4g, 122 mmol) and allyl bromide (14.8g, 122 mmol) were dissolved in MeCN (50 mL) and stirred at 80 °C for 24h. The solvent was removed under reduced pressure, resulting in 94% yield (28.2 g, 114.2 mmol) of compound **6a** as a brown viscous liquid.

¹H-NMR (400 MHz, CDCl₃): δ (ppm): 10.0 (s, 1H, N=CH-N), 7.73 (t, 1H, J = 1.7 Hz, CH=CH-N), 7.57 (t, 1H, J = 1.7 Hz, N-CH=CH), 6.12-6.07 (m, 1H, CH₂=CH-CH₂), 5.53 - 5.46 (m, 2H, CH₂=CH), 5.04 (d, 2H, J = 6.4 Hz, CH-CH₂-N), 4.61 (t, 2H, J = 4.8 Hz, N-CH₂-CH₂),

3.80 (t, 2H, $J = 4.78$ Hz, $\text{CH}_2\text{-CH}_2$ 3.38 (s, 3H, O- CH_3)

6.3 Synthesis of 1-allyl-3-(2-methoxyethyl)-1*H*-imidazolium bis(trifluoromethylsulfonyl)imide (**6b**)

Bis(trifluoromethane)sulfonimide lithium salt (7.10 g, 24.7 mmol) and compound **6a** (6.11 g, 24.7 mmol) were mixed, dissolved in water (30 mL) and stirred for 2h. Two layers were formed and the IL was separated from the aqueous layer and washed with water until the water phase gave a negative test with a silver nitrate solution. The IL was finally dried in vacuum for 48h at 60 °C, resulting in 74% yield (8.22 g, 18.4 mmol) of IL **6b** as a brown liquid.

¹H-NMR (400 MHz, CDCl_3): δ (ppm): 8.63 (s, 1H, N=CH-N), 7.46 (t, 1H, $J = 1.8$ Hz, CH=CH-N), 7.34 (t, 1H, $J = 1.8$ Hz, N⁺=CH=CH), 6.05-5.95 (m, 1H, $\text{CH}_2=\text{CH-CH}_2$), 5.50-5.44 (m, 2H, $\text{CH}_2=\text{CH}$), 4.79 (d, 2H, $J = 6.5$ Hz, CH-CH₂-N⁺), 4.36 (t, 2H, $J = 4.8$ Hz, N-CH₂-CH₂), 3.71 (t, 2H, $J = 4.8$ Hz, CH₂-CH₂-O), 3.36 (s, 3H, O-CH₃)

¹³C-NMR (400 MHz, CDCl_3): δ (ppm): 135.4 (N=CH-N), 129.3 ($\text{CH}_2=\text{CH-CH}_2$), 124.5, 121.1, 118.1, 114.9 ($\text{CF}_3\text{-SO}_2$), 123.4 (CH=CH-N), 122.7 ($\text{CH}_2=\text{CH}$), 121.9 (N⁺-CH=CH), 69.7 ($\text{CH}_2\text{-CH}_2$)-O), 58.7 (O-CH₃), 52.0 (CH-CH₂-N⁺), 49.9 (N-CH₂-CH₂)

IR (thin film, cm^{-1}): 3150.88, 3116.63, 3094.43, 2996.25, 2941.32, 2903.07, 2839.35, 1563.22, 1451.53, 1426.91, 1347.06, 1329.29, 1226.15, 1181.32, 1134.07, 1054.07, 1013.64, 993.57, 948.01, 835.91, 789.25, 761.68, 740.20,

652.99, 614.53, 570.69, 513.53, 407.97

HR-MS (ES+): calcd for C₉H₁₅N₂O [M] 167.1184, obsd: 167.1184.

HR-MS (ES-): calcd for C₂F₆NO₄S₂ [M] 279.9173, obsd: 279.9179.

Water content (ppm): 120.8

6.4 Synthesis of 1-allyl-3-(2-methoxyethyl)-1*H*-imidazolium dicyanamide (**6c**)

Compound **6a** (2.64 g, 10.7 mmol) and sodium dicyanamide (1.04 g, 11.7 mmol) were mixed, dissolved in acetone (20 mL) and stirred for 24h at room temperature. The precipitate formed was filtered off, the solvent was removed under reduced pressure and dichloromethane was added. The solution was stored in the fridge over night. The precipitate formed was filtered off, the solvent was removed under reduced pressure and the same procedure was repeated until no precipitation occurred. The IL was then dried in vacuum for 24h at 60 °C. This resulted in 62% yield (1.54 g, 6.59 mmol) of IL **6c** as a brown liquid.

¹H-NMR (400 MHz, CDCl₃): δ (ppm): 9.38 (s, 1H, N⁺=CH-N), 7.67 (s, 1H, CH=CH-N), 7.56 (s, 1H, N⁺-CH=CH), 6.13-6.03 (m, 1H, CH₂=CH-CH₂), 5.54-5.50 (m, 2H, CH₂=CH), 4.96 (d, 2H, J = 6.4 Hz, CH-CH₂-N⁺), 4.51 (t, 2H, J = 4.8 Hz, N-CH₂-CH₂), 3.80 (t, 2H, J = 4.8 Hz, CH₂-CH₂-O), 3.40 (s, 3H, O-CH₃)

¹³C-NMR (400 MHz, CDCl₃): δ (ppm): 136.1 (N⁺=CH-N), 129.7 (CH₂=CH-CH₂), 123.4 (CH=CH-N), 122.7 (CH₂=CH), 122.0 (N⁺-

CH=CH), 119.7 (NC-N⁻), 69.8 (CH₂-CH₂-O), 58.7 (O-CH₃), 52.0 (CH-CH₂-N⁺), 49.9 (N-CH₂-CH₂)

IR (thin film, cm¹): 3406.99, 3138.04, 3085.78, 2936.58, 2229.20, 2192.96, 2128.55, 1667.64, 1561.69, 1445.89, 1423.75, 1385.97, 1308.17, 1221.77, 1159.67, 1118.05, 1081.90, 1011.75, 994.81, 944.60, 833.74, 757.49, 668.64, 641.25, 622.92, 564.45, 524.

HR-MS (ES+): calcd for C₉H₁₅N₂O [M] 167.1184, obsd: 167.1184.

HR-MS (ES-): calcd for C₂N₃ [M] 66.0092, obsd: 66.0092.

Water content (ppm): 498.2

6.5 Synthesis of 1-allyl-3-(2-methoxyethyl)-1*H*-imidazolium thiocyanate (**6d**)

Following the procedure for compound **6c** with compound **6a** (2.74 g, 11.1 mmol) and sodium thiocyanate (0.99 g, 12.2 mmol) in acetone (20 mL), resulted in 74% yield (1.84 g, 8.16 mmol) of IL **6d** as a brown viscous liquid.

¹H-NMR (400 MHz, CDCl₃): δ (ppm): 9.14 (s, 1H, N⁺=CH-N), 7.65 (s, 1H, CH=CH-N), 7.50 (s, 1H, N⁺-CH=CH), 6.16-6.06 (m, 1H, CH₂=CH-CH₂), 5.55-5.48 (m, 2H, CH₂=CH), 5.00 (d, 2H, J = 6.4 Hz, CH-CH₂-N⁺), 4.57 (t, 2H, J = 4.7 Hz, N-CH₂-CH₂), 3.85 (t, 2H, J = 4.8 Hz, CH₂-CH₂-O), 3.40 (s, 3H, O-CH₃)

¹³C-NMR (400 MHz, CDCl₃): δ (ppm): 136.2 (N⁺=CH-N), 132.1 (S-CN), 129.9 (CH₂=CH-CH₂), 123.5 (CH=CH-N), 122.7 (CH₂=CH),

121.9 ($\text{N}^+ \text{-CH=CH}$), 70.1 ($\text{CH}_2 \text{-CH}_2 \text{-O}$), 59.0 (O-CH_3), 52.3 ($\text{CH}_2 \text{=CH}$), 49.9 ($\text{N-CH}_2 \text{-CH}_2$)

IR (thin film, cm^{-1}): 3411.88, 3139.21, 3100.93, 2991.62, 2938.26, 2831.47, 2050.59, 1665.38, 1561.24, 1445.08, 1423.32, 1388.20, 1349.91, 1292.39, 1157.47, 1116.75, 1079.29, 1010.20, 993.55, 943.78, 831.73, 748.22, 667.81, 638.42, 620.51, 562.47, 470.79

HR-MS (ES+): calcd for $\text{C}_9\text{H}_{15}\text{N}_2\text{O}$ [M] 167.1184, obsd: 167.1186.

HR-MS (ES-): calcd for CNS [M] 57.9751, obsd: 57.9750.

Water content (ppm): 433.9

6.6 Synthesis of 1-allyl-3-(2-methoxyethyl)-1*H*-imidazolium tetrafluoroborate (6e)

Following the procedure for **6c** with compound **6a** (2.43 g, 7.87 mmol) and sodium tetrafluoroborate (1.19g, 10.8 mmol) in acetone (20 mL), resulted in 64% yield (1.84 g, 8.16 mmol) of IL **6e** as a brown viscous liquid.

$^1\text{H-NMR}$ (400 MHz, CDCl_3): δ (ppm): 8.79 (s, 1H, $\text{N}^+ \text{=CH-N}$), 7.49 (t, 1H, $J = 1.7$ Hz, CH=CH-N), 7.37 (t, 1H, $J = 1.6$ Hz, $\text{N}^+ \text{-CH=CH}$), 6.06-5.96 (m, 1H, $\text{CH}_2 \text{=CH-CH}_2$), 5.48-5.42 (m, 2H, $\text{CH}_2 \text{=CH}$), 4.82 (d, 2H, $J = 6.4$ Hz, $\text{CH-CH}_2 \text{-N}^+$), 4.38 (t, 2H, $J = 4.8$ Hz, $\text{N-CH}_2 \text{-CH}_2$), 3.73 (t, 2H, $J = 4.8$ Hz, $\text{CH}_2 \text{-CH}_2 \text{-O}$), 3.34 (s, 3H, O-CH_3)

$^{13}\text{C-NMR}$ (400 MHz, CDCl_3): δ (ppm): 136.0 ($\text{N}^+ \text{=CH-N}$), 132.1 (S-CN), 129.9 ($\text{CH}_2 \text{=CH-CH}_2$), 123.3 (CH=CH-N), 122.5 ($\text{CH}_2 \text{=CH}$),

121.9 ($\text{N}^+ \text{-CH=CH}$), 69.9 ($\text{CH}_2 \text{-CH}_2 \text{-O}$), 58.8 (O-C_3), 52.0 ($\text{CH-CH}_2 \text{-N}^+$), 49.8 ($\text{N-CH}_2 \text{-CH}_2$)

IR (thin film, cm^{-1}): 3152.35, 3092.05, 2989.06, 2941.35, 1645.88, 1562.64, 1448.76, 1425.88, 1355.99, 1287.11, 1161.93, 1114.08, 1050.81, 947.80, 833.51, 759.73, 670.82, 642.47, 623.90, 570.62, 521.28

HR-MS (ES+): calcd for $\text{C}_9\text{H}_{15}\text{N}_2\text{O}$ [M] 167.1184, obsd: 167.1183.

HR-MS (ES-): calcd for BF_4^- [M] 87.0029, obsd: 87.0034.

Water content (ppm): 370.5

6.7 Synthesis of 1-chloro-2-(2-methoxyethoxy)ethane (1)

Diethylene glycol monomethyl ether (25.0 g, 208 mmol) and pyridine (16.5 g, 208 mmol) were dissolved in dichloromethane (50 mL) stirred under N_2 atmosphere. Thionyl chloride (24.8 g, 208 mmol) dissolved in dichloromethane (50 mL) was added dropwise to the solution. The solution was then heated to reflux and stirred over night. The solution was then cooled down to room temperature and extracted with water (3 x 50 mL). The solution was dried over MgSO_4 and the solvent was removed under reduced pressure, resulting in 85% yield (24.5 g, 177 mmol) of compound **1** as pale yellow liquid.

$^1\text{H-NMR}$ (400 MHz, CDCl_3): δ (ppm): 3.76 (t, 2H, $J = 5.9$ Hz, $\text{Cl-CH}_2 \text{-CH}_2$), 3.68-3.63 (m, 4H, $\text{CH}_2 \text{-CH}_2 \text{-O}$), 3.57-3.55 (m, 2H, $\text{CH}_2 \text{-CH}_2 \text{-O}$), 3.39 (s, 3H, O-CH_3)

6.8 Synthesis of 1-(2-(2-methoxyethoxy)ethyl)-1*H*-imidazole (4)

Following the procedure for **3** with imidazole (11.6 g, 170 mmol), compound **1** (23.53 g, 170 mmol) and NaOH (13.58 g, 340 mmol) in acetonitrile (100 mL), resulted in 94% (27.2 yield g, 160 mmol) yield of compound **4** as an orange liquid.

¹H-NMR (400 MHz, MeOD): δ (ppm): 7.68 (s, 1H, N⁺=CH-N), 7.18 (s, 1H, CH=CH-N), 6.96 (s, 1H, N⁺-CH=CH), 4.19 (t, 2H, J = 5.0 Hz, N-CH₂-CH₂), 3.76 (t, 2H, J = 5.1 Hz, CH₂-CH₂-O), 3.61-3.58 (m, 2H, O-CH₂-CH₂), 3.53-3.51 (m, 2H, CH₂-CH₂-O), 3.35 (s, 3H, O-CH₃)

6.9 Synthesis of 3-allyl-1-(2-(2-methoxyethoxy)ethyl)-1*H*-imidazolium bromide (7a)

Following the procedure for compound **6a** with compound **4** (6.25 g, 36.7 mmol) and allyl bromide (4.44 g, 36.7 mmol) in acetonitrile (30 mL), resulted in 95% yield (10.2 g, 34.9 mmol) of compound **7a** as a brown viscous liquid.

¹H-NMR (400 MHz, CDCl₃): δ (ppm): 10.1 (s, 1H, N⁺=CH-N), 7.75 (t, 1H, J = 1.7 Hz, CH=CH-N), 7.50 (t, 1H, J = 1.7 Hz, N⁺-CH-CH), 6.11-6.01 (m, 1H, CH₂=CH-CH₂), 5.52-5.47 (m, 2H, CH₂=CH), 5.01 (d, 2H, J = 6.4 Hz, CH-CH₂-N⁺), 4.64 (t, 2H, J = 4.7 Hz, N-CH₂-CH₂), 3.92 (t, 2H, J = 5.0 Hz, CH₂-CH₂-O), 3.68-3.66 (m, 2H, O-CH₂-CH₂), 3.54-3.52 (m, 2H, CH₂-CH₂-O), 3.36 (s, 3H, O-CH₃)

6.10 Synthesis of 3-all l-1-(2-methoxyethoxy)-ethyl)-1*H*-imidazolium bis(trifluoromethylsulfonyl)imide (**7b**)

Following the procedure for **6b** with compound **7a** (7.00 g, 24.0 mmol) and bis(trifluoromethane)sulfonimide lithium salt (6.90 g, 24 mmol) in water (30 mL), resulted in 88% yield (10.4 g, 21.2 mmol) of IL **7b** as a brown liquid.

¹H-NMR (400 MHz, CDCl₃): δ (ppm): 8.70 (s, 1H, N⁺=CH-N), 7.51 (t, 1H, J = 1.8 Hz, CH=CH-N)), 7.34 (t, 1H, N⁺-CH=CH), 6.05-5.95 (m, 1H, CH₂=CH-CH₂), 5.49-5.44 (m, 2H, CH₂=CH), 4.78 (d, 2H, CH-CH₂-N⁺), 4.36 (t, 2H, J = 4.8 Hz, N-CH₂-CH₂), 3.83 (t, 2H, J = 4.7 Hz, CH₂-CH₂-O), 3.65-3.63 (m, 2H, CH₂-CH₂-O), 3.53-3.52 (m, 2H, O-CH₂-CH₂), 3.35 (s, 3H, O-CH₃)

¹³C-NMR (400 MHz, CDCl₃): δ (ppm): 136.0 (N⁺=CH-N), 129.6 (CH₂=CH-CH₂), 123.4, (CH=CH-N), 122.6 (CH₂=CH), 121.2 (N⁺-CH=CH), 124.5, 121.3, 118.1, 115 (CF₃-SO₂), 71.4 (CHF₂-CH₂-O), 70.1 (O-CH₂-CH₂), 68.3 (CH₂-C₂-O), 58.7 (O-CH₃), 52.0 (CH-CH₂-N⁺), 49.7 (N-CH₂-CH₂)

IR (thin film, cm¹): 3150.65, 2883.95, 1563.88, 1452.07, 1347.96, 1330.10, 1226.33, 1178.87, 1132.10, 1051.72, 992.40, 947.61, 844.24, 788.73, 761.40, 739.64, 652.68, 612.41, 599.80, 568.90, 509.39, 406.69

HR-MS (ES+): calcd for C₁₁H₁₉N₂O₂ [M] 211.1447, obsd: 211.1443.

HR-MS (ES-): calcd for C₂NO₄F₆S₂ [M] 279.9179, obsd: 279.9173

Water content (ppm): 209.1

6.11 Synthesis of 3-allyl-1-(2-(2-methoxyethoxy)-ethyl)-1*H*-imidazolium dicyanamide (**7c**)

Following the procedure for **6c** with compound **7a** (4.72 g, 16.2 mmol) sodium dicyanamide (1.59 g, 17.8 mmol) in acetone (30 mL), resulted in 76% yield (3.42 g, 12.3 mmol) of IL **7c** as a brown liquid.

¹H-NMR (400 MHz, CDCl₃): δ (ppm): 9.36 (s, 1H, N⁺=CH-N), 7.72 (s, 1H, CH=CH-N), 7.58 (s, 1H, N⁺-CH), 6.13-6.03 (m, 1H, CH₂=CH-CH₂), 5.54-5.49 (m, 2H, CH₂=CH), 4.96 (d, 2H, J = 6.4 Hz, CH-CH₂)-N⁺), 4.52 (t, 2H, J = 4.7 Hz, N-CH₂-CH₂), 3.91 (t, 2H, J = 4.7 Hz, CH₂-CH₂-O), 3.70-3.67 (m, 2H, O-CH₂-CH₂), 3.56-3.54 (m, 2H, CH₂-CH₂-O), 3.37 (s, 3H, O-CH₃)

¹³C-NMR (400 MHz, CDCl₃): δ (ppm): 136.1 (N⁺=CH-N), 129.7 (CH₂=CH-CH₂), 123.4 (CH=CH-N), 122.5 (CH₂=CH), 122.0 (N-CH=CH), 119.6 (CN-N⁻), 71.5 (CH₂-CH₂-O), 70.2 (O-CH₂-CH₂), 68.4 (CH₂-CH₂-O), 52.0 (CH-CH₂-N⁺), 49.8 (N-CH₂-CH₂)

IR (thin film, cm¹): 3137.55, 3085.97, 2878.98, 2826.47, 2225.86, 2190.54, 2126.04, 1670.27, 1646.45, 1561.89, 1447.94, 1424.99, 1352.05, 1303.07, 1198.39, 1160.24, 1098.13, 1023.75, 993.32, 943.74, 844.21, 756.78, 668.00, 640.98, 622.36, 562.33, 522.77, 449.62

HR-MS (ES+): calcd for C₁₁H₁₉N₂O₂ [M] 211.1447, obsd: 211.1443.

HR-MS (ES-): calcd for C₂N₃ [M] 66.0092, obsd: 66.0093

Water content (ppm): 196.2

6.12 Synthesis of 3-allyl-1-(2-(2-methoxyethoxy)-ethyl)-1*H*-imidazolium thiocyanate (**7d**)

Following the procedure for **6c** with compound **7a** (3.23 g, 11.4 mmol) and sodium thiocyanate (0.90 g, 12.2 mmol) in acetone (20 mL), resulted in 74% yield (2.43 g, 9.03 mmol) of IL **7d** as a brown viscous liquid.

¹H-NMR (400 MHz, CDCl₃): δ (ppm): 9.20 (s, 1H, N⁺=CH-N), 7.72 (t, 1H, J = 1.6 Hz, CH=CH-N), 7.48 (t, 1H, J = 1.7 Hz N⁺-CH), 6.16-6.06 (m, 1H, CH₂=CH-CH₂), 5.55-5.48 (m, 2H, CH₂=CH), 5.01 (d, 2H, J = 6.4 Hz, CH-CH₂)-N⁺), 4.61 (t, 2H, J = 4.7 Hz, N-CH₂-CH₂), 3.98 (t, 2H, J = 4.7 Hz, CH₂-CH₂-O), 3.72-3.69 (m, 2H, O-CH₂-CH₂), 3.58-3.56 (m, 2H, CH₂-CH₂-O), 3.39 (s, 3H, O-CH₃)

¹³C-NMR (400 MHz, CDCl₃): δ (ppm): 136.5 (N⁺=CH-N), 132.4 (S-CN), 130.0 (CH₂=CH-CH₂), 123.6 (CH=CH-N), 122.6 (CH₂=CH), 121.8 (N-CH=CH), 71.4 (CH₂-CH₂-O), 70.2 (O-CH₂-CH₂), 68.8 (CH₂-CH₂-O), 59.0 (O-CH₃), 52.3 (CH-CH₂-N⁺), 49.8 (N-CH₂-CH₂)

IR (thin film, cm¹): 3305.87, 3136.79, 3089.89, 2879.22, 2820.97, 2052.10, 1667.55, 1560.76, 1446.26, 1423.69, 1386.91, 1351.49, 1290.78, 1244.33, 1198.53, 1158.25, 1082.02, 1024.73, 992.04, 944.19, 846.19, 752.85, 668.38, 640.43, 621.28, 564.76, 472.46

HR-MS (ES+): calcd for C₁₁H₁₉N₂O₂ [M] 211.1447, obsd: 211.1451.

HR-MS (ES-): calcd for CNS [M] 57.9751, obsd: 57.9760

Water content (ppm): 358.4

6.13 Synthesis of 3-allyl-1-(2-(2-methoxyethoxy)-ethyl)-1*H*-imidazolium tetrafluoroborate (**7e**)

Following the procedure for **6c** with compound **6a** (3.88 g, 13.3 mmol) and sodium tetrafluoroborate (1.61 g, 14.7 mmol) in acetone (20 mL), resulted in 83% yield (3.30 g, 11.1 mmol) of IL **7e** as a brown viscous liquid.

¹H-NMR (400 MHz, CDCl₃): δ (ppm): 8.81 (s, 1H, N⁺=CH-N), 7.55 (t, 1H, J = 1.7 Hz, CH=CH-N), 7.40 (t, 1H, J = 1.7 Hz N⁺-CH=CH), 6.07-5.97 (m, 1H, CH₂=CH-CH₂), 5.48-5.42 (m, 2H, CH₂=CH), 4.82 (d, 2H, J = 6.4 Hz, CH-CH₂)-N⁺), 4.40 (t, 2H, J = 4.7 Hz, N-CH₂-CH₂), 3.85 (t, 2H, J = 4.8 Hz, CH₂-CH₂-O), 3.65-3.63 (m, 2H, O-CH₂-CH₂), 3.53-3.50 (m, 2H, CH₂-CH₂-O), 3.34 (s, 3H, O-CH₃)

¹³C-NMR (400 MHz, CDCl₃): δ (ppm): 136.0 (N⁺=CH-N), 129.9 (CH₂=CH-CH₂), 123.4 (CH=CH-N), 122.3 (CH₂=CH), 121.9 (N-CH=CH), 71.5 (CH₂-CH₂-O), 70.1 (O-CH₂-CH₂), 68.5 (CH₂-CH₂-O), 58.8 (O-CH₃), 51.9 (CH-CH₂-N⁺), 49.6 (N-CH₂-CH₂)

¹⁹F-NMR (400 MHz, CDCl₃): -150.9, -151.0

IR (thin film, cm¹): 3152.76, 3114.82, 2882.31, 1647.10, 1564.44, 1451.84, 1427.07, 1353.50, 1286.47, 1199.26, 1163.05, 1047.47, 1020.12, 951.46, 844.47, 759.24, 669.91, 643.04, 623.66, 562.32, 520.28

HR-MS (ES+): calcd for C₁₁H₁₉N₂O₂ [M] 211.1447, obsd: 211.1445.

HR-MS (ES-): calcd for BF₄ [M] 86.0065 obsd: 86.0065

Water content (ppm): 466.9

6.14 Synthesis of 1-chloro-2-(2-(2-methoxyethoxy)ethoxy)ethane (2)

Following the procedure for **1** with triethylene glycol monomethyl ether (27.0 g, 164 mmol), pyridine (13.0 g, 164 mmol) and thionyl chloride (19.6 g, 164 mmol), resulted in 94% (28.2 g, 154 mmol) of compound **2** as a light brown liquid.

¹H-NMR (400 MHz, CDCl₃): δ (ppm): 3.76 (t, 2H, J = 5.8 Hz, Cl-CH₂-CH₂), 3.71-3.62 (m, 8H, O-CH₂-CH₂). 3.56-3.54 (m, 2H, CH₂-CH₂-O), 3.38 (s, 3H, O-CH₃)

6.15 Synthesis of 1-(2-(2-(2-methoxyethoxy)ethoxy)ethyl)-1*H*-imidazole (5)

Following the procedure for **3** with imidazole (9.53 g, 140 mmol), compound **2** and NaOH (11.2 g, 240 mmol) in acetonitrile (70 mL), resulted in 86% (25.7 g, 120 mmol) of compound **3** as an orange liquid.

¹H-NMR (400 MHz, CDCl₃): δ (ppm): 7.53 (s, 1H, N⁺=CH-N), 7.01 (s, 2H, CH=CH-N), 4.11 (t, 2H, J = 5.1 Hz, N-CH₂CH₂), 3.74 (t, 3H, J = 5.2 Hz, CH₂-CH₂-O), 3.61-3.58 (m, 6H, O-CH₂-CH₂), 3.55-3.52

(m, 2H, CH₂-CH₂-O), 3.37 (s, 3H, O-CH₃)

6.16 Synthesis of 3-allyl-1-(2-(2-methoxyethoxy)ethoxyethyl)-1*H*-imidazolium bromide (**8a**)

Following the procedure for **6a** with compound **5** (25.7 g, 120 mmol) and allyl bromide (14.5 g, 120 mmol), resulted in 94% yield (37.9 g, 113 mmol) of compound **8a** as a brown viscous liquid.

¹H-NMR (400 MHz, CDCl₃): δ (ppm): 9.87 (s, 1H, N⁺=CH-N), 7.90 (t, 1H, J = 1.7 Hz, CH=CH-N), 7.67 (t, 1H, N⁺-CH), 6.13-6.03 (m, 1H, CH₂=CH-CH₂), 5.52-5.45 (m, 2H, CH₂=CH), 5.05 (d, 2H, J = 6.3 Hz, CH-CH₂-N⁺), 4.63 (t, 2H, J = 4.7 Hz, N-CH₂-CH₂), 3.92 (t, 2H, J = 4.7 Hz, CH₂-CH₂-O), 3.71-3.68 (m, 2H, CH₂-CH₂-O), 3.64-3.62 (m, 4H, CH₂-CH₂-O), 3.56-3.54 (m, 2H, CH₂-CH₂-O), 3.37 (s, 3H, O-CH₃)

6.17 Synthesis of 3-allyl-1-(2-(2-methoxyethoxy)ethoxyethyl)-1*H*-imidazolium bis(trifluoromethylsulfonyl)imide (**8b**)

Following the procedure for **6b** with compound **8a** (3.25 g, 9.70 mmol) and bis(trifluoromethane)sulfonimide lithium salt (2.78 g, 9.70 mmol) in water (30 mL), resulted in 80% yield (4.17 g, 7.78 mmol) of IL **8b** as a light brown liquid.

¹H-NMR (400 MHz, CDCl₃): δ (ppm): 8.77 (s, 1H, N⁺=CH), 7.55 (t, 1H, J = 1.8 Hz, CH=CH-N), 7.30 (s, 1H, J = 1.8 Hz, N⁺-CH=CH), 6.04-5.94 (m, 1H, CH₂=CH-CH₂), 5.48-5.42 (m, 2H, CH₂=CH), 4.80 (d, 2H, J = 6.4 Hz, CH-CH₂-N⁺), 4.36 (t, 2H, J = 4.6 Hz, N-CH₂-CH₂), 3.83 (t, 2H, J = 4.7 Hz, CH₂-CH₂-O), 3.67-3.65 (m, 2H, O-CH₂-CH₂), 3.63-3.60 (m, 4H, CH₂-CH₂-O), 3.56-3.54 (m, 2H, O-CH₂-CH₂), 3.35 (s, 3H, O-CH₃)

¹³C-NMR (400 MHz, CDCl₃): 135.8 (N⁺=CH-N), 129.5 (CH₂=C-CH₂), 124.5, 121.3, 118.2, 115.0 (CF₃-SO₂), 123.7 (CH=CH-N), 122.5 (CH₂=CH), 121.7 (N⁺-CH=CH), 71.7 (CH₂-CH₂-O), 70.2 (O-CH₂-CH₂), 70.1 (CH₂-CH₂-O), 70.0 (O-CH₂-CH₂), 68.3 (CH₂-CH₂-O), 58.7 (O-CH₃), 51.9 (CH-CH₂-N⁺), 49.8 (N-CH₂-CH₂)

IR (thin film, cm¹): 3149.39, 3114.32, 2879.11, 1648.15, 1563.45, 1452.58, 1426.73, 1348.27, 1330.29, 1226.47, 1181.51, 1133.09, 1054.04, 993.01, 942.62, 848.63, 788.66, 761.46, 739.88, 652.73, 614.37, 570.21, 512.76, 406.45

HR-MS (ES+): calcd for C₁₃H₂₃N₂O₃ [M] 255.1709, obsd: 255.1708

HR-MS (ES-): calcd for C₂NO₄F₆S₂ [M] 279.9173, obsd: 279.9179

Water content (ppm): 238.2

6.18 Synthesis of 3-allyl-1-(2-(2-methoxyethoxy)ethoxy)ethyl)-*1H*-imidazolium dicyanamide (8c)

Following the procedure for **6c** with compound **8a** (3.8825 g, 11.6 mmol) and dicyanamide (1.13 g, 12.7 mmol) in acetone (20 mL), resulted in 64% yield (2.38 g, 7.40 mmol) of a light brown liquid.

¹H-NMR (400 MHz, CDCl₃): δ (ppm): 9.55 (s, 1H, N⁺=CH), 7.78 (t, 1H, J = 1.8 Hz, CH=CH-N), 7.49 (s, 1H, J = 1.8 Hz, N⁺-CH=CH), 6.11-6.01 (m, 1H, CH₂=CH-CH₂), 5.51-5.47 (m, 2H, CH₂=CH), 4.96 (d, 2H, J = 7.2 Hz, CH-CH₂-N⁺), 4.55 (t, 2H, J = 4.7 Hz, N-CH₂-CH₂), 3.91 (t, 2H, J = 4.7 Hz, CH₂-CH₂-O), 3.71-3.68 (m, 2H, O-CH₂-CH₂), 3.65-3.63 (m, 4H, CH₂-CH₂-O), 3.57-3.55 (m, 2H, O-CH₂-CH₂), 3.37 (s, 3H, O-CH₃)

¹³C-NMR (400 MHz, CDCl₃): 136.3 (N⁺=CH-N), 129.7 (CH₂=C-CH₂), 123.7 (CH=CH-N), 122.5 (CH₂=CH), 121.7 (N⁺-CH=CH), 119.7 (CN-N⁻), 71.7 (CH₂-CH₂-O), 70.2 (O-CH₂-CH₂), 70.1 (CH₂-CH₂-O), 70.0 (O-CH₂-CH₂), 68.5 (CH₂-CH₂-O), 58.8 (O-CH₃), 51.9 (CH-CH₂-N⁺), 49.8 (N-CH₂-CH₂)

IR (thin film, cm¹): 3487.14, 3138.88, 3087.21, 2876.31, 2226.93, 2191.09, 2127.17, 1645.69, 1562.02, 1448.70, 1350.79, 1303.07, 1249.26, 1199.14, 1090.80, 1025.48, 993.56, 936.98, 847.63, 757.71, 668.00, 641.43, 622.56, 561.68, 522.99

HR-MS (ES+): calcd for C₁₃H₂₃N₂O₃ [M] 255.1709, obsd: 255.1708

HR-MS (ES-): calcd for C₂N₃ [M] 66.0092, obsd: 66.0100

Water content (ppm): 358.4

6.19 Synthesis of 3-allyl-1-(2-(2-methoxyethoxy)ethoxy)ethyl)-1*H*-imidazolium thiocyanate (8d)

Following the procedure for compound **6c** using compound **8a** (3.98 g, 11.9 mmol) and sodium thiocyanate (1.06 g, 13.1 mmol) in acetone (20 ml), resulted in 80% yield (2.98 g, 9.51 mmol) in a light brown viscous liquid.

¹H-NMR (600 MHz, CDCl₃): δ (ppm): 9.52 (s, 1H, N⁺=CH), 7.79 (t, 1H, J = 1.7 Hz, CH=CH-N), 7.48 (s, 1H, J = 1.8 Hz, N⁺-CH=CH), 6.15-6.08 (m, 1H, CH₂=CH-CH₂), 5.55-5.49 (m, 2H, CH₂=CH), 5.02 (d, 2H, J = 6.4 Hz, CH-CH₂-N⁺), 4.63 (t, 2H, J = 4.7 Hz, N-CH₂-CH₂), 4.01 (t, 2H, J = 4.7 Hz, CH₂-CH₂-O), 3.74-3.73 (m, 2H, O-CH₂-CH₂), 3.69-3.66 (m, 4H, CH₂-CH₂-O), 3.58-3.57 (m, 2H, O-CH₂-CH₂), 3.40 (s, 3H, O-CH₃)

¹³C-NMR (600 MHz, CDCl₃): 136.5 (N⁺=CH-N), 132.7 (S-CN), 130.1 (CH₂=C-CH₂), 123.6 (CH=CH-N), 122.6 (CH₂=CH), 121.9 (N⁺-CH=CH), 71.3 (CH₂-CH₂-O), 70.3 (O-CH₂-CH₂), 69.7 (CH₂-CH₂-O), 69.6 (O-CH₂-CH₂), 69.0 (CH₂-CH₂-O), 59.1 (O-CH₃), 52.3 (CH-CH₂-N⁺), 50.0 (N-CH₂-CH₂)

IR (thin film, cm¹): 3136.94, 3086.06, 2875.85, 2052.24, 1668.21, 1561.02,

1447.25, 1423.77, 1349.33, 1292.49, 1246.69, 1199.65, 1158.38, 1080.84, 1024.71, 992.74, 940.30, 851.02, 752.90, 668.22, 640.53, 621.46, 564.67, 472.06

HR-MS (ES+): calcd for C₁₃H₂₃N₂O₃ [M] 255.1709, obsd: 255.1709

HR-MS (ES-): calcd for CNS [M] 57.9751, obsd: 57.9751

Water content (ppm): 238.2

6.20 Synthesis of 3-allyl-1-(2-(2-methoxyethoxy)ethoxyethyl)-1*H*-imidazolium tetrafluoroborate (**8e**)

Following the procedure for compound **6c** with compound **8a** (4.18 g, 12.5 mmol) and sodium tetrafluoroborate (1.51 g, 13.7 mmol) in acetone (30 mL), resulted in 64% yield (2.73 g, 7.98 mmol) of IL **8e** as a light brown liquid.

¹H-NMR (400 MHz, CDCl₃): δ (ppm): 8.88 (s, 1H, N⁺=CH), 7.61 (s, 1H, CH=CH-N), 7.39 (s, 1H, N⁺-CH=CH), 6.07-5.97 (m, 1H, CH₂=CH-CH₂), 5.47-5.42 (m, 2H, CH₂=CH), 4.84 (d, 2H, J = 6.1 Hz, CH-CH₂-N⁺), 4.40 (t, 2H, J = 4.4 Hz, N-CH₂-CH₂), 3.85 (t, 2H, J = 4.5 Hz, CH₂-CH₂-O), 3.66-3.61 (m, 6H, O-CH₂-CH₂), 3.56-3.53 (m, 2H, CH₂-CH₂-O), 3.35 (s, 3H, O-CH₃)

¹³C-NMR (400 MHz, CDCl₃): 136.0 (N⁺=CH-N), 130.1 (CH₂=C-CH₂), 123.5 (CH=CH-N), 122.1 (CH₂=CH), 121.8 (N⁺-CH=CH), 71.7 (CH₂-CH₂-O), 70.2 (O-CH₂-CH₂), 70.1 (O-CH₂-CH₂), 68.5 (CH₂-

CH₂-O), 58.8 (O-CH₃), 51.8 (CH-CH₂-N⁺), 49.6 (N-CH₂-CH₂)

IR (thin film, cm¹): 3150.68, 3113.37, 2877.28, 1646.28, 1563.67, 1451.55, 1426.75, 1351.55, 1286.67, 1249.06, 1200.13, 1162.21, 1051.39, 942.90, 848.53, 761.95, 669.79, 643.64, 624.27, 562.81, 521.00

¹⁹F-NMR (400 MHz, CDCl₃): -151.0, -151.1

HR-MS (ES+): calcd for C₁₃H₂₃N₂O₃ [M] 255.1709, obsd: 255.1708

HR-MS (ES-): calcd for CNS [M] 87.0029, obsd: 87.0035

Water content (ppm): 191.1

6.21 Synthesis of 3-benzyl-1-(2-methoxyethyl)-1*H*-imidazolium bromide (**9a**)

Following the procedure for compound **6a** with compound **3** (6.33 g, 50.2 mmol) and benzyl bromide (8.58 g, 50.2 mmol) in acetonitrile (30 mL), resulted in 92% yield (13.7 g, 46.1 mmol) of compound **9a** as a dark brown viscous liquid.

¹H-NMR (400 MHz, DMSO): δ (ppm): 9.57 (s, 1H, N⁺=CH-N), 7.93 (t, 1H, J = 1.6 Hz, CH=CH-N), 7.86 (t, 1H, J = 1.6 Hz, N⁺-CH=CH), 7.49-7.47 (m, 2H, H_{Ar}), 7.42-7.33 (m, 3H, H_{Ar}), 5.54 (s, 2H, CH_{Ar}-CH₂-N⁺, 4.41 (t, 2H, J = 4.9 Hz, N-CH₂-CH₂), 3.69 (t, 2H, J = 5.0 Hz, CH₂-CH₂-O), 3.24 (s, 3H, O-CH₃)

6.22 Synthesis of 3-benzyl-1-(2-methoxyethyl)-1*H*-imidazolium bis(trifluoromethylsulfonyl)imide (**9b**)

Following the procedure for **6b** with compound **9a** (2.82 g, 9.49 mmol) and bis(trifluoromethane)sulfonimide lithium salt (2.73 g, 9.49 mmol) in water (30 mL), resulted in 73% (3.45 g, 6.88 mmol) of a brown liquid.

¹H-NMR (400 MHz, DMSO): δ (ppm): 9.29 (s, 1H, N⁺=CH-N), 7.79 (t, 1H, J = 1.7 Hz, N⁺-CH=CH), 7.76 (t, 1H, J = 1.7 Hz, CH=CH-N), 7.44-7.36 (m, 5H, H_{Ar}), 5.46 (s, 2H, CH_{Ar}-CH₂-N⁺), 4.39 (t, 2H, J = 4.9 Hz, N-CH₂-CH₂), 3.70 (t, 2H, J = 4.9 Hz, CH₂-CH₂-O), 3.28 (s, 3H, O-CH₃)

¹³C-NMR (400 MHz, DMSO): δ (ppm): 136.6 (N⁺=CH-N), 134.8 (CH_{Ar}-C_q-CH_{Ar}), 129.0 (CH_{Ar}), 128.8 (CH_{Ar}), 128.3 (CH_{Ar}), 123.2 (CH=CH-N), 122.4 (N⁺-CH=CH), 69.5 (CH₂-CH₂-O), 58.0 (O-CH₃), 52.0 (CH_{Ar}-CH₂-N⁺), 50.0 (N-CH₂-CH₂)

IR (thin film, cm¹): 3149.13, 3114.86, 2936.37, 1561.91, 1498.76, 1456.19, 1347.25, 1328.84, 1225.99, 1180.79, 1133.56, 1082.20, 1053.35, 836.50, 788.88, 761.76, 739.47, 715.68, 651.28, 613.17, 570.26, 512.53, 464.21, 407.03

HR-MS (ES+): calcd for C₁₃H₁₇N₂O [M] 217.1341, obsd: 217.1337

HR-MS (ES-): calcd for C₂NO₄S₂F₆ [M] 279.9173, obsd: 279.9174

Water content (ppm): 257.7

6.23 Synthesis of 3-benzyl-1-(2-methoxyethyl)-1*H*-imidazolium dicyanamide (**9c**)

Following the procedure for **6c** with compound **9a** (4.54 g, 15.3 mmol) and sodium dicyanamide (1.50 g, 16.8 mmol) in acetone (30 mL), resulted in 71% yield (3.07 g, 10.8 mmol) of a red liquid.

¹H-NMR (400 MHz, DMSO): δ (ppm): 9.43 (s, 1H, N⁺=CH-N), 7.86 (t, 1H, J = 1.7 Hz, N⁺-CH=CH), 7.81 (t, 1H, J = 1.7 Hz, CH=CH-N), 7.46-7.37 (m, 5H, CH_{Ar}), 5.50 (s, 2H, CH_{Ar}-CH₂-N⁺), 4.40 (t, 2H, J = 5.0 Hz, N-CH₂-CH₂), 3.70 (t, 2H, J = 5.0 Hz, CH₂-CH₂-O), 3.25 (s, 3H, O-CH₃)

¹³C-NMR (400 MHz, DMSO): δ (ppm): 136.5 (N⁺=CH-N), 134.9 (CH_{Ar}-C_q-CH_{Ar}), 129.0 (CH_{Ar}), 128.7 (CH_{Ar}), 128.3 (CH_{Ar}), 123.1 (CH=CH-N), 122.3 (N⁺-CH=CH), 119.1 (NC-N⁻), 69.5 (CH₂-CH₂-O), 58.1 (O-CH₃), 51.8 (CH_{Ar}-CH₂-N⁺), 48.8 (N-CH₂-CH₂)

IR (thin film, cm¹): 3133.98, 3060.53, 2930.38, 2227.92, 2190.97, 2128.82, 1666.51, 1559.71, 1496.69, 1453.94, 1384.49, 1355.20, 1308.12, 1192.18, 1155.78, 1118.71, 1081.15, 1013.43, 969.34, 834.36, 717.97, 665.06, 644.86, 611.43, 568.29, 524.34, 461.50

HR-MS (ES+): calcd for C₁₃H₁₇N₂O [M] 217.1341, obsd: 217.1338

HR-MS (ES-): calcd for C₂N₃ [M] 66.0092, obsd: 66.0099

Water content (ppm): 475.0

6.24 Synthesis of 3-benzyl-1-(2-methoxyethyl)-1*H*-imidazolium thiocyanate (9d)

Following the procedure for **6c** with compound **9a** (4.72 g, 15.9 mmol) and sodium thiocyanate (1.42 g, 17.5 mmol) in acetone (30 mL), resulted in 65% yield (2.84 g, 10.3 mmol) of a brown viscous liquid.

¹H-NMR (400 MHz, DMSO): δ (ppm): 9.28 (s, 1H, N⁺=CH-N), 7.81 (t, 1H, J = 1.8 Hz, N⁺-CH=CH), 7.77 (t, 1H, J = 1.7 Hz, CH=CH-N), 7.43-7.38 (m, 5H, CH_{Ar}), 5.45 (s, 2H, CH_{Ar}-CH₂-N⁺), 4.38 (t, 2H, J = 5.0 Hz, N-CH₂-CH₂), 3.69 (t, 2H, J = 5.0 Hz, CH₂-CH₂-O), 3.29 (s, 3H, O-CH₃)

¹³C-NMR (400 MHz, DMSO): δ (ppm): 136.5 (N⁺=CH-N), 134.8 (CH_{Ar}-C_q-CH_{Ar}), 129.8 (S-CN), 129.0 (CH_{Ar}), 128.8 (CH_{Ar}), 128.3 (CH_{Ar}), 123.2 (CH=CH-N), 122.4 (N⁺-CH=CH), 69.5 (CH₂-CH₂-O), 58.1 (O-CH₃), 52.0 (CH_{Ar}-CH₂-N⁺), 48.9 (N-CH₂-CH₂)

IR (thin film, cm¹): 3134.61, 3064.93, 2988.75, 2931.95, 2894.13, 2816.69, 2153.54, 2052.30, 1664.96, 1604.83, 1558.73, 1496.11, 1453.77, 1388.28, 1352.10, 1192.99, 1153.50, 1117.54, 1080.20, 1028.59, 1012.04, 967.26, 833.75, 716.45, 663.83, 642.62, 610.42, 567.72, 466.99

HR-MS (ES+): calcd for C₁₃H₁₇N₂O [M] 217.1341, obsd: 217.1337

HR-MS (ES-): calcd for CNS [M] 57.9751, obsd: 57.9752

Water content (ppm): 466.9

6.25 Synthesis of 3-benzyl-1-(2-methoxyethyl)-1*H*-imidazolium tetrafluoroborate (9e)

Following the procedure for **6c** with compound **9a** (4.33 g, 14.7 mmol) and sodium tetrafluoroborate (1.76 g, 16.0 mmol) in acetone (30 mL), resulted in 69% yield (2.11 g, 6.94 mmol) of a brown viscous liquid.

¹H-NMR (400 MHz, DMSO): δ (ppm): 9.29 (s, 1H, N⁺=CH-N), 7.80 (t, 1H, J = 1.7 Hz, N⁺-CH=CH), 7.76 (t, 1H, J = 1.7 Hz, CH=CH-N), 7.44-7.37 (m, 5H, CH_{Ar}), 5.46 (s, 2H, CH_{Ar}-CH₂-N⁺), 4.38 (t, 2H, J = 4.9 Hz, N-CH₂-CH₂), 3.70 (t, 2H, J = 5.0 Hz, CH₂-CH₂-O), 3.26 (s, 3H, O-CH₃)

¹³C-NMR (400 MHz, DMSO): δ (ppm): 136.5 (N⁺=CH-N), 134.9 (CH_{Ar}-C_q-CH_{Ar}), 129.1 (CH_{Ar}), 128.8 (CH_{Ar}), 128.3 (CH_{Ar}), 123.2 (CH=CH-N), 122.4 (N⁺-CH=CH), 69.5 (CH₂-CH₂-O), 58.1 (O-CH₃), 52.0 (CH_{Ar}-CH₂-N⁺), 48.9 (N-CH₂-CH₂)

¹⁹F-NMR (400 MHz, DMSO): -148.1, -148.2

IR (thin film, cm¹): 3150.08, 3112.79, 2932.26, 2834.61, 1666.54, 1562.11, 1498.17, 1454.82, 1389.46, 1355.61, 1285.22, 1193.41, 1157.43, 1050.61, 834.46, 753.62, 717.65, 665.23, 645.32, 611.53, 571.19, 521.10, 462.48

HR-MS (ES+): calcd for C₁₃H₁₇N₂O [M] 217.1341, obsd: 217.1338

HR-MS (ES-): calcd for BF₄ [M] 87.0029, obsd: 87.0027

Water content (ppm): 419.3

6.26 Synthesis of 3-benzyl-1-(2-(2-methoxyethoxy)ethyl)-1*H*-imidazolium bromide (10a)

Following the procedure for compound **6a** with compound **4** (7.42 g, 43.6 mmol) and benzyl bromide (7.46 g, 43.6 mmol), resulted in 95% yield (14.1 g, 41.1 mmol) of compound **10a** as a brown viscous liquid.

¹H-NMR (600 MHz, DMSO): δ (ppm): 9.62 (s, 1H, N⁺=CH-N), 7.99 (s, 1H, N⁺-CH=CH), 7.91 (s, 1H, J = 1.1 Hz, CH=CH-N), 7.51 (d, 2H, J = 6.9, CH_{Ar}) 7.39-7.34 (m, 3H, CH_{Ar}), 5.59 (s, 2H, CH_{Ar}-CH₂-N⁺), 4.44 (t, 2H, J = 5.0 Hz, N-CH₂-CH₂), 3.78 (t, 2H, J = 5.0 Hz, CH₂-CH₂-O), 3.53-3.51 (m, 2H, O-CH₂-CH₂), 3.36-3.34 (m, 2H, CH₂-CH₂-O 3.14 (s, 3H, O-CH₃)

6.27 Synthesis of 3-benzyl-1-(2-(2-methoxyethoxy)ethyl)-1*H*-imidazolium bis(trifluoromethylsulfonyl)imide (10b)

Following the procedure for compound **6b** with compound **10a** (2.38 g, 6.96 mmol) and bis(trifluoromethane)sulfonimide lithium salt (2.00 g, 6.96 mmol) in water (20 mL), resulted in 82% yield (3.09 g, 5.71 mmol) of **10b** as a brown liquid.

¹H-NMR (400 MHz, DMSO): δ (ppm): 9.26 (s, 1H, N⁺=CH-N), 7.80 (s, 1H, N⁺-CH=CH), 7.76 (s, 1H, CH=CH-N), 7.44-7.37 (m,

5H, CH_{Ar}), 5.46 (s, 2H, $\text{CH}_{Ar}-\text{CH}_2-\text{N}^+$), 4.38 (t, 2H, $J = 4.9$ Hz, N- CH_2-CH_2), 3.79 (t, 2H, $J = 4.9$ Hz, $\text{CH}_2-\text{CH}_2-\text{O}$), 3.57-3.54 (m, 2H, O- CH_2-CH_2), 3.42-3.39 (m, 2H, $\text{CH}_2-\text{CH}_2-\text{O}$), 3.20 (s, 3H, O- CH_3)

$^{13}\text{C-NMR}$ (400 MHz, DMSO): 137.0 ($\text{N}^+=\text{CH}-\text{N}$), 135.2 ($\text{CH}_{Ar}-\text{C}_q-$ CH_{Ar}), 129.4 (CH_{Ar}), 129.2 (CH_{Ar}), 128.6 (CH_{Ar}), 123.5 ($\text{CH}=\text{CH}-\text{N}$), 122.8 ($\text{N}^+-\text{CH}=\text{CH}$), 71.5 ($\text{CH}_2-\text{CH}_2-\text{O}$), 69.8 (O- CH_2-CH_2), 68.8 (CH₂-CH₂), 58.4 (O-CH₃), 52.5 ($\text{C}_q-\text{CH}_2-\text{N}^+$), 49.5 (N-CH₂-CH₂)

IR (thin film, cm¹): 3148.60, 2884.11, 1597.42, 1563.14, 1499.73, 1457.33, 1348.01, 1329.58, 1226.40, 1179.54, 1132.07, 1100.48, 1051.22, 925.33, 844.79, 822.40, 788.39, 761.32, 739.46, 715.30, 696.88, 652.42, 611.97, 599.22, 568.83, 508.86, 462.24, 406.39

HR-MS (ES+): calcd for C₁₅H₂₁N₂O₂ [M] 261.1603, obsd: 261.1605

HR-MS (ES-): calcd for C₂NO₄S₂F₆ [M] 279.9173, obsd: 279.9180

Water content (ppm): 237.8

6.28 Synthesis of 3-benzyl-1-(2-(2-methoxyethoxy)ethyl)-1*H*-imidazolium dicyanamide (10c)

Following the procedure for compound **6c** with compound **10a** (2.56 g, 7.50 mmol) and sodium dicyanamide (0.73 g, 8.25 mmol) in acetone (30 mL) resulted in 68% yield (1.67 g, 5.10 mmol) of IL **10c** as a dark red liquid.

$^1\text{H-NMR}$ (400 MHz, DMSO): δ (ppm): 9.38 (s, 1H, $\text{N}^+=\text{CH}-\text{N}$),

7.87 (s, 1H, N⁺-CH=CH), 7.81 (s, 1H, CH=CH-N), 7.46-7.37 (m, 5H, CH_{Ar}), 5.50 (s, 2H, CH_{Ar}-CH₂-N⁺), 4.39 (t, 2H, J = 4.9 Hz, N-CH₂-CH₂), 3.78 (t, 2H, J = 5.0 Hz, CH₂-CH₂-O), 3.54-3.52 (m, 2H, O-CH₂-CH₂), 3.39-3.37 (m, 2H, CH₂-CH₂-O), 3.17 (s, 3H, O-CH₃)

¹³C-NMR (400 MHz, DMSO): 137.0 (N⁺=CH-N), 135.4 (CH_{Ar}-C_q-CH_{Ar}), 129.4 (CH_{Ar}), 129.2 (CH_{Ar}), 128.8 (CH_{Ar}), 123.6 (CH=CH-N), 122.8 (N⁺-CH=CH), 119.6 (NC-N⁻), 71.5 (CH₂-CH₂-O), 69.8 (O-CH₂-CH₂), 68.4 (CH₂-CH₂), 58.5 (O-CH₃), 52.3 (C_q-CH₂-N⁺), 49.4 (N-CH₂-CH₂)

IR (thin film, cm¹): 3133.76, 3061.18, 2876.54, 2226.43, 2190.08, 2128.00, 1559.44, 1496.72, 1453.90, 1351.80, 1304.66, 1197.94, 1154.66, 1099.66, 1027.72, 903.45, 846.37, 821.56, 717.75, 664.82, 644.86, 611.09, 569.70, 523.33, 462.40

HR-MS (ES+): calcd for C₁₅H₂₁N₂O₂ [M] 261.1603, obsd: 261.1599

HR-MS (ES-): calcd for C₂NO₄S₂F₆ [M] 66.0092, obsd: 66.0096

Water content (ppm): 433.9

6.29 Synthesis of 3-benzyl-1-(2-(2-methoxyethoxy)ethyl)-1*H*-imidazolium thiocyanate (**10d**)

Following the procedure for compound **6c** with compound **10a** (3.10 g, 9.10 mmol) and sodium thiocyanate (0.81 g, 10.0 mmol) in acetone (30 mL), resulted in 71% yield (2.06 g, 6.46 mmol) of IL **10d** as a brown

viscous liquid.

¹H-NMR (400 MHz, DMSO): δ (ppm): 9.25 (s, 1H, N⁺=CH-N), 7.81 (t, 1H, J = 1.8 Hz N⁺-CH=CH), 7.77 (t, 1H, J = 1.7 Hz, CH=CH-N), 7.43-7.38 (m, 5H, CH_{Ar}), 5.46 (s, 2H, CH_{Ar}-CH₂-N⁺), 4.37 (t, 2H, J = 4.9 Hz, N-CH₂-CH₂), 3.77 (t, 2H, J = 5.0 Hz, CH₂-CH₂-O), 3.54-3.52 (m, 2H, O-CH₂-CH₂), 3.40-3.37 (m, 2H, CH₂-CH₂-O), 3.17 (s, 3H, O-CH₃)

¹³C-NMR (400 MHz, DMSO): 137.0 (N⁺=CH-N), 135.3 (CH_{Ar}-C_q-CH_{Ar}), 130.3 (S-CN), 129.5 (CH_{Ar}), 129.2 (CH_{Ar}), 128.7 (CH_{Ar}), 123.6 (CH=CH-N), 122.8 (N⁺-CH=CH), 71.5 (CH₂-CH₂-O), 69.8 (O-CH₂-CH₂), 68.4 (CH₂-CH₂), 58.5 (O-CH₃), 52.4 (C_q-CH₂-N⁺), 49.5 (N-CH₂-CH₂)

IR (thin film, cm¹): 3134.91, 3091.21, 2923.67, 2822.93, 2050.54, 1670.79, 1604.27, 1559.71, 1496.74, 1453.71, 1351.20, 1286.67, 1245.65, 1199.32, 1153.66, 1079.50, 1026.86, 928.51, 847.80, 820.78, 750.15, 713.31, 661.65, 642.09, 609.96, 583.41, 560.11, 464.00

HR-MS (ES+): calcd for C₁₅H₂₁N₂O₂ [M] 261.1603, obsd: 261.1605

HR-MS (ES-): calcd for C₂NO₄S₂F₆ [M] 57.9751, obsd: 57.9760

Water content (ppm): 358.4

6.30 Synthesis of 3-benzyl-1-(2-(2-methoxyethoxy)ethyl)-1*H*-imidazolium tetrafluoroborate (10e)

Following the procedure for compound **6c** with compound **10a** (2.70 g, 7.92 mmol) and sodium tetrafluoroborate (0.96 g, 8.71 mmol) in acetone (30 mL), resulted in 80% yield (2.21 g, 6.34 mmol) of IL **10e** as a brown viscous liquid.

¹H-NMR (400 MHz, DMSO): δ (ppm): 9.26 (s, 1H, N⁺=CH-N), 7.81 (t, 1H, J = 1.7 Hz, N⁺-CH=CH), 7.76 (t, 1H, J = 1.7 Hz, CH=CH-N), 7.44-7.39 (m, 5H, CH_{Ar}), 5.46 (s, 2H, CH_{Ar}-CH₂-N⁺), 4.37 (t, 2H, J = 4.9 Hz, N-CH₂-CH₂), 3.78 (t, 2H, J = 5.0 Hz, CH₂-CH₂-O), 3.55-3.53 (m, 2H, O-CH₂-CH₂), 3.40-3.38 (m, 2H, CH₂-CH₂-O), 3.18 (s, 3H, O-CH₃)

¹³C-NMR (400 MHz, DMSO): 137.0 (N⁺=CH-N), 135.3 (CH_{Ar}-C_q-CH_{Ar}), 129.5 (CH_{Ar}), 129.2 (CH_{Ar}), 128.7 (CH_{Ar}), 123.6 (CH=CH-N), 122.8 (N⁺-CH=CH), 71.5 (CH₂-CH₂-O), 69.8 (O-CH₂-CH₂), 68.4 (CH₂-CH₂-O), 58.5 (O-CH₃), 52.4 (C_q-CH₂-N⁺), 49.4 (N-CH₂-CH₂)

IR (thin film, cm¹): 3378.14, 3149.96, 3111.62, 2921.23, 1669.47, 1562.32, 1498.17, 1455.18, 1383.55, 1352.06, 1285.48, 1244.55, 1198.63, 1157.32, 1053.79, 847.80, 822.85, 718.65, 665.15, 645.49, 611.66, 559.24, 521.23, 462.66

HR-MS (ES+): calcd for C₁₅H₂₁N₂O₂ [M] 261.1603, obsd: 261.1604

HR-MS (ES-): calcd for BF₄ [M] 87.0030, obsd: 87.0033

Water content (ppm): 312.7

6.31 Synthesis of 3-benzyl-1-(2-(2-methoxyethoxy)ethoxyethyl)-1*H*-imidazolium bromide (**11a**)

Following the procedure for **6a** with compound **5** (10.2 g, 47.6 mmol) and benzyl bromide (8.14 g, 47.6 mmol) in acetonitrile (50 mL) resulted in 96% yield (17.6 g, 45.7 mmol) of compound **11a** as a dark brown liquid.

¹H-NMR (400 MHz, DMSO): δ (ppm): 9.53 (s, 1H, N⁺=CH-N), 7.93 (s, 1H, N⁺-CH=CH), 7.86 (s, 1H, CH=CH-N), 7.50-7.34 (m, 5H, CH_{Ar}), 5.54 (s, 2H, CH_{Ar}-CH₂-N⁺), 4.41 (t, 2H, J = 4.8 Hz, N-CH₂-CH₂), 3.78 (t, 2H, J = 4.9 Hz, CH₂-CH₂-O), 3.54-3.36 (m, 8H, O-CH₂-CH₂), 3.20 (s, 3H, O-CH₃)

6.32 Synthesis of 3-benzyl-1-(2-(2-methoxyethoxy)ethoxyethyl)-1*H*-imidazolium bis(trifluoromethyl-sulfonyl)imide (**11b**)

Following the procedure for **6b** with compound **11a** (2.52 g, 6.54 mmol) and bis(trifluoromethane)sulfonimide lithium salt (1.88 g, 6.54 mmol), resulted in 77% yield (2.95 g, 5.04 mmol) of IL **11b** as a brown liquid.

¹H-NMR (400 MHz, DMSO): δ (ppm): 9.25 (s, 1H, N⁺=CH-N), 7.79 (t, 2H, J = 1.7 Hz, N⁺-CH=CH), 7.77 (t, 1H, J = 1.7 Hz, CH=CH-N),

7.44-7.39 (m, 5H, CH_{Ar}), 5.46 (s, 2H, $\text{CH}_{Ar}-\text{CH}_2-\text{N}^+$), 4.39 (t, 2H, $J = 4.8$ Hz, N- CH_2-CH_2), 3.80 (t, 2H, $J = 4.9$ Hz, $\text{CH}_2-\text{CH}_2-\text{O}$), 3.58-3.41 (m, 8H, O- CH_2-CH_2), 3.23 (s, 3H, O- CH_3)

$^{13}\text{C-NMR}$ (400 MHz, DMSO): 137.0 ($\text{N}^+=\text{CH}-\text{N}$), 135.2 ($\text{CH}_{Ar}-\text{C}_q-\text{CH}_{Ar}$), 129.4 (CH_{Ar}), 129.2 (CH_{Ar}), 128.6 (CH_{Ar}), 123.6 ($\text{CH}=\text{CH}-\text{N}$), 122.7, ($\text{N}^+-\text{CH}=\text{CH}$), 124.8, 121.6, 118.4, 115.2 (CF_3-SO_2) 71.7 ($\text{CH}_2-\text{CH}_2-\text{O}$), 70.0 ($\text{CH}_2-\text{CH}_2-\text{O}$) 69.9 (O- CH_2-CH_2), 68.5 ($\text{CH}_2-\text{CH}_2-\text{O}$), 58.4 (O- CH_3), 52.4 ($\text{C}_q-\text{CH}_2-\text{N}^+$), 49.4 (N- CH_2-CH_2)

IR (thin film, cm^{-1}): 3147.15, 3113.35, 2880.90, 1562.31, 1498.89, 1456.59, 1348.26, 1330.11, 1226.31, 1179.43, 1132.06, 1051.90, 932.20, 849.37, 822.47, 788.28, 761.43, 739.15, 715.84, 651.94, 611.84, 599.42, 568.83, 509.33, 462.11, 405.99

HR-MS (ES+): calcd for $\text{C}_{17}\text{H}_{25}\text{N}_2\text{O}_3$ [M] 305.1865, obsd: 305.1861

HR-MS (ES-): calcd for $\text{C}_2\text{NO}_4\text{S}_2\text{F}_6$ [M] 279.9173, obsd: 279.9172

Water content (ppm): 273.9 pm

6.33 Synthesis of 3-benzyl-1-(2-(2-(2-methoxyethoxy)ethoxy)ethyl)-1*H*-imidazolium dicyanamide (11c)

Following the procedure for **6c** with compound **11a** (3.42 g, 8.88 mmol) and sodium dicyanamide (0.87 g, 9.76 mmol) in acetone (30 mL), resulted in 75% yield (2.47 g, 6.67 mmol) of IL **11c** as a dark red liquid.

$^1\text{H-NMR}$ (400 MHz, DMSO): δ (ppm): 9.35 (s, 1H, $\text{N}^+=\text{CH}-\text{N}$),

7.86-7.81 (m, 2H, N⁺-CH=CH), 7.44-7.40 (m, 5H, CH_{Ar}), 5.48 (s, 2H, CH_{Ar}-CH₂-N⁺), 4.38 (s, 2H, N-CH₂-CH₂), 3.78 (s, CH₂-CH₂-O), 3.54-3.39 (m, 8H, O-CH₂-CH₂), 3.22-3.19 (m, 3H, O-CH₃)

¹³C-NMR (400 MHz, DMSO): 136.9 (N⁺=CH-N), 135.4 (CH_{Ar}-C_q-CH_{Ar}), 129.5 (CH_{Ar}), 129.2 (CH_{Ar}), 128.7 (CH_{Ar}), 123.6 (CH=CH-N), 122.7 (N⁺-CH=CH), 119.6 (NC-N⁻), 71.7 (CH₂-CH₂-O), 70.0 (CH₂-CH₂-O), 69.9 (O-CH₂-CH₂), 68.5 (CH₂-CH₂-O), 58.4 (O-CH₃), 52.4 (C_q-CH₂-N⁺), 49.4 (N-CH₂-CH₂)

IR (thin film, cm¹): 3135.14, 3064.84, 2874.83, 2226.29, 2189.97, 2127.18, 1669.85, 1560.51, 1497.12, 1454.39, 1350.92, 1302.71, 1248.99, 1198.78, 1090.24, 1027.68, 930.29, 848.62, 822.42, 715.87, 664.14, 644.00, 610.72, 568.37, 522.37, 461.48

HR-MS (ES+): calcd for C₁₇H₂₅N₂O₃ [M] 305.1863, obsd: 305.1865

HR-MS (ES-): calcd for C₂N₃ [M] 66.0092, obsd: 66.0092

Water content (ppm): 400.3 pm

6.34 Synthesis of 3-benzyl-1-(2-(2-(2-methoxyethoxy)ethoxy)ethyl)-1*H*-imidazolium thiocyanate (**11d**)

Following the procedure for **6c** with compound **11a** (3.68 g, 9.56 mmol) and sodium thiocyanate (0.85 g, 10.5mmol) in acetone (30 mL), resulted in 62% yield (2.15 g, 5.92 mmol) of IL **11d** as a brown viscous liquid.

¹H-NMR (400 MHz, DMSO): δ (ppm): 9.24 (s, 1H, N⁺=CH-N), 7.80 (t, 2H, J = 1.7 Hz, N⁺-CH=CH), 7.77 (t, 1H, J = 1.7 Hz, CH=CH-N), 7.42-7.38 (m, 5H, CH_{Ar}), 5.45 (s, 2H, CH_{Ar}-CH₂-N⁺), 4.37 (t, 2H, J = 4.9 Hz, N-CH₂-CH₂), 3.78 (t, 2H, J = 4.9 Hz, CH₂-CH₂-O), 3.55-3.44 (m, 8H, O-CH₂-CH₂), 3.40 (s, 3H, O-CH₃)

¹³C-NMR (400 MHz, DMSO): 136.9 (N⁺=CH-N), 135.3 (CH_{Ar}-C_q-CH_{Ar}), 130.3 (S-CN), 129.5 (CH_{Ar}), 129.2 (CH_{Ar}), 128.7 (CH_{Ar}), 123.7 (CH=CH-N), 122.7 (N⁺-CH=CH), 71.7 (CH₂-CH₂-O), 70.0 (CH₂-CH₂-O), 69.9 (O-CH₂-CH₂), 68.5 (CH₂-CH₂-O), 58.5 (O-CH₃), 52.4 (C_q-CH₂-N⁺), 49.4 (N-CH₂-CH₂)

IR (thin film, cm¹): 3421.27, 3134.14, 3088.79, 2915.66, 2823.94, 2051.36, 1669.03, 1559.64, 1496.90, 1454.25, 1349.11, 1295.08, 1246.75, 1199.92, 1153.36, 1078.09, 1025.43, 929.62, 852.48, 821.68, 751.07, 715.44, 663.45, 642.12, 610.09, 569.21, 539.66, 507.68, 465.49

HR-MS (ES+): calcd for C₁₇H₂₅N₂O₃ [M] 305.1864, obsd: 305.1865

HR-MS (ES-): calcd for C₂N₃ [M] 57.9751, obsd: 57.9753

Water content (ppm): 342.2

6.35 Synthesis of 3-benzyl-1-(2-(2-(2-methoxyethoxy)ethoxy)ethyl)-1*H*-imidazolium tetrafluoroborate (11e)

Following the procedure for **6b** with compound **11a** (2.73 g, 7.09 mmol) and sodium tetrafluoroborate (0.86 g, 7.80 mmol) in acetone (30 mL),

resulted in 60% yield (1.67 g, 4.25 mmol) of IL **11e** as a brown liquid.

¹H-NMR (400 MHz, DMSO): δ (ppm): 9.23 (s, 1H, N⁺=CH-N), 7.80 (s, 2H, J = 1.7 Hz, N⁺-CH=CH), 7.77 (t, 1H, J = 1.7 Hz, CH=CH-N), 7.43-7.39 (m, 5H, CH_{Ar}), 5.45 (s, 2H, CH_{Ar}-CH₂-N⁺), 4.37 (t, 2H, J = 4.8 Hz, N-CH₂-CH₂), 3.78 (t, 2H, J = 4.9 Hz, CH₂-CH₂-O), 3.56-3.39 (m, 8H, O-CH₂-CH₂), 3.22 (s, 3H, O-CH₃)

IR (thin film, cm¹): 3149.64, 3112.00, 2878.97, 1672.49, 1562.69, 1498.56, 1455.76, 1351.67, 1285.73, 1249.05, 1199.29, 1048.45, 1029.56, 932.76, 849.00, 823.02, 761.07, 716.49, 664.77, 645.09, 611.50, 520.23, 461.81, 408.83

Due to time restriction and technical problems, a full characterization of IL **11e** could not be performed.

6.36 Synthesis of 1-(2-methoxyethyl)-1*H*-benzoimidazole (**12**)

Following the procedure for **3** with benzimidazole (10.5 g, 88.9 mmol), 2-chloroethyl methyl ether (8.40 g, 88.9 mmol) and NaOH (7.11 g, 177.8 mmol) in acetonitrile (60 mL), resulted in 97% yield (15.2 g, 86.2 mmol) of compound **12** as a yellow liquid.

¹H-NMR (400 MHz, CDCl₃): 7.90 (s, 1H, N-CH-N), 7.79-7.77 (m, 1H, CH_{Ar}), 7.36-7.32 (m, 1H, CH_{Ar}), 7.27-7.22 (m, 2H, CH_{Ar}), 4.17 (t, 2H, J = 5.2 Hz, N-CH₂-CH₂), 3.58 (t, 2H, J = 5.2 Hz, CH₂-CH₂-O), 3.21 (s, 3H, O-CH₃)

6.37 1-(2-(2-methoxyethoxy)ethyl)- 1*H*-benzoimidazole(13)

Following the procedure for **3** with benzimidazole (13.8 g, 117 mmol), compound **1** (16.2 g, 117 mmol) and NaOH (9.33 g, 233 mmol) in acetonitrile (100 mL), resulted in 94% yield (24.2 g, 110 mmol) of compound **13** as a yellow liquid.

¹H-NMR (600 MHz, DMSO): 8.22 (s, 1H, N-CH-N), 7.71 (d, 1H, J = 8.1 Hz, CH_{Ar}), 7.62 (d, 1H, J = 7.8 Hz, CH_{Ar}), 7.28-7.21 (m, 2H, CH_{Ar}), 4.40 (t, 2H, J = 5.3 Hz, N-CH₂-CH₂), 3.76 (t, 2H, J = 5.3 Hz, CH₂-CH₂-O), 3.50-3.48 (m, 2H, O-CH₂-CH₂), 3.37-3.35 (m, 2H, CH₂-CH₂-O), 3.18 (s, 3H, O-CH₃)

6.38 Synthesis of 1-(2-(2-(2-methoxyethoxy)ethoxy)ethyl)-1*H*-benzoimidazole (14)

Following the procedure for **3** with benzimidazole (11.1 g, 94.0 mmol), compound **2** (17.2 g, 94.0 mmol) and NaOH (7.52 g, 188 mmol) in acetonitrile (100 mL), resulted in 90% yield (22.4 g, 84.6 mmol) of compound **13** as a yellow liquid.

¹H-NMR (400 MHz, DMSO): 8.20 (s, 1H, N-CH-N), 7.69-7.67 (m, 1H, CH_{Ar}), 7.62-7.61 (m, 1H, CH_{Ar}), 7.27-7.19 (m, 2H, CH_{Ar}), 4.41 (t, 2H, J = 5.2 Hz, N-CH₂-CH₂), 3.76 (t, 2H, J = 5.2 Hz, CH₂-CH₂-O), 3.51-3.49 (m, 2H, O-CH₂-CH₂), 3.45-3.41 (m, 4H, CH₂-CH₂-O),

3.37-3.36 (m, 2H, CH₂-CH₂-O), 3.21 (s, 3H, O-CH₃)

6.39 Synthesis of 3-allyl-1-(2-methoxyethyl)-1*H*-benzoimidazolium bromide (**15a**)

Following the procedure for **6a** with compound **12** (11.4 g, 64.8 mmol) and allyl bromide (7.84 g, 64.8 mmol) in acetonitrile (60 mL), resulted in 96% yield (18.5 g, 62.2 mmol) of compound **15a** as a light brown solid.

¹H-NMR (400 MHz, DMSO): δ (ppm): 9.82 (s, 1H, N⁺=CH-N), 8.13-8.11 (m, 1H, CH_{Ar}), 8.02-7.99 (m, 1H, CH_{Ar}), 7.72-7.67 (m, 2H, CH_{Ar}), 6.17-6.07 (m, 1H, CH₂=CH-CH₂), 5.40-5.36 (m, 2H, CH₂=CH), 5.23 (d, 2H, J = 4.9 Hz, CH-CH₂-N⁺), 4.73 (t, 2H, J = 4.9 Hz, N-CH₂-CH₂), 3.80 (t, 2H, J = 4.9 Hz, CH₂-CH₂-O), 3.27 (s, 3H, O-CH₃)

6.40 Synthesis of 3-allyl-1-(2-methoxyethyl)-1*H*-benzoimidazolium bis(trifluoromethylsulfonyl)imide (**15b**)

Following the procedure for **6b** with compound **15a** (2.76 g, 12.7 mmol) and bis(trifluoromethane)sulfonimide lithium salt (3.65 g, 12.7 mmol) in water (30 mL), resulted in 85% yield (3.93 g, 7.89 mmol) of IL **15b** as a light brown liquid.

¹H-NMR (400 MHz, DMSO): δ (ppm): 9.77 (s, 1H, N⁺=CH-N), 8.11-8.09 (m, 1H, CH_{Ar}), 8.00-7.98 (m, 1H, CH_{Ar}), 7.72-7.66 (m, 2H,

CH_{Ar}), 6.18-6.08 (m, 1H, $\text{CH}_2=\text{CH-CH}_2$), 5.43-5.38 (m, 2H, $\text{CH}_2=\text{CH}$), 5.23 (d, 2H, $J = 8.7$ Hz, $\text{CH-CH}_2-\text{N}^+$), 4.74 (t, 2H, $J = 4.9$ Hz, $\text{N-CH}_2-\text{CH}_2$), 3.82 (t, 2H, $J = 4.9$ Hz, $\text{CH}_2-\text{CH}_2-\text{O}$), 3.39 (s, 3H, O-CH_3)

$^1\text{C-NMR}$ (400 MHz, DMSO): 143.1 ($\text{N}^+=\text{CH-N}$), 131.9 ($\text{CH}_{Ar}-\text{C}_q-\text{N}$), 131.4 ($\text{CH}_2=\text{CH-CH}_2$), 131.3 ($\text{CH}_{Ar}-\text{C}_q-\text{N}^+$), 127.0 (CH_{Ar}), 124.8, 121.6, 118.4, 115.2 (CF_3-SO_2), 121.0 ($\text{CH}_2=\text{CH}$), 114.4 (CH_{Ar}), 114.2 (CH_{Ar}), 69.5 ($\text{CH}_2-\text{CH}_2-\text{O}$), 58.6 (O-CH_3), 49.3 ($\text{CH-CH}_2-\text{N}^+$), 47.1 ($\text{N-CH}_2-\text{CH}_2$)

IR (thin film, cm^{-1}): 3146.51, 3083.58, 2935.08, 1729.84, 1647.43, 1612.33, 1565.76, 1483.39, 1452.07, 1426.10, 1346.46, 1329.23, 1225.75, 1182.42, 1133.61, 1054.54, 993.25, 947.58, 840.51, 788.60, 749.86, 701.64, 653.88, 616.25, 570.96, 513.73, 423.99, 408.49

HR-MS (ES+): calcd for $\text{C}_{13}\text{H}_{17}\text{N}_2\text{O}$ [M] 217.1341, obsd: 217.1337

HR-MS (ES-): calcd for $\text{C}_2\text{NO}_4\text{F}_6\text{S}_2$ [M] 279.9173, obsd: 279.9174

Water content (ppm): 170.7

6.41 Synthesis of 3-allyl-1-(2-methoxyethyl)-1*H*-benzoimidazolium dicyanamide (15c)

Following the procedure for **6c** with compound **15a** (3.47 g, 11.7 mmol) and sodium dicyanamide (1.14 g, 12.8 mmol) in acetone (30 mL), resulted in 70% yield (2.32 g, 8.17 mmol) of IL **15c** as a brown solid.

$^1\text{H-NMR}$ (600 MHz, DMSO): δ (ppm): 9.78 (s, 1H, $\text{N}^+=\text{CH-N}$), 8.12-8.10 (m, 1H, CH_{Ar}), 8.00-7.99 (m, 1H, CH_{Ar}), 7.72-7.67 (m, 2H,

CH_{Ar}), 6.15-6.08 (m, 1H, $\text{CH}_2=\text{CH-CH}_2$), 5.41-5.37 (m, 2H, $\text{CH}_2=\text{CH}$), 5.22 (d, 2H, $J = 5.8$ Hz, $\text{CH-CH}_2-\text{N}^+$), 4.73 (t, 2H, $J = 5.0$ Hz, $\text{N-CH}_2-\text{CH}_2$), 3.81 (t, 2H, $J = 5.0$ Hz, $\text{CH}_2-\text{CH}_2-\text{O}$), 3.27 (s, 3H, O-CH_3)

$^1\text{C-NMR}$ (600 MHz, DMSO): 143.1 ($\text{N}^+=\text{CH-N}$), 131.9 ($\text{CH}_{Ar}-\text{C}_q-\text{N}$), 131.5 ($\text{CH}_2=\text{CH-CH}_2$), 131.3 ($\text{CH}_{Ar}-\text{C}_q-\text{N}^+$), 127.0 (CH_{Ar}), 120.8 ($\text{CH}_2=\text{CH}$), 119.6 (NC-N^-), 114.5 (CH_{Ar}), 114.3 (CH_{Ar}), 69.5 ($\text{CH}_2-\text{CH}_2-\text{O}$), 58.7 (O-CH_3), 49.3 ($\text{CH-CH}_2-\text{N}^+$), 47.1 ($\text{N-CH}_2-\text{CH}_2$)

IR (thin film, cm^{-1}): 3483.63, 3130.63, 3064.25, 2941.03, 2895.68, 2836.29, 2237.65, 2224.85, 2189.57, 2126.53, 1643.19, 1614.94, 1558.52, 1483.32, 1444.47, 1425.45, 1368.39, 1312.79, 1301.79, 1290.63, 1208.56, 1191.23, 1110.41, 1083.26, 1028.35, 1011.57, 990.55, 974.72, 943.53, 903.72, 884.10, 835.02, 754.41, 705.76, 664.32, 632.48, 591.64, 556.69, 522.77, 440.83, 424.17

HR-MS (ES+): calcd for $\text{C}_{13}\text{H}_{17}\text{N}_2\text{O}$ [M] 217.1341, obsd: 217.1337

HR-MS (ES-): calcd for C_2N_3 [M] 66.0092, obsd: 66.0096

Water content (ppm): 370.5

6.42 Synthesis of 3-allyl-1-(2-methoxyethyl)-1*H*-benzoimidazolium thiocyanate (**15d**)

Following the procedure for **6c** with compound **15a** (3.69 g, 12.4 mmol) and sodium thiocyanate (1.11 g, 13.7 mmol) in acetone (30 mL), resulted in 65% yield (2.22 g, 8.07 mmol) of IL **15d** as a brown solid.

$^1\text{H-NMR}$ (600 MHz, DMSO): δ (ppm): 9.75 (s, 1H, $\text{N}^+=\text{CH-N}$),

8.11-8.10 (m, 1H, CH_{Ar}), 8.00-7.99 (m, 1H, CH_{Ar}), 7.72-7.67 (m, 2H, CH_{Ar}), 6.15-6.09 (m, 1H, $\text{CH}_2=\text{CH-CH}_2$), 5.41-5.37 (m, 2H, $\text{CH}_2=\text{CH}$), 5.22 (d, 2H, $J = 5.8$ Hz, $\text{CH-CH}_2-\text{N}^+$), 4.73 (t, 2H, $J = 5.0$ Hz, N- CH_2-CH_2), 3.81 (t, 2H, $J = 5.0$ Hz, $\text{CH}_2-\text{CH}_2-\text{O}$), 3.27 (s, 3H, O- CH_3)

$^1\text{C-NMR}$ (600 MHz, DMSO): 143.1 ($\text{N}^+=\text{CH-N}$), 131.9 ($\text{CH}_{Ar}-\text{C}_q-\text{N}$), 131.5 ($\text{CH}_2=\text{CH-CH}_2$), 131.3 ($\text{CH}_{Ar}-\text{C}_q-\text{N}^+$), 130.1 (S-CN), 127.1 (CH_{Ar}), 120.8 ($\text{CH}_2=\text{CH}$), 114.5 (CH_{Ar}), 114.3 (CH_{Ar}), 69.5 ($\text{CH}_2-\text{CH}_2-\text{O}$), 58.7 (O- CH_3), 49.3 ($\text{CH-CH}_2-\text{N}^+$), 47.1 (N- CH_2-CH_2)

IR (thin film, cm^{-1}): 3453.45, 3135.95, 3063.52, 3024.75, 2988.06, 2893.46, 2814.67, 2050.07, 1644.59, 1615.04, 1560.53, 1485.72, 1444.97, 1426.39, 1389.31, 1369.13, 1351.14, 1287.34, 1205.95, 1191.17, 1164.87, 1114.14, 1080.61, 1030.49, 1012.36, 986.38, 943.56, 869.76, 839.70, 783.34, 755.48, 704.26, 630.63, 618.00, 586.54, 556.08, 512.08, 467.97, 424.44

HR-MS (ES+): calcd for $\text{C}_{13}\text{H}_{17}\text{N}_2\text{O}$ [M] 217.1341, obsd: 217.1337

HR-MS (ES-): calcd for CNS [M] 57.9751, obsd: 57.9760

Water content (ppm): 521.4

6.43 Synthesis of 3-allyl-1-(2-methoxyethyl)-1*H*-benzoimidazolium tetrafluoroborate (15e)

Following the procedure for **6c** with compound **15a** (3.12 g, 10.5 mmol) and sodium tetrafluoroborate (127 g, 11.5 mmol) in acetone (30 mL) resulted in 78% yield (2.49 g, 8.19 mmol) of IL **15e** as a brown solid.

$^1\text{H-NMR}$ (400 MHz, DMSO): δ (ppm): 9.73 (s, 1H, $\text{N}^+=\text{CH-N}$),

8.11-8.10 (m, 1H, CH_{Ar}), 8.00-7.98 (m, 1H, CH_{Ar}), 7.72-7.67 (m, 2H, CH_{Ar}), 6.16-6.07 (m, 1H, $\text{CH}_2=\text{CH-CH}_2$), 5.41-5.35 (m, 2H, $\text{CH}_2=\text{CH}$), 5.21 (d, 2H, $J = 5.8$ Hz, $\text{CH-CH}_2-\text{N}^+$), 4.71 (t, 2H, $J = 4.9$ Hz, N- CH_2-CH_2), 3.80 (t, 2H, $J = 5.0$ Hz, $\text{CH}_2-\text{CH}_2-\text{O}$), 3.27 (s, 3H, O- CH_3)

$^1\text{C-NMR}$ (400 MHz, DMSO): 143.1 ($\text{N}^+=\text{CH-N}$), 131.8 ($\text{CH}_{Ar}-\text{C}_q-\text{N}$), 131.5 ($\text{CH}_2=\text{CH-CH}_2$), 131.3 ($\text{CH}_{Ar}-\text{C}_q-\text{N}^+$), 127.1 (CH_{Ar}), 120.8 ($\text{CH}_2=\text{CH}$), 114.5 (CH_{Ar}), 114.3 (CH_{Ar}), 69.5 ($\text{CH}_2-\text{CH}_2-\text{O}$), 58.7 (O- CH_3), 49.3 ($\text{CH-CH}_2-\text{N}^+$), 47.1 (N- CH_2-CH_2)

IR (thin film, cm^{-1}): 3376.70, 3155.61, 3097.04, 2989.68, 2947.80, 2831.72, 1661.84, 1620.77, 1562.05, 1484.31, 1449.64, 1424.51, 1391.92, 1368.94, 1352.87, 1290.71, 1203.16, 1167.33, 1093.56, 1046.54, 1034.94, 978.08, 940.88, 869.99, 850.13, 834.19, 783.56, 753.11, 704.57, 633.51, 592.66, 556.37, 520.22, 483.58, 444.37, 421.81

HR-MS (ES+): calcd for $\text{C}_{13}\text{H}_{17}\text{N}_2\text{O}$ [M] 217.1341, obsd: 217.1337

HR-MS (ES-): calcd for BF_4^- [M] 86.0065, obsd: 86.0061

Water content (ppm): 385.7

6.44 Synthesis of 3-allyl-1-(2-(2-methoxyethoxy)-ethyl)-1*H*-benzoimidazolium bromide (16a)

Following the procedure for **6a** with compound **13** (12.7 g, 57.9 mmol) and allyl bromide (7.00 g, 57.9 mmol) in acetonitrile (50 mL), resulted in 94% yield (18.6 g, 54.4 mmol) of a brown viscous liquid.

$^1\text{H-NMR}$ (600 MHz, DMSO): δ (ppm): 10.0 (s, 1H, $\text{N}^+=\text{CH-N}$),

8.18-8.15 (m, 1H, CH_{Ar}), 8.05-8.03 (m, 1H, CH_{Ar}), 7.67-7.64 (m, 2H, CH_{Ar}), 6.15-6.09 (m, 1H, $\text{CH}_2=\text{CH-CH}_2$), 5.43-5.35 (m, 2H, $\text{CH}_2=\text{CH}$), 5.31 (d, 2H, $J = 5.8$ Hz, $\text{CH-CH}_2-\text{N}^+$), 4.78 (t, 2H, $J = 4.9$ Hz, $\text{N-CH}_2-\text{CH}_2$), 3.90 (t, 2H, $J = 5.0$ Hz, $\text{CH}_2-\text{CH}_2-\text{O}$), 3.55-3.53 (m, 2H, $\text{O-CH}_2\text{CH}_2$), 3.34-3.33 (m, 2H, $\text{CH}_2-\text{CH}_2-\text{O}$), 3.09 (s, 3H, O-CH_3)

6.45 Synthesis of 3-allyl-1-(2-(2-methoxyethoxy)-ethyl)-1*H*benzoimidazolium bis(trifluoromethylsulfonyl)imide (**16b**)

Following the procedure for **6b** with compound **16a** (2.51 g, 11.4 mmol) and bis(trifluoromethane)sulfonimide lithium salt (3.28 g, 11.4 mmol) in water (30 mL), resulted in 81% yield (5.00 g, 9.24 mmol) of IL **16b** as a light brown liquid.

¹H-NMR (600 MHz, DMSO): δ (ppm): 9.72 (s, 1H, $\text{N}^+=\text{CH-N}$), 8.12-8.10 (m, 1H, CH_{Ar}), 7.99-7.98 (m, 1H, CH_{Ar}), 7.71-7.67 (m, 2H, CH_{Ar}), 6.16-6.10 (m, 1H, $\text{CH}_2=\text{CH-CH}_2$), 5.43-5.39 (m, 2H, $\text{CH}_2=\text{CH}$), 5.22 (d, 2H, $J = 5.8$ Hz, $\text{CH-CH}_2-\text{N}^+$), 4.73 (t, 2H, $J = 5.0$ Hz, $\text{N-CH}_2-\text{CH}_2$), 3.91 (t, 2H, $J = 5.0$ Hz, $\text{CH}_2-\text{CH}_2-\text{O}$), 3.57-3.56 (m, 2H, $\text{O-CH}_2\text{CH}_2$), 3.38-3.37 (m, 2H, $\text{CH}_2-\text{CH}_2-\text{O}$), 3.14 (s, 3H, O-CH_3)

¹³C-NMR (600 MHz, DMSO): δ (ppm): 143.2 ($\text{N}^+=\text{CH-N}$), 143.1 ($\text{CH}_{Ar}-\text{C}_q-\text{N}^+$), 131.8 ($\text{CH}_{Ar}-\text{C}_q-(\text{CH}_{Ar})$), 131.3 ($\text{CH}_2=\text{CH-CH}_2$), 127.0 (CH_{Ar}), 123.2, 121.1, 118.9, 116.8 ($\text{CF}_3\text{-SO}_2$), 120.7 ($\text{CH}_2=\text{CH}$), 114.4 (CH_{Ar}), 114.1 (CH_{Ar}), 71.5 ($\text{CH}_2-\text{CH}_2-\text{O}$), 69.9 ($\text{CH}_2-\text{CH}_2-\text{O}$), 67.9 ($\text{O-CH}_2-\text{CH}_2$), 58.4 (O-CH_3), 49.2 ($\text{CH-CH}_2-\text{N}^+$), 47.3 ($\text{N-CH}_2-\text{CH}_2$)

IR (thin film, cm¹): 3147.51, 3083.84, 2884.18, 2833.47, 1612.99, 1566.04, 1483.89, 1453.37, 1347.18, 1329.29, 1225.90, 1178.55, 1131.05, 1051.45, 992.07, 945.87, 846.20, 788.04, 748.58, 700.64, 653.36, 612.89, 599.45, 568.77, 509.08, 423.31, 406.71

HR-MS (ES+): calcd for C₁₅H₂₁N₂O₂ [M] 261.1603, obsd: 261.1598

HR-MS (ES-): calcd for C₂NO₄F₆S₂ [M] 279.9173, obsd: 279.9173

Water content (ppm): 191.1

6.46 Synthesis of 3-allyl-1-(2-(2-methoxyethoxy)-ethyl)-1*H*-benzoimidazolium dicyanamide (16c)

Following the procedure for **6c** with compound **16a** (3.96 g, 18.0 mmol) and sodium dicyanamide (1.76 g, 19.8 mmol) in acetone (30 mL), resulted in 50% yield (2.96 g, 9.04 mmol) of IL **16c** as a brown liquid.

¹H-NMR (600 MHz, DMSO): δ (ppm): 9.80 (s, 1H, N⁺=CH-N), 8.13-8.12 (m, 1H, CH_{Ar}), 8.01-8.00 (m, 1H, CH_{Ar}), 7.70-7.67 (m, 2H, CH_{Ar}), 6.16-6.09 (m, 1H, CH₂=CH-CH₂), 5.41-5.38 (m, 2H, CH₂=CH), 5.24 (d, 2H, J = 5.8 Hz, CH-CH₂-N⁺), 4.74 (t, 2H, J = 5.0 Hz, N-CH₂-CH₂), 3.90 (t, 2H, J = 5.0 Hz, CH₂-CH₂-O), 3.56-3.54 (m, 2H, O-CH₂CH₂), 3.38-3.35 (m, 2H, CH₂-CH₂-O), 3.12 (s, 3H, O-CH₃)

¹³C-NMR (600 MHz, DMSO): δ (ppm): 143.2 (N⁺=CH-N), 131.8 (CH_{Ar}-C_q-N), 131.5 (CH_{Ar}-C_q-N⁺), 131.3 (CH₂=CH-CH₂), 127.0 (CH_{Ar}),

120.8 ($\text{CH}_2=\text{CH}$), 114.5 (CH_{Ar}), 114.2 (CH_{Ar}), 71.6 ($\text{CH}_2\text{-CH}_2\text{-O}$), 69.9 ($\text{CH}_2\text{-CH}_2\text{-O}$), 67.9 ($\text{O}\text{-CH}_2\text{-CH}_2$), 58.5 ($\text{O}\text{-CH}_3$), 49.2 ($\text{CH}\text{-CH}_2\text{-N}^+$), 47.3 ($\text{N}\text{-CH}_2\text{-CH}_2$)

IR (thin film, cm^{-1}): 3484.07, 3131.53, 3067.35, 3028.45, 2986.52, 2940.44, 2891.66, 2835.13, 2237.94, 2225.89, 2190.58, 2127.06, 1643.12, 1615.10, 1558.77, 1483.83, 1446.41, 1424.97, 1368.74, 1313.52, 1208.67, 1191.85, 1111.15, 1084.30, 1028.38, 1011.95, 990.73, 974.49, 943.62, 904.05, 882.71, 842.27, 754.14, 705.35, 664.11, 632.76, 591.69, 556.43, 522.83, 423.97

HR-MS (ES+): calcd for $\text{C}_{15}\text{H}_{21}\text{N}_2\text{O}_2$ [M] 261.1603, obsd: 261.1601

HR-MS (ES-): calcd for C_2N_3 [M] 66.0092, obsd: 66.0093

Water content (ppm): 370.5

6.47 Synthesis of 3-allyl-1-(2-(2-methoxyethoxy)-ethyl)-1*H*-benzoimidazolium thiocyanate (16d)

Following the procedure for **6b** with compound **16a** (4.23 g, 19.2 mmol) and sodium thiocyanate (1.71 g, 21.2 mmol) in acetone (30 mL), resulted in 61% yield of IL **16d** (3.74 g, 11.7 mmol) as a dark brown viscous liquid.

$^1\text{H-NMR}$ (600 MHz, DMSO): δ (ppm): 9.71 (s, 1H, $\text{N}^+=\text{CH-N}$), 8.11-8.10 (m, 1H, CH_{Ar}), 8.00-7.98 (m, 1H, CH_{Ar}), 7.70-7.66 (m, 2H, CH_{Ar}), 6.15-6.08 (m, 1H, $\text{CH}_2=\text{CH-CH}_2$), 5.40-5.37 (m, 2H, $\text{CH}_2=\text{CH}$),

5.22 (d, 2H, J = 5.8 Hz, CH-CH₂-N⁺), 4.72 (t, 2H, J = 5.0 Hz, N-CH₂-CH₂), 3.89 (t, 2H, J = 5.0 Hz, CH₂-CH₂-O), 3.55-3.53 (m, 2H, O-CH₂CH₂), 3.35-3.34 (m, 2H, CH₂-CH₂-O), 3.11 (s, 3H, O-CH₃)

¹³C-NMR (600 MHz, DMSO): δ (ppm): 143.2 (N⁺=CH-N), 131.8 (CH_{Ar}-C_q-N), 131.5 (CH_{Ar}-C_q-N⁺), 131.3 (CH₂=CH-CH₂), 130.4 (S-CN), 127.0 (CH_{Ar}), 120.8 (CH₂=CH), 114.5 (CH_{Ar}), 114.2 (CH_{Ar}), 71.6 (CH₂-CH₂-O), 69.9 (CH₂-CH₂-O), 67.9 (O-CH₂-CH₂), 58.5 (O-CH₃), 49.2 (CH-CH₂-N⁺), 47.3 (N-CH₂-CH₂)

IR (thin film, cm¹): 3414.50, 3133.10, 3033.42, 2879.98, 2819.29, 2051.98, 1727.13, 1666.85, 1644.39, 1611.02, 1561.80, 1481.10, 1447.77, 1425.61, 1351.60, 1286.25, 1244.01, 1198.41, 1084.93, 1025.64, 992.18, 944.65, 849.25, 752.84, 700.48, 626.13, 559.79, 472.58, 424.15

HR-MS (ES+): calcd for C₁₅H₂₁N₂O₂ [M] 261.1603, obsd: 261.1602

HR-MS (ES-): calcd for CNS [M] 57.9751, obsd: 57.9754

Water content (ppm): 273.4

6.48 Synthesis of 3-allyl-1-(2-(2-methoxyethoxy)-ethyl)-1*H*benzoimidazolium tetrafluoroborate (16e)

Following the procedure for **6b** with compound **16a** (3.24 g, 14.7 mmol) and sodium tetrafluoroborate (1.78 g, 16.2 mmol) in acetone (30 mL), resulted in 56% yield (3.16 g, 9.07 mmol) of IL **16e** as a brown viscous liquid.

¹H-NMR (600 MHz, DMSO): δ (ppm): 9.67 (s, 1H, N⁺=CH-N), 8.09-8.08 (m, 1H, CH_{Ar}), 7.97-7.96 (m, 1H, CH_{Ar}), 7.66-7.65 (m, 2H, CH_{Ar}), 6.16-6.10 (m, 1H, CH₂=CH-CH₂), 5.44-5.40 (m, 2H, CH₂=CH), 5.22 (d, 2H, J = 5.8 Hz, CH-CH₂-N⁺), 4.73 (t, 2H, J = 4.9 Hz, N-CH₂-CH₂), 3.92 (t, 2H, J = 4.8 Hz, CH₂-CH₂-O), 3.57-3.55 (m, 2H, O-CH₂CH₂), 3.37-3.36 (m, 2H, CH₂-CH₂-O), 3.12 (s, 3H, O-CH₃)

¹³C-NMR (600 MHz, DMSO): δ (ppm): 143.2 (N⁺=CH-N), 131.8 (CH_{Ar}-C_q-N), 131.5 (CH_{Ar}-C_q-N⁺), 131.3 (CH₂=CH-CH₂), 130.4 (S-CN), 127.0 (CH_{Ar}), 120.8 (CH₂=CH), 114.5 (CH_{Ar}), 114.2 (CH_{Ar}), 71.6 (CH₂-CH₂-O), 69.9 (CH₂-CH₂-O), 67.9 (O-CH₂-CH₂), 58.5 (O-CH₃), 49.2 (CH-CH₂-N⁺), 47.3 (N-CH₂-CH₂)

IR (thin film, cm¹): 3150.55, 3087.55, 2881.79, 1645.88, 1616.58, 1565.10, 1483.79, 1451.75, 1429.55, 1352.84, 1286.60, 1202.76, 1047.69, 1027.01, 949.42, 845.81, 751.67, 702.25, 628.28, 558.61, 520.43, 424.74

HR-MS (ES+): calcd for C₁₅H₂₁N₂O₂ [M] 261.1603, obsd: 261.1604

HR-MS (ES-): calcd for BF₄ [M] 87.0029, obsd: 87.0034

Water content (ppm): 218.19

6.49 Synthesis of 3-allyl-1-(2-(2-methoxyethoxy)-ethyl)-1*H*-benzoimidazolium bromide (**17a**)

Following the procedure for **6a** with compound **14** (16.5 g, 62.5 mmol) and allyl bromide (7.56 g, 62.5 mmol), resulted in 97% yield (20.7 g, 60.6 mmol) of compound **17a** as a brown viscous liquid.

¹H-NMR (400 MHz, DMSO): δ (ppm): 9.93 (s, 1H, N⁺=CH-N), 8.17-8.15 (m, 1H, CH_{Ar}), 8.05-8.03 (m, 1H, CH_{Ar}), 7.70-7.67 (m, 2H, CH_{Ar}), 6.18-6.08 (m, 1H, CH₂=CH-CH₂), 5.43-5.37 (m, 2H, CH₂=CH), 5.28 (d, 2H, J = 5.8 Hz, CH-CH₂-N⁺), 4.77 (t, 2H, J = 4.9 Hz, N-CH₂-CH₂), 3.91 (t, 2H, J = 4.9 Hz, CH₂-CH₂-O), 3.57-3.55 (m, 2H, O-CH₂CH₂), 3.46-3.44 (m, 2H, CH₂-CH₂-O), 3.41-3.39 (m, 2H, CH₂-CH₂-O), 3.34-3.33 (O-CH₂-CH₂), 3.18 (s, 3H, O-CH₃)

6.50 Synthesis of 3-allyl-1-(2-(2-methoxyethoxy)-ethyl)-1*H*-benzoimidazolium bis(trifluoromethylsulfonyl)imide (**17b**)

Following the procedure for **6b** with compound **17a** (3.20 g, 8.31 mmol) and bis(trifluoromethane)sulfonimide lithium salt (2.38 g, 8.31 mmol) in water (30 mL), resulted in 80% yield (3.60 g, 6.64 mmol) of IL **17b** as a brown liquid.

¹H-NMR (600 MHz, DMSO): δ (ppm): 9.74 (s, 1H, N⁺=CH-N), 8.13-8.11 (m, 1H, CH_{Ar}), 8.00-7.99 (m, 1H, CH_{Ar}), 7.77-7.68 (m, 2H, CH_{Ar}), 6.18-6.12 (m, 1H, CH₂=CH-CH₂), 5.44-5.41 (m, 2H, CH₂=CH), 5.24 (d, 2H, J = 5.8 Hz, CH-CH₂-N⁺), 4.75 (t, 2H, J = 4.9 Hz, N-CH₂-CH₂), 3.94 (t, 2H, J = 4.9 Hz, CH₂-CH₂-O), 3.61-3.50 (m, 2H, O-CH₂CH₂), 3.51-3.49 (m, 2H, CH₂-CH₂-O), 3.45-3.44 (m, 2H, CH₂-CH₂-O), 3.38-3.36 (m, 2H, CH₂-CH₂-O), 3.18 (s, 3H, O-CH₃)

¹³C-NMR (600 MHz, DMSO): δ (ppm): 143.1 (N⁺=CH-N), 131.9 (C_q), 131.3 (CH₂=CH-CH₂), 127.0 (CH_{Ar}), 123.2, 121.1, 118.9, 116.8

(CF₃-SO₂), 120.7 (CH₂=CH), 114.4 (C_HAr), 114.1 (C)H_{Ar}), 71.6 (CH₂-CH₂-O), 70.2 (O-CH₂-CH₂), 70.1 (CH₂-CH₂-O), 70.0 (O-CH₂-CH₂), 67.9 (CH₂-CH₂-O), 58.3 (O-CH₃), 49.2 (CH-CH₂-N⁺), 47.3 (N-CH₂-CH₂)

IR (thin film, cm¹): 3143.47, 3080.81, 2880.53, 1565.43, 1483.24, 1452.89, 1347.83, 1329.96, 1226.01, 1179.01, 1131.20, 1051.89, 992.58, 939.80, 850.06, 787.66, 748.98, 700.50, 653.20, 613.21, 599.70, 568.97, 509.89, 423.91, 406.15

HR-MS (ES+): calcd for C₁₇H₂₅N₂O₃ [M] 305.1865, obsd: 305.1860

HR-MS (ES-): calcd for C₂NO₄F₆S₂ [M] 279.9173, obsd: 279.9179

Water content (ppm): 98.2

6.51 Synthesis of 3-allyl-1-(2-(2-methoxyethoxy)-ethyl)-1*H*-benzoimidazolium dicyanamide (17c)

Following the procedure for **6c** with compound **17a** (3.45 g, 8.95 mmol) and sodium dicyanamide (0.88 g, 9.84 mmol) in acetone (30 mL), resulted in 57% yield (1.67 g, 5.10 mmol) of IL **17c** as a brown liquid.

¹H-NMR (600 MHz, DMSO): δ (ppm): 9.80 (s, 1H, N⁺=CH-N), 8.15-8.13 (m, 1H, CH_{Ar}), 8.02-8.01 (m, 1H, CH_{Ar}), 7.77-7.68 (m, 2H, CH_{Ar}), 6.17-6.10 (m, 1H, CH₂=CH-CH₂), 5.42-5.39 (m, 2H, CH₂=CH), 5.25 (d, 2H, J = 5.8 Hz, CH-CH₂-N⁺), 4.75 (t, 2H, J = 5.0 Hz, N-CH₂-CH₂), 3.92 (t, 2H, J = 5.0 Hz, CH₂-CH₂-O), 3.58-3.56 (m, 2H,

O-CH₂CH₂), 3.47-3.46 (m, 2H, CH₂-CH₂-O), 3.42-3.41 (m, 2H, CH₂-CH₂-O), 3.35-3.33 (m, 2H, CH₂-CH₂-O), 3.19 (s, 3H, O-CH₃)

¹³C-NMR (600 MHz, DMSO): δ (ppm): 143.2 (N⁺=CH-N), 131.8 (CH_{Ar}-C_q-N⁺), 131.5 (CH₂=CH-CH₂), 131.3 (CH_{Ar}-C_q-N) 127.0 (CH_{Ar}), 120.8 (CH₂=CH), 119.5 (CN-N⁻), 114.6 (C_HAr), 114.2 (C)H_{Ar}), 71.7 (CH₂-CH₂-O), 70.2 (O-CH₂-CH₂), 70.1 (CH₂-CH₂-O), 70.0 (O-CH₂-CH₂), 68.0 (CH₂-CH₂-O), 58.5 (O-CH₃), 49.2 (CH-CH₂-N⁺), 47.3 (N-CH₂-CH₂)

IR (thin film, cm¹): 3132.52, 2873.66, 2223.45, 2188.64, 2126.24, 1726.36, 1669.13, 1644.71, 1611.33, 1561.93, 1482.83, 1448.89, 1428.15, 1351.42, 1301.55, 1246.29, 1199.40, 1102.33, 1028.74, 994.25, 939.63, 849.84, 753.62, 701.62, 627.44, 560.73, 523.54, 425.41

HR-MS (ES+): calcd for C₁₇H₂₅N₂O₃ [M] 305.1865, obsd: 305.1862

HR-MS (ES-): calcd for C₂N₃ [M] 66.0092, obsd: 66.0093

Water content (ppm): 113.2

6.52 Synthesis of 3-allyl-1-(2-(2-methoxyethoxy)-ethyl)-1*H*-benzoimidazolium thiocyanate (**17d**)

Following the procedure for **6c** with compound **17a** (3.73 g, 9.68 mmol) and thiocyanate (0.86 g, 10.6 mmol) in acetone (30 mL), resulted in 71% yield (2.20 g, 6.87 mmol) of IL **17d** as a brown viscous liquid.

¹H-NMR (600 MHz, DMSO): δ (ppm): 9.72 (s, 1H, N⁺=CH-N), 8.13-8.11 (m, 1H, CH_{Ar}), 8.01-8.00 (m, 1H, CH_{Ar}), 7.77-7.67 (m, 2H,

CH_{Ar}), 6.17-6.10 (m, 1H, $\text{CH}_2=\text{CH-CH}_2$), 5.42-5.38 (m, 2H, $\text{CH}_2=\text{CH}$), 5.24 (d, 2H, $J = 5.9$ Hz, $\text{CH-CH}_2\text{-N}^+$), 4.74 (t, 2H, $J = 4.9$ Hz, N- $\text{CH}_2\text{-CH}_2$), 3.91 (t, 2H, $J = 5.0$ Hz, $\text{CH}_2\text{-CH}_2\text{-O}$), 3.59-3.55 (m, 2H, O- CH_2CH_2), 3.46-3.45 (m, 2H, $\text{CH}_2\text{-CH}_2\text{-O}$), 3.41-3.39 (m, 2H, $\text{CH}_2\text{-CH}_2\text{-O}$), 3.33-3.32 (m, 2H, $\text{CH}_2\text{-CH}_2\text{-O}$), 3.17 (s, 3H, O- CH_3)

$^{13}\text{C-NMR}$ (600 MHz, DMSO): δ (ppm): 143.1 ($\text{N}^+=\text{CH-N}$), 131.8 ($\text{CH}_{Ar}\text{-C}_q\text{-N}^+$), 131.5 ($\text{CH}_2=\text{CH-CH}_2$), 131.2 ($\text{CH}_{Ar}\text{-C}_q\text{-N}$), 130.4 (S-CN), 127.0 (CH_{Ar}), 120.8 ($\text{CH}_2=\text{CH}$), 114.5 (C_HAr), 114.2 (CH_{Ar}), 71.6 ($\text{CH}_2\text{-CH}_2\text{-O}$), 70.2 (O- $\text{CH}_2\text{-CH}_2$), 70.1 ($\text{CH}_2\text{-CH}_2\text{-O}$), 70.0 (O- $\text{CH}_2\text{-CH}_2$), 68.0 ($\text{CH}_2\text{-CH}_2\text{-O}$), 58.5 (O- CH_3), 49.2 ($\text{CH-CH}_2\text{-N}^+$), 47.3 (N- $\text{CH}_2\text{-CH}_2$)

IR (thin film, cm^{-1}): 3433.82, 3135.68, 3034.97, 2921.10, 2821.49, 2051.36, 1644.44, 1611.90, 1561.80, 1481.34, 1447.43, 1425.42, 1351.52, 1286.19, 1244.48, 1198.16, 1083.99, 1025.13, 991.58, 943.57, 848.45, 750.73, 626.19, 558.61, 472.05, 423.94

HR-MS (ES+): calcd for $\text{C}_{17}\text{H}_{25}\text{N}_2\text{O}_3$ [M] 305.1865, obsd: 305.1864

HR-MS (ES-): calcd for CNS [M] 57.9751, obsd: 57.9753

Water content (ppm): 198.5

6.53 Synthesis of 3-allyl-1-(2-(2-methoxyethoxy)-ethyl)-1*H*-benzoimidazolium tetrafluoroborate (**17e**)

Following the procedure for **6c** with compound **17a** (3.12 g, 8.10 mmol) and sodium tetrafluoroborate (0.98 g, 8.91 mmol) in acetone (30 mL), resulted in 65% yield (1.83 g, 5.26 mmol) of IL **17e** as a brown viscous liquid.

¹H-NMR (600 MHz, DMSO): δ (ppm): 9.70 (s, 1H, N⁺=CH-N), 8.13-8.12 (m, 1H, CH_{Ar}), 8.01-8.00 (m, 1H, CH_{Ar}), 7.77-7.70 (m, 2H, CH_{Ar}), 6.16-6.10 (m, 1H, CH₂=CH-CH₂), 5.42-5.38 (m, 2H, CH₂=CH), 5.23 (d, 2H, J = 5.8 Hz, CH-CH₂-N⁺), 4.73 (t, 2H, J = 5.0 Hz, N-CH₂-CH₂), 3.91 (t, 2H, J = 5.0 Hz, CH₂-CH₂-O), 3.58-3.56 (m, 2H, O-CH₂CH₂), 3.48-3.46 (m, 2H, CH₂-CH₂-O), 3.43-3.41 (m, 2H, CH₂-CH₂-O), 3.36-3.34 (m, 2H, CH₂-CH₂-O), 3.20 (s, 3H, O-CH₃)

¹³C-NMR (600 MHz, DMSO): δ (ppm): 143.1 (N⁺=CH-N), 131.9 (CH_{Ar}-C_q-N⁺), 131.5 (CH₂=CH-CH₂), 131.3 (CH_{Ar}-C_q-N), 127.1 (CH_{Ar}), 120.7 (CH₂=CH), 114.5 (C_HAr), 114.2 (C)H_{Ar}), 71.7 (CH₂-CH₂-O), 70.1 (O-CH₂-CH₂), 70.0 (CH₂-CH₂-O), 69.9 (O-CH₂-CH₂), 68.0 (CH₂-CH₂-O), 58.5 (O-CH₃), 49.2 (CH-CH₂-N⁺), 47.3 (N-CH₂-CH₂)

IR (thin film, cm¹): 3148.29, 3084.32, 2877.16, 1645.41, 1615.38, 1564.41, 1483.24, 1451.52, 1429.08, 1352.12, 1286.57, 1249.34, 1202.05, 1049.92, 943.38, 849.79, 754.30, 702.11, 628.29, 559.58, 520.74, 425.35

HR-MS (ES+): calcd for C₁₇H₂₅N₂O₃ [M] 305.1865, obsd: 305.1861

HR-MS (ES-): calcd for BF_4^- [M] 87.0029, obsd: 87.0034

Water content (ppm): 246.3

References

- (1) Martínez-Palou, R.; Luque, R. *Energy Environ. Sci.* **2014**, *7*, 2414–2447.
- (2) Kulkarni, P. S.; Afonso, C. A. *Green Chemistry* **2010**, *12*, 1139–1149.
- (3) Yu, F.; Liu, C.; Yuan, B.; Xie, P.; Xie, C.; Yu, S. *Fuel* **2016**, *177*, 39–45.
- (4) Bhutto, A. W.; Abro, R.; Gao, S.; Abbas, T.; Chen, X.; Yu, G. *Journal of the Taiwan Institute of Chemical Engineers* **2016**, *62*, 84–97.
- (5) Ren, Z.; Zhou, Z.; Li, M.; Zhang, F.; Wei, L.; Liu, W. *ACS Sustainable Chemistry & Engineering* **2019**, *7*, 1890–1900.
- (6) Robinson, P. R.; Dolbear, G. E. In *Practical Advances in Petroleum Processing*; Springer New York: New York, NY, 2006, pp 177–218.
- (7) Ibrahim, M. H.; Hayyan, M.; Hashim, M. A.; Hayyan, A. *Renewable and Sustainable Energy Reviews* **2017**, *76*, 1534–1549.
- (8) Abro, R.; Abdeltawab, A. A.; Al-Deyab, S. S.; Yu, G.; Qazi, A. B.; Gao, S.; Chen, X. *RSC Adv.* **2014**, *4*, 35302–35317.
- (9) Raj, J. J.; Magaret, S.; Pranesh, M.; Lethesh, K. C.; Devi, W. C.; Mutalib, M. A. *Journal of Cleaner Production* **2019**, *213*, 989–998.
- (10) Safa, M.; Mokhtarani, B.; Mortaheb, H. R. *Chemical Engineering Research and Design* **2016**, *111*, 323–331.

- (11) Wellens, S.; Thijs, B.; Binnemans, K. *Green Chemistry* **2013**, *15*, 3484.
- (12) Zhang, C.; Zhu, L.; Wang, J.; Wang, J.; Zhou, T.; Xu, Y.; Cheng, C. *Ecotoxicology and Environmental Safety* **2017**, *140*, 235–240.
- (13) Ko, N. H.; Lee, J. S.; Huh, E. S.; Lee, H.; Jung, K. D.; Kim, H. S.; Cheong, M. *Energy & Fuels* **2008**, *22*, 1687–1690.
- (14) Sintra, T. E.; Nasirpour, M.; Siopa, F.; Rosatella, A. A.; Gonçalves, F.; Coutinho, J. A.; Afonso, C. A.; Ventura, S. P. *Ecotoxicology and Environmental Safety* **2017**, *143*, 315–321.
- (15) Dharaskar, S.; Sillanpaa, M.; Tadi, K. K. *Environmental Science and Pollution Research* **2018**, *25*, 17156–17167.
- (16) Duarte, F. A.; Mello, P. D. A.; Bizzi, C. A.; Nunes, M. A. G.; Moreira, E. M.; Alencar, M. S.; Motta, H. N.; Dressler, V. L.; Flores, É. M. M. *Fuel* **2011**, *90*, 2158–2164.
- (17) Wasserscheid, P.; Welton, T. T., *Ionic Liquids in Synthesis*. Wiley-VCH: 2007, p 749.
- (18) Raj, J. J.; Magaret, S.; Pranesh, M.; Lethesh, K. C.; Devi, W. C.; Mutalib, M. A. *Separation and Purification Technology* **2018**, *196*, 115–123.
- (19) Tang, S.; Baker, G. A.; Zhao, H. *Chemical Society Reviews* **2012**, *41*, 4030.
- (20) Królikowski, M.; Lipińska, A. *Fluid Phase Equilibria* **2019**, *482*, 11–23.
- (21) Kianpour, E.; Azizian, S. *Fuel* **2014**, *137*, 36–40.
- (22) Domańska, U.; Włazło, M. *Fuel* **2014**, *134*, 114–125.

- (23) Francisco, M.; Arce, A.; Soto, A. *Fluid Phase Equilibria* **2010**, *294*, 39–48.
- (24) Ghandi, K. *Green and Sustainable Chemistry* **2014**, *04*, 44–53.
- (25) Mochizuki, Y.; Sugawara, K. *Energy & Fuels* **2008**, *22*, 3303–3307.
- (26) Wilfred, C. D.; Kiat, C. F.; Man, Z.; Bustam, M. A.; Mutalib, M. I. M.; Phak, C. Z. *Fuel Processing Technology* **2012**, *93*, 85–89.
- (27) Li, X.; Asumana, C.; Chen, X.; Yu, G.; Liu, G.; Zhao, J. *Green Chemistry* **2010**, *12*, 2030.
- (28) Ibrahim, J. J.; Gao, S.; Abdeltawab, A. A.; Al-Deyab, S. S.; Yu, L.; Yu, G.; Chen, X.; Yong, X. *Separation Science and Technology* **2015**, *50*, 1166–1174.
- (29) *Ionic Liquids in Synthesis*; Wasserscheid, P., Welton, T., Eds.; Wiley-VCH Verlag GmbH & Co. KGaA: Weinheim, FRG, 2002.
- (30) Laus, G.; Bentivoglio, G.; Schottenberger, H.; Kahlenberg, V. *Lenzinger Berichte* **2005**, *84*, 71–85.
- (31) Koel, M., *Ionic liquids in chemical analysis*; CRC Press: 2009, p 414.
- (32) Cui, G.; Wang, J.; Zhang, S. *Chem. Soc. Rev* **2016**, *45*, 4307.
- (33) Aghaie, M.; Rezaei, N.; Zendehboudi, S. *Renewable and Sustainable Energy Reviews* **2018**, *96*, 502–525.
- (34) Riisager, A.; Wasserscheid, P.; Van Hal, R.; Fehrman, R. *Journal of Catalysis* **2003**, *219*, 452–455.
- (35) Vekariya, R. L. *Journal of Molecular Liquids* **2017**, *227*, 44–60.

- (36) Hallett, J. P.; Welton, T. *Chemical Reviews* **2011**, *111*, 3508–3576.
- (37) Dong, B.; Wang, W.-J.; Pan, W.; Kang, G.-J. *Materials Chemistry and Physics* **2019**, *226*, 244–249.
- (38) Eftekhari, A.; Liu, Y.; Chen, P. *Journal of Power Sources* **2016**, *334*, 221–239.
- (39) Xing, S. H.; Dai, S.; Yang, Q.; Zhang, Z.; Sun, X.-G.; Hu, Y.-S.; Xing, H. *Chem. Soc. Rev* **2018**, *47*, 2020.
- (40) Mallakpour, S.; Dinari, M. In *Green Solvents II*; Springer Netherlands: Dordrecht, 2012, pp 1–32.
- (41) Mumford, K. A.; Mirza, N. R.; Stevens, G. W. *Energy Procedia* **2017**, *114*, 2671–2674.
- (42) Sawant, A.; Raut, D.; Darvatkar, N.; Salunkhe, M. *Green Chemistry Letters and Reviews* **2011**, *4*, 41–54.
- (43) Yuan, J.; Mecerreyes, D.; Antonietti, M. *Progress in Polymer Science* **2013**, *38*, 1009–1036.
- (44) Wickramanayake, S.; Hopkinson, D.; Myers, C.; Hong, L.; Feng, J.; Seol, Y.; Plasynski, D.; Zeh, M.; Luebke, D. *Journal of Membrane Science* **2014**, *470*, 52–59.
- (45) Greaves, T. L.; Calum, D. J. *Chemical Reviews* **2007**, *108*, 206–237.
- (46) Wilkes, J. S.; Zaworotko, M. J. *Journal of the Chemical Society, Chemical Communications* **1992**, 965–967.
- (47) Holbrey, J. D.; Seddon, K. R. *Clean Technologies and Environmental Policy* **1999**, *1*, 223–236.

- (48) McIntosh, A. J.; Griffith, J.; Gräsvik, J. *Application, Purification, and Recovery of Ionic Liquids* **2016**, 59–99.
- (49) Bösmann, A.; Datsevich, L.; Jess, A.; Lauter, A.; Schmitz, C.; Wasserscheid, P. *Chemical Communications* **2001**, 0, 2494–2495.
- (50) Chen, X.; Guan, Y.; Abdeltawab, A. A.; Al-Deyab, S. S.; Yuan, X.; Wang, C.; Yu, G. *Fuel* **2015**, 146, 6–12.
- (51) NIE, Y.; YUAN, X. *Journal of Theoretical and Computational Chemistry* **2011**, 10, 31–40.
- (52) Holbrey, J. D.; Reichert, W. M.; Nieuwenhuyzen, M.; Shepard, O.; Hardacre, C.; Rogers, R. D. *Chemical Communications* **2003**, 0, 476–477.
- (53) Otsuki, S.; Nonaka, T.; Takashima, N.; Qian, W.; Ishihara, A.; Imai, T.; Kabe, T. *Energy & Fuels* **2000**, 14, 1232–1239.
- (54) Tam, P. S.; Kittrell, J. R.; Eldridge, J. W. *Industrial & Engineering Chemistry Research* **1990**, 29, 321–324.
- (55) Brégeault, J.-M. *Dalton Trans.* **2003**, 0, 3289–3302.
- (56) Molaei Dehkordi, A.; Kiaei, Z.; Amin Sobati, M. *Fuel Processing Technology* **2008**, 90, 435–445.
- (57) Borah, D.; Baruah, M. K.; Haque, I. *Fuel* **2001**, 80, 1475–1488.
- (58) Campos-Martin, J.; Capel-Sanchez, M.; Perez-Presas, P.; Fierro, J. *Journal of Chemical Technology & Biotechnology* **2010**, 85, 879–890.
- (59) Capel-Sanchez, M.; Perez-Presas, P.; Campos-Martin, J.; Fierro, J. *Catalysis Today* **2010**, 157, 390–396.
- (60) Jiang, X.; Li, H.; Zhu, W.; He, L.; Shu, H.; Lu, J. *Fuel* **2009**, 88, 431–436.

- (61) José da Silva, M.; Faria dos Santos, L. *Journal of Applied Chemistry* **2013**, *2013*, 1–7.
- (62) Prasad, V.; Jeong, K.-E.; Chae, H.-J.; Kim, C.-U.; Jeong, S.-Y. *Catalysis Communications* **2008**, *9*, 1966–1969.
- (63) Muhammad, Y.; Shoukat, A.; Rahman, A. U.; Rashid, H. U.; Ahmad, W. *Chinese Journal of Chemical Engineering* **2018**, *26*, 593–600.
- (64) Sharipov, A. K.; Nigmatullin, V. R. *Chemistry and Technology of Fuels and Oils* **2005**, *41*, 309–312.
- (65) García-Gutiérrez, J. L.; Fuentes, G. A.; Hernández-Terán, M. E.; Murrieta, F.; Navarrete, J.; Jiménez-Cruz, F. *Applied Catalysis A: General* **2006**, *305*, 15–20.
- (66) Zhu, W.; Li, H.; Jiang, X.; Yan, Y.; Lu, J.; He, L.; Xia, J. *Green Chemistry* **2008**, *10*, 641.
- (67) Jin, W.; Tian, Y.; Wang, G.; Zeng, D.; Xu, Q.; Cui, J. *RSC Advances* **2017**, *7*, 48208–48213.
- (68) Lo, W.-H.; Yang, H.-Y.; Wei, G.-T. *Green Chemistry* **2003**, *5*, 639.
- (69) Mohebali, G.; Ball, A. S. *International Biodeterioration & Biodegradation* **2016**, *110*, 163–180.
- (70) Singh, S.; Schwan, A. *Comprehensive Biotechnology* **2011**, 257–271.
- (71) Xu, P.; Yu, B.; Li, F. L.; Cai, X. F.; Ma, C. Q. *Trends in Microbiology* **2006**, *14*, 398–405.

- (72) Díaz, E.; García, J. L. In *Handbook of Hydrocarbon and Lipid Microbiology*; Springer Berlin Heidelberg: Berlin, Heidelberg, 2010, pp 2787–2801.
- (73) Ohshiro, T.; Izumi, Y. *Bioscience, Biotechnology, and Biochemistry* **1999**, *63*, 1–9.
- (74) Oldfield, C.; Wood, N. T.; Gilbert, S. C.; Murray, F. D.; Faure, F. R. *Antonie van Leeuwenhoek* **1998**, *74*, 119–132.
- (75) Li, W.; Zhang, Y.; Wang, M. D.; Shi, Y. *FEMS Microbiology Letters* **2005**, *247*, 45–50.
- (76) Bhatia, S.; Sharma, D. K. *Journal of Industrial Microbiology & Biotechnology* **2010**, *37*, 425–429.
- (77) Solomons, T. W. G. *Organic chemistry.*, Singapore, 2014.
- (78) Reid, E. E.; Ruhoff, J. R.; Burnett, R. E. *Organic Syntheses* **1935**, *15*, 24.
- (79) Carey, F. A. *Advanced Organic Chemistry : Part B: Reactions and Synthesis.*, Boston, MA, 2007.
- (80) Chen, S.; Izgorodina, E. I. *Phys. Chem. Chem. Phys* **2017**, *19*, 17411.
- (81) Beyersdorff, T.; Schubert, T. J. S.; Welz-Biermann, U.; Pitner, W.; Abbott, A. P.; McKenzie, K. J.; Ryder, K. S. In *Electrodeposition from Ionic Liquids*; Wiley-VCH Verlag GmbH & Co. KGaA: Weinheim, Germany, 2017; Chapter 2, pp 17–53.
- (82) Gao, H.; Zeng, S.; Liu, X.; Nie, Y.; Zhang, X.; Zhang, S. *RSC Advances* **2015**, *5*, 30234–30238.
- (83) Gao, H.; Guo, C.; Xing, J.; Zhao, J.; Liu, H. *Green Chemistry* **2010**, *12*, 1220.

- (84) Ren, Z.; Wei, L.; Zhou, Z.; Zhang, F.; Liu, W. *Energy & Fuels* **2018**, *32*, 9172–9181.
- (85) Rashid, T.; Kait, C. F.; Murugesan, T. *Chinese Journal of Chemical Engineering* **2017**, *25*, 1266–1272.
- (86) Bui, T. T. L.; Nguyen, D. D.; Ho, S. V.; Nguyen, B. T.; Uong, H. T. N. *Fuel* **2017**, *191*, 54–61.
- (87) Chen, Z. J.; Xue, T.; Lee, J.-M. *RSC Advances* **2012**, *2*, 10564.
- (88) Zhang, X.; Gong, Z.; Li, J.; Lu, T. *Journal of Chemical Information and Modeling* **2015**, *55*, 2138–2153.
- (89) Li, J.; Lei, X.-J.; Tang, X.-D.; Zhang, X.-P.; Wang, Z.-Y.; Jiao, S. *Energy & Fuels* **2019**, *33*, 4079–4088.
- (90) Ahmed, O. U.; Mjalli, F. S.; Al-Wahaibi, T.; Al-Wahaibi, Y.; Alnashef, I. M. *Industrial & Engineering Chemistry Research* **2015**, *54*, 6540–6550.
- (91) Yao, T.; Yao, S.; Pan, C.; Dai, X.; Song, H. *Energy & Fuels* **2016**, *30*, 4740–4749.
- (92) Dharaskar, S. A.; Wasewar, K. L.; Varma, M. N.; Shende, D. Z.; Yoo, C. *Arabian Journal of Chemistry* **2016**, *9*, 578–587.
- (93) Moghadam, F. R.; Azizian, S.; Kianpour, E.; Yarie, M.; Bayat, M.; Zolfigol, M. A. *Chemical Engineering Journal* **2017**, *309*, 480–488.
- (94) Dharaskar, S. A.; Wasewar, K. L.; Varma, M. N.; Shende, D. Z. *Journal of Energy* **2013**, *2013*, 1–4.
- (95) Su, B.-M.; Zhang, S.; Zhang, Z. C. *The Journal of Physical Chemistry* **2004**, *108*, 19510–19517.

- (96) Kermanioryani, M.; Mutalib, M. I. A.; Kurnia, K. A.; Lethesh, K. C.; Krishnan, S.; Leveque, J.-M. *Journal of Cleaner Production* **2016**, *137*, 1149–1157.

Appendix

Contents

1	^1H-NMR spectrum of compound 1	I
2	^1H-NMR spectrum of compound 2	II
3	^1H-NMR spectrum of compound 3	III
4	Spectra of IL 6b	IV
4.1	^1H -NMR spectrum of IL 6b	IV
4.2	^{13}C -NMR spectrum of IL 6b	V
4.3	COSY-spectrum of IL 6b	VI
4.4	HSQC-spectrum of IL 6b	VII
4.5	HMBC-spectrum of IL 6b	VIII
4.6	IR-spectrum of IL 6b	IX
4.7	HR-MS positive mode spectrum of IL 6b	X
4.8	HR-MS negative mode spectrum of IL 6b	XI
5	Spectra of IL 6c	XII
5.1	^1H -NMR spectrum of IL 6c	XII
5.2	^{13}C -NMR spectrum of IL 6c	XIII
5.3	COSY-spectrum of IL 6c	XIV
5.4	HSQC-spectrum of IL 6c	XV
5.5	HMBC-spectrum of IL 6c	XVI
5.6	IR-spectrum of IL 6c	XVII
5.7	HR-MS positive mode spectrum of IL 6c	XVIII
5.8	HR-MS negative mode spectrum of IL 6c	XIX

6 Spectra of IL 6d	XX
6.1 ^1H -NMR spectrum of IL 6d	XX
6.2 ^{13}C -NMR spectrum of IL 6d	XXI
6.3 COSY-spectrum of IL 6d	XXII
6.4 HSQC-spectrum of IL 6d	XXIII
6.5 HMBC-spectrum of IL 6d	XXIV
6.6 IR-spectrum of IL 6d	XXV
6.7 HR-MS positive mode spectrum of IL 6d	XXVI
6.8 HR-MS negative mode spectrum of IL 6d	XXVII
7 Spectra of IL 6e	XXVIII
7.1 ^1H -NMR spectrum of IL 6e	XXVIII
7.2 ^{13}C -NMR spectrum of IL 6e	XXIX
7.3 ^{19}F -NMR spectrum of IL 6e	XXX
7.4 COSY-spectrum of IL 6e	XXXI
7.5 HSQC-spectrum of IL 6e	XXXII
7.6 HMBC-spectrum of IL 6e	XXXIII
7.7 IR-spectrum of IL 6e	XXXIV
7.8 HR-MS positive mode spectrum of IL 6e	XXXV
7.9 HR-MS negative mode spectrum of IL 6e	XXXVI
8 ^1H-NMR spectrum of compound 4	XXXVII
9 Spectra of IL 7b	XXXVIII
9.1 ^1H -NMR spectrum of IL 7b	XXXVIII
9.2 ^{13}C -NMR spectrum of IL 7b	XXXIX
9.3 COSY-spectrum of IL 7b	XL

9.4	HSQC-spectrum of IL 7b	XLI
9.5	HMBC-spectrum of IL 7b	XLII
9.6	IR-spectrum of IL 7b	XLIII
9.7	HR-MS positive mode spectrum of IL 7b	XLIV
9.8	HR-MS negative mode spectrum of IL 7b	XLV
10	Spectra of IL 7c	XLVI
10.1	¹ H-NMR spectrum of IL 7c	XLVI
10.2	¹³ C-NMR spectrum of IL 7c	XLVII
10.3	COSY-spectrum of IL 7c	XLVIII
10.4	HSQC-spectrum of IL 7c	XLIX
10.5	HMBC-spectrum of IL 7c	L
10.6	IR-spectrum of IL 7c	LI
10.7	HR-MS positive mode spectrum of IL 7c	LII
10.8	HR-MS negative mode spectrum of IL 7c	LIII
11	Spectra of IL 7d	LIV
11.1	¹ H-NMR spectrum of IL 7d	LIV
11.2	¹³ C-NMR spectrum of IL 7d	LV
11.3	COSY-spectrum of IL 7d	LVI
11.4	HSQC-spectrum of IL 7d	LVII
11.5	HMBC-spectrum of IL 7d	LVIII
11.6	IR-spectrum of IL 7d	LIX
11.7	HR-MS positive mode spectrum of IL 7d	LX
11.8	HR-MS negative mode spectrum of IL 7d	LXI
12	Spectra of IL 7e	LXII

12.1 ^1H -NMR spectrum of IL 7e	LXII
12.2 ^{13}C -NMR spectrum of IL 7e	LXIII
12.3 ^{19}F -NMR spectrum of IL 7e	LXIV
12.4 COSY-spectrum of IL 7e	LXV
12.5 HSQC-spectrum of IL 7e	LXVI
12.6 HMBC-spectrum of IL 7e	LXVII
12.7 IR-spectrum of IL 7e	LXVIII
12.8 HR-MS positive mode spectrum of IL 7e	LXIX
12.9 HR-MS negative mode spectrum of IL 7e	LXX
13 ^1H-NMR spectrum of compound 5	LXXI
14 Spectra of IL 8b	LXXII
14.1 ^1H -NMR spectrum of IL 8b	LXXII
14.2 ^{13}C -NMR spectrum of IL 8b	LXXIII
14.3 COSY-spectrum of IL 8b	LXXIV
14.4 HSQC-spectrum of IL 8b	LXXV
14.5 HMBC-spectrum of IL 8b	LXXVI
14.6 IR-spectrum of IL 8b	LXXVII
14.7 HR-MS positive mode spectrum of IL 8b	LXXVIII
14.8 HR-MS negative mode spectrum of IL 8b	LXXIX
15 Spectra of IL 8c	LXXX
15.1 ^1H -NMR spectrum of IL 8c	LXXX
15.2 ^{13}C -NMR spectrum of IL 8c	LXXXI
15.3 COSY-spectrum of IL 8c	LXXXII
15.4 HSQC-spectrum of IL 8c	LXXXIII

15.5	HMBC-spectrum of IL 8c	LXXXIV
15.6	IR-spectrum of IL 8c	LXXXV
15.7	HR-MS positive mode spectrum of IL 8c	LXXXVI
15.8	HR-MS negative mode spectrum of IL 8c	LXXXVII

16 Spectra of IL **8d** LXXXVIII

16.1	¹ H-NMR spectrum of IL 8d	LXXXVIII
16.2	¹³ C-NMR spectrum of IL 8d	LXXXIX
16.3	COSY-spectrum of IL 8d	XC
16.4	HSQC-spectrum of IL 8d	XCI
16.5	HMBC-spectrum of IL 8d	XCII
16.6	IR-spectrum of IL 8d	XCIII
16.7	HR-MS positive mode spectrum of IL 8d	XCIV
16.8	HR-MS negative mode spectrum of IL 8d	XCV

17 Spectra of IL **8e** XCVI

17.1	¹ H-NMR spectrum of IL 8e	XCVI
17.2	¹³ C-NMR spectrum of IL 8e	XCVII
17.3	¹⁹ F-NMR spectrum of IL 8e	XCVIII
17.4	COSY-spectrum of IL 8e	XCIX
17.5	HSQC-spectrum of IL 8e	C
17.6	HMBC-spectrum of IL 8e	CI
17.7	IR-spectrum of IL 8e	CII
17.8	HR-MS positive mode spectrum of IL 8e	CIII
17.9	HR-MS negative mode spectrum of IL 8e	CIV

18 ¹H-NMR spectrum of compound **9a** CV

19 Spectra of IL 9b	CVI
19.1 ^1H -NMR spectrum of IL 9b	CVI
19.2 ^{13}C -NMR spectrum of IL 9b	CVII
19.3 COSY-spectrum of IL 9b	CVIII
19.4 HSQC-spectrum of IL 9b	CIX
19.5 HMBC-spectrum of IL 9b	CX
19.6 IR-spectrum of IL 9b	CXI
19.7 HR-MS positive mode spectrum of IL 9b	CXII
19.8 HR-MS negative mode spectrum of IL 9b	CXIII
20 Spectra of IL 9c	CXIV
20.1 ^1H -NMR spectrum of IL 9c	CXIV
20.2 ^{13}C -NMR spectrum of IL 9c	CXV
20.3 COSY-spectrum of IL 9c	CXVI
20.4 HSQC-spectrum of IL 9c	CXVII
20.5 HMBC-spectrum of IL 9c	CXVIII
20.6 IR-spectrum of IL 9c	CXIX
20.7 HR-MS positive mode spectrum of IL 9c	CXX
20.8 HR-MS negative mode spectrum of IL 9c	CXXI
21 Spectra of IL 9d	CXXII
21.1 ^1H -NMR spectrum of IL 9d	CXXII
21.2 ^{13}C -NMR spectrum of IL 9d	CXXIII
21.3 COSY-spectrum of IL 9d	CXXIV
21.4 HSQC-spectrum of IL 9d	CXXV
21.5 HMBC-spectrum of IL 9d	CXXVI
21.6 IR-spectrum of IL 9d	CXXVII

21.7	HR-MS positive mode spectrum of IL 9d	CXXVIII
21.8	HR-MS negative mode spectrum of IL 9d	CXXIX
22	Spectra of IL 9e	CXXX
22.1	¹ H-NMR spectrum of IL 9e	CXXX
22.2	¹³ C-NMR spectrum of IL 9e	CXXXI
22.3	COSY-spectrum of IL 9e	CXXXII
22.4	HSQC-spectrum of IL 9e	CXXXIII
22.5	HMBC-spectrum of IL 9e	CXXXIV
22.6	IR-spectrum of IL 9e	CXXXV
22.7	HR-MS positive mode spectrum of IL 9e	CXXXVI
22.8	HR-MS negative mode spectrum of IL 9e	CXXXVII
23	¹H-NMR spectrum of compound 10a	CXXXVIII
24	Spectra of IL 10b	CXXXIX
24.1	¹ H-NMR spectrum of IL 10b	CXXXIX
24.2	¹³ C-NMR spectrum of IL 10b	CXL
24.3	COSY-spectrum of IL 10b	CXLI
24.4	HSQC-spectrum of IL 10b	CXLII
24.5	HMBC-spectrum of IL 10b	CXLIII
24.6	IR-spectrum of IL 10b	CXLIV
24.7	HR-MS positive mode spectrum of IL 10b	CXLV
24.8	HR-MS negative mode spectrum of IL 10b	CXLVI
25	Spectra of IL 10c	CXLVII
25.1	¹ H-NMR spectrum of IL 10c	CXLVII
25.2	¹³ C-NMR spectrum of IL 10c	CXLVIII

25.3 COSY-spectrum of IL 10c	CXLIX
25.4 HSQC-spectrum of IL 10c	CL
25.5 HMBC-spectrum of IL 10c	CLI
25.6 IR-spectrum of IL 10c	CLII
25.7 HR-MS positive mode spectrum of IL 10c	CLIII
25.8 HR-MS negative mode spectrum of IL 10c	CLIV
26 Spectra of IL 10d	CLV
26.1 ^1H -NMR spectrum of IL 10d	CLV
26.2 ^{13}C -NMR spectrum of IL 10d	CLVI
26.3 COSY-spectrum of IL 10d	CLVII
26.4 HSQC-spectrum of IL 10d	CLVIII
26.5 HMBC-spectrum of IL 10d	CLIX
26.6 IR-spectrum of IL 10d	CLX
26.7 HR-MS positive mode spectrum of IL 10d	CLXI
26.8 HR-MS negative mode spectrum of IL 10d	CLXII
27 Spectra of IL 10e	CLXIII
27.1 ^1H -NMR spectrum of IL 10e	CLXIII
27.2 ^{13}C -NMR spectrum of IL 10e	CLXIV
27.3 ^{19}F -NMR spectrum of IL 10e	CLXV
27.4 COSY-spectrum of IL 10e	CLXVI
27.5 HSQC-spectrum of IL 10e	CLXVII
27.6 HMBC-spectrum of IL 10e	CLXVIII
27.7 IR-spectrum of IL 10e	CLXIX
27.8 HR-MS positive mode spectrum of IL 10e	CLXX
27.9 HR-MS negative mode spectrum of IL 10e	CLXXI

28 ^1H-NMR spectrum of compound 11a	CLXXII
29 Spectra of IL 11b	CLXXIII
29.1 ^1H -NMR spectrum of IL 11b	CLXXIII
29.2 ^{13}C -NMR spectrum of IL 11b	CLXXIV
29.3 COSY-spectrum of IL 11b	CLXXV
29.4 HSQC-spectrum of IL 11b	CLXXVI
29.5 HMBC-spectrum of IL 11b	CLXXVII
29.6 IR-spectrum of IL 11b	CLXXVIII
29.7 HR-MS positive mode spectrum of IL 11b	CLXXIX
29.8 HR-MS negative mode spectrum of IL 11b	CLXXX
30 Spectra of IL 11c	CLXXXI
30.1 ^1H -NMR spectrum of IL 11c	CLXXXI
30.2 ^{13}C -NMR spectrum of IL 11c	CLXXXII
30.3 COSY-spectrum of IL 11c	CLXXXIII
30.4 HSQC-spectrum of IL 11c	CLXXXIV
30.5 HMBC-spectrum of IL 11c	CLXXXV
30.6 IR-spectrum of IL 11c	CLXXXVI
30.7 HR-MS positive mode spectrum of IL 11c	CLXXXVII
30.8 HR-MS negative mode spectrum of IL 11c	CLXXXVIII
31 Spectra of IL 11d	CLXXXIX
31.1 ^1H -NMR spectrum of IL 11d	CLXXXIX
31.2 ^{13}C -NMR spectrum of IL 11d	CXC
31.3 COSY-spectrum of IL 11d	CXCI
31.4 HSQC-spectrum of IL 11d	CXCII

31.5	HMBC-spectrum of IL 11d	CXCIII
31.6	IR-spectrum of IL 11d	CXCIV
31.7	HR-MS positive mode spectrum of IL 11d	CXCV
31.8	HR-MS negative mode spectrum of IL 11d	CXCVI
32	¹H-NMR spectrum of compound 12	CXCVII
33	¹H-NMR spectrum of compound 13	CXCVIII
34	¹H-NMR spectrum of compound 14	CXCIX
35	¹H-NMR spectrum of compound 15a	CC
36	Spectra of IL 15b	CCI
36.1	¹ H-NMR spectrum of IL 15b	CCI
36.2	¹³ C-NMR spectrum of IL 15b	CCII
36.3	COSY-spectrum of IL 15b	CCIII
36.4	HSQC-spectrum of IL 15b	CCIV
36.5	HMBC-spectrum of IL 15b	CCV
36.6	IR-spectrum of IL 15b	CCVI
36.7	HR-MS positive mode spectrum IL 15b	CCVII
36.8	HR-MS negative mode spectrum IL 15b	CCVIII
37	Spectra of IL 15c	CCIX
37.1	¹ H-NMR spectrum of IL 15c	CCIX
37.2	¹³ C-NMR spectrum of IL 15c	CCX
37.3	COSY-spectrum of IL 15c	CCXI
37.4	HSQC-spectrum of IL 15c	CCXII
37.5	HMBC-spectrum of IL 15c	CCXIII

37.6 IR-spectrum of IL 15c	CCXIV
37.7 HR-MS positive mode spectrum of IL 15c	CCXV
38 Spectra of IL 15d	CCXVI
38.1 ^1H -NMR spectrum of IL 15d	CCXVI
38.2 ^{13}C -NMR spectrum of IL 15d	CCXVII
38.3 COSY-spectrum of IL 15d	CCXVIII
38.4 HSQC-spectrum of IL 15d	CCXIX
38.5 HMBC-spectrum of IL 15d	CCXX
38.6 IR-spectrum of IL 15c	CCXXI
38.7 HR-MS positive mode spectrum of IL 15d	CCXXII
38.8 HR-MS negative mode spectrum of IL 15d	CCXXIII
39 Spectra of IL 15e	CCXXIV
39.1 ^1H -NMR spectrum of IL 15e	CCXXIV
39.2 ^{13}C -NMR spectrum of IL 15e	CCXXV
39.3 COSY-spectrum of IL 15e	CCXXVI
39.4 HSQC-spectrum of IL 15e	CCXXVII
39.5 HMBC-spectrum of IL 15e	CCXXVIII
39.6 IR-spectrum of IL 15c	CCXXIX
39.7 HR-MS positive mode spectrum of IL 15e	CCXXX
39.8 HR-MS negative mode spectrum of IL 15e	CCXXXI
40 ^1H-NMR spectrum of compound 16a	CCXXXII
41 Spectra of IL 16b	CCXXXIII
41.1 ^1H -NMR spectrum of IL 16b	CCXXXIII
41.2 ^{13}C -NMR spectrum of IL 16b	CCXXXIV

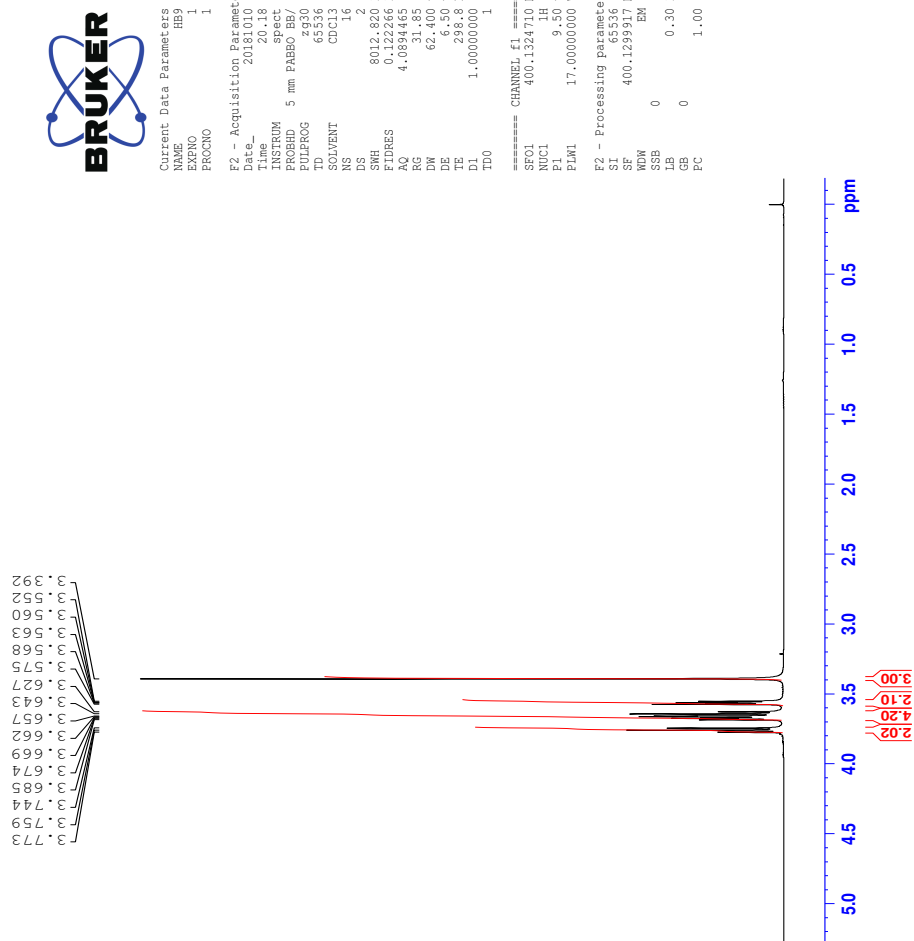
41.3 COSY-spectrum of IL 16b	CCXXXV
41.4 HSQC-spectrum of IL 16b	CCXXXVI
41.5 HMBC-spectrum of IL 16b	CCXXXVII
41.6 IR-spectrum of IL 16b	CCXXXVIII
41.7 HR-MS positive mode spectrum of IL 16b	CCXXXIX
41.8 HR-MS negative mode spectrum of IL 16b	CCXL
42 Spectra of IL 16c	CCXLI
42.1 ^1H -NMR spectrum of IL 16c	CCXLI
42.2 ^{13}C -NMR spectrum of IL 16c	CCXLII
42.3 COSY-spectrum of IL 16c	CCXLIII
42.4 HSQC-spectrum of IL 16c	CCXLIV
42.5 HMBC-spectrum of IL 16c	CCXLV
42.6 IR-spectrum of IL 16c	CCXLVI
42.7 HR-MS positive mode spectrum of IL 16c	CCXLVII
42.8 HR-MS negative mode spectrum of IL 16c	CCXLVIII
43 Spectra of IL 16d	CCXLIX
43.1 ^1H -NMR spectrum of IL 16d	CCXLIX
43.2 ^{13}C -NMR spectrum of IL 16d	CCL
43.3 COSY-spectrum of IL 16d	CCLI
43.4 HSQC-spectrum of IL 16d	CCLII
43.5 HMBC-spectrum of IL 16d	CCLIII
43.6 IR-spectrum of IL 16d	CCLIV
43.7 HR-MS positive mode spectrum of IL 16d	CCLV
43.8 HR-MS negative mode spectrum of IL 16d	CCLVI

44 Spectra of IL 16e	CCLVII
44.1 ^1H -NMR spectrum of IL 16e	CCLVII
44.2 ^{13}C -NMR spectrum of IL 16e	CCLVIII
44.3 COSY-spectrum of IL 16e	CCLIX
44.4 HSQC-spectrum of IL 16e	CCLX
44.5 HMBC-spectrum of IL 16e	CCLXI
44.6 ^{19}F -NMR of IL 16e	CCLXII
44.7 IR-spectrum of IL 16e	CCLXIII
44.8 HR-MS positive mode spectrum of IL 16e	CCLXIV
44.9 HR-MS negative mode spectrum of IL 16e	CCLXV
45 ^1H-NMR spectrum of compound 17a	CCLXVI
46 Spectra of IL 17b	CCLXVII
46.1 ^1H -NMR spectrum of IL 17b	CCLXVII
46.2 ^{13}C -NMR spectrum of IL 17b	CCLXVIII
46.3 COSY-spectrum of IL 17b	CCLXIX
46.4 HSQC-spectrum of IL 17b	CCLXX
46.5 HMBC-spectrum of IL 17b	CCLXXI
46.6 IR-spectrum of IL 17b	CCLXXII
46.7 HR-MS positive mode spectrum of IL 17b	CCLXXIII
46.8 HR-MS negative mode spectrum of IL 17b	CCLXXIV
47 Spectra of IL 17c	CCLXXV
47.1 ^1H -NMR spectrum of IL 17c	CCLXXV
47.2 ^{13}C -NMR spectrum of IL 17c	CCLXXVI
47.3 COSY-spectrum of IL 17c	CCLXXVII

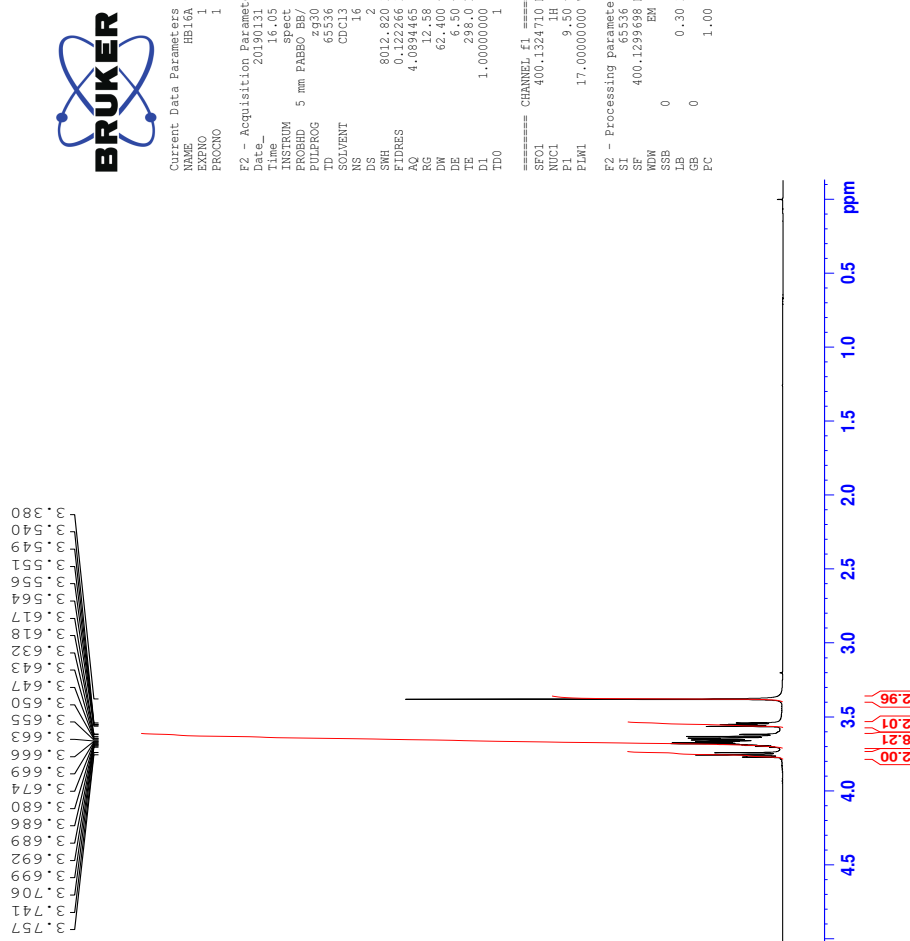
47.4	HSQC-spectrum of IL 17c	CCLXXVIII
47.5	HMBC-spectrum of IL 17c	CCLXXIX
47.6	IR-spectrum of IL 17c	CCLXXX
47.7	HR-MS positive mode spectrum of IL 17c	CCLXXXI
47.8	HR-MS negative mode spectrum of IL 17c	CCLXXXII
48	Spectra of IL 17d	CCLXXXIII
48.1	^1H -NMR spectrum of IL 17d	CCLXXXIII
48.2	^{13}C -NMR spectrum of IL 17d	CCLXXXIV
48.3	COSY-spectrum of IL 17d	CCLXXXV
48.4	HSQC-spectrum of IL 17d	CCLXXXVI
48.5	HMBC-spectrum of IL 17d	CCLXXXVII
48.6	IR-spectrum of IL 17d	CCLXXXVIII
48.7	HR-MS positive mode spectrum of IL 17d	CCLXXXIX
48.8	HR-MS negative mode spectrum of IL 17d	CCXC
49	Spectra of IL 17e	CCXCI
49.1	^1H -NMR spectrum of IL 17e	CCXCI
49.2	^{13}C -NMR spectrum of IL 17e	CCXCII
49.3	COSY-spectrum of IL 17e	CCXCIII
49.4	HSQC-spectrum of IL 17e	CCXCIV
49.5	HMBC-spectrum of IL 17e	CCXCV
49.6	IR-spectrum of IL 17e	CCXCVI
49.7	HR-MS positive mode spectrum of IL 17e	CCXCVII
49.8	HR-MS negative mode spectrum of IL 17e	CCXCVIII
50	HPLC-data	CCXCIX

50.1 HPLC-data for ILs 6-8	CCXCIX
50.2 HPLC-data for optimization studies of IL 8c	CCC
50.3 HPLC-data for ILs 9-11	CCCII
50.4 HPLC-data for ILs 15-17	CCCIII

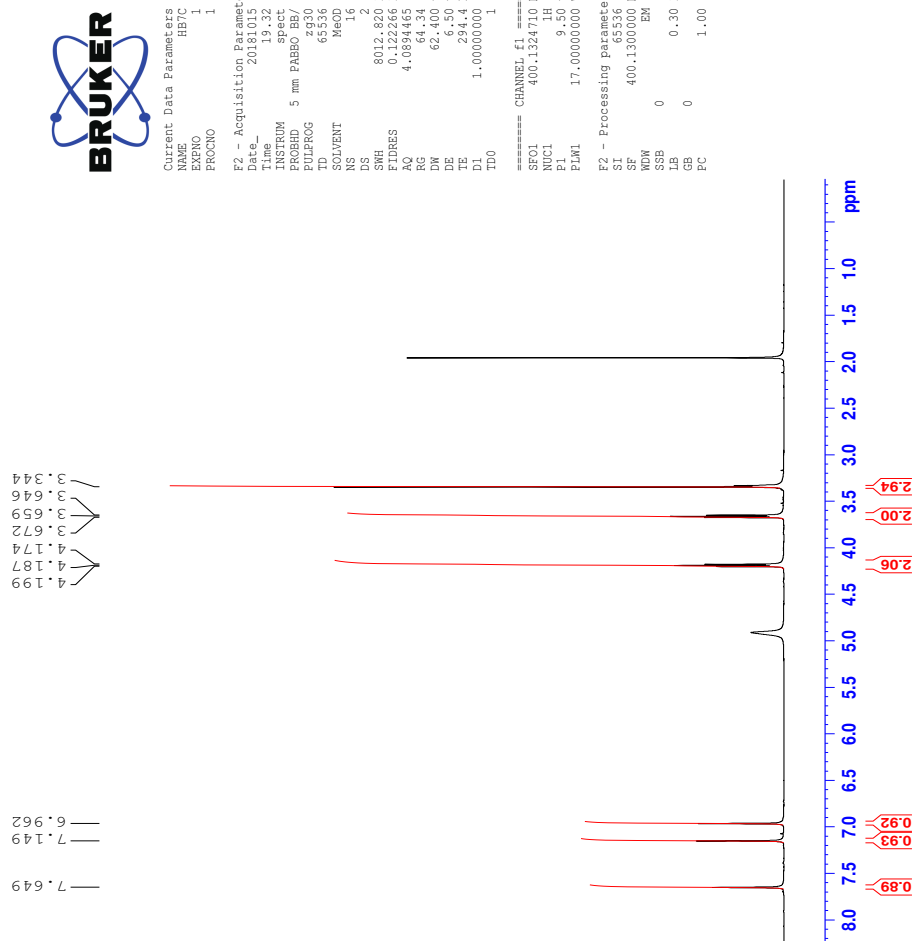
1 ^1H -NMR spectrum of compound 1



2 ^1H -NMR spectrum of compound 2



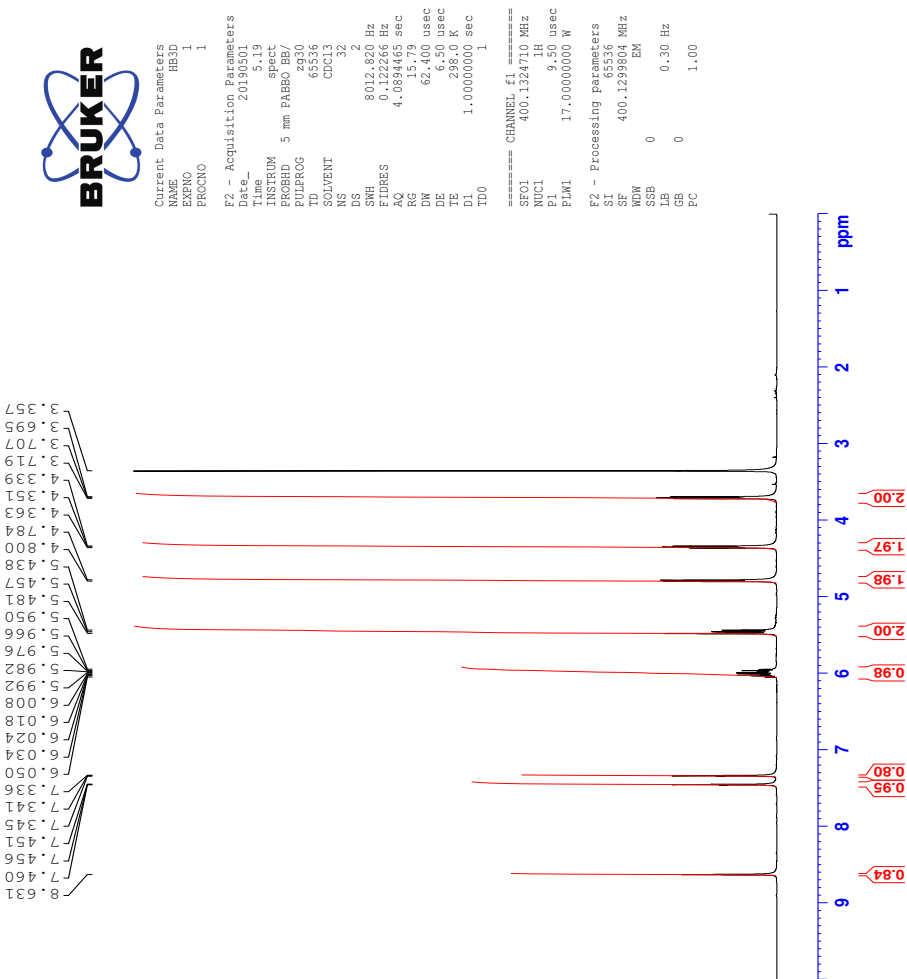
3 $^1\text{H-NMR}$ spectrum of compound 3



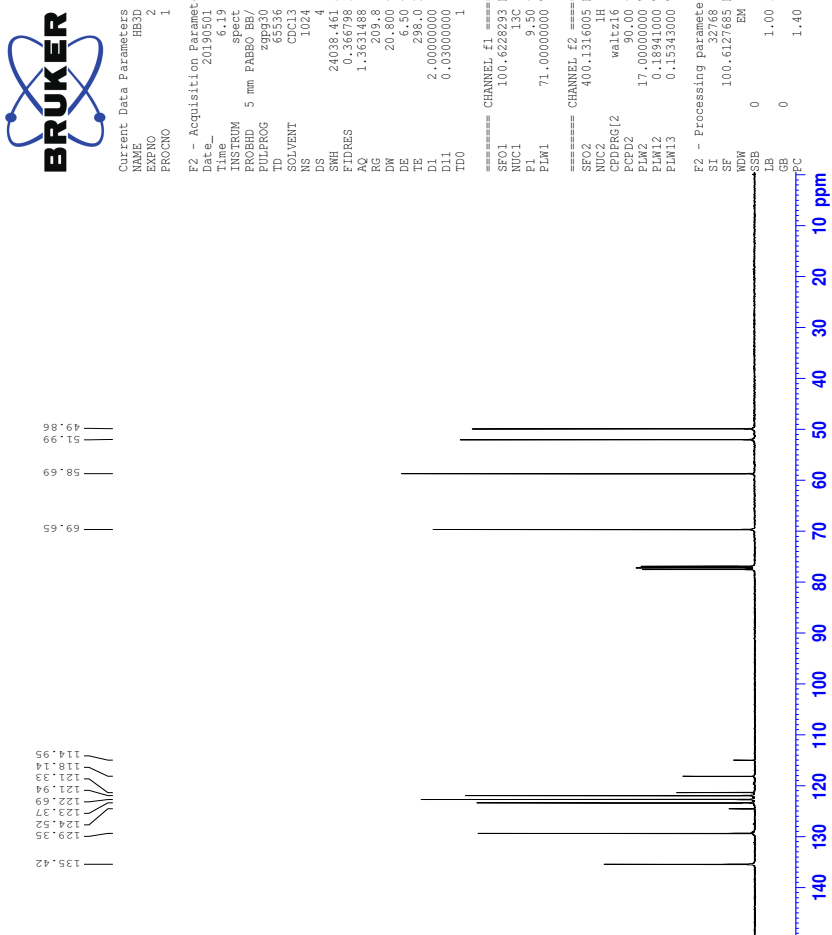
III

4 Spectra of IL 6b

4.1 ^1H -NMR spectrum of IL 6b

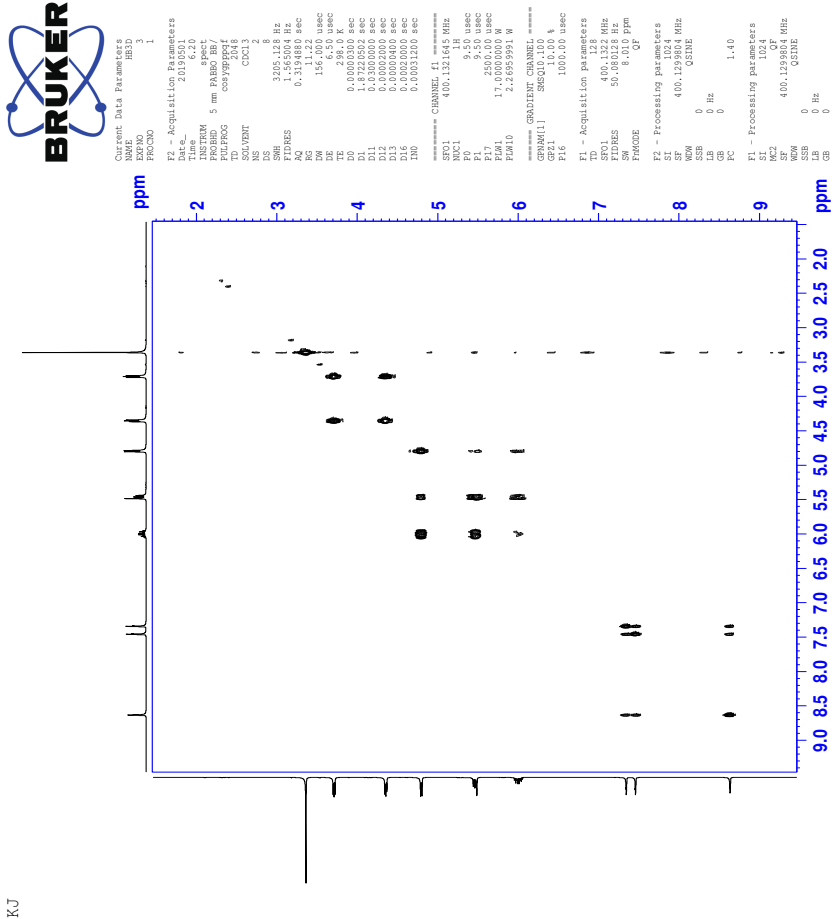


4.2 ^{13}C -NMR spectrum of IL 6b



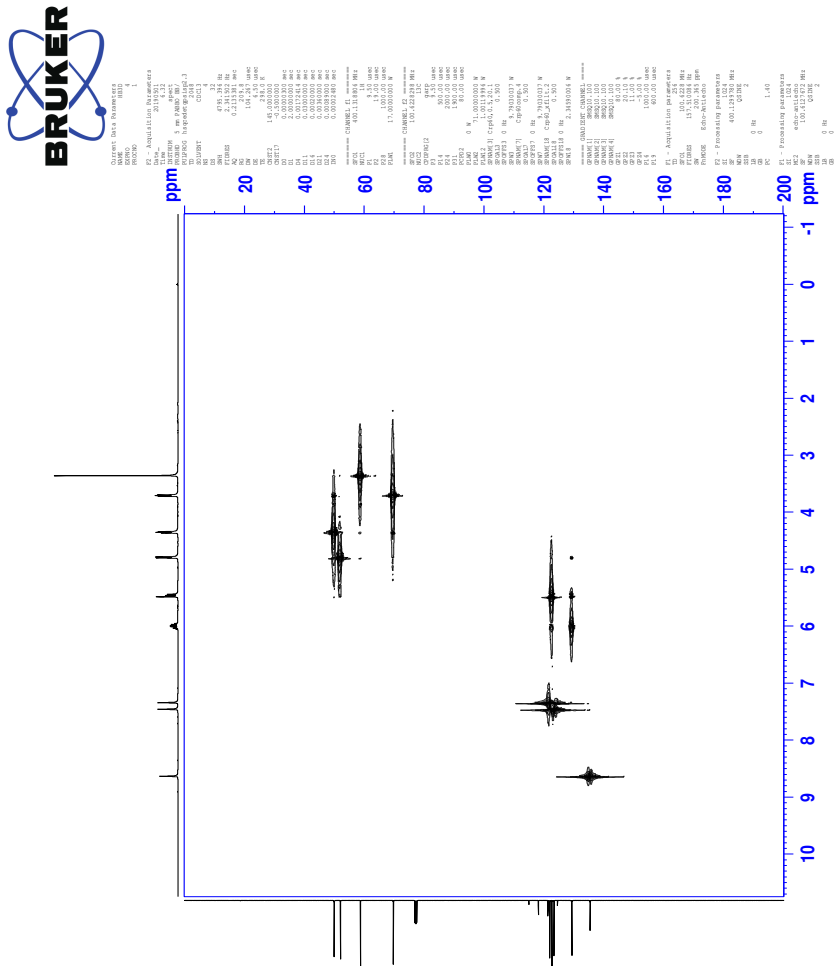
V

4.3 COSY-spectrum of IL 6b



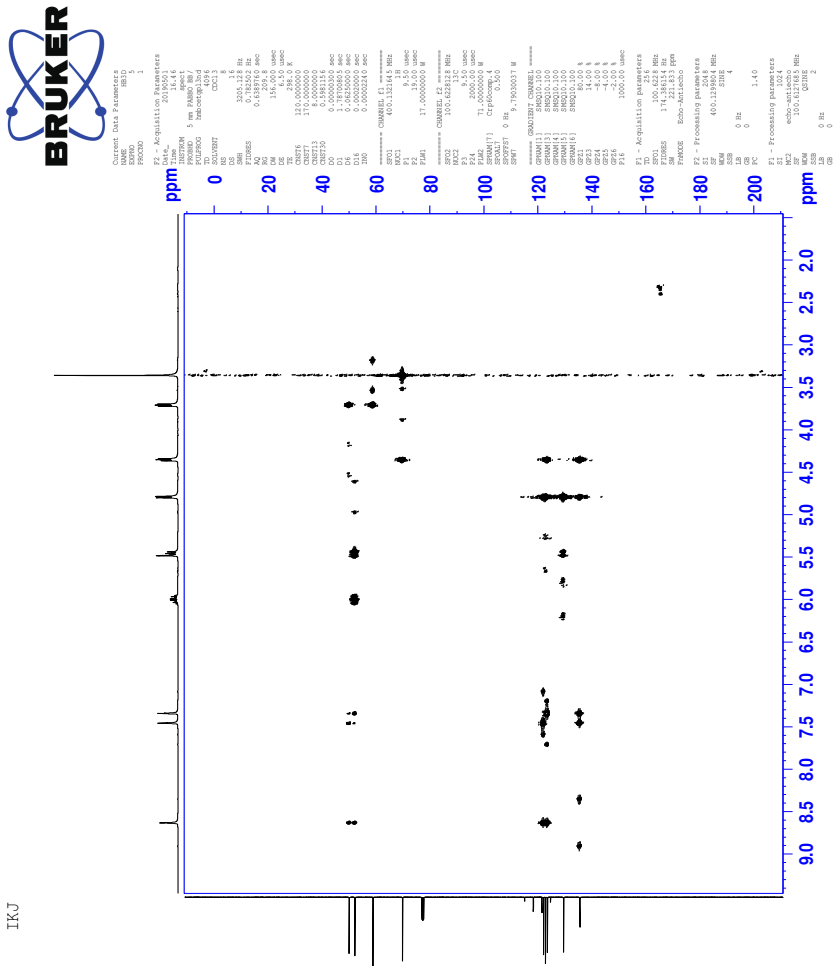
TKJ

4.4 HSQC-spectrum of IL 6b

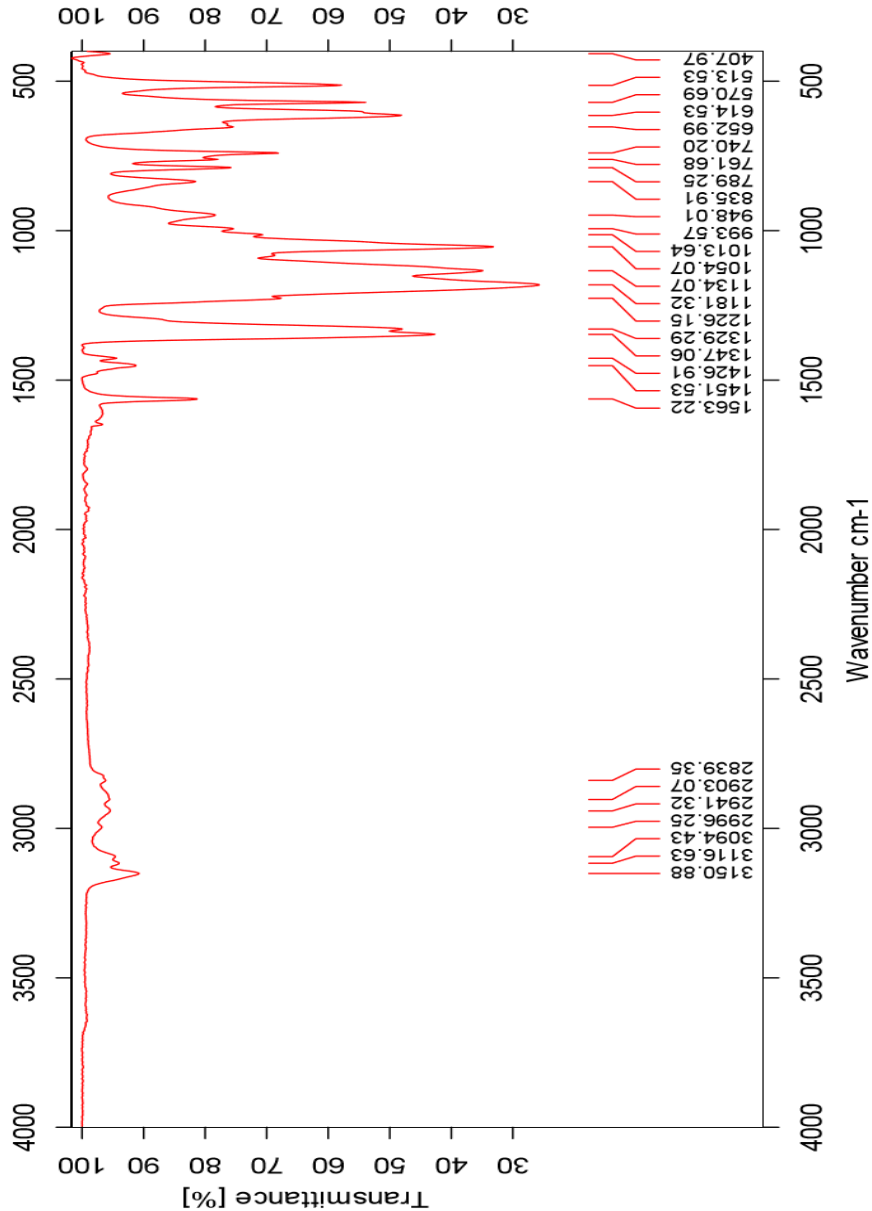


4.5 HMBC-spectrum of IL 6b

TKJ



4.6 IR-spectrum of IL 6b



4.7 HR-MS positive mode spectrum of IL 6b

Elemental Composition Report

Page 1

Single Mass Analysis

Tolerance = 2.0 PPM / DBE: min = -50.0, max = 50.0

Element prediction: Off

Number of isotope peaks used for i-FIT = 3

Monoisotopic Mass, Even Electron Ions

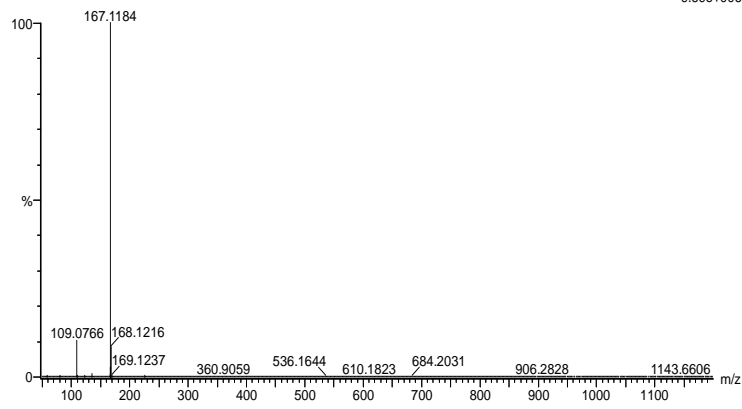
328 formula(e) evaluated with 1 results within limits (all results (up to 1000) for each mass)

Elements Used:

C: 0-100 H: 0-150 N: 0-5 O: 0-10 Au: 0-3

2019-416_RERUN 30 (0.568) AM2 (Ar,35000.0,0.00,0.00); Cr (30:36)
1: TOF MS ES+

9.69e+006



Minimum: -50.0
Maximum: 5.0 2.0 50.0

Mass	Calc. Mass	mDa	PPM	DBE	i-FIT	Norm	Conf (%)	Formula
167.1184	167.1184	0.0	0.0	3.5	2222.2	n/a	n/a	C9 H15 N2 O

4.8 HR-MS negative mode spectrum of IL 6b

Elemental Composition Report

Page 1

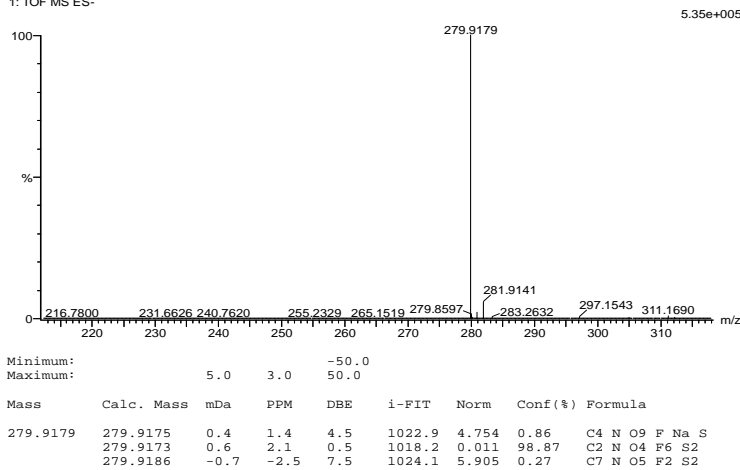
Single Mass Analysis

Tolerance = 3.0 PPM / DBE: min = -50.0, max = 50.0
Element prediction: Off
Number of isotope peaks used for i-FIT = 3

Monoisotopic Mass, Even Electron Ions
604 formula(e) evaluated with 3 results within limits (all results (up to 1000) for each mass)

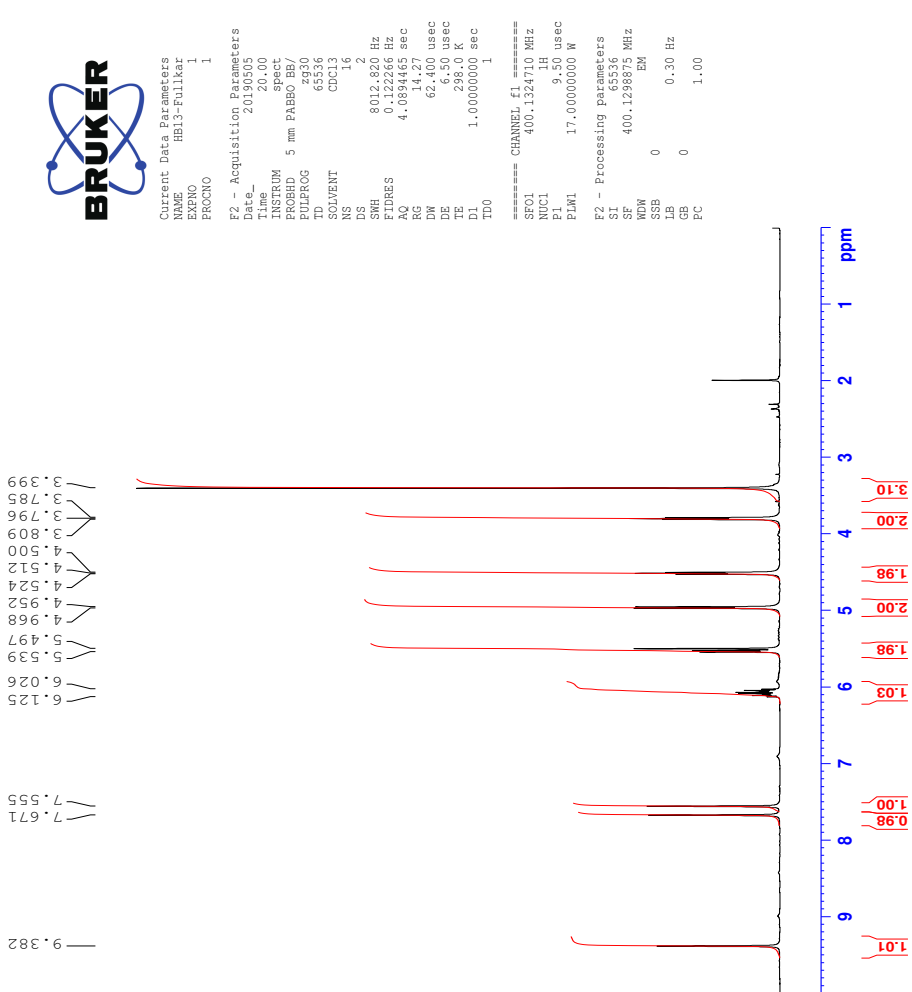
Elements Used:

C: 0-100 N: 0-10 O: 0-10 F: 0-6 Na: 0-1 S: 0-3
2019-417neg.20 (0.237) AM2 (Ar,35000.0,0.00,0.00); Cm (18:20)
1: TOF MS ES-

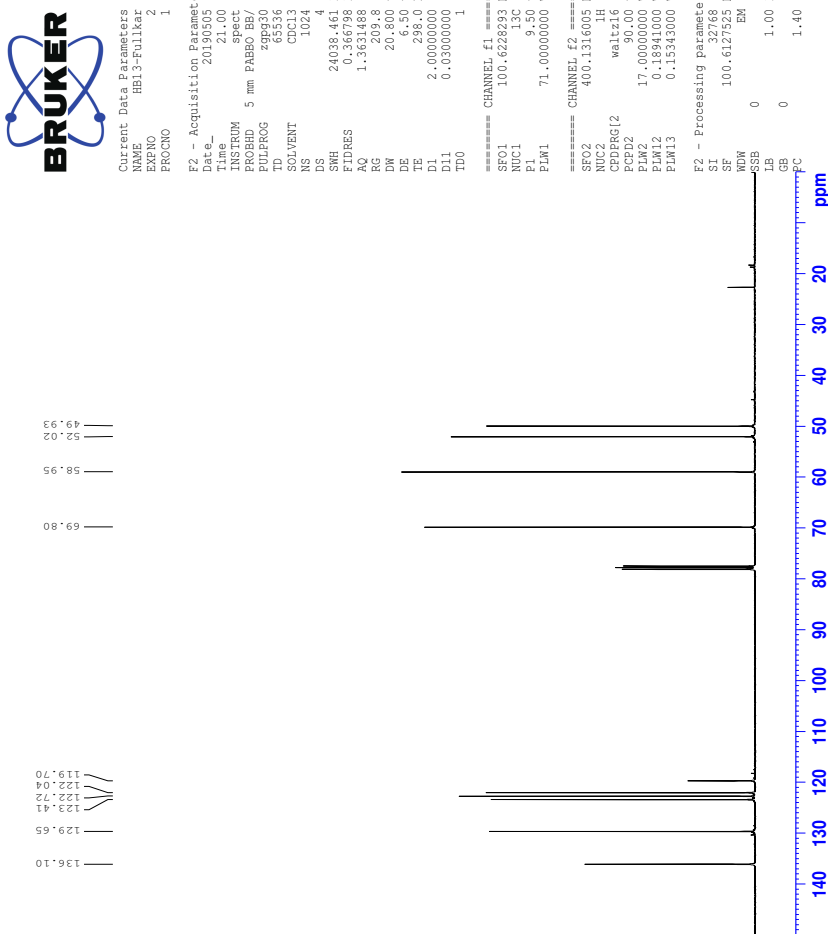


5 Spectra of IL 6c

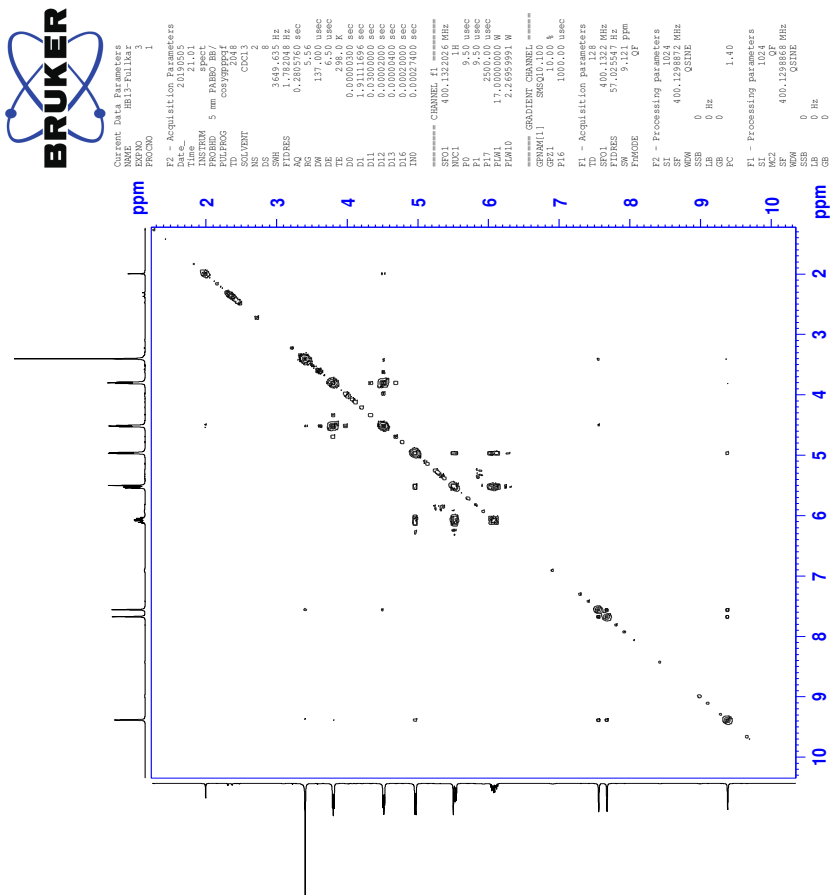
5.1 ^1H -NMR spectrum of IL 6c



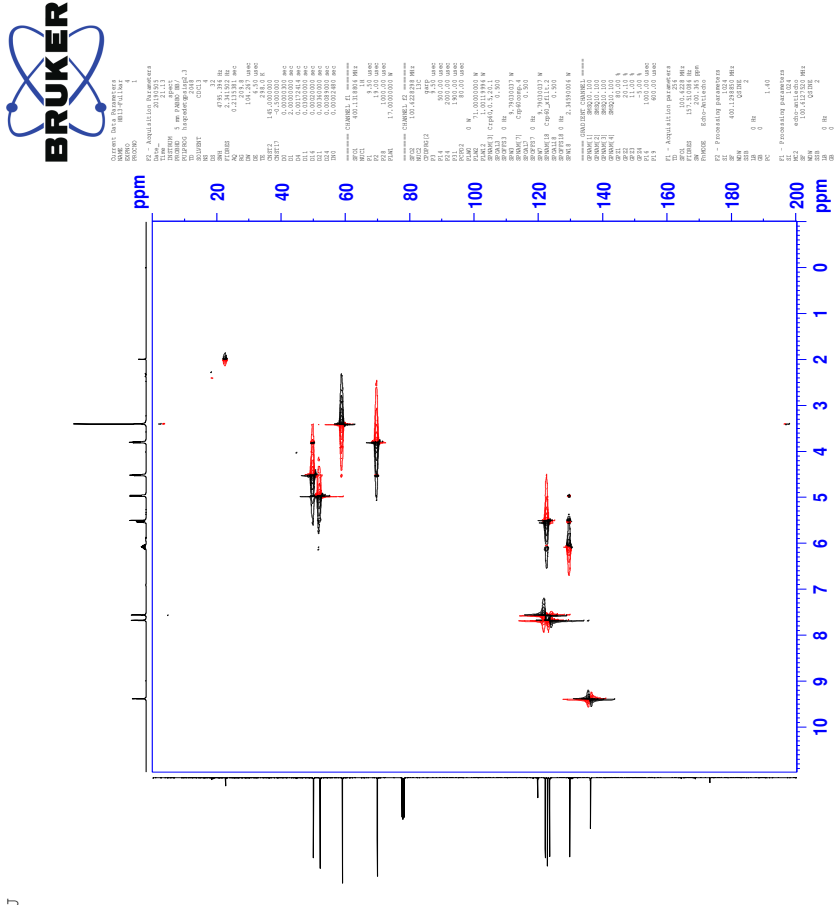
5.2 ^{13}C -NMR spectrum of IL 6c



5.3 COSY-spectrum of IL 6c

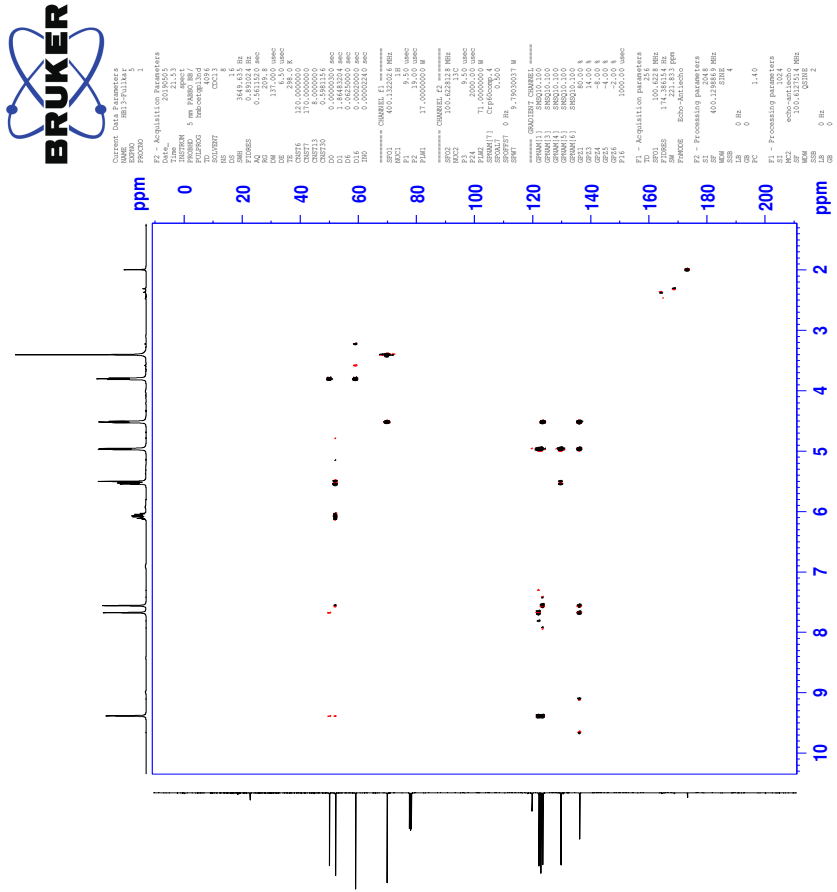


5.4 HSQC-spectrum of IL 6c

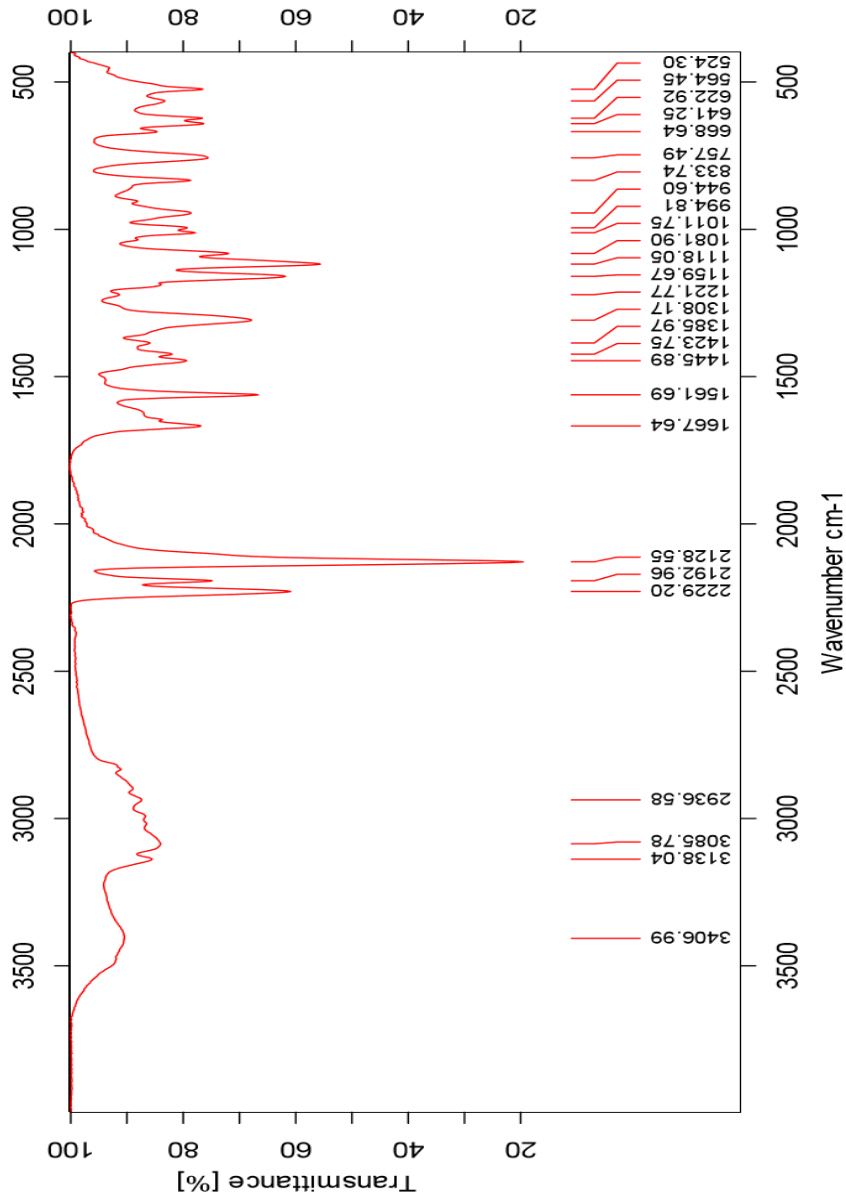


TKU

5.5 HMBC-spectrum of IL 6c



5.6 IR-spectrum of IL 6c



5.7 HR-MS positive mode spectrum of IL 6c

Elemental Composition Report

Page 1

Single Mass Analysis

Tolerance = 5.0 PPM / DBE: min = -50.0, max = 50.0

Element prediction: Off

Number of isotope peaks used for i-FIT = 3

Monoisotopic Mass, Even Electron Ions

600 formula(e) evaluated with 1 results within limits (all results (up to 1000) for each mass)

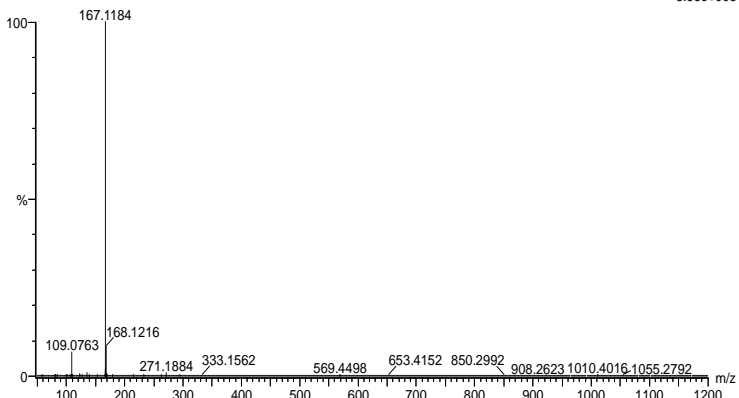
Elements Used:

C: 0-100 H: 0-150 N: 0-10 O: 0-5 Na: 0-1

2019-440 31 (0.361) AM2 (Ar,35000.0,0.00,0.00); Cm (31)

1: TOF MS ES+

3.66e+005



Minimum: -50.0
Maximum: 5.0 5.0 50.0

Mass	Calc. Mass	mDa	PPM	DBE	i-FIT	Norm	Conf (%)	Formula
167.1184	167.1184	0.0	0.0	3.5	1123.6	n/a	n/a	C9 H15 N2 O

5.8 HR-MS negative mode spectrum of IL 6c

Elemental Composition Report

Page 1

Single Mass Analysis

Tolerance = 5.0 PPM / DBE: min = -50.0, max = 50.0

Element prediction: Off

Number of isotope peaks used for i-FIT = 3

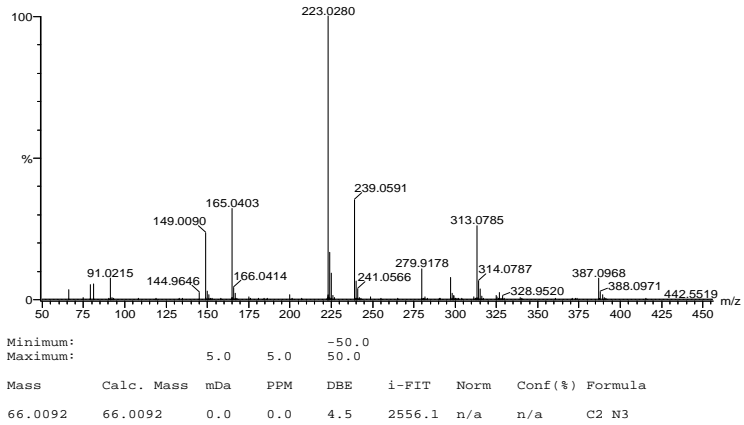
Monoisotopic Mass, Even Electron Ions

58 formula(e) evaluated with 1 results within limits (all results (up to 1000) for each mass)

Elements Used:

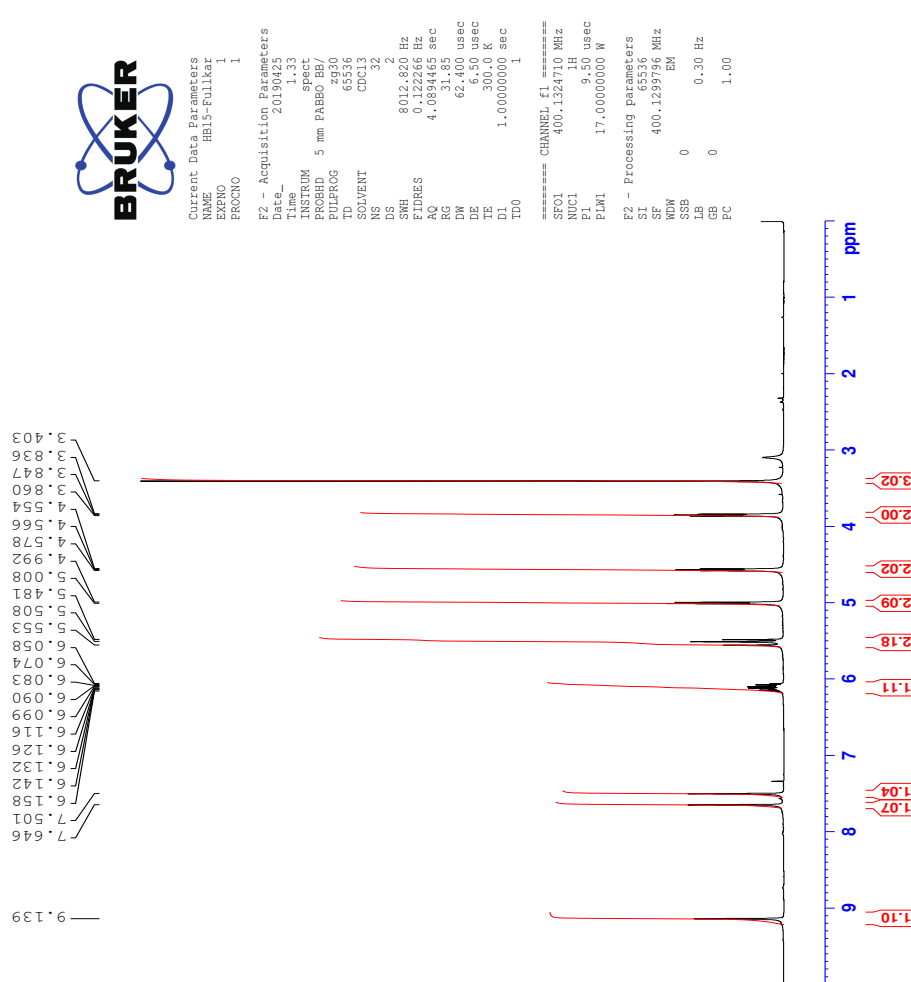
C: 0-100 H: 0-150 N: 0-10 O: 0-5 Na: 0-1
2019-441 26 (0.488) AM2 (Ar,35000.0,0.00,0.00); Cm (25.27)
1: TOF MS ES-

6.74e+005

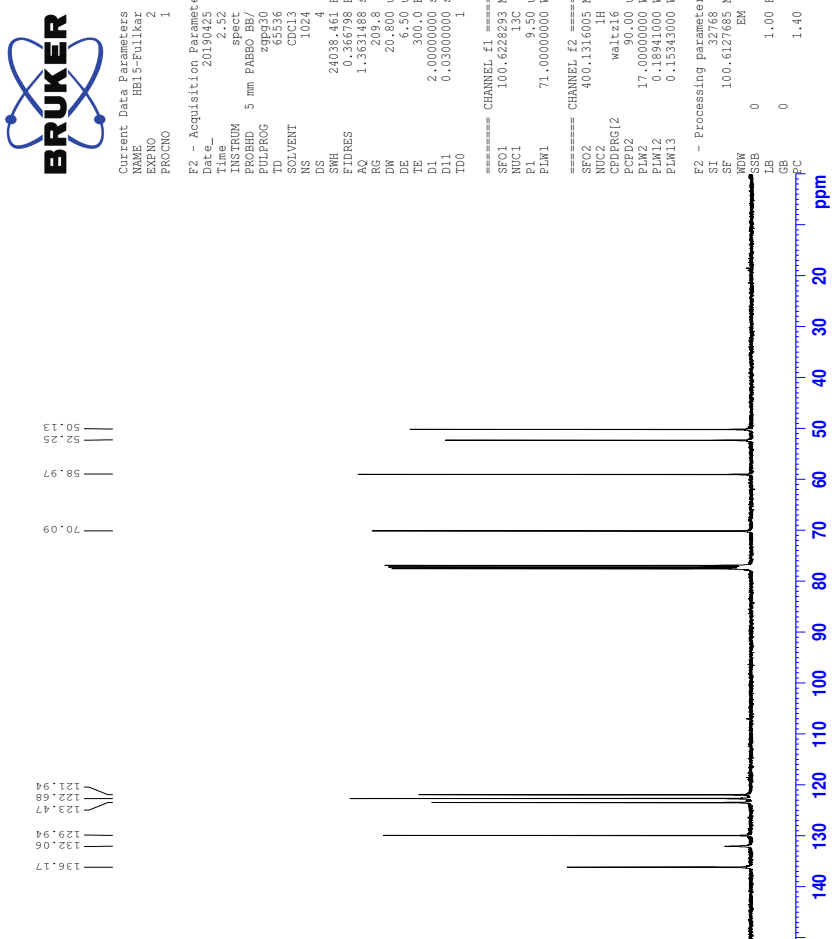


6 Spectra of IL 6d

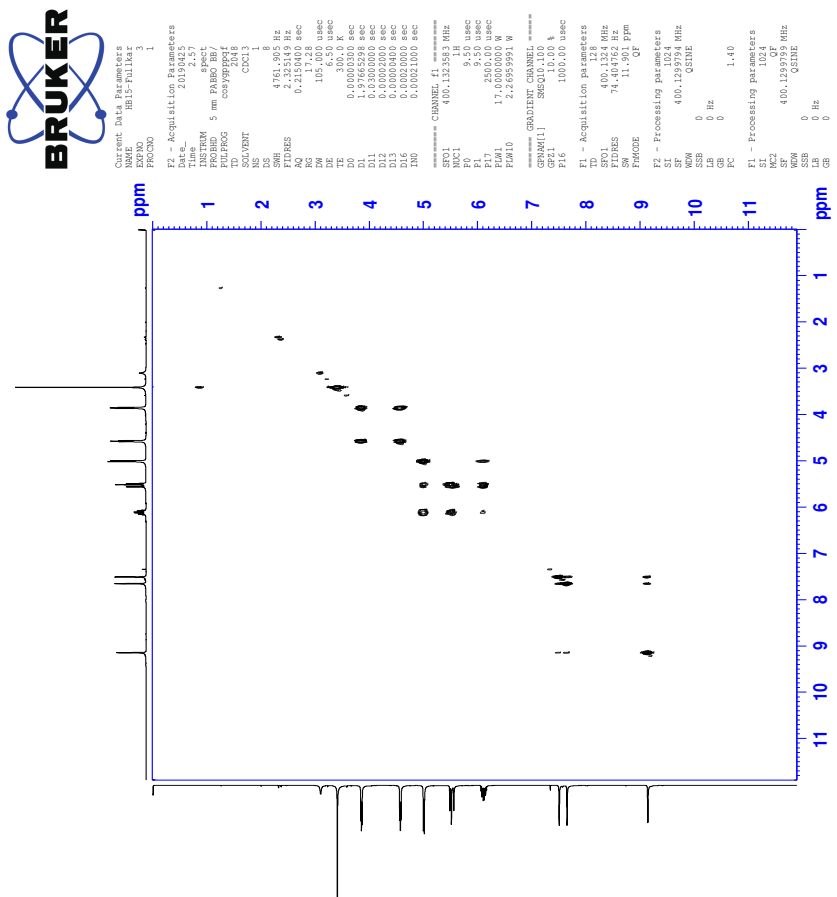
6.1 ^1H -NMR spectrum of IL 6d



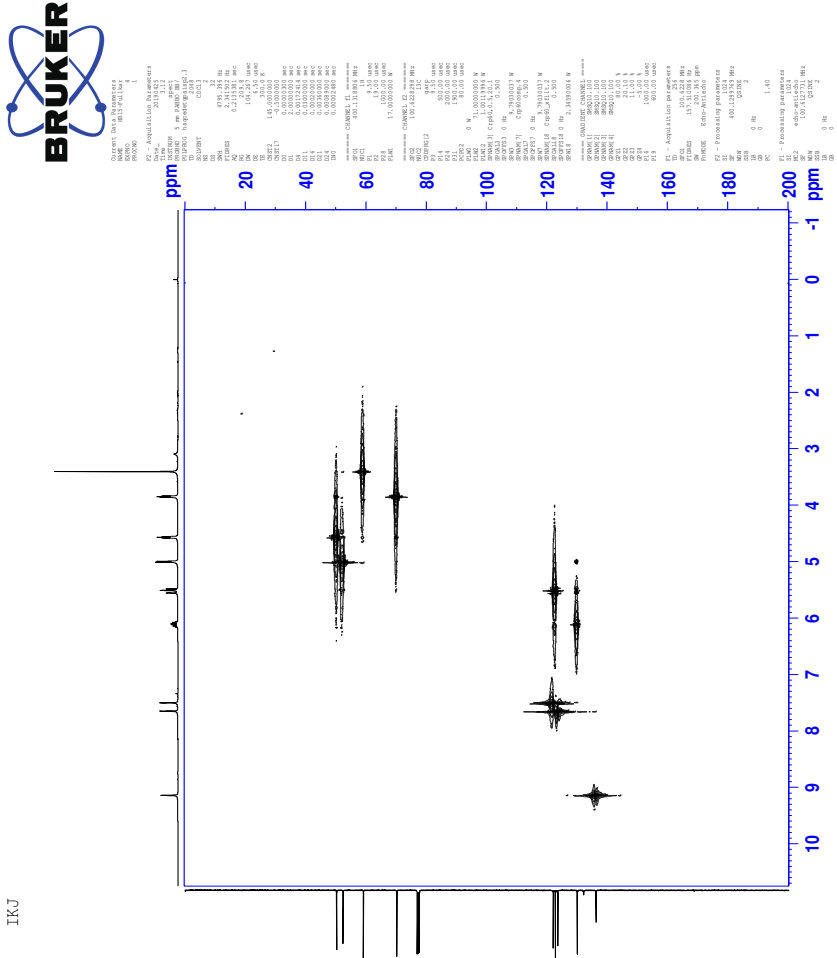
6.2 ^{13}C -NMR spectrum of IL 6d



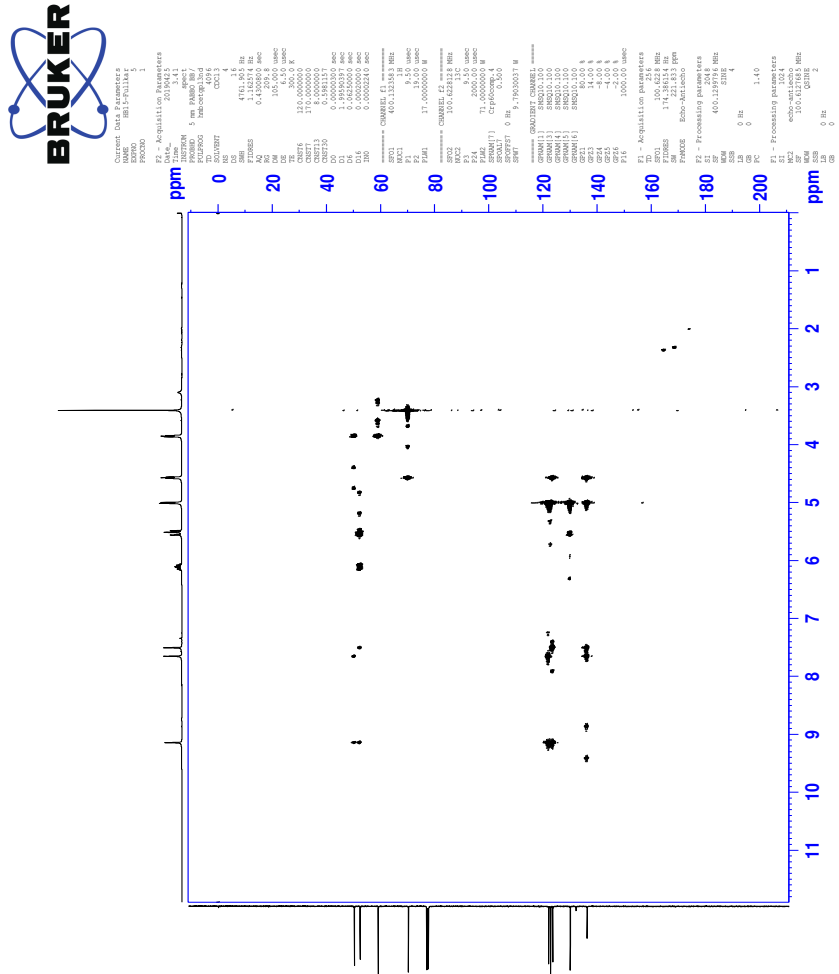
6.3 COSY-spectrum of IL 6d



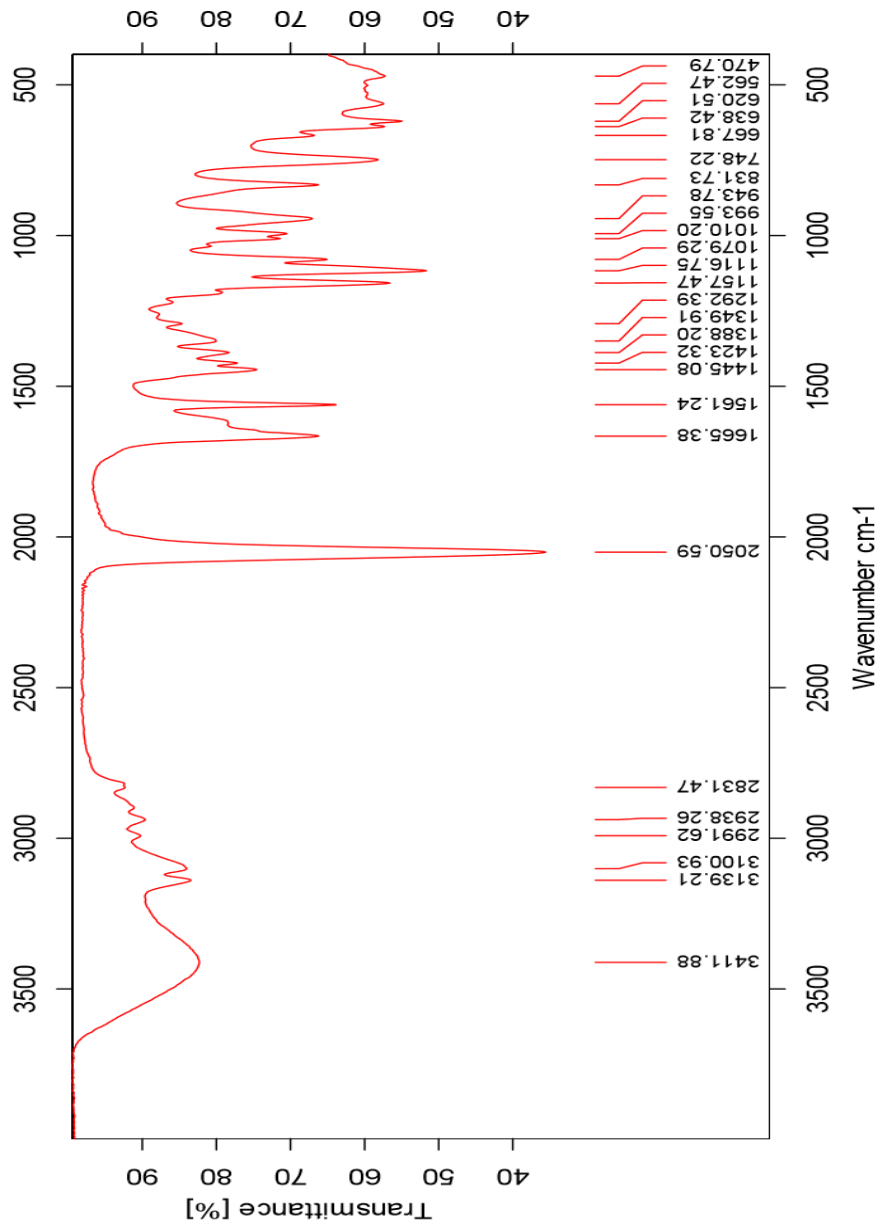
6.4 HSQC-spectrum of IL 6d



6.5 HMBC-spectrum of IL 6d



6.6 IR-spectrum of IL 6d



6.7 HR-MS positive mode spectrum of IL 6d

Elemental Composition Report

Page 1

Single Mass Analysis

Tolerance = 5.0 PPM / DBE: min = -50.0, max = 50.0

Element prediction: Off

Number of isotope peaks used for i-FIT = 3

Monoisotopic Mass, Even Electron Ions

600 formula(e) evaluated with 1 results within limits (all results (up to 1000) for each mass)

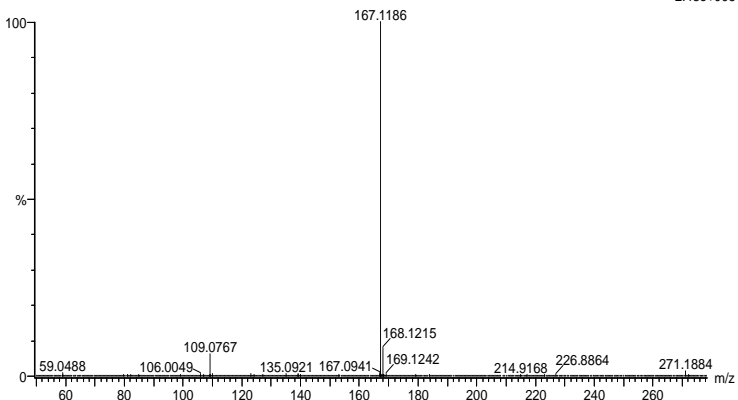
Elements Used:

C: 0-100 H: 0-150 N: 0-10 O: 0-5 Na: 0-1

2019-442 30 (0.342) AM2 (Ar,35000.0,0.00,0.00); Cm (30)

1: TOF MS ES+

2.48e+005



Minimum: -50.0
Maximum: 5.0 5.0 50.0

Mass	Calc. Mass	mDa	PPM	DBE	i-FIT	Norm	Conf (%)	Formula
167.1186	167.1184	0.2	1.2	3.5	1034.4	n/a	n/a	C9 H15 N2 O

6.8 HR-MS negative mode spectrum of IL 6d

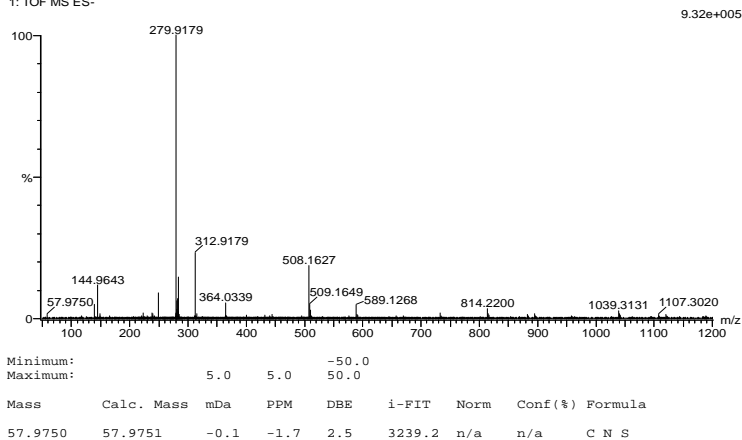
Elemental Composition Report

Page 1

Single Mass Analysis

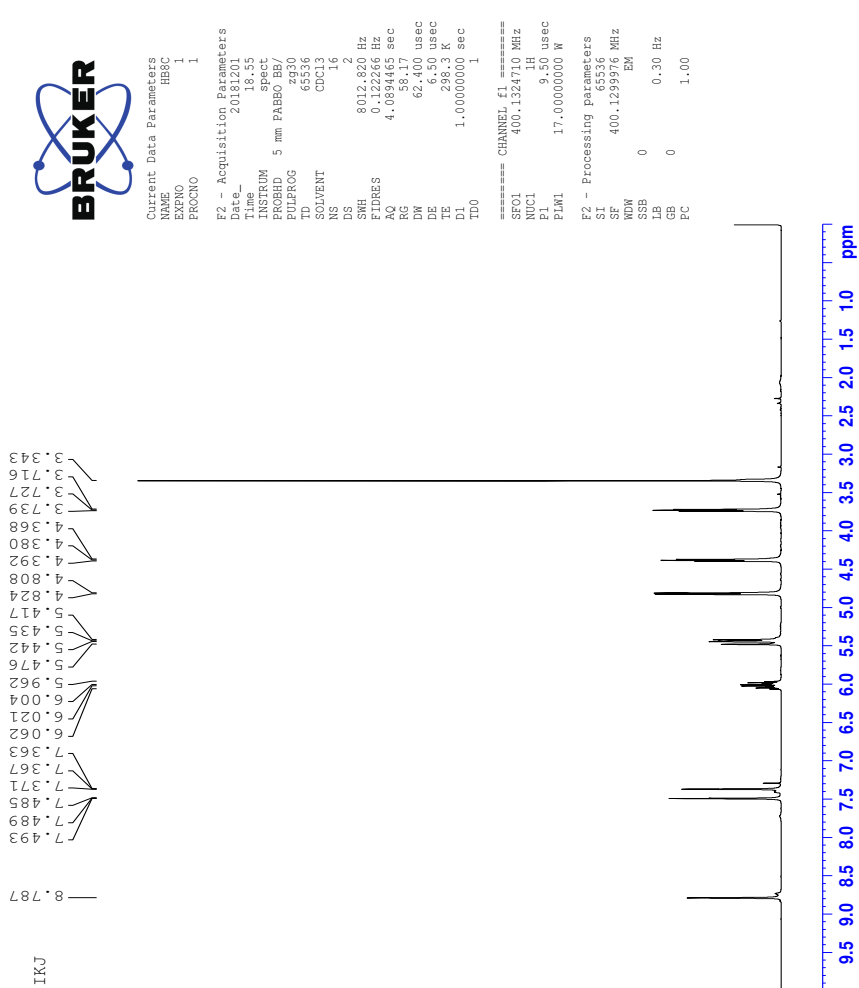
Tolerance = 5.0 PPM / DBE: min = -50.0, max = 50.0
Element prediction: Off
Number of isotope peaks used for i-FIT = 3

Monoisotopic Mass, Even Electron Ions
48 formula(e) evaluated with 1 results within limits (all results (up to 1000) for each mass)
Elements Used:
C: 0-100 H: 0-150 N: 0-10 O: 0-5 Na: 0-1 S: 0-3
2019-443 32 (0.603) AM2 (Ar:35000.0,0.00,0.00); Cm (26.32)
1: TOF MS ES-

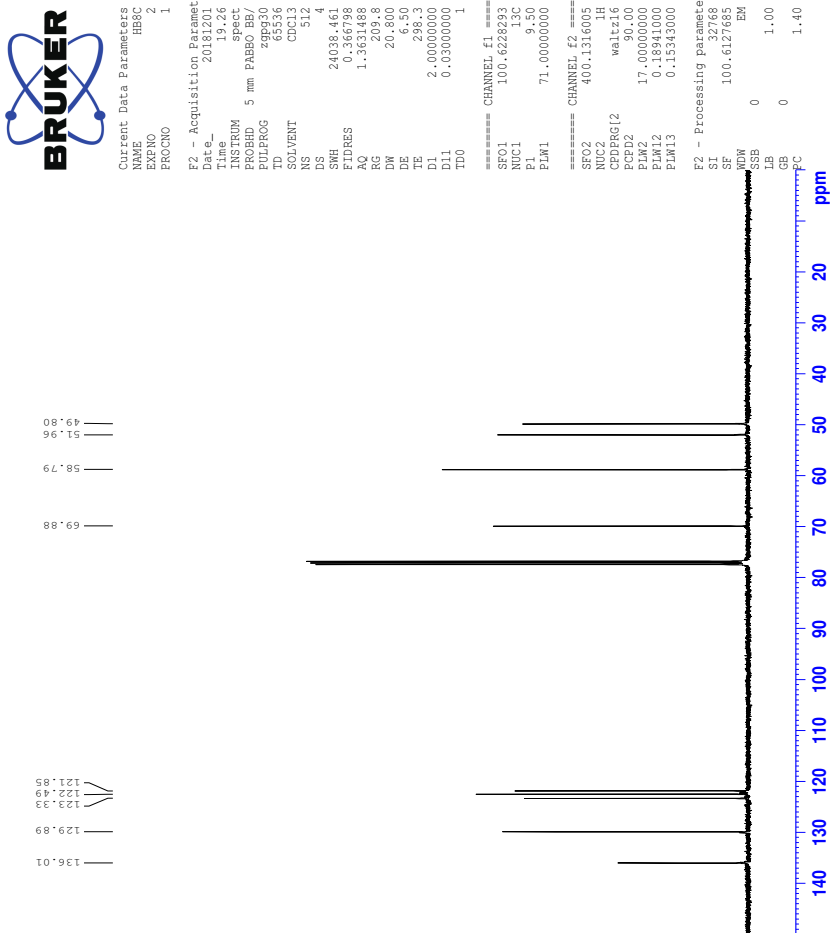


7 Spectra of IL 6e

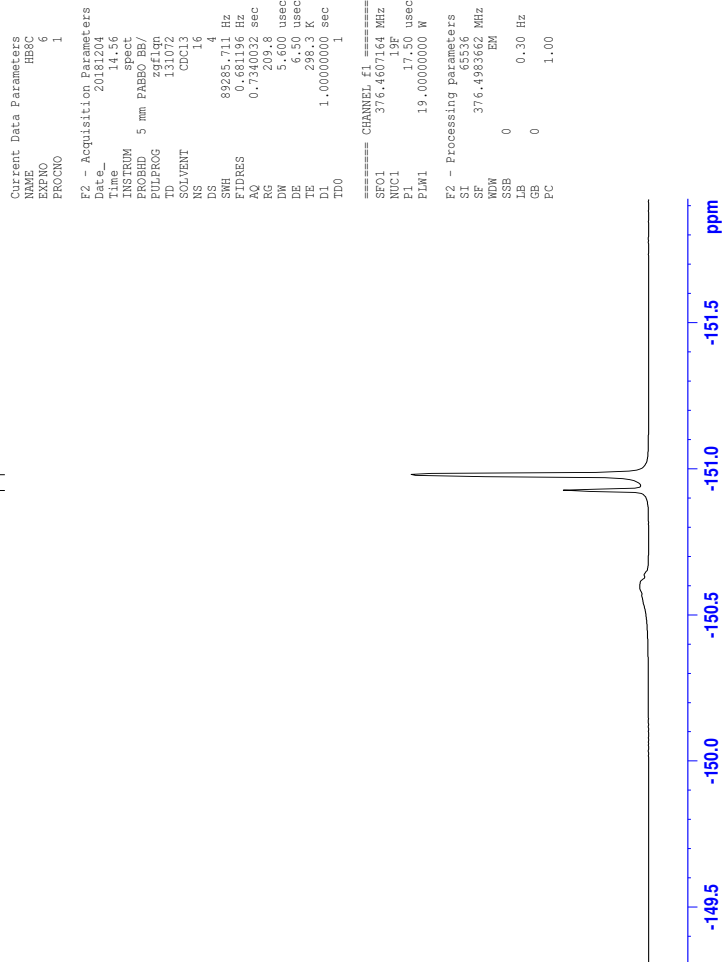
7.1 ^1H -NMR spectrum of IL 6e



7.2 ^{13}C -NMR spectrum of IL 6e

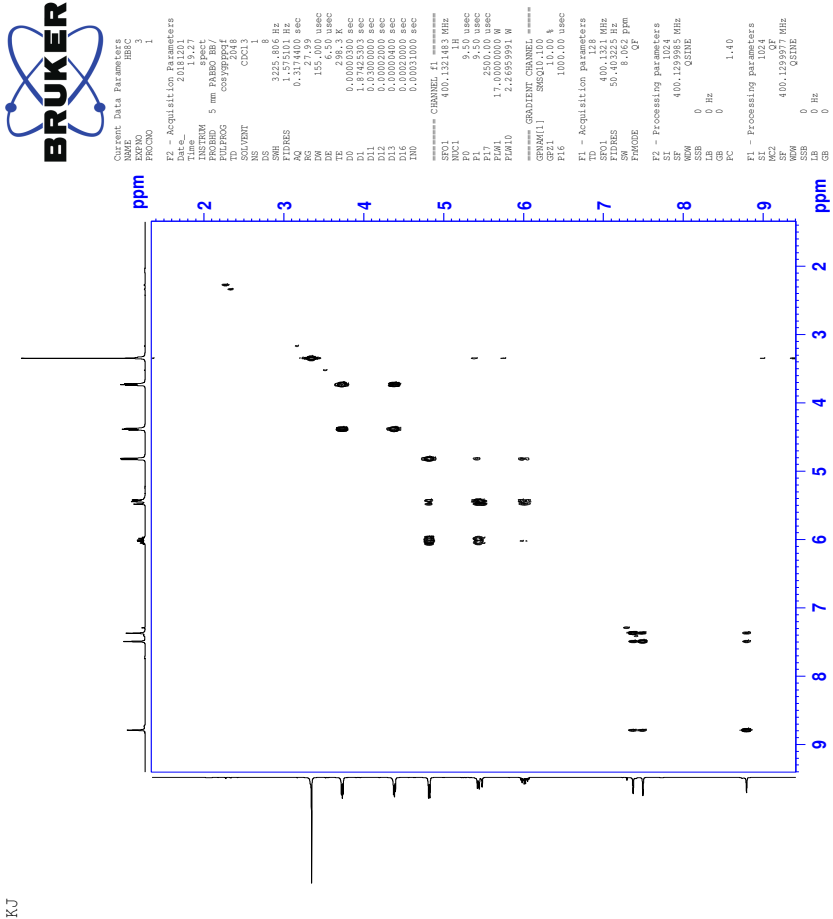


7.3 ^{19}F -NMR spectrum of IL 6e



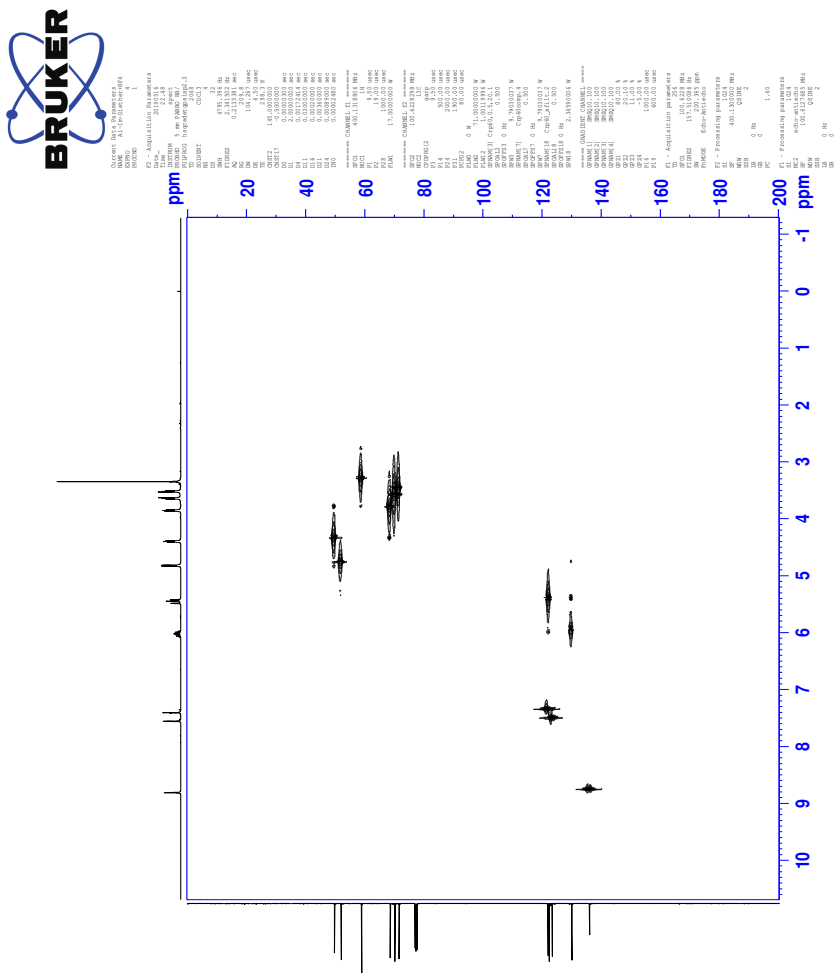
XXX

7.4 COSY-spectrum of IL 6e

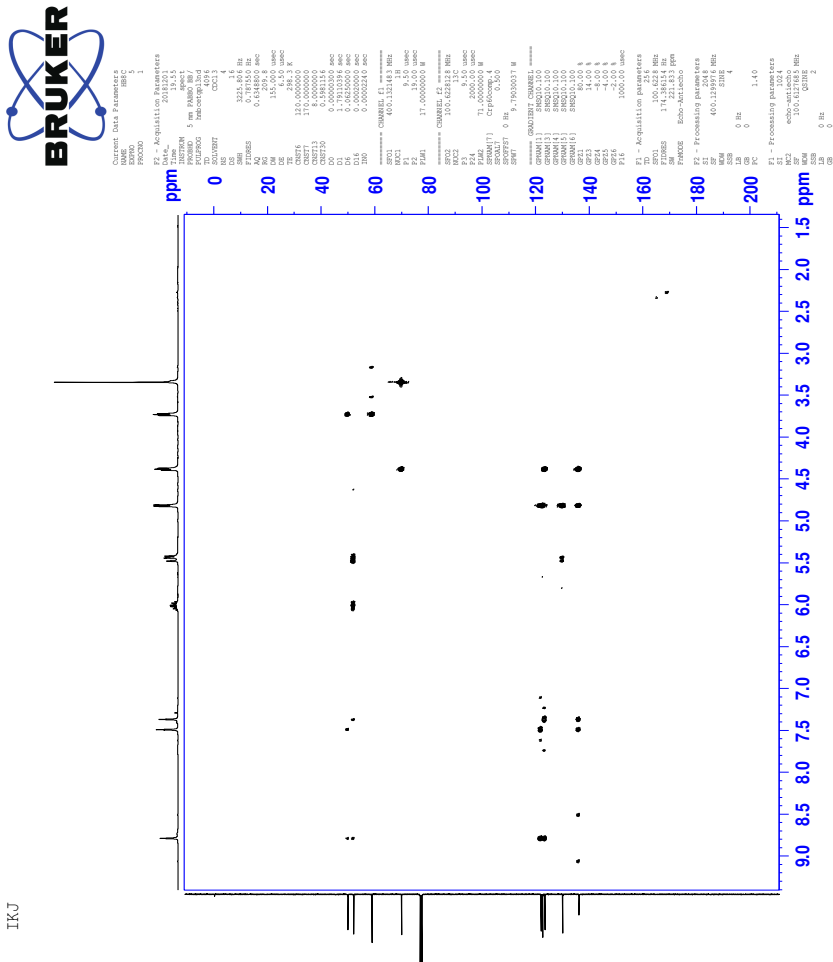


TKJ

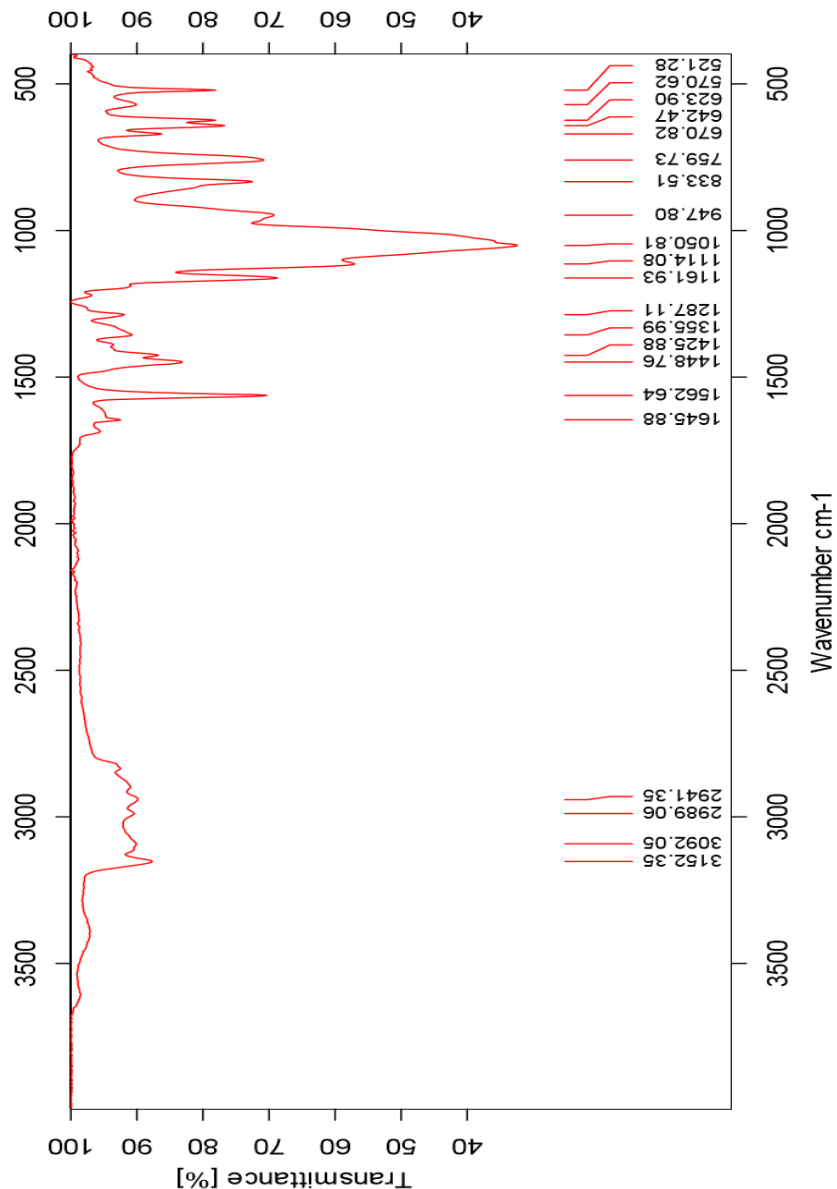
7.5 HSQC-spectrum of IL 6e



7.6 HMBC-spectrum of IL 6e



7.7 IR-spectrum of IL 6e



7.8 HR-MS positive mode spectrum of IL 6e

Elemental Composition Report

Page 1

Single Mass Analysis

Tolerance = 5.0 PPM / DBE: min = -50.0, max = 50.0

Element prediction: Off

Number of isotope peaks used for i-FIT = 3

Monoisotopic Mass, Even Electron Ions

688 formula(e) evaluated with 1 results within limits (all results (up to 1000) for each mass)

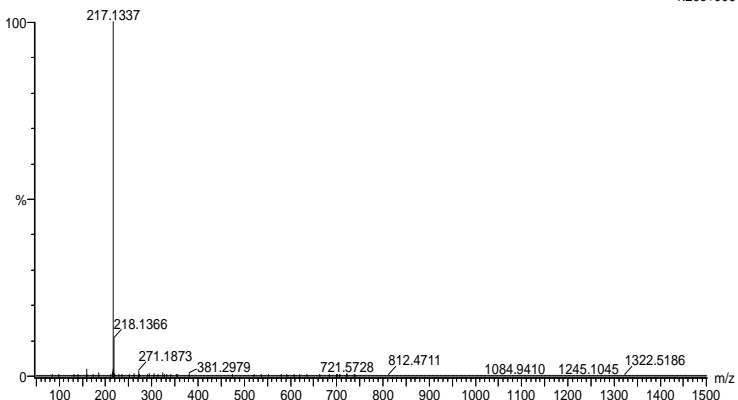
Elements Used:

C: 0-100 H: 0-150 N: 0-10 O: 0-10

2019_512FIA79 (1.466) AM2 (Ar,35000.0,0.00,0.00); Cm (79:81)

1: TOF MS ES+

1.20e+006



Minimum: -50.0

Maximum: 5.0 5.0 50.0

Mass	Calc. Mass	mDa	PPM	DBE	i-FIT	Norm	Conf (%)	Formula
217.1337	217.1341	-0.4	-1.8	6.5	1395.9	n/a	n/a	C13 H17 N2 O

7.9 HR-MS negative mode spectrum of IL 6e

Elemental Composition Report

Page 1

Single Mass Analysis

Tolerance = 10.0 PPM / DBE: min = -50.0, max = 50.0

Element prediction: Off

Number of isotope peaks used for i-FIT = 3

Monoisotopic Mass, Even Electron Ions

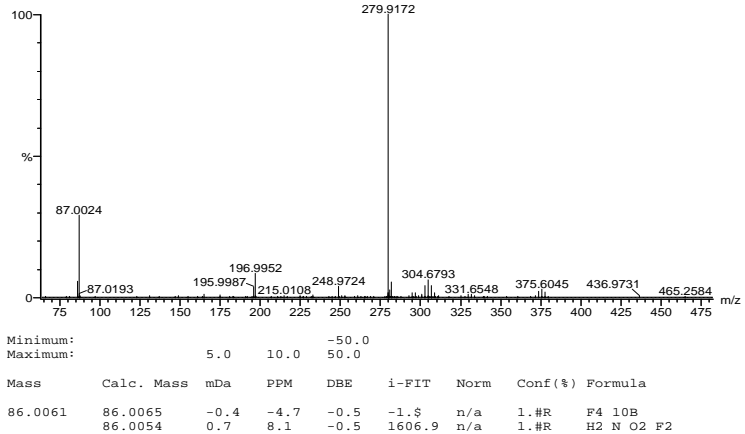
423 formula(e) evaluated with 2 results within limits (all results (up to 1000) for each mass)

Elements Used:

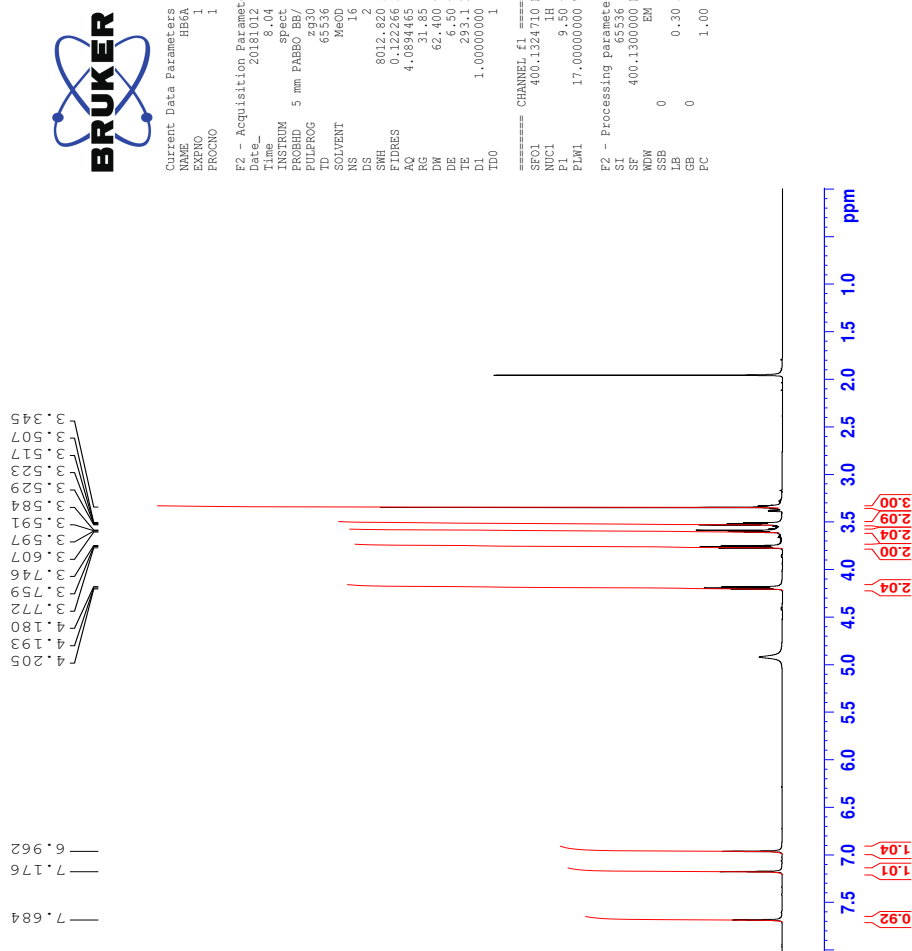
C: 0-100 H: 0-150 N: 0-10 O: 0-10 F: 0-8 10B: 0-1

2019_513FIA76 (0.857) AM2 (Ar,35000.0,0.00,0.00); Cm (64:76)
1: TOF MS ES-

3.60e+005

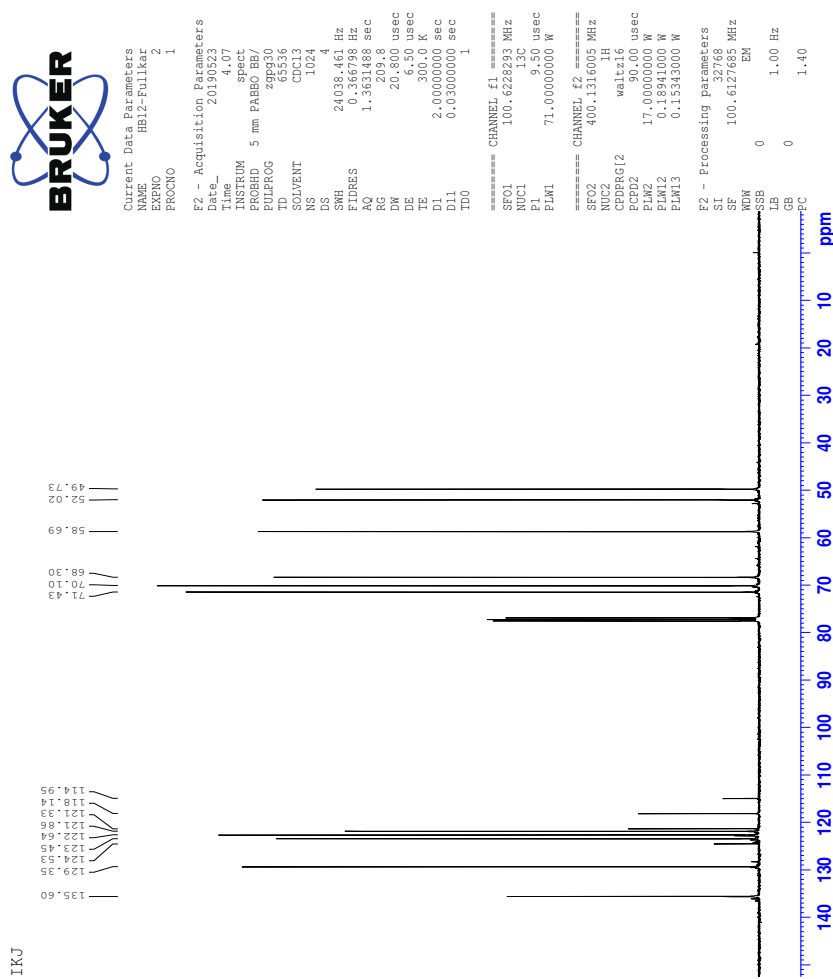


8 $^1\text{H-NMR}$ spectrum of compound 4

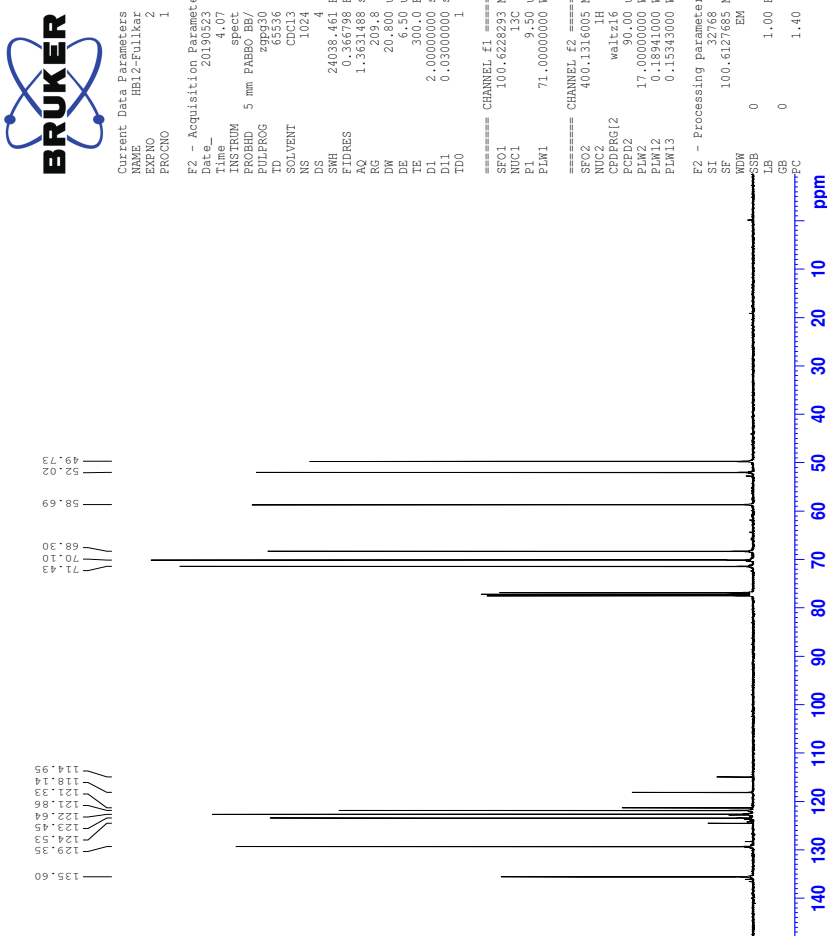


9 Spectra of IL 7b

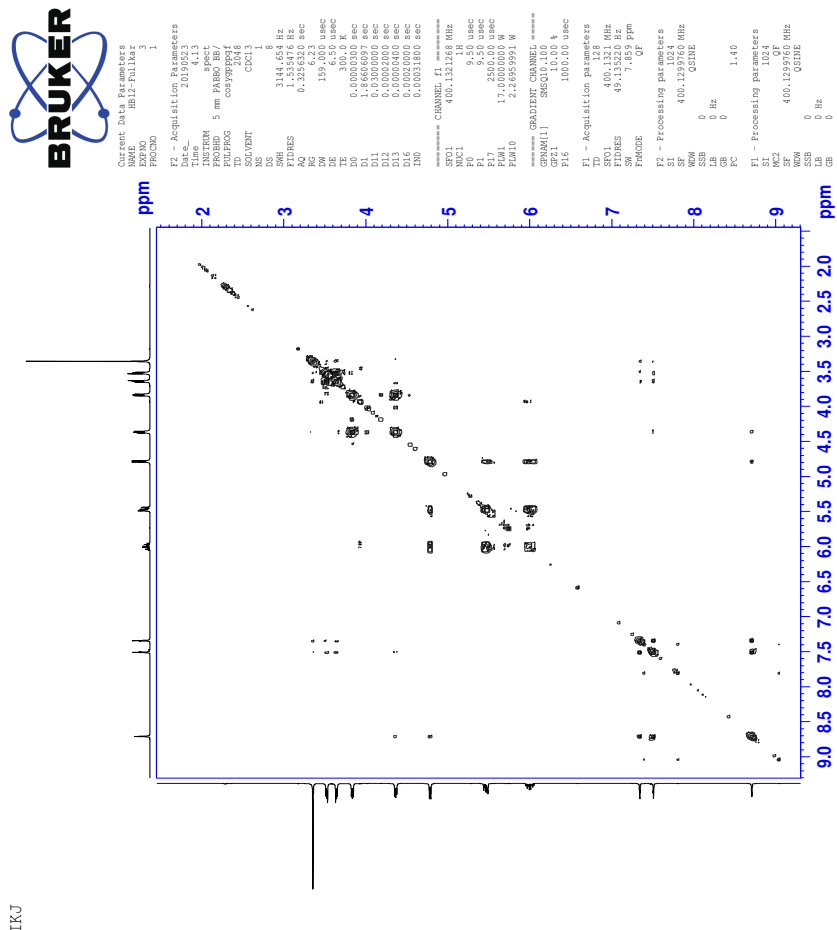
9.1 ^1H -NMR spectrum of IL 7b



9.2 ^{13}C -NMR spectrum of IL 7b



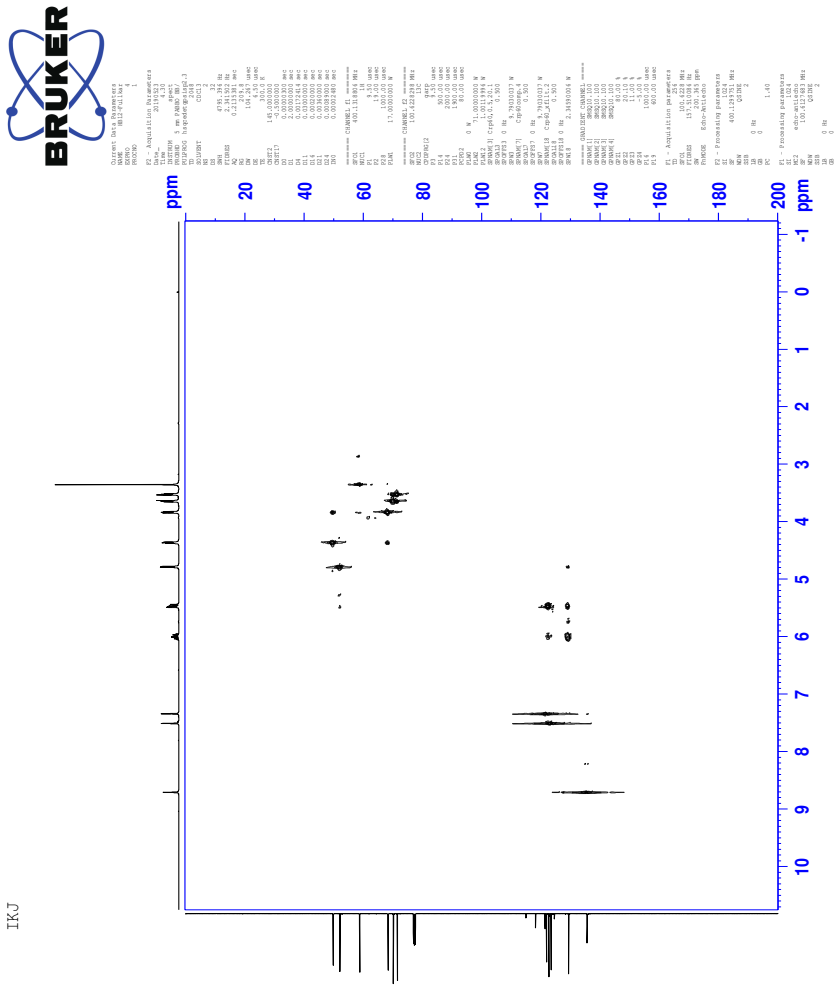
9.3 COSY-spectrum of IL 7b



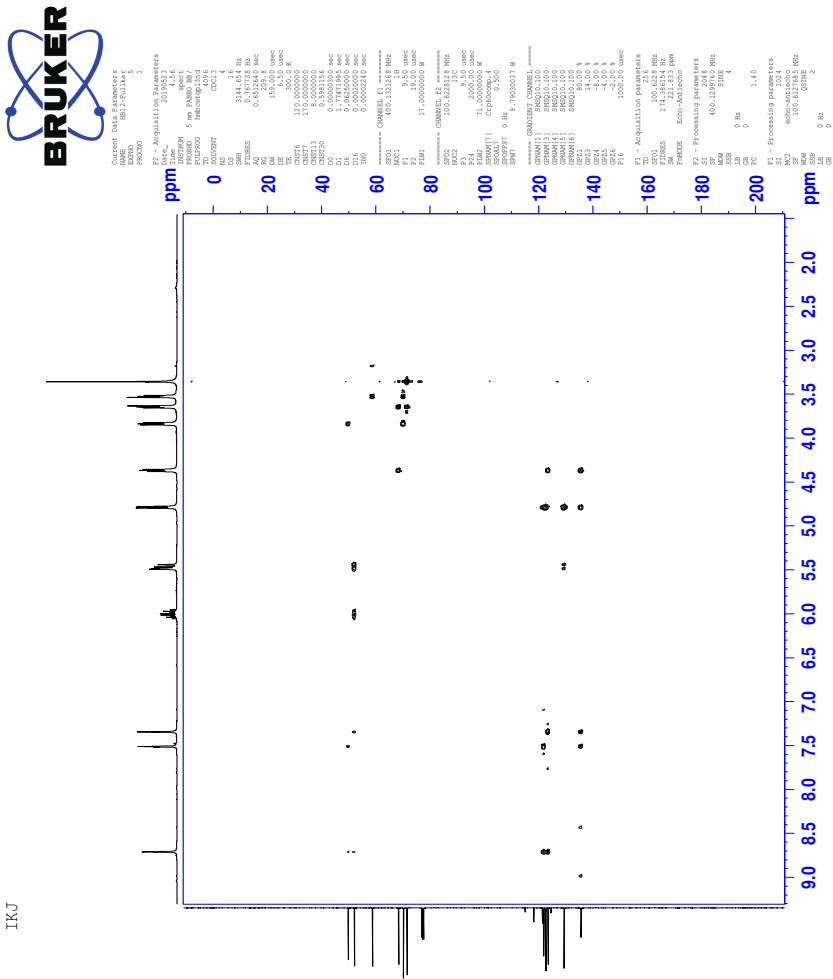
TKJ

XL

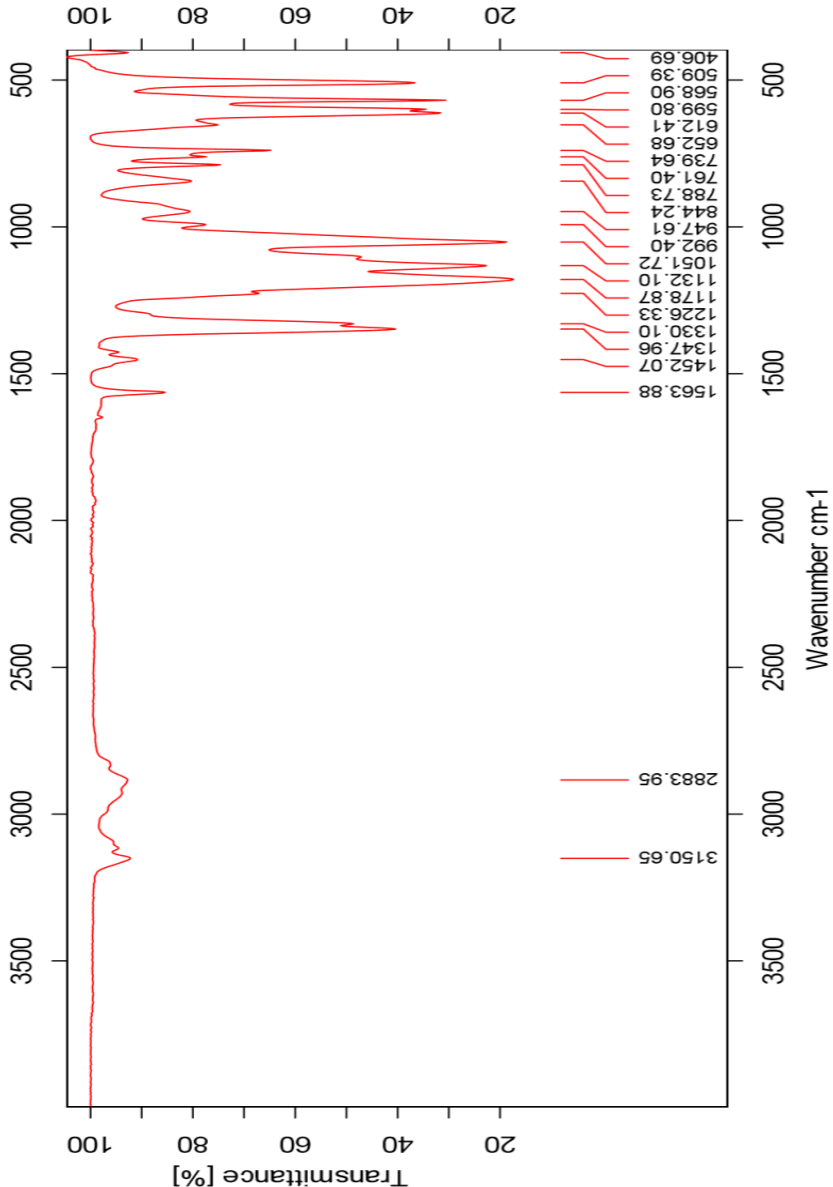
9.4 HSQC-spectrum of IL 7b



9.5 HMBC-spectrum of IL 7b



9.6 IR-spectrum of IL 7b



9.7 HR-MS positive mode spectrum of IL 7b

Elemental Composition Report

Page 1

Single Mass Analysis

Tolerance = 3.0 PPM / DBE: min = -50.0, max = 50.0

Element prediction: Off

Number of isotope peaks used for i-FIT = 3

Monoisotopic Mass, Even Electron Ions

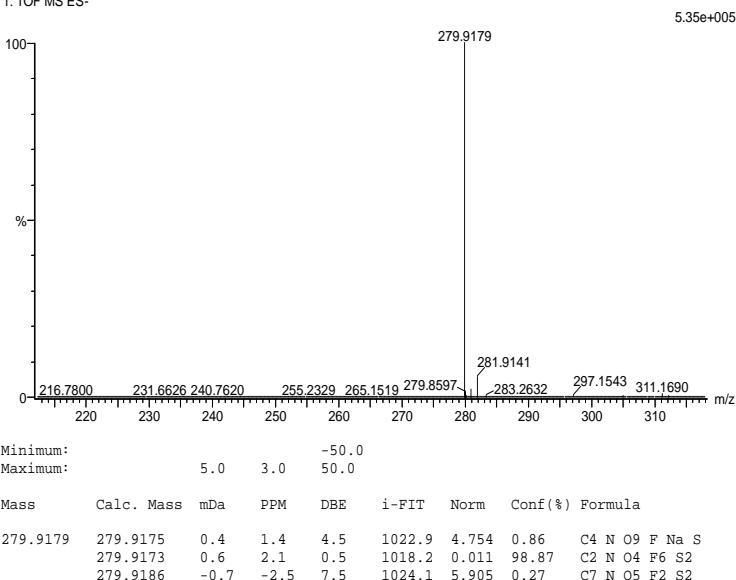
604 formula(e) evaluated with 3 results within limits (all results (up to 1000) for each mass)

Elements Used:

C: 0-100 N: 0-10 O: 0-10 F: 0-6 Na: 0-1 S: 0-3

2019-417\neq 20 (0.237) AM2 (Ar,35000.0,0.00,0.00); Cr (18:20)

1: TOF MS ES-



9.8 HR-MS negative mode spectrum of IL 7b

Elemental Composition Report

Page 1

Single Mass Analysis

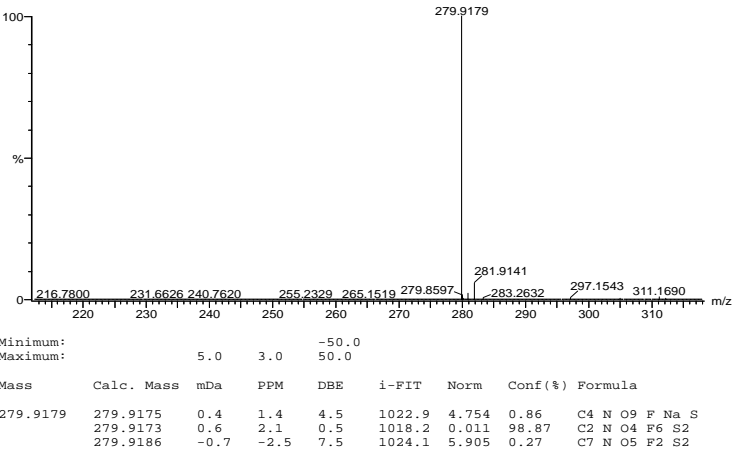
Tolerance = 3.0 PPM / DBE: min = -50.0, max = 50.0
 Element prediction: Off
 Number of isotope peaks used for i-FIT = 3

Monoisotopic Mass, Even Electron Ions
 604 formula(e) evaluated with 3 results within limits (all results (up to 1000) for each mass)

Elements Used:

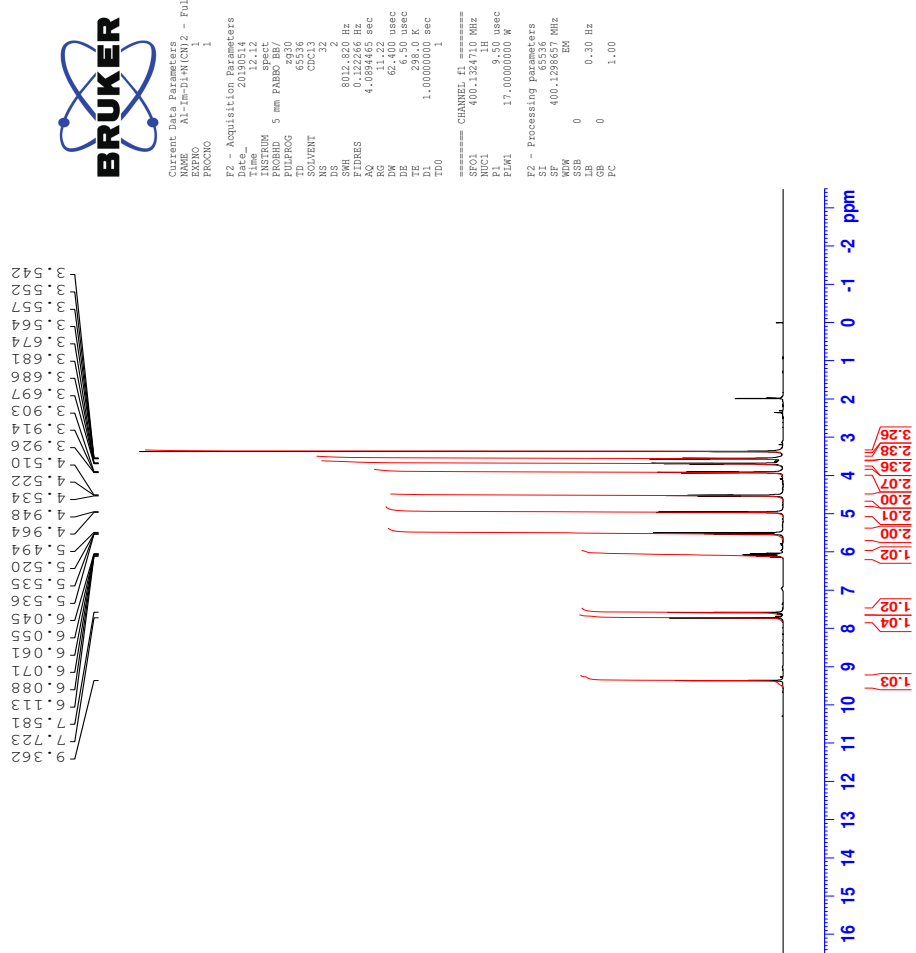
C: 0-100 N: 0-10 O: 0-10 F: 0-6 Na: 0-1 S: 0-3
 2019-417neg.20 (0.237) AM2 (Ar,35000.0,0.00,0.00); Cm (18:20)
 1: TOF MS ES-

5.35e+005

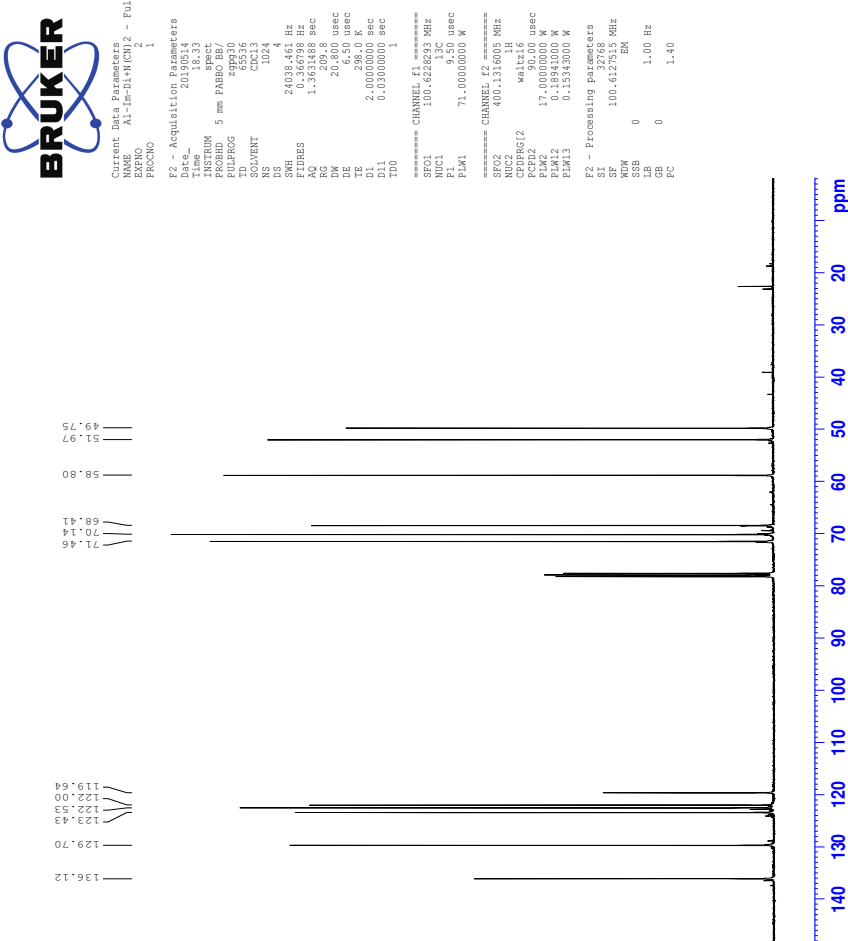


10 Spectra of IL 7c

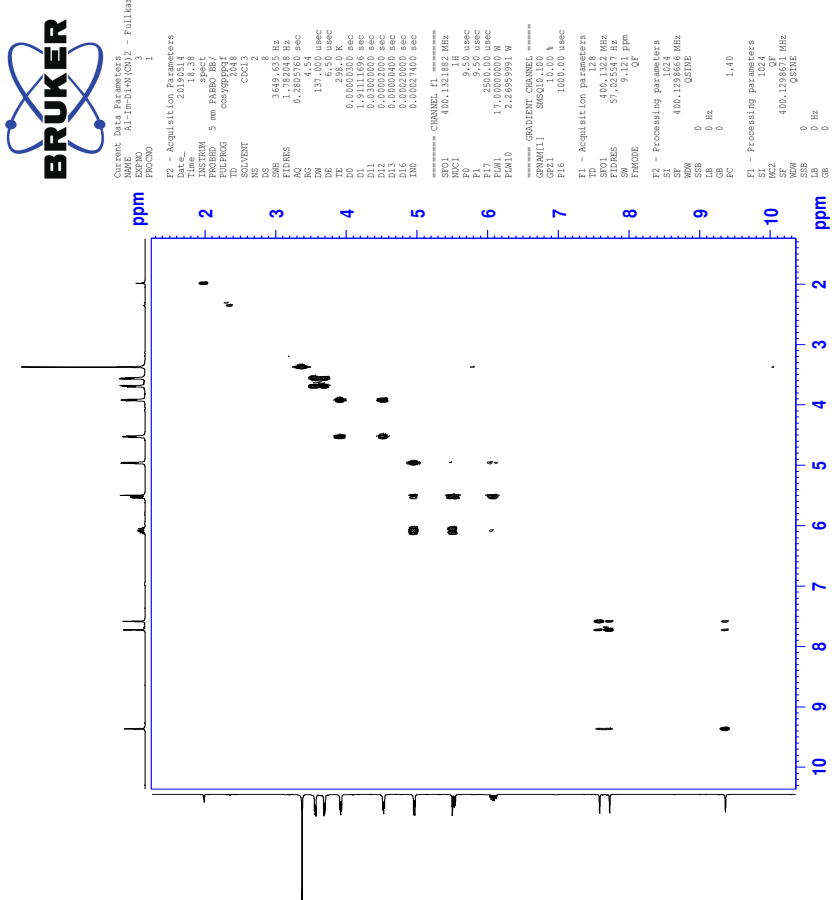
10.1 ^1H -NMR spectrum of IL 7c



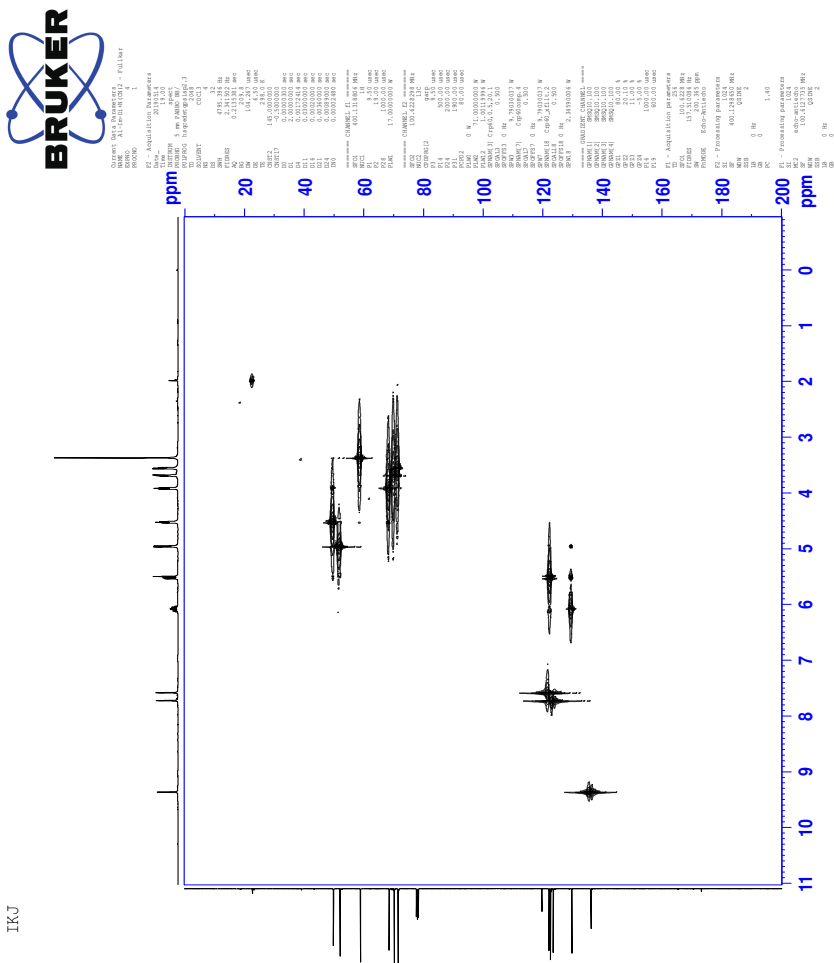
10.2 ^{13}C -NMR spectrum of IL 7c



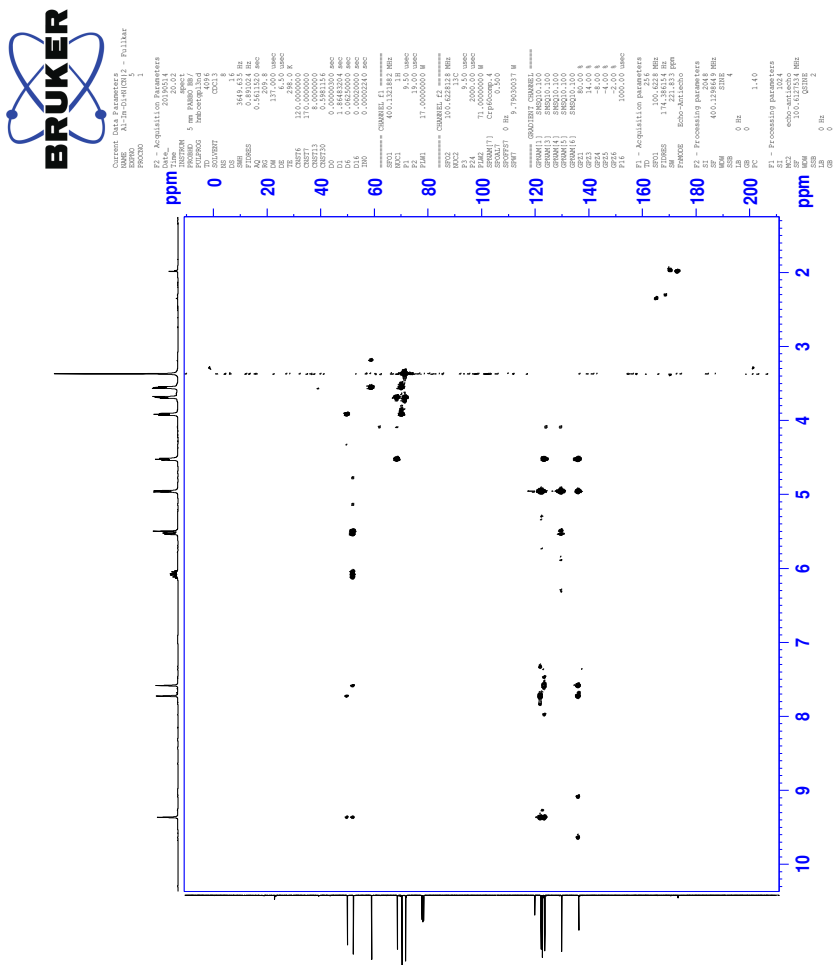
10.3 COSY-spectrum of IL 7c



10.4 HSQC-spectrum of IL 7c

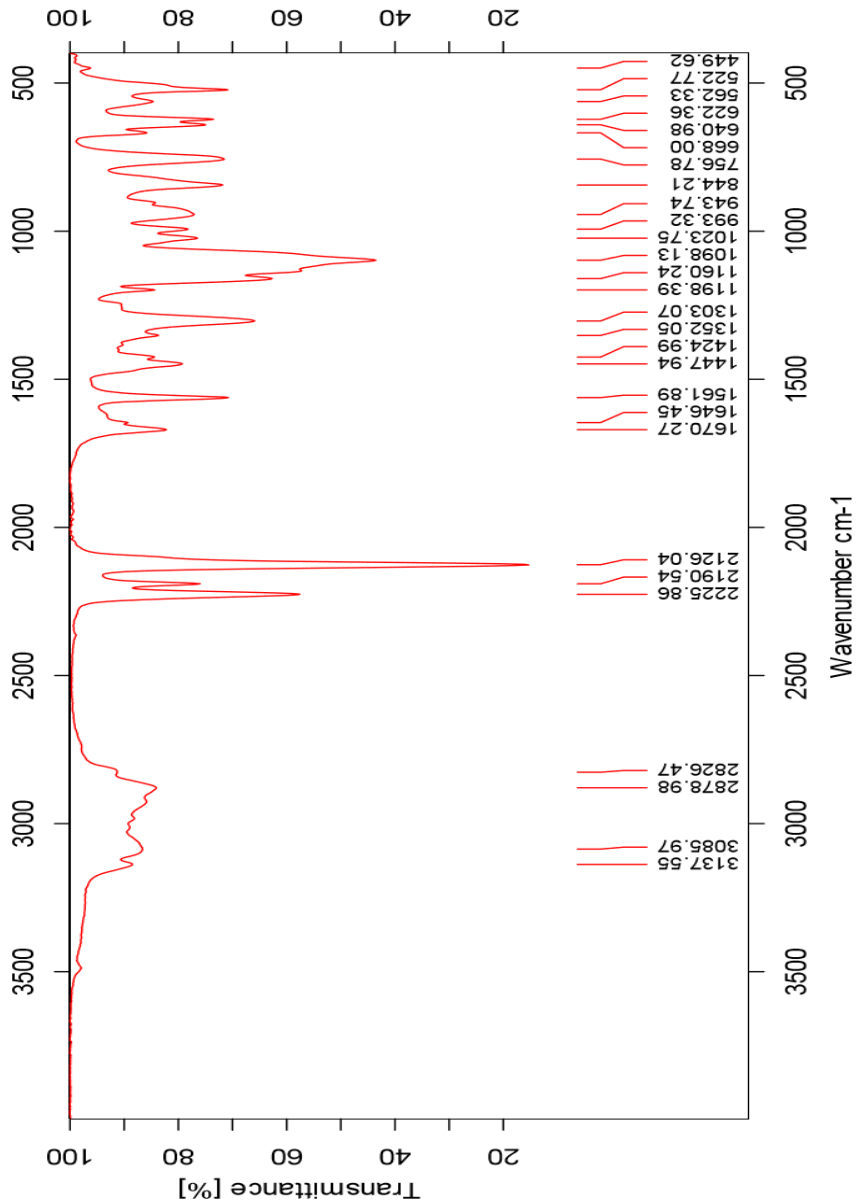


10.5 HMBC-spectrum of IL 7c



L

10.6 IR-spectrum of IL 7c



10.7 HR-MS positive mode spectrum of IL 7c

Elemental Composition Report

Page 1

Single Mass Analysis

Tolerance = 5.0 PPM / DBE: min = -50.0, max = 50.0

Element prediction: Off

Number of isotope peaks used for i-FIT = 3

Monoisotopic Mass, Even Electron Ions

660 formula(e) evaluated with 1 results within limits (all results (up to 1000) for each mass)

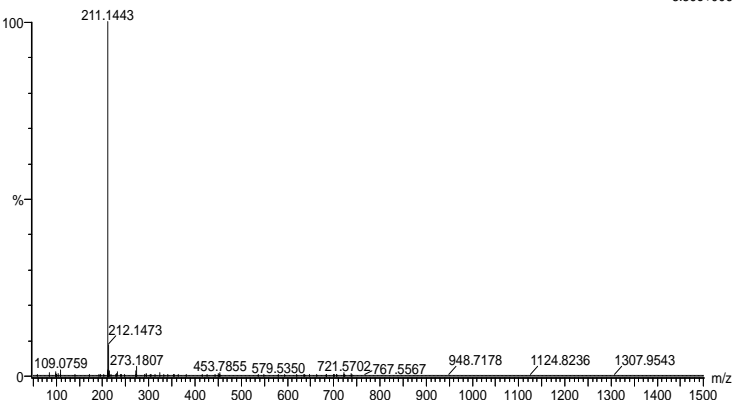
Elements Used:

C: 0-100 H: 0-150 N: 0-10 O: 0-10

2019_496FIA 100 (1.859) AM2 (Ar,35000.0,0.00,0.00); Cm (100:108)

1: TOF MS ES+

3.39e+006



Minimum: -50.0

Maximum: 5.0 5.0 50.0

Mass	Calc. Mass	mDa	PPM	DBE	i-FIT	Norm	Conf (%)	Formula
211.1443	211.1447	-0.4	-1.9	3.5	1770.2	n/a	n/a	C11 H19 N2 O2

10.8 HR-MS negative mode spectrum of IL 7c

Elemental Composition Report

Page 1

Single Mass Analysis

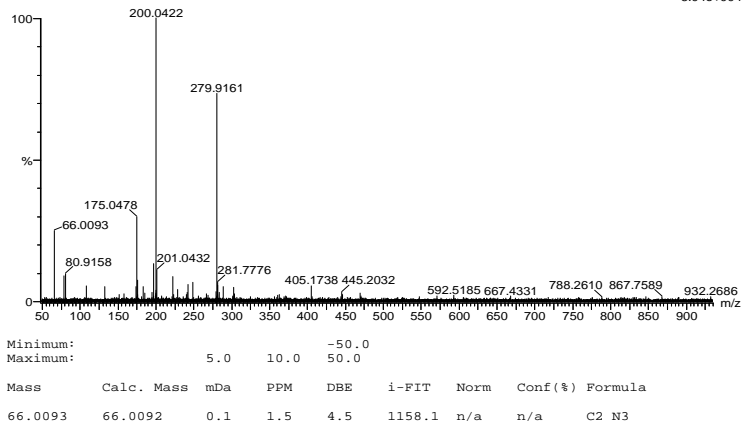
Tolerance = 10.0 PPM / DBE: min = -50.0, max = 50.0
Element prediction: Off
Number of isotope peaks used for i-FIT = 3

Monoisotopic Mass, Even Electron Ions
182 formula(e) evaluated with 1 results within limits (all results (up to 1000) for each mass)

Elements Used:

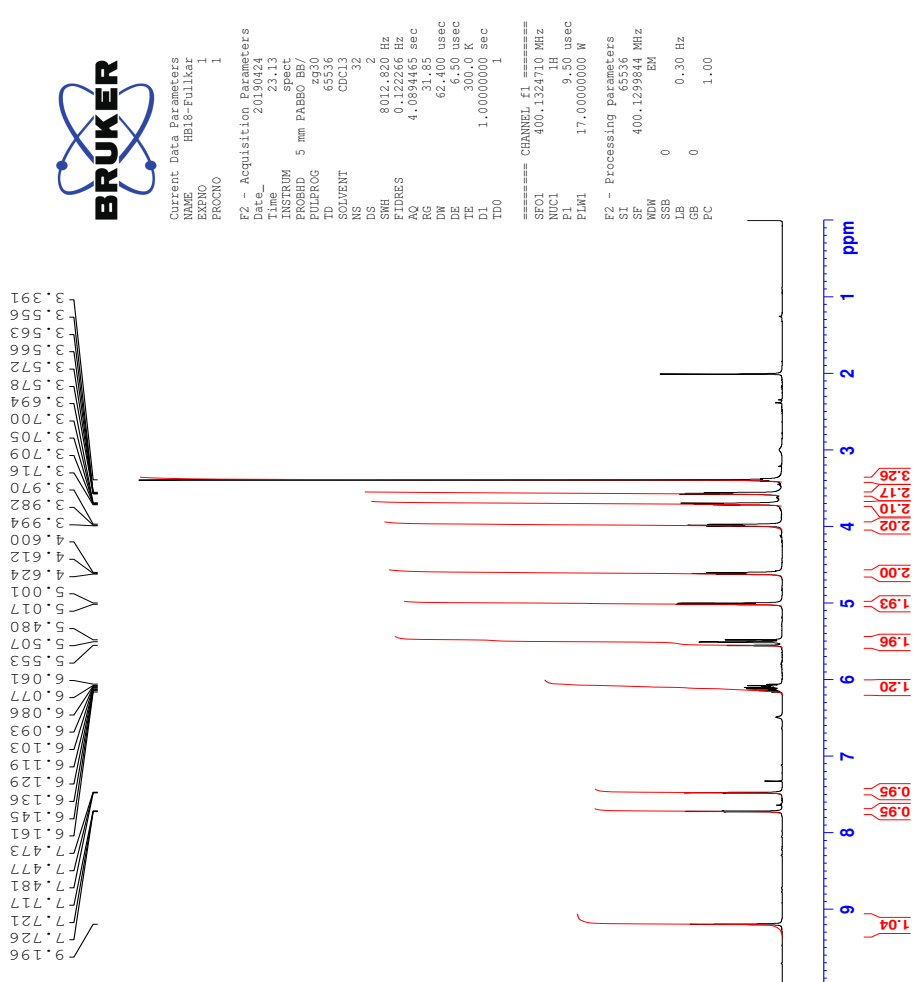
C: 0-100 H: 0-150 10B: 0-1 11B: 0-1 N: 0-10 O: 0-10 F: 0-8
2019_497neg 52 (0.589) AM2 (Ar,35000.0,0.00,0.00); Cm (39:57)
1: TOF MS ES-

3.04e+004

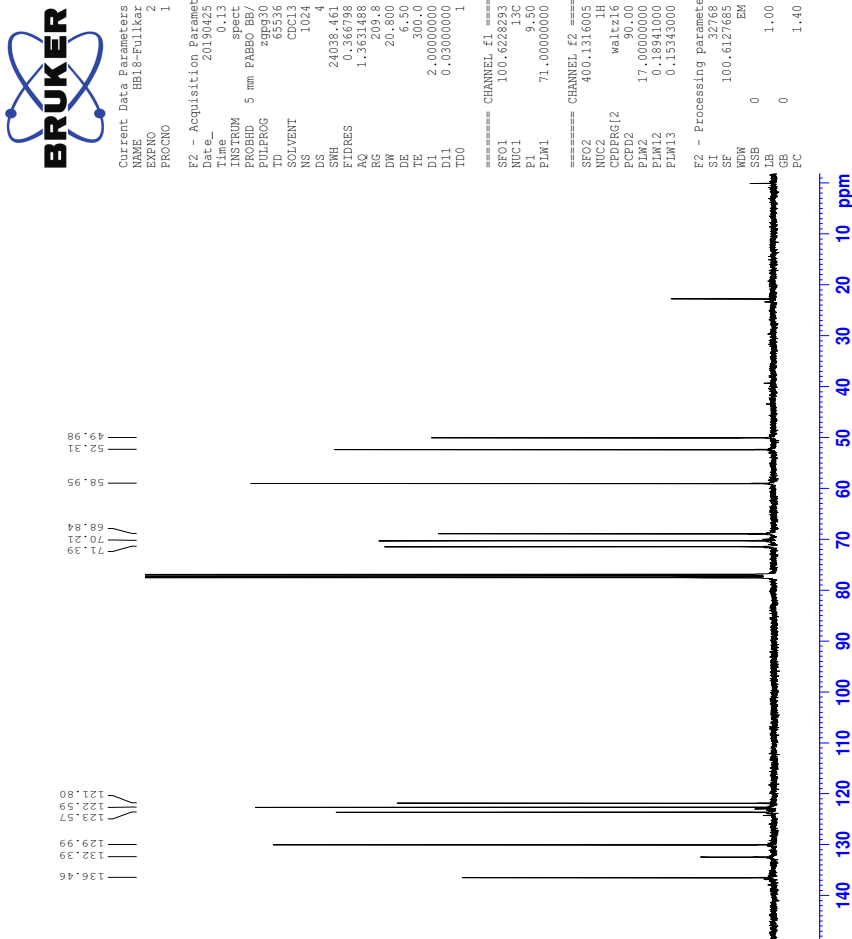


11 Spectra of IL 7d

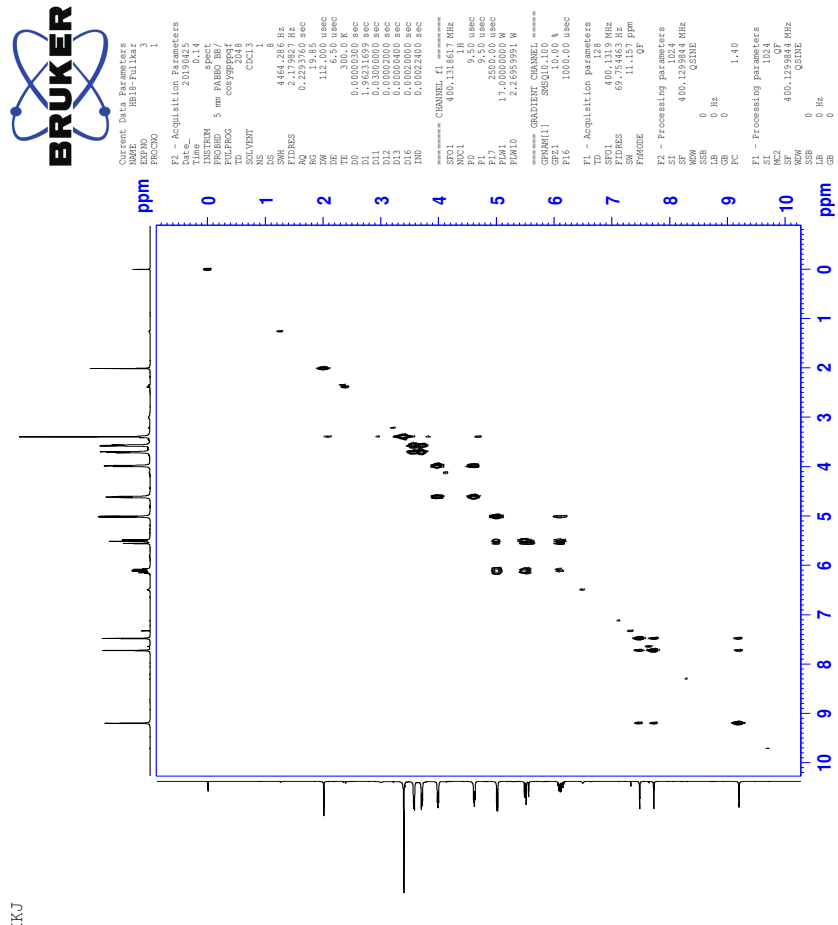
11.1 ^1H -NMR spectrum of IL 7d



11.2 ^{13}C -NMR spectrum of IL 7d



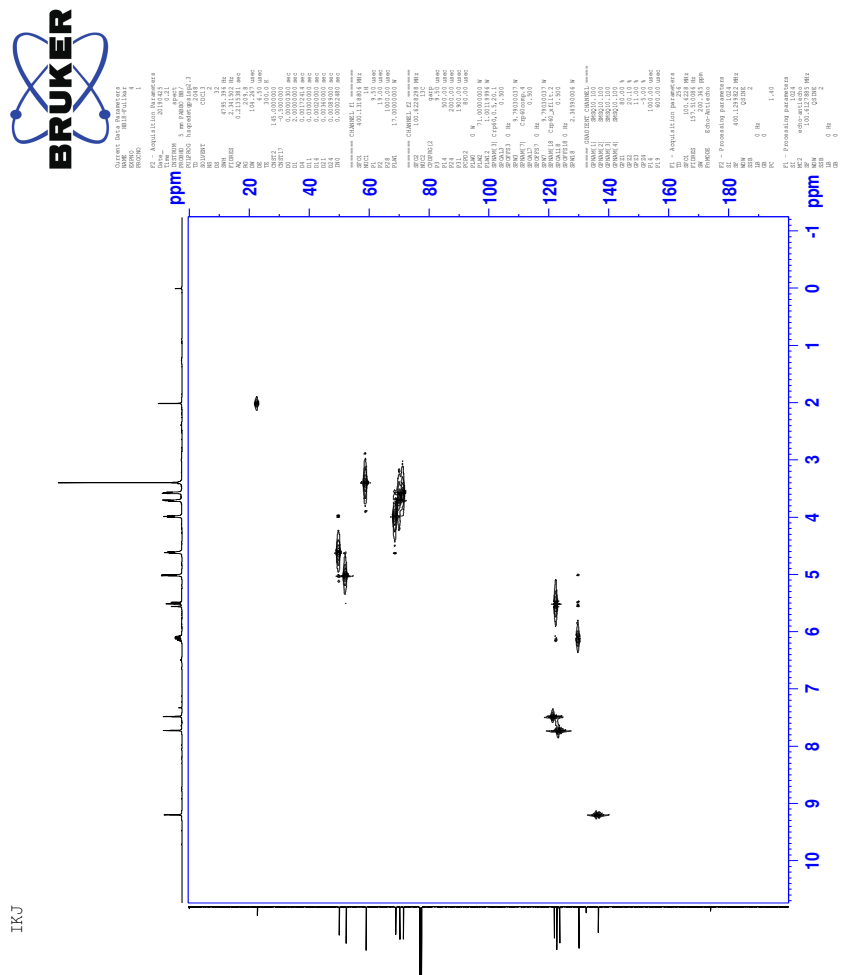
11.3 COSY-spectrum of IL 7d



TKJ

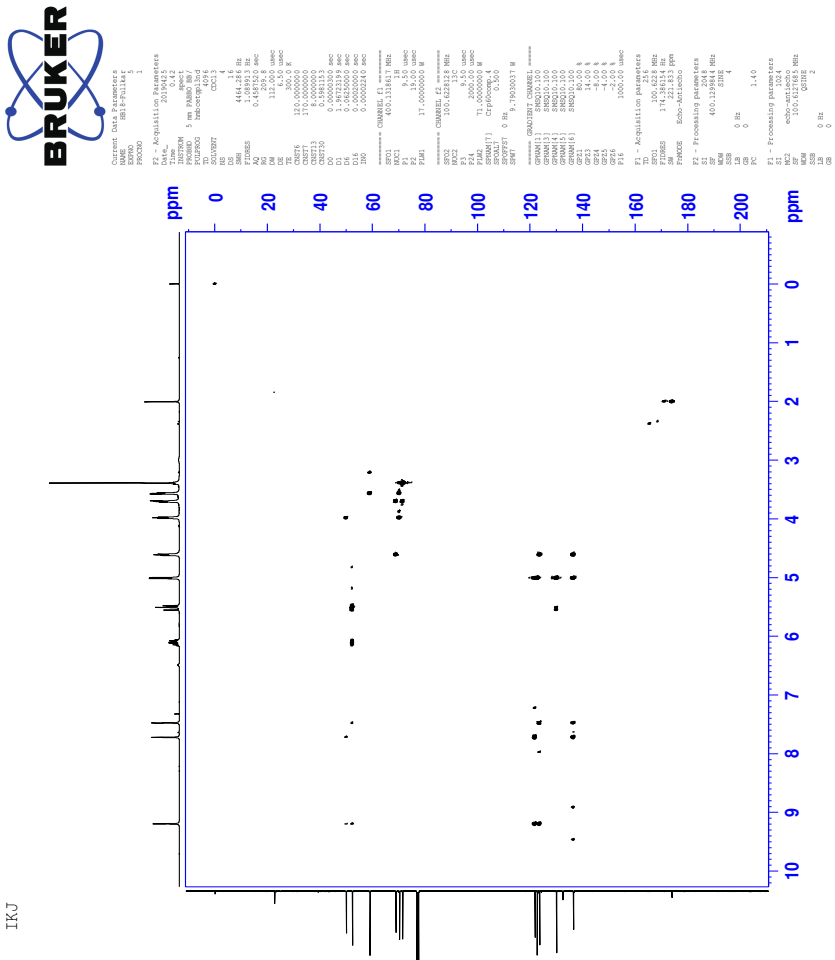
LVI

11.4 HSQC-spectrum of IL 7d

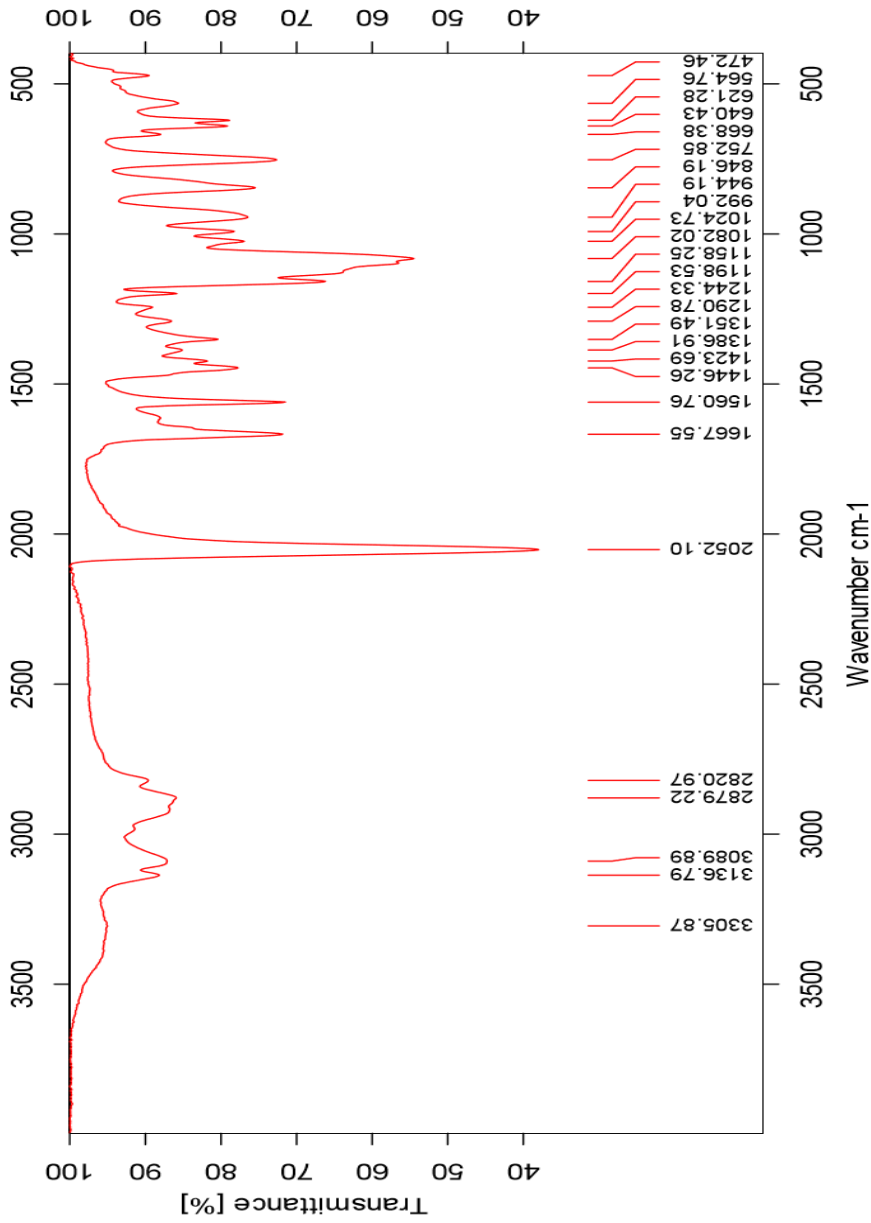


11.5 HMBC-spectrum of IL 7d

TKJ



11.6 IR-spectrum of IL 7d



11.7 HR-MS positive mode spectrum of IL 7d

Elemental Composition Report

Page 1

Single Mass Analysis

Tolerance = 5.0 PPM / DBE: min = -1.5, max = 50.0

Element prediction: Off

Number of isotope peaks used for i-FIT = 3

Monoisotopic Mass, Even Electron Ions

397 formula(e) evaluated with 1 results within limits (up to 50 closest results for each mass)

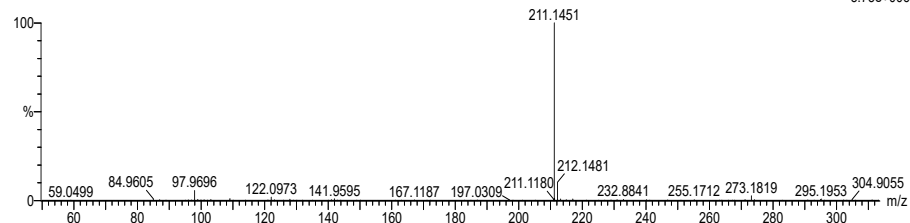
Elements Used:

C: 0-500 H: 0-1000 N: 0-10 O: 0-10 Na: 0-1

svg_20190211_73_2_75 (1.396) AM2 (Ar:35000.0.00.0.00); Cm (75:80)

1: TOF MS ES+

3.75e+006



Minimum: -1.5
Maximum: 5.0 5.0 50.0

Mass	Calc. Mass	mDa	PPM	DBE	i-FIT	Norm	Conf(%)	Formula
211.1451	211.1447	0.4	1.9	3.5	1648.9	n/a	n/a	C11 H19 N2 O2

11.8 HR-MS negative mode spectrum of IL 7d

Elemental Composition Report

Page 1

Single Mass Analysis

Tolerance = 25.0 PPM / DBE: min = -2.0, max = 50.0

Element prediction: Off

Number of isotope peaks used for i-FIT = 3

Monoisotopic Mass, Even Electron Ions

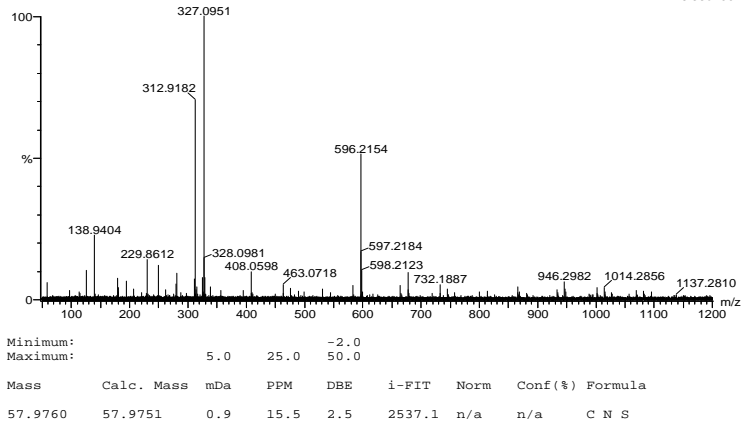
48 formula(e) evaluated with 1 results within limits (all results (up to 1000) for each mass)

Elements Used:

C: 0-100 H: 0-150 B: 0-2 N: 0-10 O: 0-8 S: 0-2 Cl: 0-2 Br: 0-3

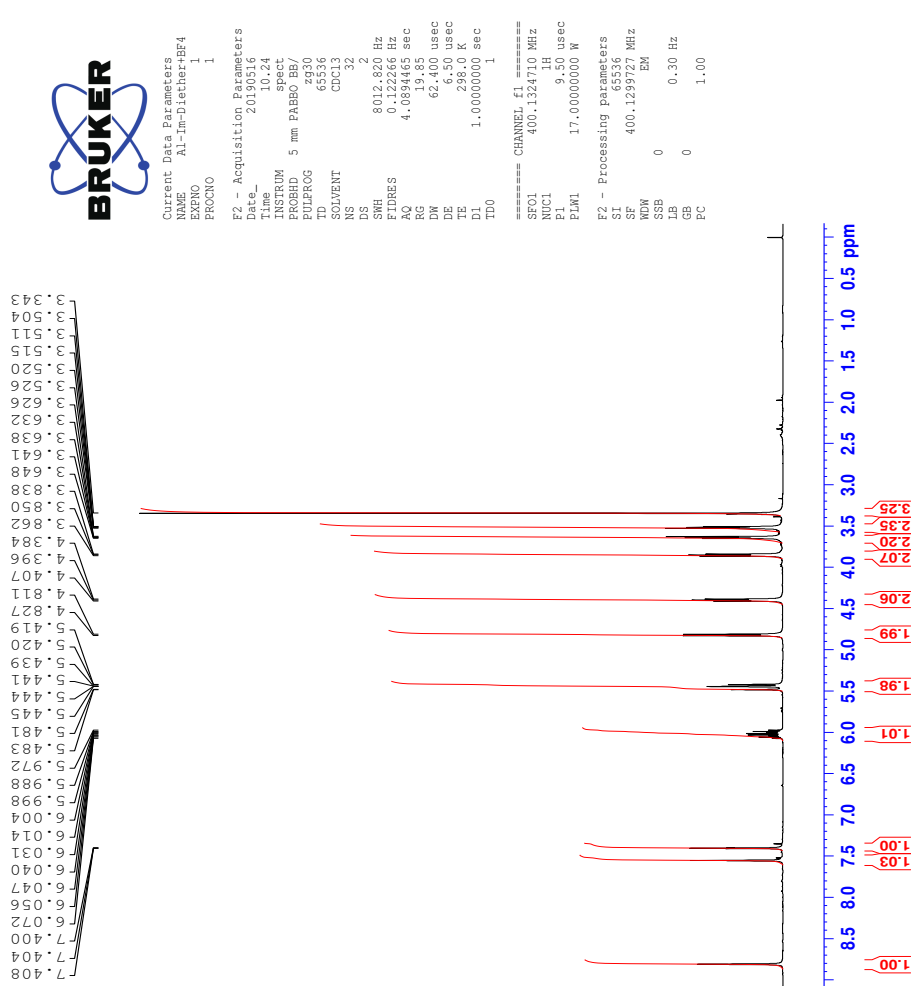
svg_20190211_74X 48 (0.547) AM2 (Ar,35000.0,0.00,0.00); Cm (48:51)
1: TOF MS ES-

5.33e+004

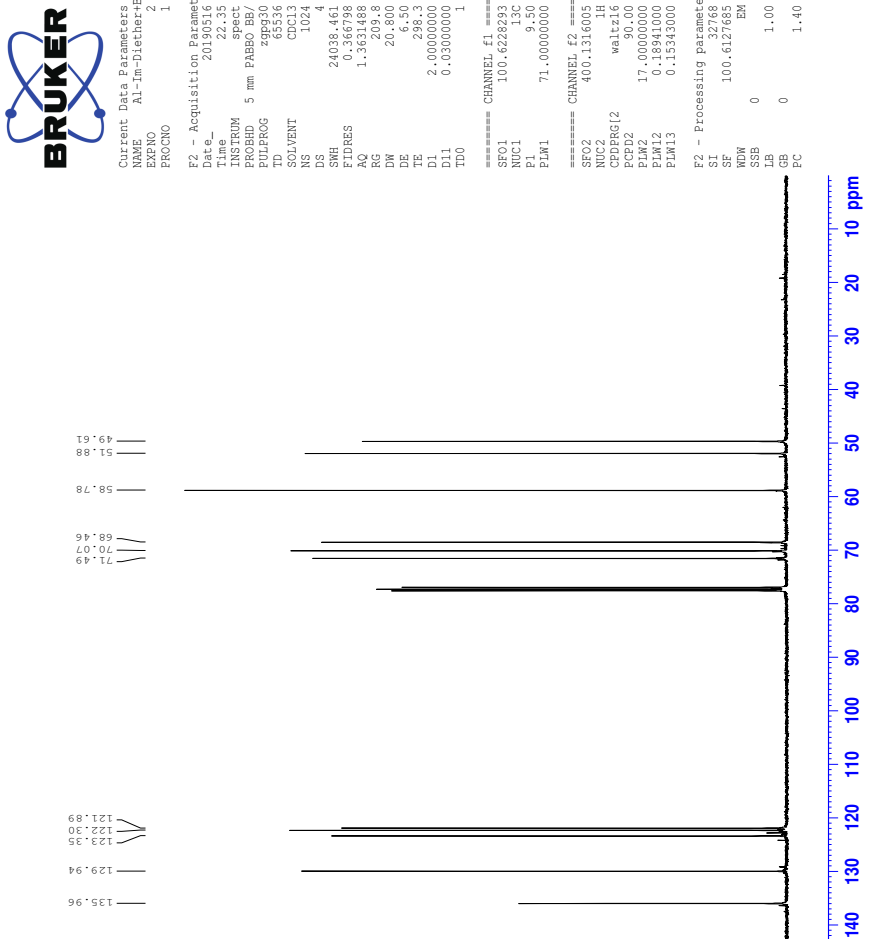


12 Spectra of IL 7e

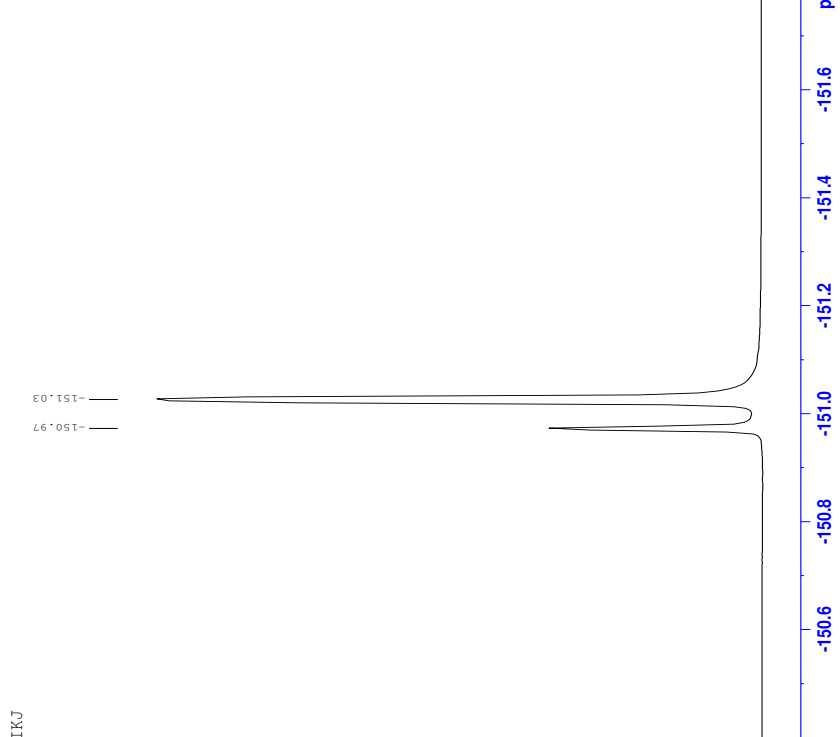
12.1 ^1H -NMR spectrum of IL 7e



12.2 ^{13}C -NMR spectrum of IL 7e

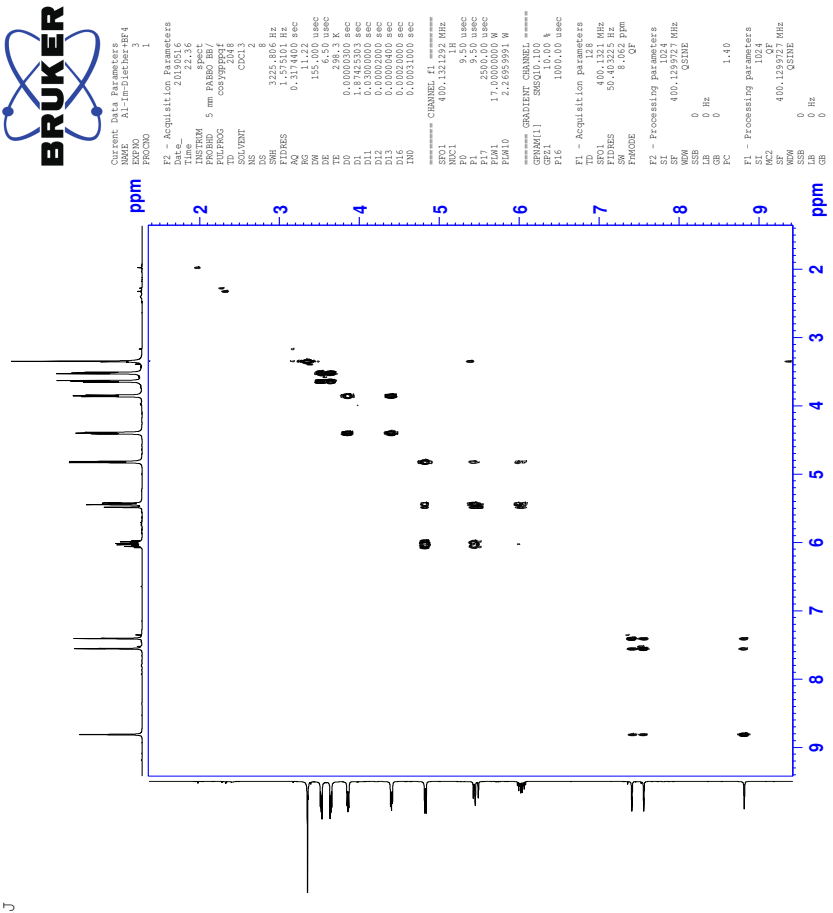


12.3 ^{19}F -NMR spectrum of IL 7e



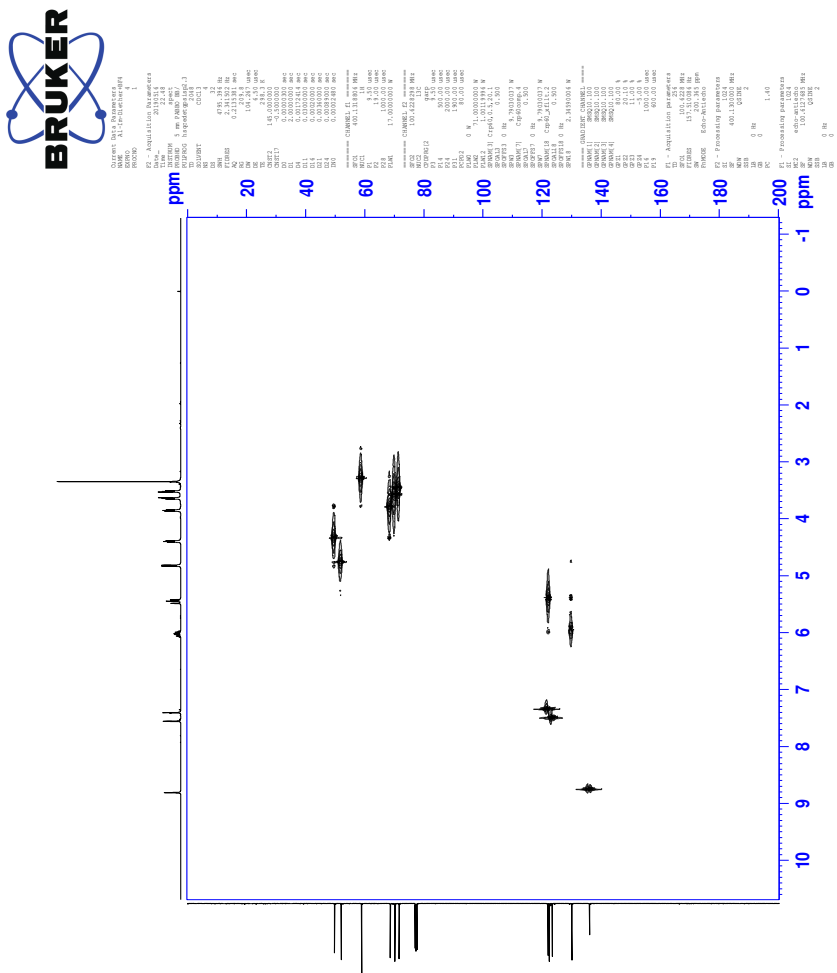
TKJ

12.4 COSY-spectrum of IL 7e

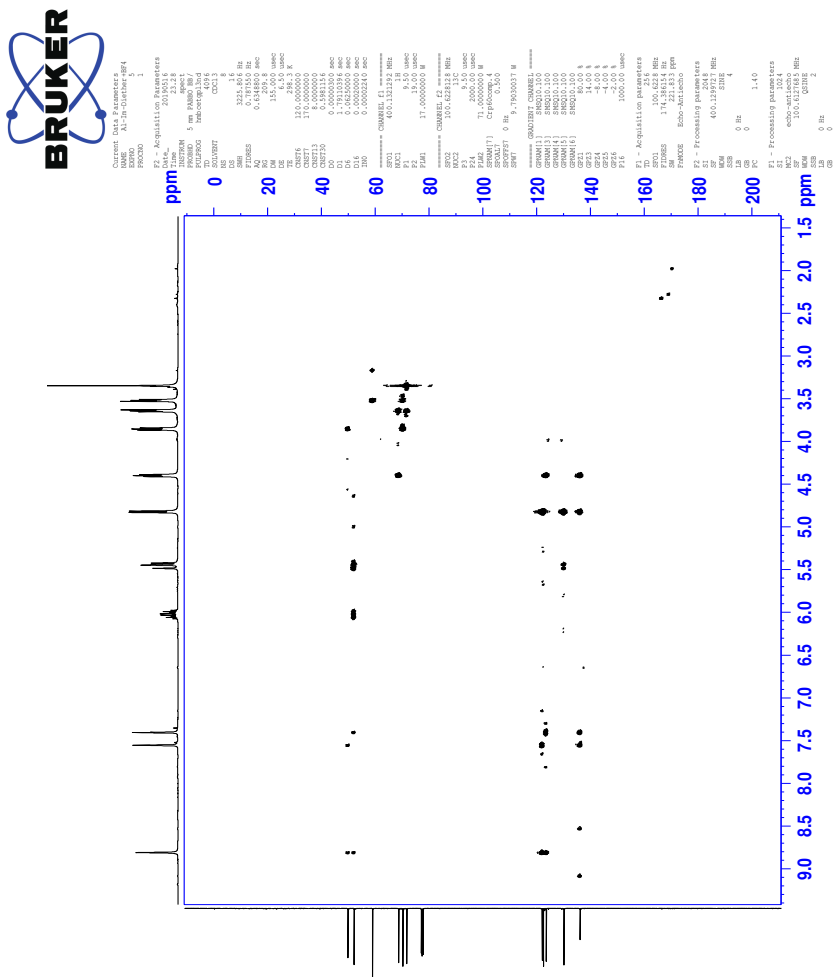


TKJ

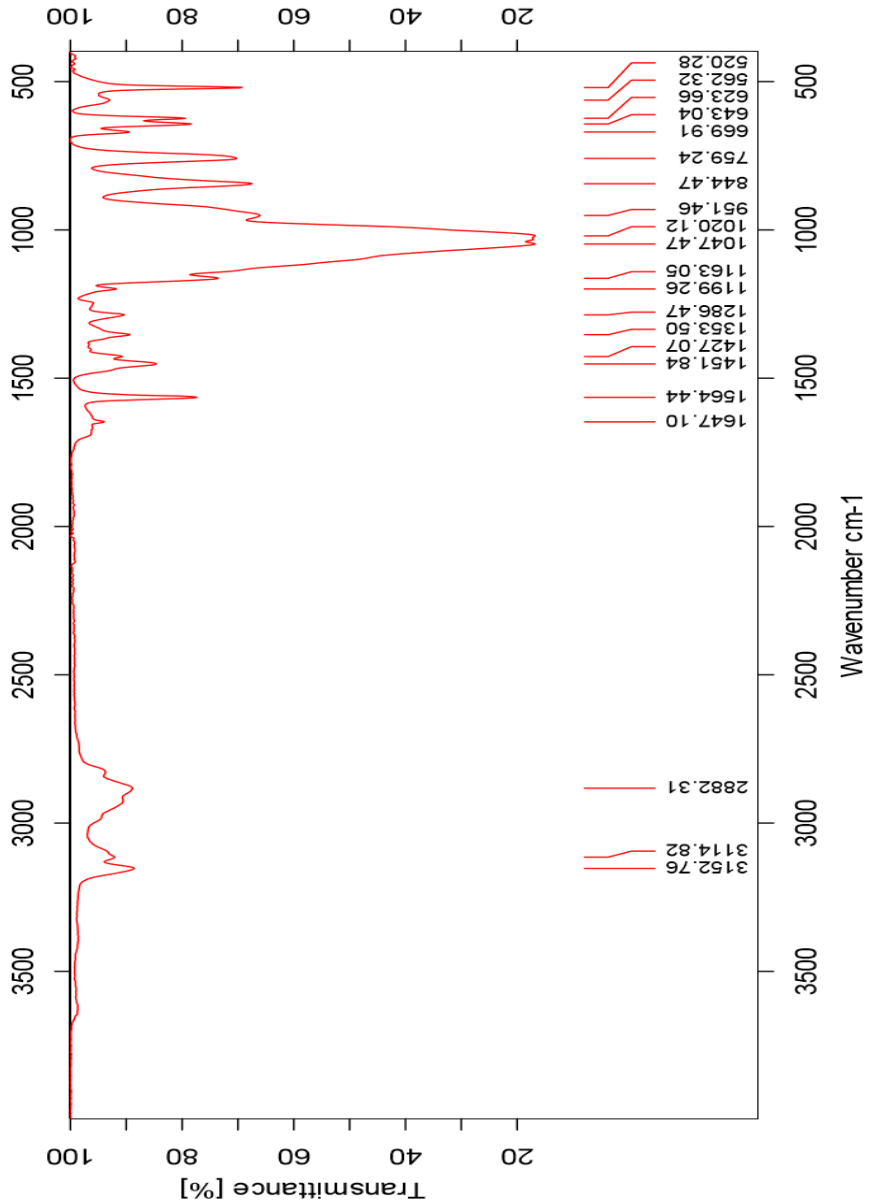
12.5 HSQC-spectrum of IL 7e



12.6 HMBC-spectrum of IL 7e



12.7 IR-spectrum of IL 7e



12.8 HR-MS positive mode spectrum of IL 7e

Elemental Composition Report

Page 1

Single Mass Analysis

Tolerance = 2.0 PPM / DBE: min = -50.0, max = 50.0

Element prediction: Off

Number of isotope peaks used for i-FIT = 3

Monoisotopic Mass, Even Electron Ions

660 formula(e) evaluated with 1 results within limits (all results (up to 1000) for each mass)

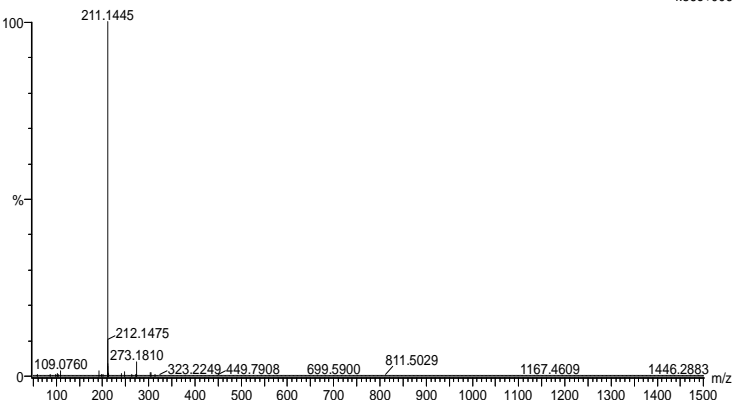
Elements Used:

C: 0-100 H: 0-150 N: 0-10 O: 0-10

2019_498FIA18 (0.339) AM2 (Ar,35000.0,0.00,0.00); Cm (10:18)

1: TOF MS ES+

4.86e+006



Minimum: -50.0

Maximum: 5.0 2.0 50.0

Mass	Calc. Mass	mDa	PPM	DBE	i-FIT	Norm	Conf (%)	Formula
211.1445	211.1447	-0.2	-0.9	3.5	1823.0	n/a	n/a	C11 H19 N2 O2

12.9 HR-MS negative mode spectrum of IL 7e

Elemental Composition Report

Page 1

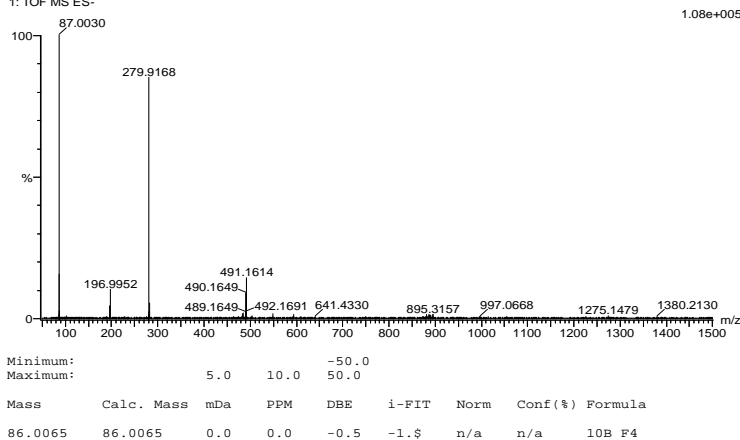
Single Mass Analysis

Tolerance = 10.0 PPM / DBE: min = -50.0, max = 50.0
Element prediction: Off
Number of isotope peaks used for i-FIT = 3

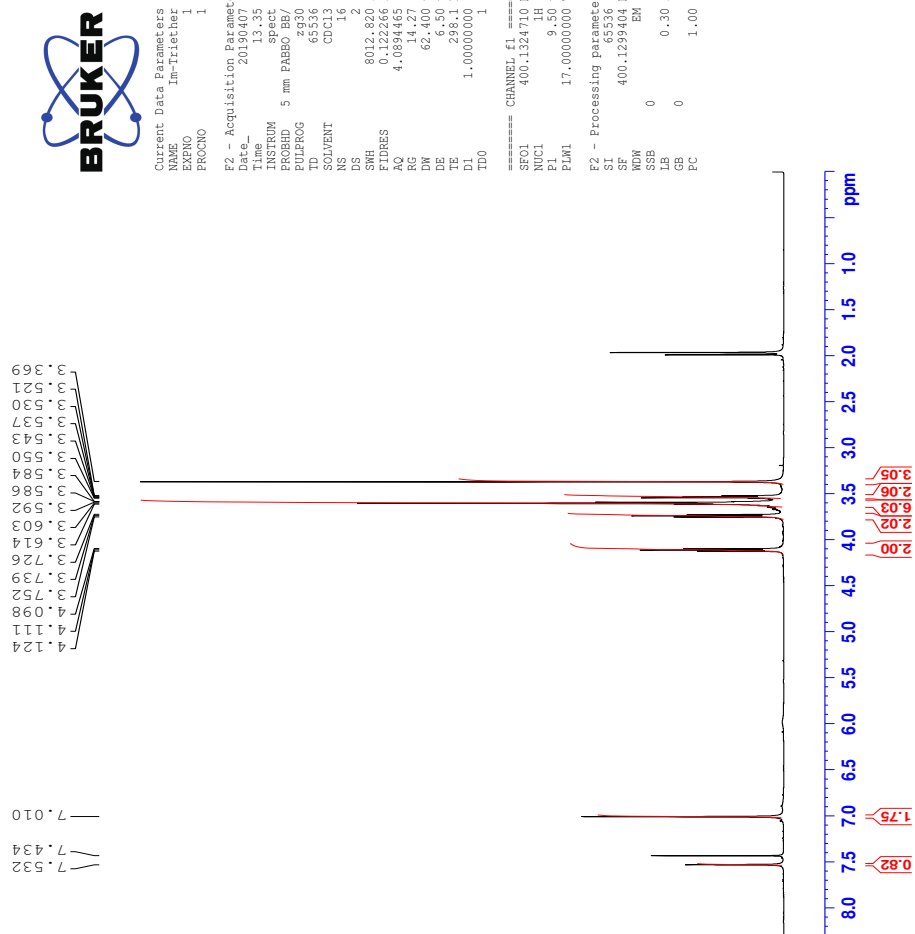
Monoisotopic Mass, Even Electron Ions
423 formula(e) evaluated with 1 results within limits (all results up to 1000) for each mass

Elements Used:

C: 0-100 H: 0-150 10B: 0-1 11B: 0-1 N: 0-10 O: 0-10 F: 0-8
2019_499neg 61 (0.691) AM2 (Ar,35000.0,0.00,0.00); Cm (61.66)
1: TOF MS ES-

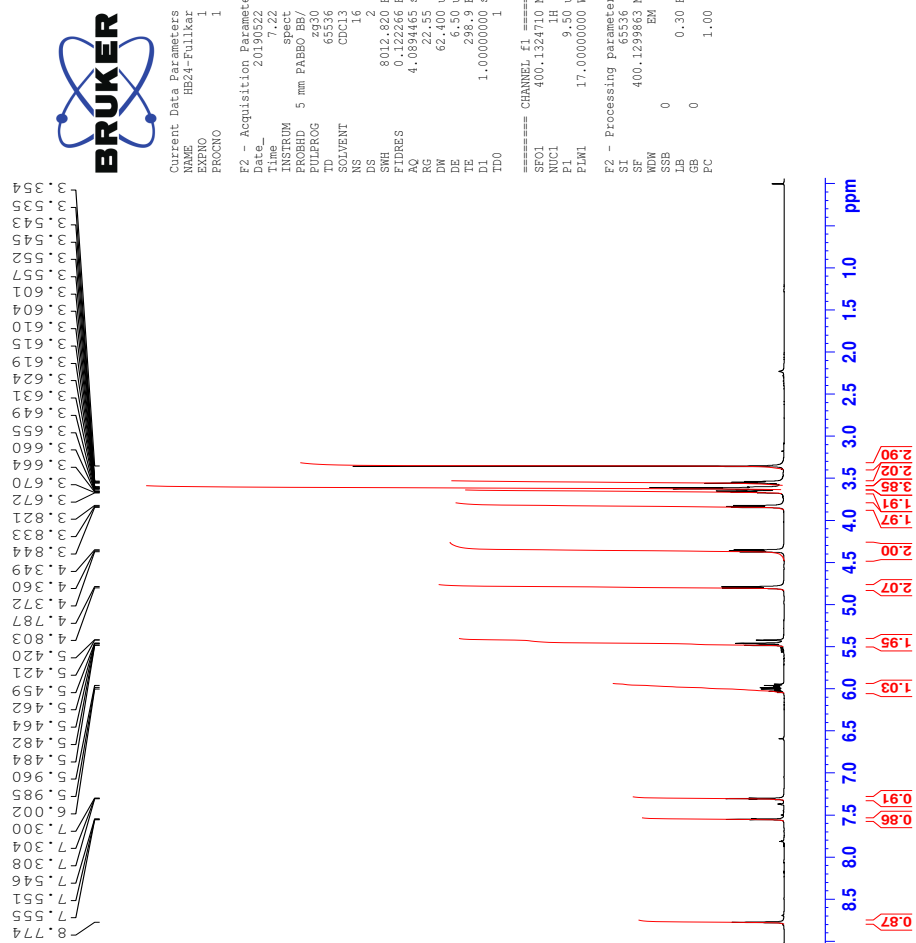


13 $^1\text{H-NMR}$ spectrum of compound 5

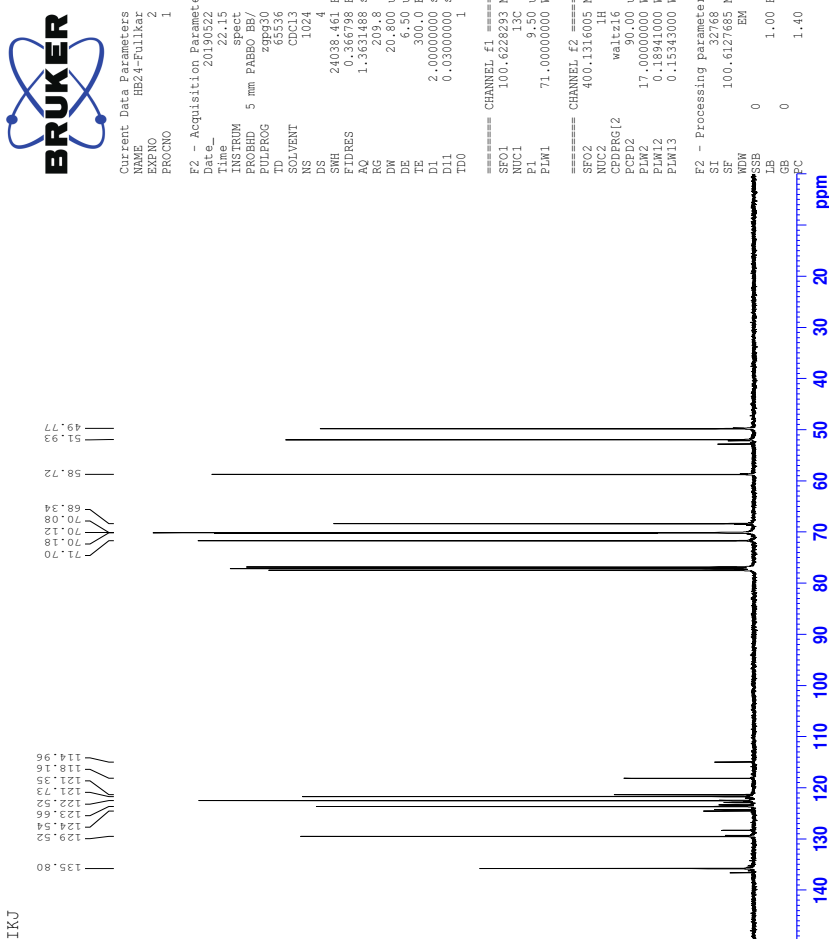


14 Spectra of IL 8b

14.1 ^1H -NMR spectrum of IL 8b

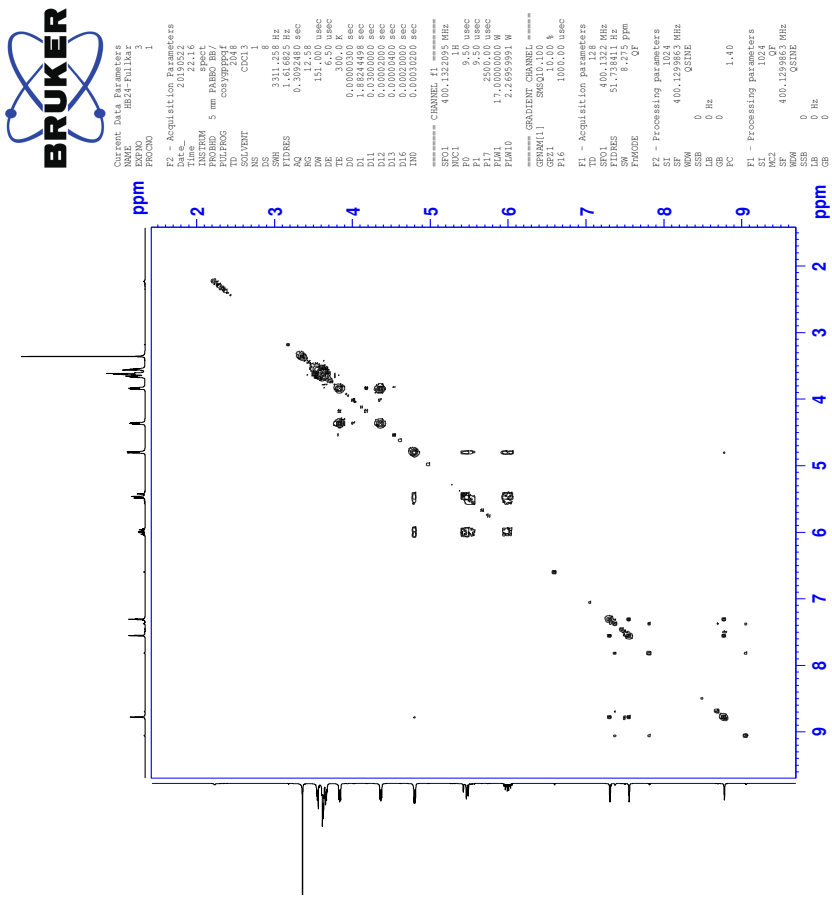


14.2 ^{13}C -NMR spectrum of IL 8b

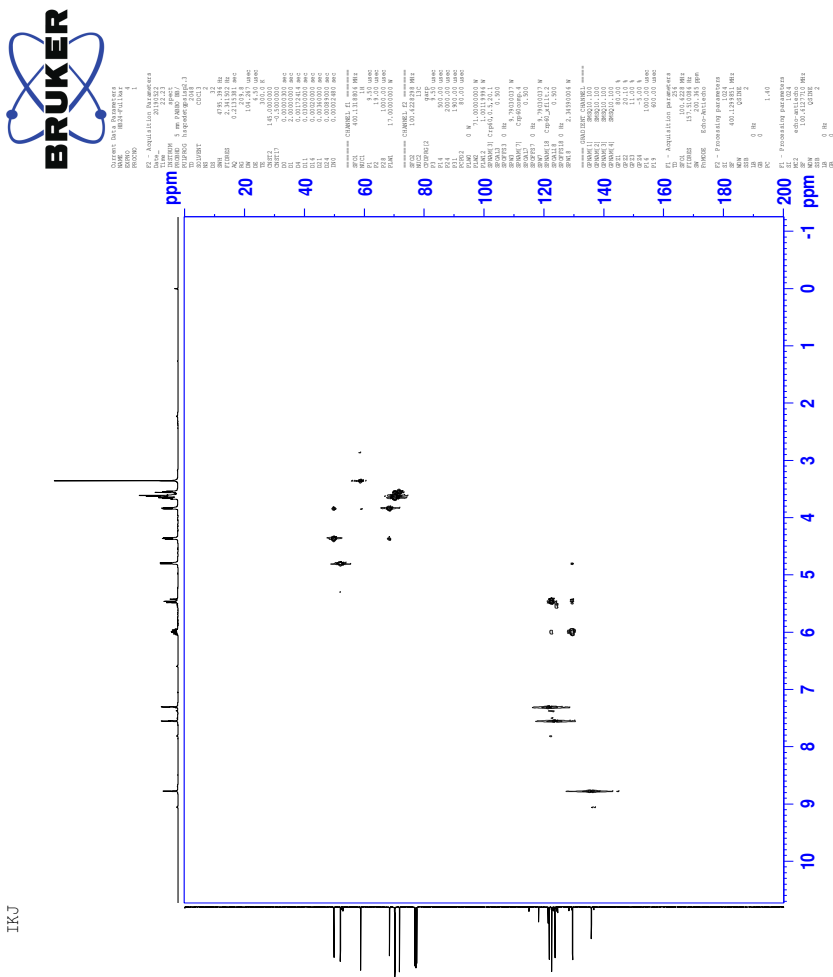


14.3 COSY-spectrum of IL 8b

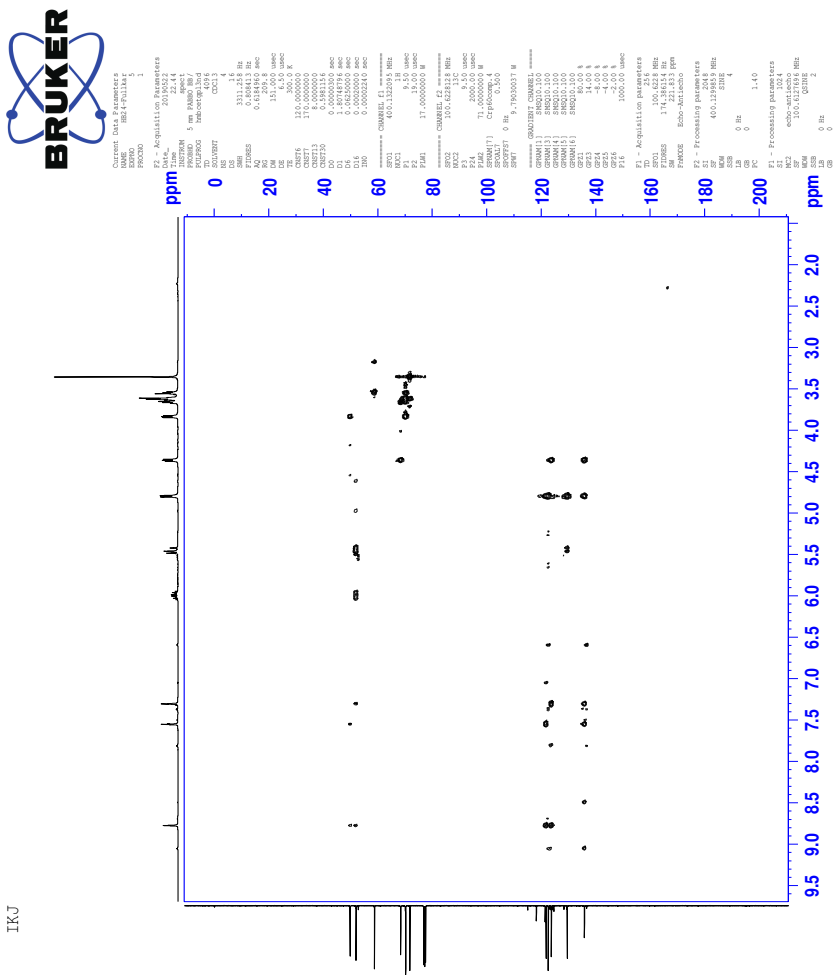
TKJ



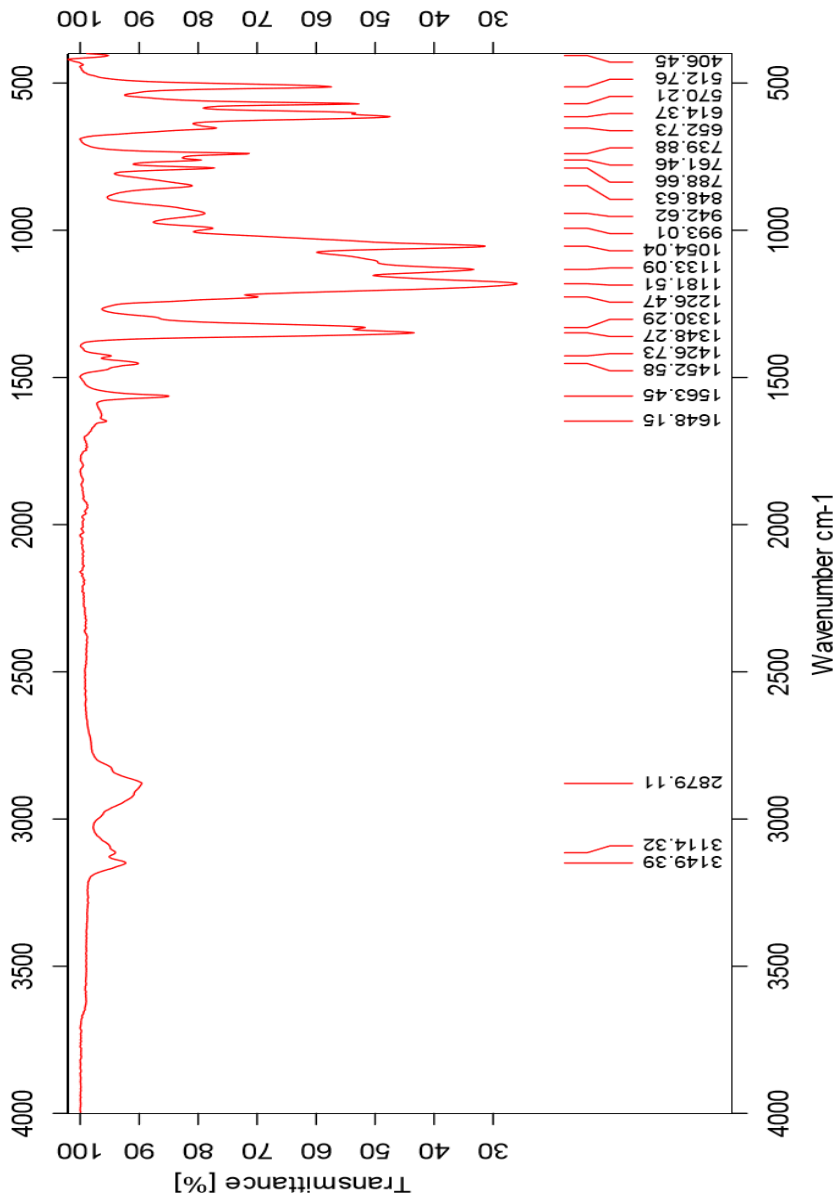
14.4 HSQC-spectrum of IL 8b



14.5 HMBC-spectrum of IL 8b



14.6 IR-spectrum of IL 8b



14.7 HR-MS positive mode spectrum of IL 8b

Elemental Composition Report

Page 1

Single Mass Analysis

Tolerance = 5.0 PPM / DBE: min = -1.5, max = 50.0

Element prediction: Off

Number of isotope peaks used for i-FIT = 3

Monoisotopic Mass, Even Electron Ions

554 formula(e) evaluated with 1 results within limits (up to 50 closest results for each mass)

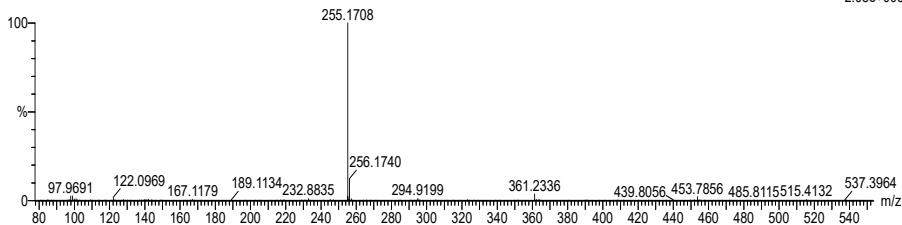
Elements Used:

C: 0-500 H: 0-1000 N: 0-10 O: 0-10 Na: 0-1

svg_20190211_75_18 (0.339) AM2 (Ar,35000.0,0.00,0.00); Cm (13:18)

1: TOF MS ES+

2.08e+006



Minimum: -1.5
Maximum: 5.0 5.0 50.0

Mass	Calc. Mass	mDa	PPM	DBE	i-FIT	Norm	Conf(%)	Formula
255.1708	255.1709	-0.1	-0.4	3.5	1469.1	n/a	n/a	C ₁₃ H ₂₃ N ₂ O ₃

14.8 HR-MS negative mode spectrum of IL 8b

Elemental Composition Report

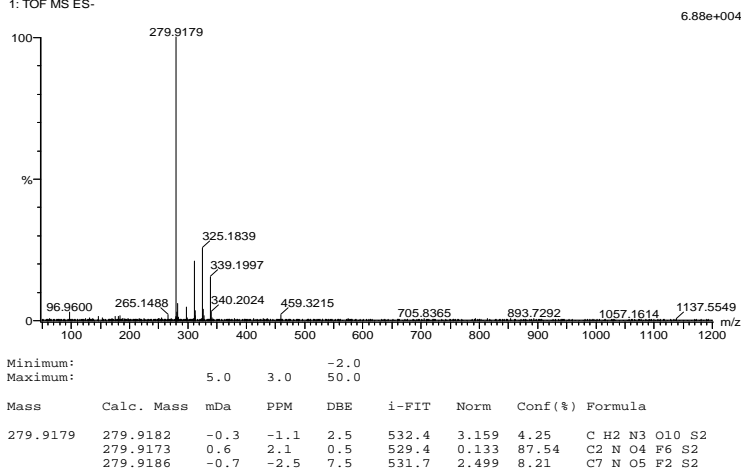
Page 1

Single Mass Analysis

Tolerance = 3.0 PPM / DBE: min = -2.0, max = 50.0
 Element prediction: Off
 Number of isotope peaks used for i-FIT = 3

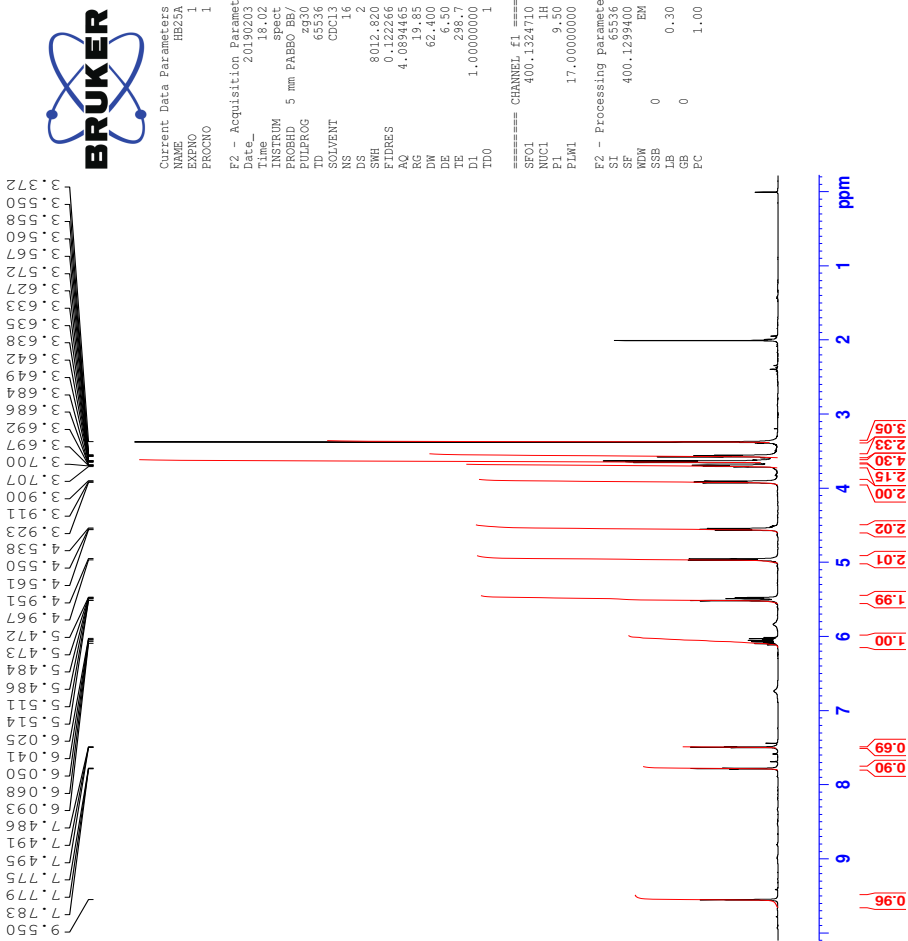
Monoisotopic Mass, Even Electron Ions
 4155 formula(e) evaluated with 3 results within limits (all results (up to 1000) for each mass)
 Elements Used:

C: 0-100 H: 0-150 N: 0-10 O: 0-10 F: 0-10 S: 0-2
 svg_20190211_76X24 (0.278) AM2 (Ar,35000.0,0.00,0.00)
 1: TOF MS ES-

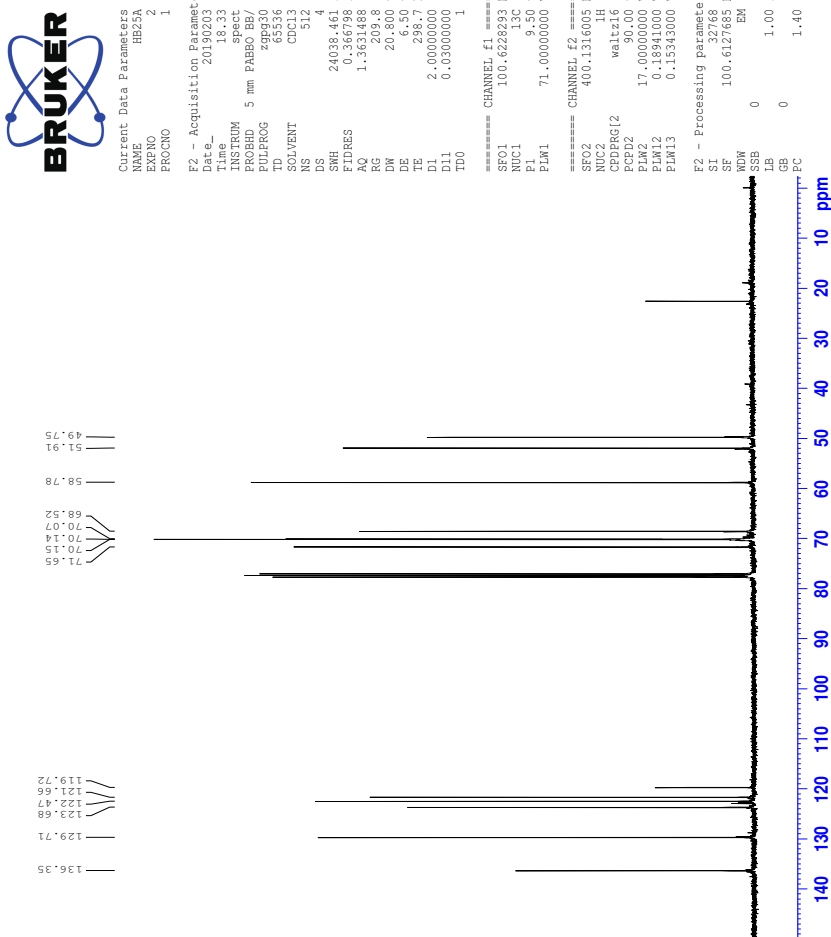


15 Spectra of IL 8c

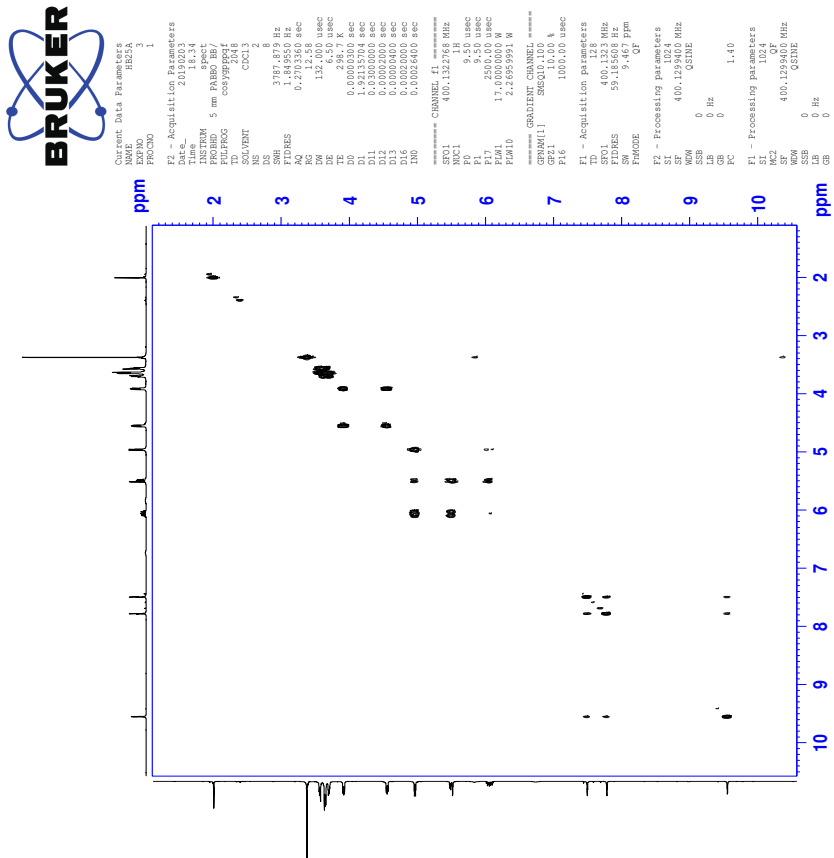
15.1 ^1H -NMR spectrum of IL 8c



15.2 ^{13}C -NMR spectrum of IL 8c

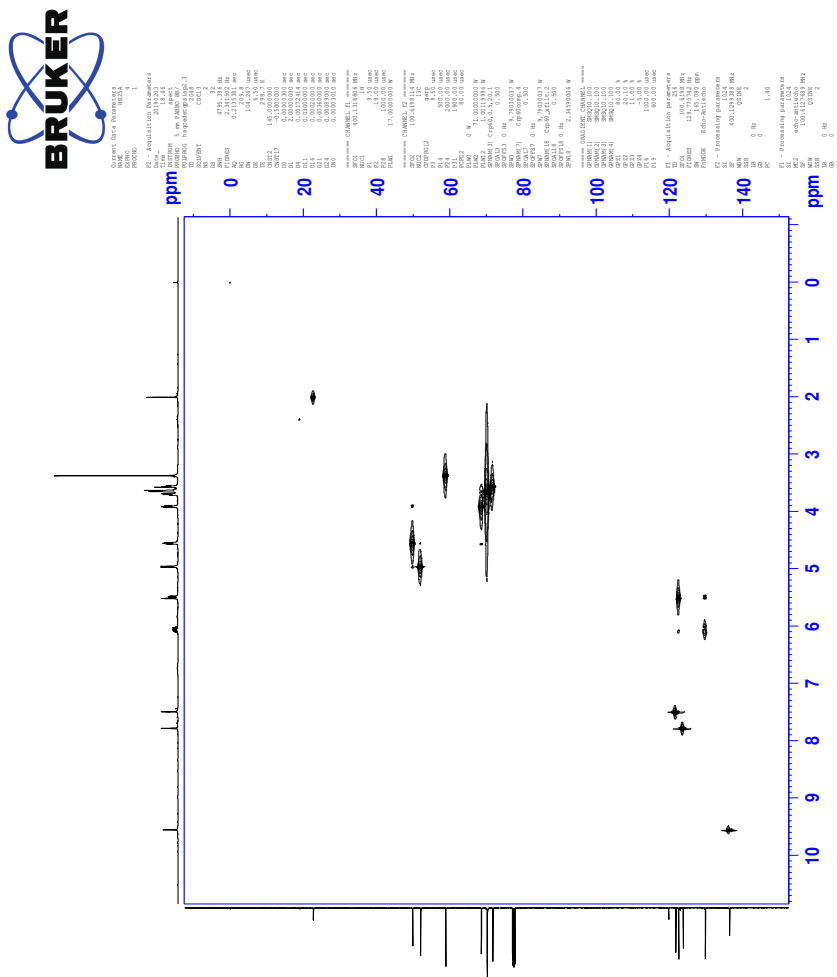


15.3 COSY-spectrum of IL 8c

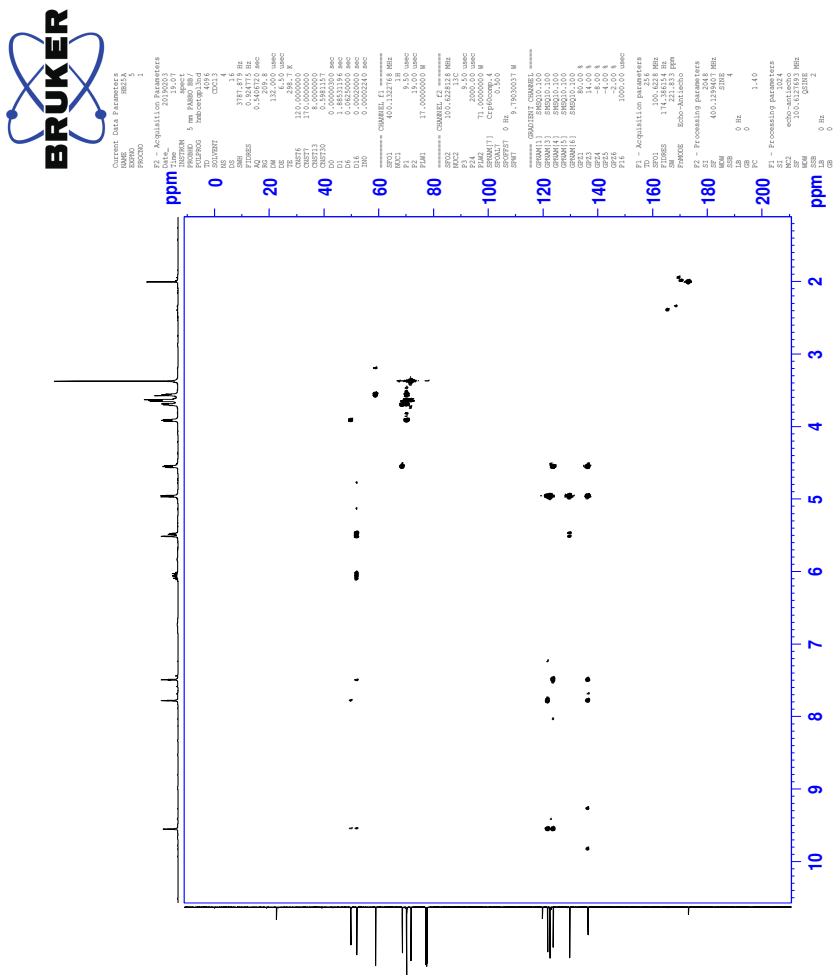


TKJ

15.4 HSQC-spectrum of IL 8c



15.5 HMBC-spectrum of IL 8c



15.6 IR-spectrum of IL 8c

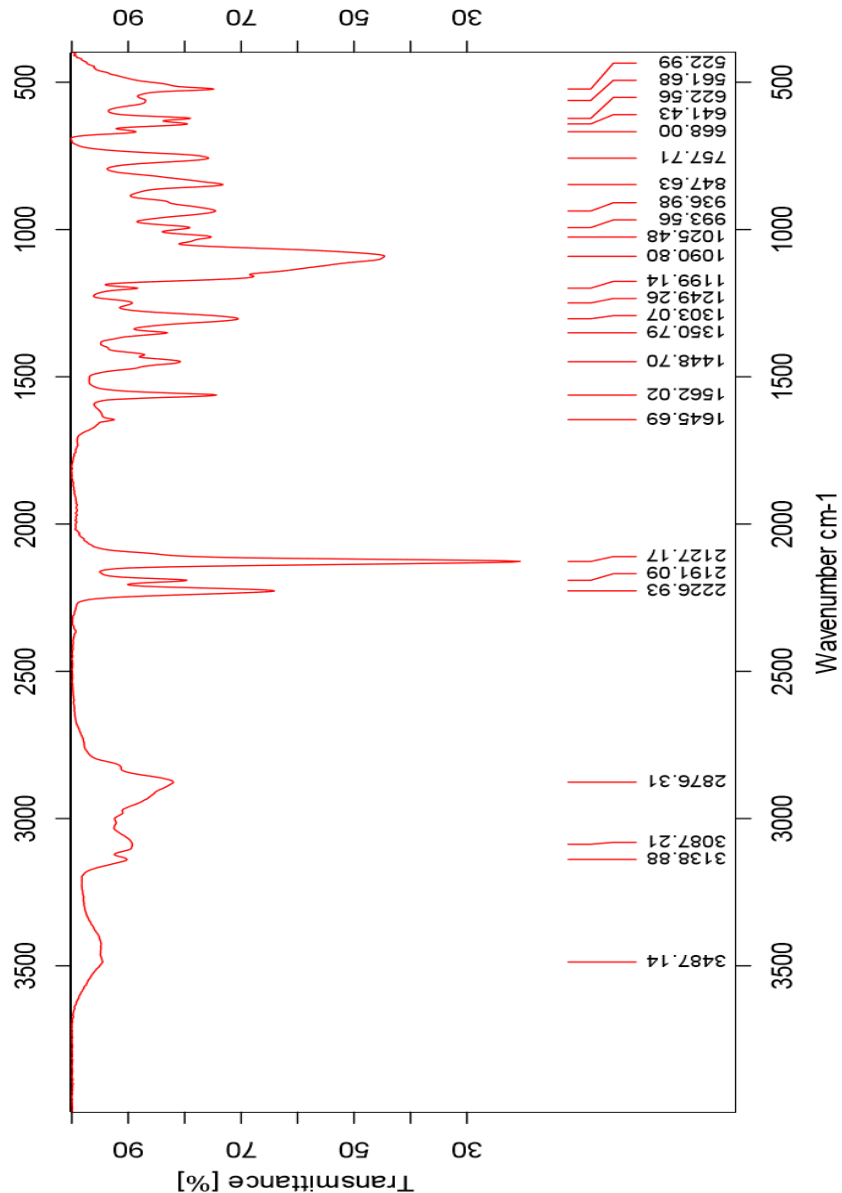


Figure 1: Caption

15.7 HR-MS positive mode spectrum of IL 8c

Elemental Composition Report

Page 1

Single Mass Analysis

Tolerance = 5.0 PPM / DBE: min = -1.5, max = 50.0

Element prediction: Off

Number of isotope peaks used for i-FIT = 3

Monoisotopic Mass, Even Electron Ions

554 formula(e) evaluated with 1 results within limits (up to 50 closest results for each mass)

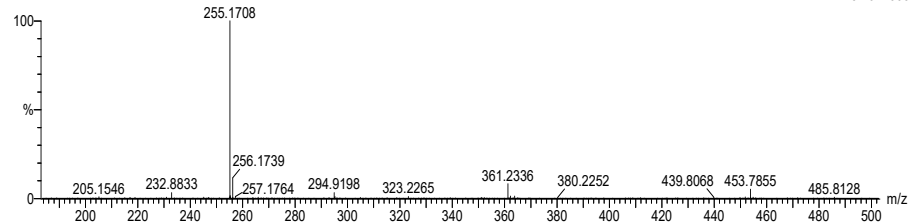
Elements Used:

C: 0-500 H: 0-1000 N: 0-10 O: 0-10 Na: 0-1

svg_20190211_77_17 (0.322) AM2 (Ar:35000.0.00.0.00); Cm (12:17)

1: TOF MS ES+

8.76e+005



Minimum: -1.5
Maximum: 5.0 5.0 50.0

Mass	Calc. Mass	mDa	PPM	DBE	i-FIT	Norm	Conf(%)	Formula
255.1708	255.1709	-0.1	-0.4	3.5	1296.2	n/a	n/a	C13 H23 N2 O3

15.8 HR-MS negative mode spectrum of IL 8c

Elemental Composition Report

Page 1

Single Mass Analysis

Tolerance = 50.0 PPM / DBE: min = -1.5, max = 50.0

Element prediction: Off

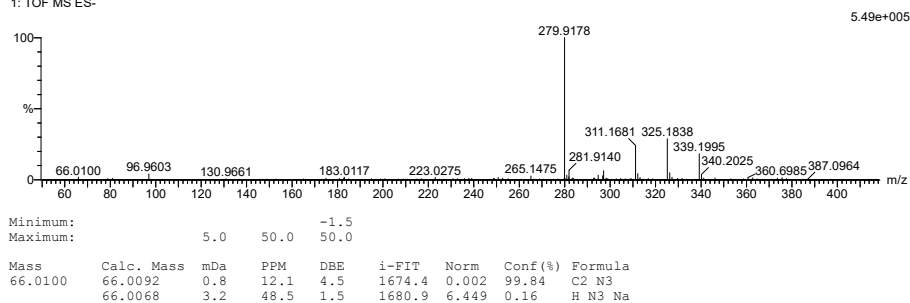
Number of isotope peaks used for i-FIT = 3

Monoisotopic Mass, Even Electron Ions

37 formula(e) evaluated with 2 results within limits (up to 50 closest results for each mass)

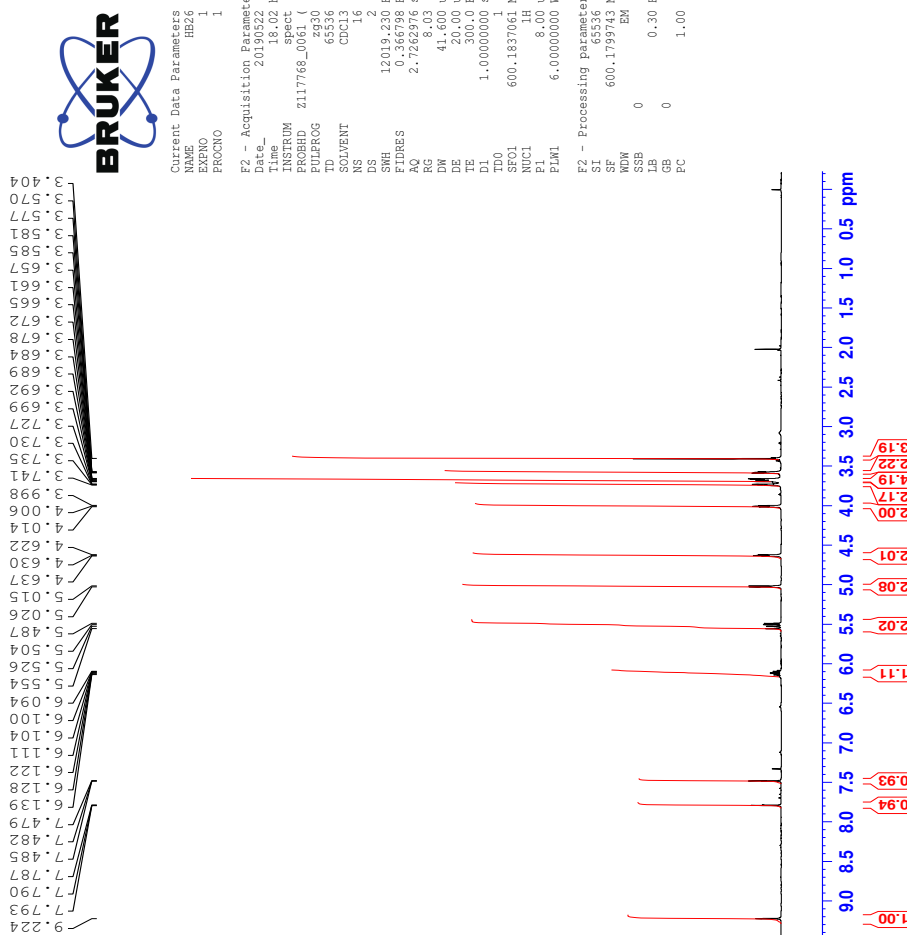
Elements Used:

C: 0-500 H: 0-1000 N: 0-10 O: 0-10 Na: 0-1 S: 0-3
svg_20190211_78X76 (0.856) AM2 (Ar,35000.0,0.00,0.00); Cr (68:80)
1: TOF MS ES⁻

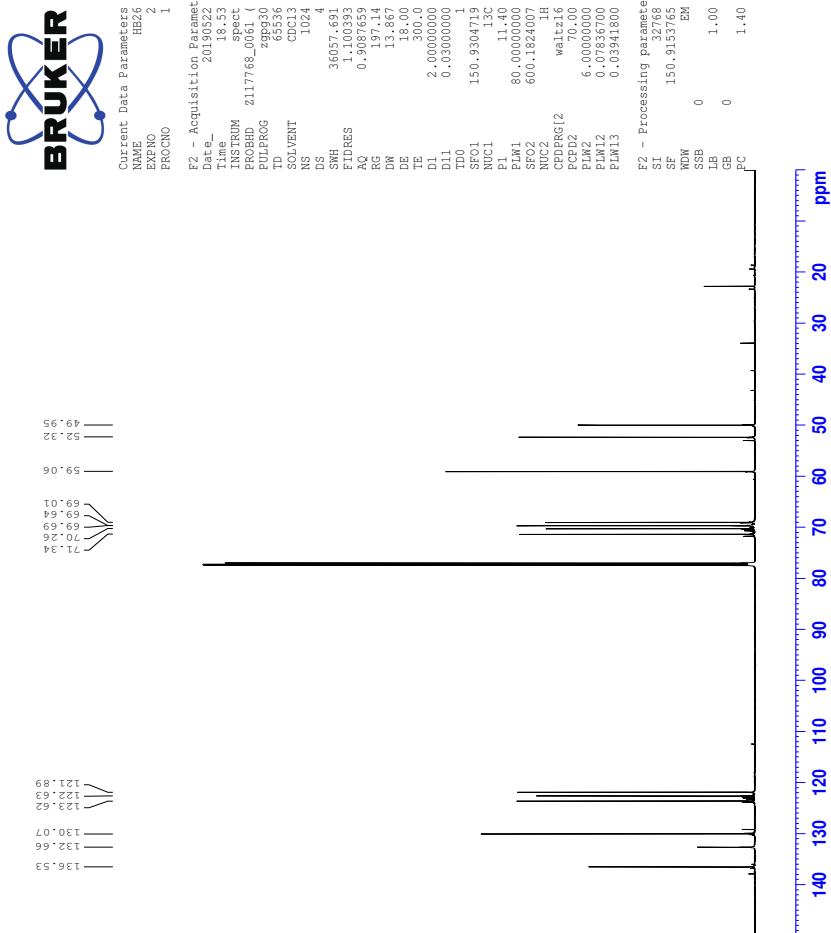


16 Spectra of IL 8d

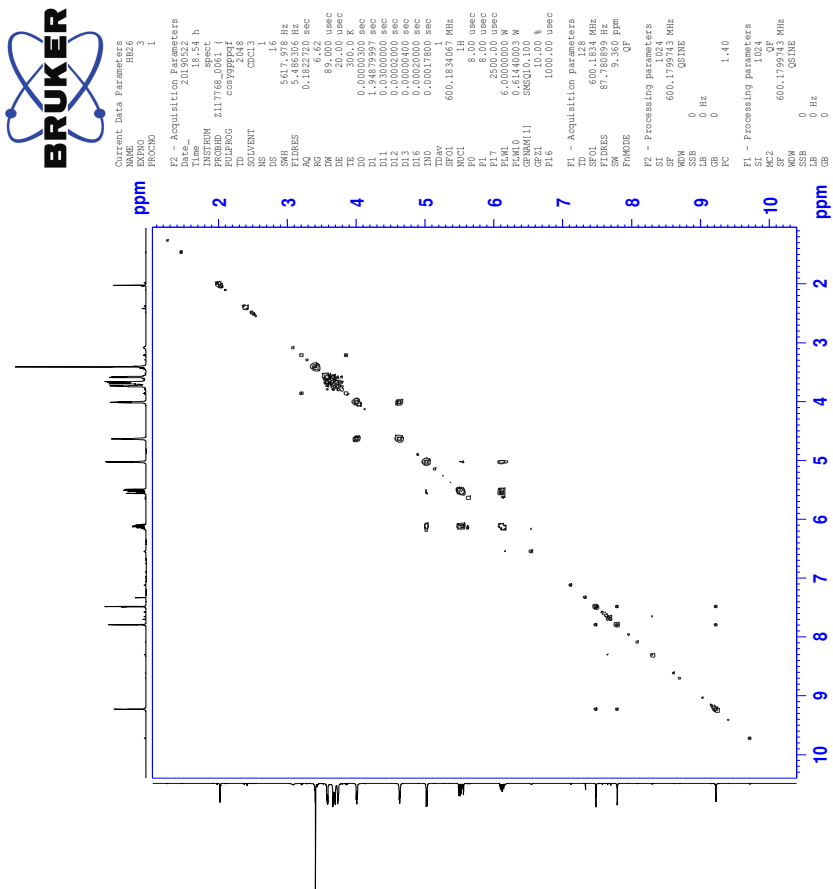
16.1 ^1H -NMR spectrum of IL 8d



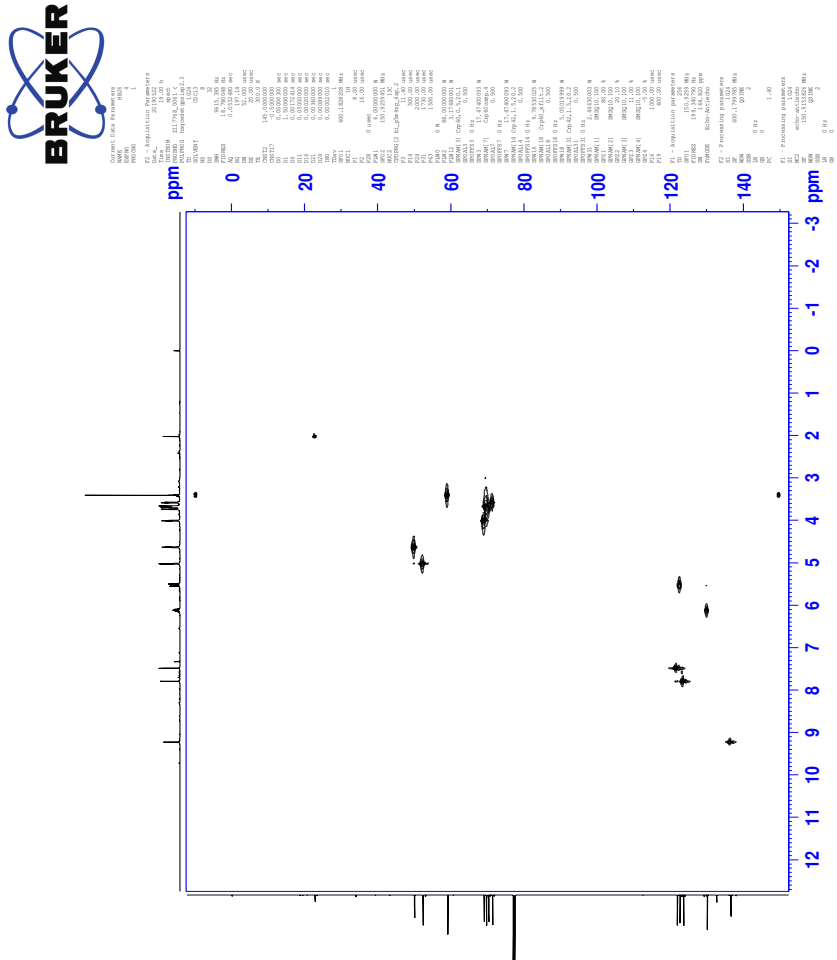
16.2 ^{13}C -NMR spectrum of IL 8d



16.3 COSY-spectrum of IL 8d

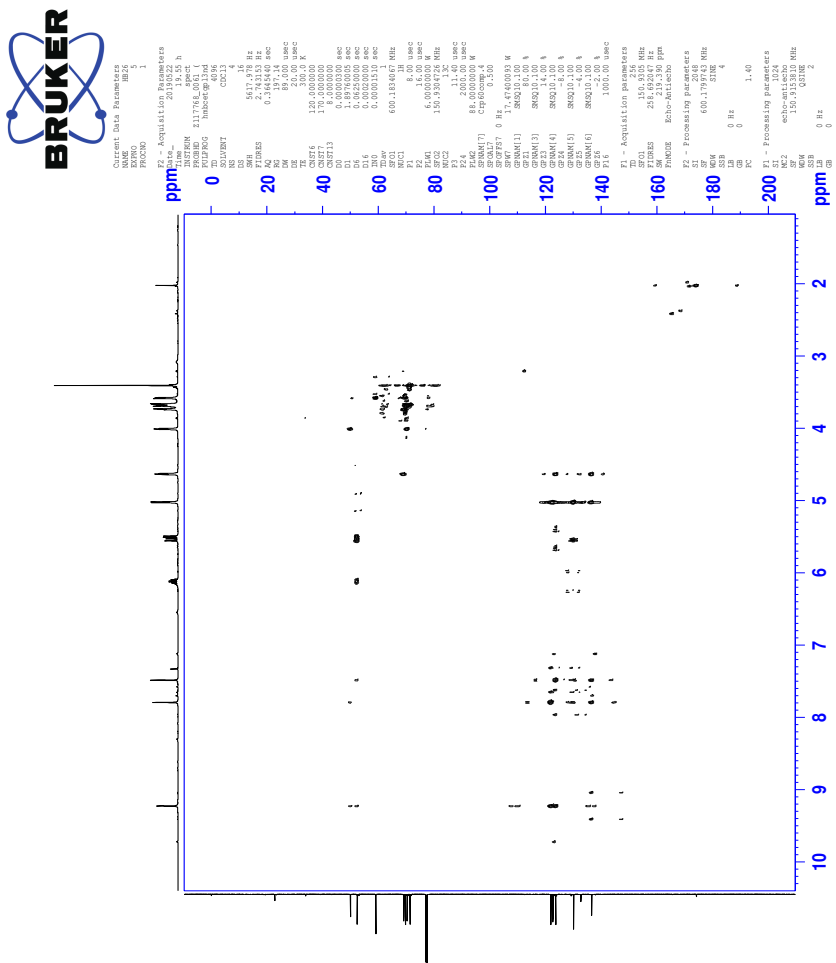


16.4 HSQC-spectrum of IL 8d



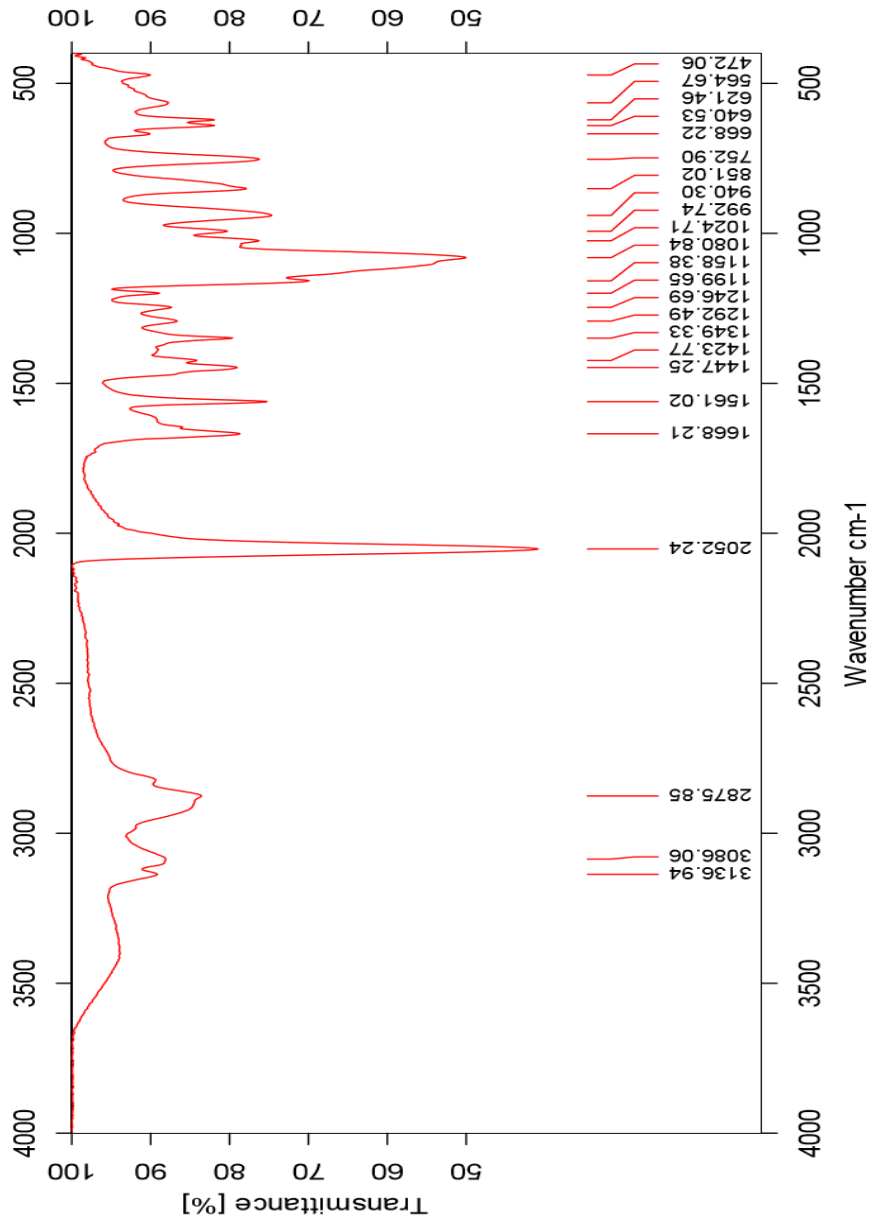
XCI

16.5 HMBC-spectrum of IL 8d



XCII

16.6 IR-spectrum of IL 8d



16.7 HR-MS positive mode spectrum of IL 8d

Elemental Composition Report

Page 1

Single Mass Analysis

Tolerance = 5.0 PPM / DBE: min = -2.0, max = 50.0

Element prediction: Off

Number of isotope peaks used for i-FIT = 3

Monoisotopic Mass, Even Electron Ions

925 formula(e) evaluated with 2 results within limits (all results (up to 1000) for each mass)

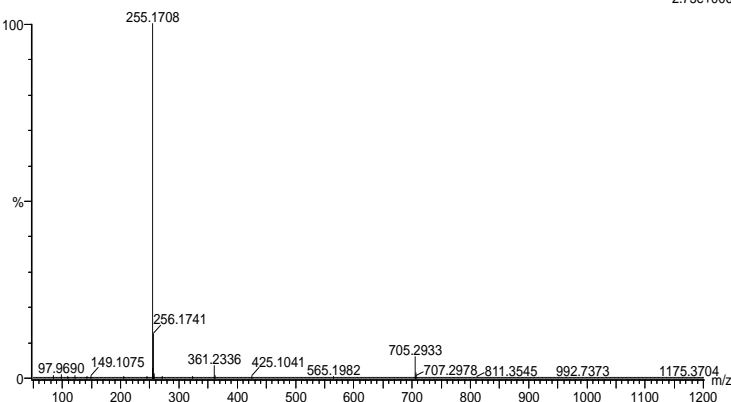
Elements Used:

C: 0-100 H: 0-150 N: 0-10 O: 0-10 P: 0-3

svg_20190211_79 94 (1.745) AM2 (Ar,35000.0,0.00,0.00); Cm (94.95)

1: TOF MS ES+

2.75e+006



Minimum: -2.0
Maximum: 5.0 5.0 50.0

Mass	Calc. Mass	mDa	PPM	DBE	i-FIT	Norm	Conf (%)	Formula
255.1708	255.1709	-0.1	-0.4	3.5	1484.8	0.046	95.50	C13 H23 N2 O3
	255.1698	1.0	3.9	-0.5	1487.8	3.100	4.50	C7 H24 N6 O2 P

16.8 HR-MS negative mode spectrum of IL 8d

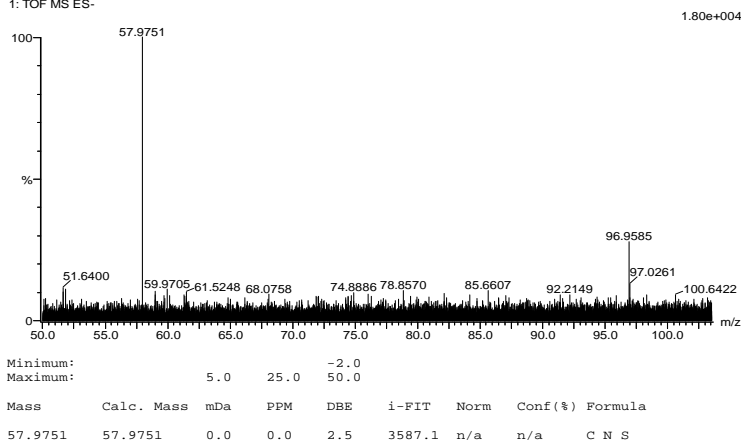
Elemental Composition Report

Page 1

Single Mass Analysis

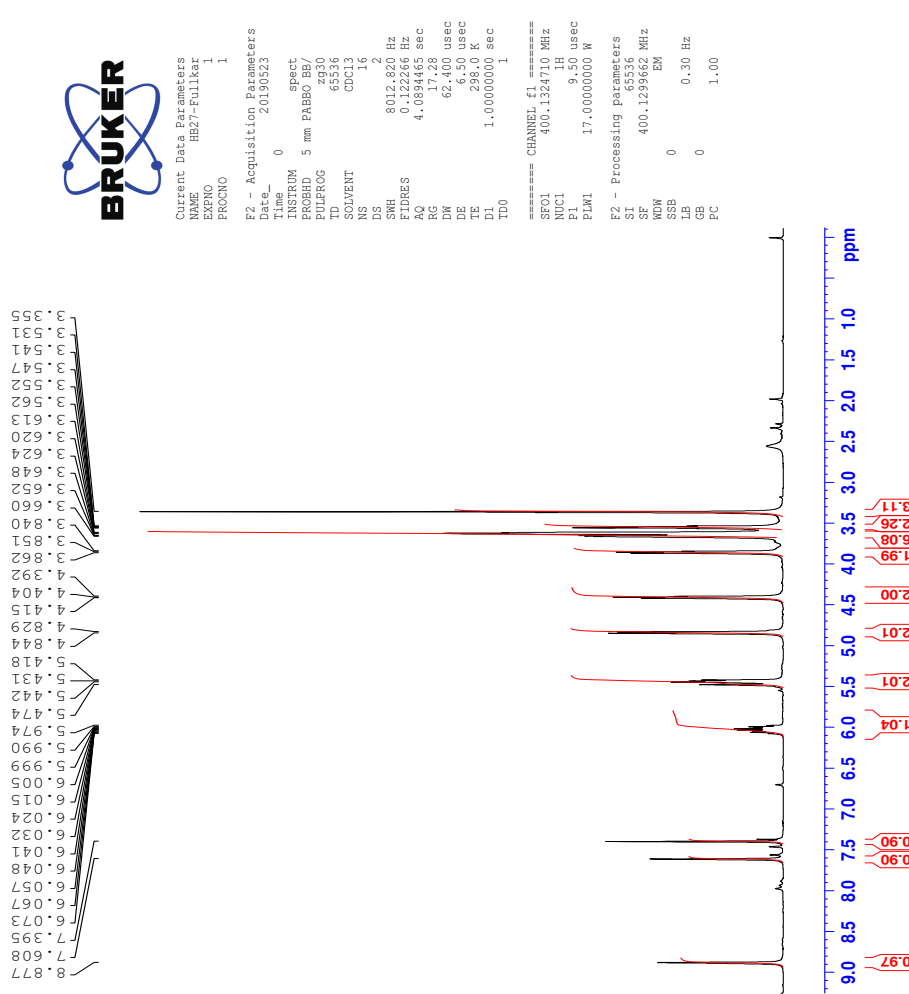
Tolerance = 25.0 PPM / DBE: min = -2.0, max = 50.0
Element prediction: Off
Number of isotope peaks used for i-FIT = 3

Monoisotopic Mass, Even Electron Ions
9 formula(e) evaluated with 1 results within limits (all results (up to 1000) for each mass)
Elements Used:
C: 0-100 B: 0-2 N: 0-10 O: 0-8 F: 0-10 Na: 0-1 S: 0-2
svg_20190211_80_48 (0.546) AM2 (Ar,35000.0,0.00,0.00); Cm (42:63)
1: TOF MS ES-

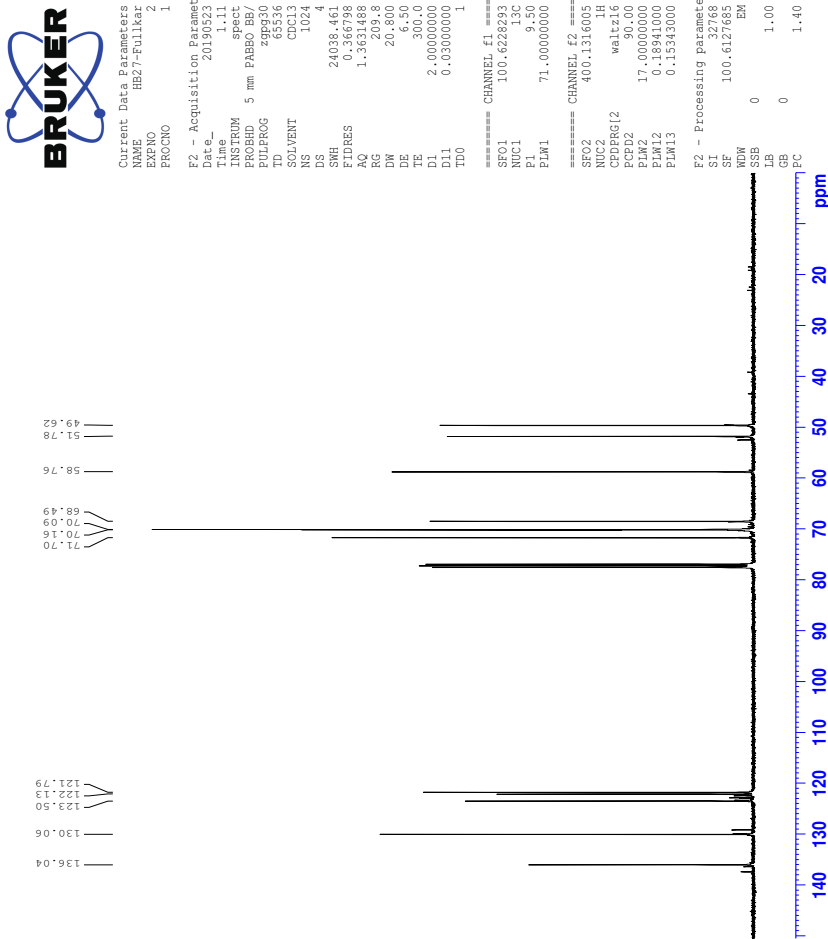


17 Spectra of IL 8e

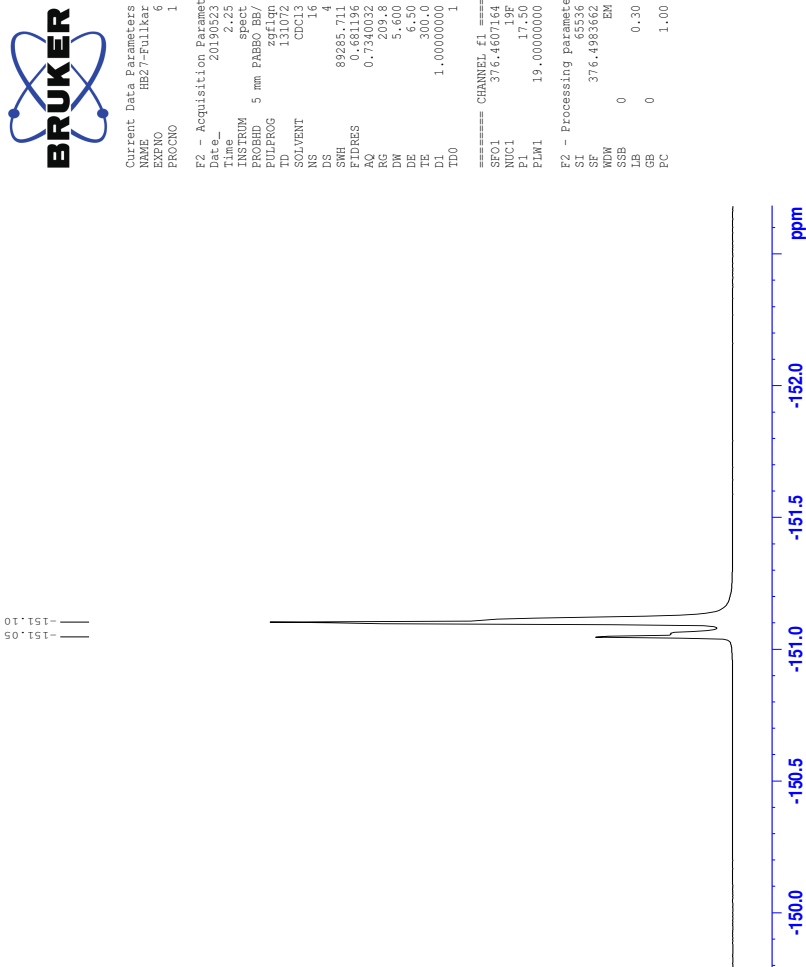
17.1 ^1H -NMR spectrum of IL 8e



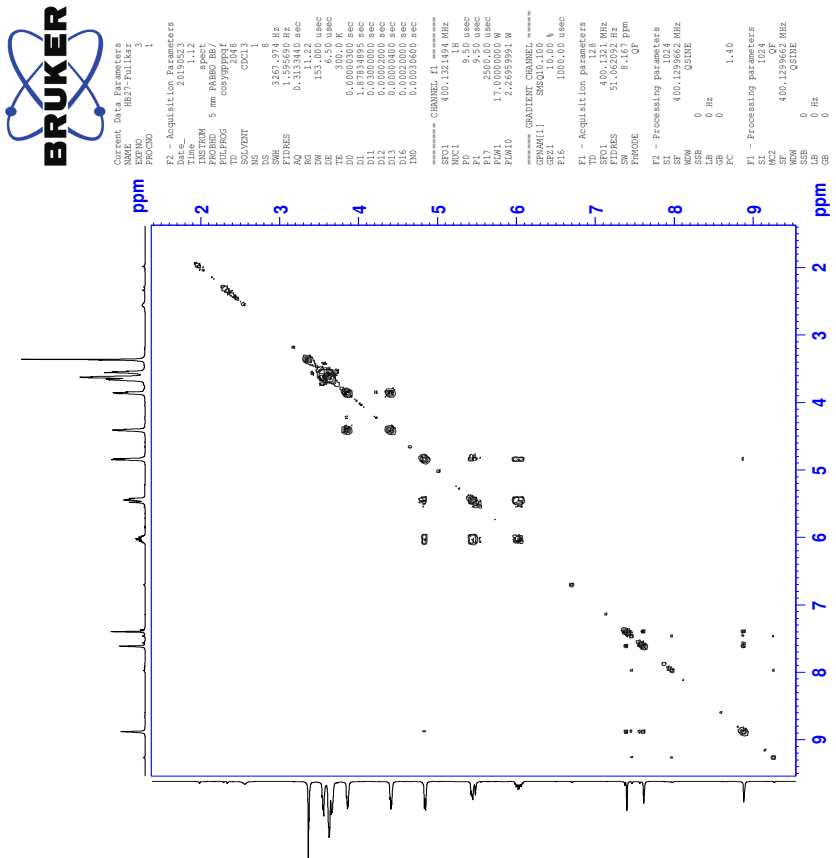
17.2 ^{13}C -NMR spectrum of IL 8e



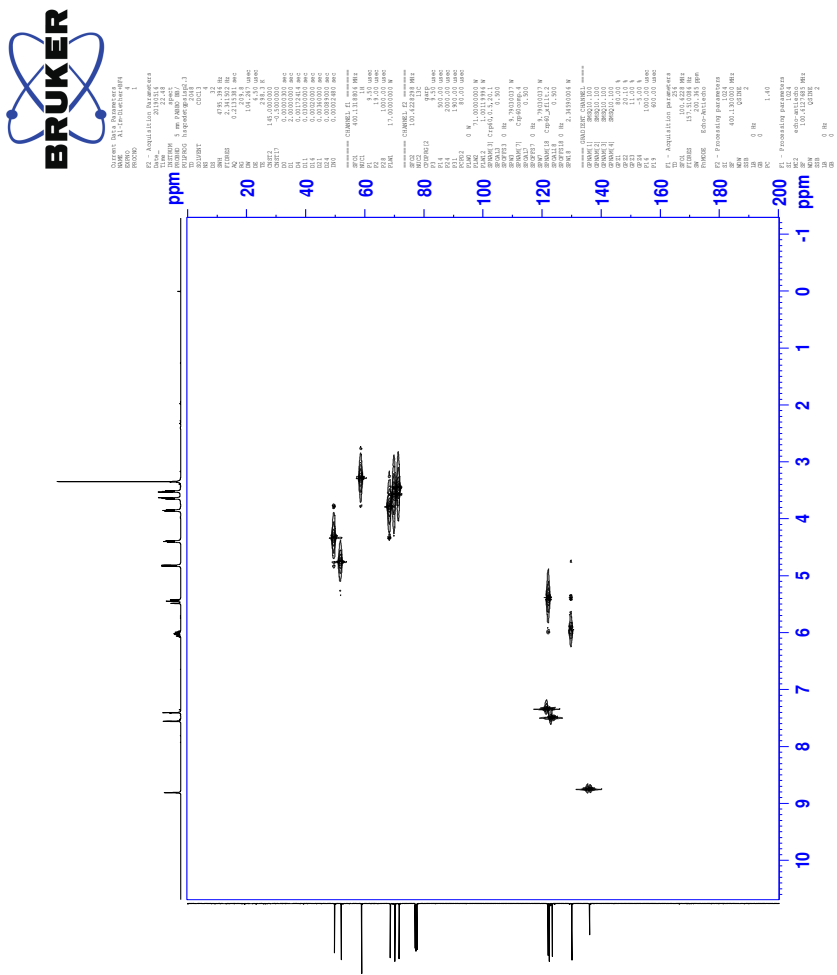
17.3 ^{19}F -NMR spectrum of IL 8e



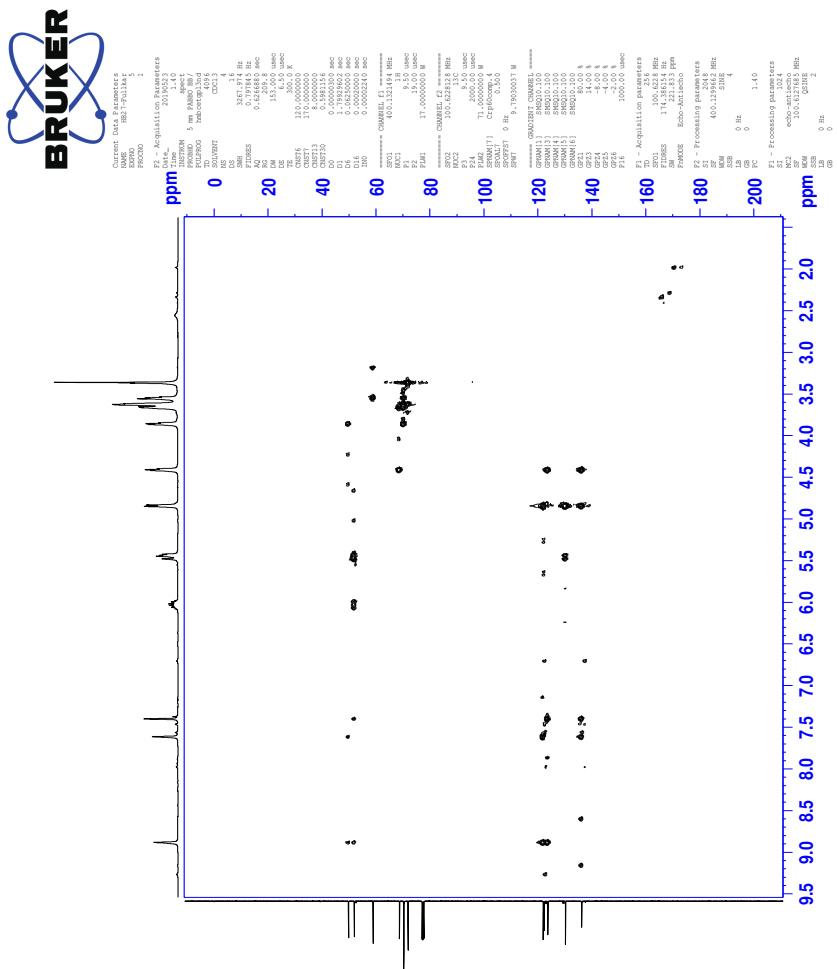
17.4 COSY-spectrum of IL 8e



17.5 HSQC-spectrum of IL 8e

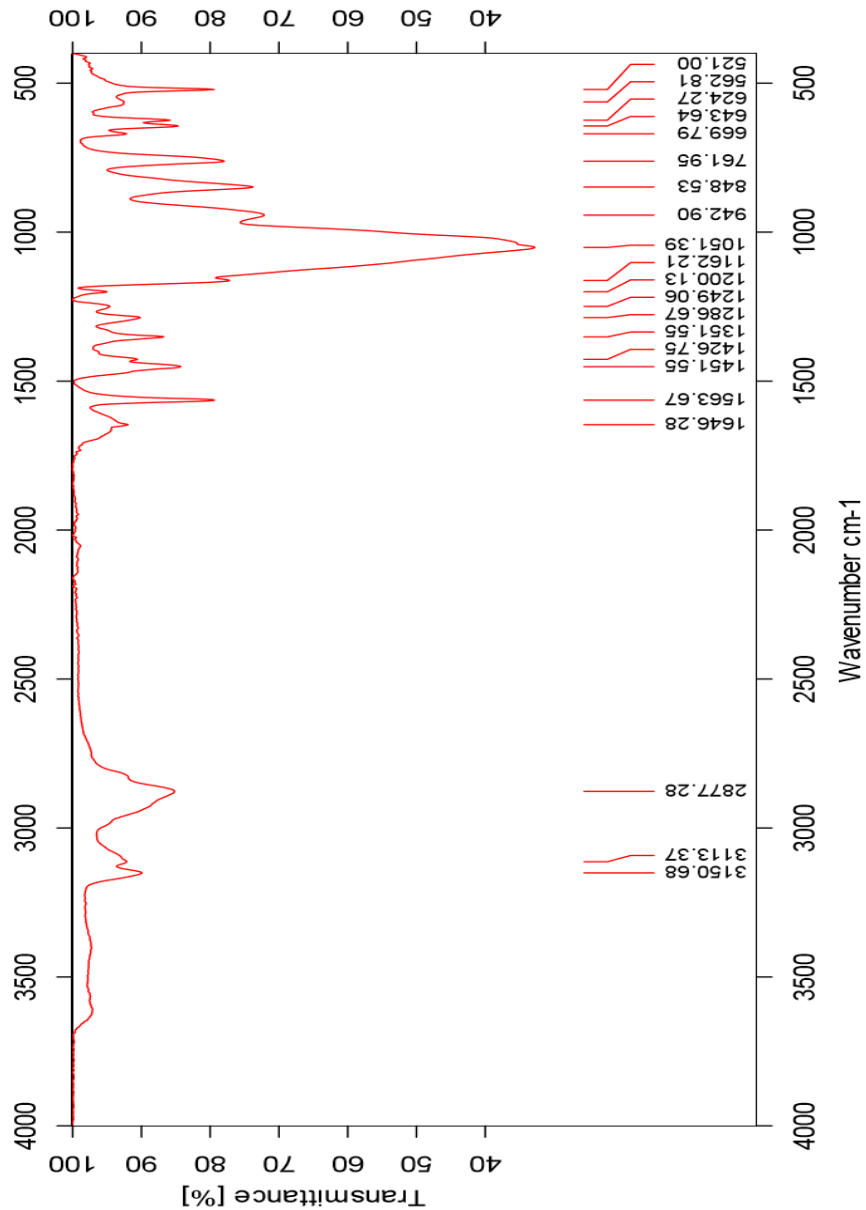


17.6 HMBC-spectrum of IL 8e



CI

17.7 IR-spectrum of IL 8e



17.8 HR-MS positive mode spectrum of IL 8e

Elemental Composition Report

Page 1

Single Mass Analysis

Tolerance = 3.0 PPM / DBE: min = -50.0, max = 50.0

Element prediction: Off

Number of isotope peaks used for i-FIT = 3

Monoisotopic Mass, Even Electron Ions

2175 formula(e) evaluated with 3 results within limits (all results (up to 1000) for each mass)

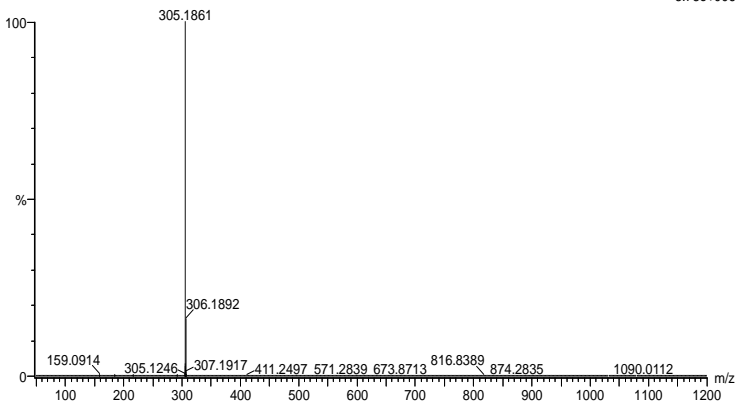
Elements Used:

C: 0-100 H: 0-150 N: 0-10 O: 0-10 Na: 0-1

2019-425 16 (0.305) AM2 (Ar,35000.0,0.00,0.00); Cm (15:16)

1: TOF MS ES+

3.73e+006



Minimum: -50.0
Maximum: 5.0 3.0 50.0

Mass	Calc. Mass	mDa	PPM	DBE	i-FIT	Norm	Conf (%)	Formula
305.1861	305.1860	0.1	0.3	-9.5	1401.3	7.111	0.08	C3 H30 N4 O10 Na
	305.1865	-0.4	-1.3	6.5	1394.2	0.001	99.92	C17 H25 N2 O3
	305.1857	0.4	1.3	-5.5	1404.8	10.604	0.00	C H25 N10 O8

17.9 HR-MS negative mode spectrum of IL 8e

Elemental Composition Report

Page 1

Single Mass Analysis

Tolerance = 10.0 PPM / DBE: min = -50.0, max = 50.0

Element prediction: Off

Number of isotope peaks used for i-FIT = 3

Monoisotopic Mass, Even Electron Ions

454 formula(e) evaluated with 3 results within limits (all results (up to 1000) for each mass)

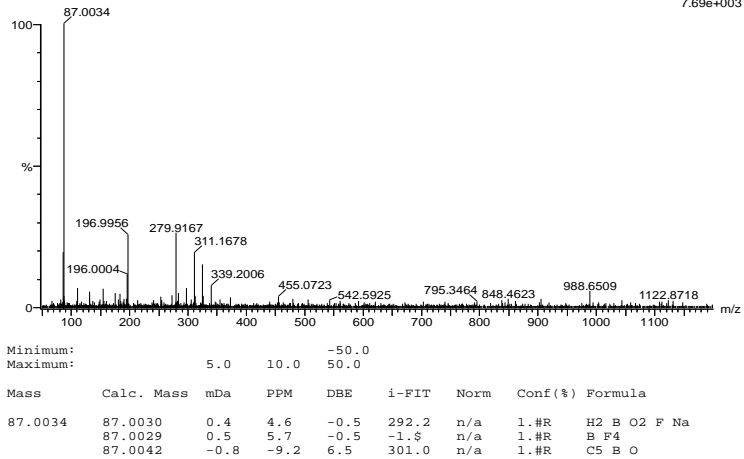
Elements Used:

C: 0-100 H: 0-150 B: 0-2 N: 0-10 O: 0-10 F: 0-7 Na: 0-1

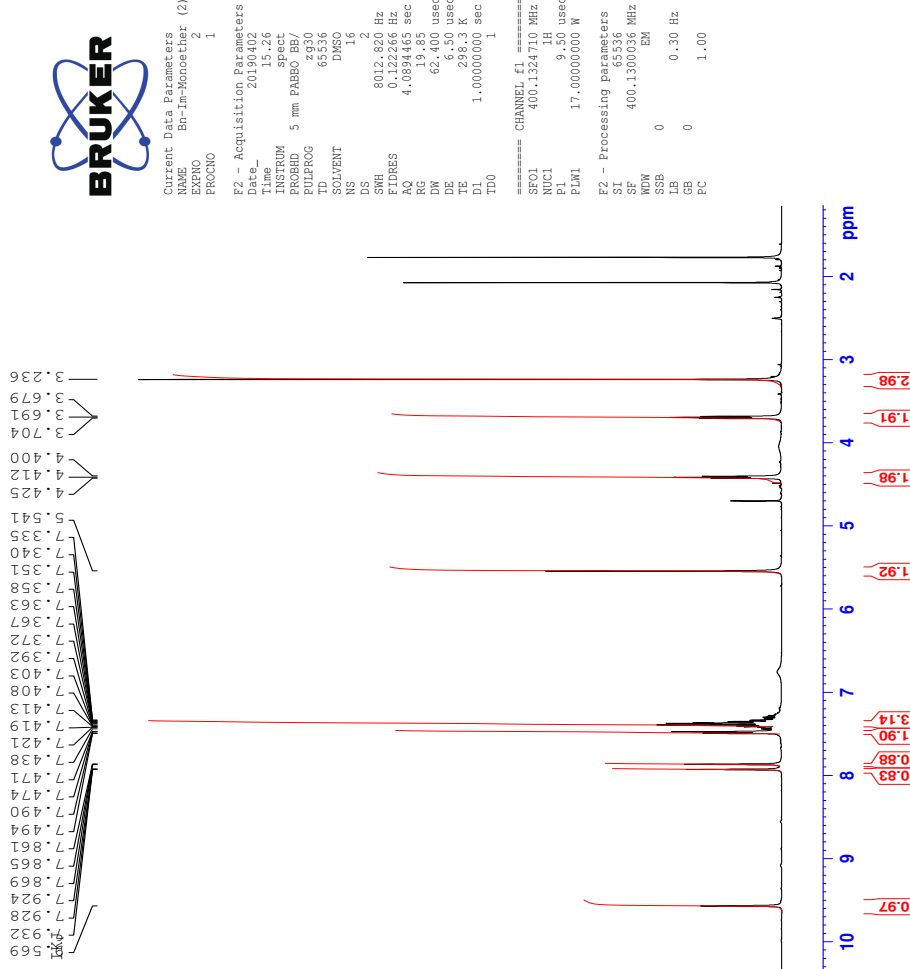
2019-405neg.30 (0.341) AM2 (Ar,35000.0,0.00,0.00); Cm (29:30)

1: TOF MS ES-

7.69e+003



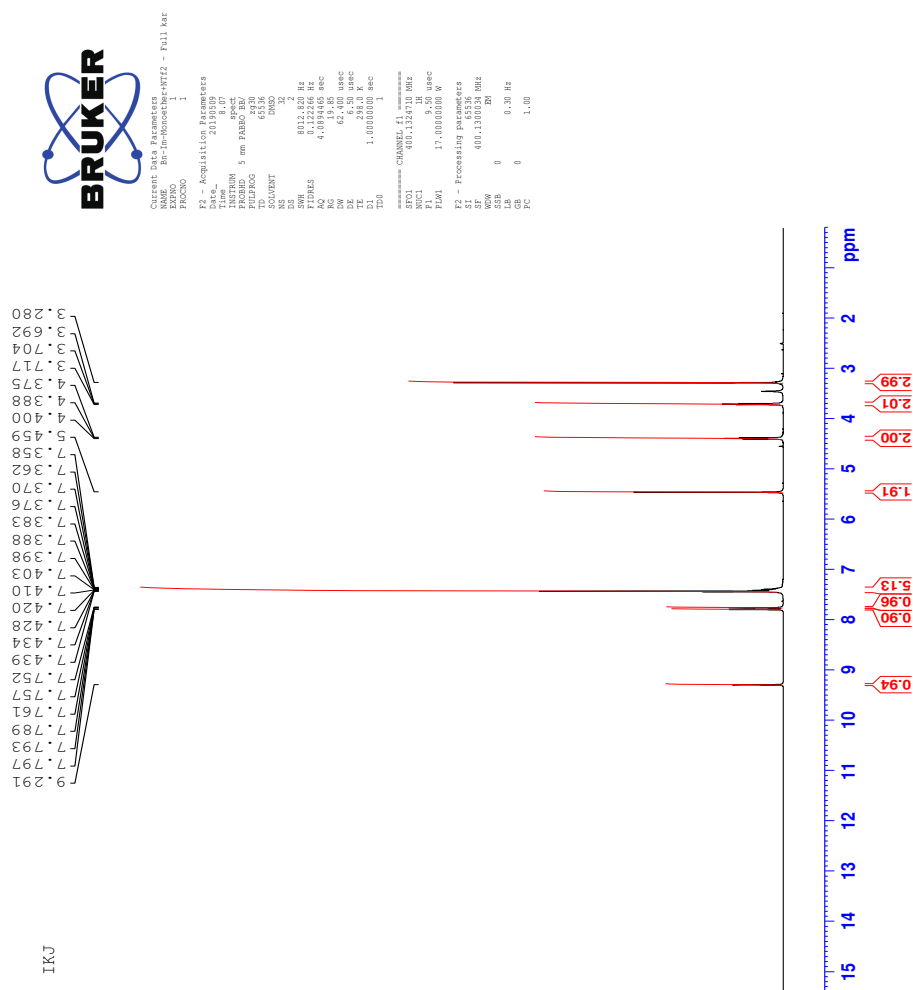
18 $^1\text{H-NMR}$ spectrum of compound 9a



CV

19 Spectra of IL 9b

19.1 ^1H -NMR spectrum of IL 9b

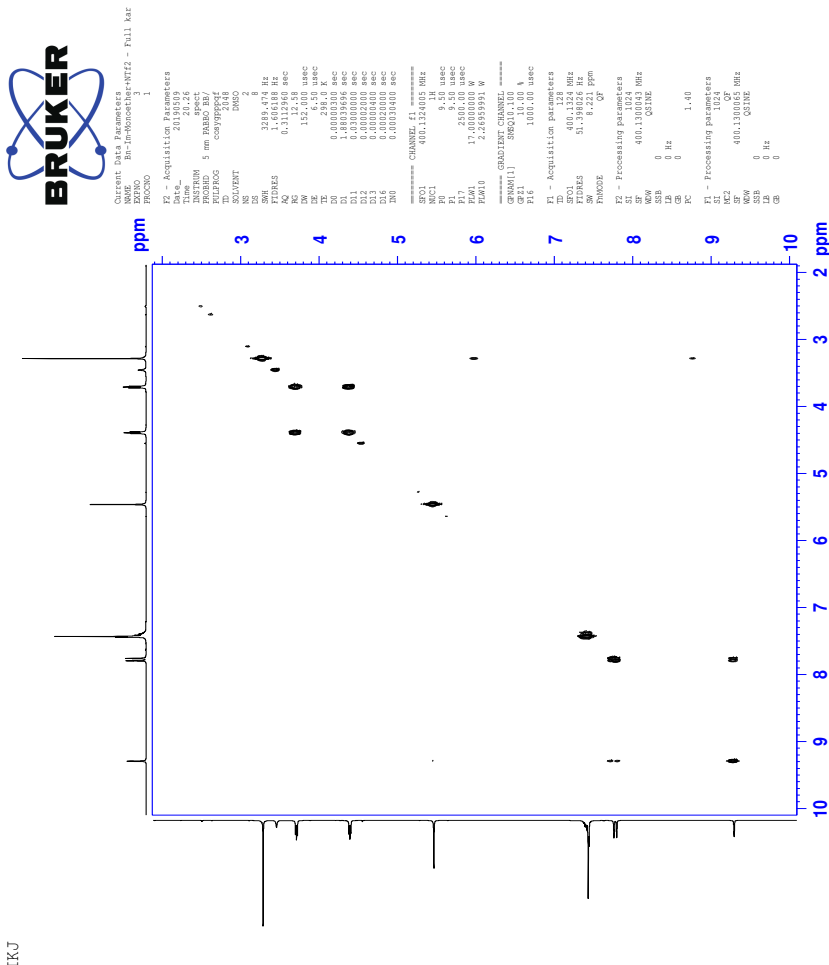


19.2 ^{13}C -NMR spectrum of IL 9b

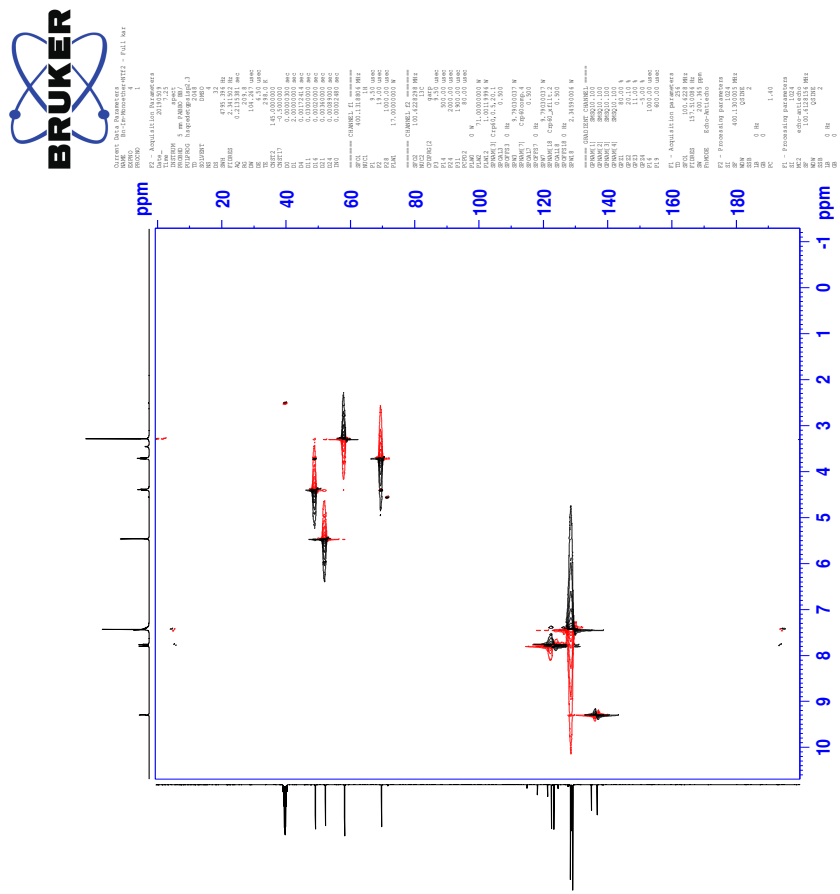
II KJ

CVII

19.3 COSY-spectrum of IL 9b



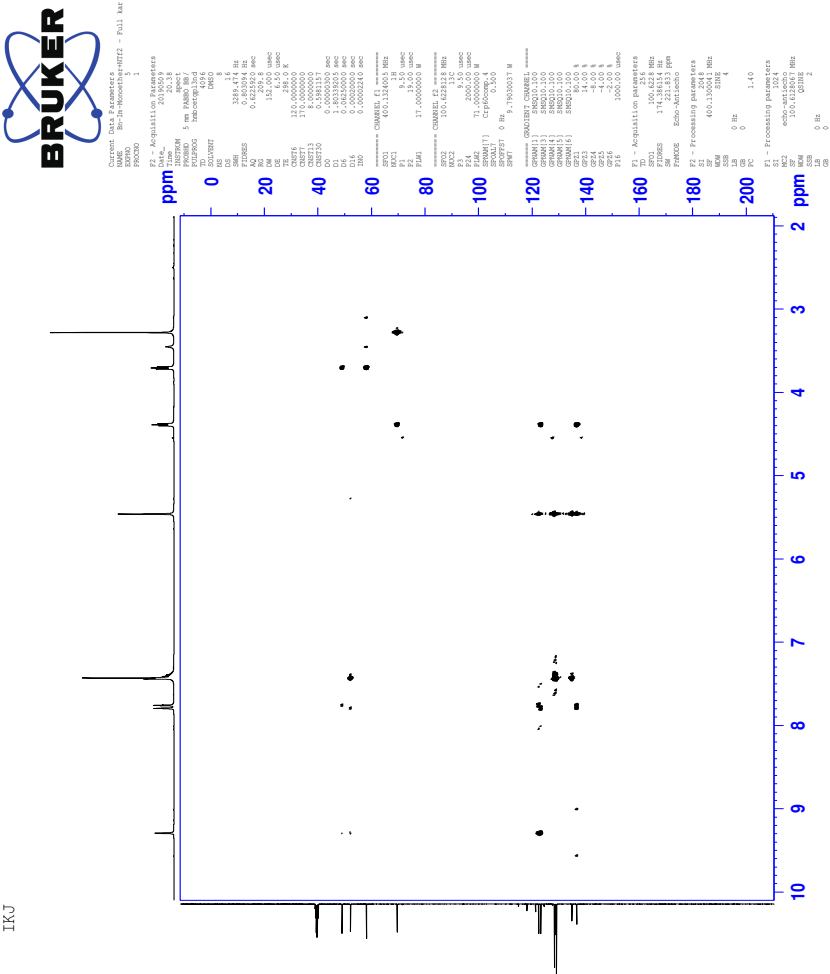
19.4 HSQC-spectrum of IL 9b



TKJ

CIX

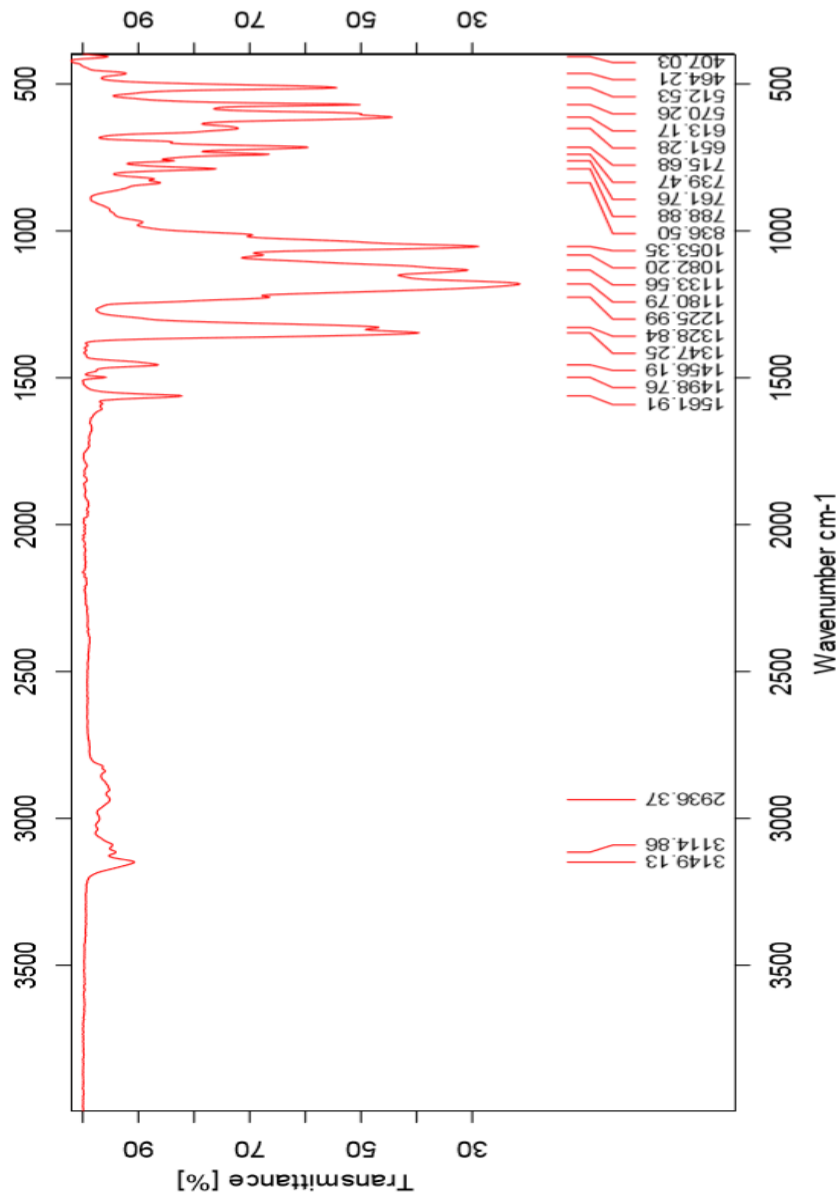
19.5 HMBC-spectrum of IL 9b



IIKJ

CX

19.6 IR-spectrum of IL 9b



19.7 HR-MS positive mode spectrum of IL 9b

Elemental Composition Report

Page 1

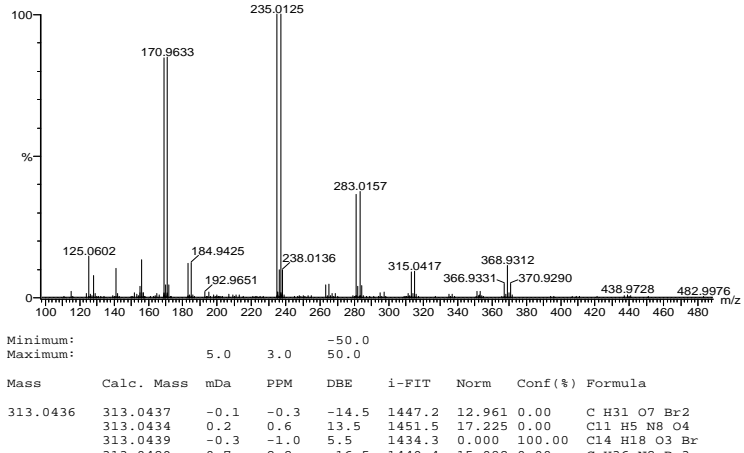
Single Mass Analysis

Tolerance = 3.0 PPM / DBE: min = -50.0, max = 50.0
 Element prediction: Off
 Number of isotope peaks used for i-FIT = 3

Monoisotopic Mass, Even Electron Ions
 2331 formula(e) evaluated with 4 results within limits (all results up to 1000) for each mass
 Elements Used:
 C: 0-100 H: 0-150 N: 0-10 O: 0-10 Br: 0-3

2019-468 50 (1.001) AM2 (Ar,35000.0,0.00,0.00); Cm (49.57)
 1: TOF MS ASAP+

5.36e+006



19.8 HR-MS negative mode spectrum of IL 9b

Elemental Composition Report

Page 1

Single Mass Analysis

Tolerance = 2.0 PPM / DBE: min = -50.0, max = 50.0

Element prediction: Off

Number of isotope peaks used for i-FIT = 3

Monoisotopic Mass, Even Electron Ions

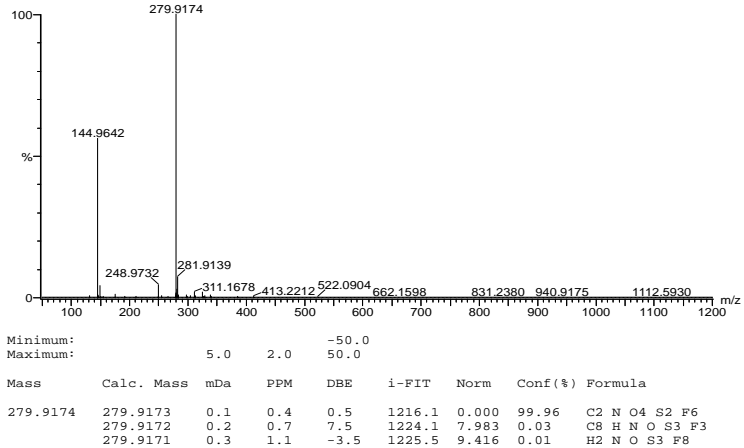
14728 formula(e) evaluated with 3 results within limits (all results (up to 1000) for each mass)

Elements Used:

C: 0-100 H: 0-150 N: 0-10 O: 0-10 S: 0-4 F: 0-8

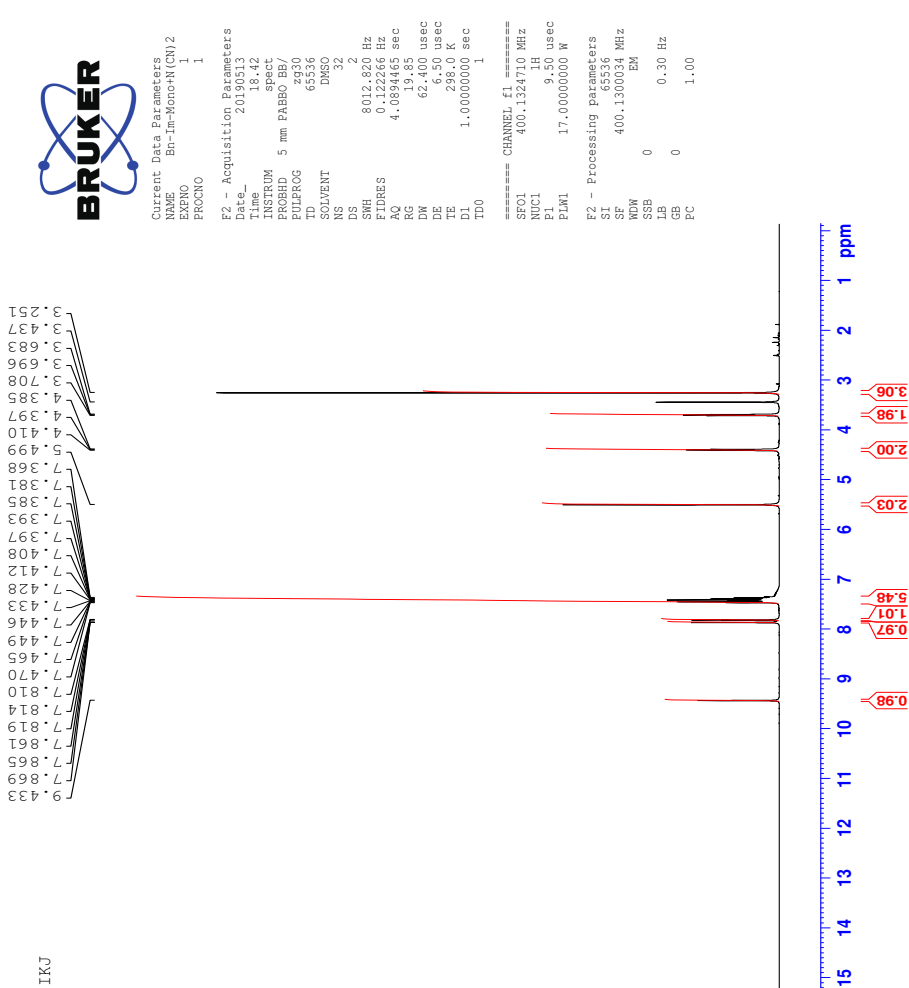
2019-458 16 (0.306) AM2 (Ar,35000.0,0.00,0.00); Cm (13:16)
1: TOF MS ES-

1.03e+006

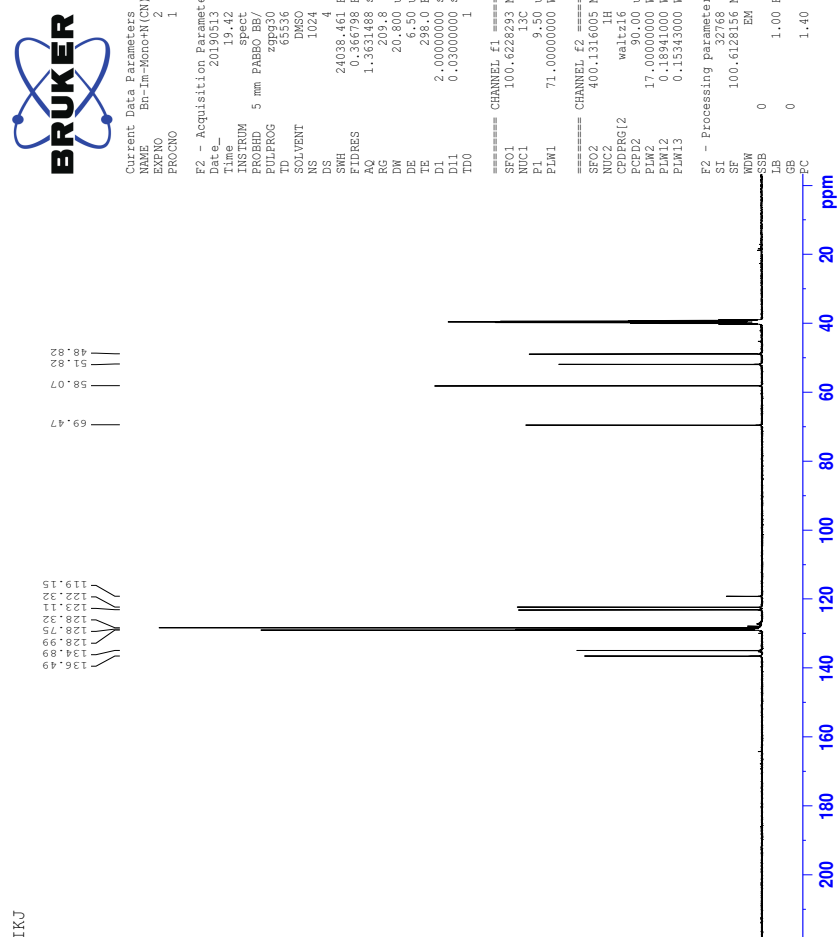


20 Spectra of IL 9c

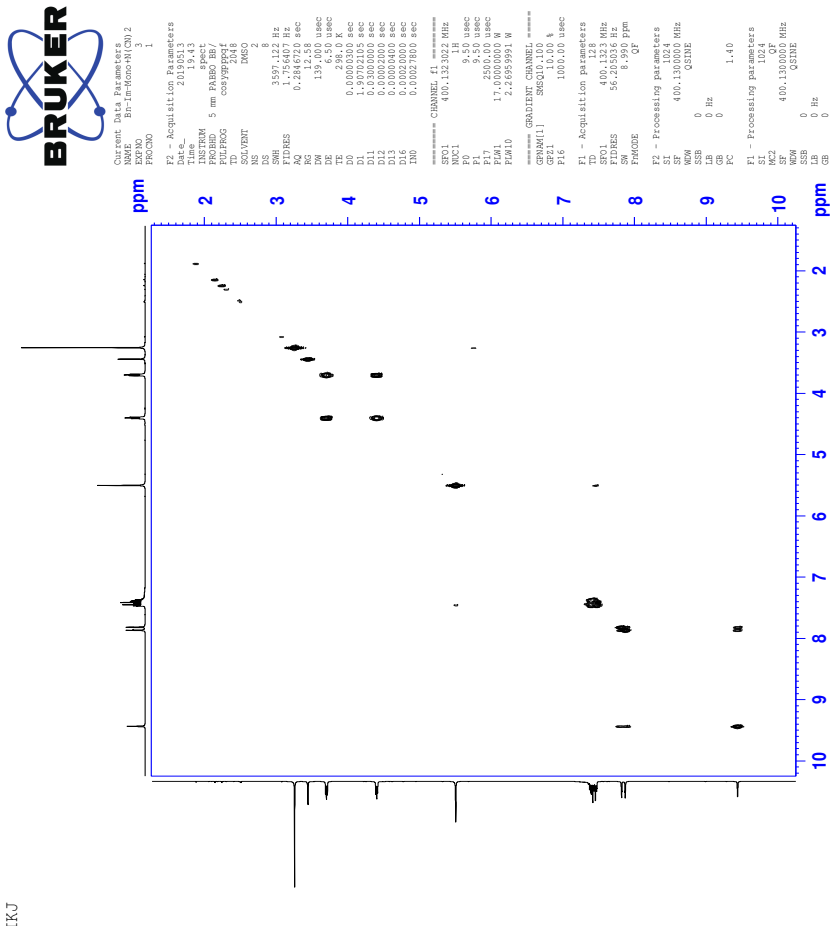
20.1 ^1H -NMR spectrum of IL 9c



20.2 ^{13}C -NMR spectrum of IL 9c



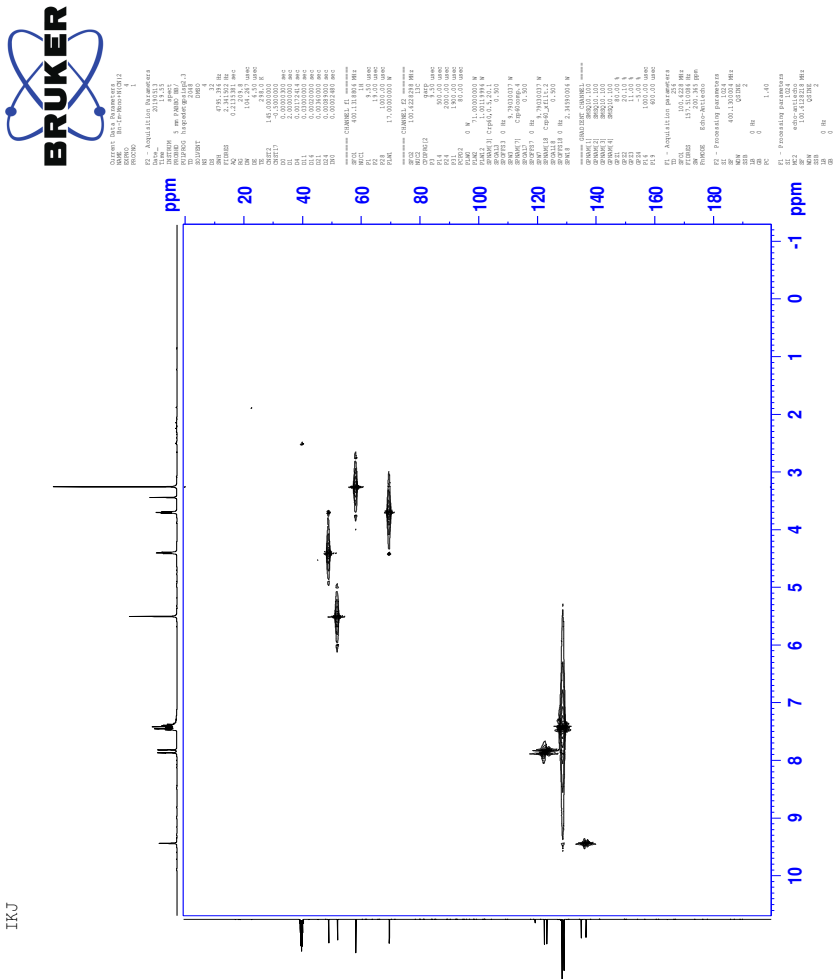
20.3 COSY-spectrum of IL 9c



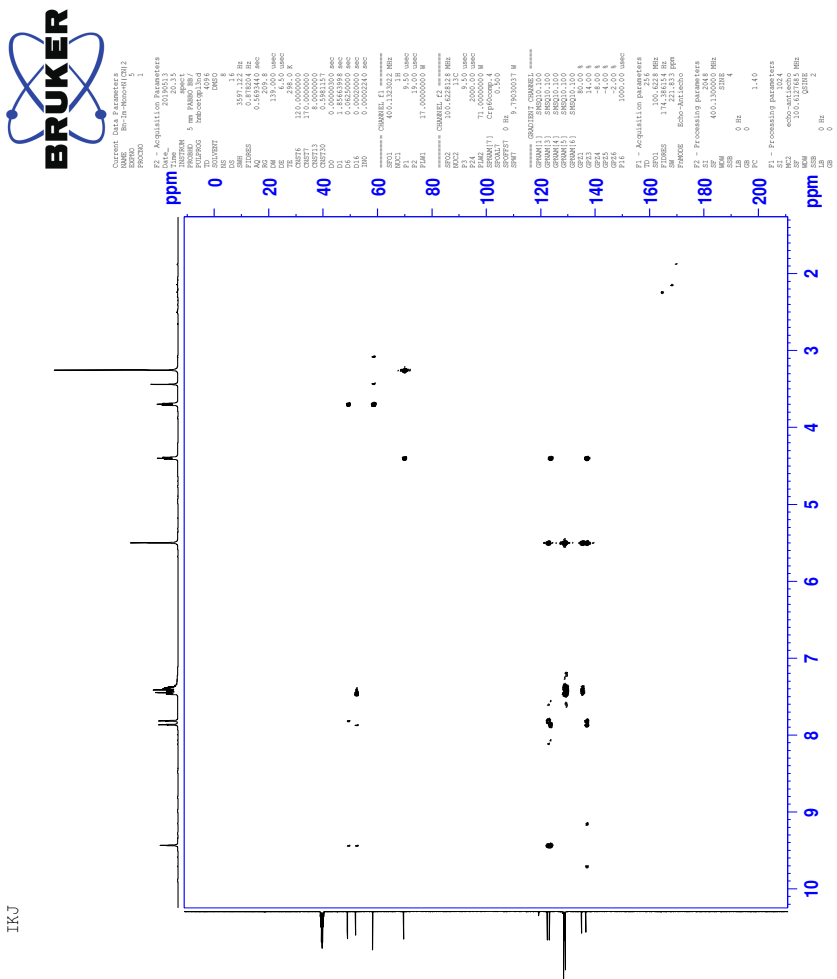
TKJ

20.4 HSQC-spectrum of IL 9c

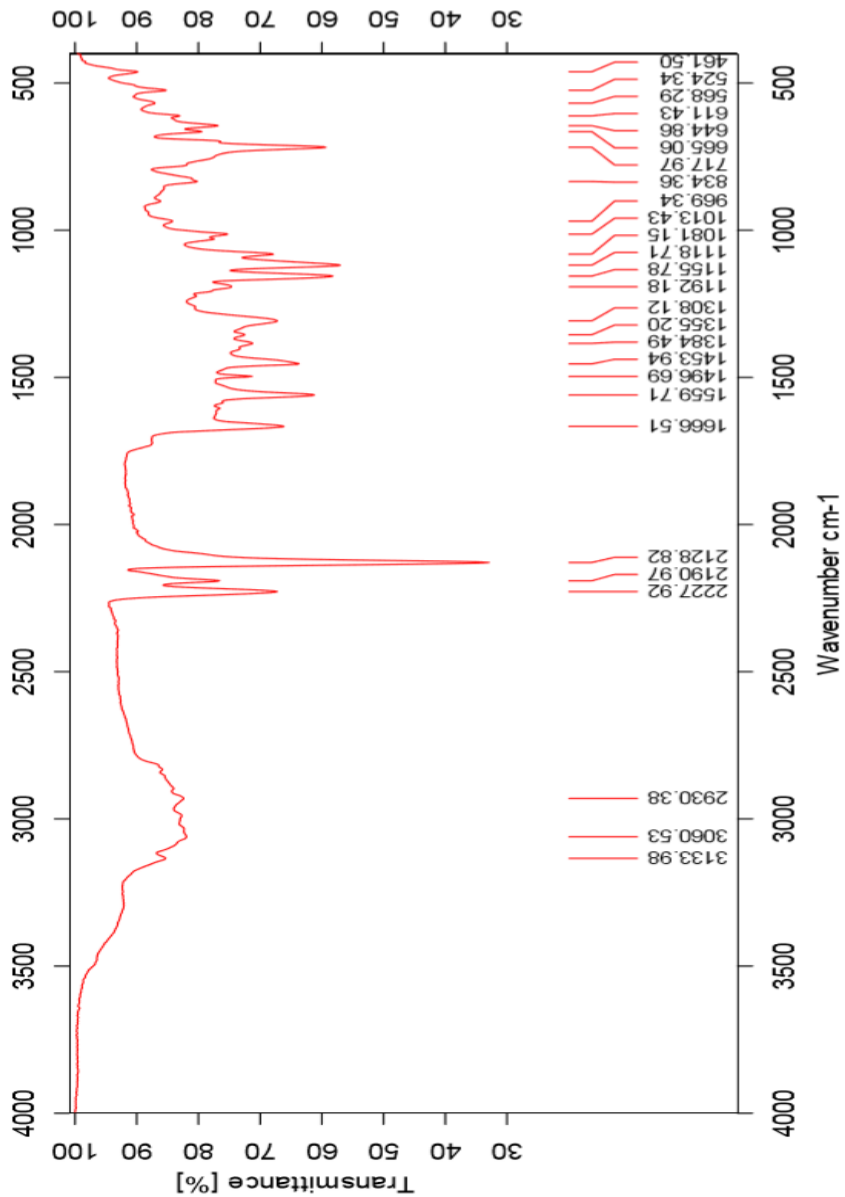
IKJ



20.5 HMBC-spectrum of IL 9c



20.6 IR-spectrum of IL 9c



20.7 HR-MS positive mode spectrum of IL 9c

Elemental Composition Report

Page 1

Single Mass Analysis

Tolerance = 5.0 PPM / DBE: min = -50.0, max = 50.0

Element prediction: Off

Number of isotope peaks used for i-FIT = 3

Monoisotopic Mass, Even Electron Ions

688 formula(e) evaluated with 1 results within limits (all results (up to 1000) for each mass)

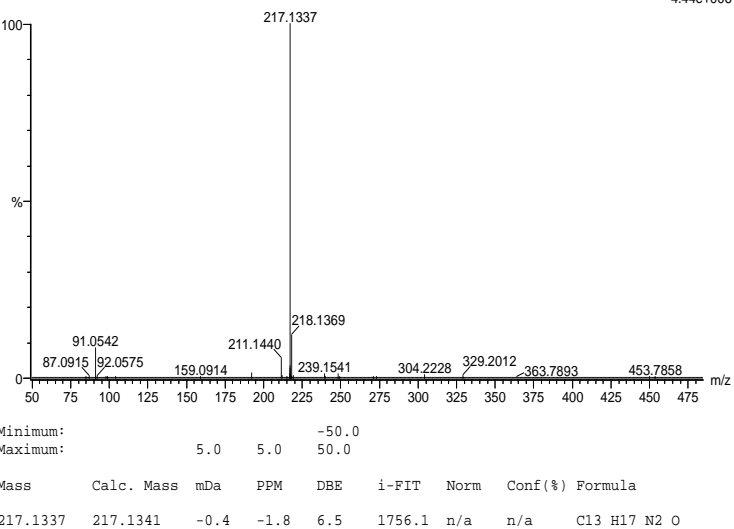
Elements Used:

C: 0-100 H: 0-150 N: 0-10 O: 0-10

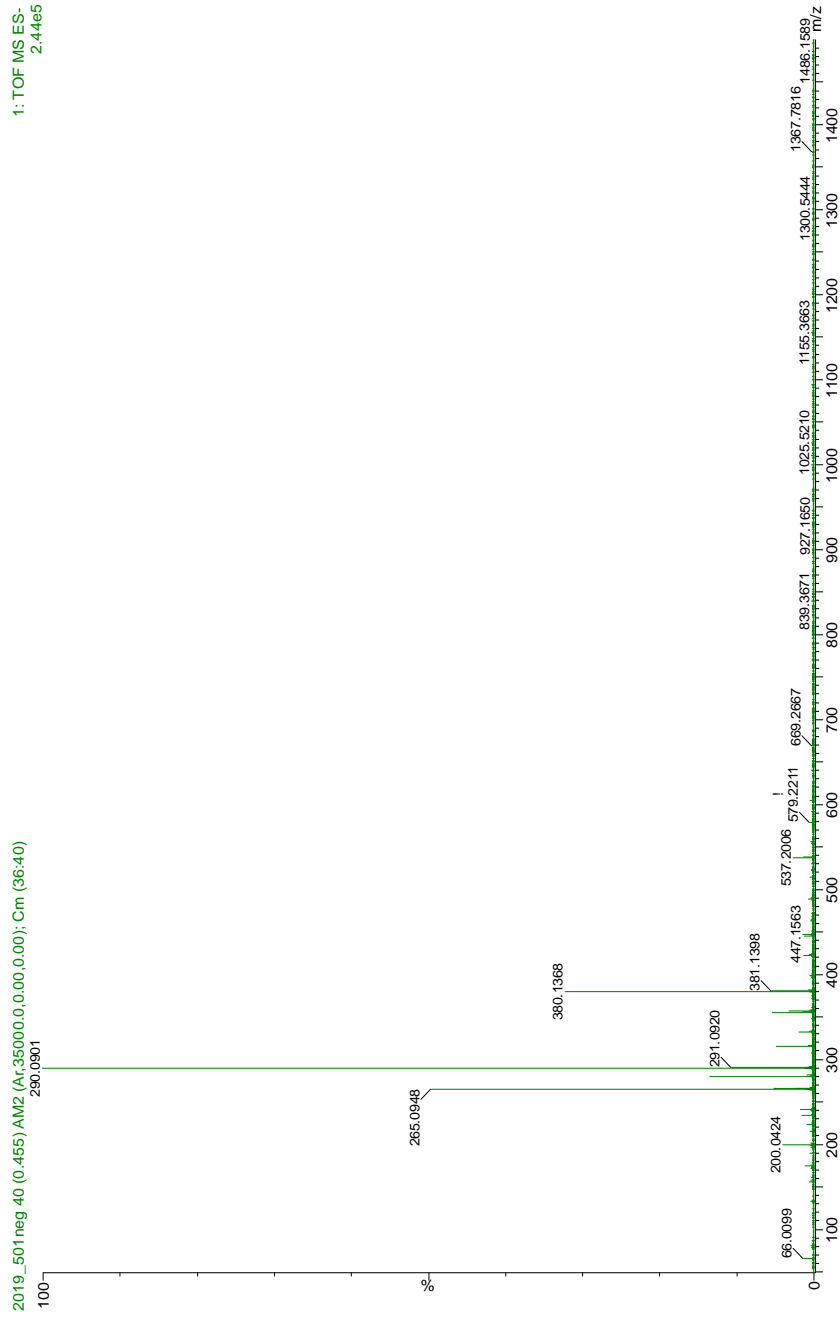
2019_500FIA 18 (0.339) AM2 (Ar,35000.0,0.00,0.00); Cm (10:18)

1: TOF MS ES+

4.44e+006

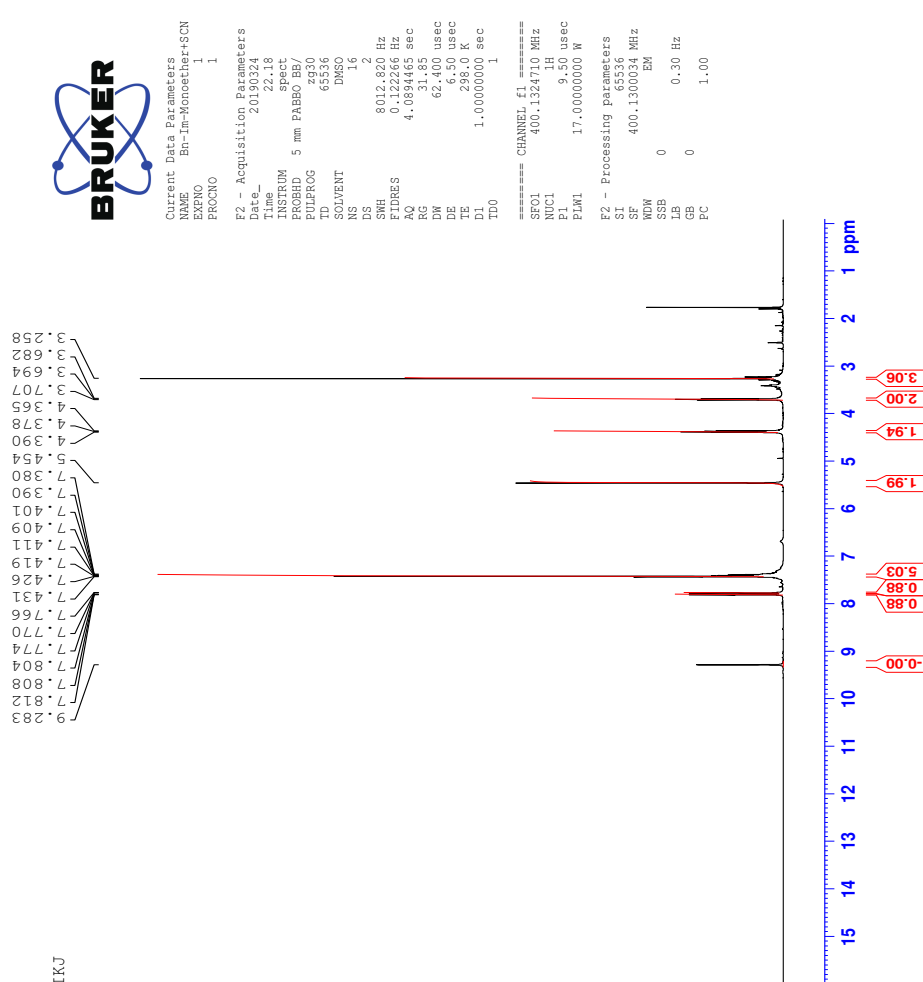


20.8 HR-MS negative mode spectrum of IL 9c



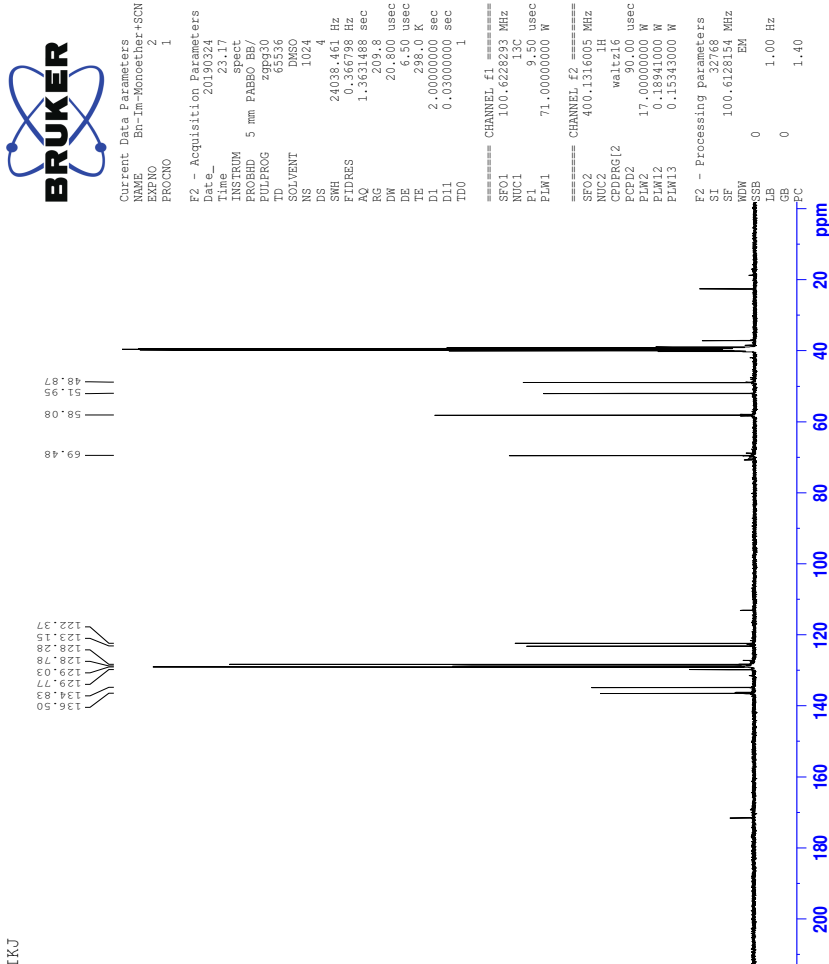
21 Spectra of IL 9d

21.1 ^1H -NMR spectrum of IL 9d



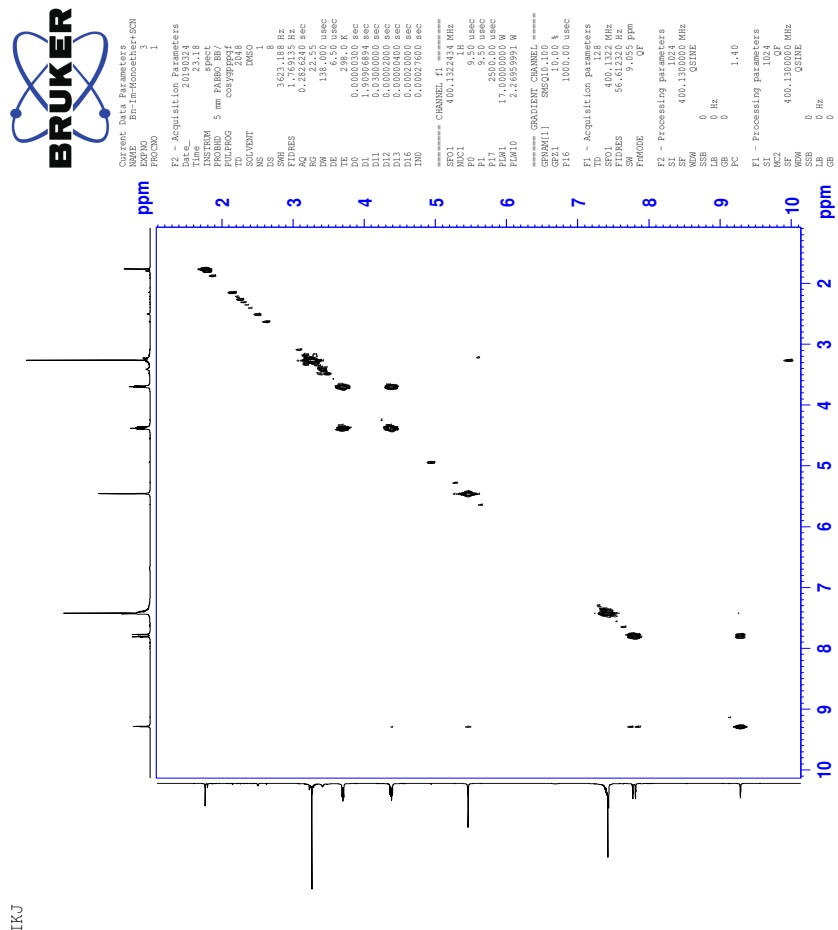
IKJ

21.2 ^{13}C -NMR spectrum of IL 9d



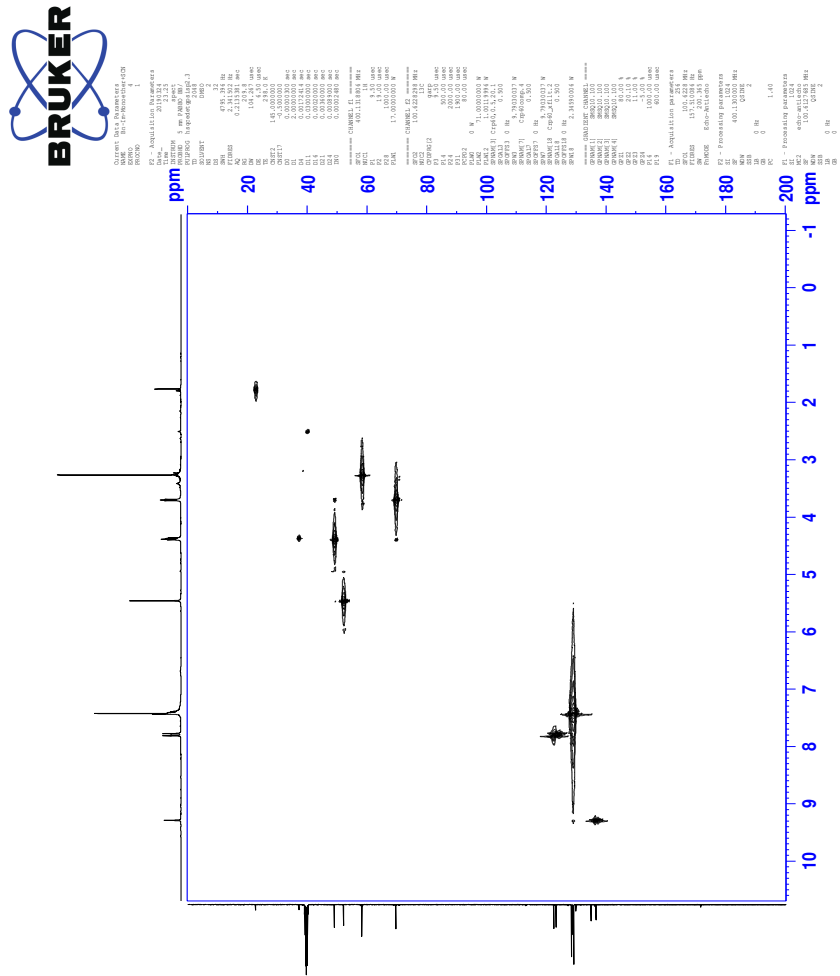
IJKJ

21.3 COSY-spectrum of IL 9d

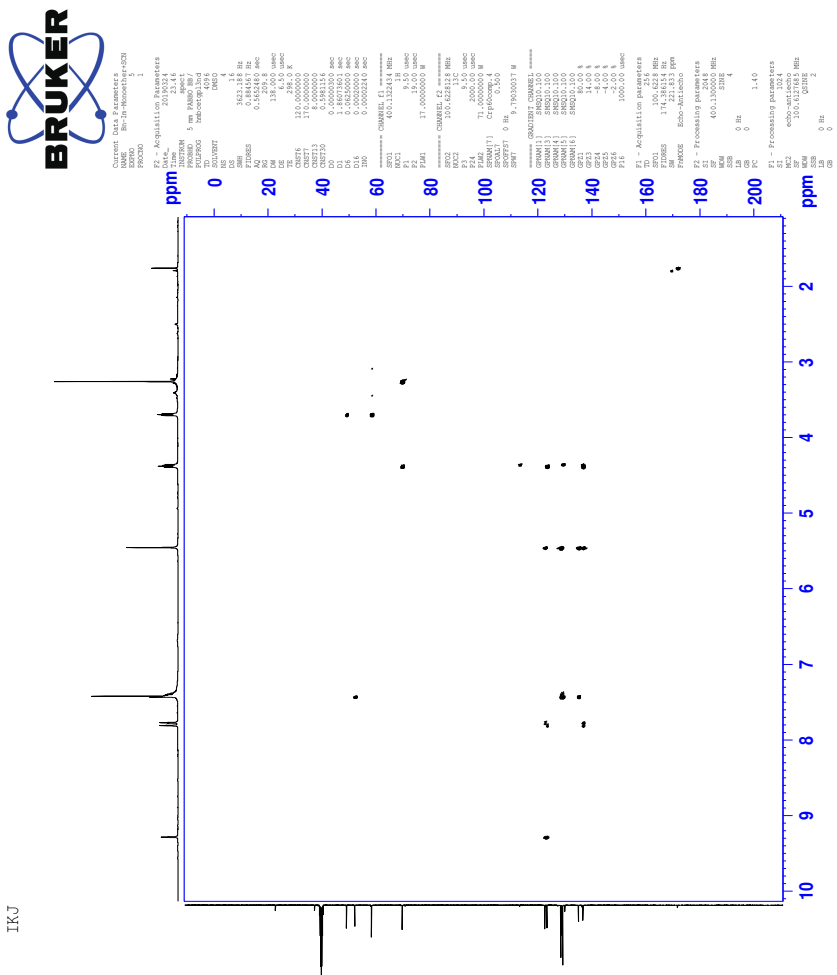


TKJ

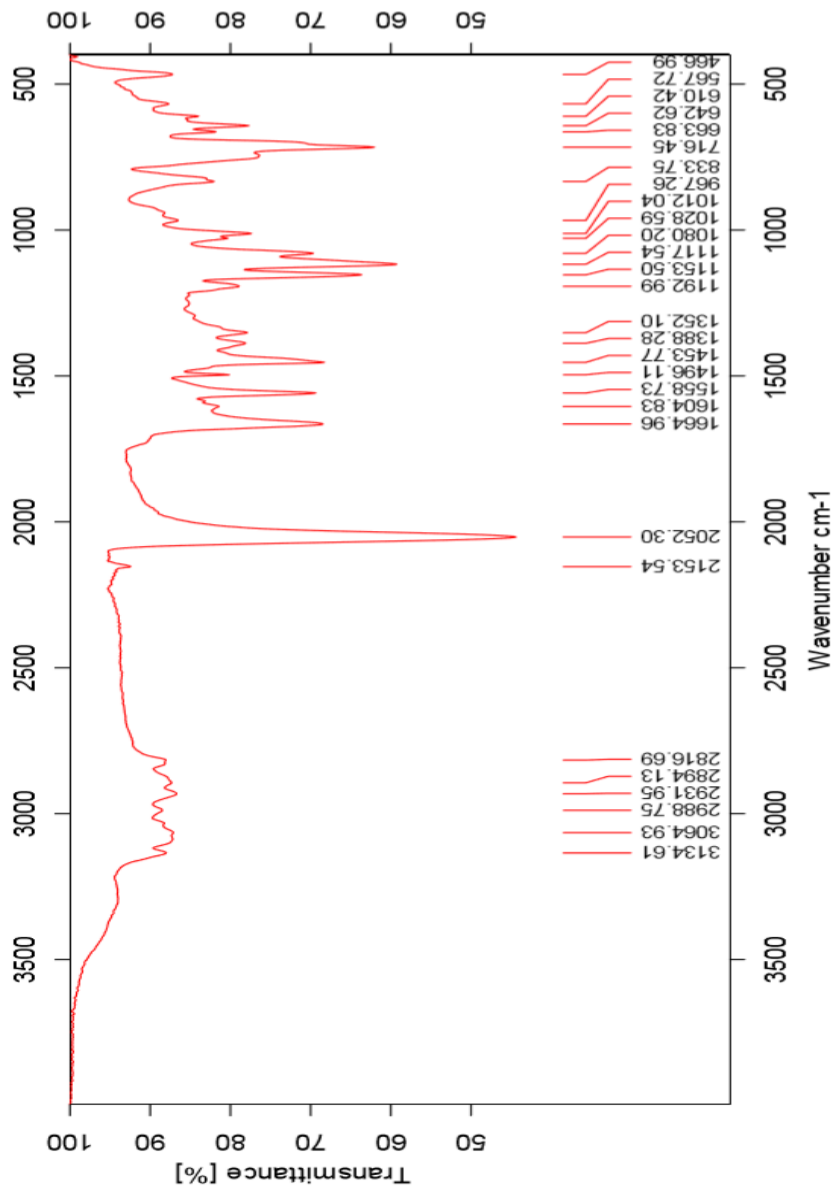
21.4 HSQC-spectrum of IL 9d



21.5 HMBC-spectrum of IL 9d



21.6 IR-spectrum of IL 9d



21.7 HR-MS positive mode spectrum of IL 9d

Elemental Composition Report

Page 1

Single Mass Analysis

Tolerance = 5.0 PPM / DBE: min = -50.0, max = 50.0

Element prediction: Off

Number of isotope peaks used for i-FIT = 3

Monoisotopic Mass, Even Electron Ions

688 formula(e) evaluated with 1 results within limits (all results (up to 1000) for each mass)

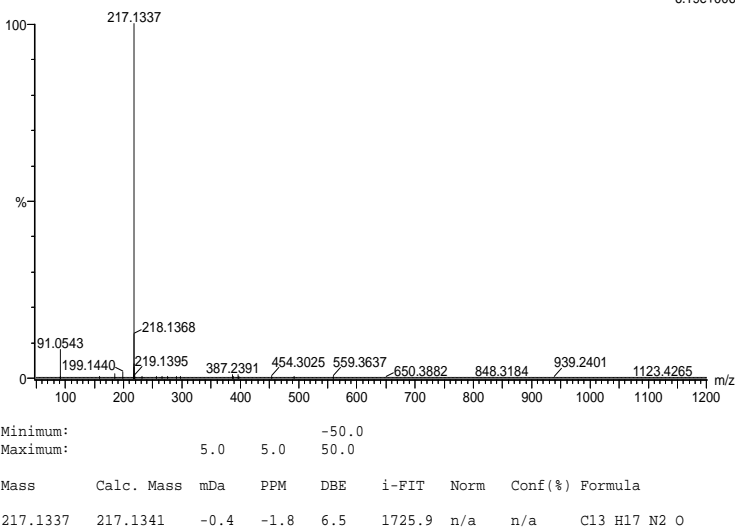
Elements Used:

C: 0-100 H: 0-150 N: 0-10 O: 0-10

svg_20190423_2019_350 23 (0.436) AM2 (Ar,35000.0,0.00,0.00); Crm (23:25)

1: TOF MS ES+

6.19e+006



21.8 HR-MS negative mode spectrum of IL 9d

Elemental Composition Report

Page 1

Single Mass Analysis

Tolerance = 10.0 PPM / DBE: min = -50.0, max = 50.0

Element prediction: Off

Number of isotope peaks used for i-FIT = 3

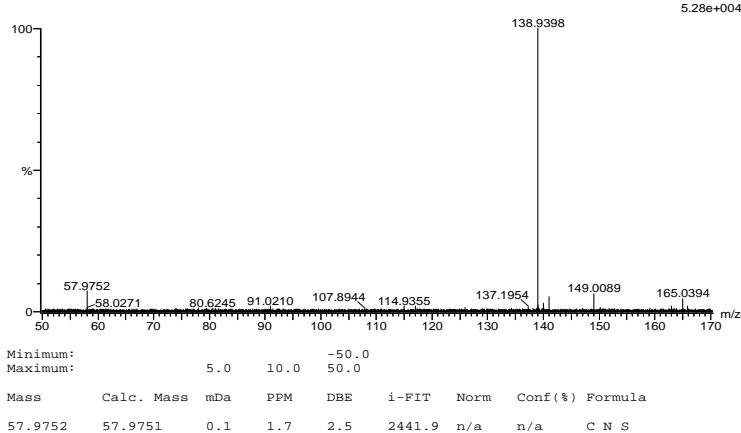
Monoisotopic Mass, Even Electron Ions

47 formula(e) evaluated with 1 results within limits (all results (up to 1000) for each mass)

Elements Used:

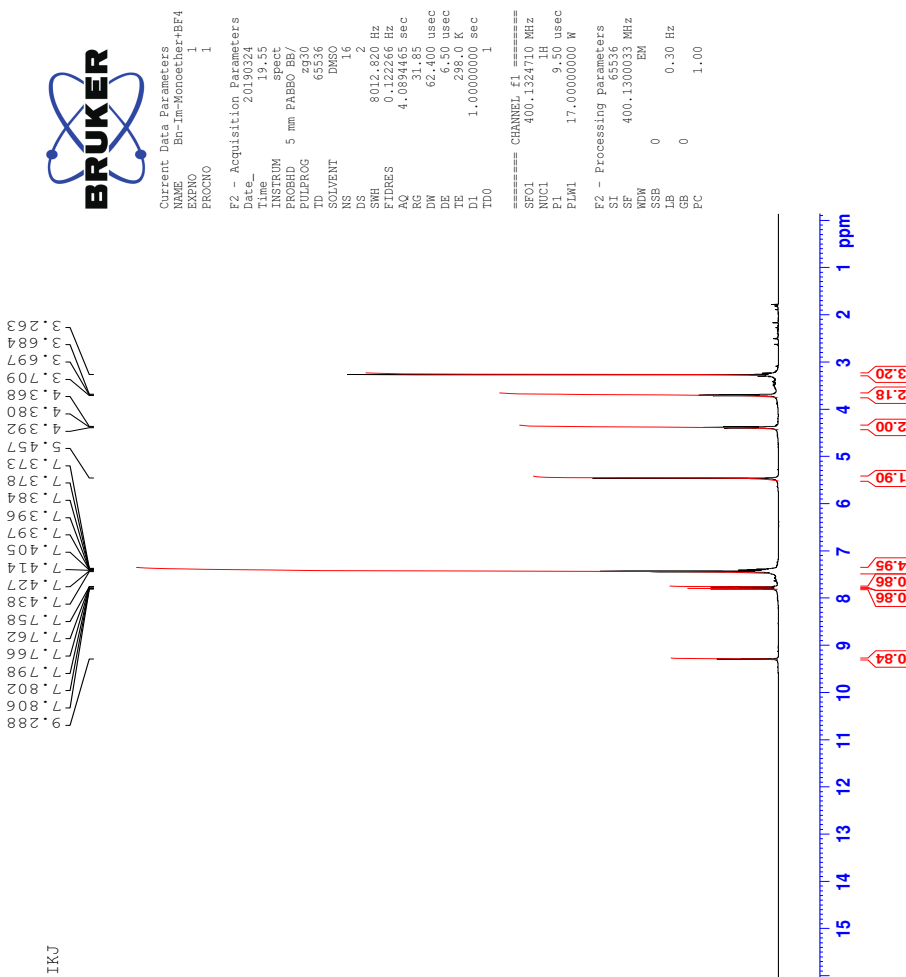
C: 0-100 H: 0-150 N: 0-3 O: 0-10 Na: 0-1 S: 0-2 Au: 0-3

svg_20190423_2019_351_2 65 (0.733) AM2 (Ar,35000.0,0.00,0.00); Cm (65.71)
1: TOF MS ES-

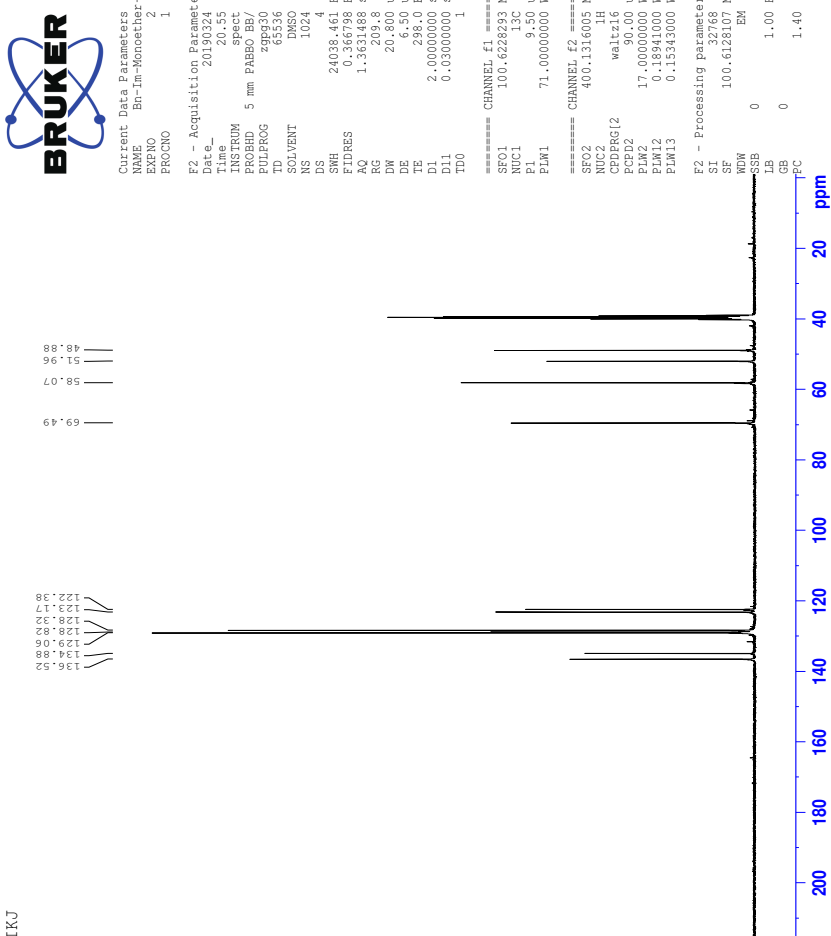


22 Spectra of IL 9e

22.1 ^1H -NMR spectrum of IL 9e

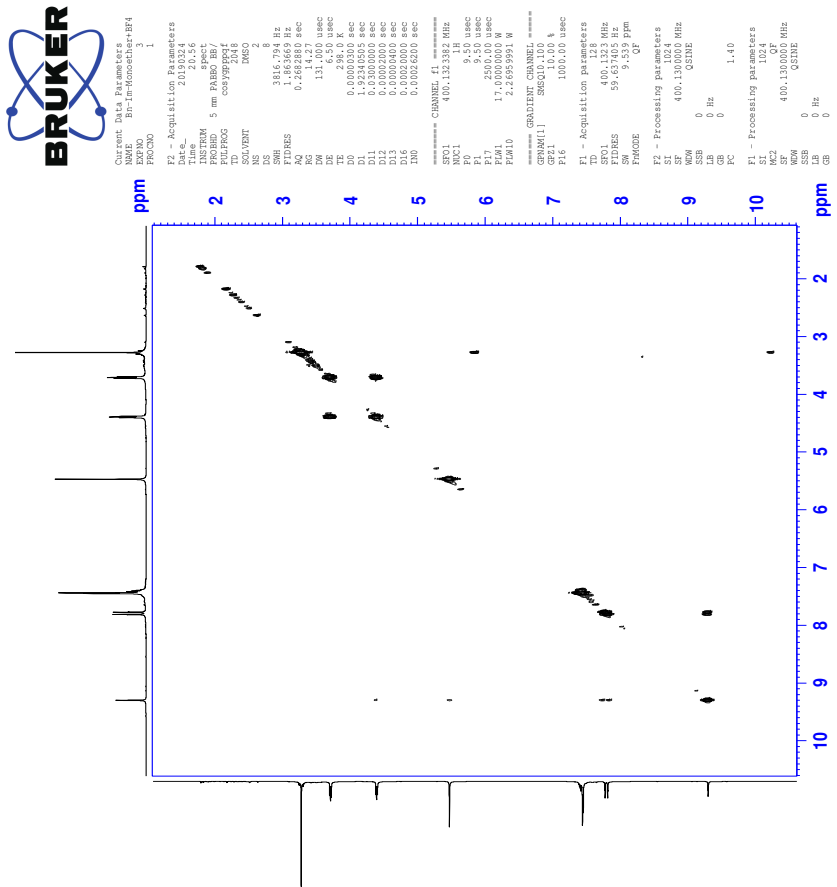


22.2 ^{13}C -NMR spectrum of IL 9e

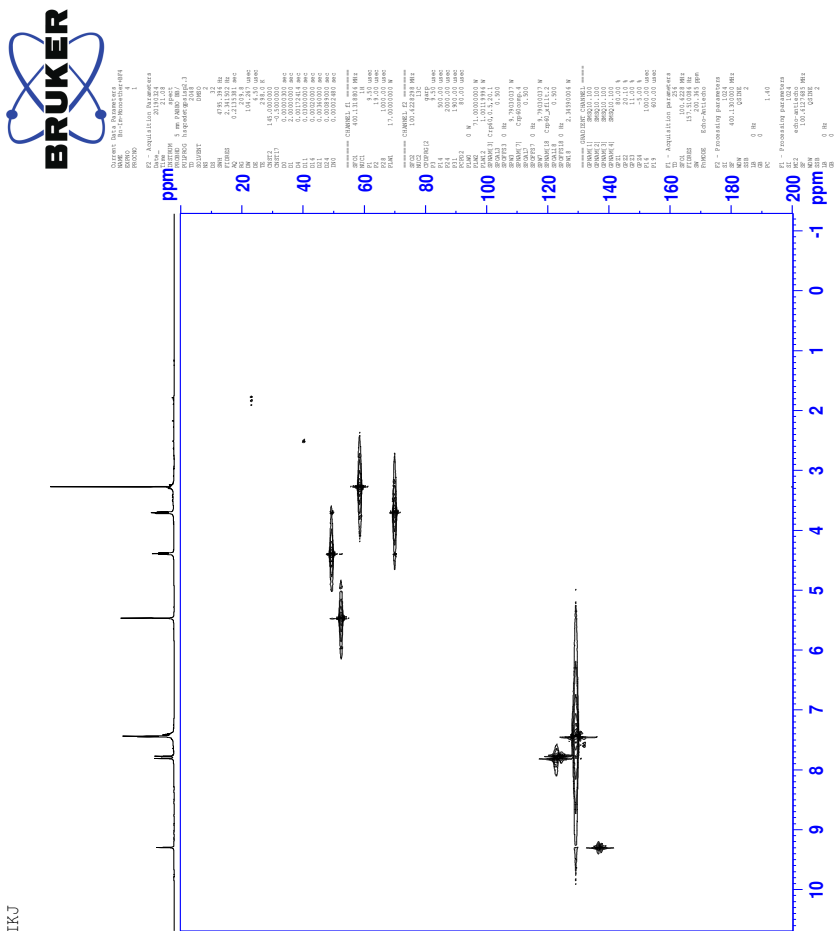


IKJ

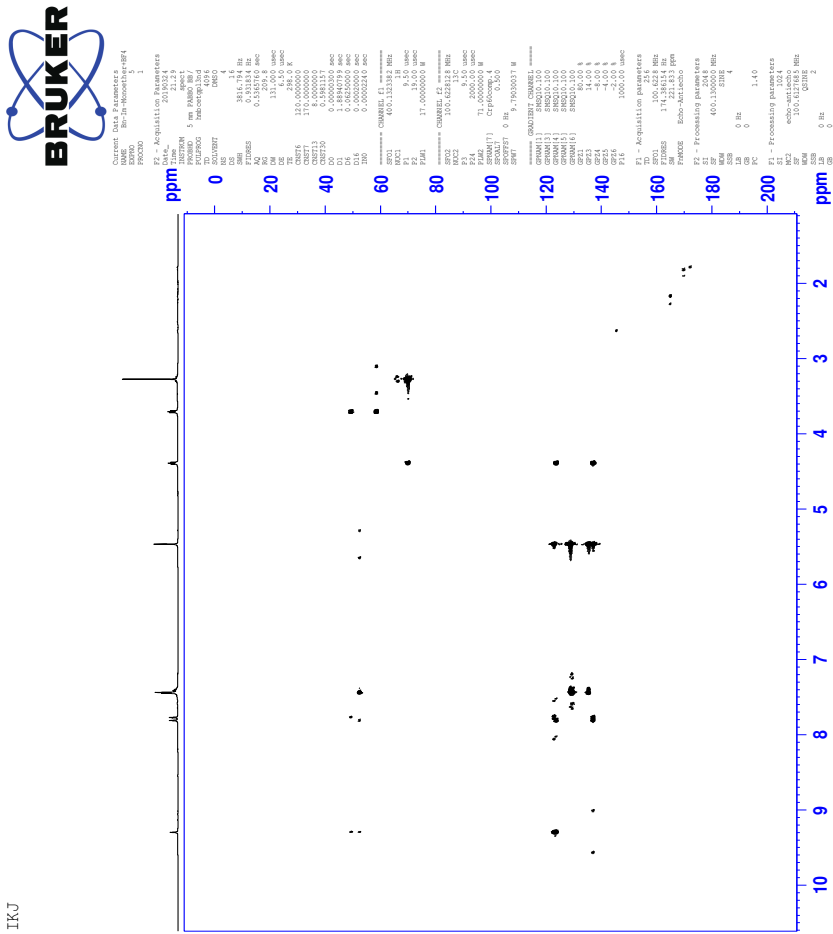
22.3 COSY-spectrum of IL 9e



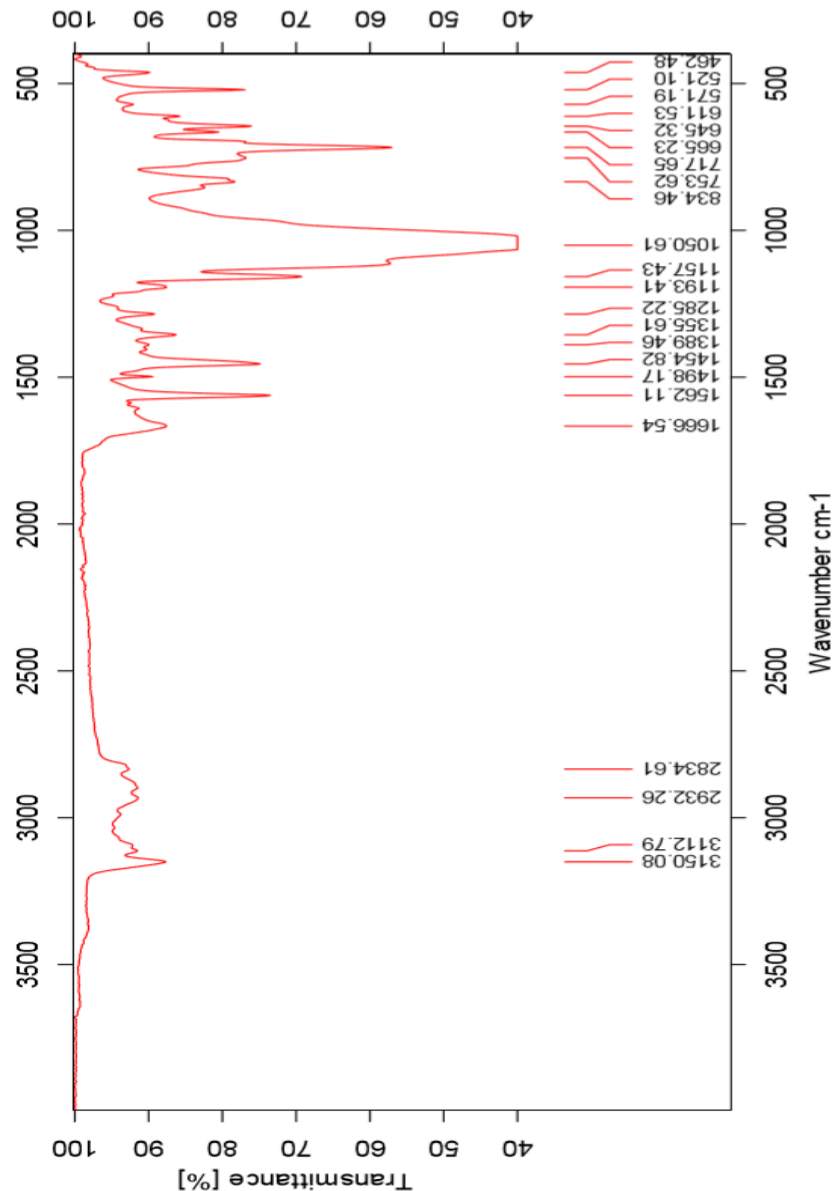
22.4 HSQC-spectrum of IL 9e



22.5 HMBC-spectrum of IL 9e



22.6 IR-spectrum of IL 9e



22.7 HR-MS positive mode spectrum of IL 9e

Elemental Composition Report

Page 1

Single Mass Analysis

Tolerance = 5.0 PPM / DBE: min = -50.0, max = 50.0

Element prediction: Off

Number of isotope peaks used for i-FIT = 3

Monoisotopic Mass, Even Electron Ions

688 formula(e) evaluated with 1 results within limits (all results (up to 1000) for each mass)

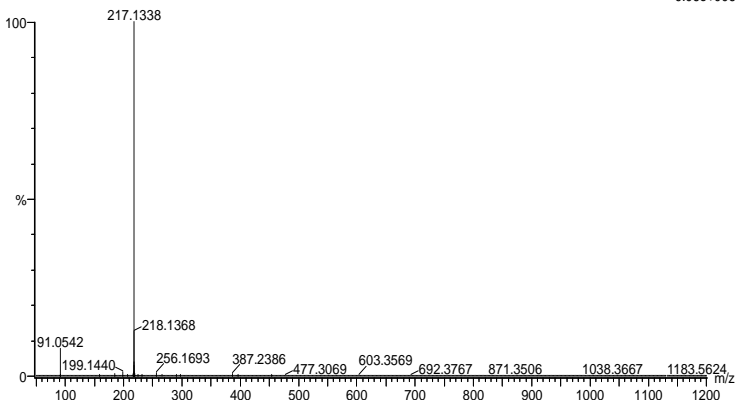
Elements Used:

C: 0-100 H: 0-150 N: 0-10 O: 0-10

svg_20190423_2019_348 22 (0.419) AM2 (Ar,35000.0,0.00,0.00); Crm (19:22)

1: TOF MS ES+

9.06e+006



Minimum: -50.0

Maximum: 5.0 5.0 50.0

Mass	Calc. Mass	mDa	PPM	DBE	i-FIT	Norm	Conf (%)	Formula
217.1338	217.1341	-0.3	-1.4	6.5	1749.8	n/a	n/a	C13 H17 N2 O

22.8 HR-MS negative mode spectrum of IL 9e

Elemental Composition Report

Page 1

Single Mass Analysis

Tolerance = 2.5 PPM / DBE: min = -50.0, max = 50.0

Element prediction: Off

Number of isotope peaks used for i-FIT = 3

Monoisotopic Mass, Even Electron Ions

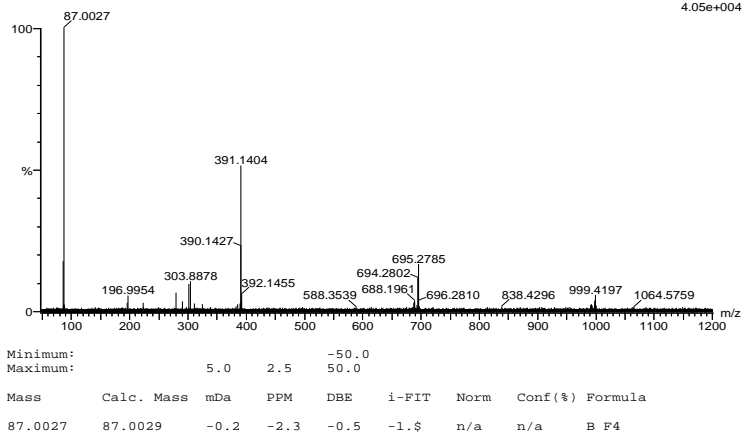
403 formula(e) evaluated with 1 results within limits (all results (up to 1000) for each mass)

Elements Used:

C: 0-100 H: 0-150 B: 0-2 N: 0-3 O: 0-10 F: 0-8 S: 0-2
svg_20190423_2019_349 43 (0.486) AM2 (Ar,35000,0,0.00,0.00); Cm (39:52)

1: TOF MS ES-

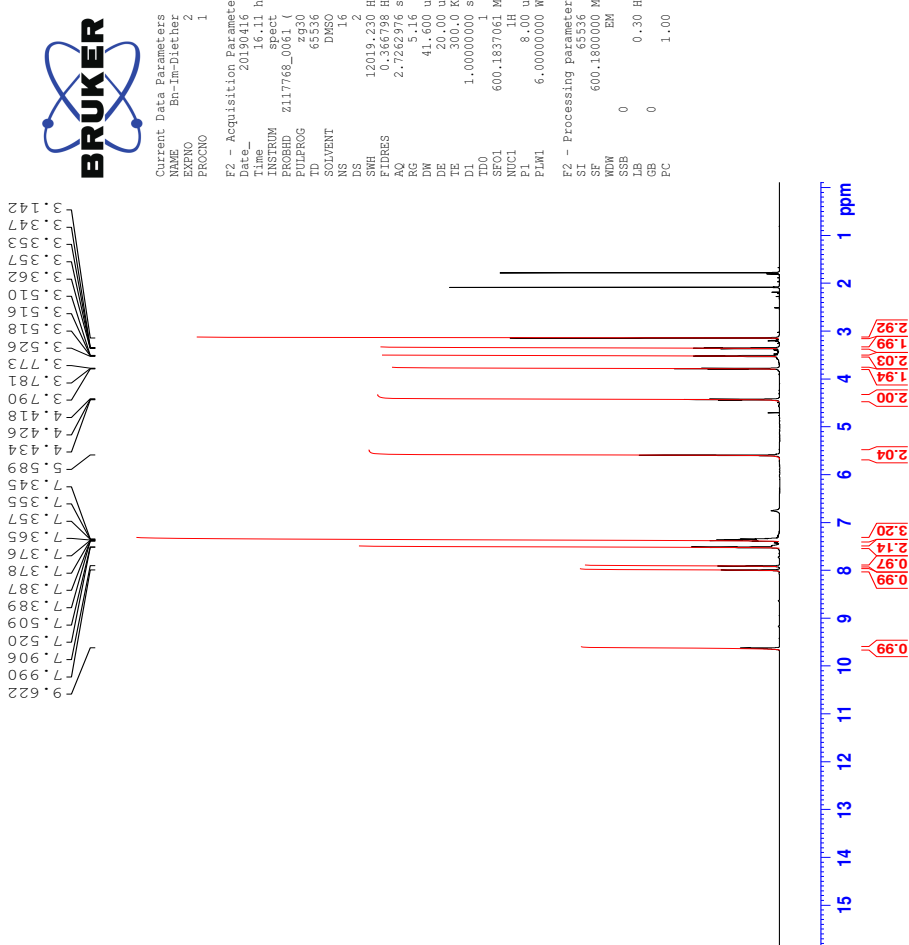
4.05e+004



Minimum: 5.0 Maximum: 2.5 -50.0

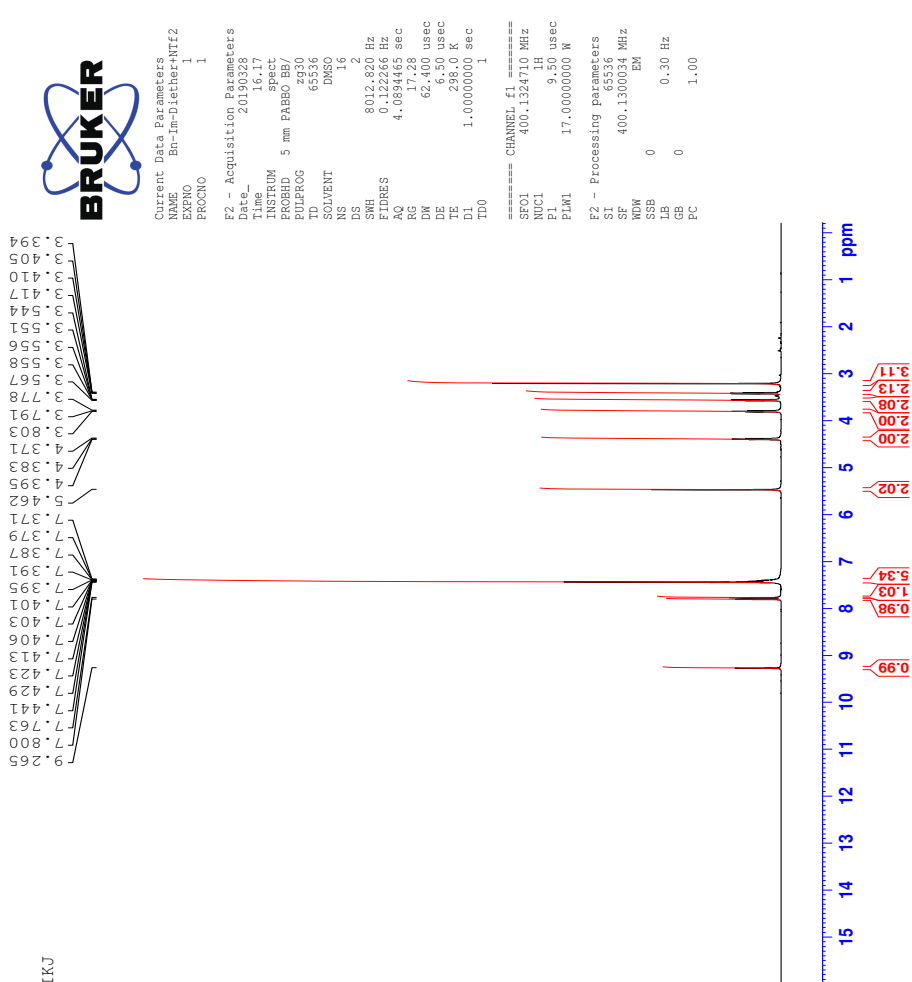
Mass	Calc. Mass	mDa	PPM	DBE	i-FIT	Norm	Conf (%)	Formula
87.0027	87.0029	-0.2	-2.3	-0.5	-1.5	n/a	n/a	B F4

23 ^1H -NMR spectrum of compound 10a

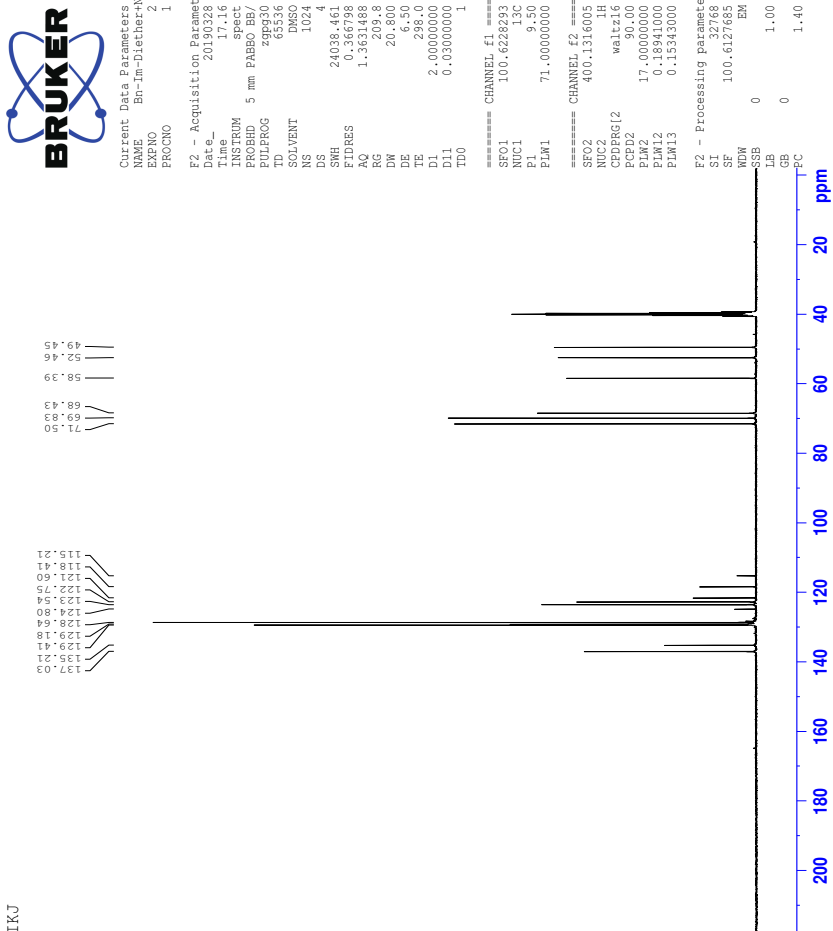


24 Spectra of IL 10b

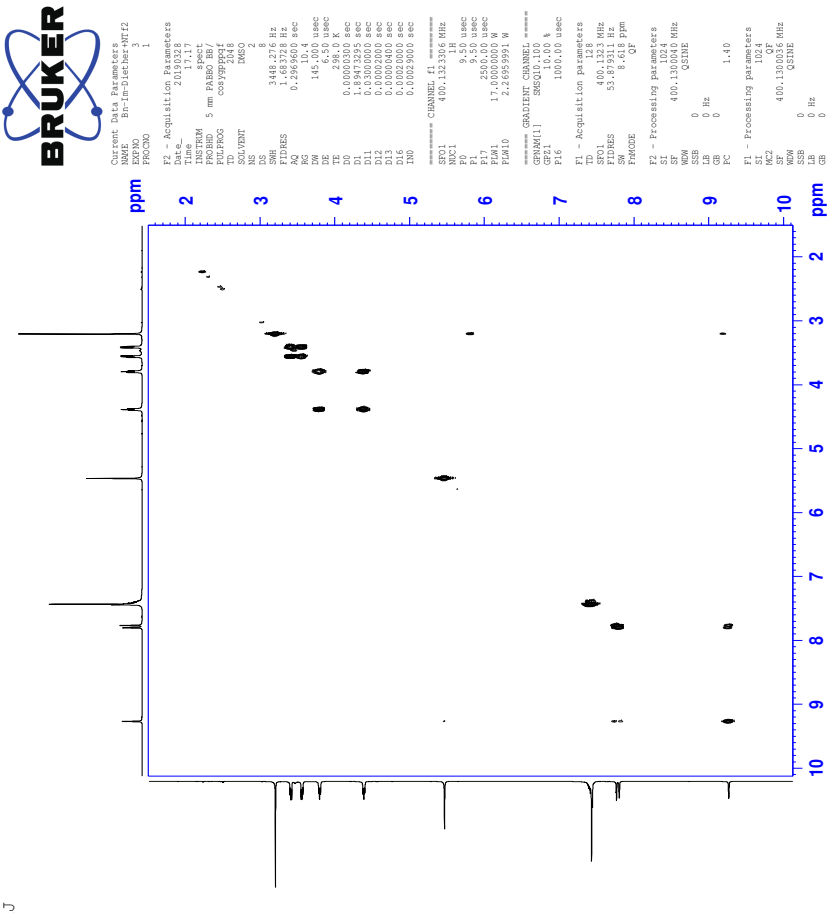
24.1 ^1H -NMR spectrum of IL 10b



24.2 ^{13}C -NMR spectrum of IL 10b



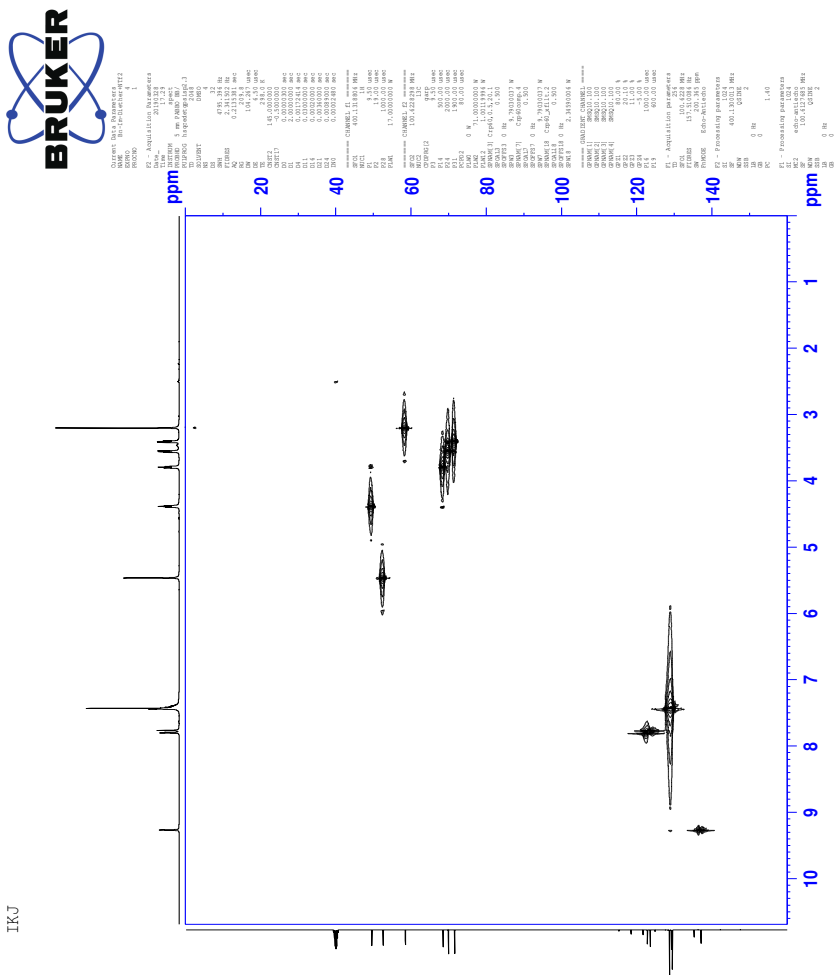
24.3 COSY-spectrum of IL 10b



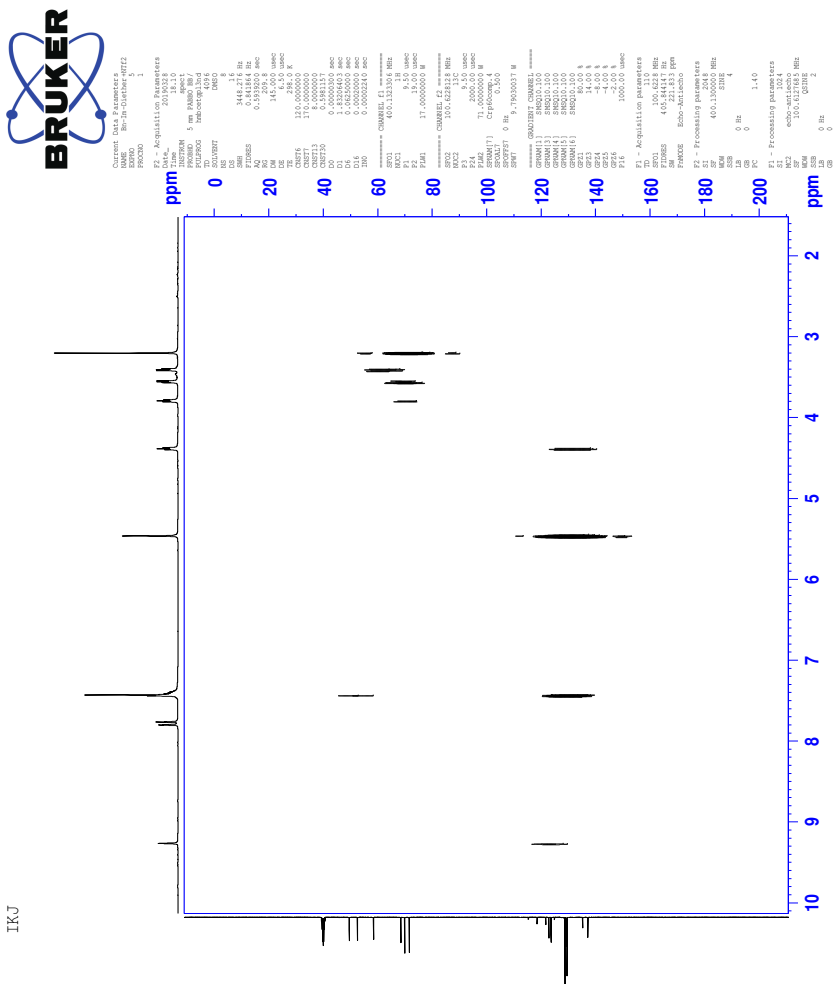
TKJ

CXLI

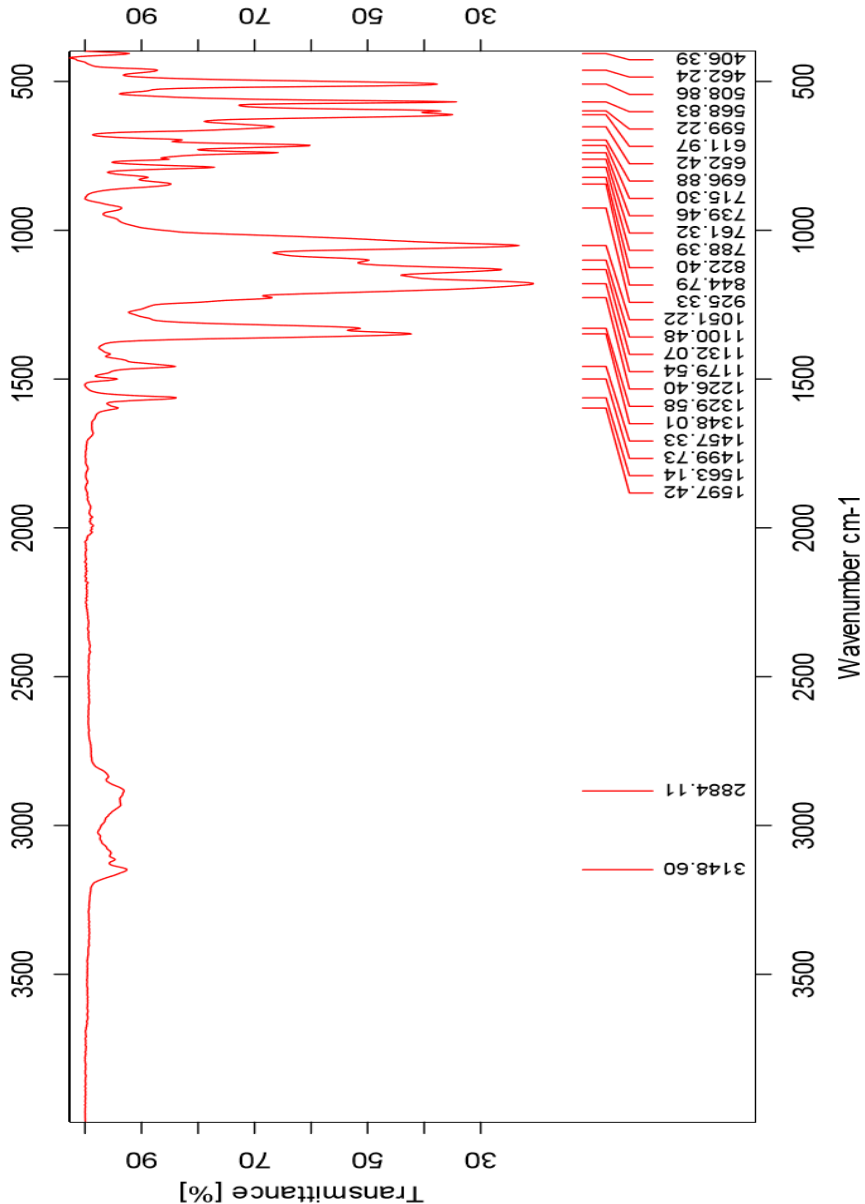
24.4 HSQC-spectrum of IL 10b



24.5 HMBC-spectrum of IL 10b



24.6 IR-spectrum of IL 10b



24.7 HR-MS positive mode spectrum of IL 10b

Elemental Composition Report

Page 1

Single Mass Analysis

Tolerance = 2.0 PPM / DBE: min = -50.0, max = 50.0

Element prediction: Off

Number of isotope peaks used for i-FIT = 3

Monoisotopic Mass, Even Electron Ions

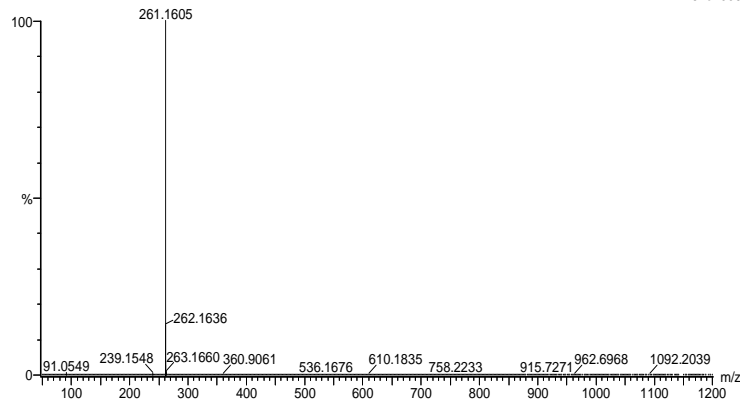
656 formula(e) evaluated with 2 results within limits (all results (up to 1000) for each mass)

Elements Used:

C: 0-100 H: 0-150 N: 0-5 O: 0-10 Au: 0-3

2019-408_RERUN 30 (0.568) AM2 (Ar,35000.0,0.00,0.00); Cm (30:31)
1: TOF MS ES+

4.62e+006



Minimum: -50.0
Maximum: 5.0 2.0 50.0

Mass	Calc. Mass	mDa	PPM	DBE	i-FIT	Norm	Conf (%)	Formula
261.1605	261.1605	0.0	0.0	-8.5	1482.7	11.367	0.00	C H24 N2 Au
261.1603	261.1603	0.2	0.8	6.5	1471.4	0.000	100.00	C15 H21 N2 O2

24.8 HR-MS negative mode spectrum of IL 10b

Elemental Composition Report

Page 1

Single Mass Analysis

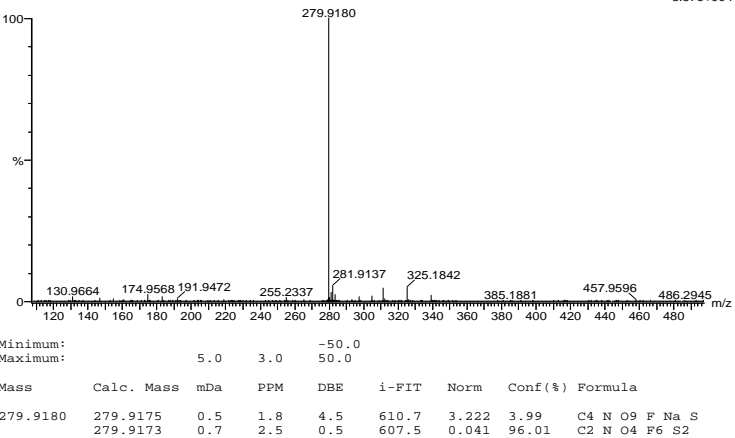
Tolerance = 3.0 PPM / DBE: min = -50.0, max = 50.0
Element prediction: Off
Number of isotope peaks used for i-FIT = 3

Monoisotopic Mass, Even Electron Ions
1959 formula(e) evaluated with 2 results within limits (all results (up to 1000) for each mass)

Elements Used:

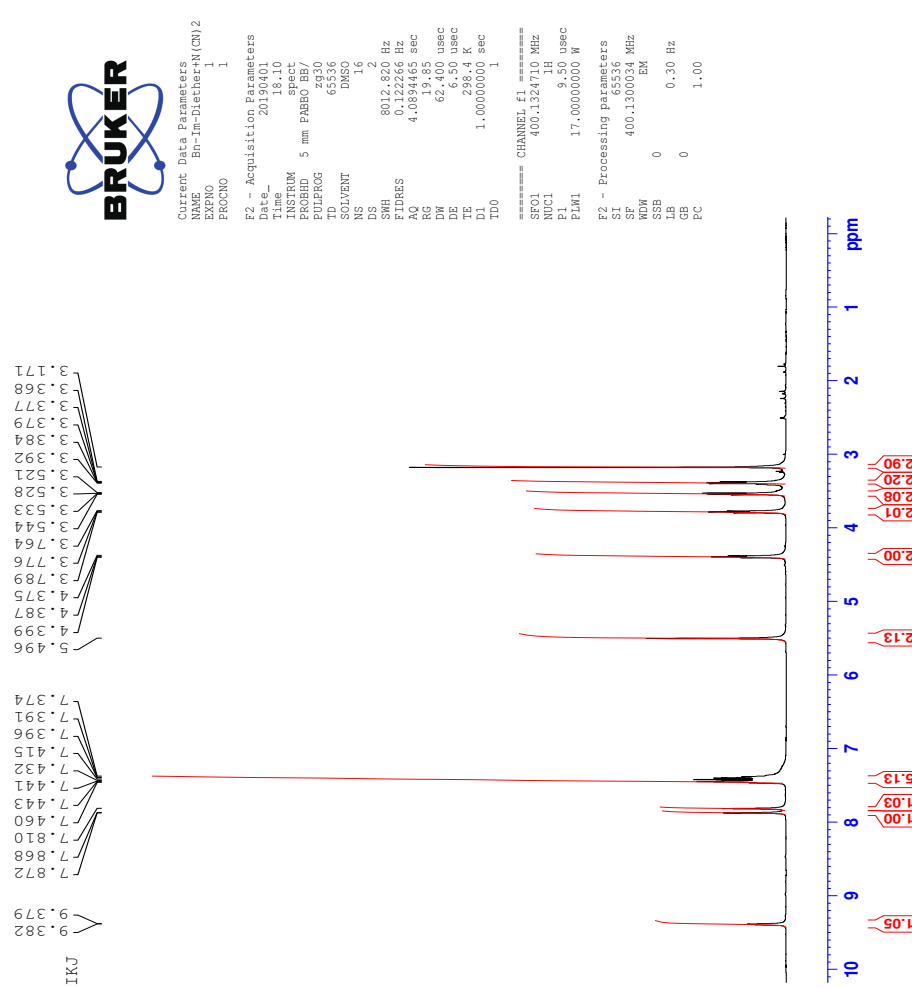
C: 0-5 N: 0-10 O: 0-10 F: 0-7 Na: 0-1 S: 0-3
2019-409neg.13 (0.156) AM2 (Ar,35000.0,0.00,0.00); Cm (13:15)
1: TOF MS ES-

8.67e+004

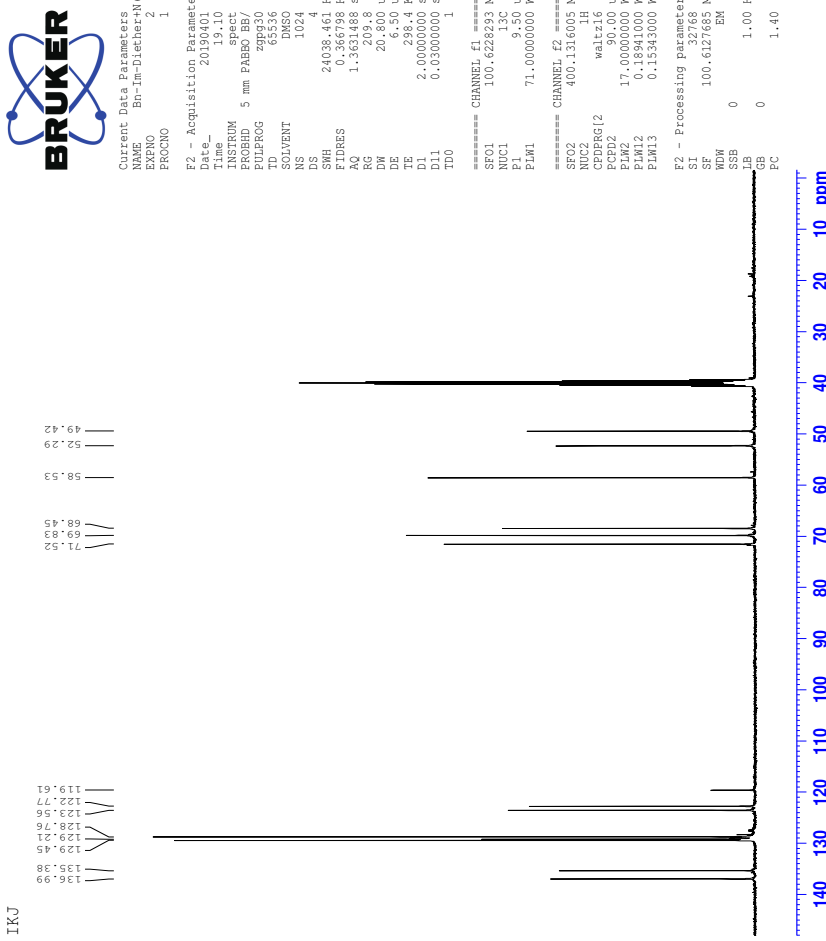


25 Spectra of IL 10c

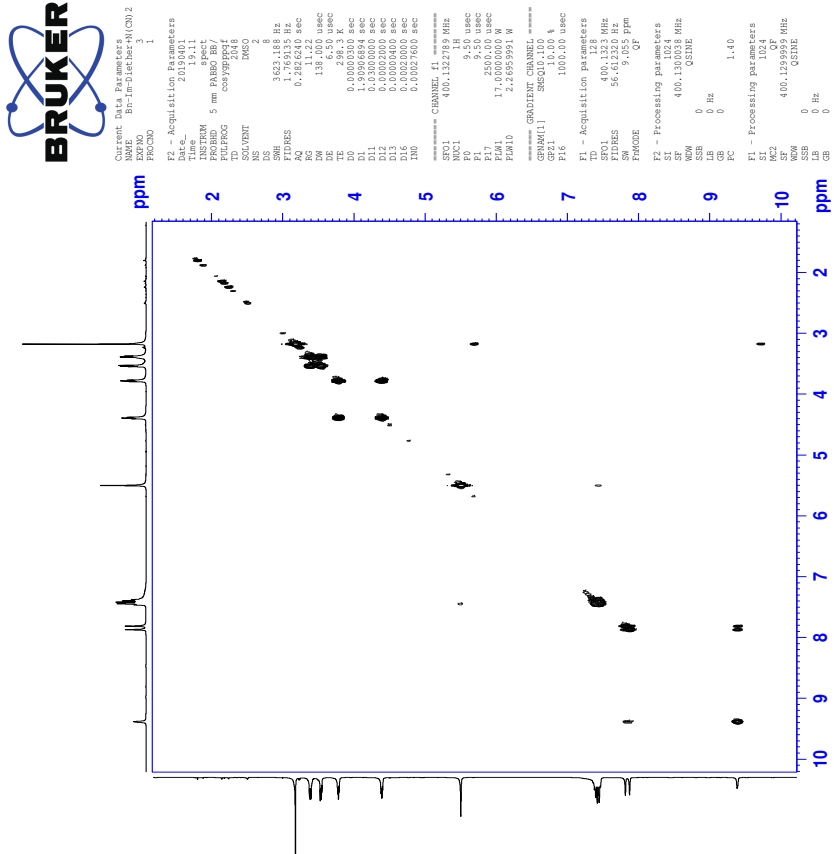
25.1 ^1H -NMR spectrum of IL 10c



25.2 ^{13}C -NMR spectrum of IL 10c

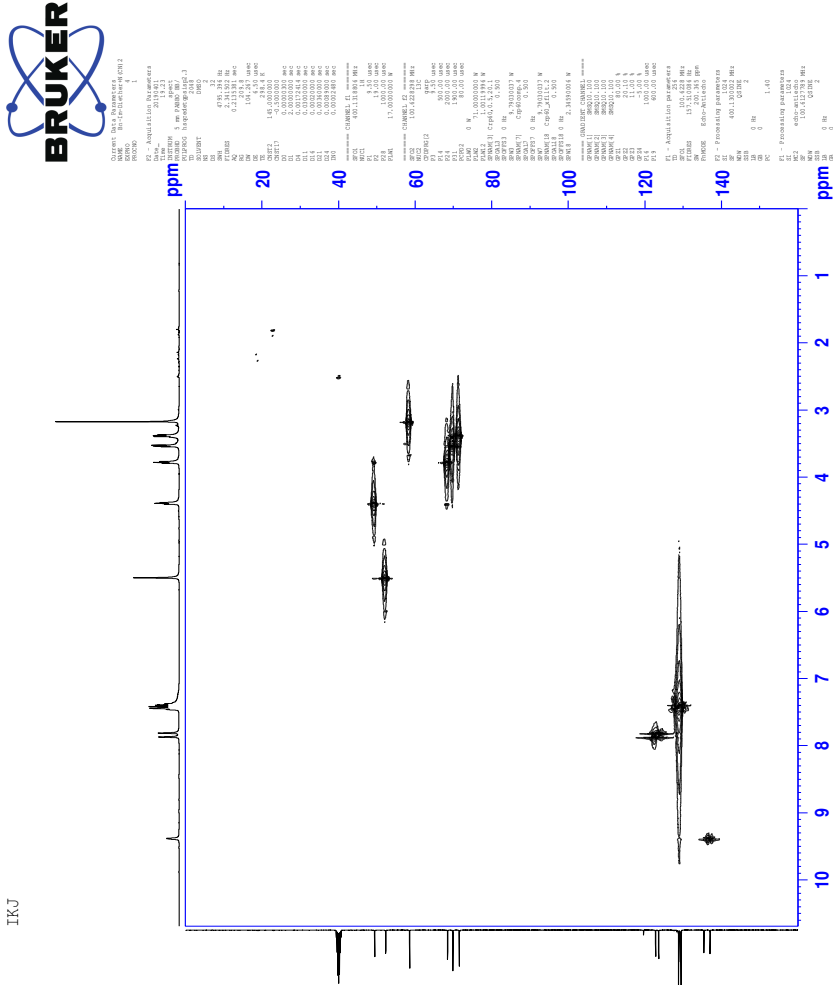


25.3 COSY-spectrum of IL 10c



TKJ

25.4 HSQC-spectrum of IL 10c

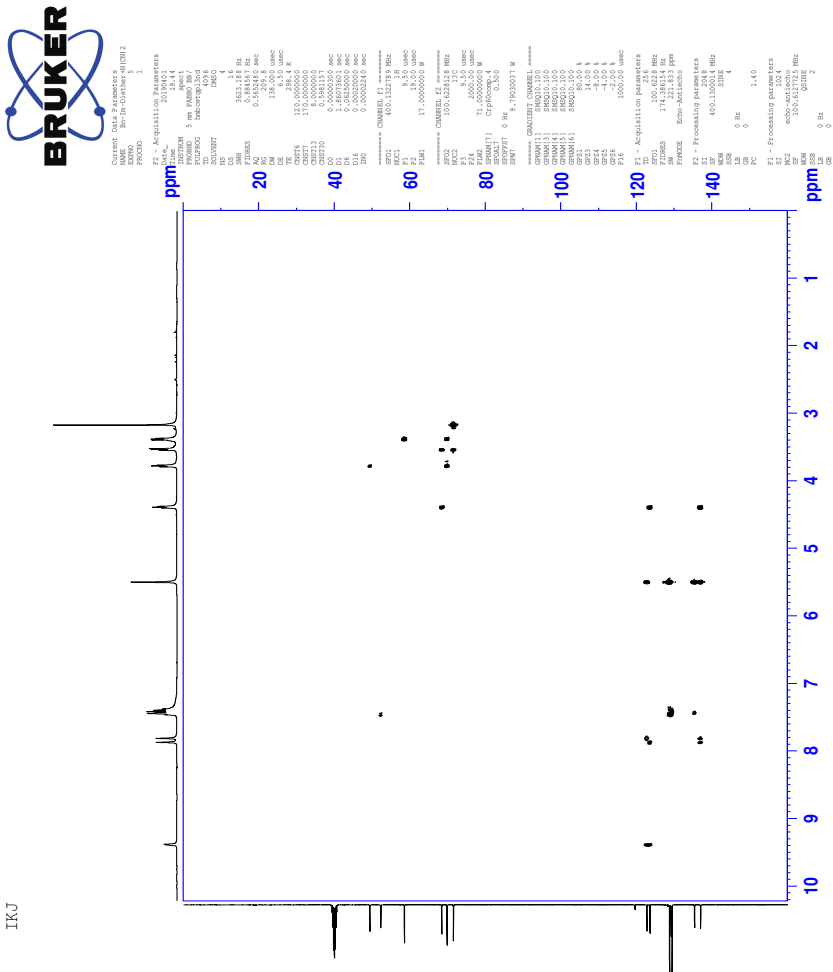


TKJ

CL

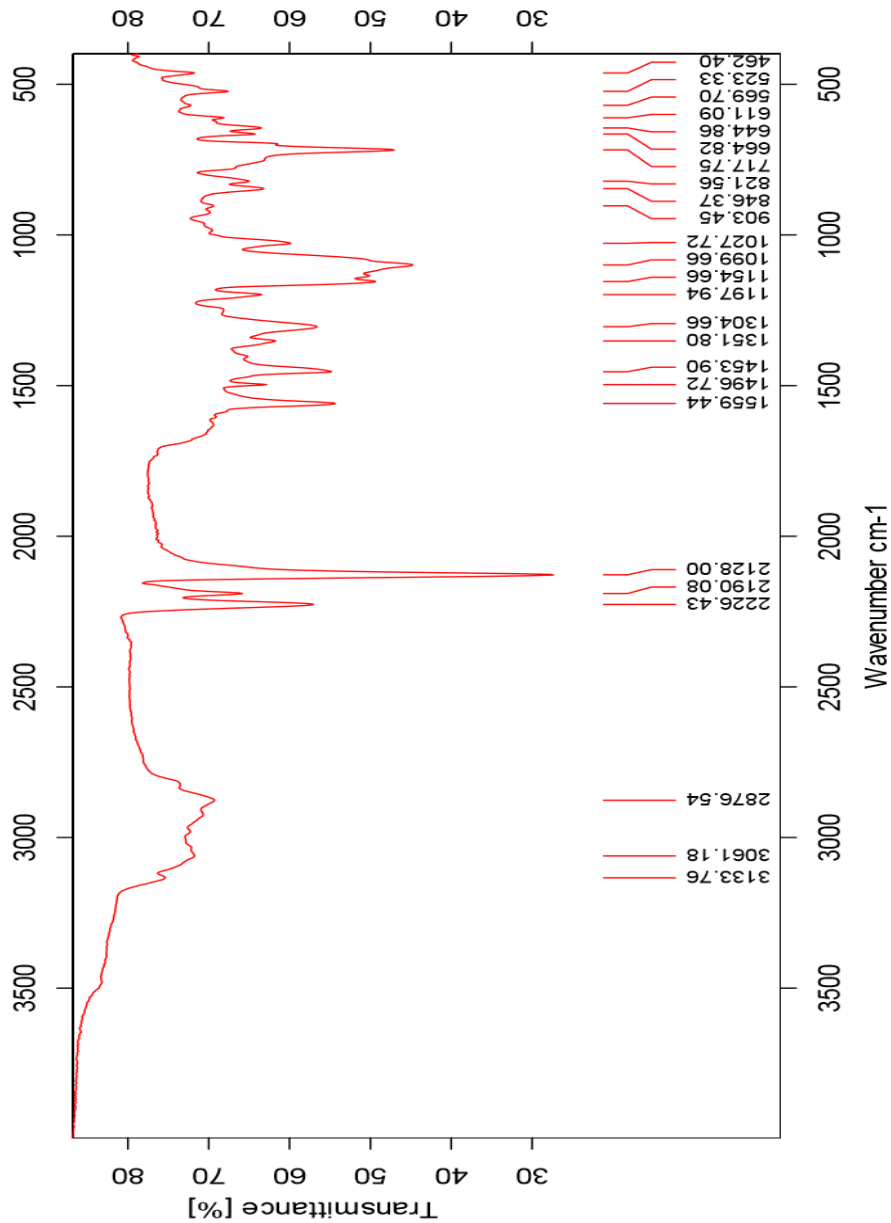
25.5 HMBC-spectrum of IL 10c

TKJ



CLI

25.6 IR-spectrum of IL 10c



25.7 HR-MS positive mode spectrum of IL 10c

Elemental Composition Report

Page 1

Single Mass Analysis

Tolerance = 5.0 PPM / DBE: min = -50.0, max = 50.0

Element prediction: Off

Number of isotope peaks used for i-FIT = 3

Monoisotopic Mass, Even Electron Ions

943 formula(e) evaluated with 1 results within limits (all results (up to 1000) for each mass)

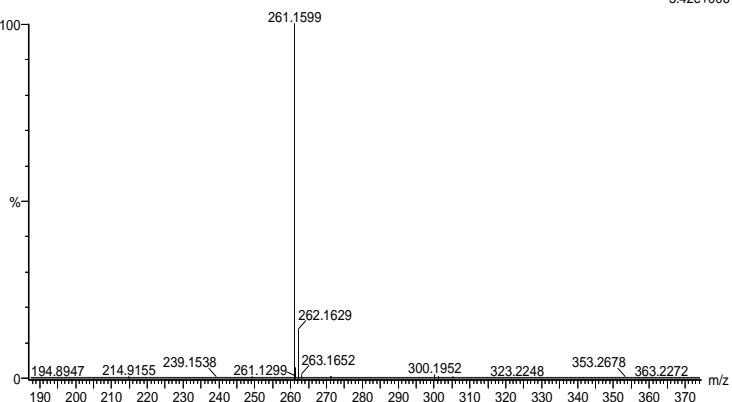
Elements Used:

C: 0-100 H: 0-150 N: 0-10 O: 0-10

2019_518FIA17 (0.323) AM2 (Ar,35000.0,0.00,0.00); Cm (11:17)

1: TOF MS ES+

3.42e+006

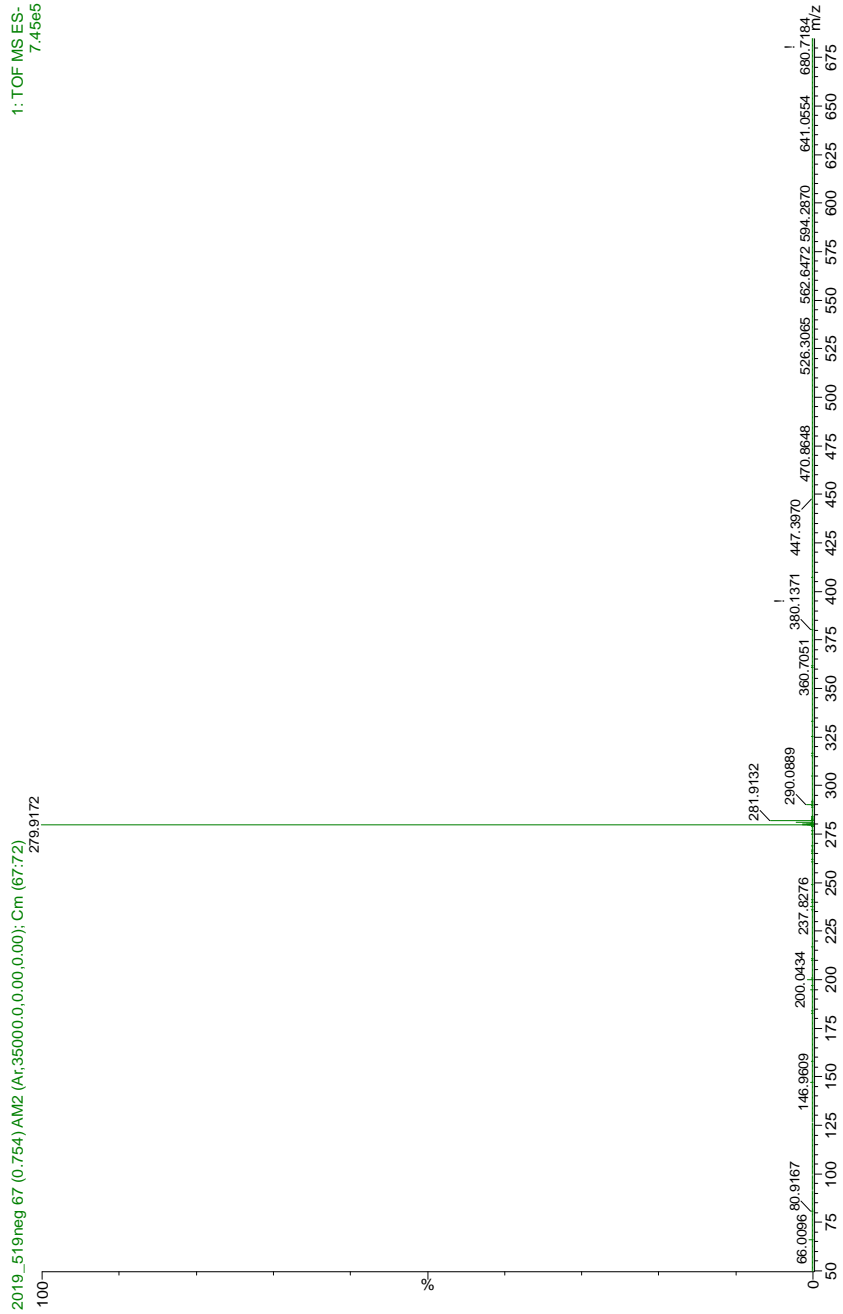


Minimum: -50.0

Maximum: 5.0 5.0 50.0

Mass	Calc. Mass	mDa	PPM	DBE	i-FIT	Norm	Conf (%)	Formula
261.1599	261.1603	-0.4	-1.5	6.5	1500.9	n/a	n/a	C15 H21 N2 O2

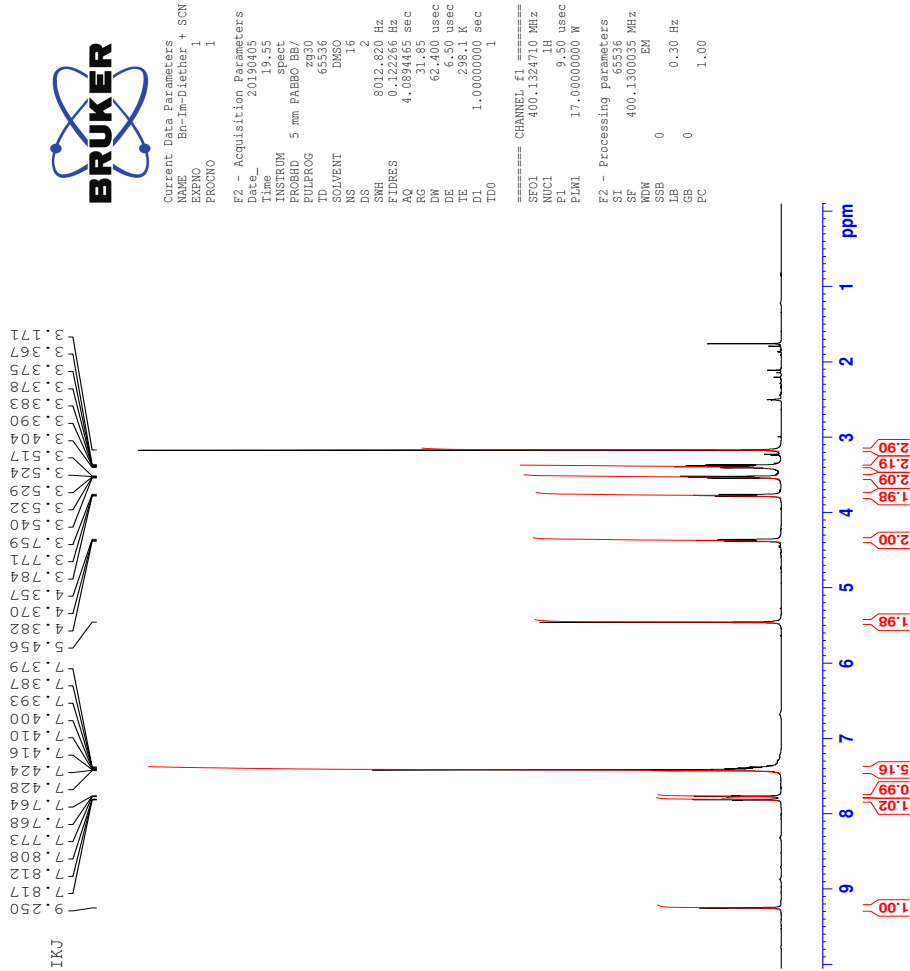
25.8 HR-MS negative mode spectrum of IL 10c



CLIV

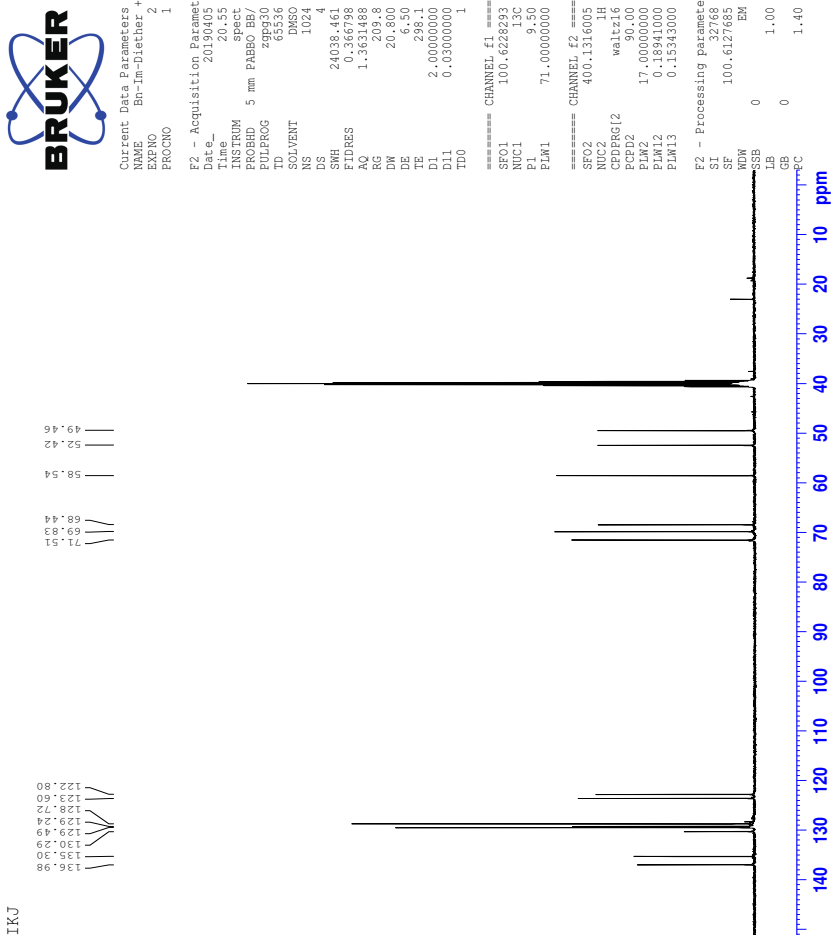
26 Spectra of IL 10d

26.1 ^1H -NMR spectrum of IL 10d

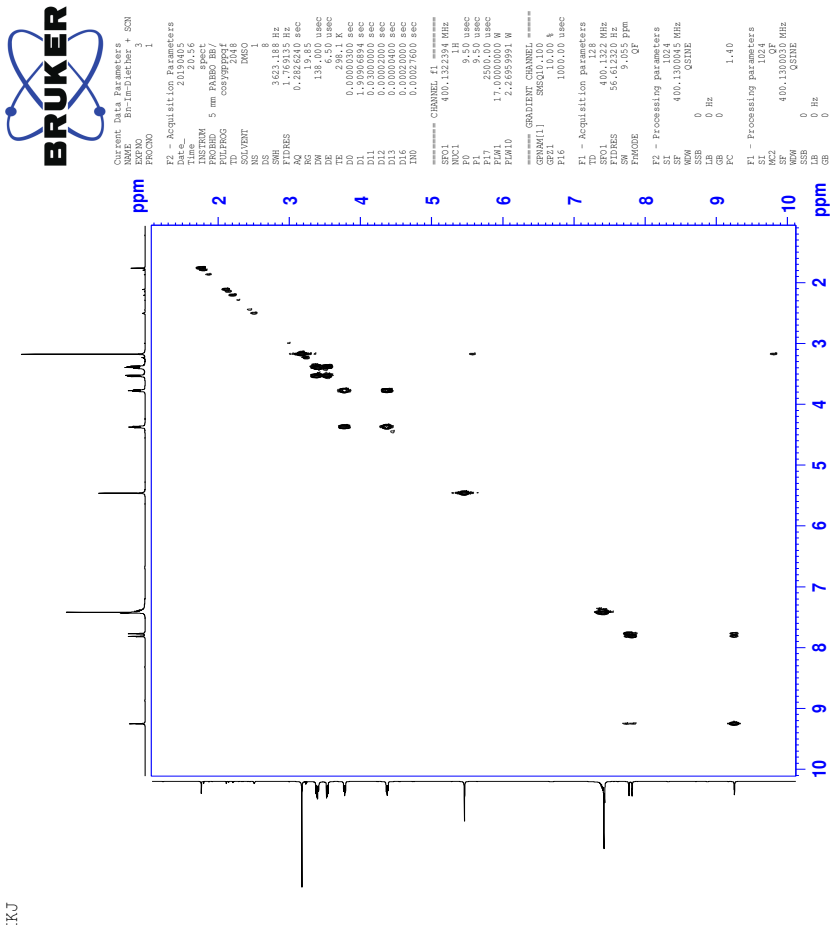


CLV

26.2 ^{13}C -NMR spectrum of IL 10d

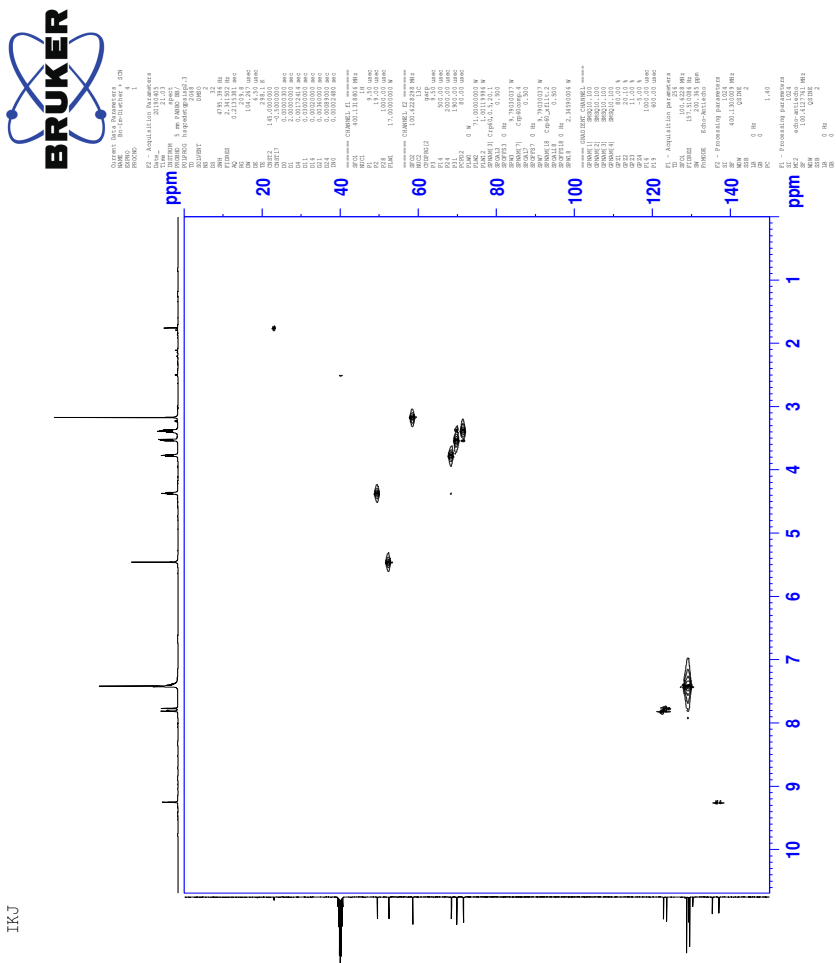


26.3 COSY-spectrum of IL 10d



TKJ

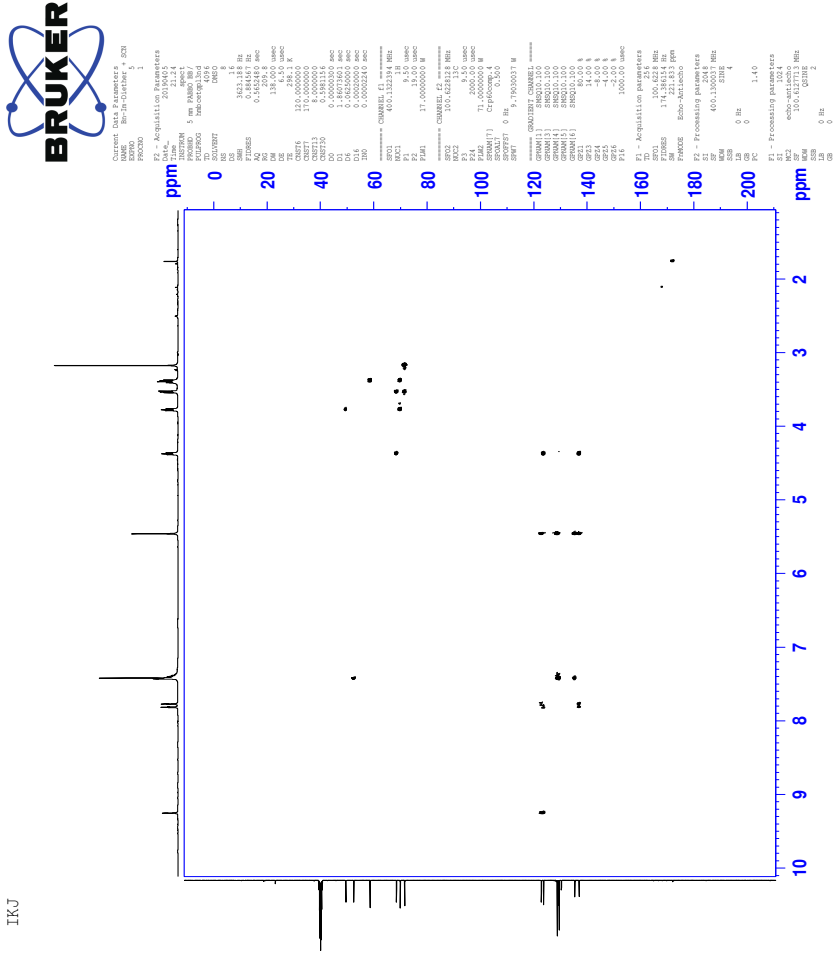
26.4 HSQC-spectrum of IL 10d



TKJ

CLVIII

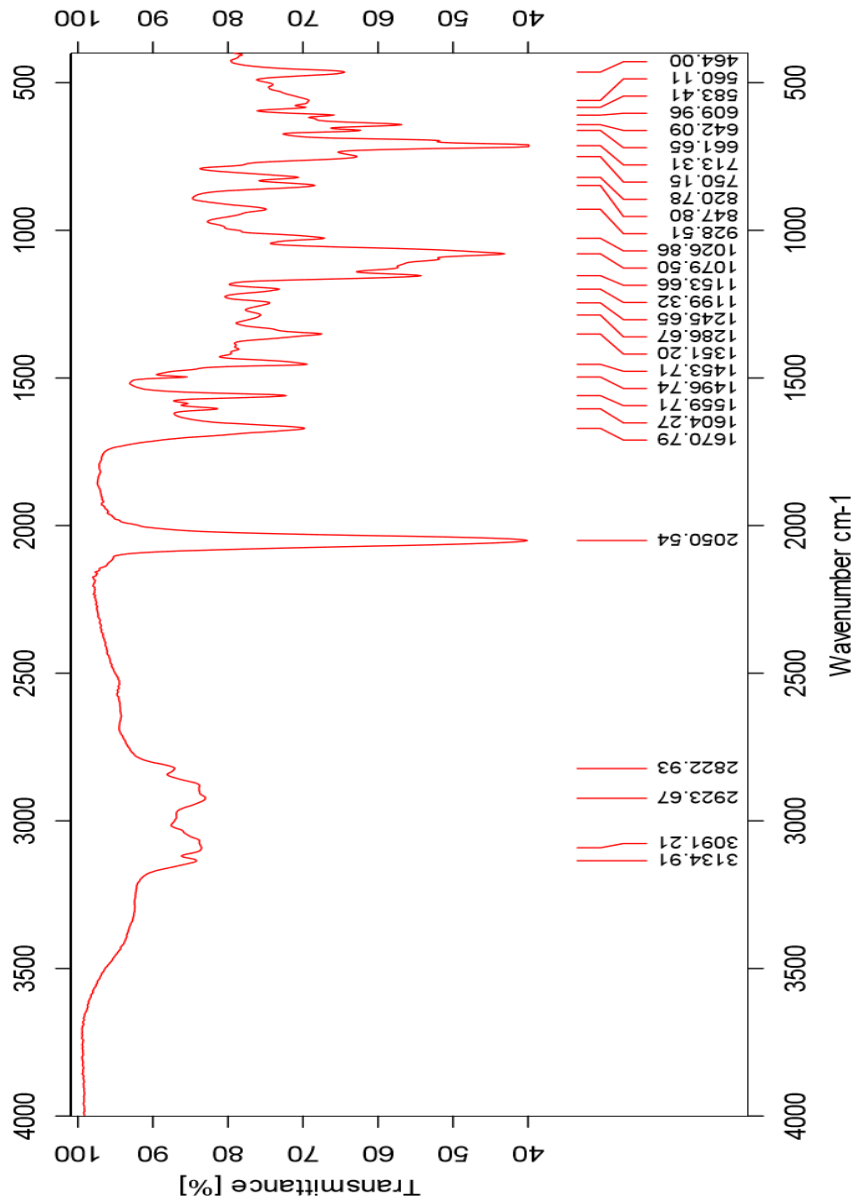
26.5 HMBC-spectrum of IL 10d



TKJ

CLIX

26.6 IR-spectrum of IL 10d



26.7 HR-MS positive mode spectrum of IL 10d

Elemental Composition Report

Page 1

Single Mass Analysis

Tolerance = 2.0 PPM / DBE: min = -50.0, max = 50.0

Element prediction: Off

Number of isotope peaks used for i-FIT = 3

Monoisotopic Mass, Even Electron Ions

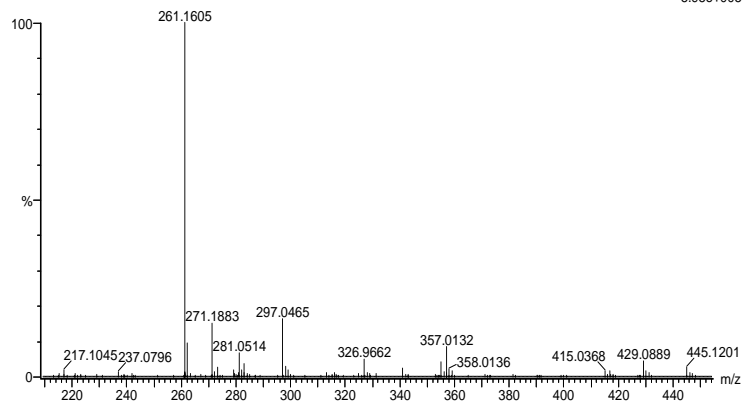
656 formula(e) evaluated with 2 results within limits (all results (up to 1000) for each mass)

Elements Used:

C: 0-100 H: 0-150 N: 0-5 O: 0-10 Au: 0-3

2019-412_RERUN 32 (0.602) AM2 (Ar,35000.0,0.00,0.00); Cr (28:33)
1: TOF MS ES+

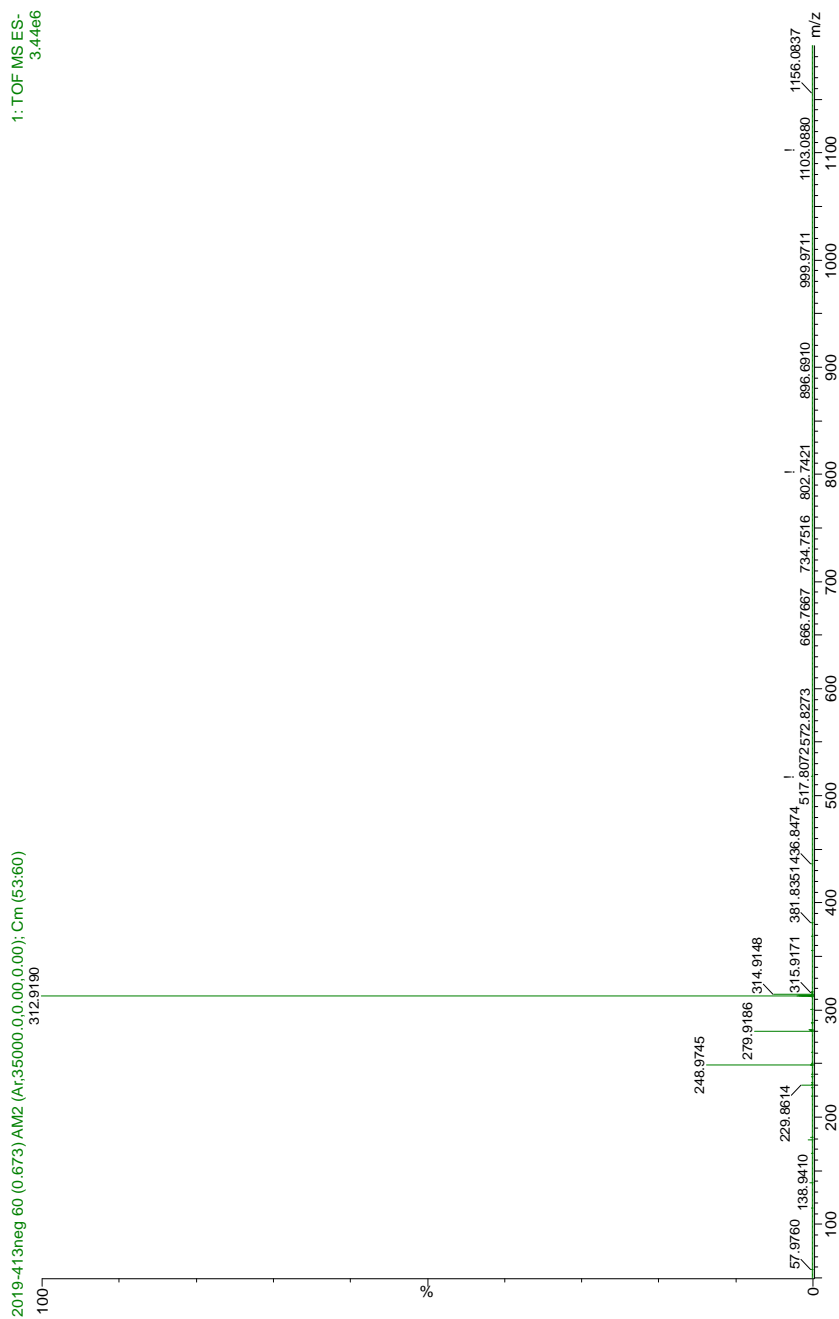
5.95e+005



Minimum: -50.0
Maximum: 5.0 2.0 50.0

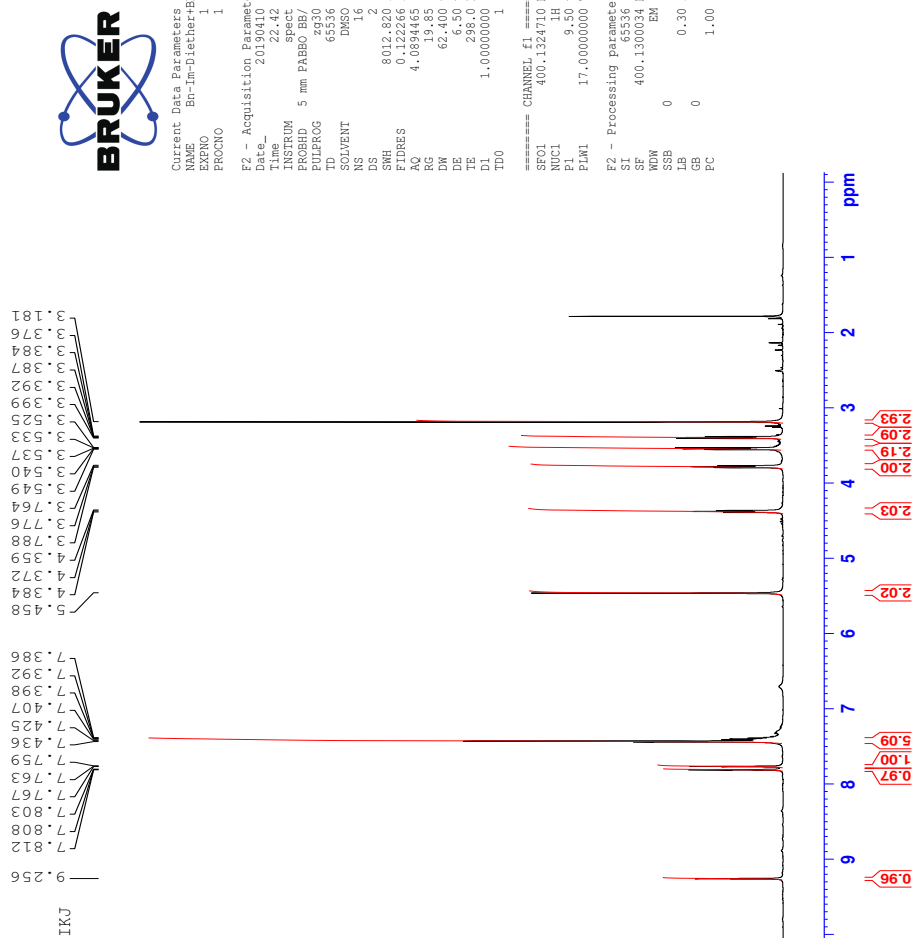
Mass	Calc. Mass	mDa	PPM	DBE	i-FIT	Norm	Conf (%)	Formula
261.1605	261.1605	0.0	0.0	-8.5	1125.2	1.249	28.69	C H24 N2 Au
261.1603	261.1603	0.2	0.8	6.5	1124.3	0.338	71.31	C15 H21 N2 O2

26.8 HR-MS negative mode spectrum of IL 10d

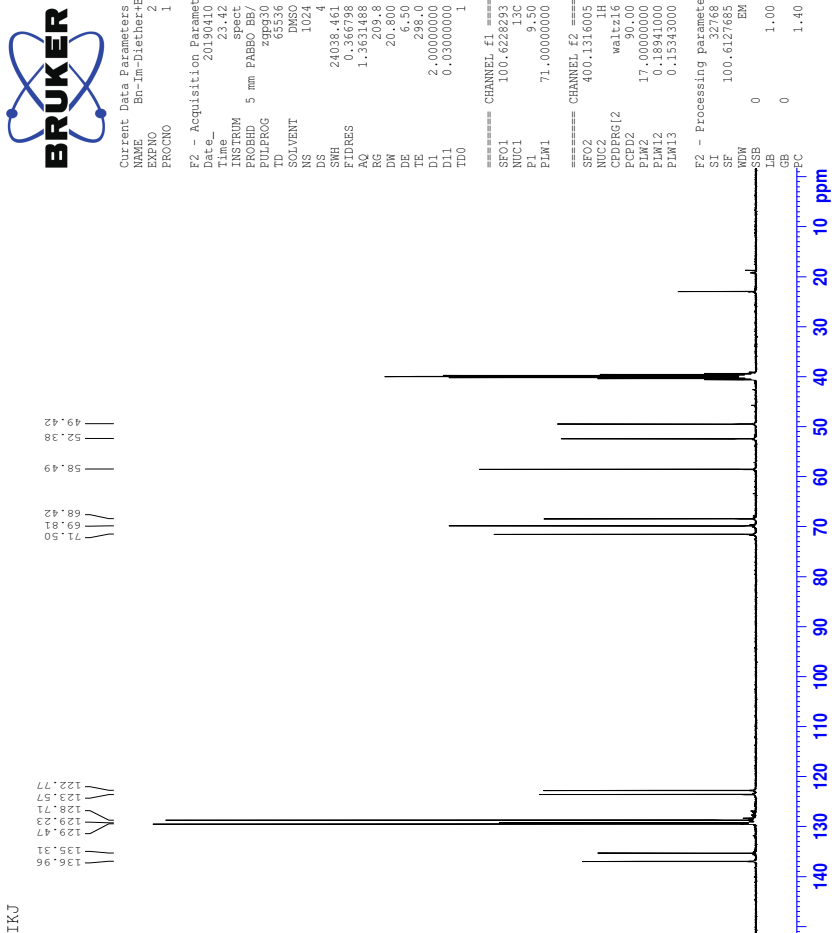


27 Spectra of IL 10e

27.1 ^1H -NMR spectrum of IL 10e



27.2 ^{13}C -NMR spectrum of IL 10e



27.3 ^{19}F -NMR spectrum of IL 10e

BRUKER

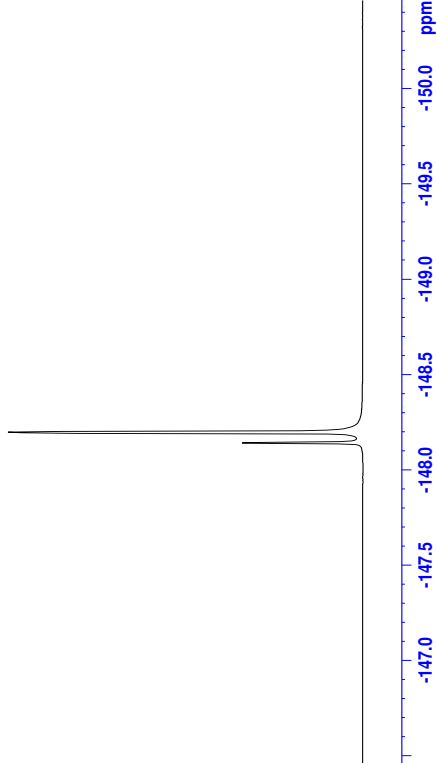
Current	Data Parameters
NAME	Bn-Im-Dietlner+BF4
EXP NO	6
PROCNO	1

```

===== CHANNEL F1 =====
SF01      376.460164 MHz
NUC1      1.9F
P1        17.000 usec
PLW1      19.00000000 W

F2 - Processing parameters
SI        65535
SF        376.498662 MHz
WDW      EM
SSB      0
LB        0.30 Hz
GB        0
PC      1.00

```

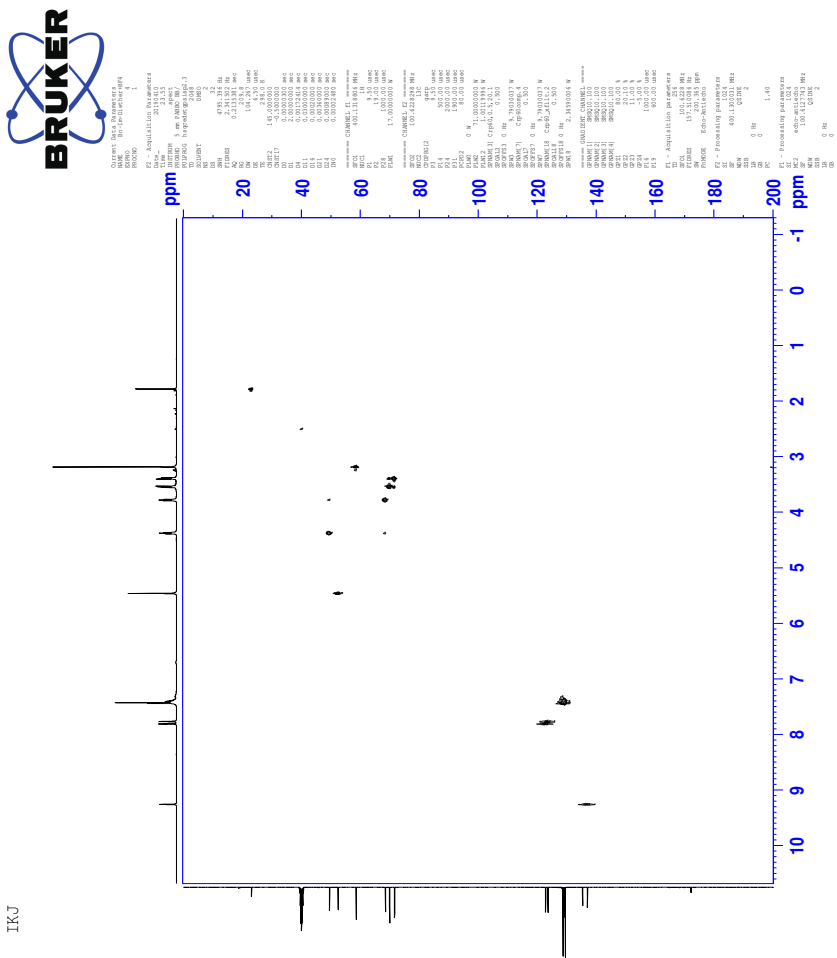


TKJ

27.4 COSY-spectrum of IL 10e

TKJ

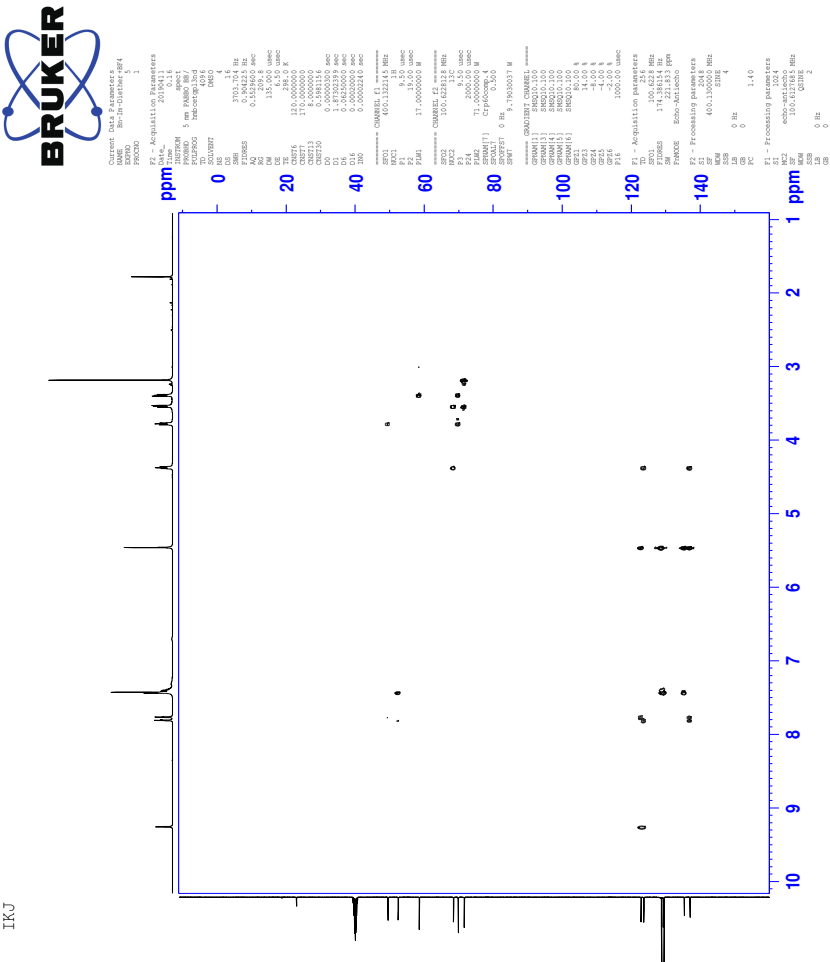
27.5 HSQC-spectrum of IL 10e



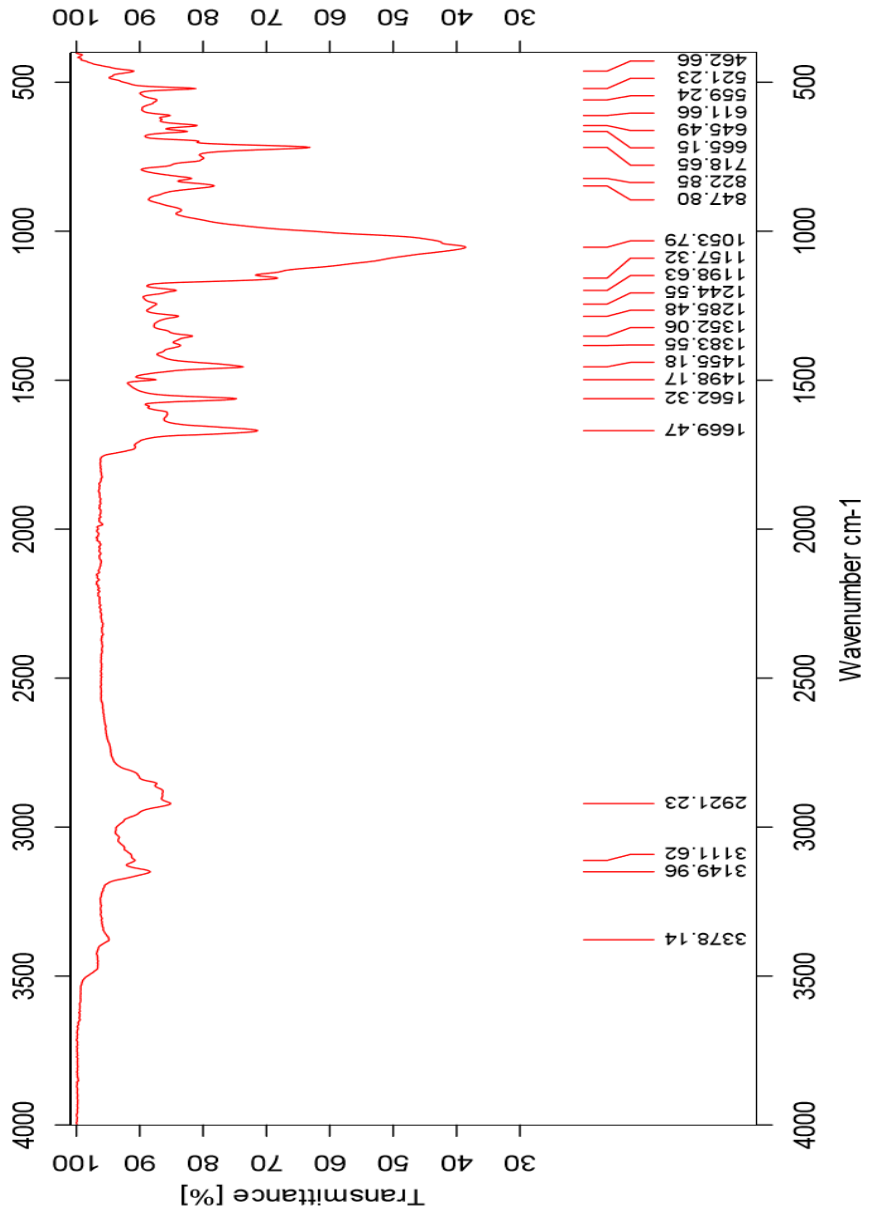
TKJ

CLXVII

27.6 HMBC-spectrum of IL 10e



27.7 IR-spectrum of IL 10e



27.8 HR-MS positive mode spectrum of IL 10e

Elemental Composition Report

Page 1

Single Mass Analysis

Tolerance = 2.0 PPM / DBE: min = -50.0, max = 50.0

Element prediction: Off

Number of isotope peaks used for i-FIT = 3

Monoisotopic Mass, Even Electron Ions

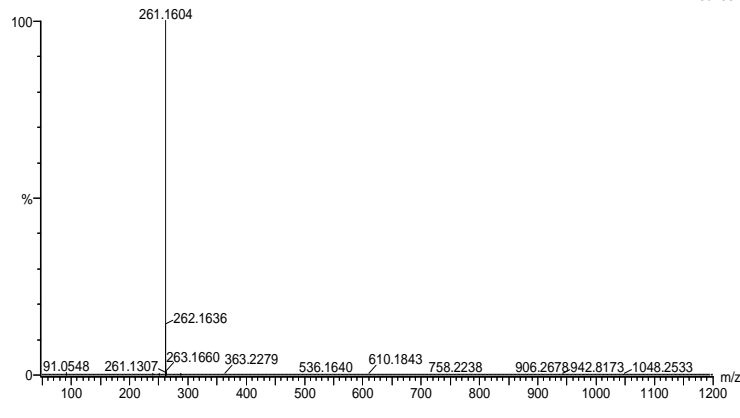
656 formula(e) evaluated with 2 results within limits (all results (up to 1000) for each mass)

Elements Used:

C: 0-100 H: 0-150 N: 0-5 O: 0-10 Au: 0-3

2019-414_RERUN 37 (0.699) AM2 (Ar,35000.0,0.00,0.00); Cr (37:41)
1: TOF MS ES+

1.48e+007



Minimum: -50.0

Maximum: 5.0 2.0 50.0

Mass	Calc. Mass	mDa	PPM	DBE	i-FIT	Norm	Conf (%)	Formula
------	------------	-----	-----	-----	-------	------	----------	---------

261.1604	261.1605	-0.1	-0.4	-8.5	1753.7	12.107	0.00	C H24 N2 Au
	261.1603	0.1	0.4	6.5	1741.6	0.000	100.00	C15 H21 N2 O2

27.9 HR-MS negative mode spectrum of IL 10e

Elemental Composition Report

Page 1

Single Mass Analysis

Tolerance = 5.0 PPM / DBE: min = -50.0, max = 50.0

Element prediction: Off

Number of isotope peaks used for i-FIT = 3

Monoisotopic Mass, Even Electron Ions

563 formula(e) evaluated with 2 results within limits (all results (up to 1000) for each mass)

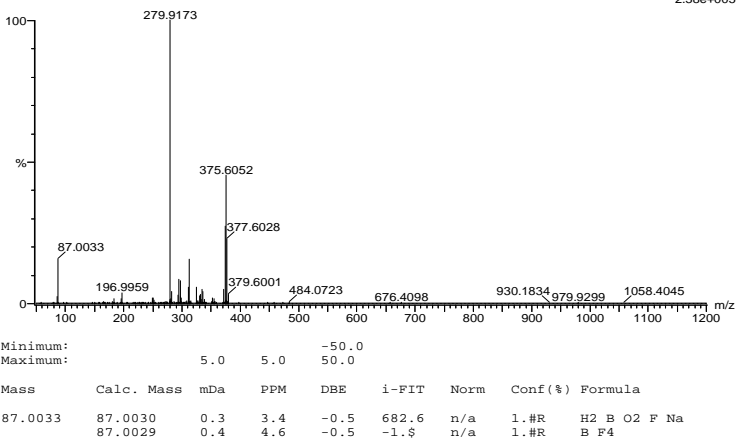
Elements Used:

C: 0-100 H: 0-150 B: 0-2 N: 0-10 O: 0-10 F: 0-5 Na: 0-1 S: 0-3

2019-415neg.127 (1.416) AM2 (Ar,35000.0,0.00,0.00); Cm (126:129)

1: TOF MS ES-

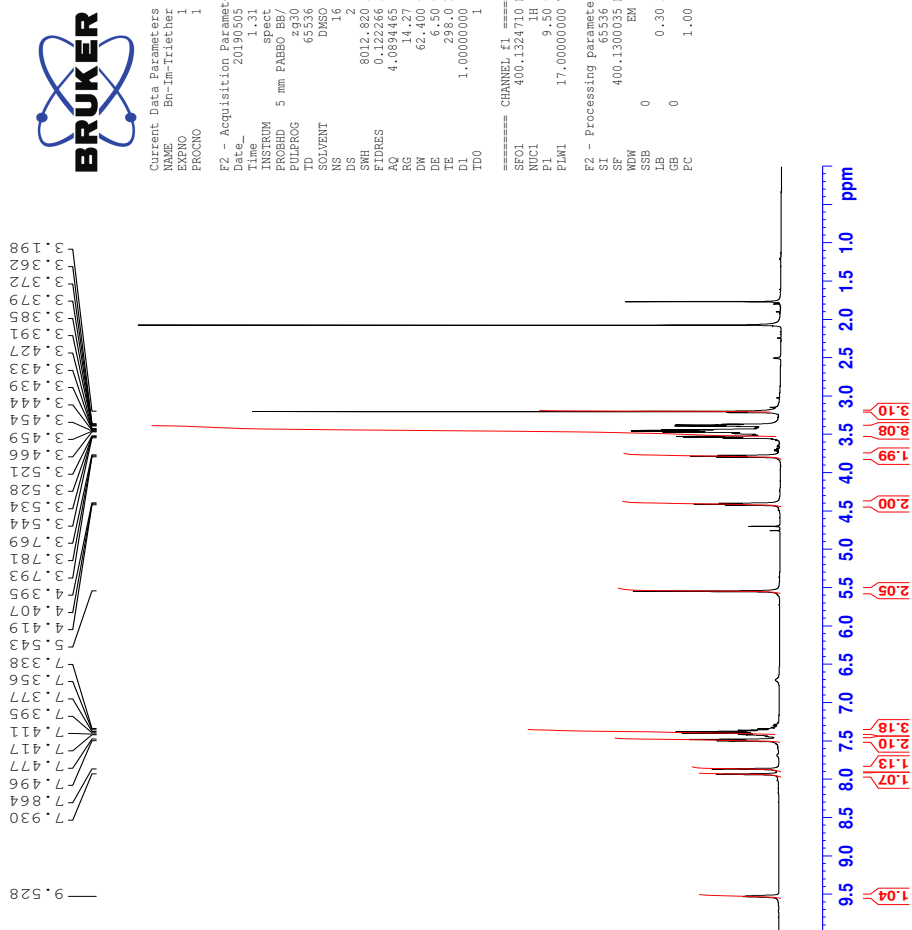
2.38e+005



Minimum: 5.0 Maximum: 5.0 -50.0

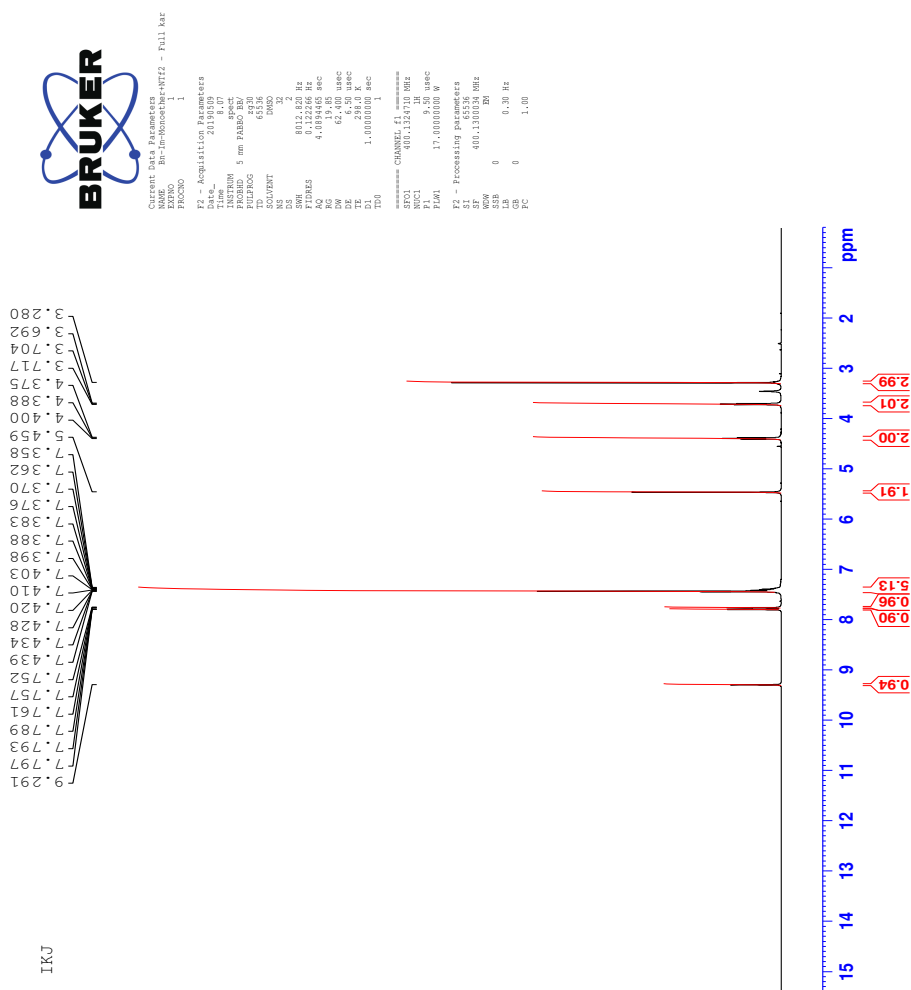
Mass	Calc. Mass	mDa	PPM	DBE	i-FIT	Norm	Conf (%)	Formula
87.0033	87.0030	0.3	3.4	-0.5	682.6	n/a	1.#R	H ₂ B O ₂ F Na
	87.0029	0.4	4.6	-0.5	-1.5	n/a	1.#R	B F ₄

28 $^1\text{H-NMR}$ spectrum of compound 11a



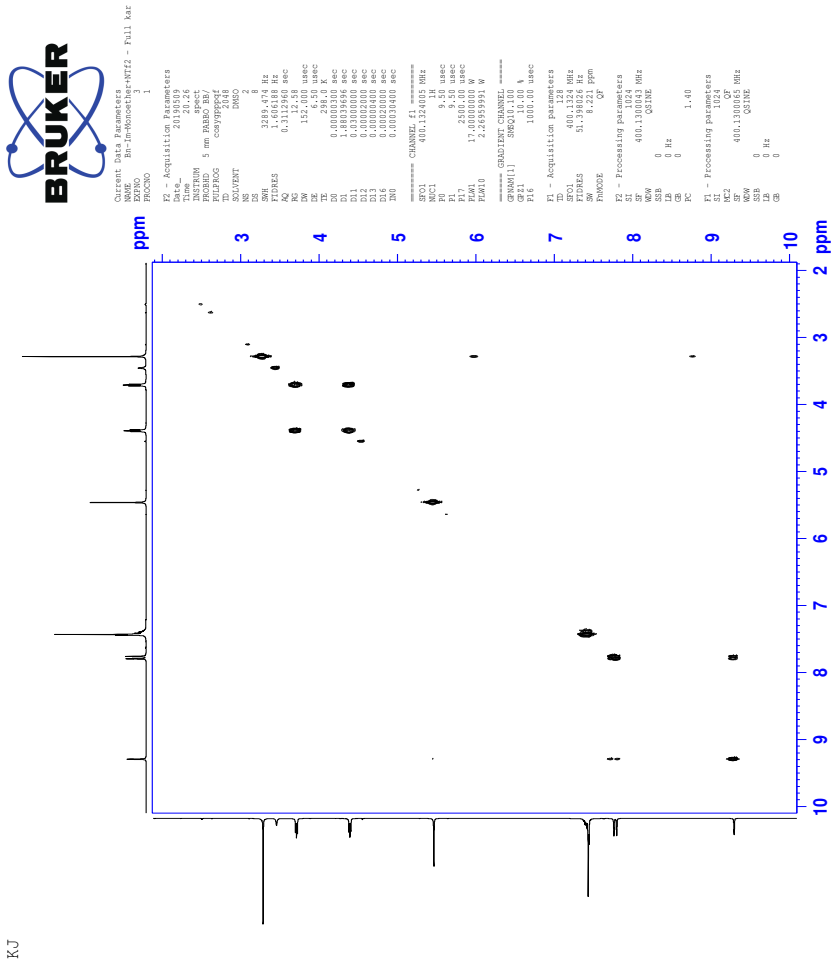
29 Spectra of IL 11b

29.1 ^1H -NMR spectrum of IL 11b

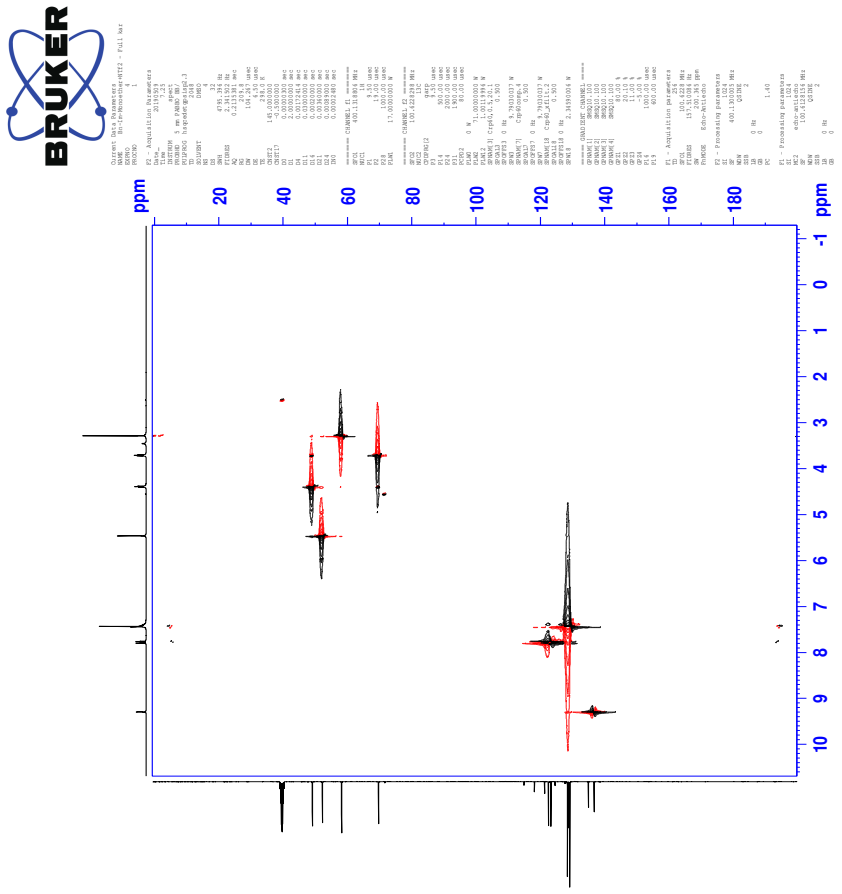


29.2 ^{13}C -NMR spectrum of IL 11b

29.3 COSY-spectrum of IL 11b



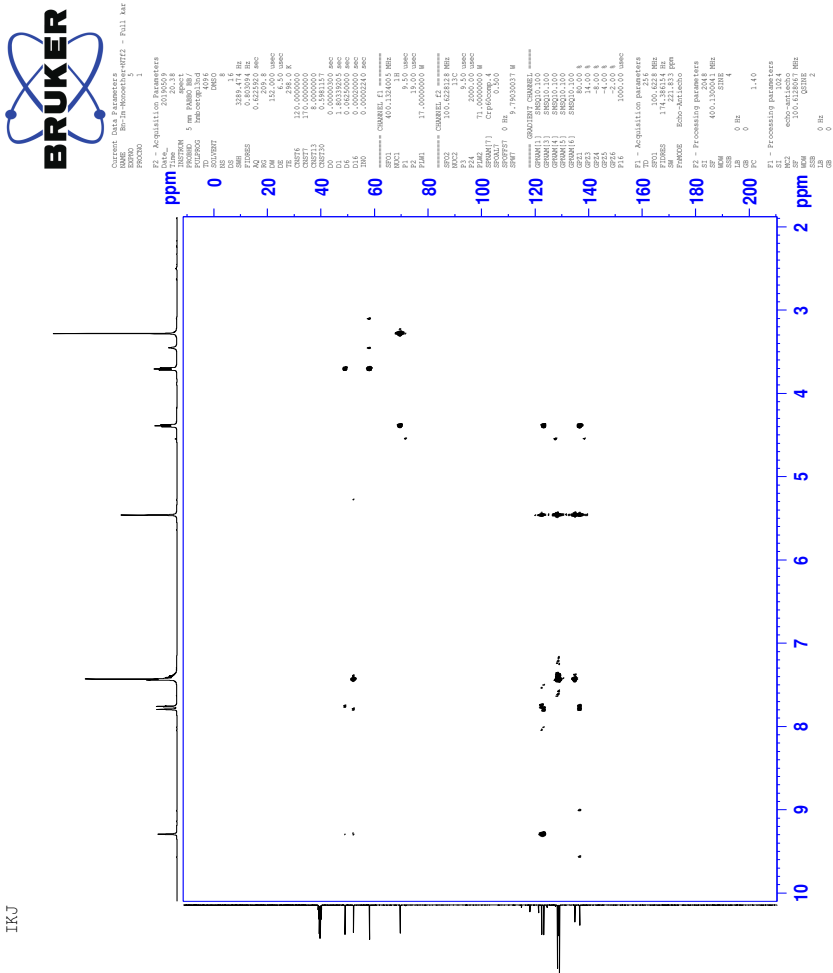
29.4 HSQC-spectrum of IL 11b



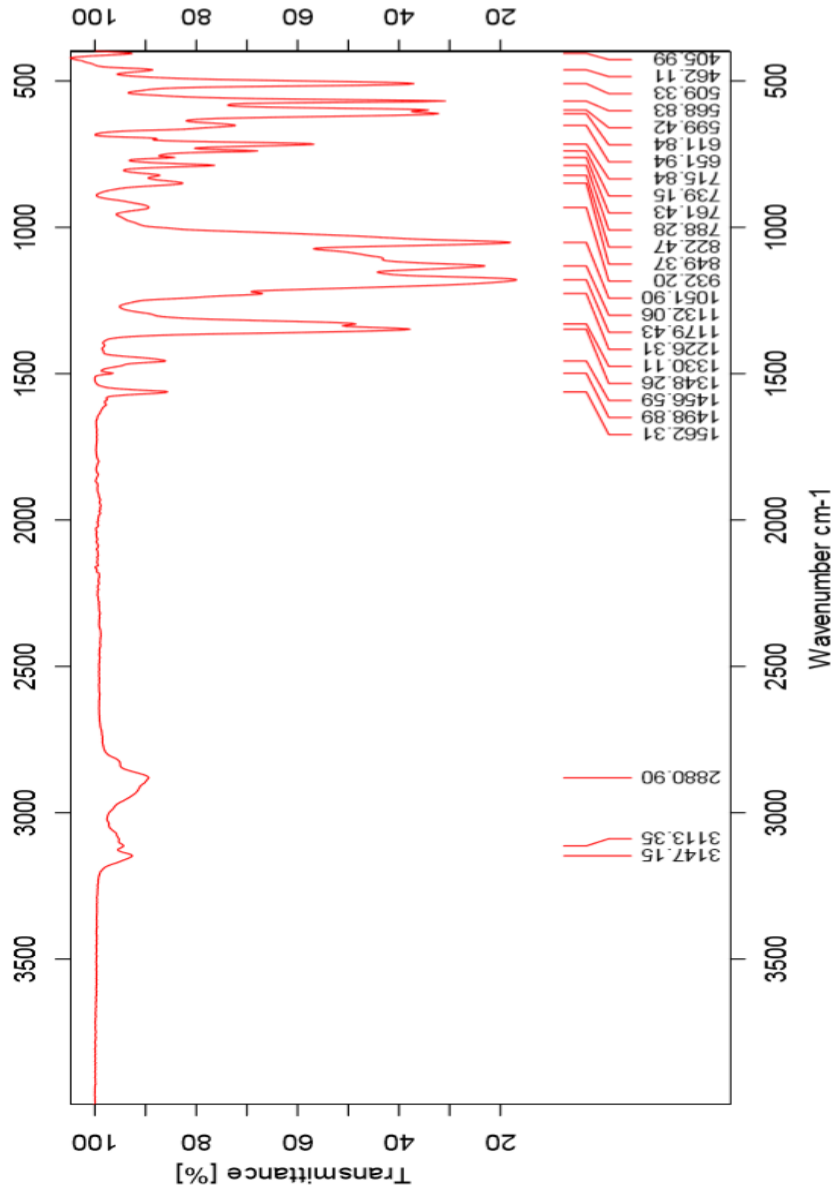
TKJ

29.5 HMBC-spectrum of IL 11b

IKJ



29.6 IR-spectrum of IL 11b



29.7 HR-MS positive mode spectrum of IL 11b

Elemental Composition Report

Page 1

Single Mass Analysis

Tolerance = 2.0 PPM / DBE: min = -50.0, max = 50.0

Element prediction: Off

Number of isotope peaks used for i-FIT = 3

Monoisotopic Mass, Even Electron Ions

1144 formula(e) evaluated with 2 results within limits (all results (up to 1000) for each mass)

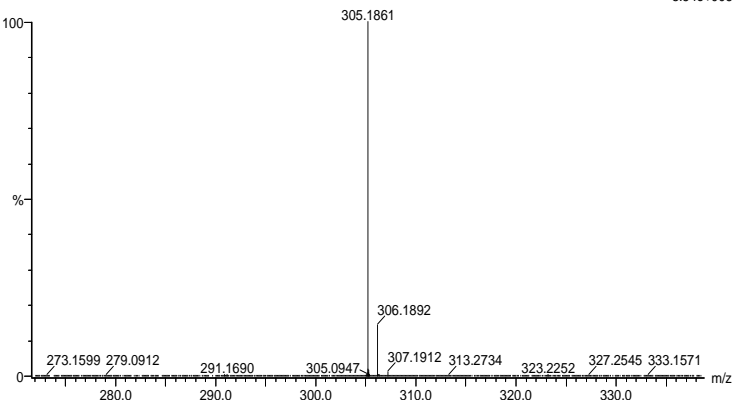
Elements Used:

C: 0-100 H: 0-150 N: 0-10 O: 0-10

2019_508FIA15 (0.288) AM2 (Ar,35000.0,0.00,0.00); Crm (13:15)

1: TOF MS ES+

8.54e+005



Minimum: -50.0
Maximum: 5.0 2.0 50.0

Mass	Calc. Mass	mDa	PPM	DBE	i-FIT	Norm	Conf (%)	Formula
305.1861	305.1865	-0.4	-1.3	6.5	1134.3	0.001	99.92	C17 H25 N2 O3
	305.1857	0.4	1.3	-5.5	1141.4	7.106	0.08	C H25 N10 O8

29.8 HR-MS negative mode spectrum of IL 11b

Elemental Composition Report

Page 1

Single Mass Analysis

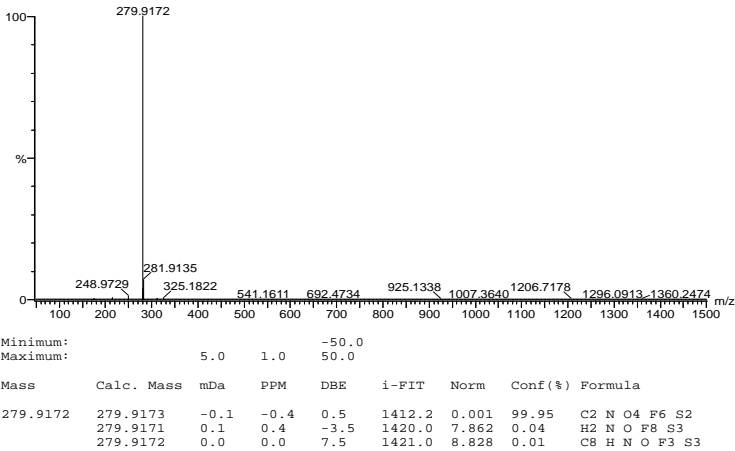
Tolerance = 1.0 PPM / DBE: min = -50.0, max = 50.0
Element prediction: Off
Number of isotope peaks used for i-FIT = 3

Monoisotopic Mass, Even Electron Ions
14728 formula(e) evaluated with 3 results within limits (all results (up to 1000) for each mass)

Elements Used:

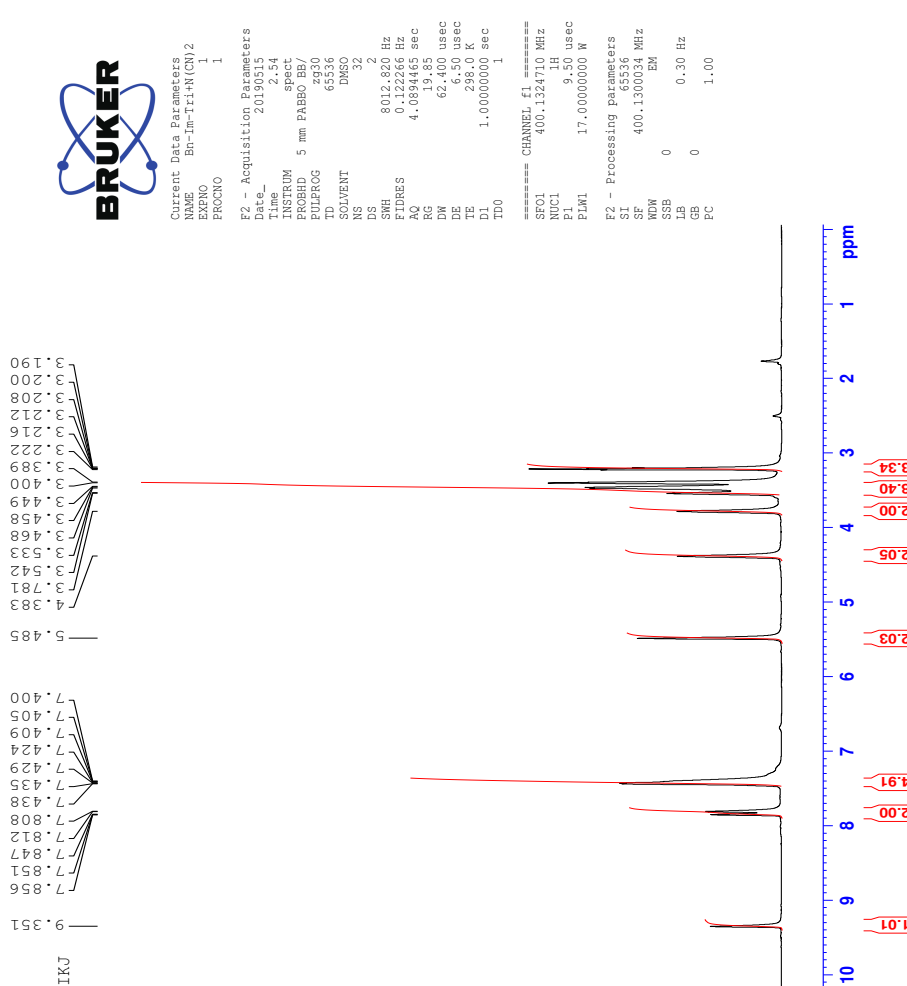
C: 0-100 H: 0-150 N: 0-10 O: 0-10 F: 0-8 S: 0-4
2019_509FIA27 (0.311) AM2 (Ar,35000.0,0.00,0.00); Cm (22.27)
1: TOF MS ES-

2.74e+006

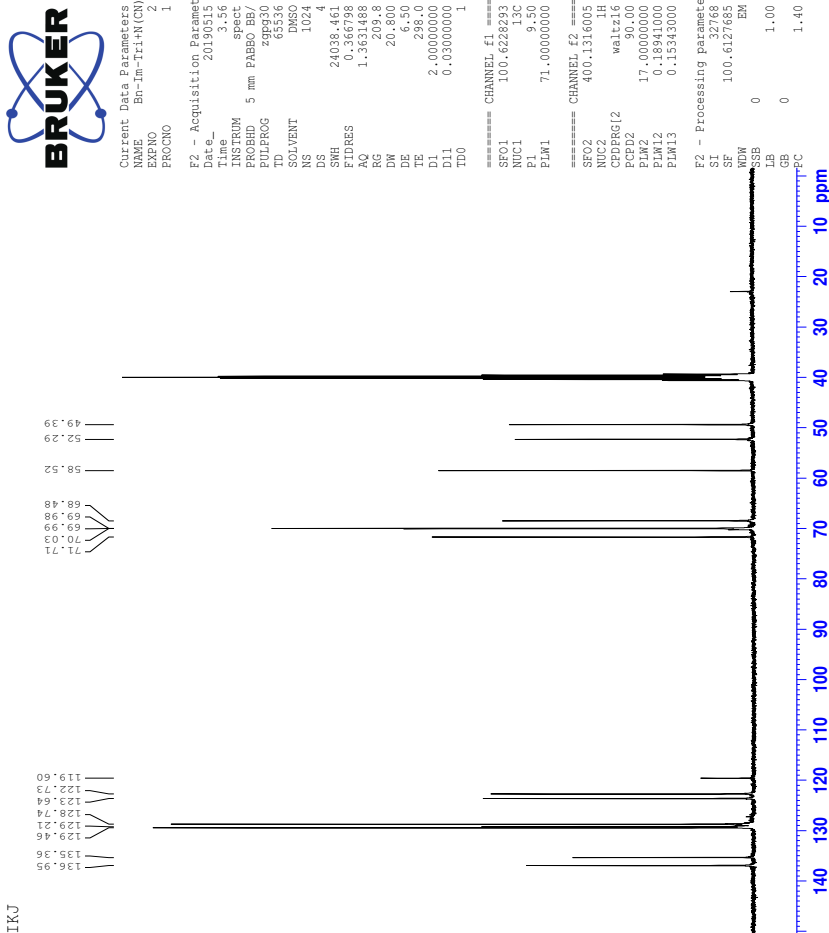


30 Spectra of IL 11c

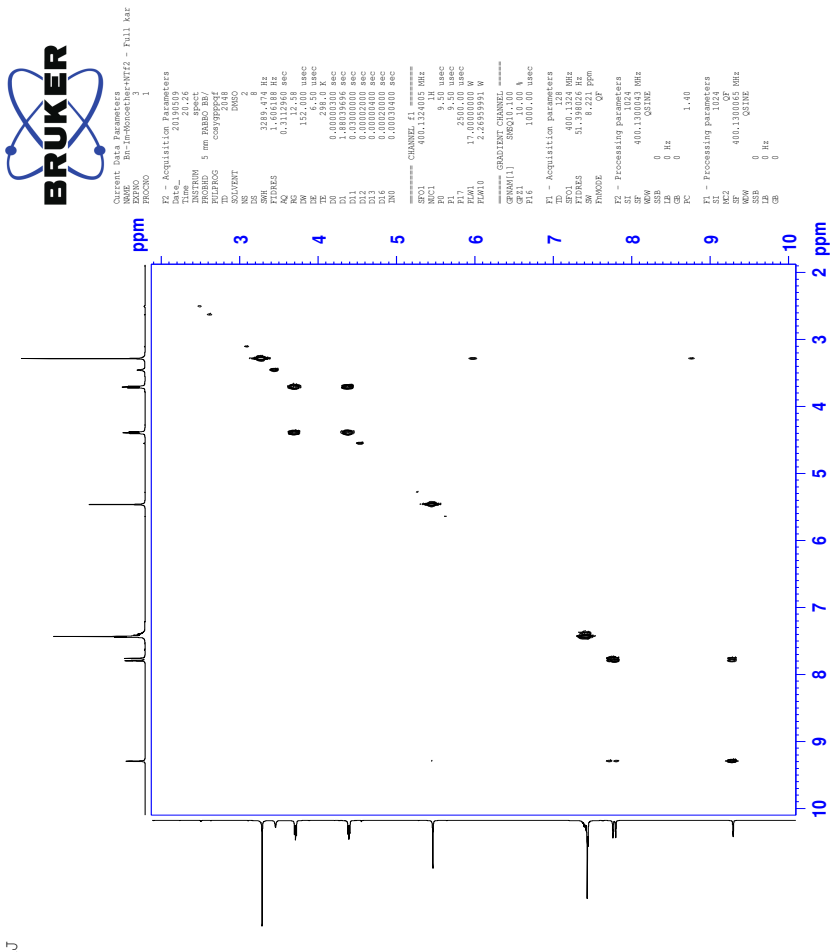
30.1 ^1H -NMR spectrum of IL 11c



30.2 ^{13}C -NMR spectrum of IL 11c

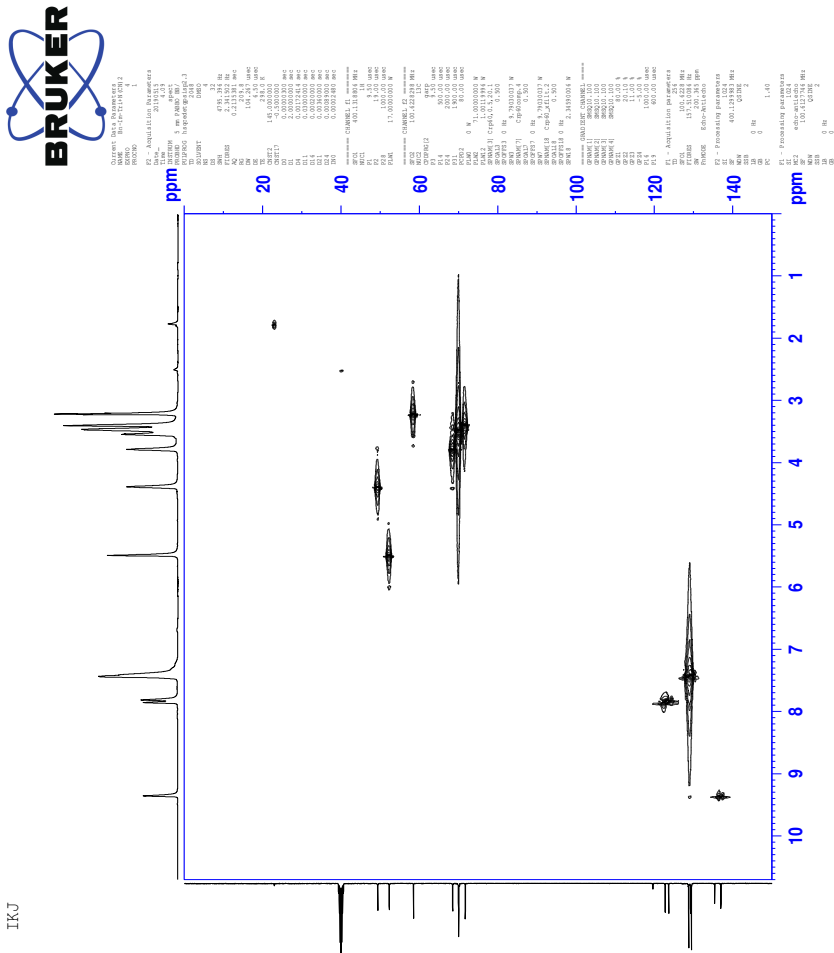


30.3 COSY-spectrum of IL 11c

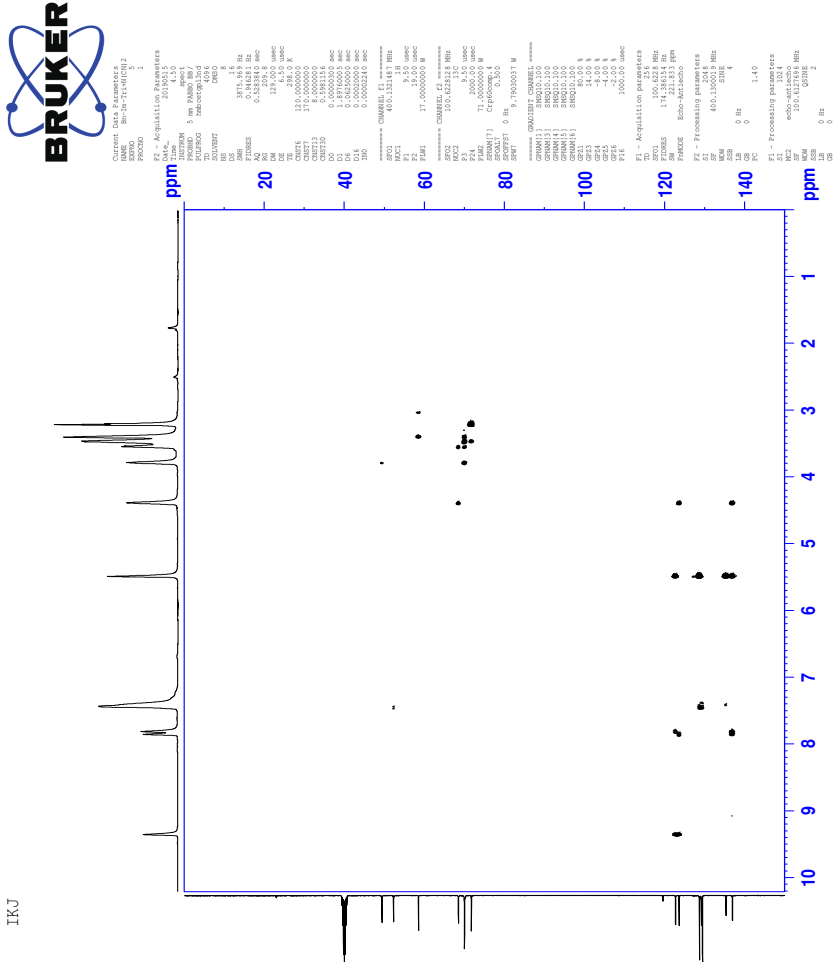


TKJ

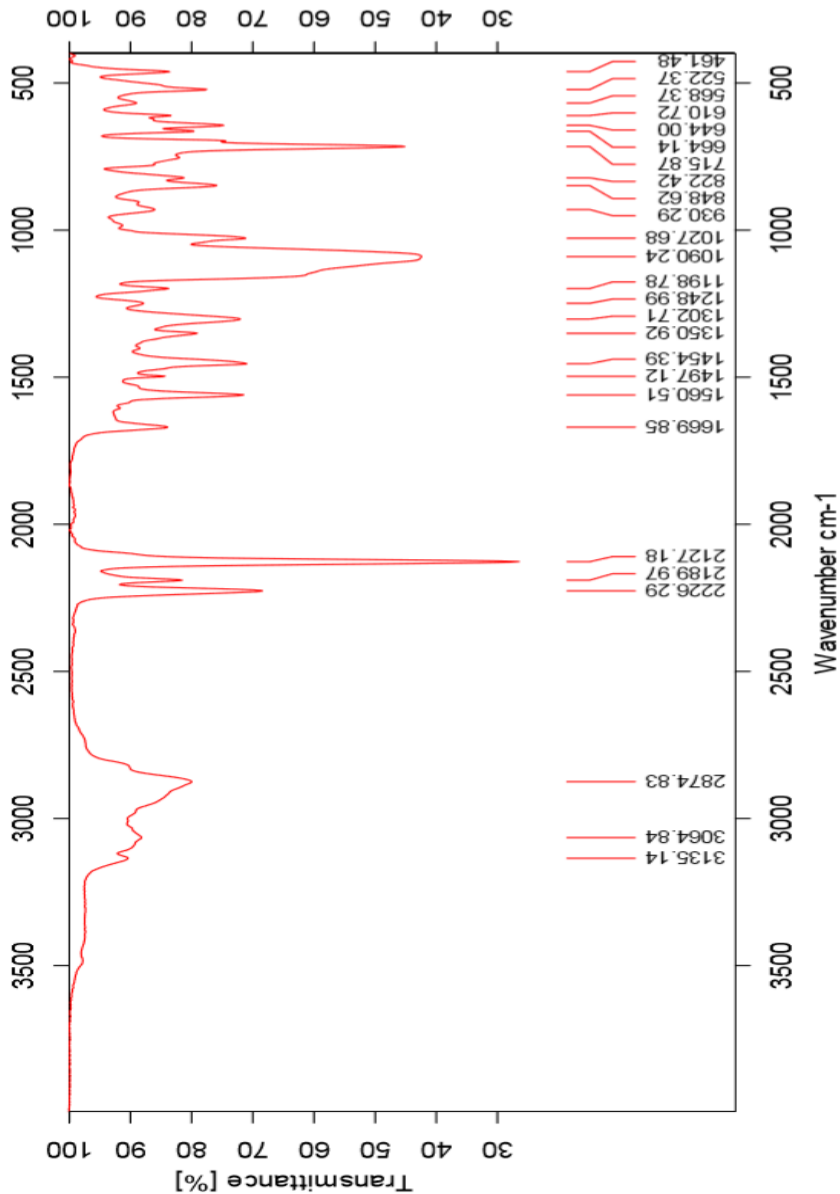
30.4 HSQC-spectrum of IL 11c



30.5 HMBC-spectrum of IL 11c



30.6 IR-spectrum of IL 11c



30.7 HR-MS positive mode spectrum of IL 11c

Elemental Composition Report

Page 1

Single Mass Analysis

Tolerance = 1.0 PPM / DBE: min = -50.0, max = 50.0

Element prediction: Off

Number of isotope peaks used for i-FIT = 3

Monoisotopic Mass, Even Electron Ions

1144 formula(e) evaluated with 1 results within limits (all results (up to 1000) for each mass)

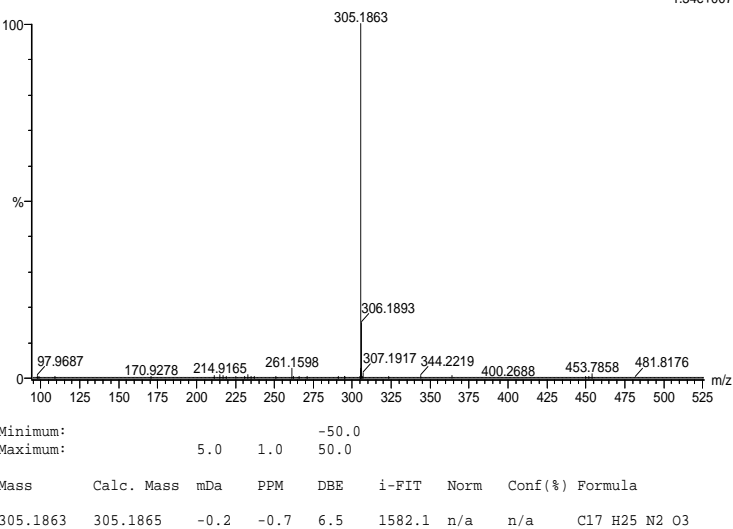
Elements Used:

C: 0-100 H: 0-150 N: 0-10 O: 0-10

2019_504FIA 87 (1.613) AM2 (Ar,35000.0,0.00,0.00); Cm (87:101)

1: TOF MS ES+

1.34e+007



30.8 HR-MS negative mode spectrum of IL 11c

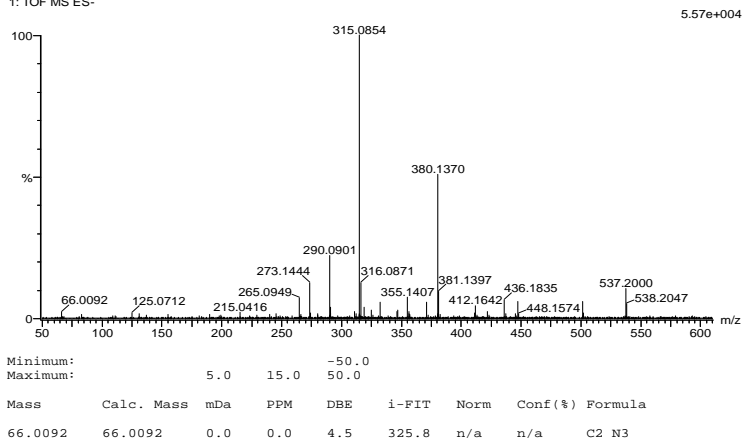
Elemental Composition Report

Page 1

Single Mass Analysis

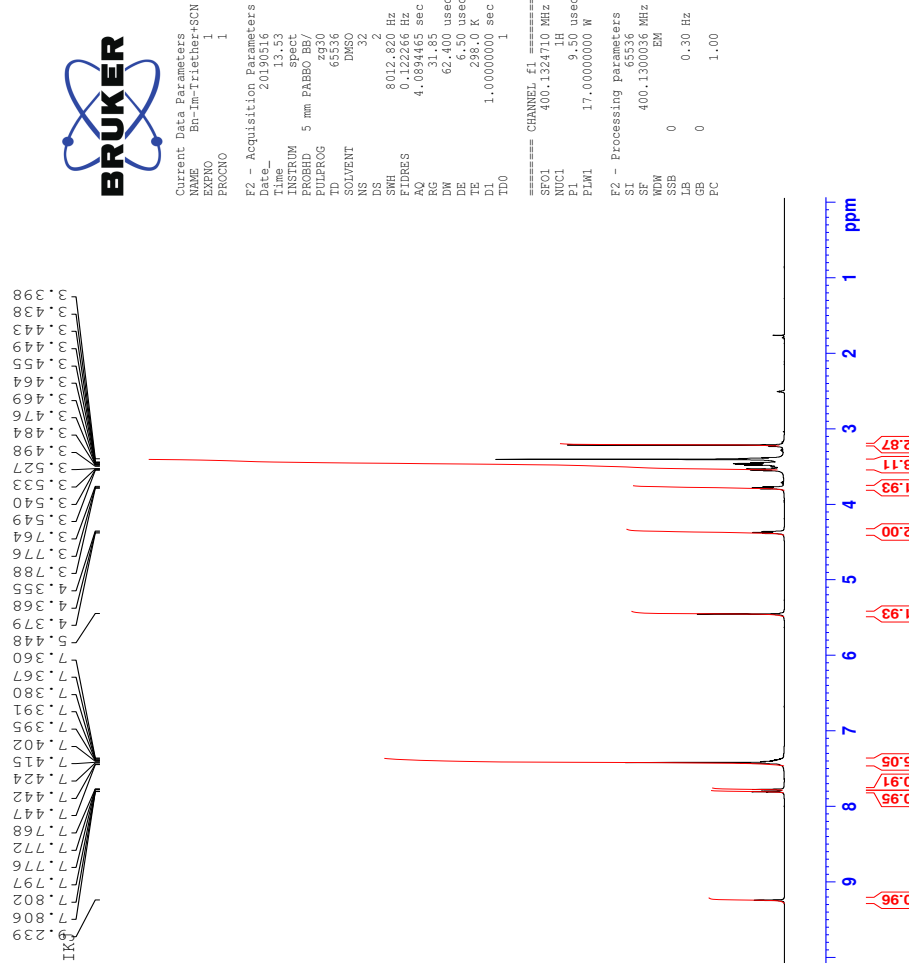
Tolerance = 15.0 PPM / DBE: min = -50.0, max = 50.0
Element prediction: Off
Number of isotope peaks used for i-FIT = 3

Monoisotopic Mass, Even Electron Ions
41 formula(e) evaluated with 1 results within limits (all results (up to 1000) for each mass)
Elements Used:
C: 0-100 H: 0-150 N: 0-10 O: 0-10
2019_505neg 28 (0.321) AM2 (Ar,35000.0,0.00,0.00); Cr (26:28)
1: TOF MS ES-

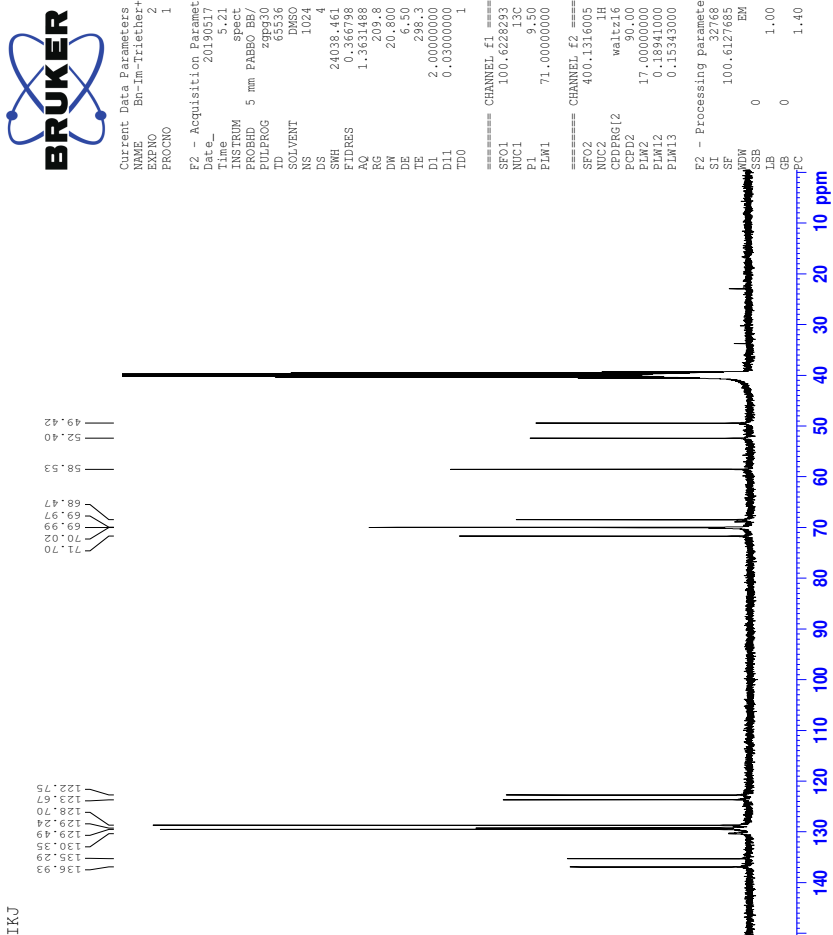


31 Spectra of IL 11d

31.1 ^1H -NMR spectrum of IL 11d



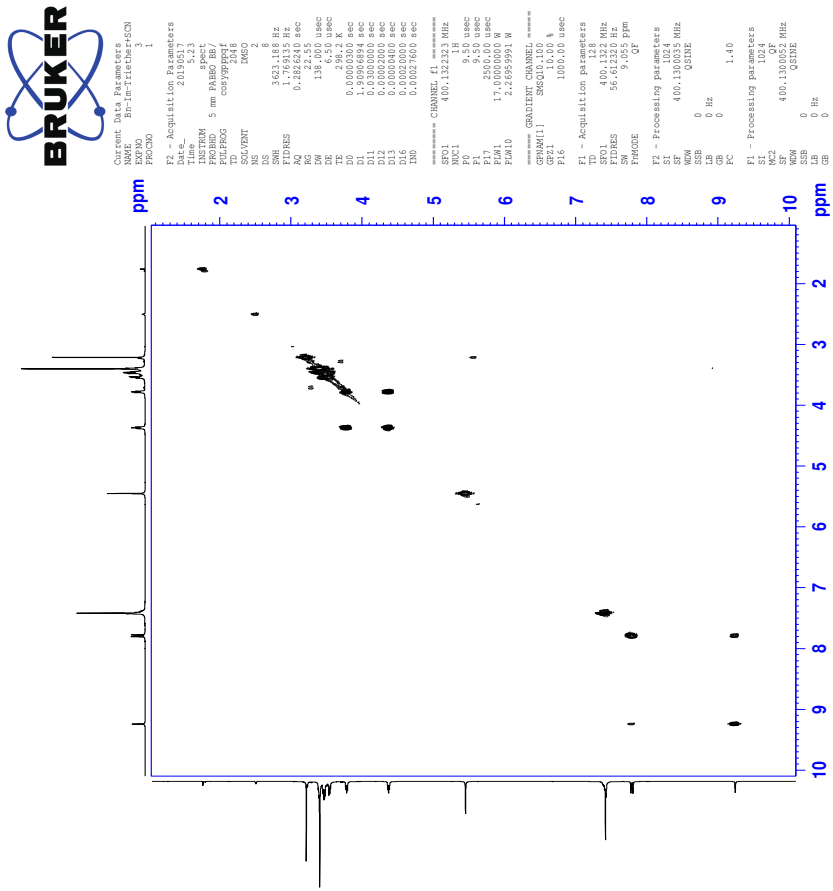
31.2 ^{13}C -NMR spectrum of IL 11d



CXC

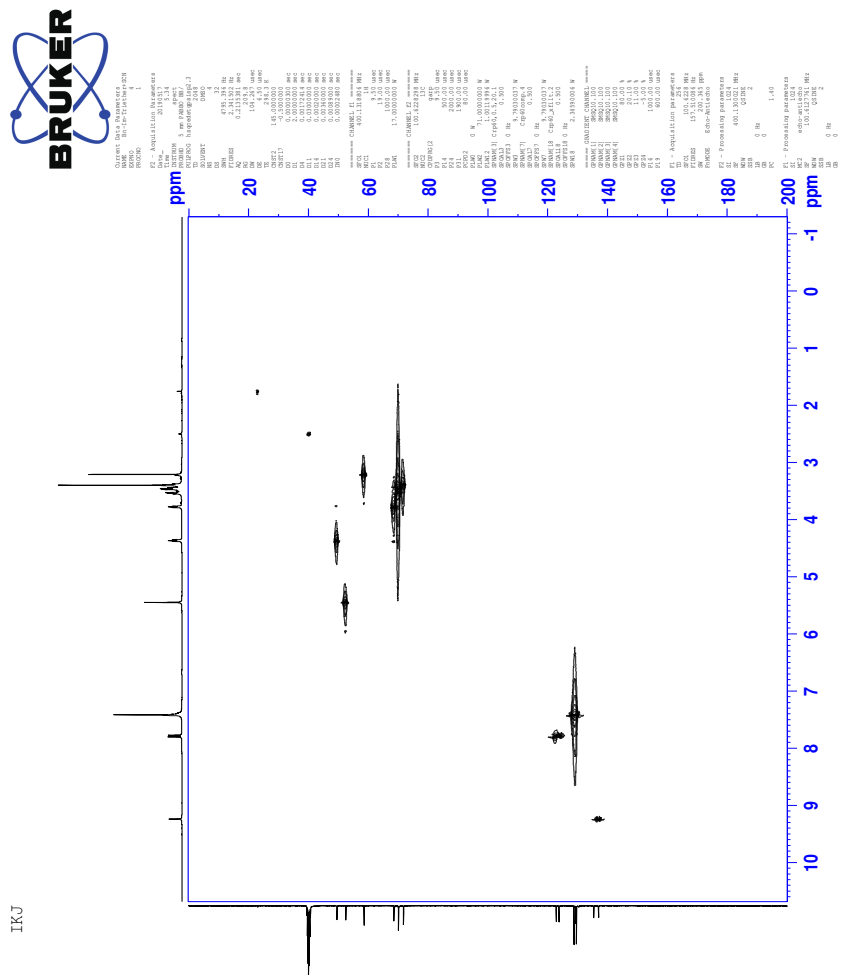
31.3 COSY-spectrum of IL 11d

TKJ



CXCI

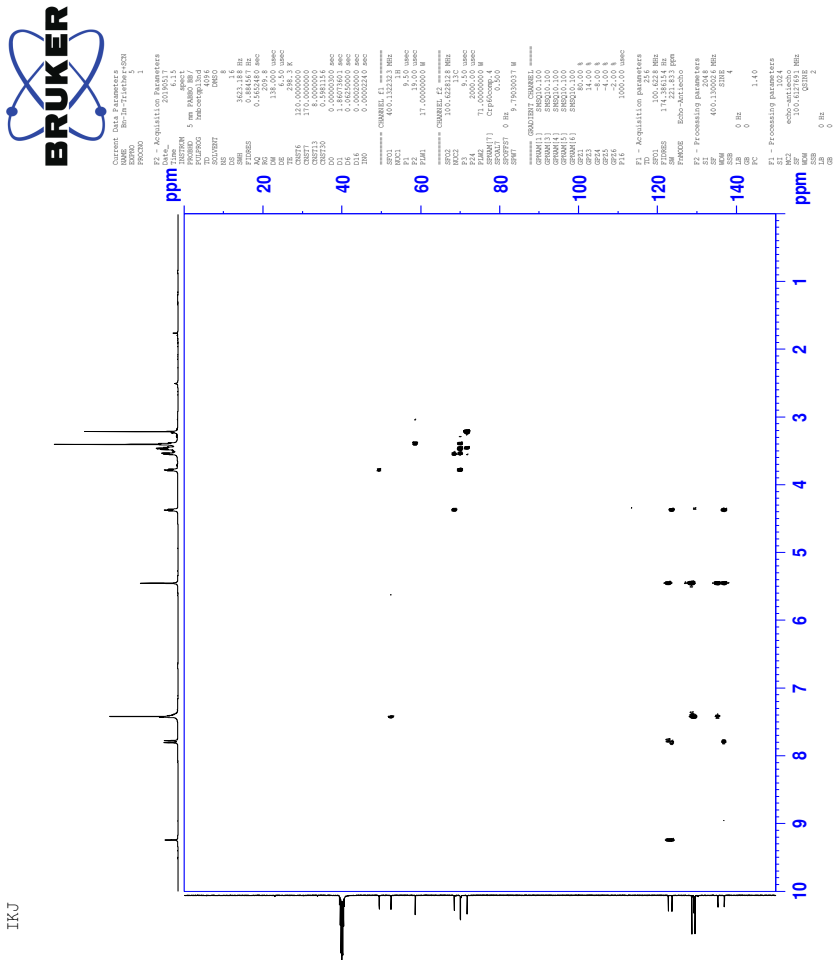
31.4 HSQC-spectrum of IL 11d



TKJ

CXCII

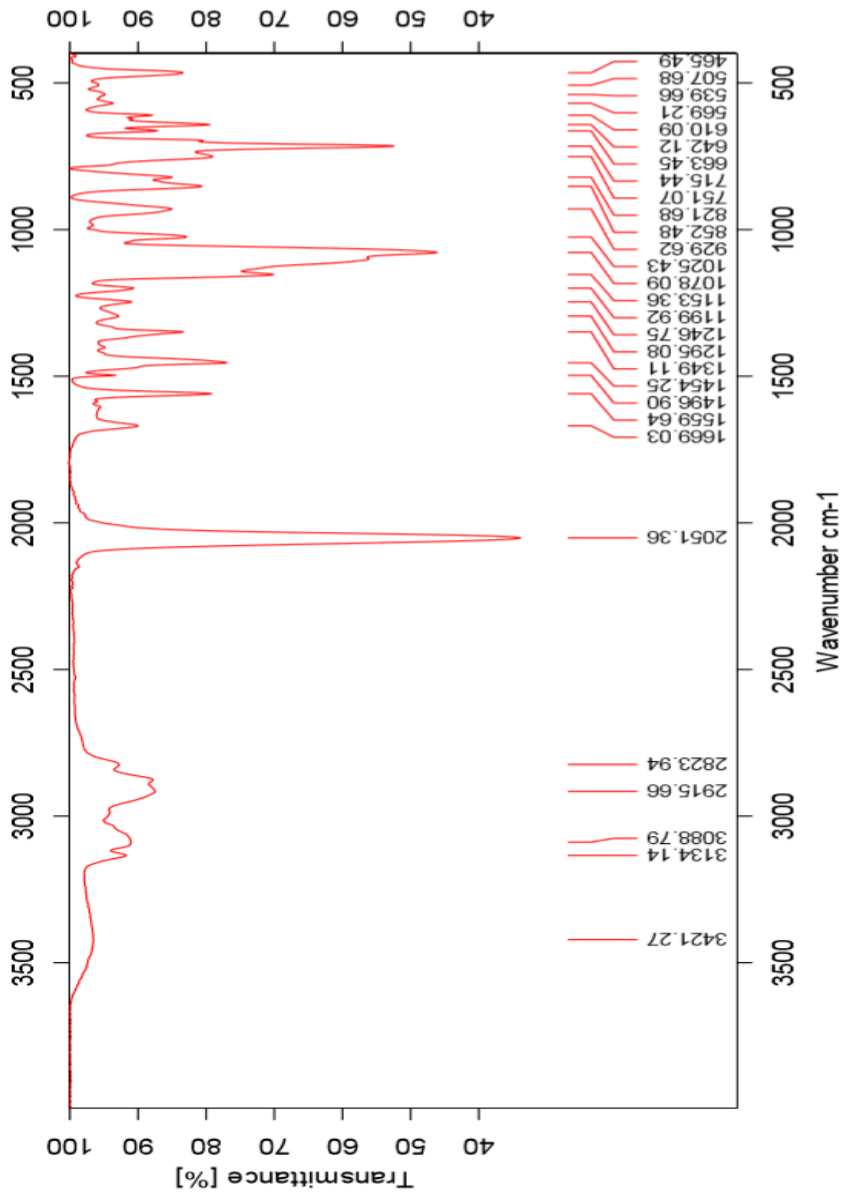
31.5 HMBC-spectrum of IL 11d



TKJ

CXCIII

31.6 IR-spectrum of IL 11d



31.7 HR-MS positive mode spectrum of IL 11d

Elemental Composition Report

Page 1

Single Mass Analysis

Tolerance = 5.0 PPM / DBE: min = -50.0, max = 50.0

Element prediction: Off

Number of isotope peaks used for i-FIT = 3

Monoisotopic Mass, Even Electron Ions

1750 formula(e) evaluated with 3 results within limits (all results (up to 1000) for each mass)

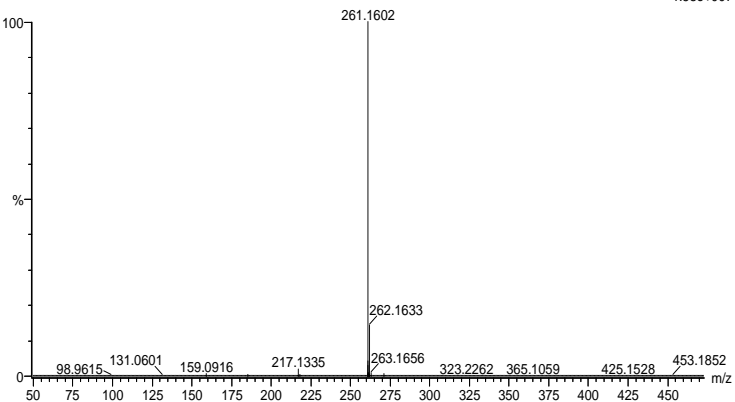
Elements Used:

C: 0-100 H: 0-150 N: 0-10 O: 0-10 Na: 0-1

2019-396 98 (1.814) AM2 (Ar,35000.0,0.00,0.00); Cm (98:103)

1: TOF MS ES+

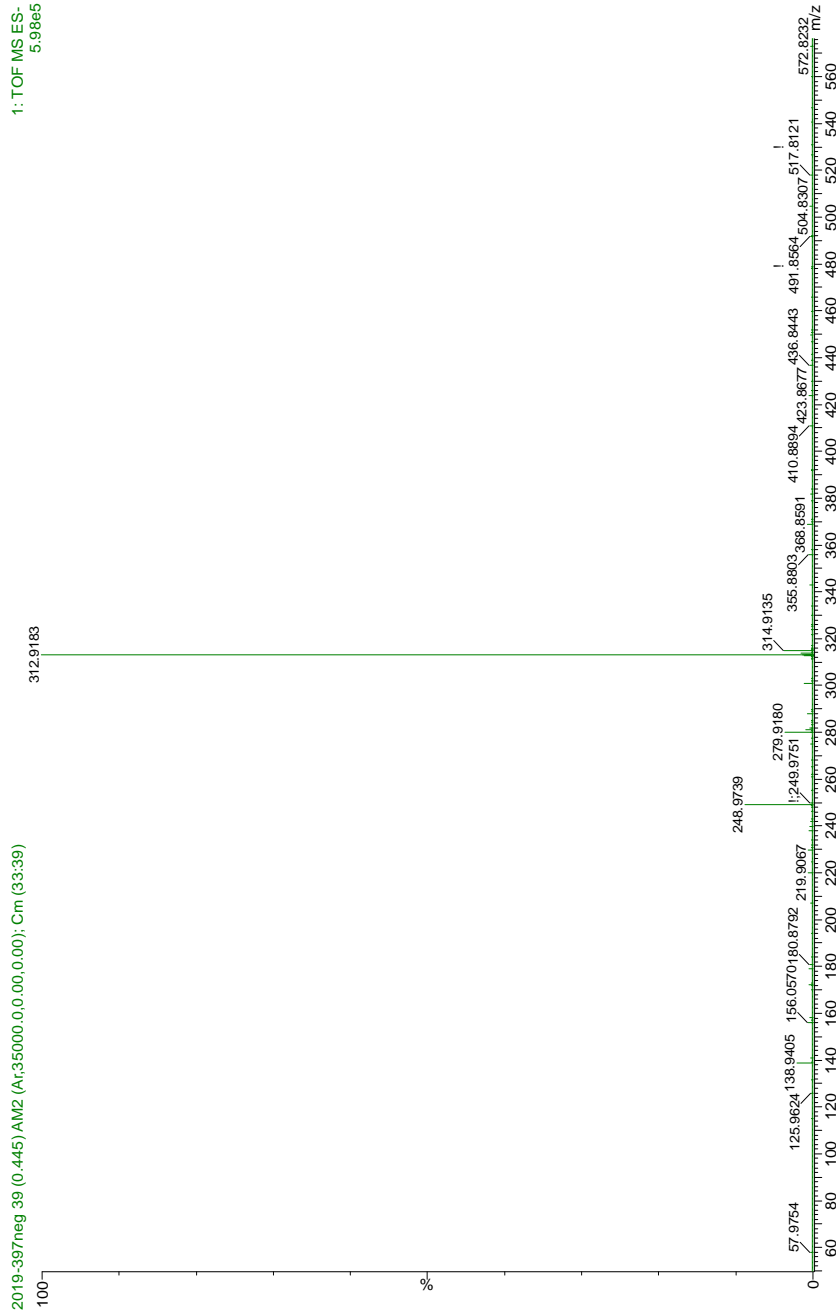
1.58e+007



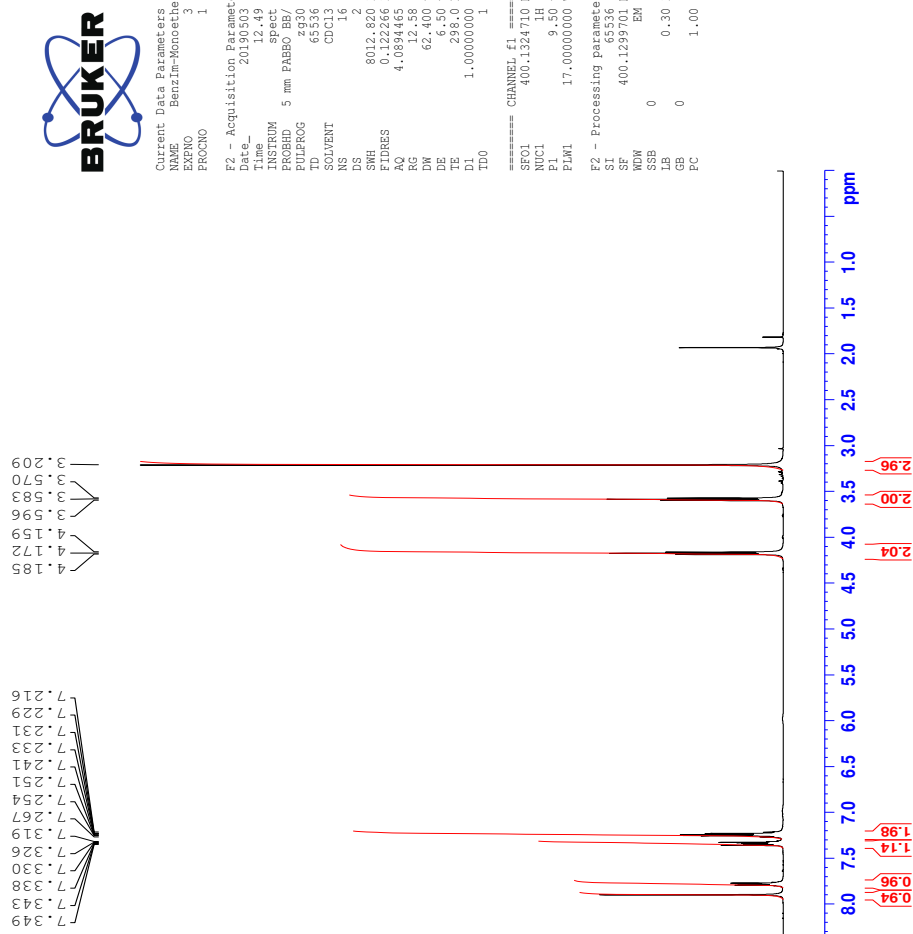
Minimum: -50.0
Maximum: 5.0 5.0 50.0

Mass	Calc. Mass	mDa	PPM	DBE	i-FIT	Norm	Conf (%)	Formula
261.1602	261.1603	-0.1	-0.4	6.5	1817.1	0.000	99.98	C15 H21 N2 O2
	261.1597	0.5	1.9	-9.5	1826.8	9.753	0.01	C H26 N4 O9 Na
	261.1611	-0.9	-3.4	-4.5	1826.2	9.095	0.01	C2 H22 N8 O5 Na

31.8 HR-MS negative mode spectrum of IL 11d

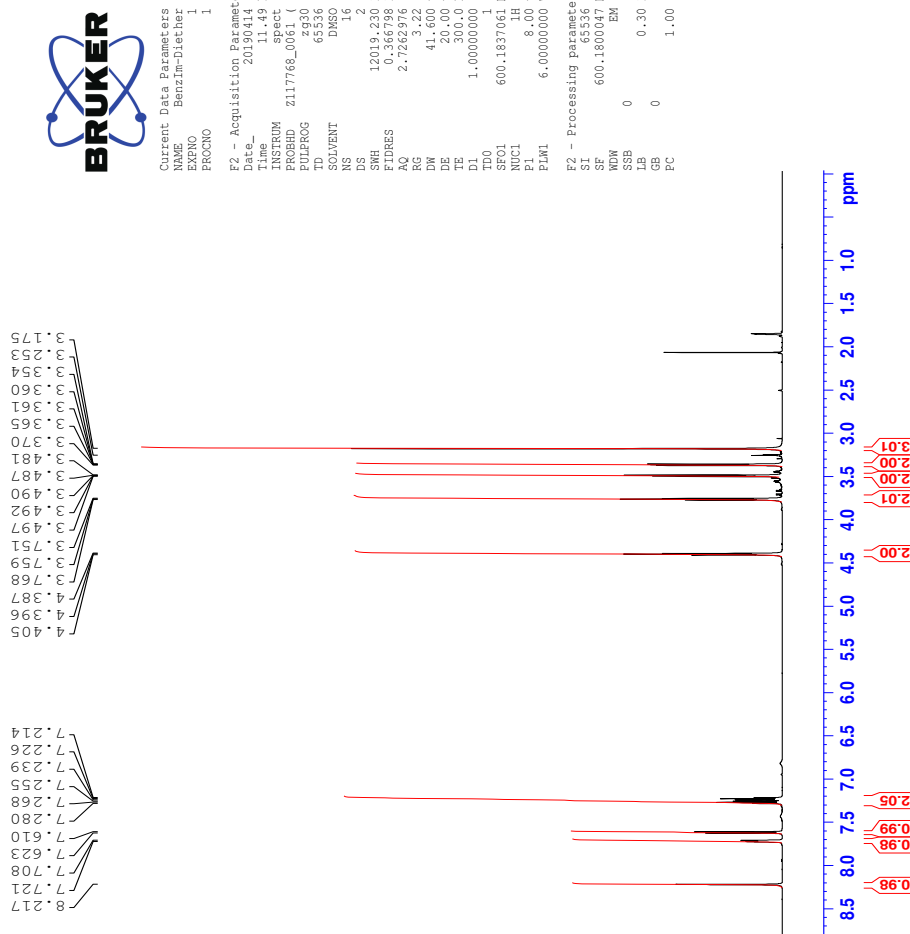


32 $^1\text{H-NMR}$ spectrum of compound 12

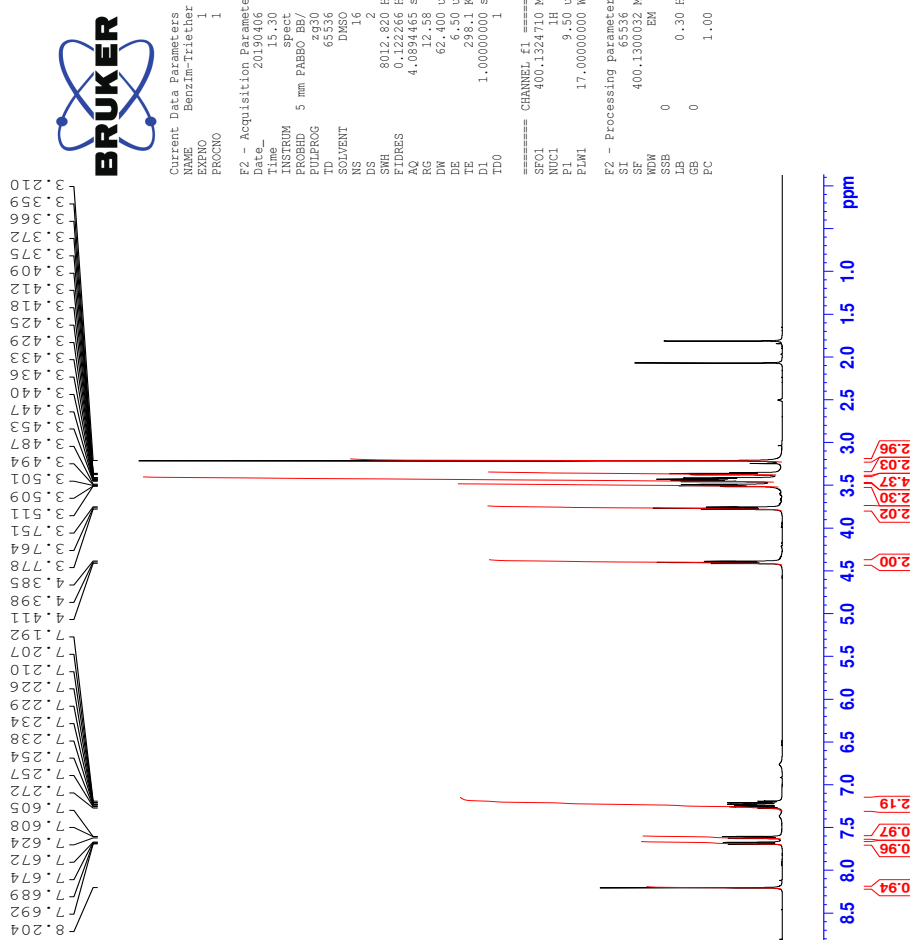


CXCVII

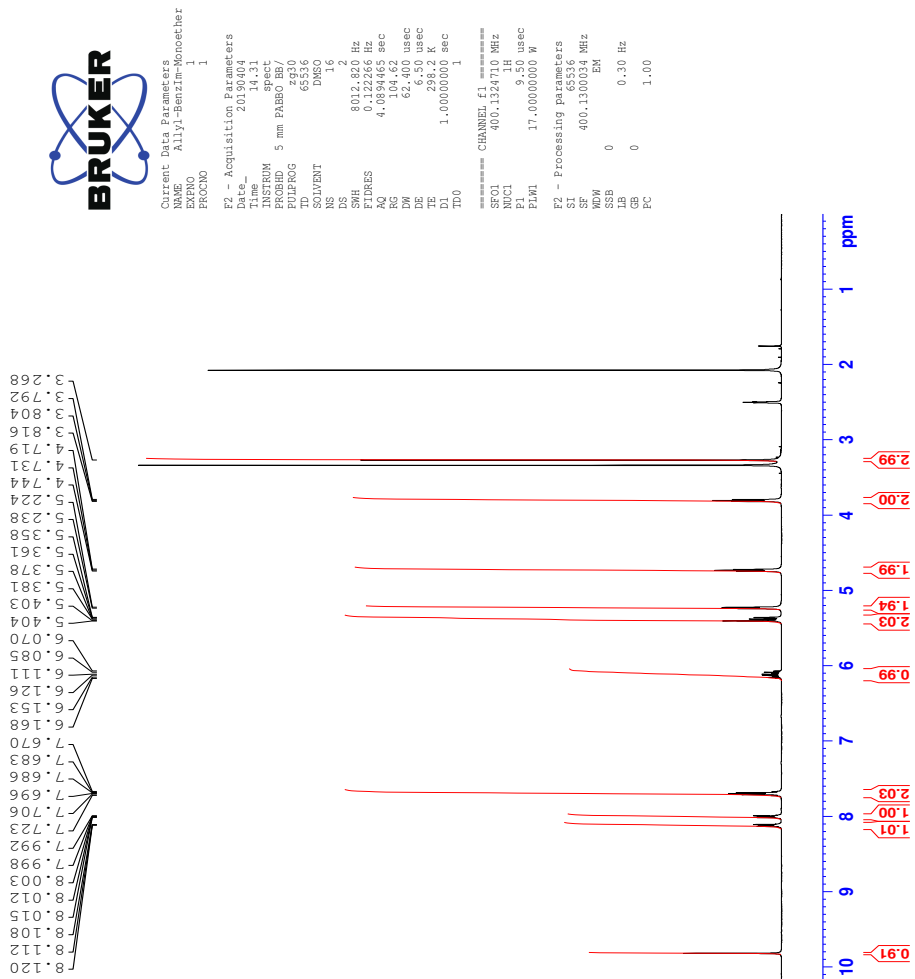
33 $^1\text{H-NMR}$ spectrum of compound 13



34 ^1H -NMR spectrum of compound 14



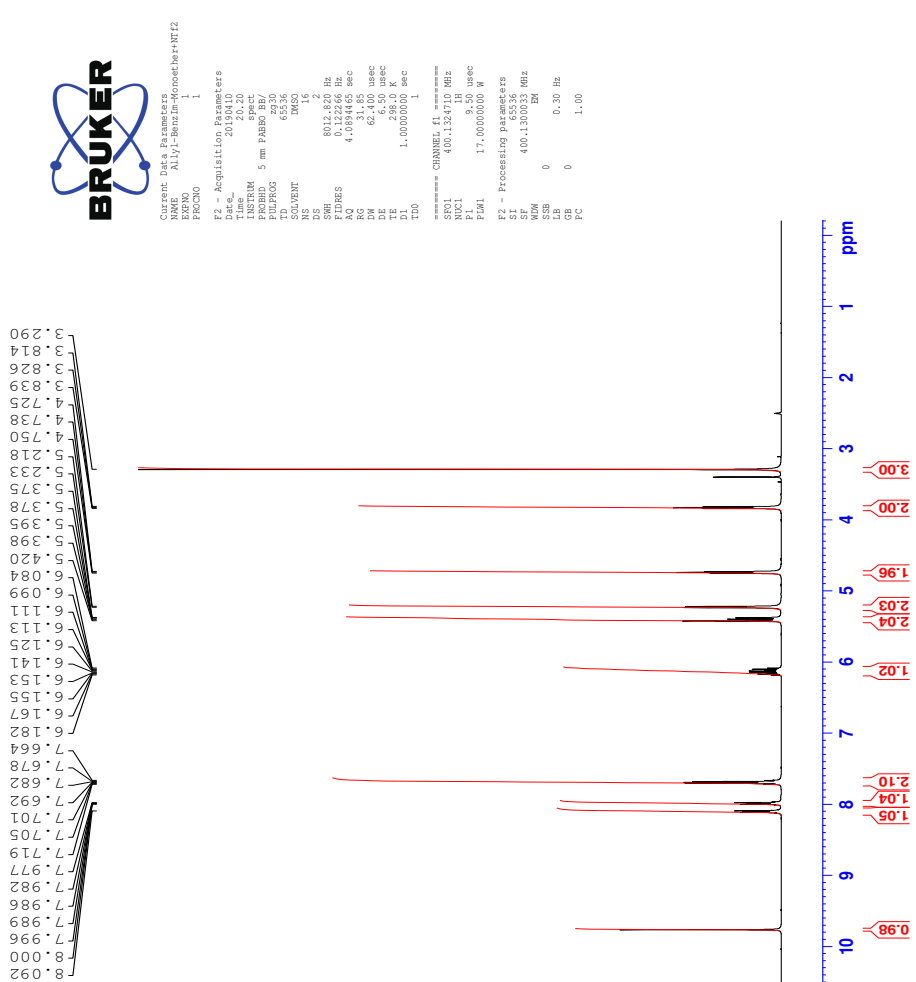
35 ^1H -NMR spectrum of compound 15a



CC

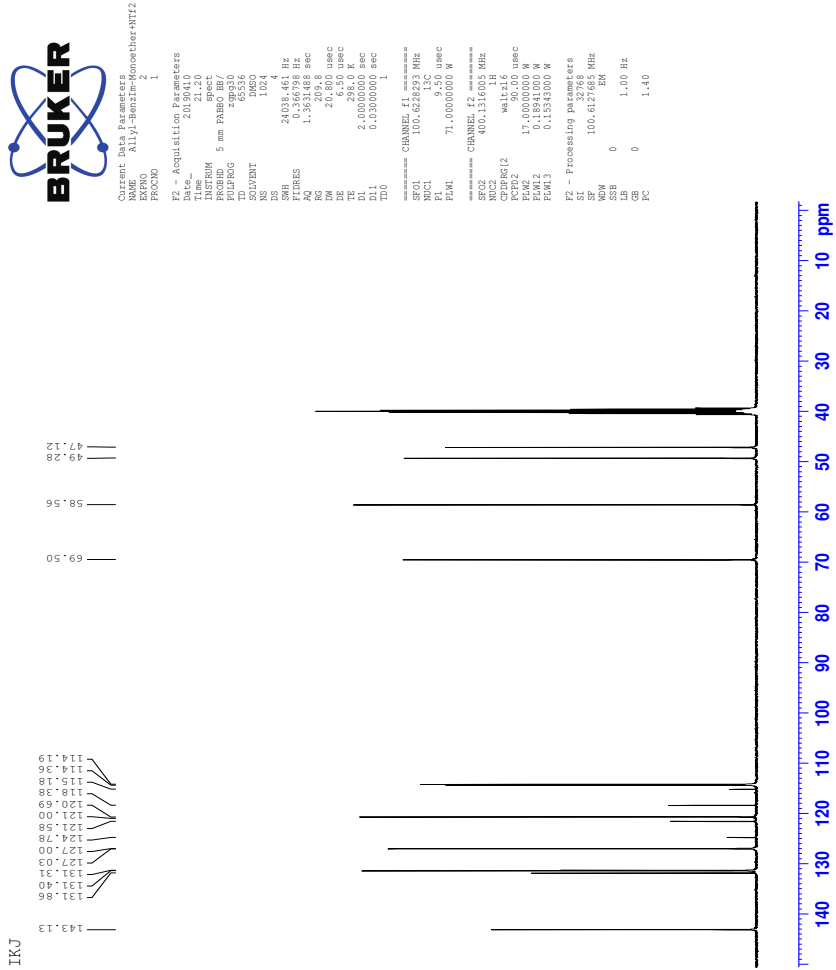
36 Spectra of IL 15b

36.1 ^1H -NMR spectrum of IL 15b



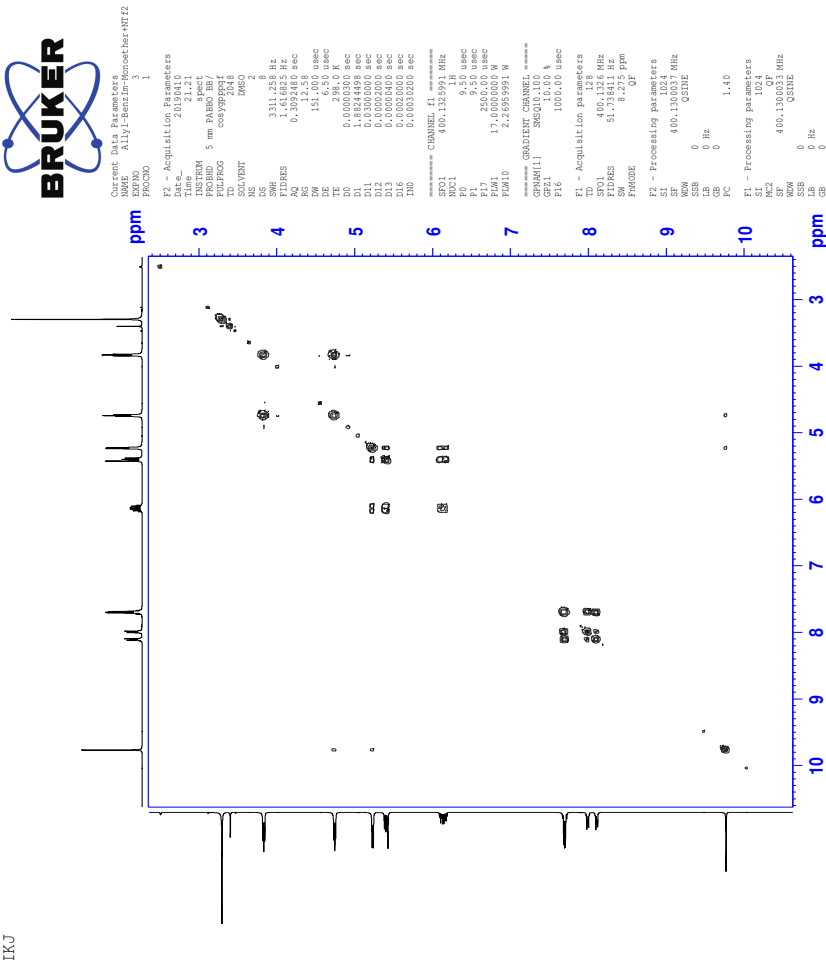
CCI

36.2 ^{13}C -NMR spectrum of IL 15b



CCII

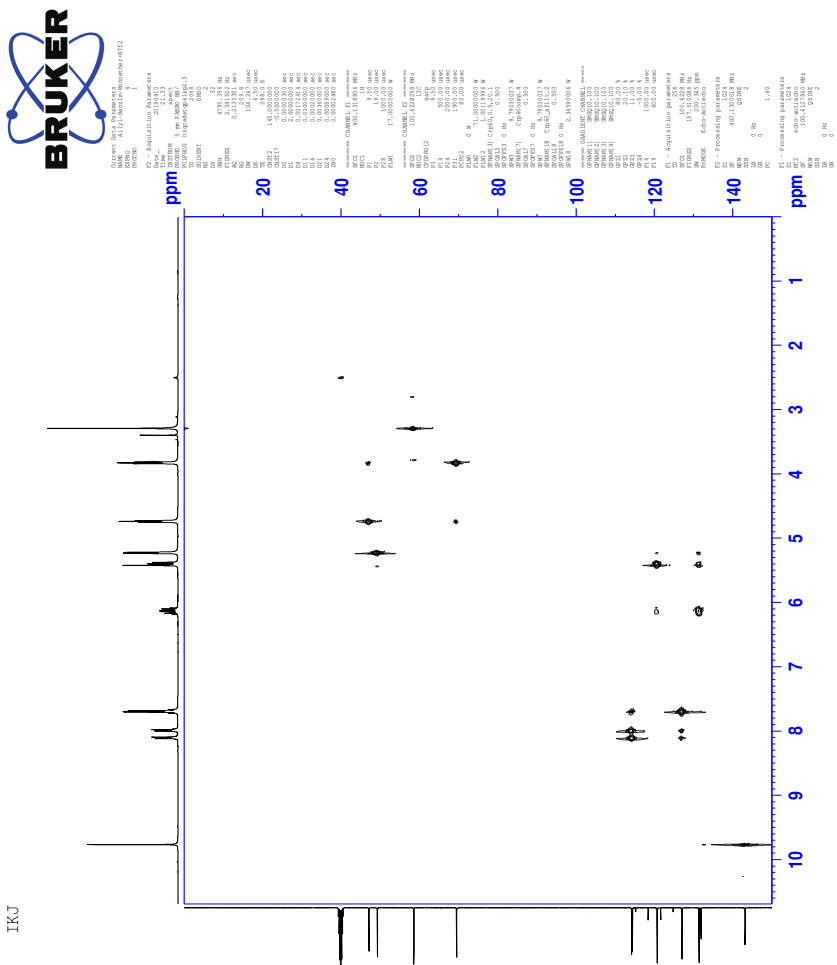
36.3 COSY-spectrum of IL 15b



TKJ

CCIII

36.4 HSQC-spectrum of IL 15b

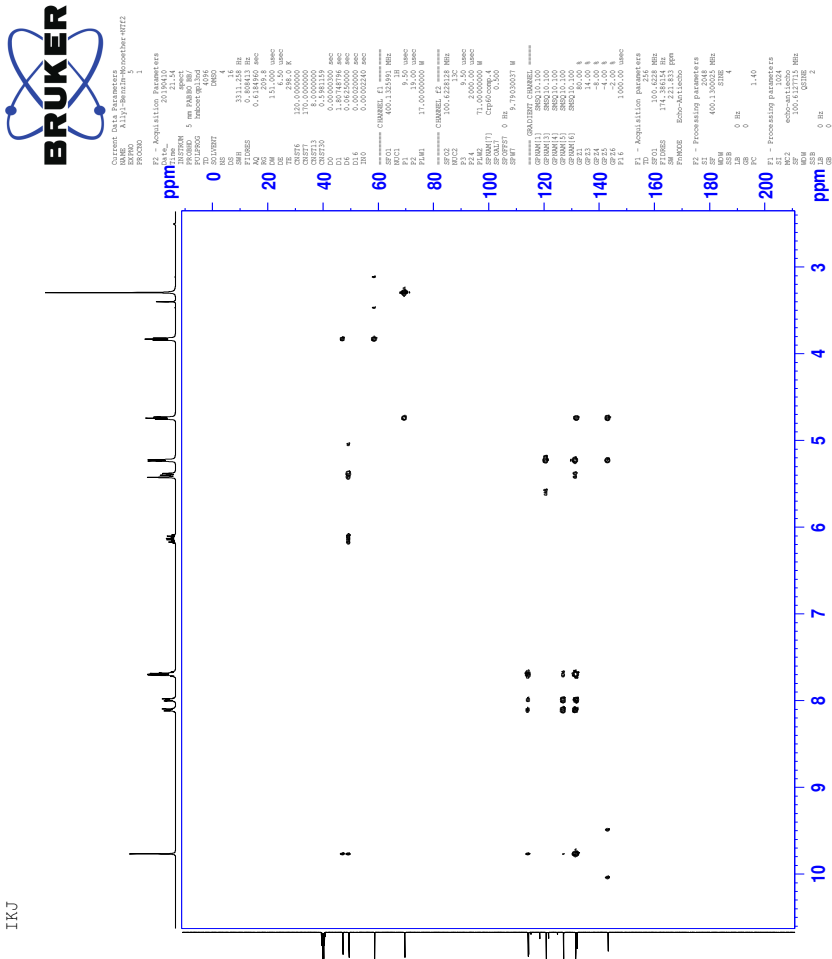


IIKJ

CCIV

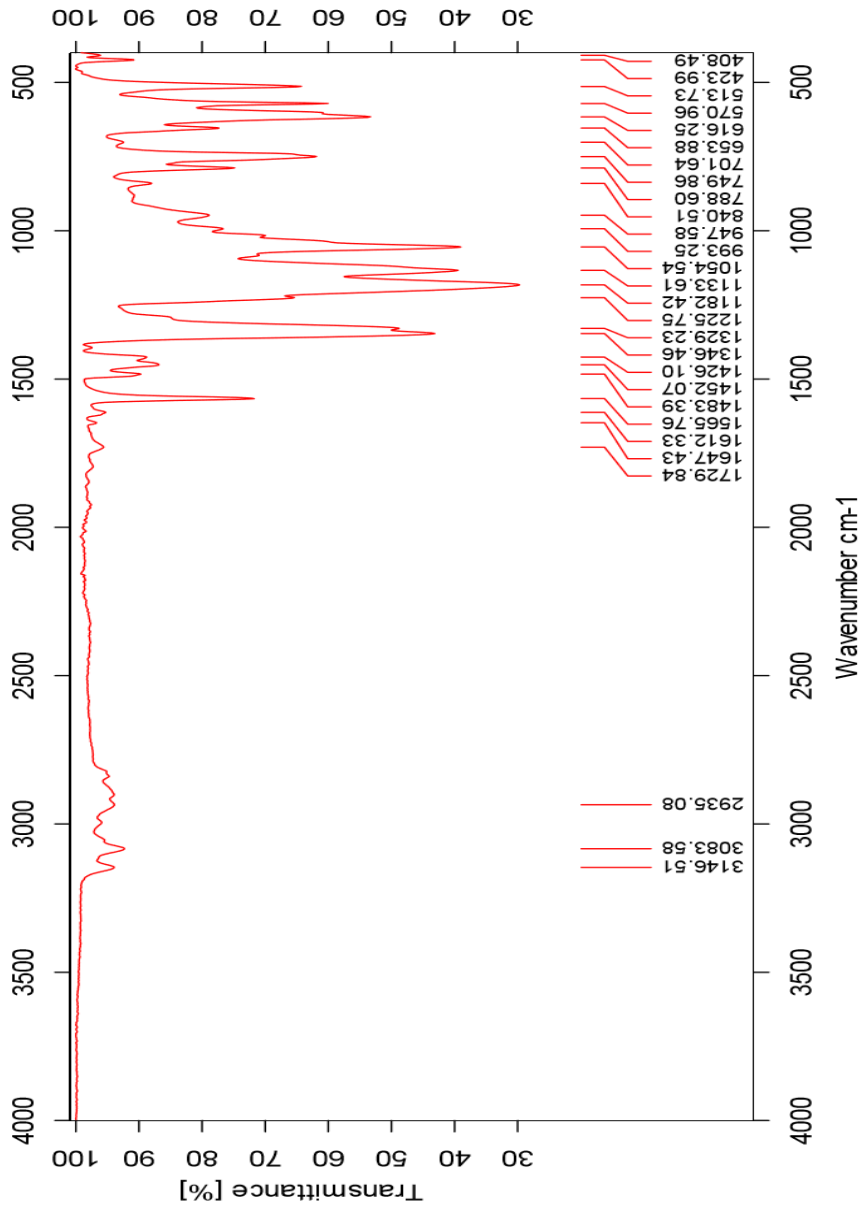
36.5 HMBC-spectrum of IL 15b

IKJ



CCV

36.6 IR-spectrum of IL 15b



36.7 HR-MS positive mode spectrum IL 15b

Elemental Composition Report

Page 1

Single Mass Analysis

Tolerance = 5.0 PPM / DBE: min = -50.0, max = 50.0

Element prediction: Off

Number of isotope peaks used for i-FIT = 3

Monoisotopic Mass, Even Electron Ions

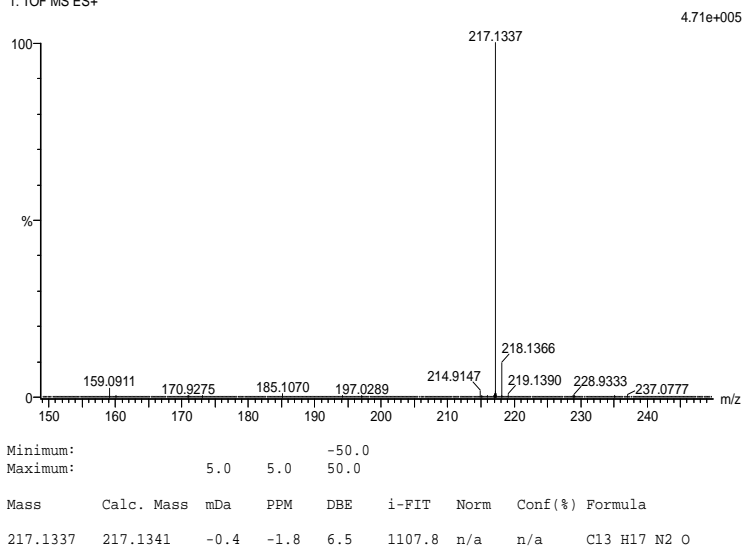
1234 formula(e) evaluated with 1 results within limits (all results (up to 1000) for each mass)

Elements Used:

C: 0-100 H: 0-150 N: 0-10 O: 0-10 Na: 0-1

2019-398 13 (0.253) AM2 (Ar,35000.0,0.00,0.00); Crm (9:13)

1: TOF MS ES+



36.8 HR-MS negative mode spectrum IL 15b

Elemental Composition Report

Page 1

Single Mass Analysis

Tolerance = 2.0 PPM / DBE: min = -50.0, max = 50.0

Element prediction: Off

Number of isotope peaks used for i-FIT = 3

Monoisotopic Mass, Even Electron Ions

14316 formula(e) evaluated with 4 results within limits (all results (up to 1000) for each mass)

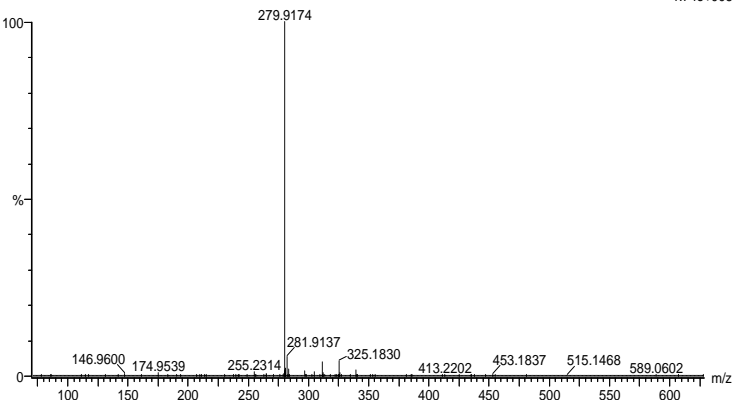
Elements Used:

C: 0-100 H: 0-150 N: 0-5 O: 0-5 F: 0-7 Na: 0-1 S: 0-3

2019-399neg 22 (0.258) AM2 (Ar,35000.0,0.00,0.00); Cm (15:22)

1: TOF MS ES-

1.74e+005

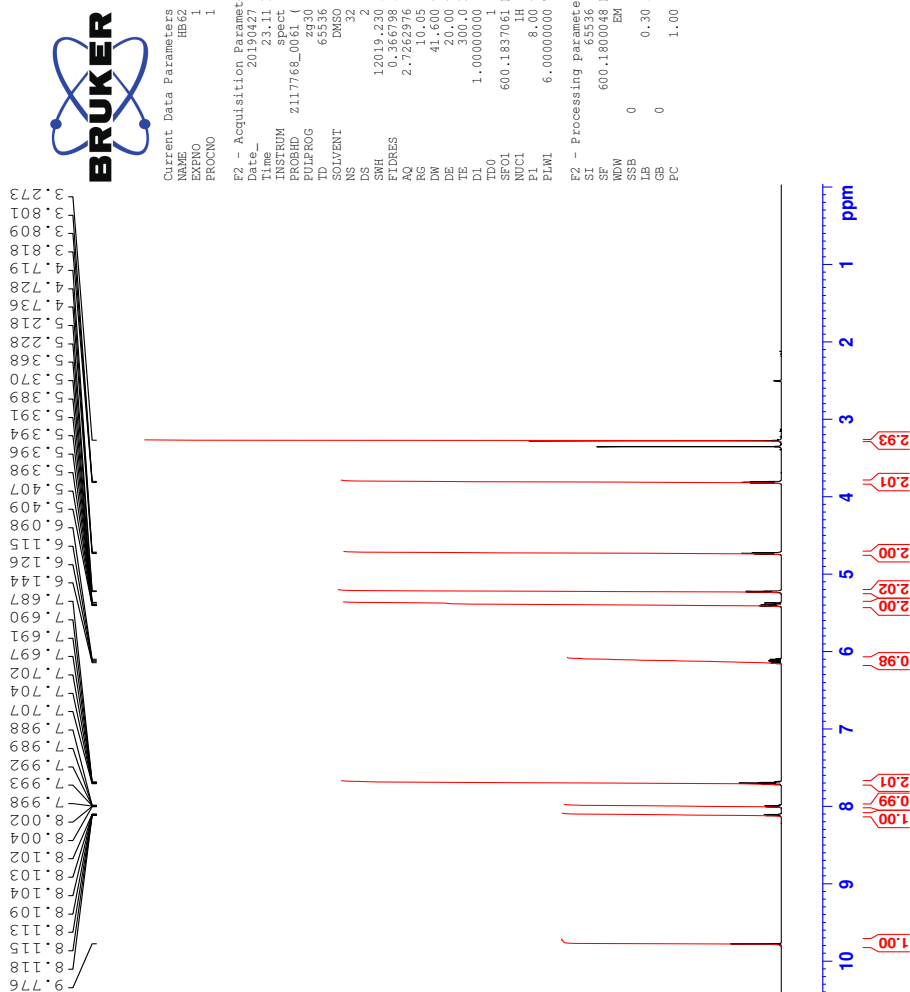


Minimum: -50.0
Maximum: 5.0 2.0 50.0

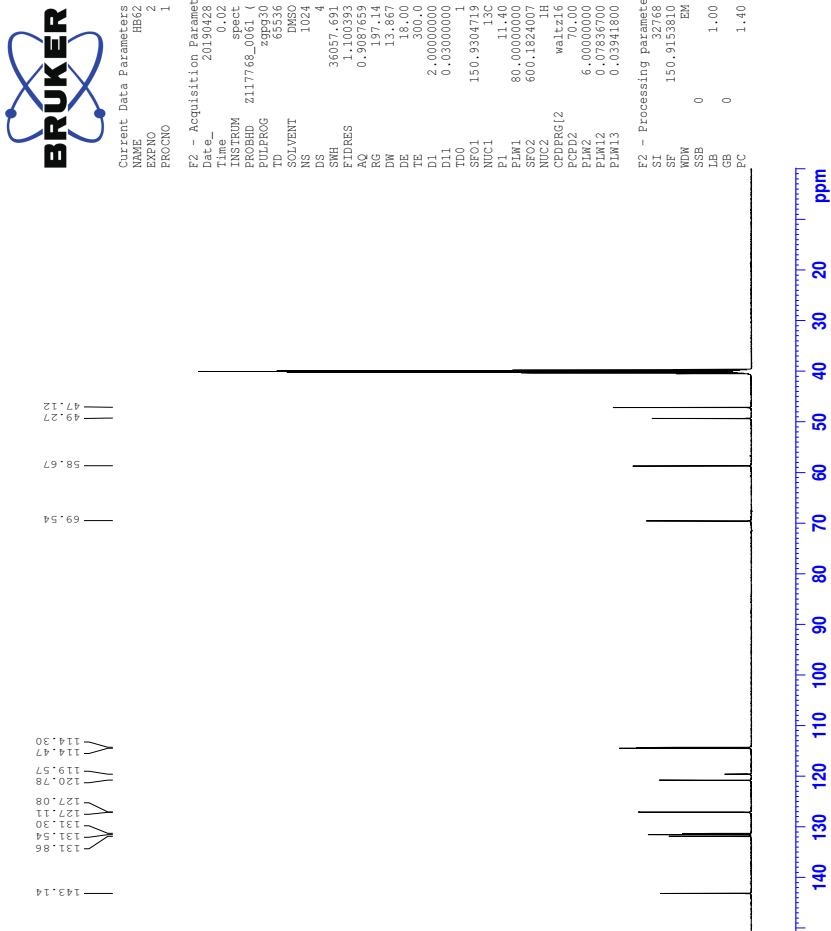
Mass	Calc. Mass	mDa	PPM	DBE	i-FIT	Norm	Conf (%)	Formula
279.9174	279.9173	0.1	0.4	0.5	732.0	0.005	99.50	C ₂ N O ₄ F ₆ S ₂
	279.9173	0.1	0.4	7.5	738.0	5.996	0.25	C ₈ H ₃ N O ₃ Na
							S ₃	
279.9172	0.2	0.7	7.5	738.1	6.115	0.22		C ₈ H N O F ₃ S ₃
279.9171	0.3	1.1	-3.5	740.0	8.004	0.03		H ₄ N O ₃ F ₅ Na
							S ₃	

37 Spectra of IL 15c

37.1 ^1H -NMR spectrum of IL 15c



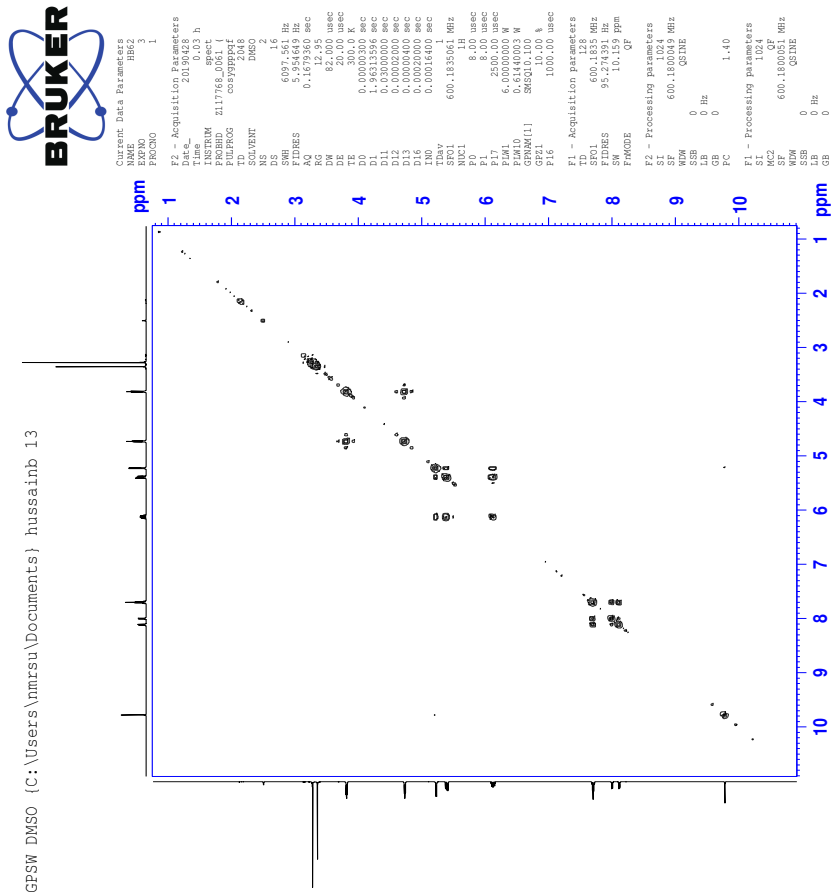
37.2 ^{13}C -NMR spectrum of IL 15c



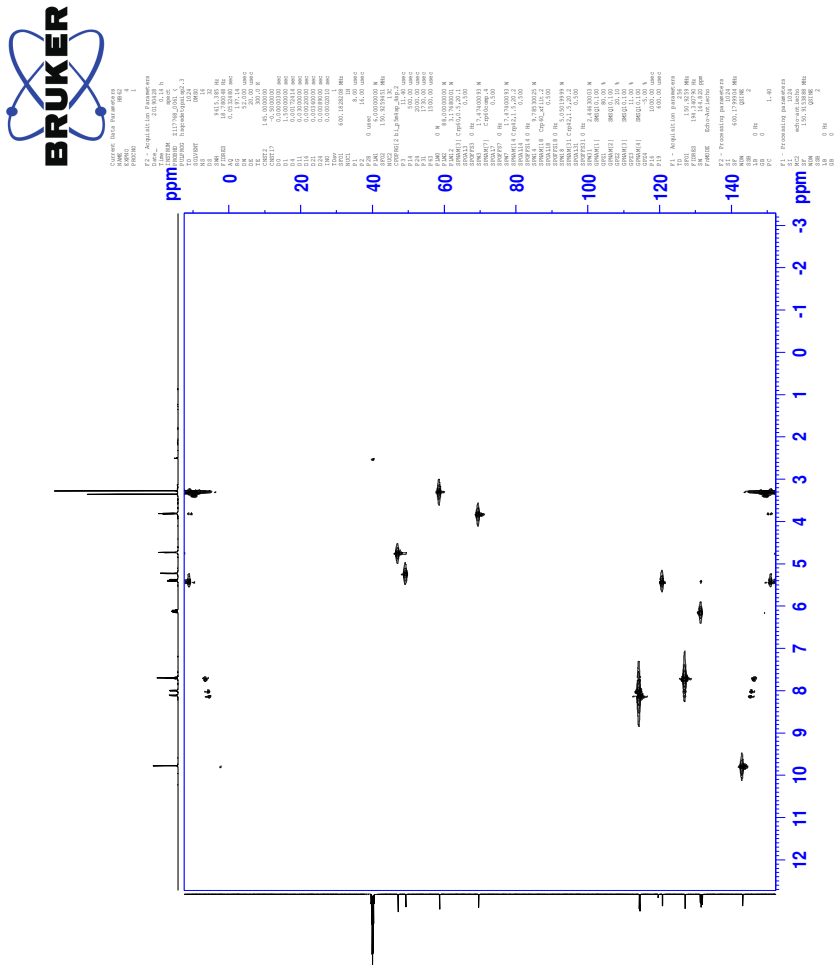
CCX

37.3 COSY-spectrum of IL 15c

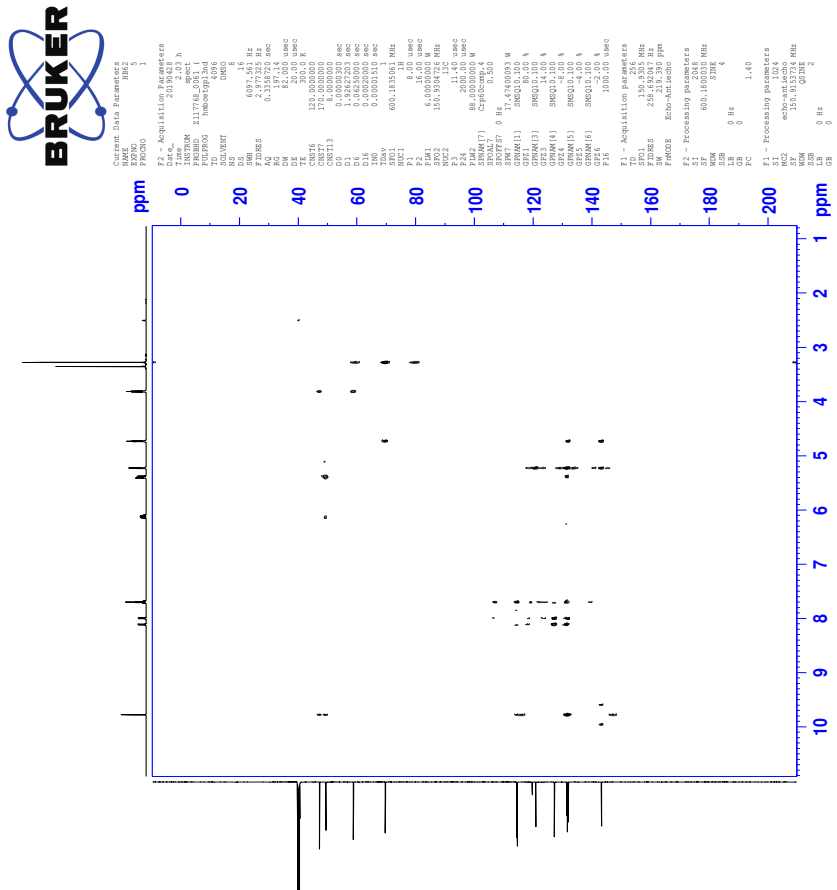
COSYGPSW DMSO {C:\Users\nmrsu\Documents} hussainb 13



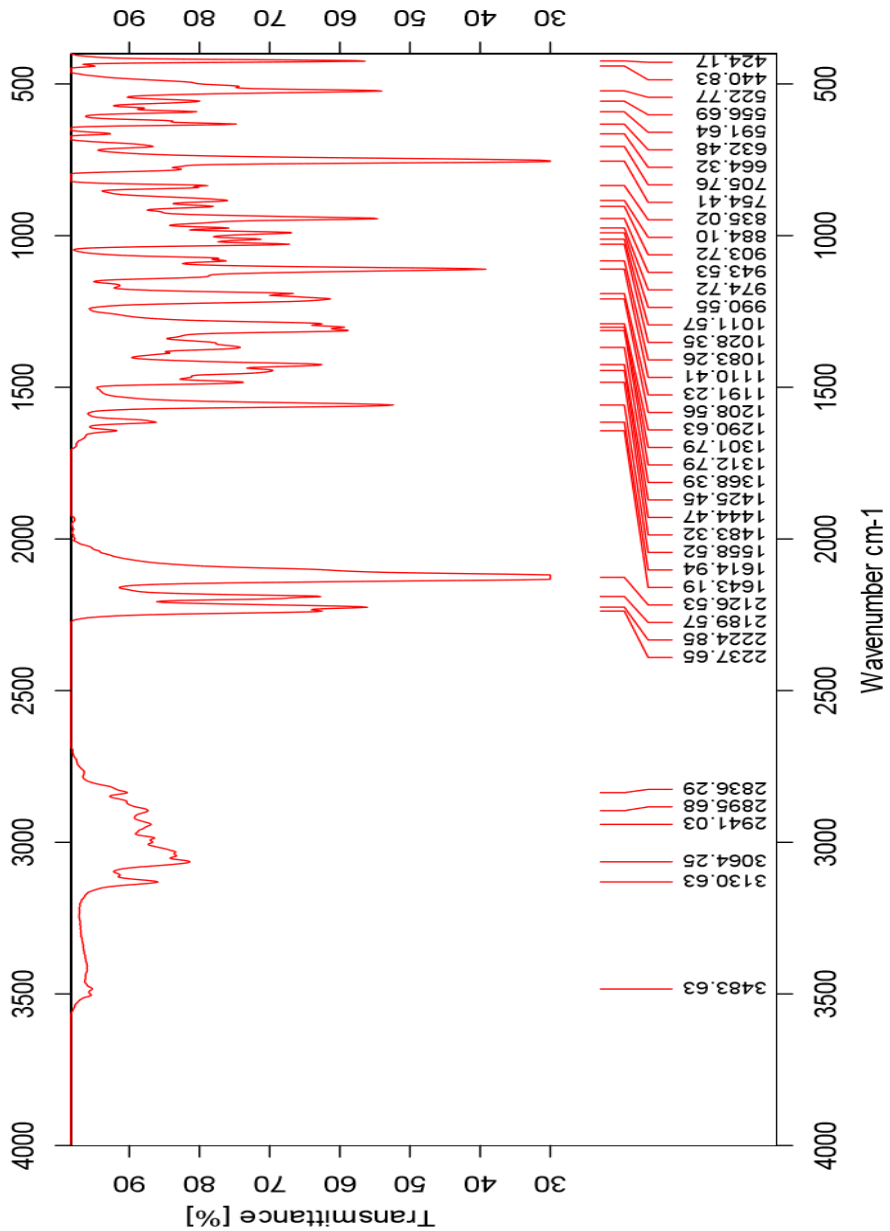
37.4 HSQC-spectrum of IL 15c



37.5 HMBC-spectrum of IL 15c



37.6 IR-spectrum of IL 15c



37.7 HR-MS positive mode spectrum of IL 15c

Elemental Composition Report

Page 1

Single Mass Analysis

Tolerance = 2.0 PPM / DBE: min = -50.0, max = 50.0

Element prediction: Off

Number of isotope peaks used for i-FIT = 3

Monoisotopic Mass, Even Electron Ions

1234 formula(e) evaluated with 1 results within limits (all results (up to 1000) for each mass)

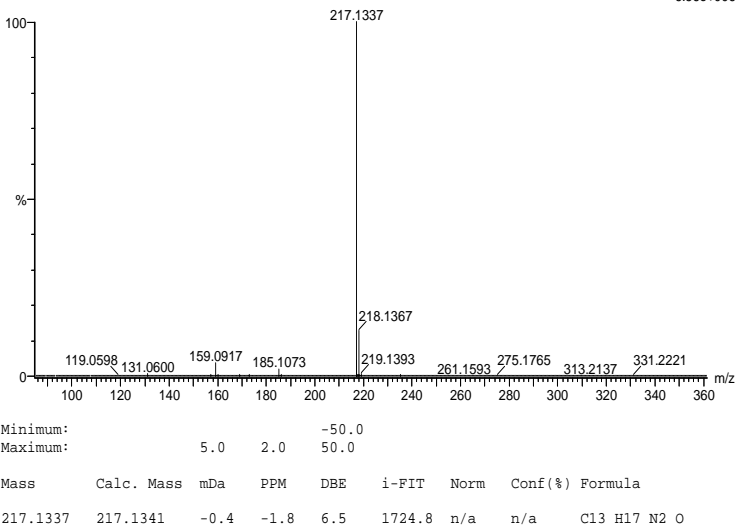
Elements Used:

C: 0-100 H: 0-150 N: 0-10 O: 0-10 Na: 0-1

2019-392 66 (1.231) AM2 (Ar,35000.0,0.00,0.00); Cm (65:66)

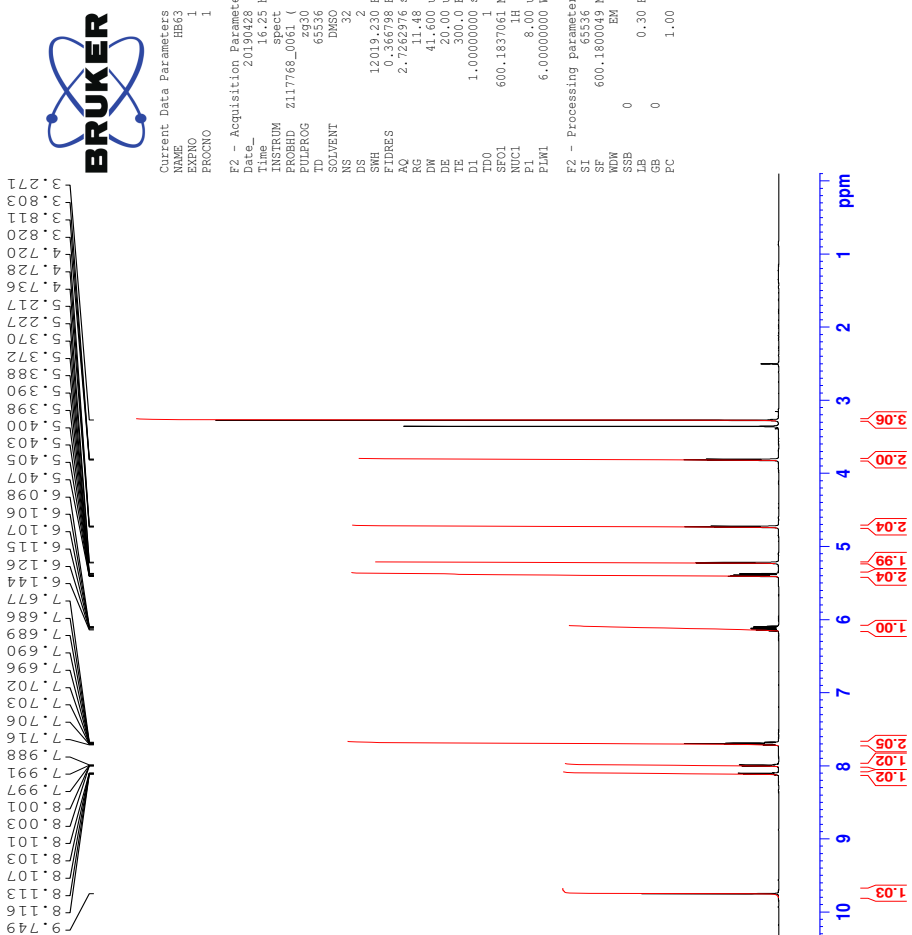
1: TOF MS ES+

6.56e+006

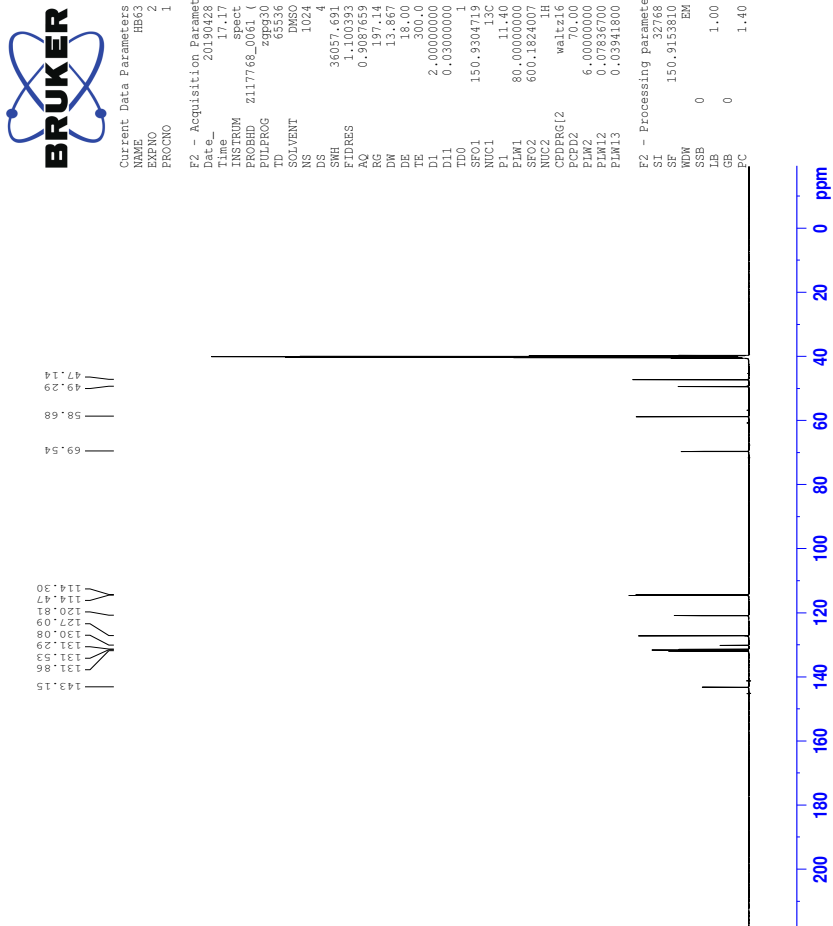


38 Spectra of IL 15d

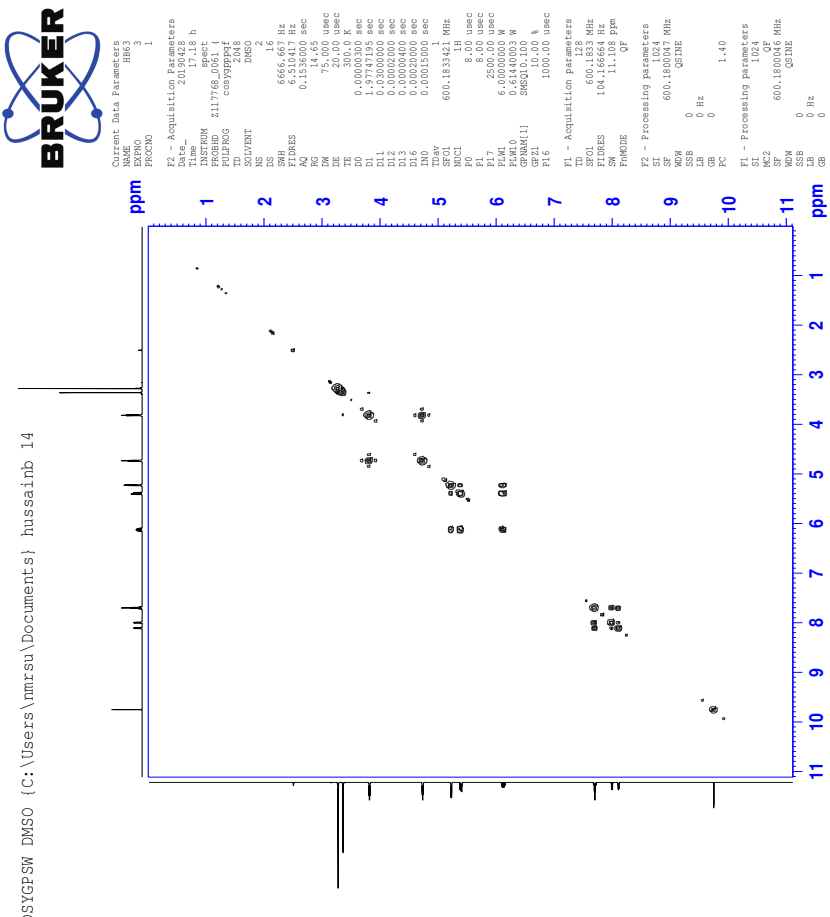
38.1 ^1H -NMR spectrum of IL 15d



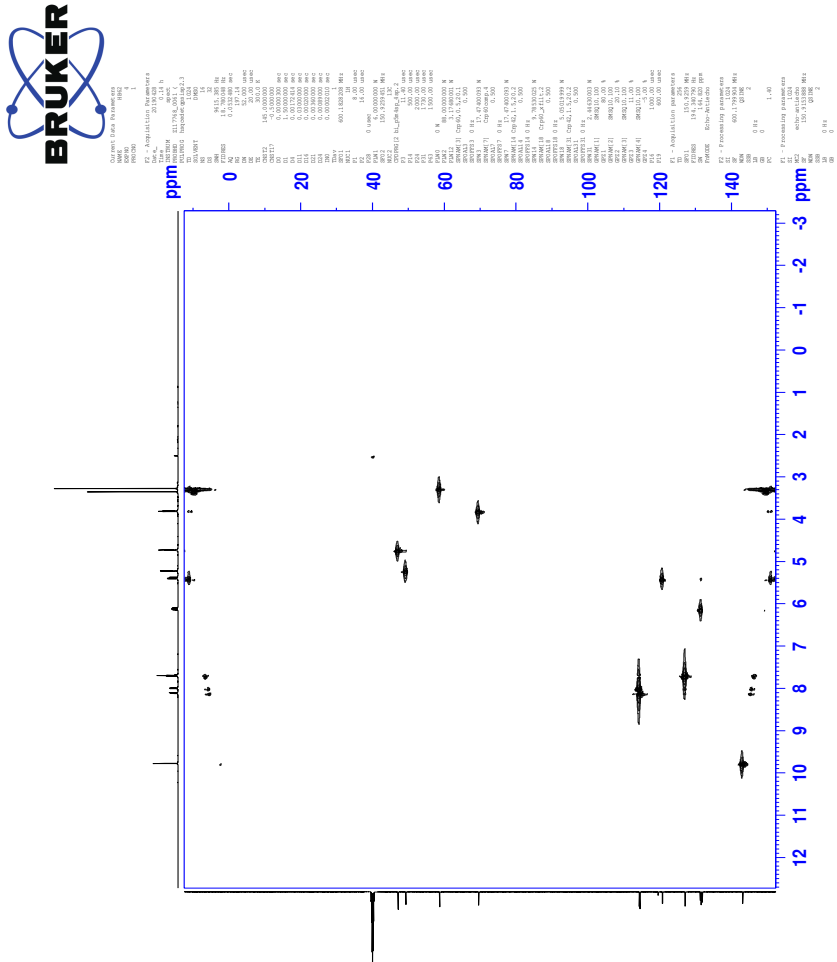
38.2 ^{13}C -NMR spectrum of IL 15d



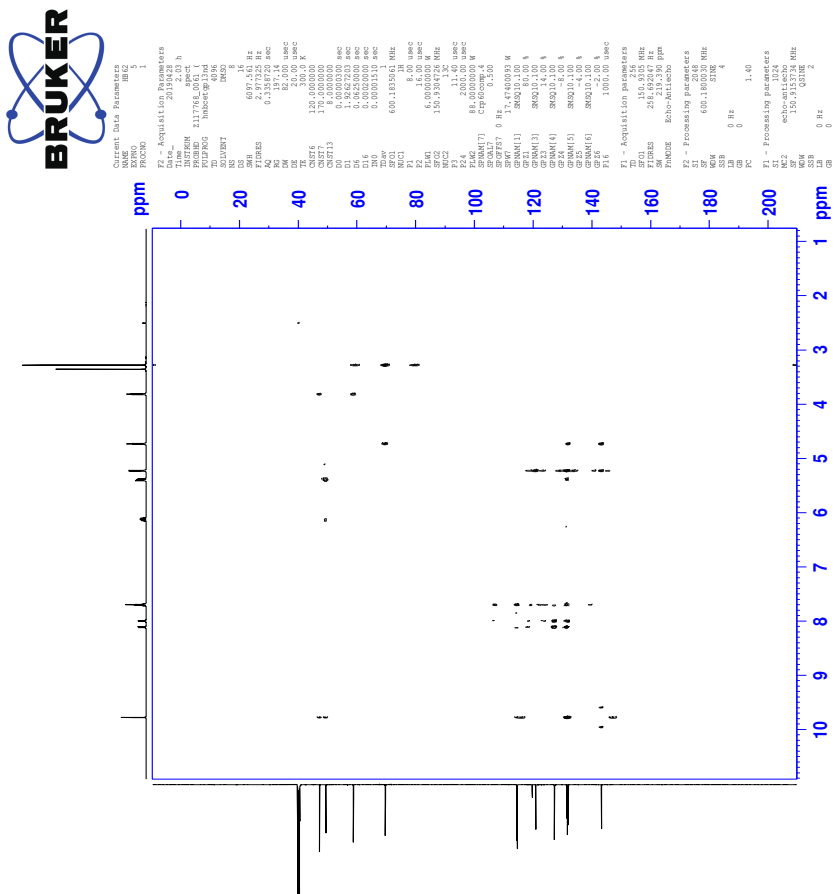
38.3 COSY-spectrum of IL 15d



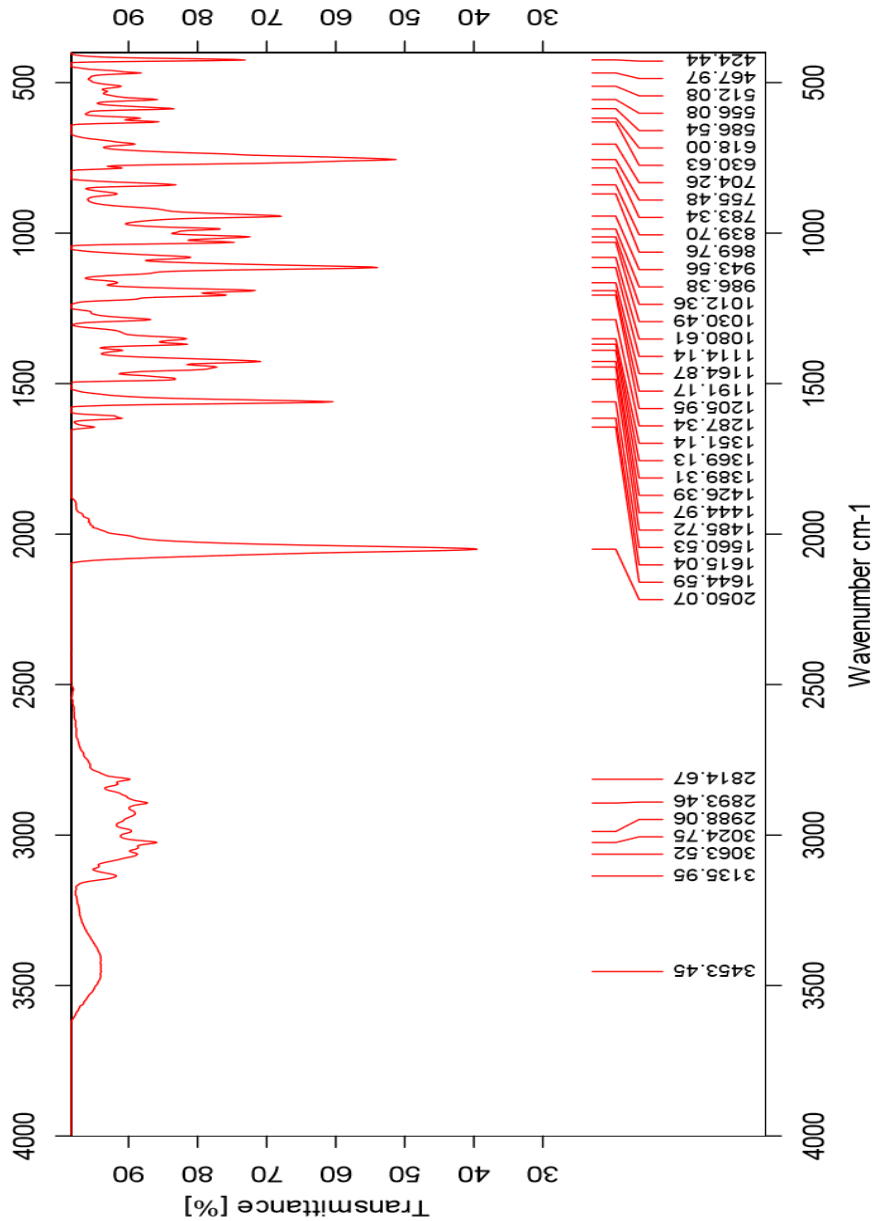
38.4 HSQC-spectrum of IL 15d



38.5 HMBC-spectrum of IL 15d



38.6 IR-spectrum of IL 15c



38.7 HR-MS positive mode spectrum of IL 15d

Elemental Composition Report

Page 1

Single Mass Analysis

Tolerance = 2.0 PPM / DBE: min = -50.0, max = 50.0

Element prediction: Off

Number of isotope peaks used for i-FIT = 3

Monoisotopic Mass, Even Electron Ions

1234 formula(e) evaluated with 1 results within limits (all results (up to 1000) for each mass)

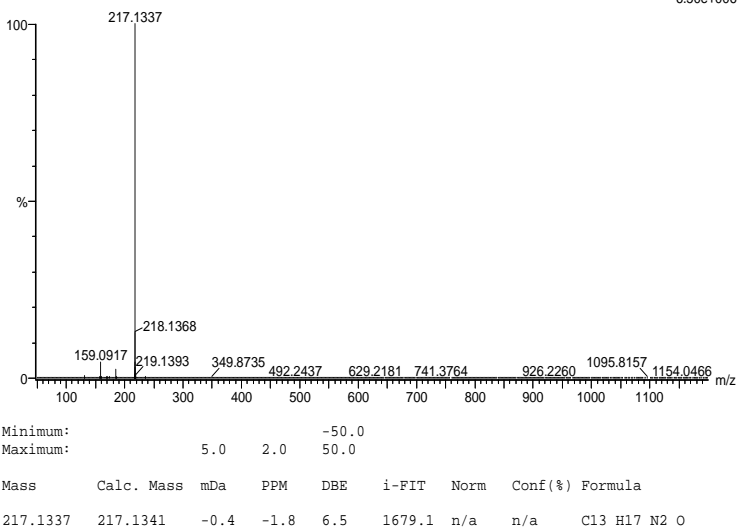
Elements Used:

C: 0-100 H: 0-150 N: 0-10 O: 0-10 Na: 0-1

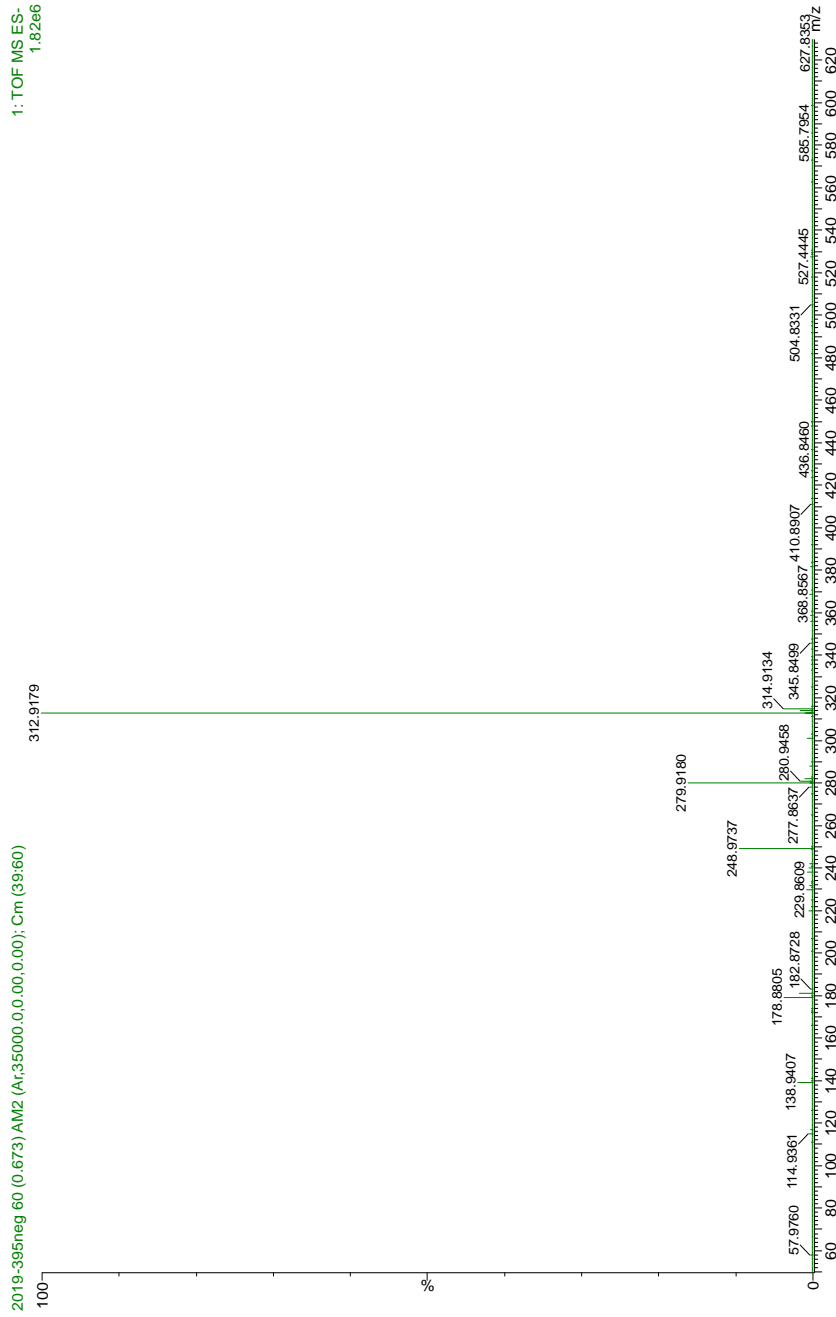
2019-394 20 (0.385) AM2 (Ar,35000.0,0.00,0.00); Cm (19:20)

1: TOF MS ES+

6.50e+006

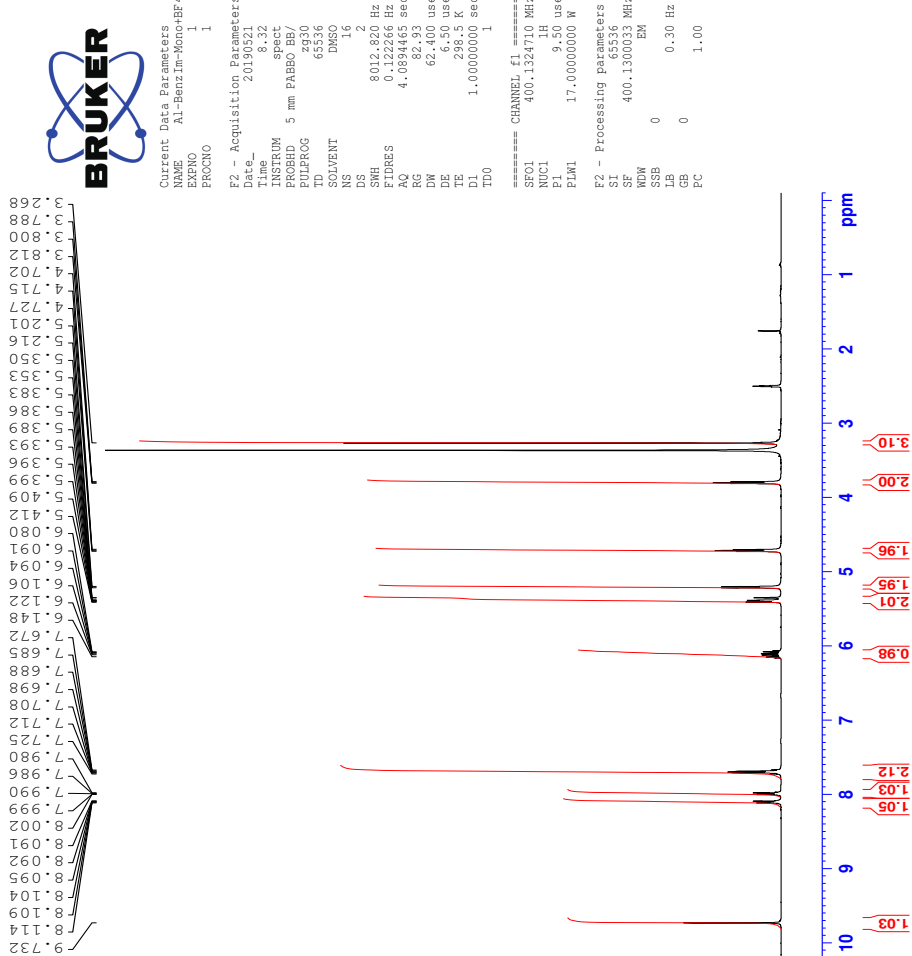


38.8 HR-MS negative mode spectrum of IL 15d

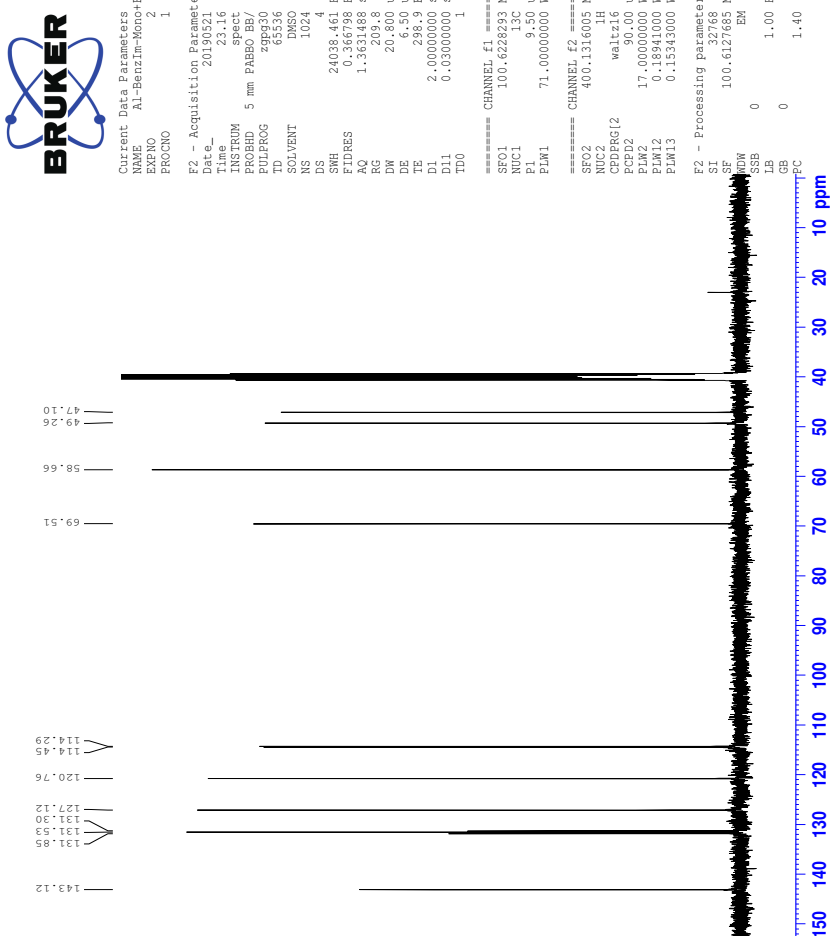


39 Spectra of IL 15e

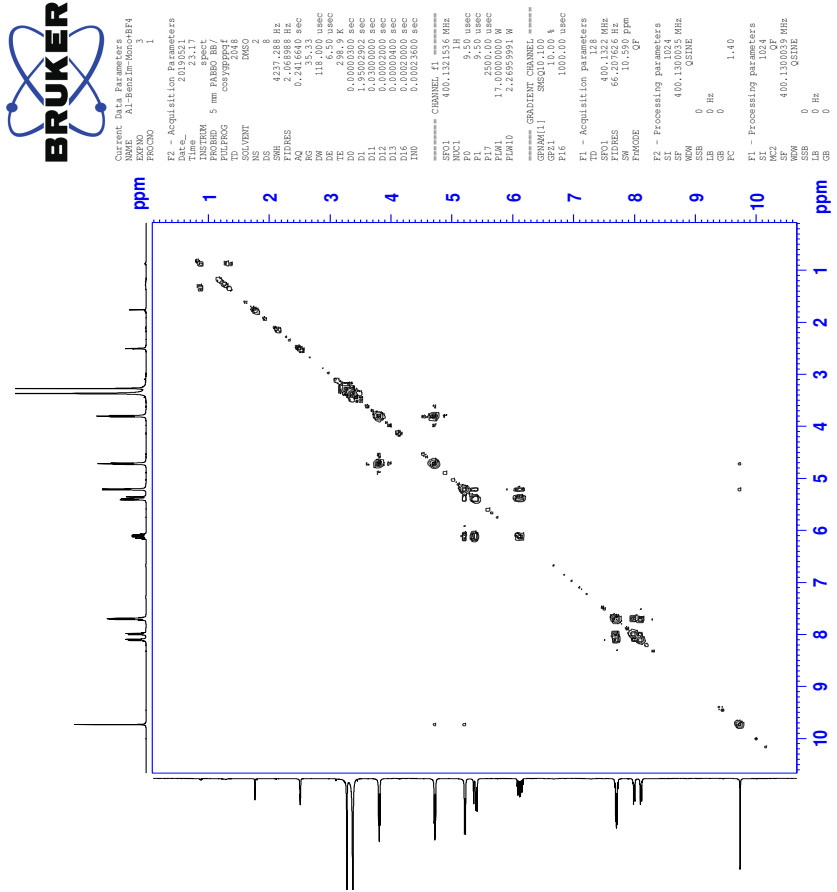
39.1 ^1H -NMR spectrum of IL 15e



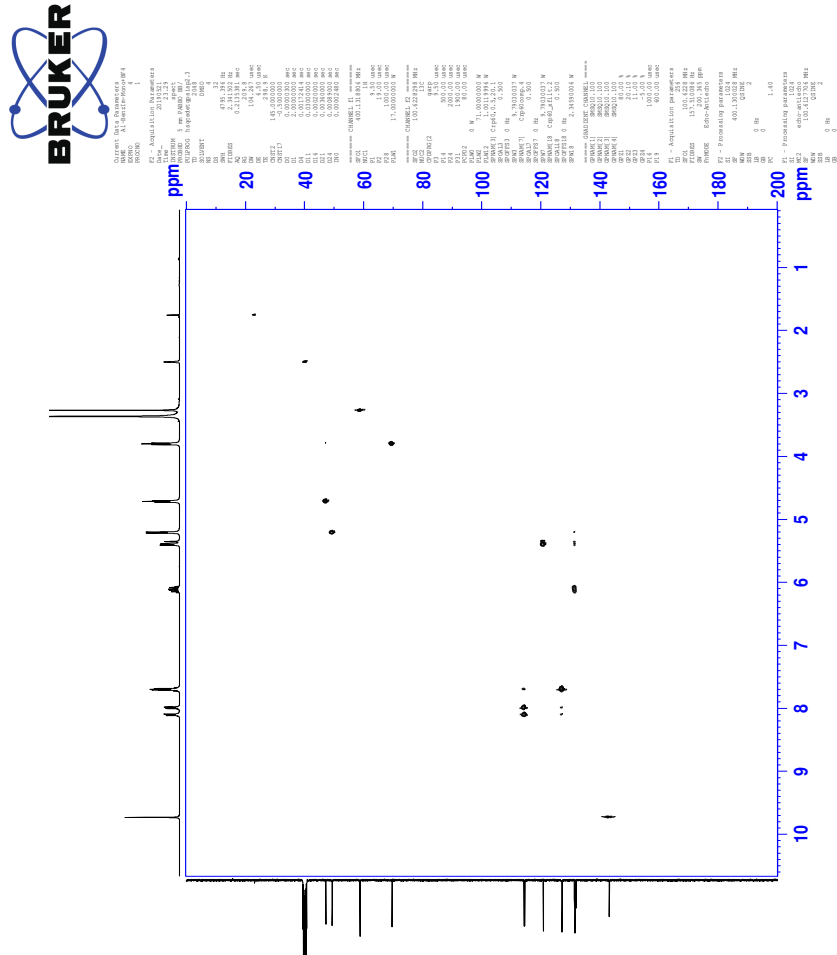
39.2 ^{13}C -NMR spectrum of IL 15e



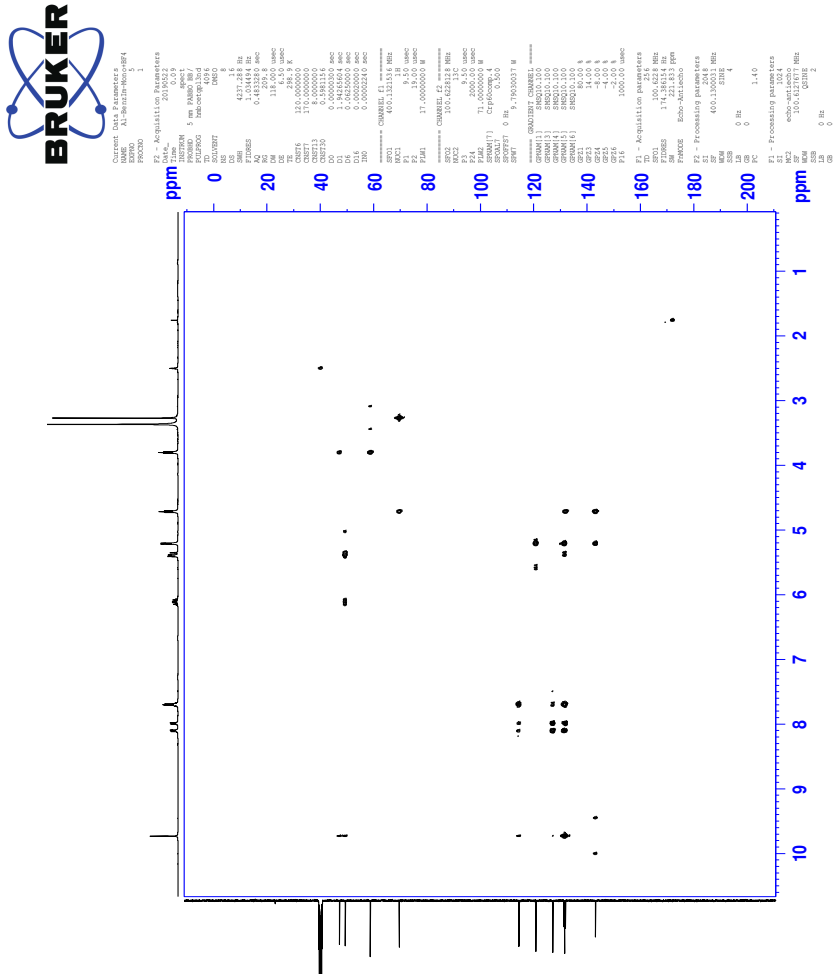
39.3 COSY-spectrum of IL 15e



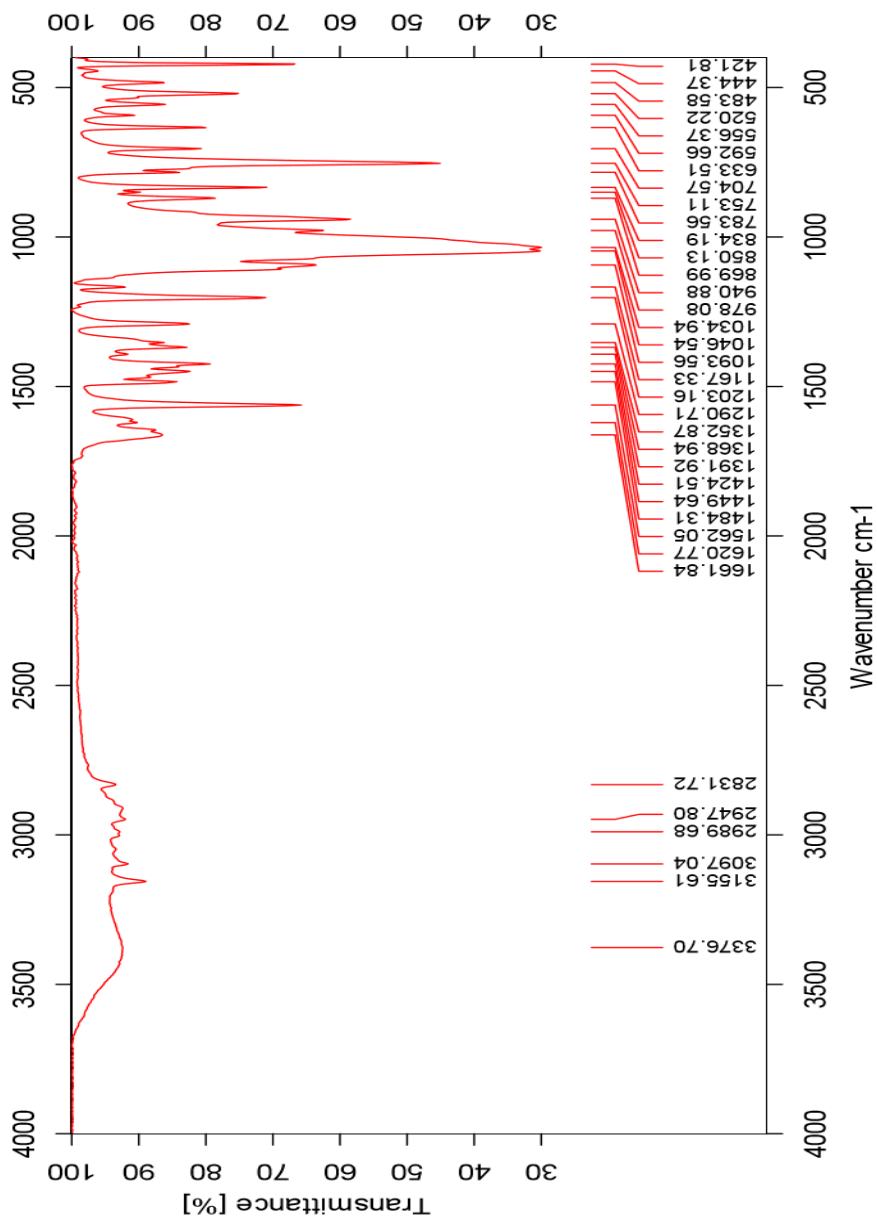
39.4 HSQC-spectrum of IL 15e



39.5 HMBC-spectrum of IL 15e



39.6 IR-spectrum of IL 15c



39.7 HR-MS positive mode spectrum of IL 15e

Elemental Composition Report

Page 1

Single Mass Analysis

Tolerance = 5.0 PPM / DBE: min = -50.0, max = 50.0

Element prediction: Off

Number of isotope peaks used for i-FIT = 3

Monoisotopic Mass, Even Electron Ions

688 formula(e) evaluated with 1 results within limits (all results (up to 1000) for each mass)

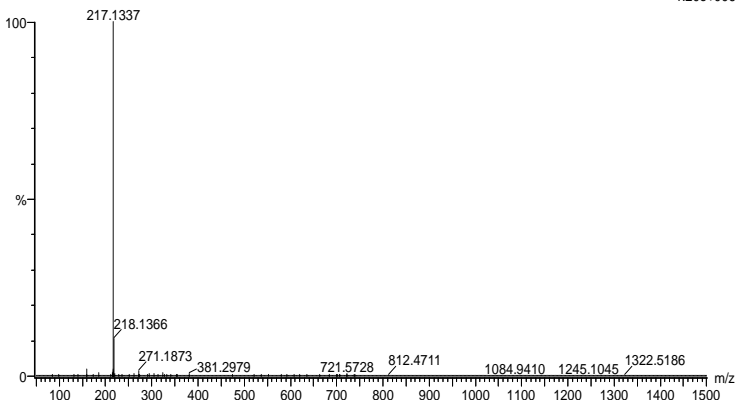
Elements Used:

C: 0-100 H: 0-150 N: 0-10 O: 0-10

2019_512FIA79 (1.466) AM2 (Ar,35000.0,0.00,0.00); Cm (79:81)

1: TOF MS ES+

1.20e+006



Minimum: -50.0
Maximum: 5.0 5.0 50.0

Mass	Calc. Mass	mDa	PPM	DBE	i-FIT	Norm	Conf (%)	Formula
217.1337	217.1341	-0.4	-1.8	6.5	1395.9	n/a	n/a	C13 H17 N2 O

39.8 HR-MS negative mode spectrum of IL 15e

Elemental Composition Report

Page 1

Single Mass Analysis

Tolerance = 10.0 PPM / DBE: min = -50.0, max = 50.0

Element prediction: Off

Number of isotope peaks used for i-FIT = 3

Monoisotopic Mass, Even Electron Ions

423 formula(e) evaluated with 2 results within limits (all results (up to 1000) for each mass)

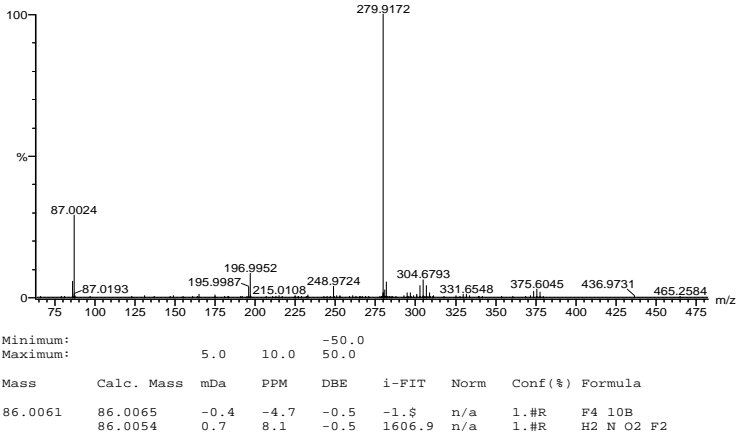
Elements Used:

C: 0-100 H: 0-150 N: 0-10 O: 0-10 F: 0-8 10B: 0-1

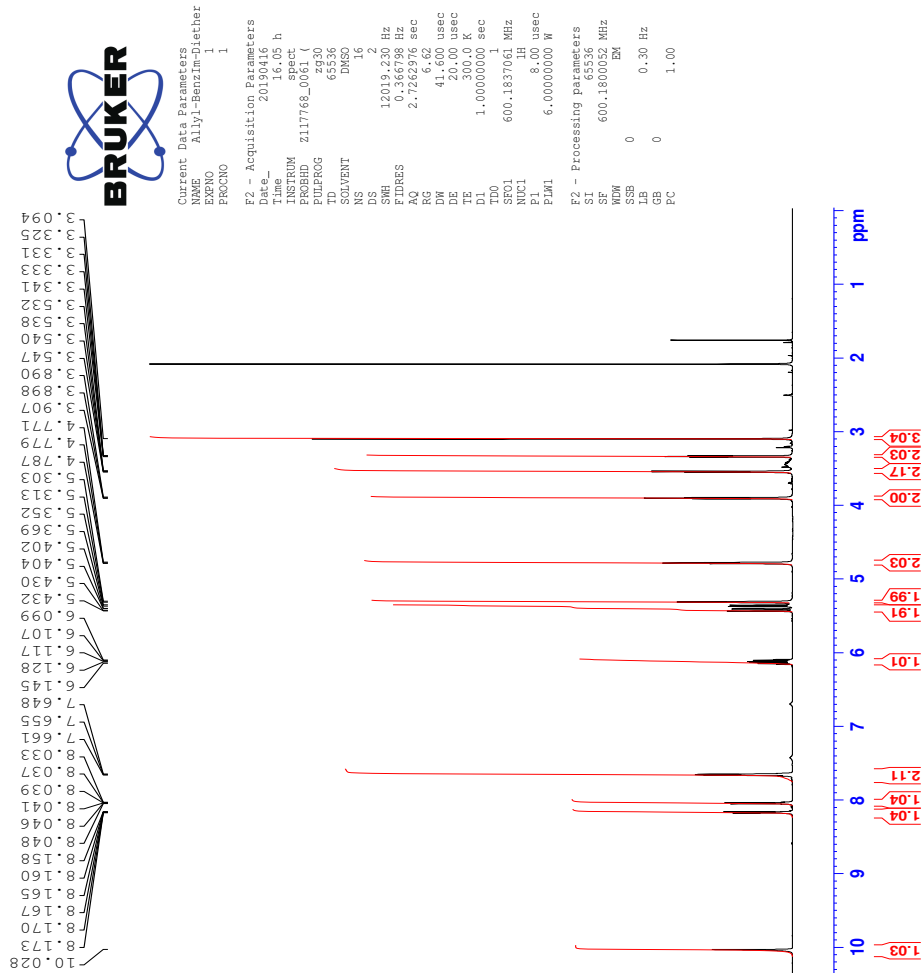
2019_513FIA76 (0.857) AM2 (Ar,35000.0,0.00,0.00); Cm (64:76)

1: TOF MS ES-

3.60e+005

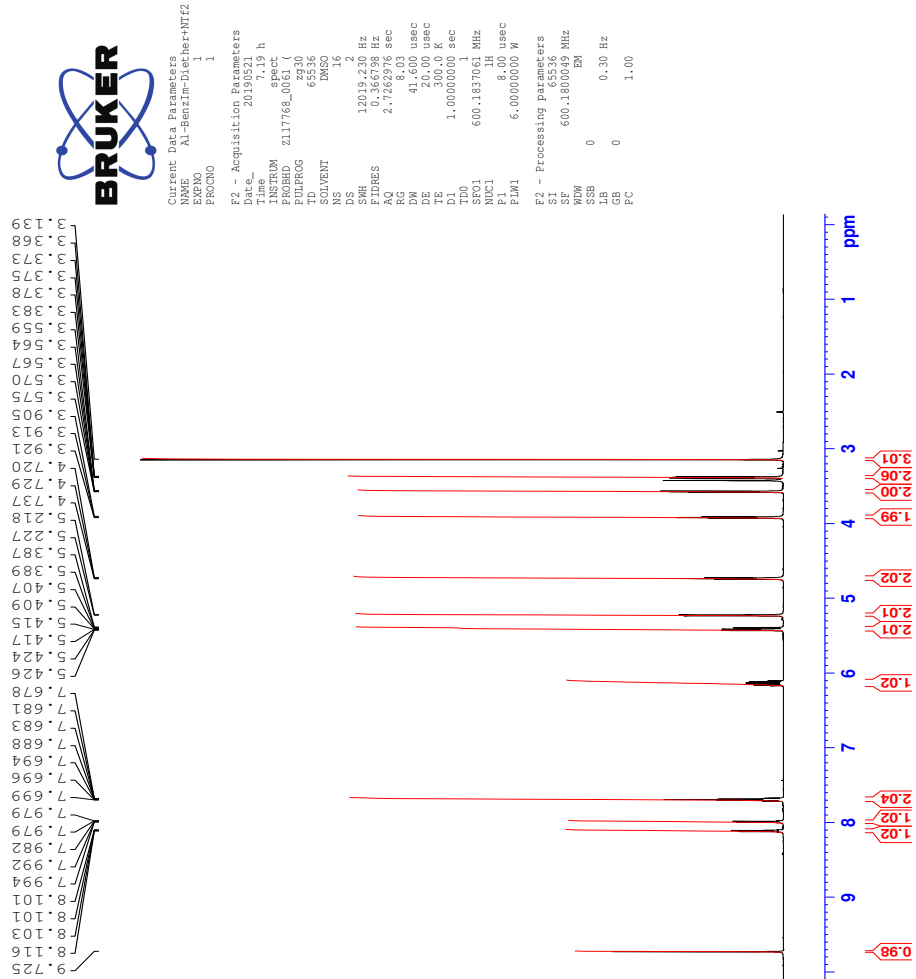


40 ^1H -NMR spectrum of compound 16a

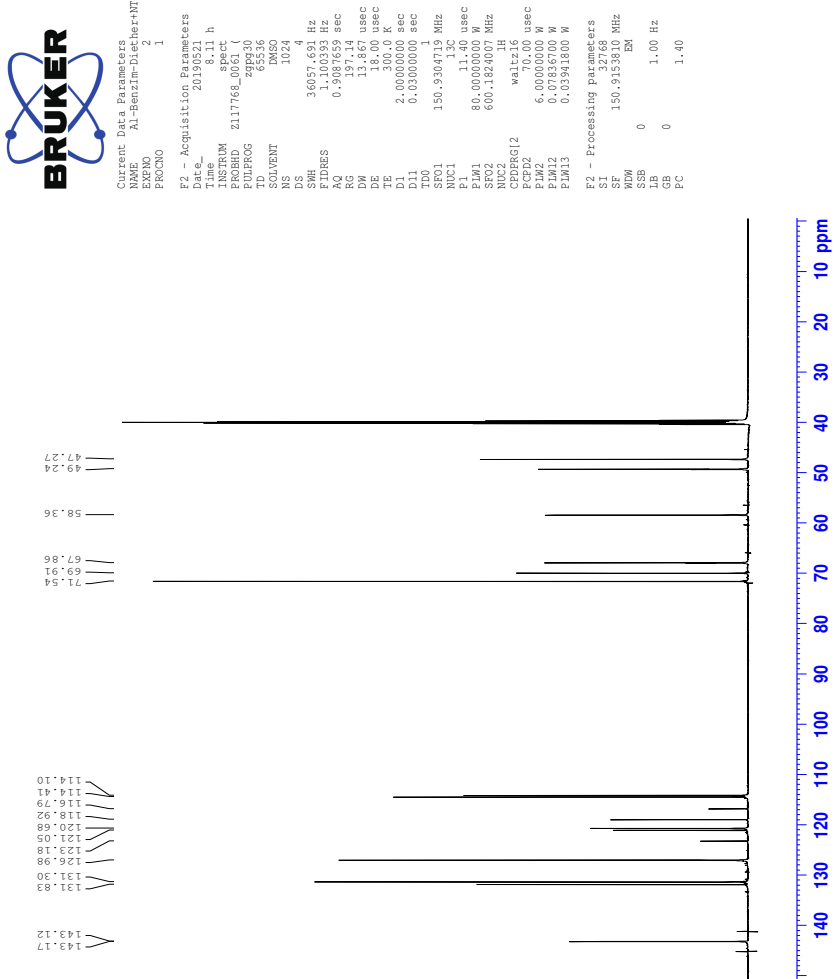


41 Spectra of IL 16b

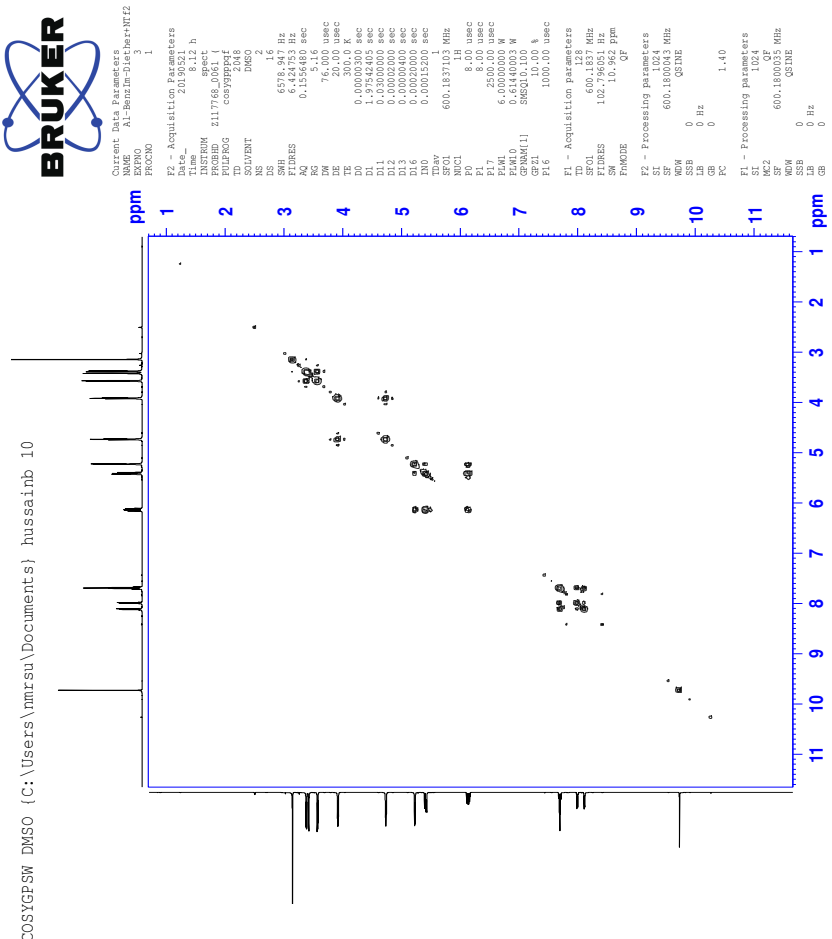
41.1 ^1H -NMR spectrum of IL 16b



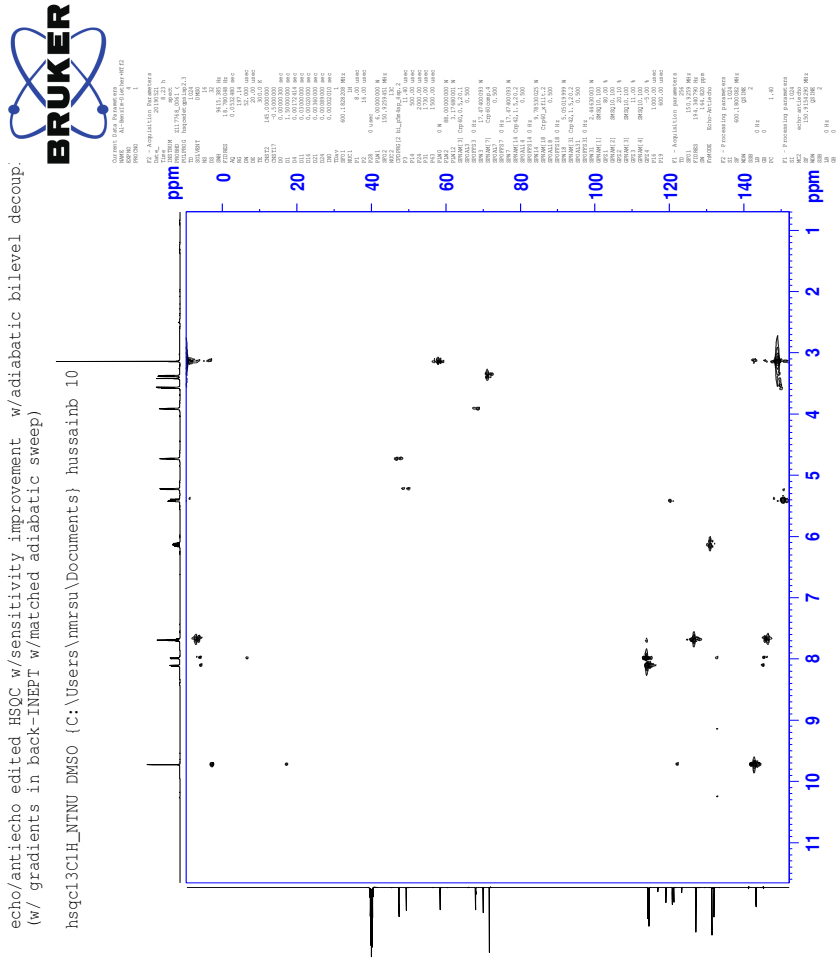
41.2 ^{13}C -NMR spectrum of IL 16b



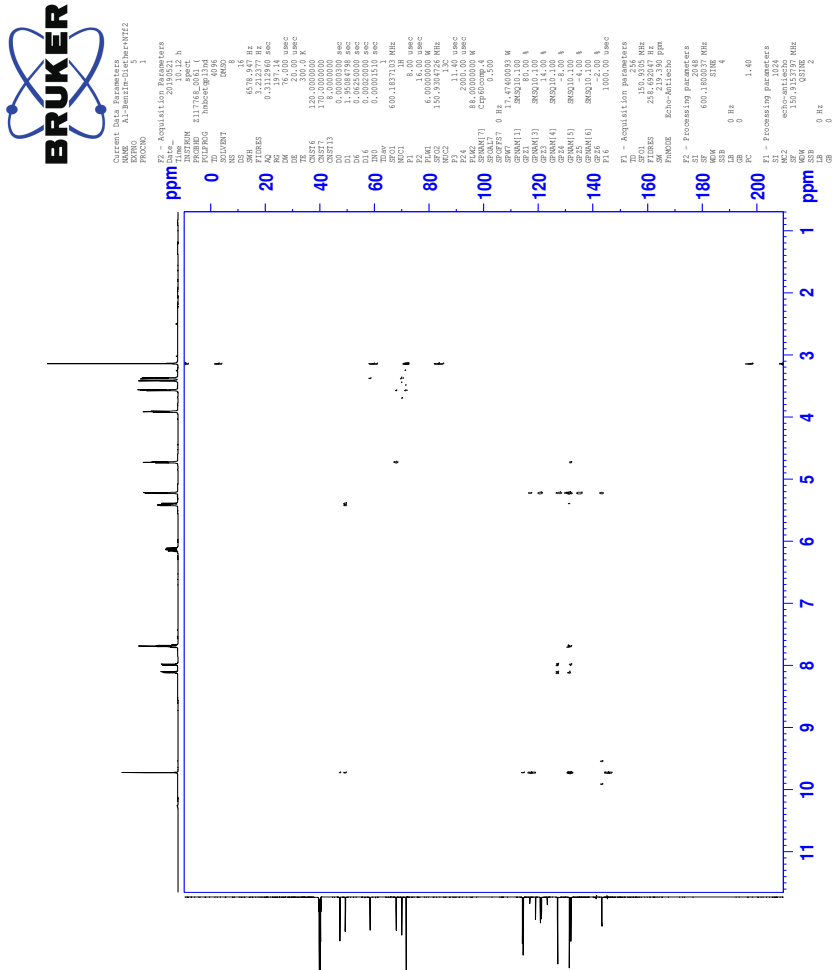
41.3 COSY-spectrum of IL 16b



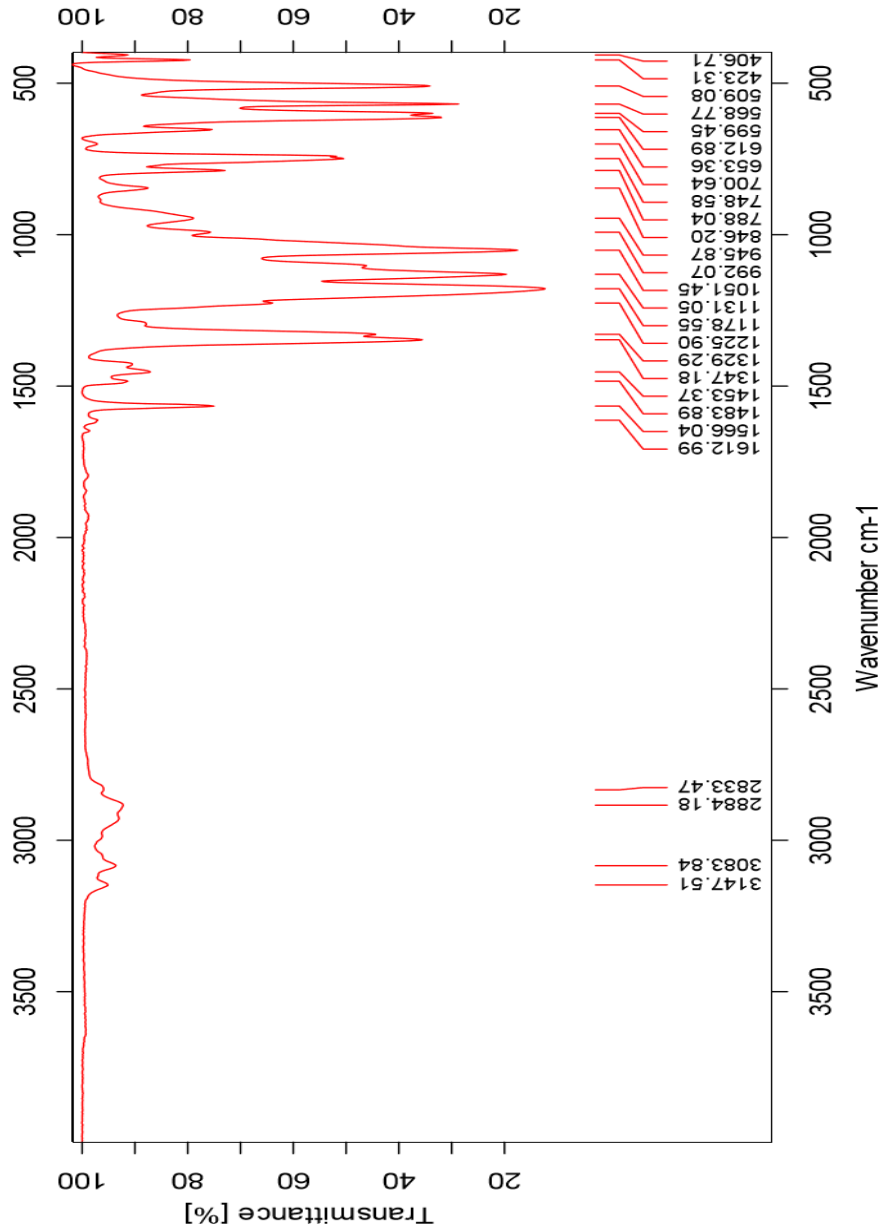
41.4 HSQC-spectrum of IL 16b



41.5 HMBC-spectrum of IL 16b



41.6 IR-spectrum of IL 16b



41.7 HR-MS positive mode spectrum of IL 16b

Elemental Composition Report

Page 1

Single Mass Analysis

Tolerance = 5.0 PPM / DBE: min = -50.0, max = 50.0

Element prediction: Off

Number of isotope peaks used for i-FIT = 3

Monoisotopic Mass, Even Electron Ions

943 formula(e) evaluated with 1 results within limits (all results (up to 1000) for each mass)

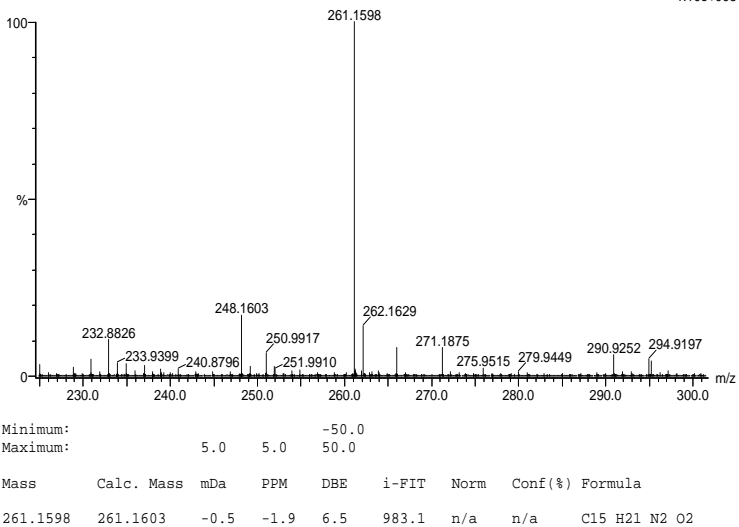
Elements Used:

C: 0-100 H: 0-150 N: 0-10 O: 0-10

2019_506FIA 19 (0.367) AM2 (Ar,35000.0,0.00,0.00); Cm (13:19)

1: TOF MS ES+

1.10e+005



41.8 HR-MS negative mode spectrum of IL 16b

Elemental Composition Report

Page 1

Single Mass Analysis

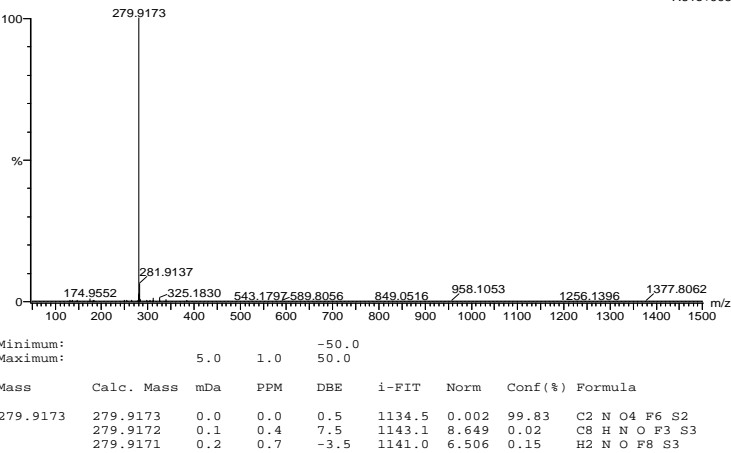
Tolerance = 1.0 PPM / DBE: min = -50.0, max = 50.0
Element prediction: Off
Number of isotope peaks used for i-FIT = 3

Monoisotopic Mass, Even Electron Ions
14728 formula(e) evaluated with 3 results within limits (all results (up to 1000) for each mass)

Elements Used:

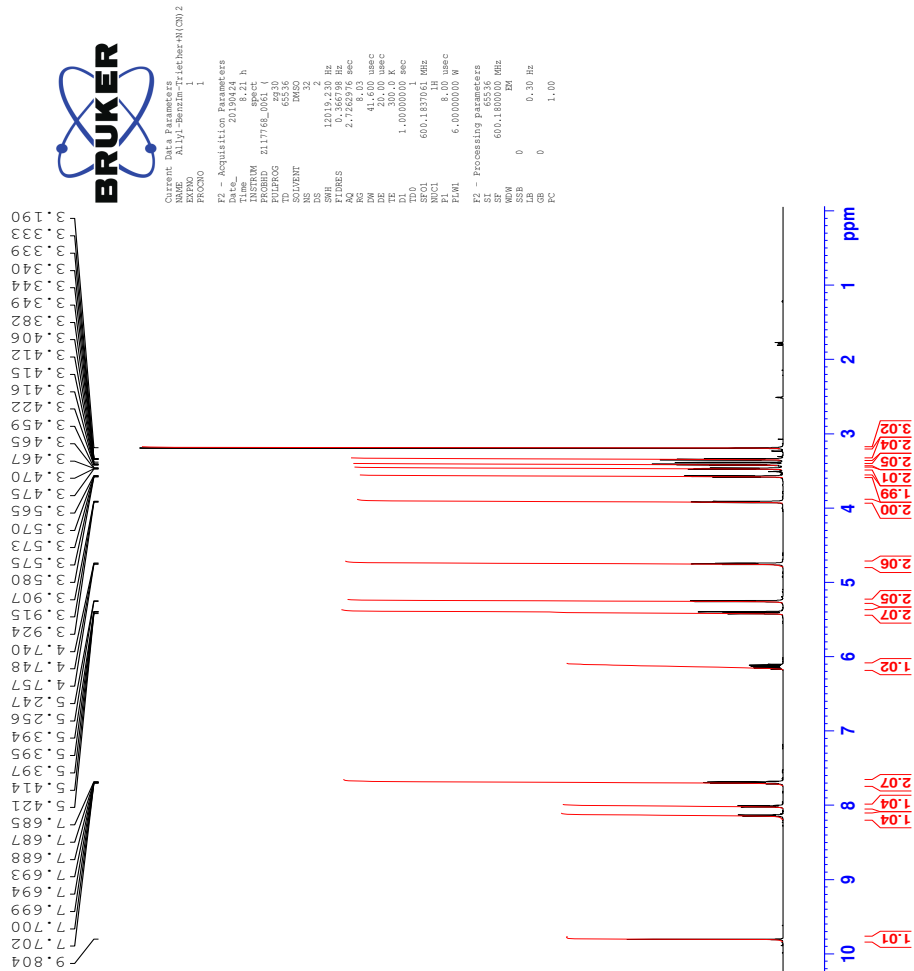
C: 0-100 H: 0-150 N: 0-10 O: 0-10 F: 0-8 S: 0-4
2019_507neg 22 (0.258) AM2 (Ar,35000.0,0.00,0.00); Cm (16:22)
1: TOF MS ES-

7.61e+005

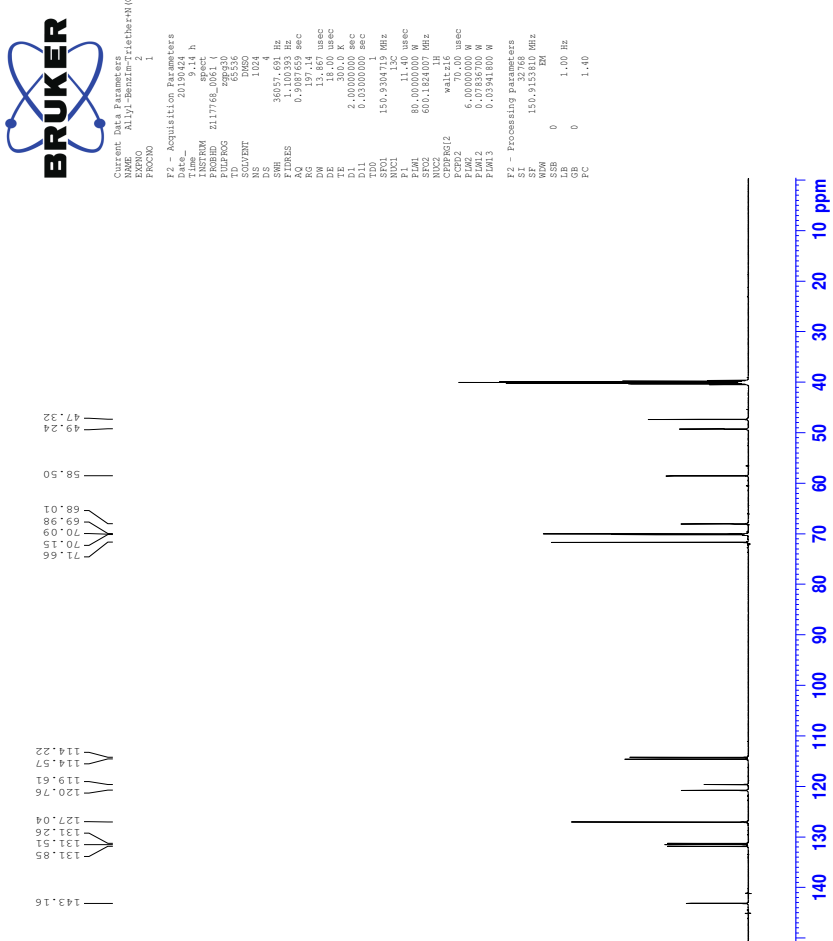


42 Spectra of IL 16c

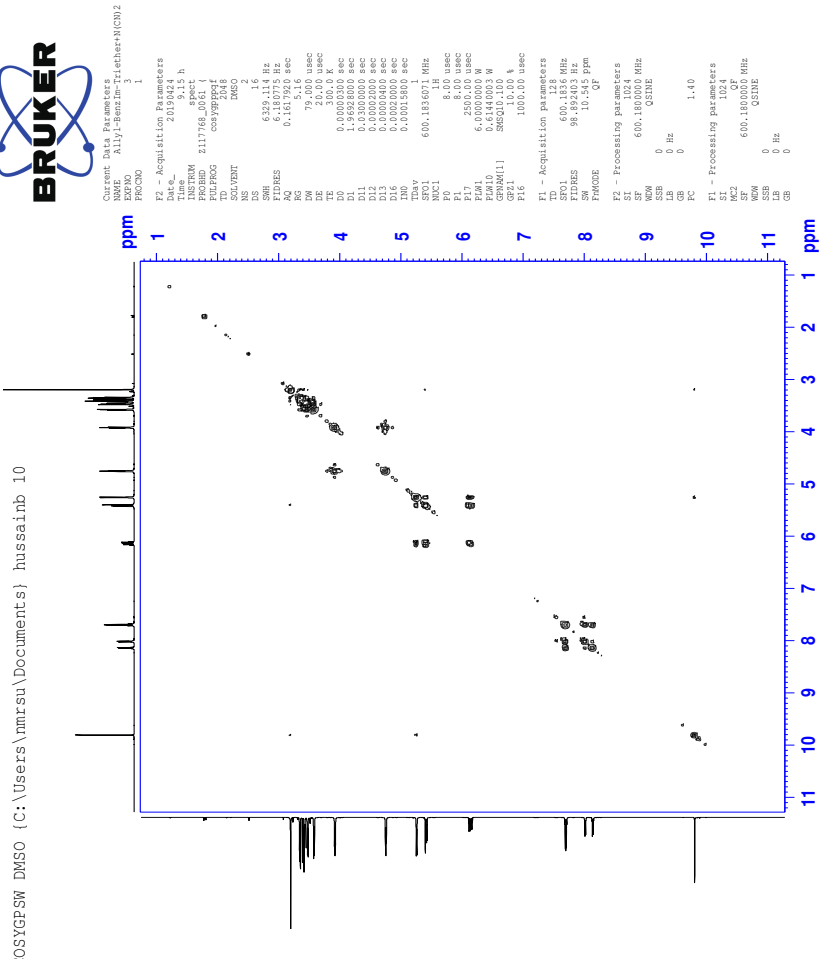
42.1 ^1H -NMR spectrum of IL 16c



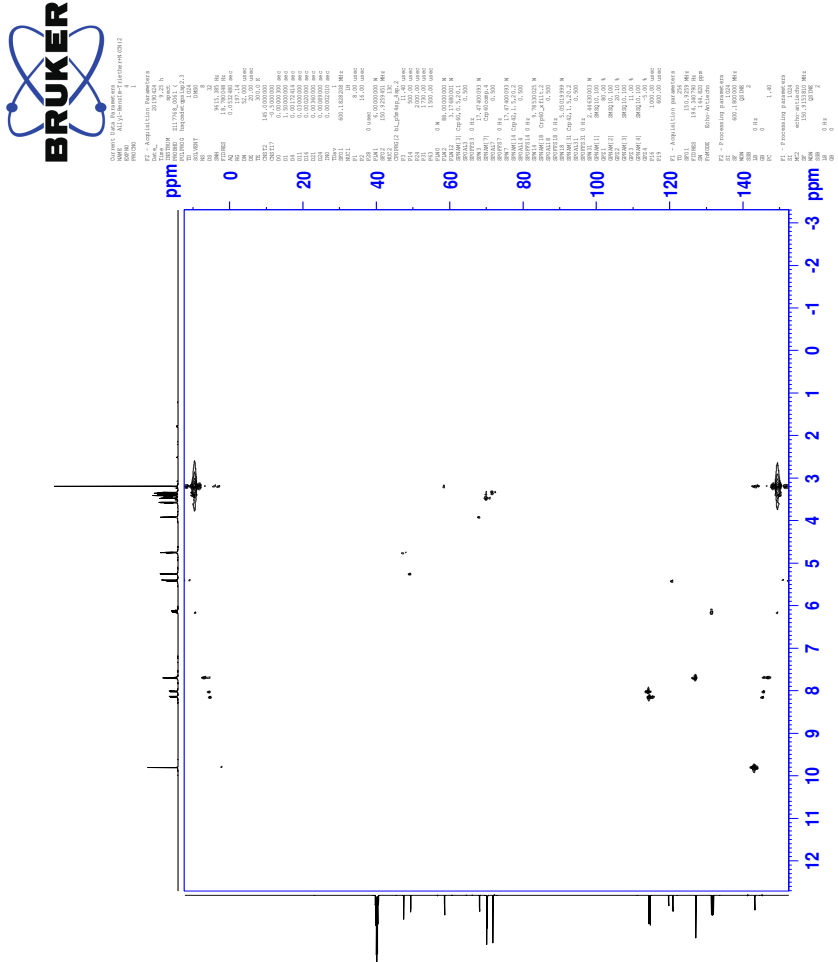
42.2 ^{13}C -NMR spectrum of IL 16c



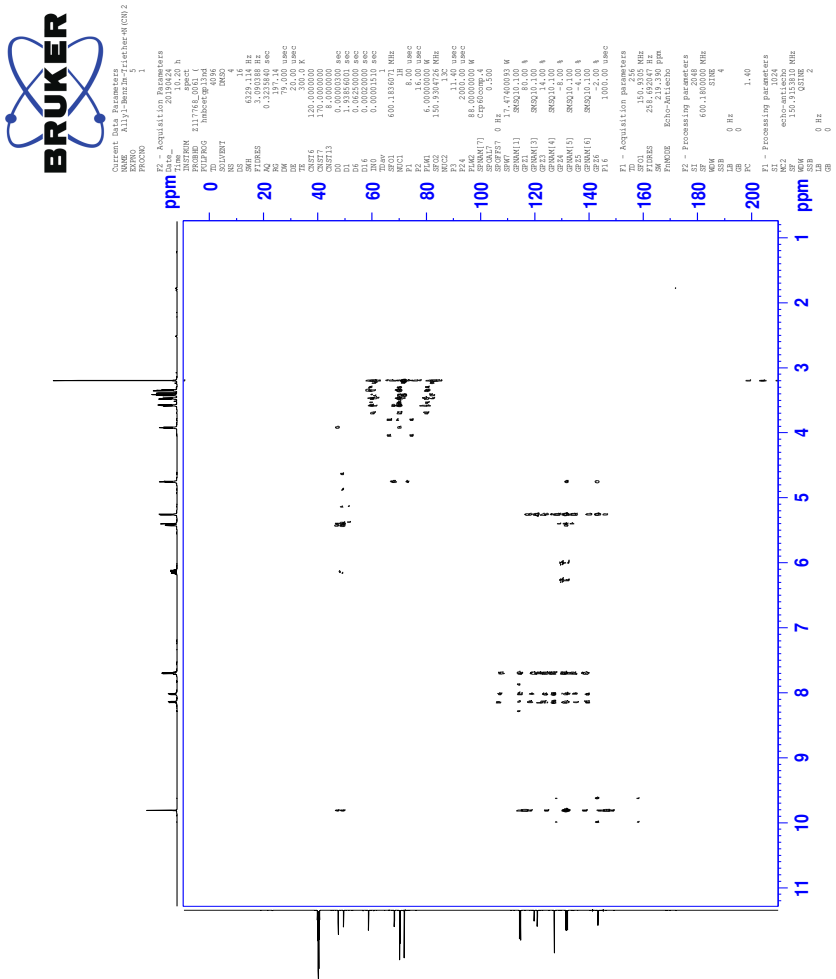
42.3 COSY-spectrum of IL 16c



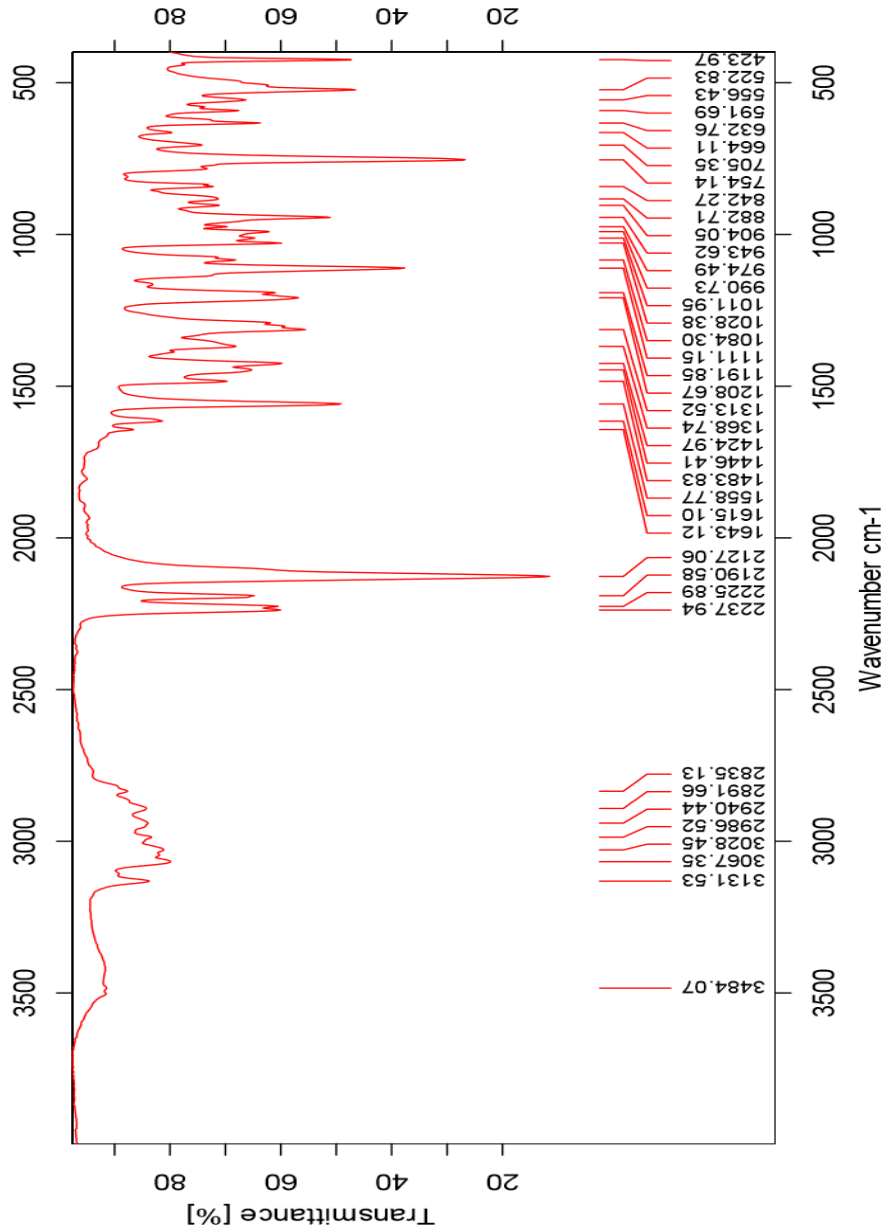
42.4 HSQC-spectrum of IL 16c



42.5 HMBC-spectrum of IL 16c



42.6 IR-spectrum of IL 16c



42.7 HR-MS positive mode spectrum of IL 16c

Elemental Composition Report

Page 1

Single Mass Analysis

Tolerance = 2.0 PPM / DBE: min = -50.0, max = 50.0

Element prediction: Off

Number of isotope peaks used for i-FIT = 3

Monoisotopic Mass, Even Electron Ions

1144 formula(e) evaluated with 2 results within limits (all results (up to 1000) for each mass)

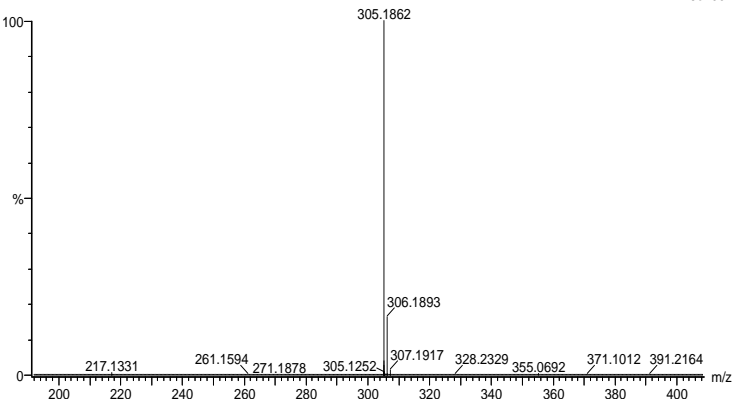
Elements Used:

C: 0-100 H: 0-150 N: 0-10 O: 0-10

svg_20190423_2019_352 18 (0.339) AM2 (Ar,35000.0,0.00,0.00); Crn (10:18)

1: TOF MS ES+

1.13e+007



Minimum: -50.0
Maximum: 5.0 2.0 50.0

Mass	Calc. Mass	mDa	PPM	DBE	i-FIT	Norm	Conf (%)	Formula
305.1862	305.1865	-0.3	-1.0	6.5	1604.3	0.000	100.00	C17 H25 N2 O3
	305.1857	0.5	1.6	-5.5	1615.3	11.015	0.00	C H25 N10 O8

42.8 HR-MS negative mode spectrum of IL 16c

Elemental Composition Report

Page 1

Single Mass Analysis

Tolerance = 2.0 PPM / DBE: min = -50.0, max = 50.0

Element prediction: Off

Number of isotope peaks used for i-FIT = 3

Monoisotopic Mass, Even Electron Ions

41 formula(e) evaluated with 1 results within limits (all results (up to 1000) for each mass)

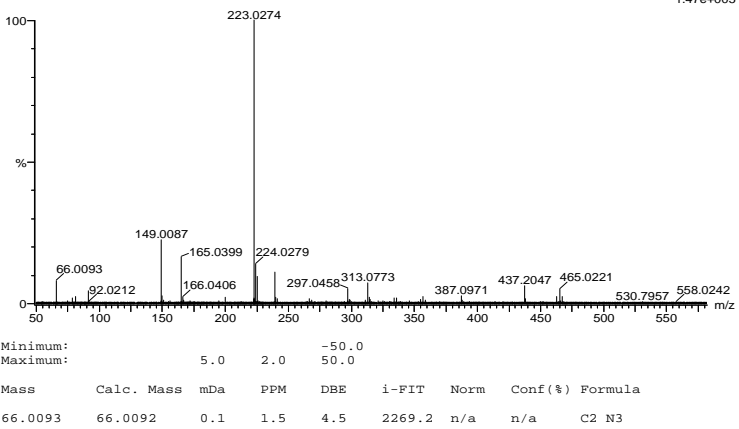
Elements Used:

C: 0-100 H: 0-150 N: 0-10 O: 0-10

svg_20190423_2019_353_2 61 (0.691)AM2 (Ar,35000.0,0.00,0.00); Cm (56.71)

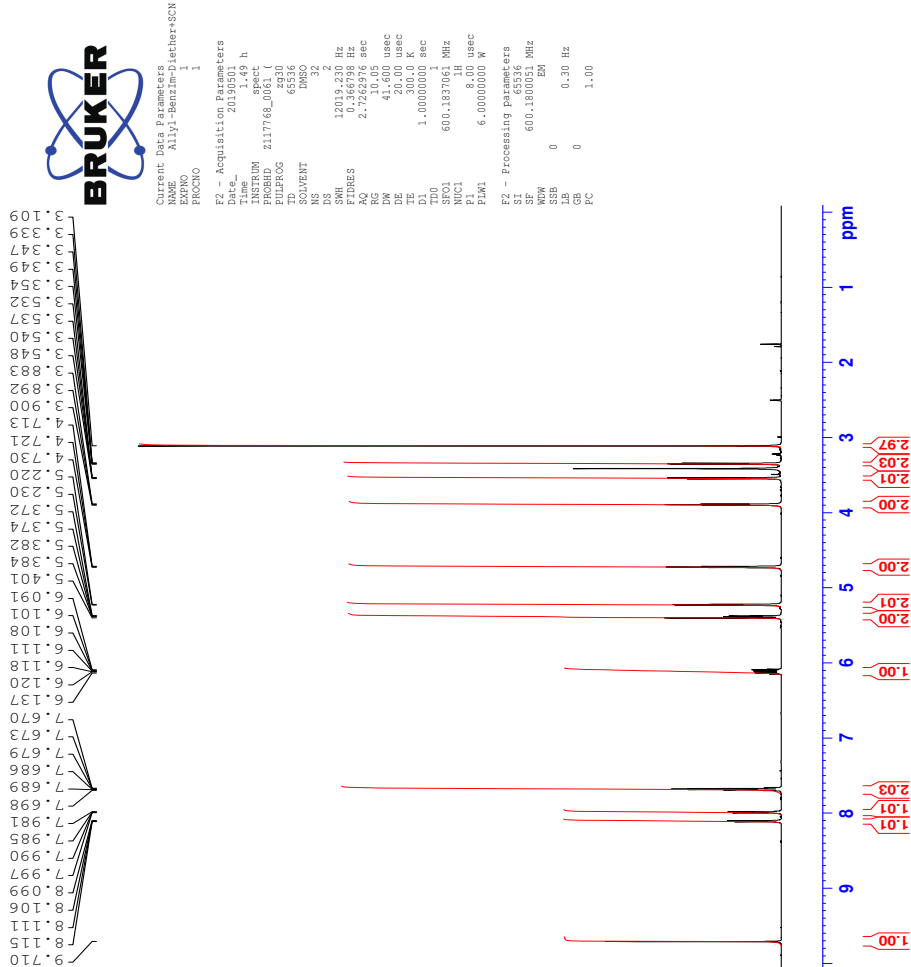
1: TOF MS ES-

1.47e+005

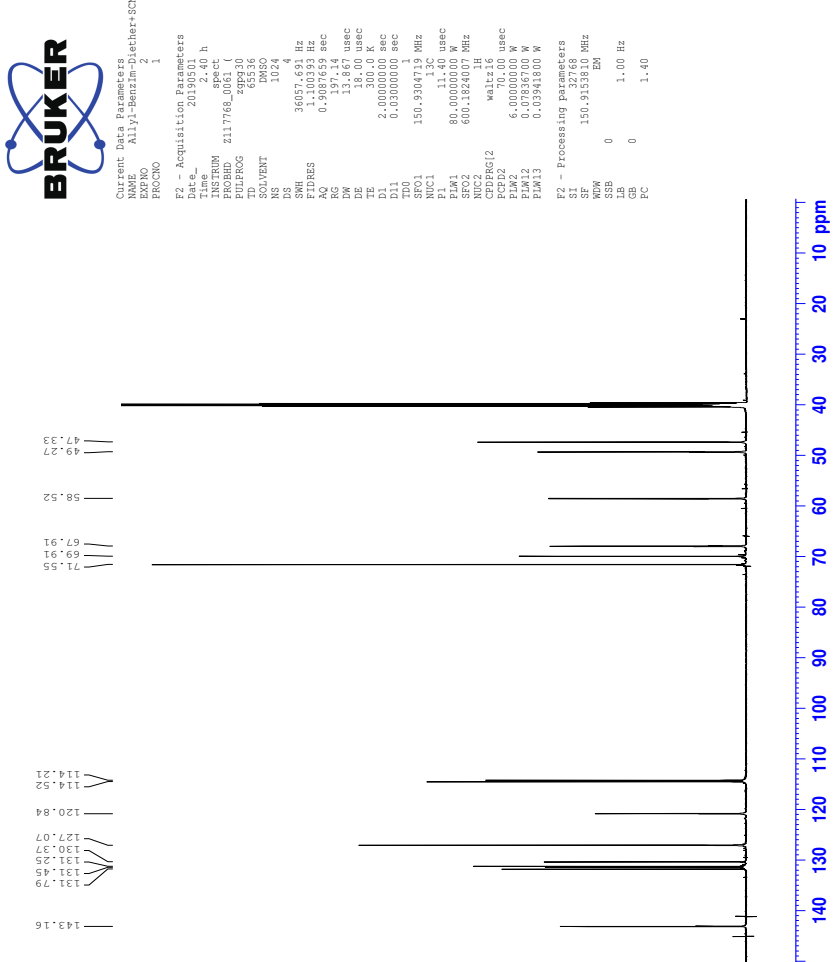


43 Spectra of IL 16d

43.1 ^1H -NMR spectrum of IL 16d

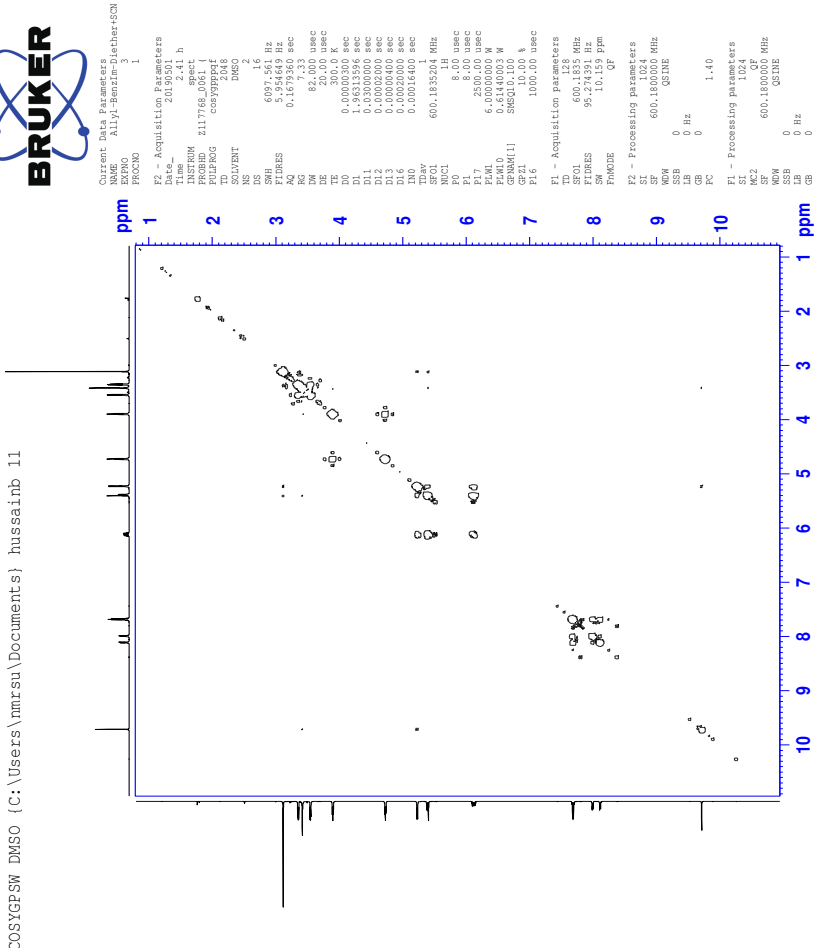


43.2 ^{13}C -NMR spectrum of IL 16d

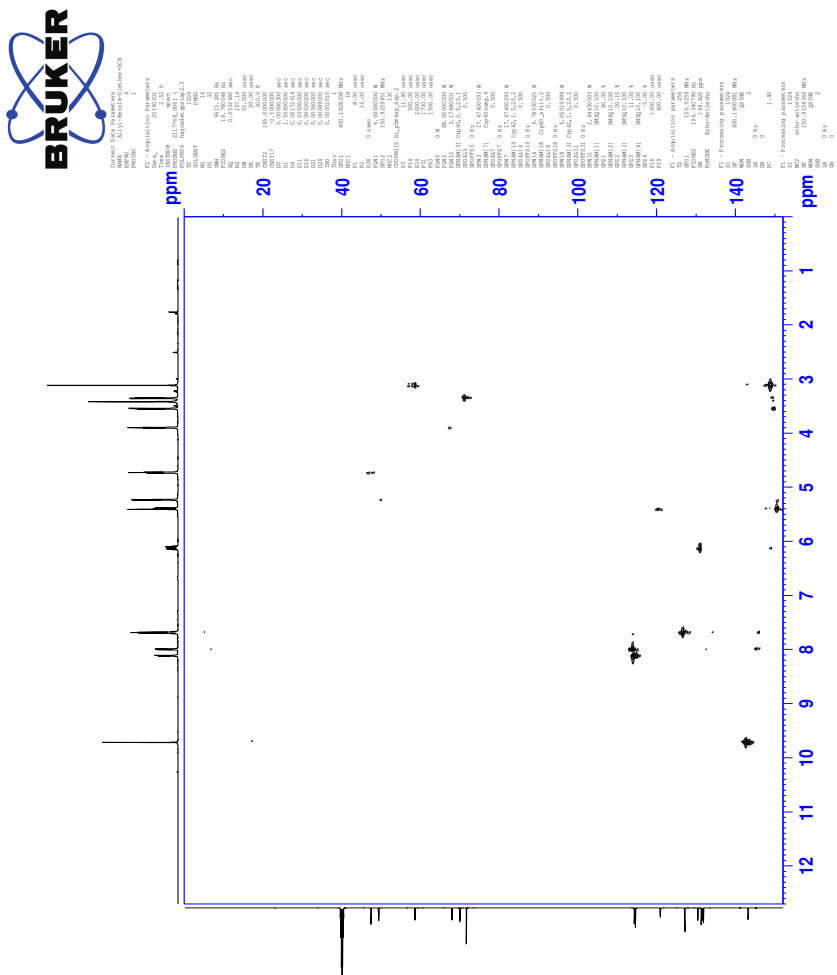


CCL

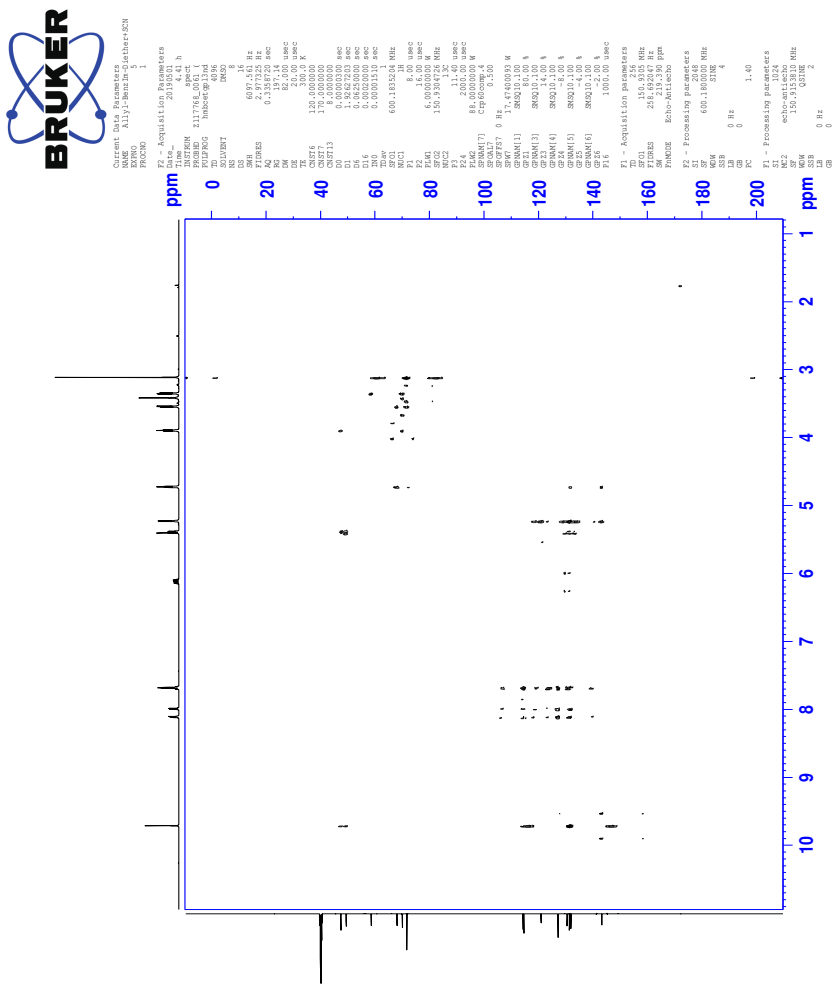
43.3 COSY-spectrum of IL 16d



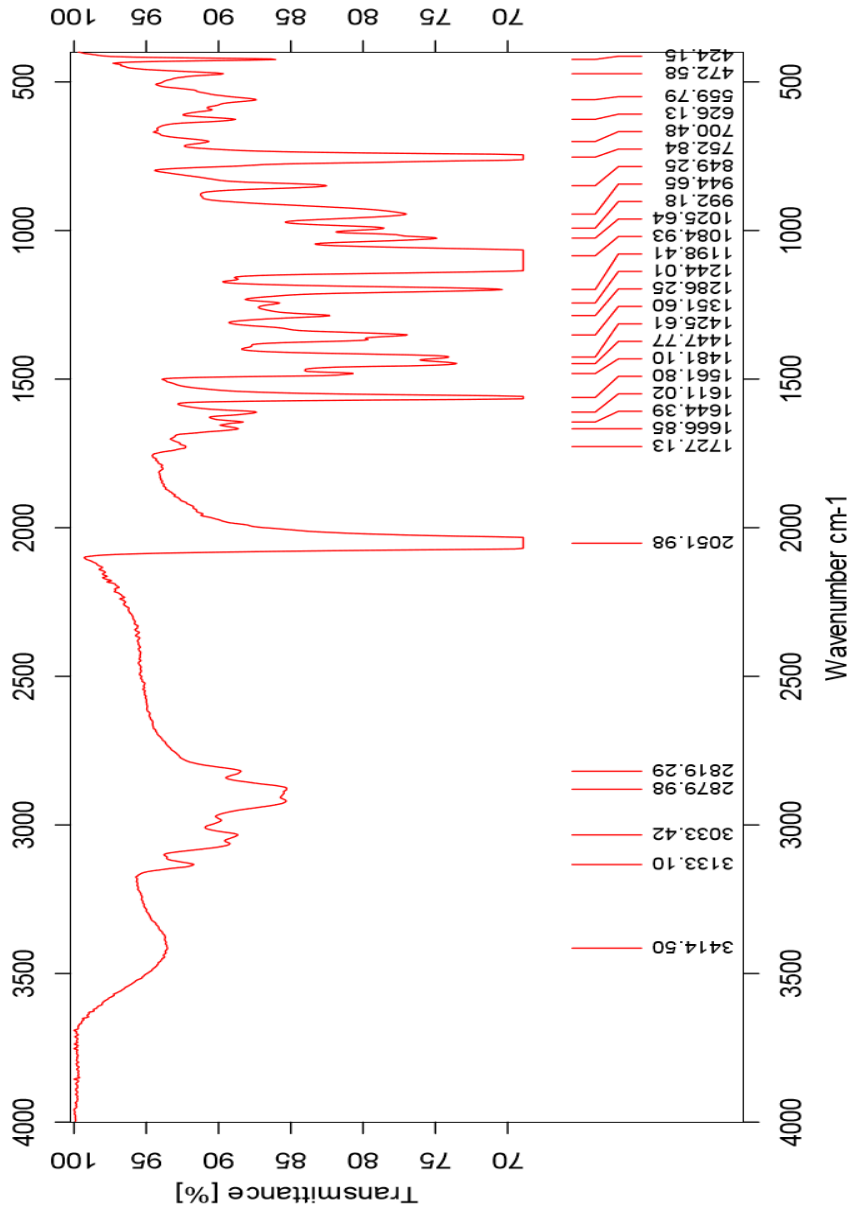
43.4 HSQC-spectrum of IL 16d



43.5 HMBC-spectrum of IL 16d



43.6 IR-spectrum of IL 16d



43.7 HR-MS positive mode spectrum of IL 16d

Elemental Composition Report

Page 1

Single Mass Analysis

Tolerance = 5.0 PPM / DBE: min = -50.0, max = 50.0

Element prediction: Off

Number of isotope peaks used for i-FIT = 3

Monoisotopic Mass, Even Electron Ions

1750 formula(e) evaluated with 3 results within limits (all results (up to 1000) for each mass)

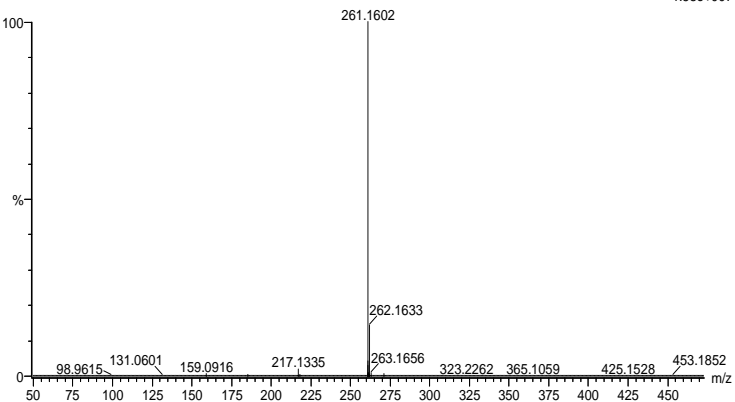
Elements Used:

C: 0-100 H: 0-150 N: 0-10 O: 0-10 Na: 0-1

2019-396 98 (1.814) AM2 (Ar,35000.0,0.00,0.00); Cm (98:103)

1: TOF MS ES+

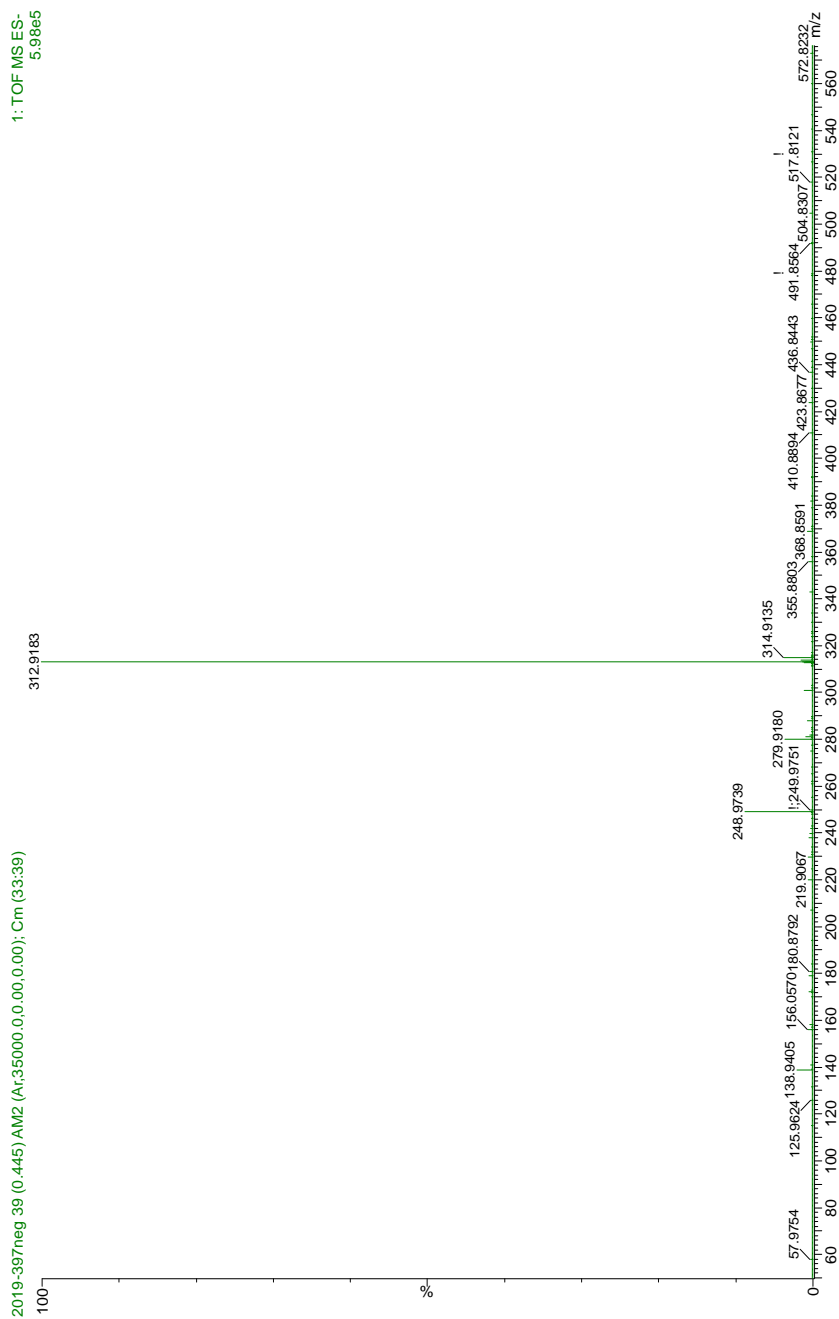
1.58e+007



Minimum: -50.0
Maximum: 5.0 5.0 50.0

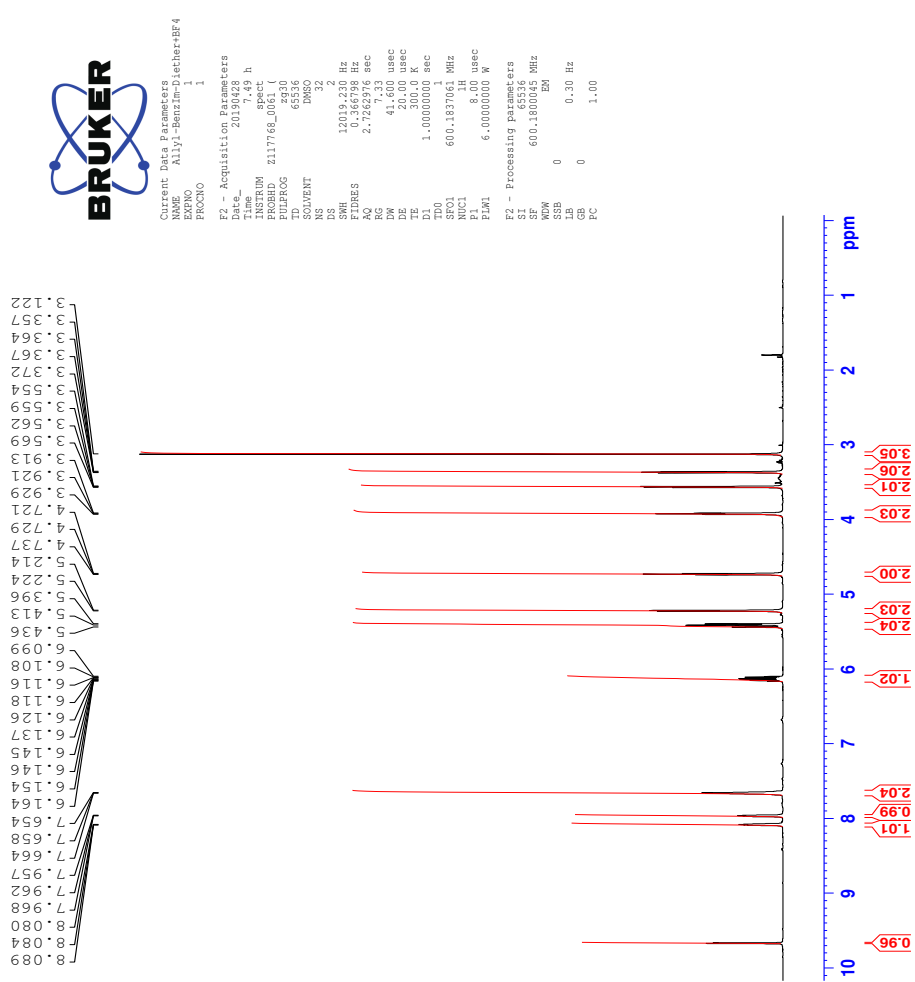
Mass	Calc. Mass	mDa	PPM	DBE	i-FIT	Norm	Conf (%)	Formula
261.1602	261.1603	-0.1	-0.4	6.5	1817.1	0.000	99.98	C15 H21 N2 O2
	261.1597	0.5	1.9	-9.5	1826.8	9.753	0.01	C H26 N4 O9 Na
	261.1611	-0.9	-3.4	-4.5	1826.2	9.095	0.01	C2 H22 N8 O5 Na

43.8 HR-MS negative mode spectrum of IL 16d

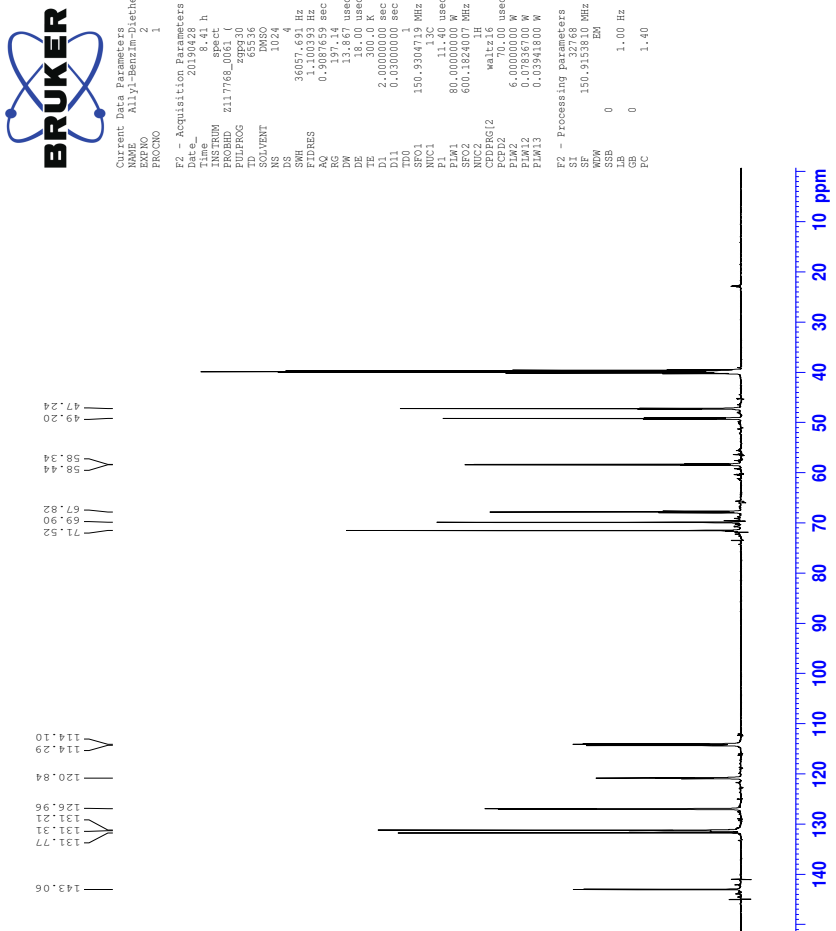


44 Spectra of IL 16e

44.1 ^1H -NMR spectrum of IL 16e

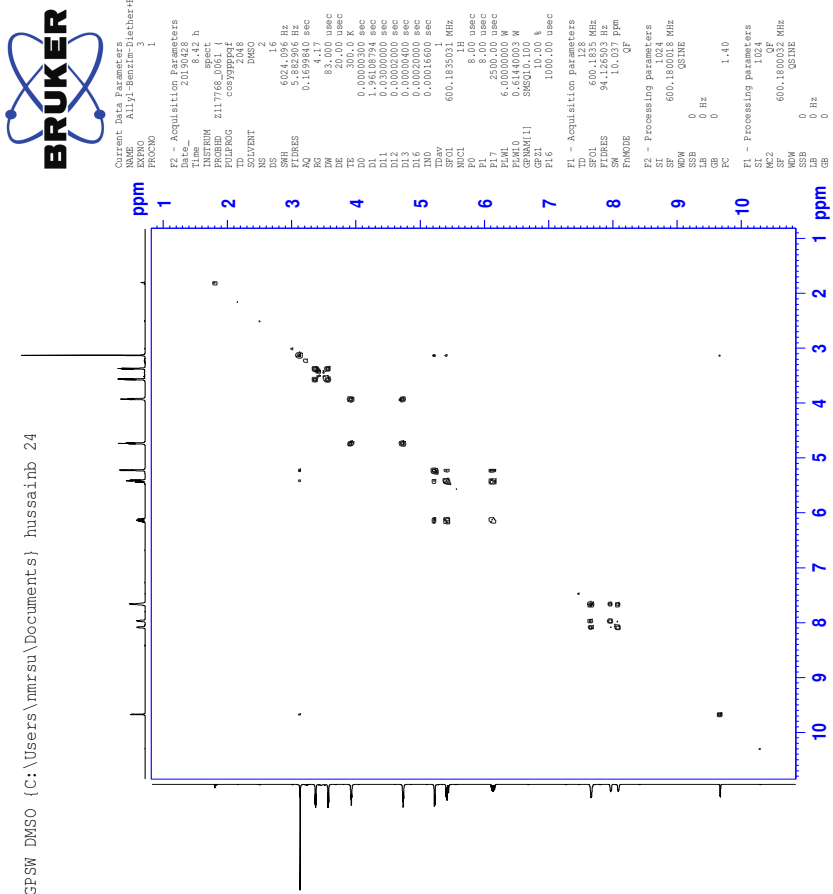


44.2 ^{13}C -NMR spectrum of IL 16e

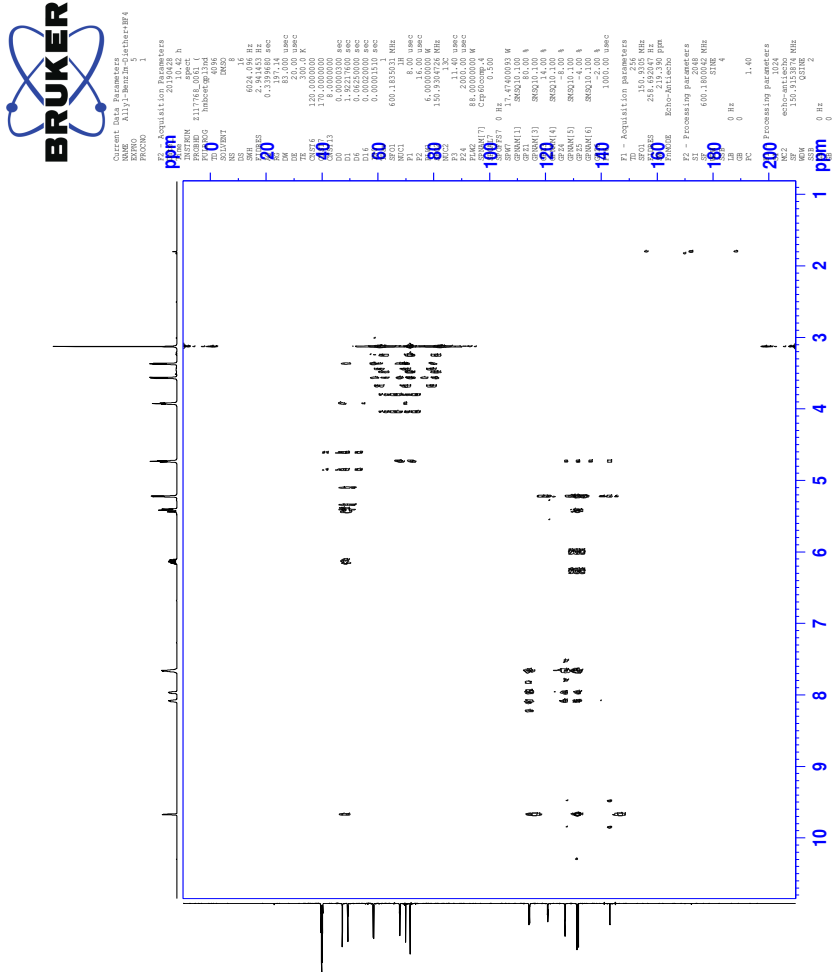


44.3 COSY-spectrum of IL 16e

COSYPSW DMSO { C:\Users\nmrsv\Documents\} hussainb 24

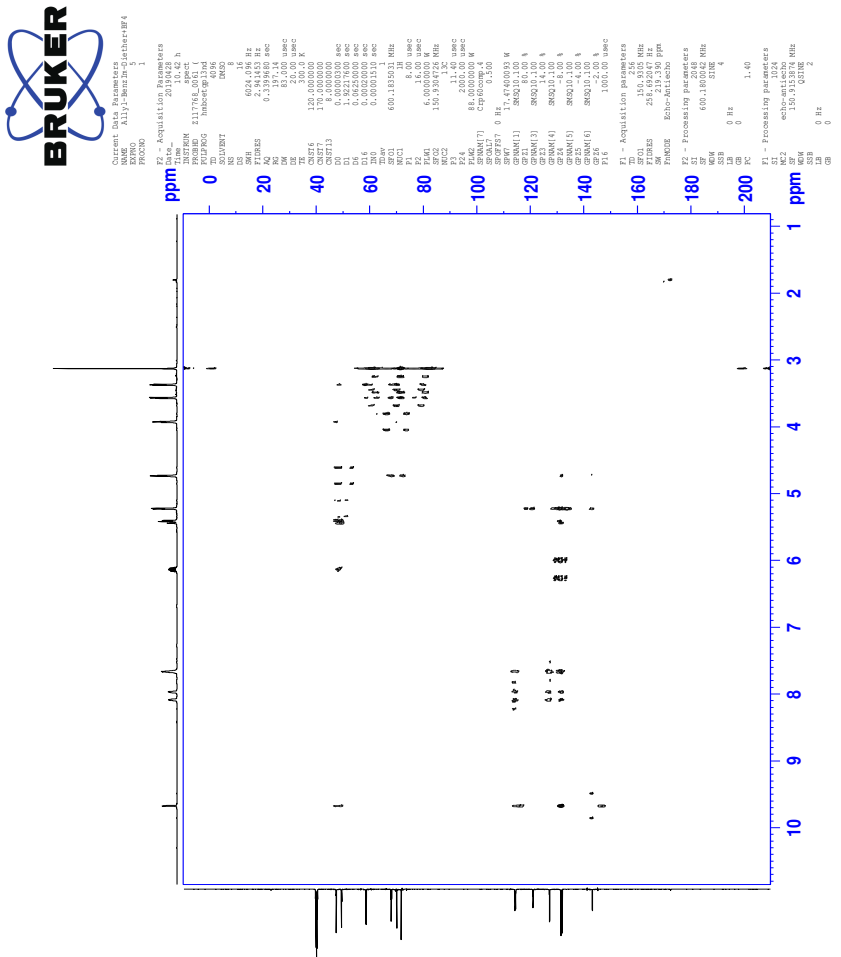


44.4 HSQC-spectrum of IL 16e

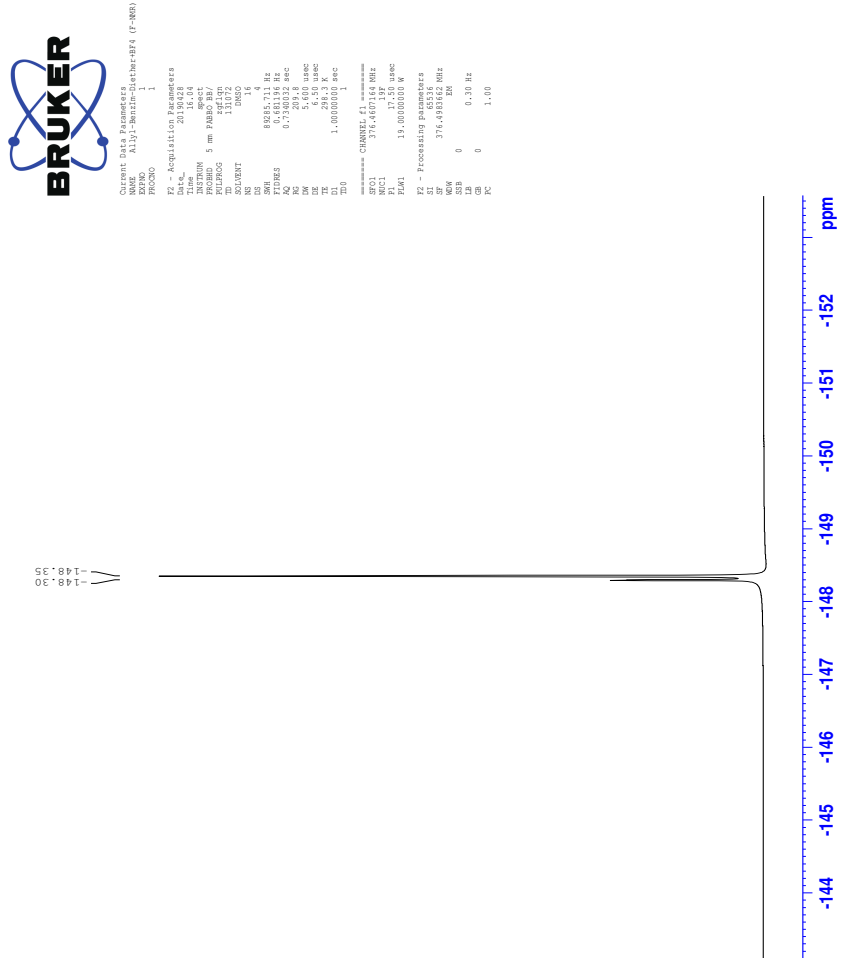


CCLX

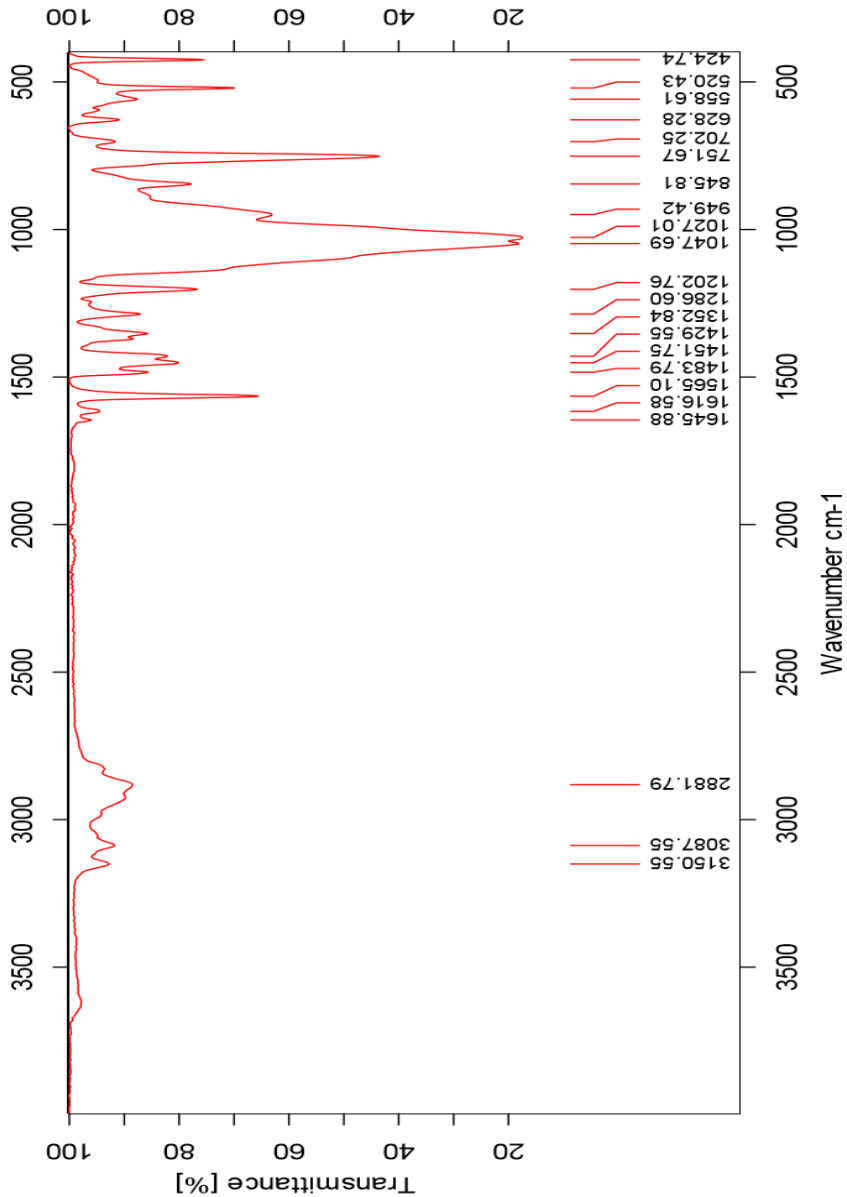
44.5 HMBC-spectrum of IL 16e



44.6 ^{19}F -NMR of IL 16e



44.7 IR-spectrum of IL 16e



44.8 HR-MS positive mode spectrum of IL 16e

Elemental Composition Report

Page 1

Single Mass Analysis

Tolerance = 2.0 PPM / DBE: min = -50.0, max = 50.0

Element prediction: Off

Number of isotope peaks used for i-FIT = 3

Monoisotopic Mass, Even Electron Ions

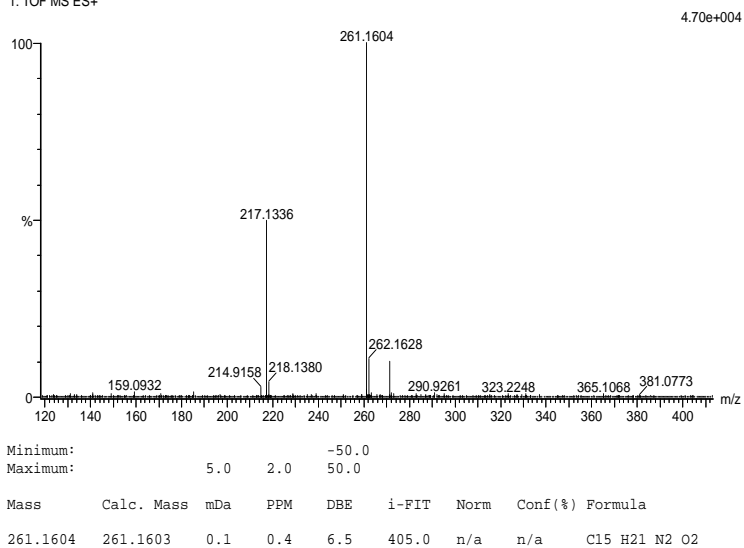
3384 formula(e) evaluated with 1 results within limits (all results (up to 1000) for each mass)

Elements Used:

C: 0-100 H: 0-150 11B: 0-1 N: 0-10 O: 0-10 Na: 0-1

2019-400 11 (0.219) AM2 (Ar,35000.0,0.00,0.00); Cm (11)

1: TOF MS ES+



44.9 HR-MS negative mode spectrum of IL 16e

Elemental Composition Report

Page 1

Single Mass Analysis

Tolerance = 10.0 PPM / DBE: min = -50.0, max = 50.0

Element prediction: Off

Number of isotope peaks used for i-FIT = 3

Monoisotopic Mass, Even Electron Ions

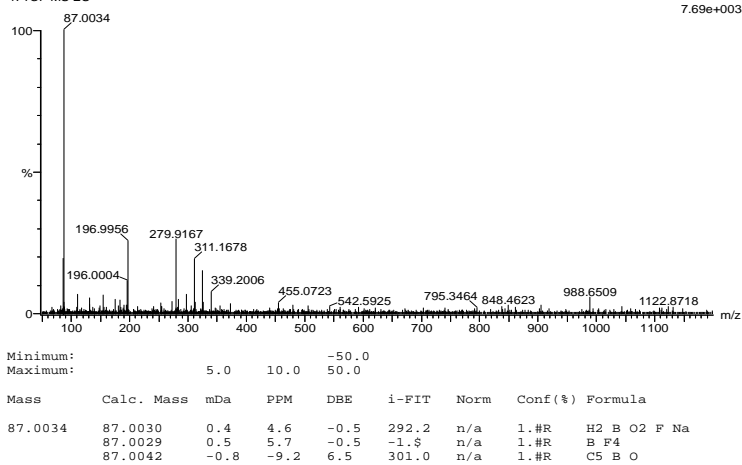
454 formula(e) evaluated with 3 results within limits (all results (up to 1000) for each mass)

Elements Used:

C: 0-100 H: 0-150 B: 0-2 N: 0-10 O: 0-10 F: 0-7 Na: 0-1

2019-405neg.30 (0.341) AM2 (Ar,35000.0,0.00,0.00); Cm (29:30)

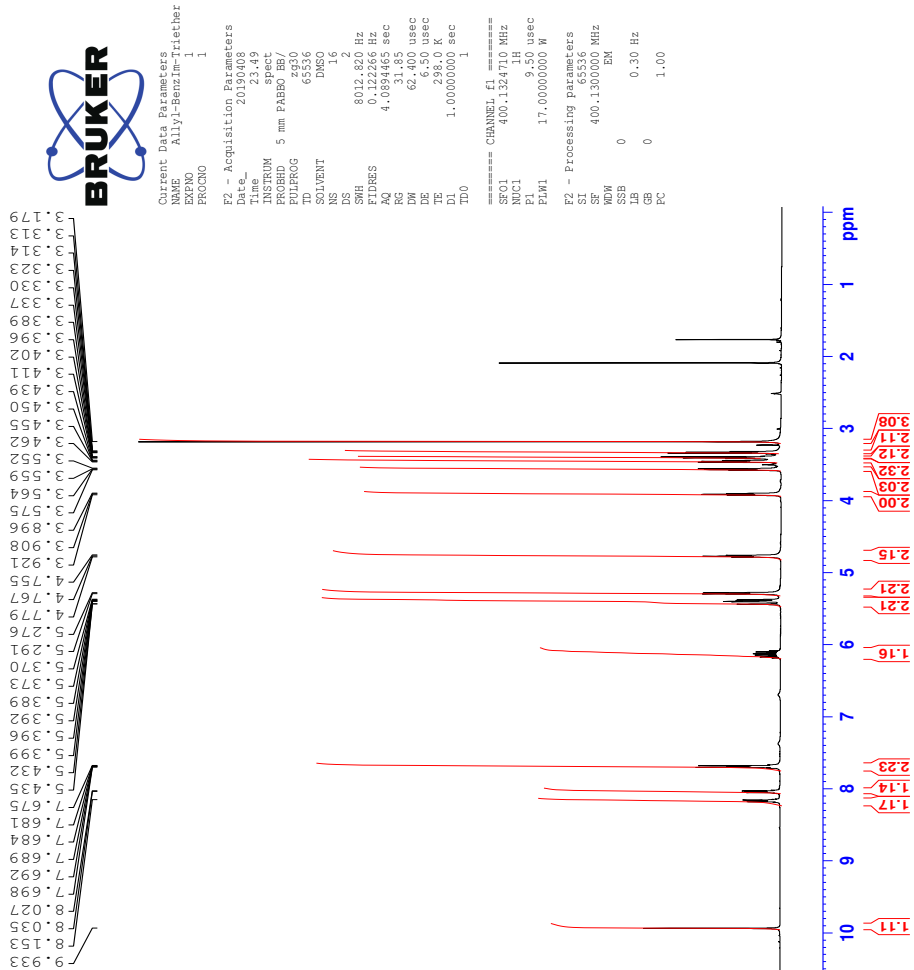
1: TOF MS ES-



Minimum: 5.0 Maximum: 50.0

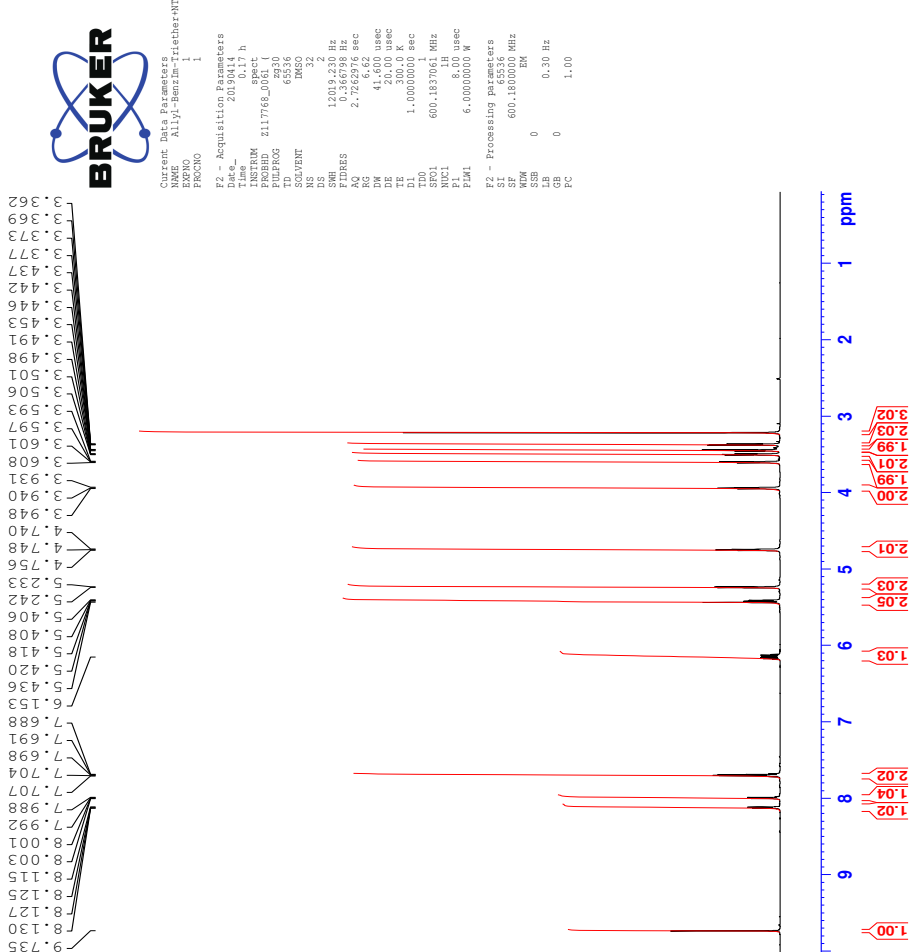
Mass	Calc. Mass	mDa	PPM	DBE	i-FIT	Norm	Conf (%)	Formula
87.0034	87.0030	0.4	4.6	-0.5	292.2	n/a	1.#R	H2 B O2 F Na
	87.0029	0.5	5.7	-0.5	-1.8	n/a	1.#R	B F4
	87.0042	-0.8	-9.2	6.5	301.0	n/a	1.#R	C5 B O

45 $^1\text{H-NMR}$ spectrum of compound 17a

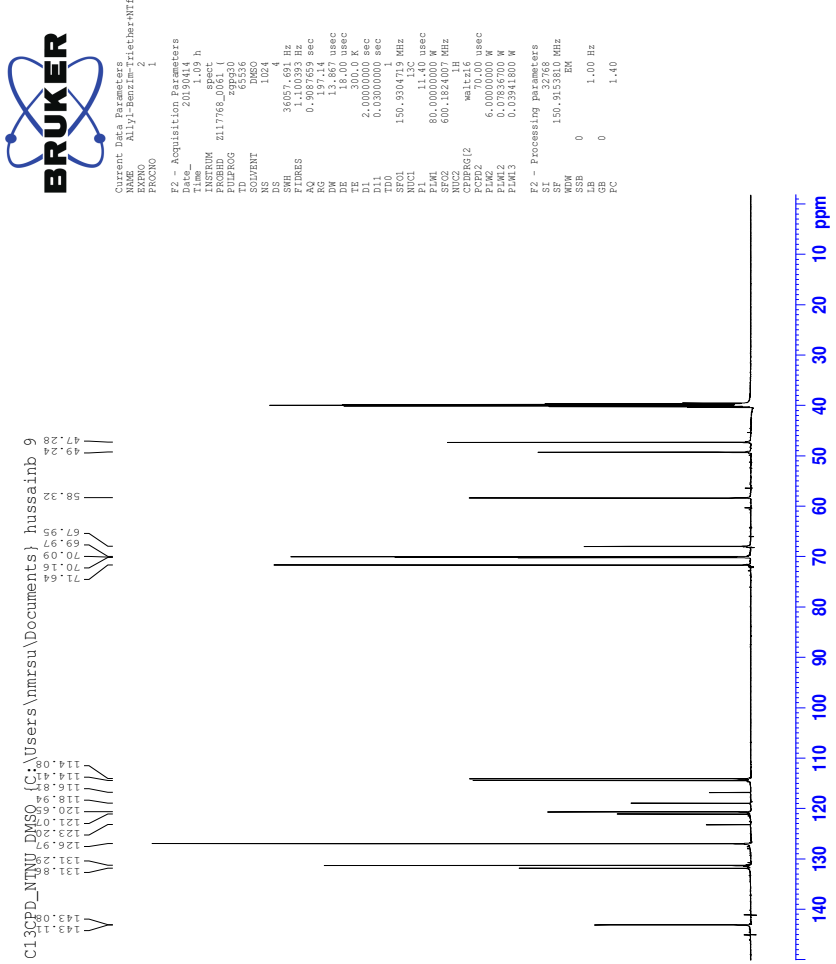


46 Spectra of IL 17b

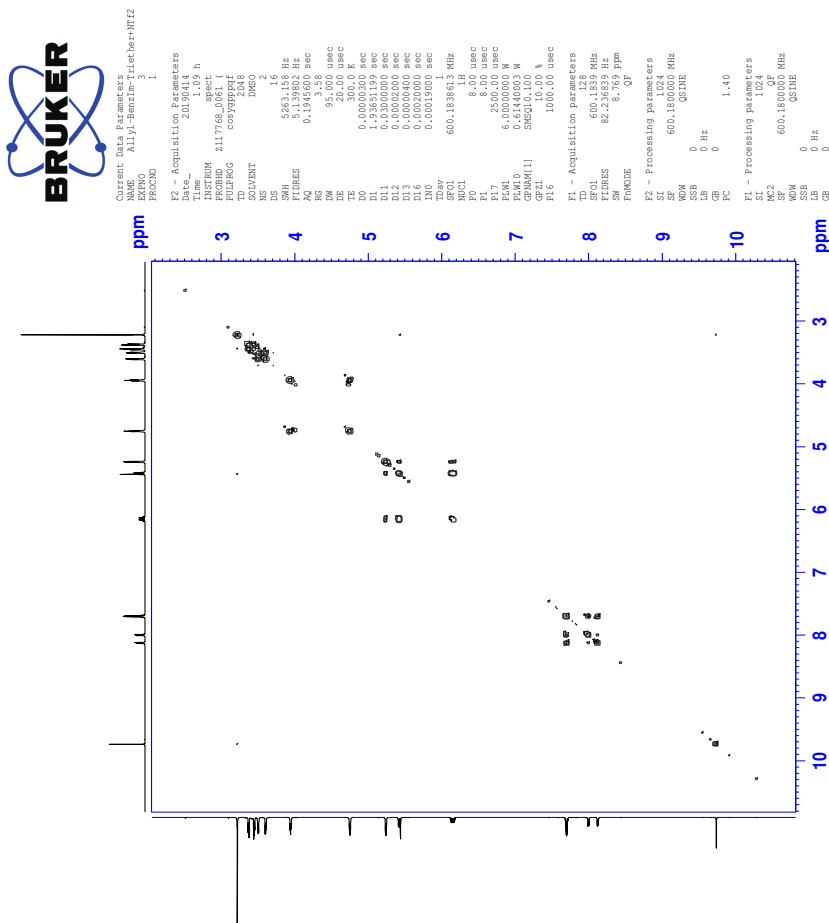
46.1 ^1H -NMR spectrum of IL 17b



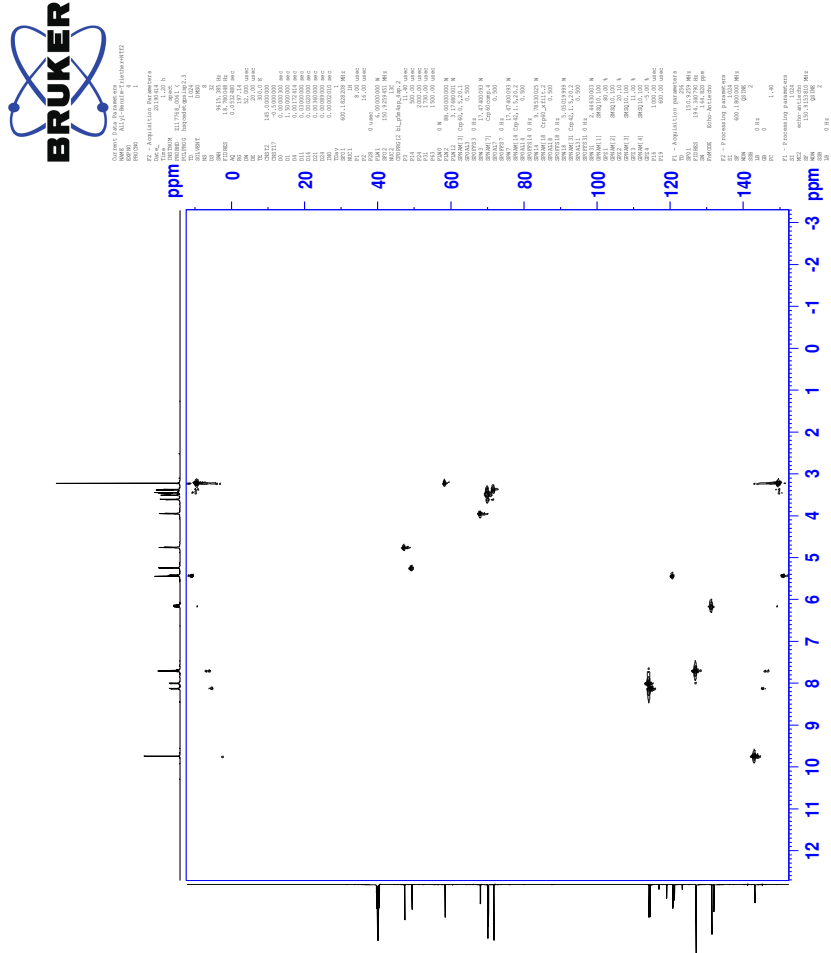
46.2 ^{13}C -NMR spectrum of IL 17b



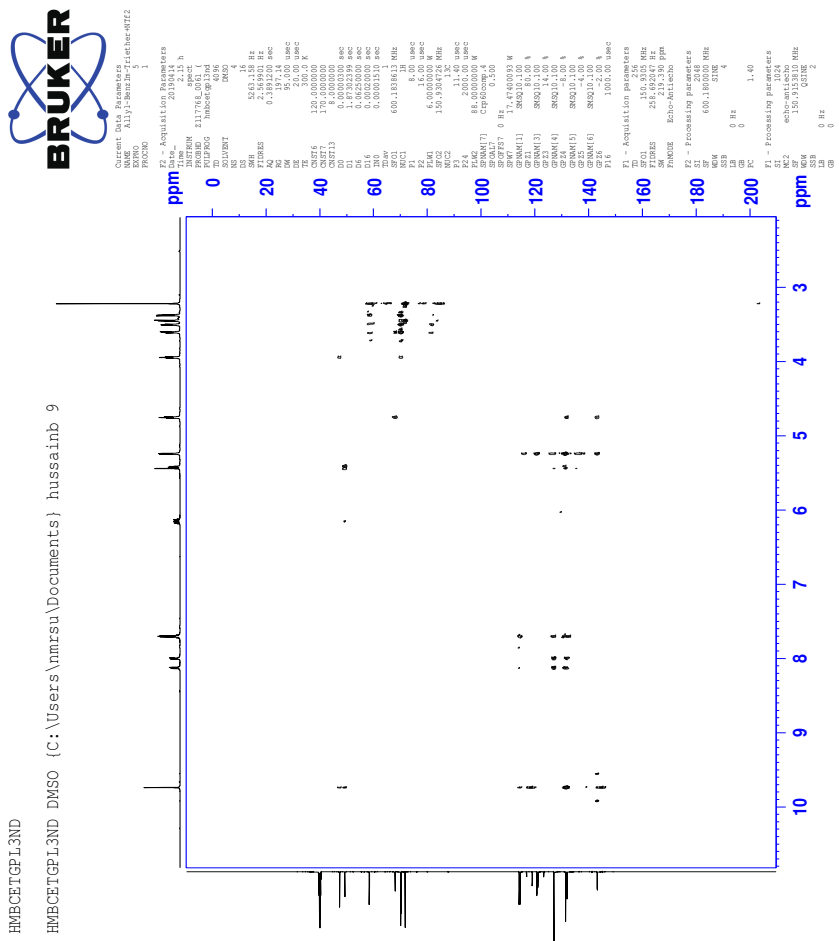
46.3 COSY-spectrum of IL 17b



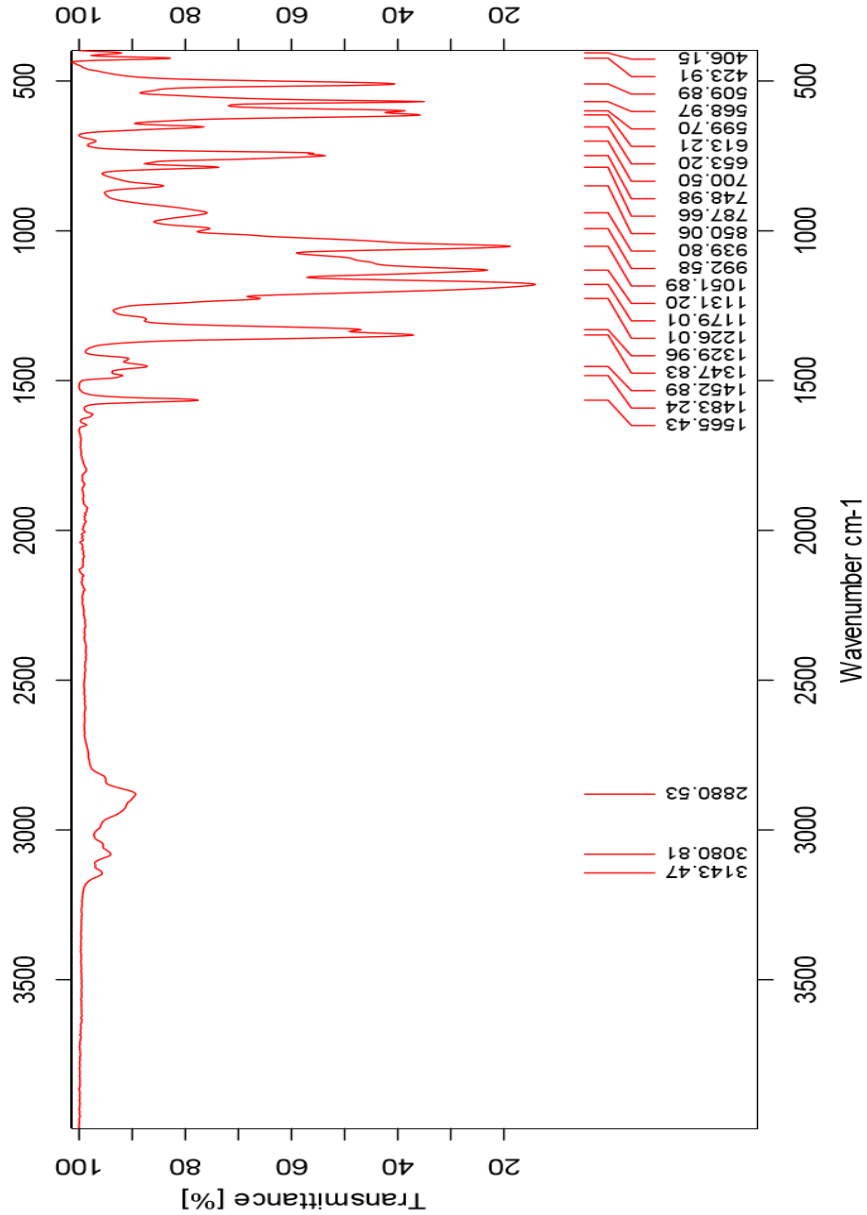
46.4 HSQC-spectrum of IL 17b



46.5 HMBC-spectrum of IL 17b



46.6 IR-spectrum of IL 17b



46.7 HR-MS positive mode spectrum of IL 17b

Elemental Composition Report

Page 1

Single Mass Analysis

Tolerance = 2.0 PPM / DBE: min = -50.0, max = 50.0

Element prediction: Off

Number of isotope peaks used for i-FIT = 3

Monoisotopic Mass, Even Electron Ions

2175 formula(e) evaluated with 3 results within limits (all results (up to 1000) for each mass)

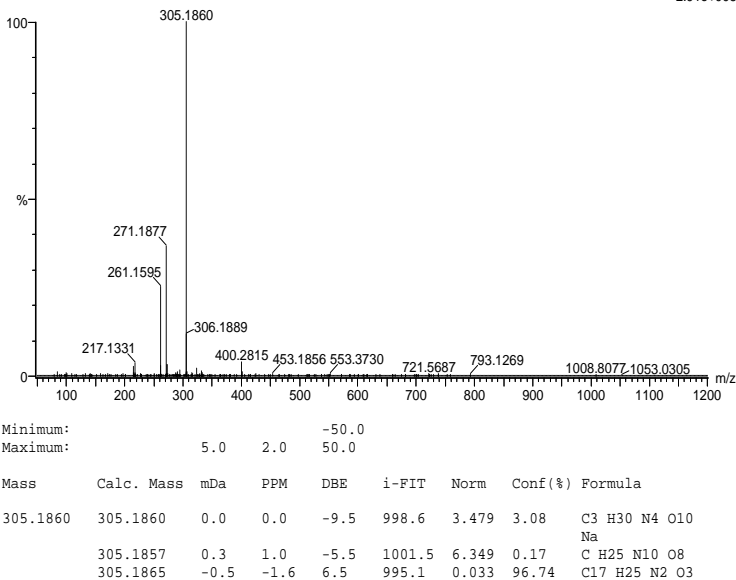
Elements Used:

C: 0-100 H: 0-150 N: 0-10 O: 0-10 Na: 0-1

2019-406 102 (1.894) AM2 (Ar,35000.0,0.00,0.00); Cm (102:103)

1: TOF MS ES+

2.91e+005



46.8 HR-MS negative mode spectrum of IL 17b

Elemental Composition Report

Page 1

Single Mass Analysis

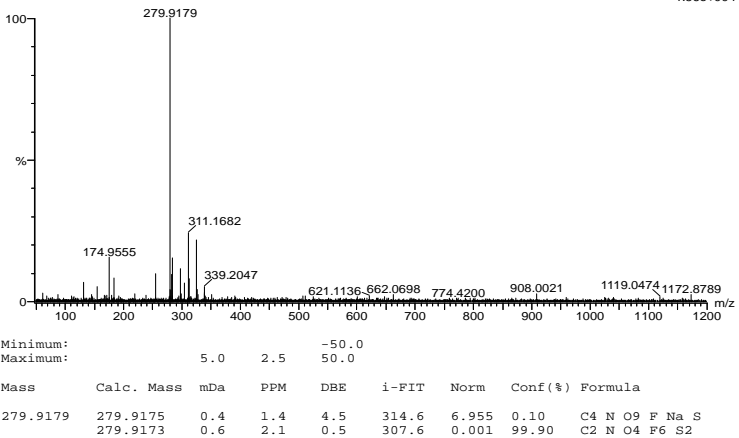
Tolerance = 2.5 PPM / DBE: min = -50.0, max = 50.0
Element prediction: Off
Number of isotope peaks used for i-FIT = 3

Monoisotopic Mass, Even Electron Ions
1958 formula(e) evaluated with 2 results within limits (all results (up to 1000) for each mass)

Elements Used:

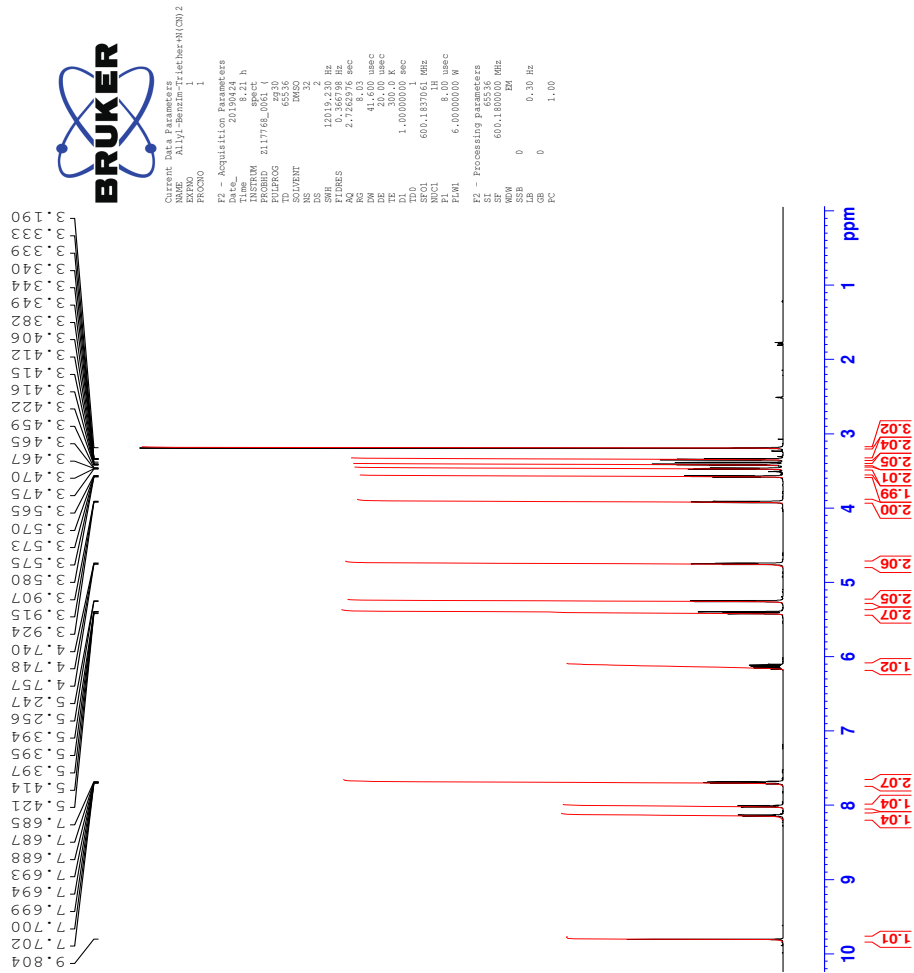
C: 0-5 N: 0-10 O: 0-10 F: 0-7 Na: 0-1 S: 0-3
2019-407neg.20 (0.237) AM2 (Ar,35000.0.00.0.00); Cm (18:20)
1: TOF MS ES-

1.56e+004

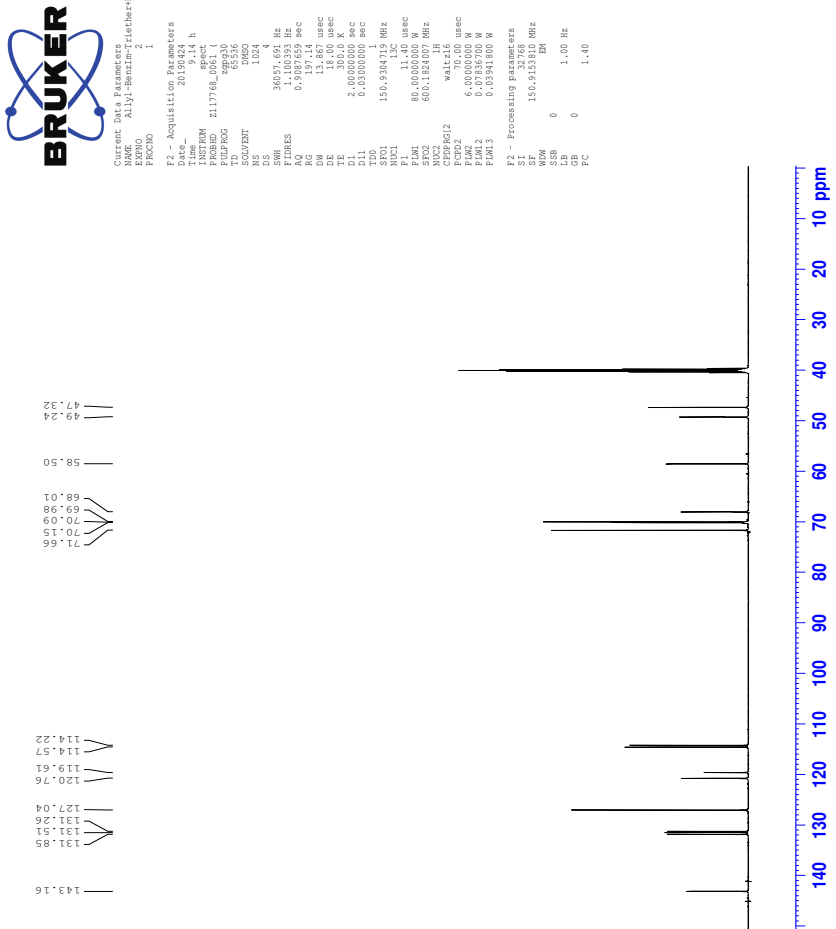


47 Spectra of IL 17c

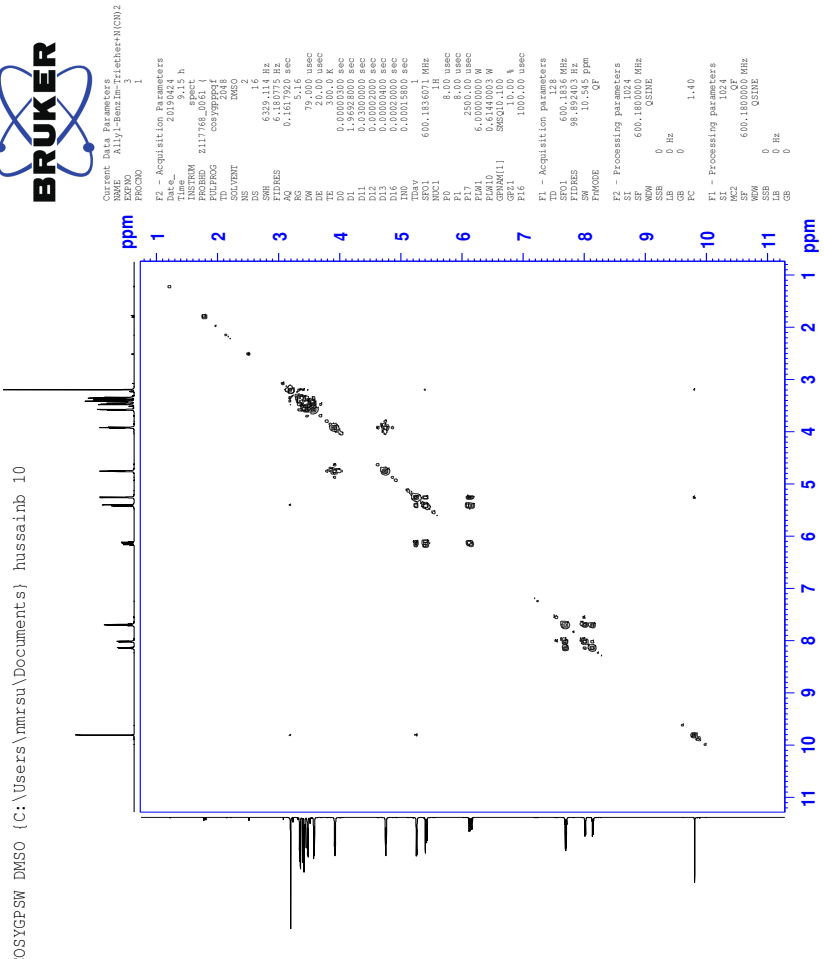
47.1 ^1H -NMR spectrum of IL 17c



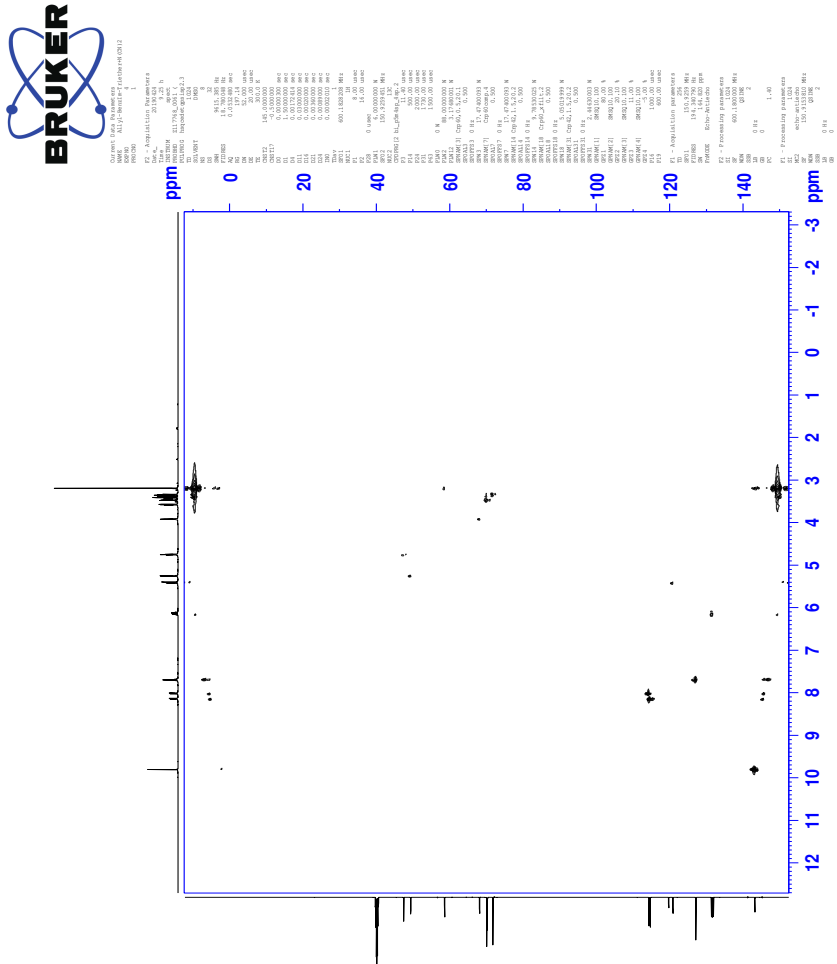
47.2 ^{13}C -NMR spectrum of IL 17c



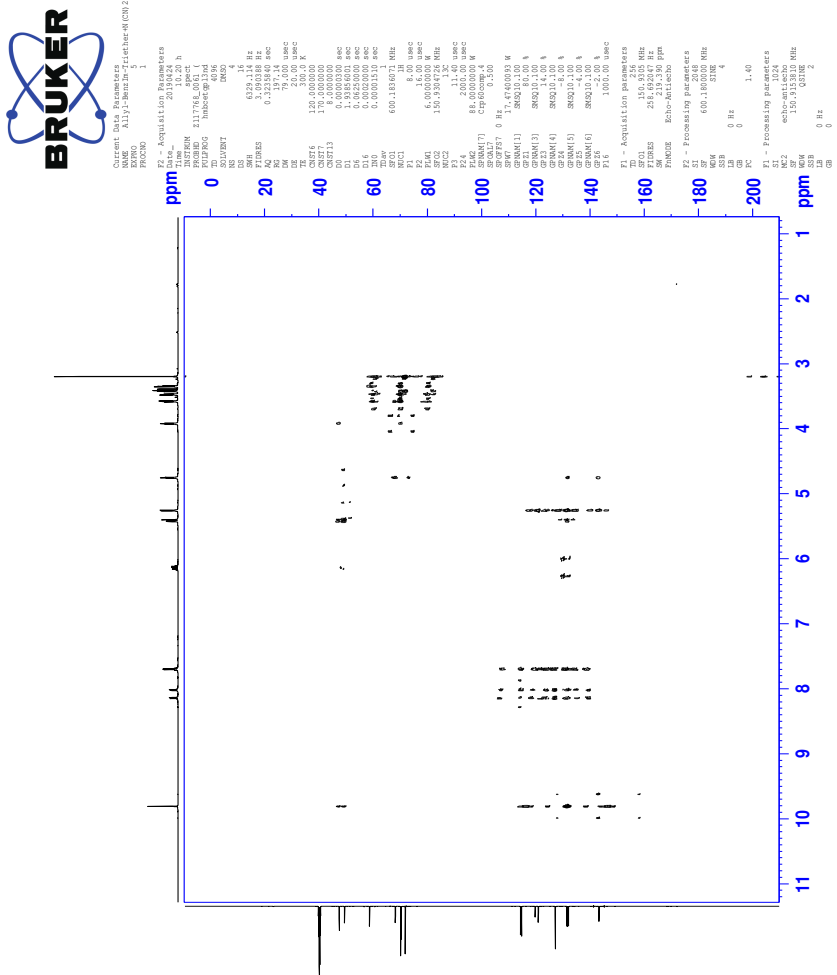
47.3 COSY-spectrum of IL 17c



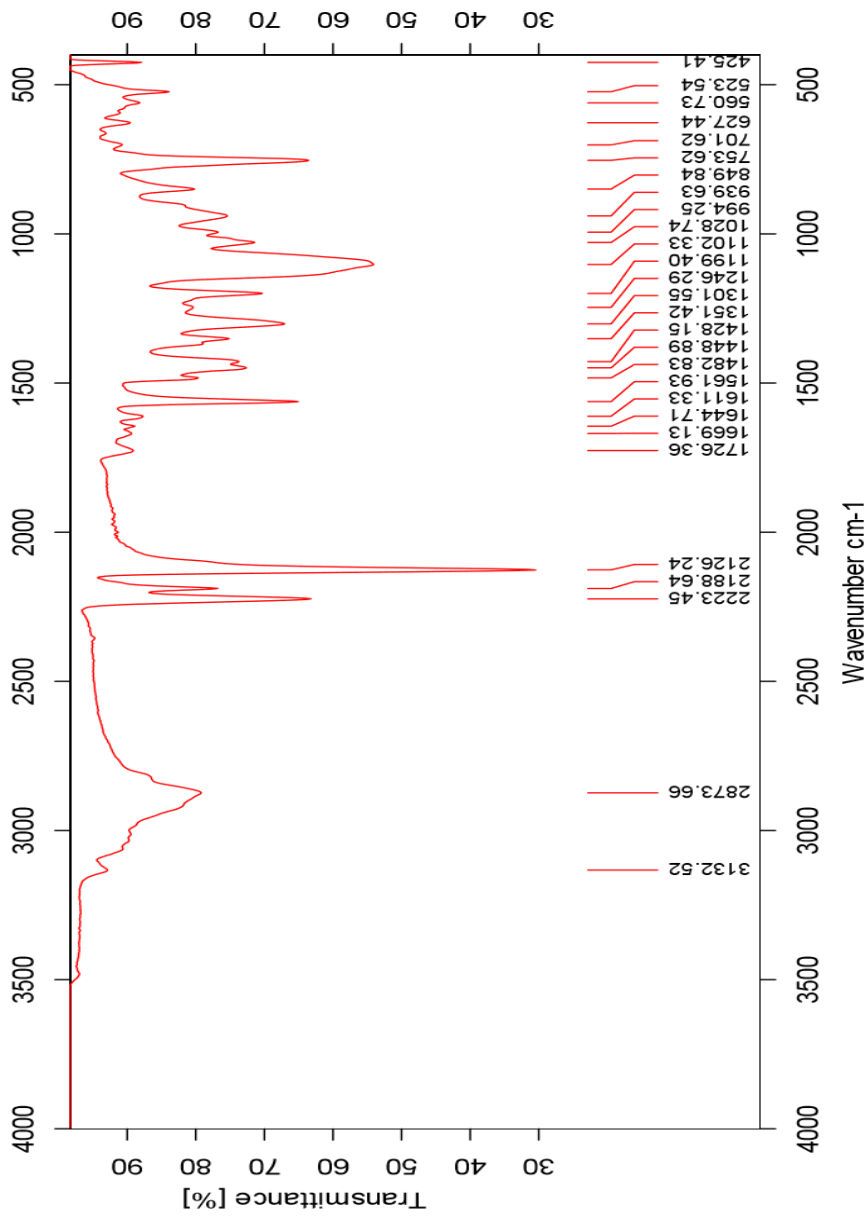
47.4 HSQC-spectrum of IL 17c



47.5 HMBC-spectrum of IL 17c



47.6 IR-spectrum of IL 17c



47.7 HR-MS positive mode spectrum of IL 17c

Elemental Composition Report

Page 1

Single Mass Analysis

Tolerance = 2.0 PPM / DBE: min = -50.0, max = 50.0

Element prediction: Off

Number of isotope peaks used for i-FIT = 3

Monoisotopic Mass, Even Electron Ions

1144 formula(e) evaluated with 2 results within limits (all results (up to 1000) for each mass)

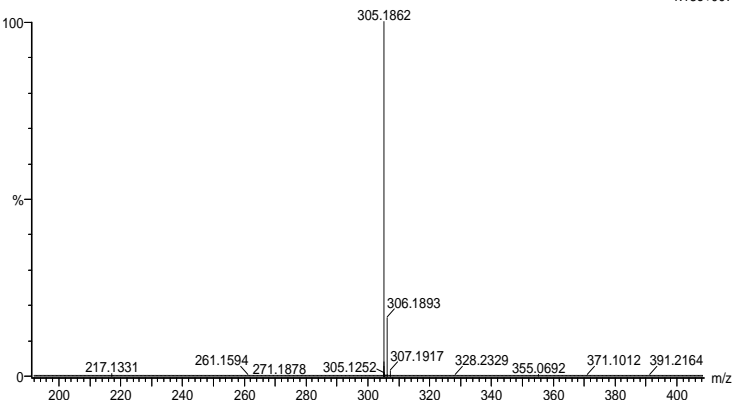
Elements Used:

C: 0-100 H: 0-150 N: 0-10 O: 0-10

svg_20190423_2019_352 18 (0.339) AM2 (Ar,35000.0,0.00,0.00); Crn (10:18)

1: TOF MS ES+

1.13e+007



Minimum: -50.0
Maximum: 5.0 2.0 50.0

Mass	Calc. Mass	mDa	PPM	DBE	i-FIT	Norm	Conf (%)	Formula
305.1862	305.1865	-0.3	-1.0	6.5	1604.3	0.000	100.00	C17 H25 N2 O3
	305.1857	0.5	1.6	-5.5	1615.3	11.015	0.00	C H25 N10 O8

47.8 HR-MS negative mode spectrum of IL 17c

Elemental Composition Report

Page 1

Single Mass Analysis

Tolerance = 2.0 PPM / DBE: min = -50.0, max = 50.0

Element prediction: Off

Number of isotope peaks used for i-FIT = 3

Monoisotopic Mass, Even Electron Ions

41 formula(e) evaluated with 1 results within limits (all results (up to 1000) for each mass)

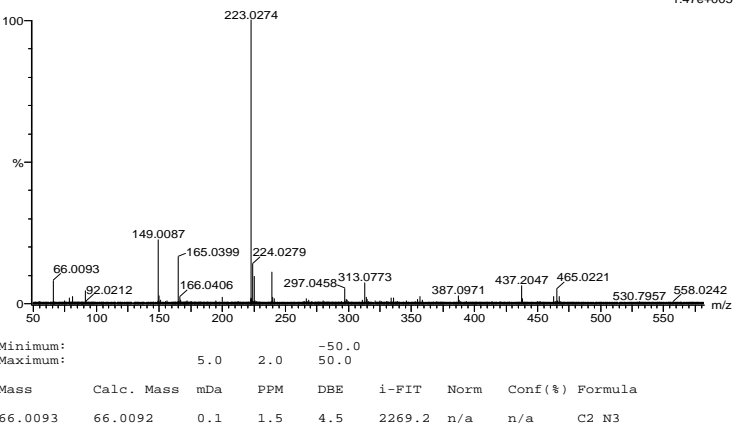
Elements Used:

C: 0-100 H: 0-150 N: 0-10 O: 0-10

svg_20190423_2019_353_2 61 (0.691)AM2 (Ar,35000.0,0.00,0.00); Cm (56.71)

1: TOF MS ES-

1.47e+005

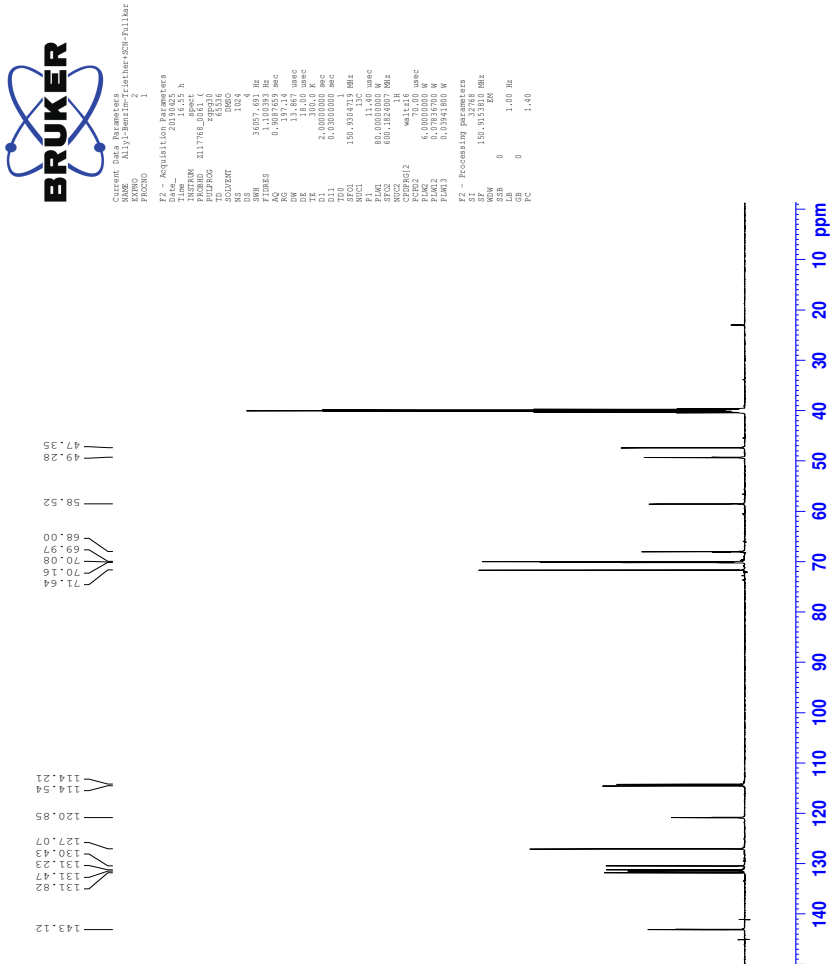


Minimum: 5.0 Maximum: 50.0

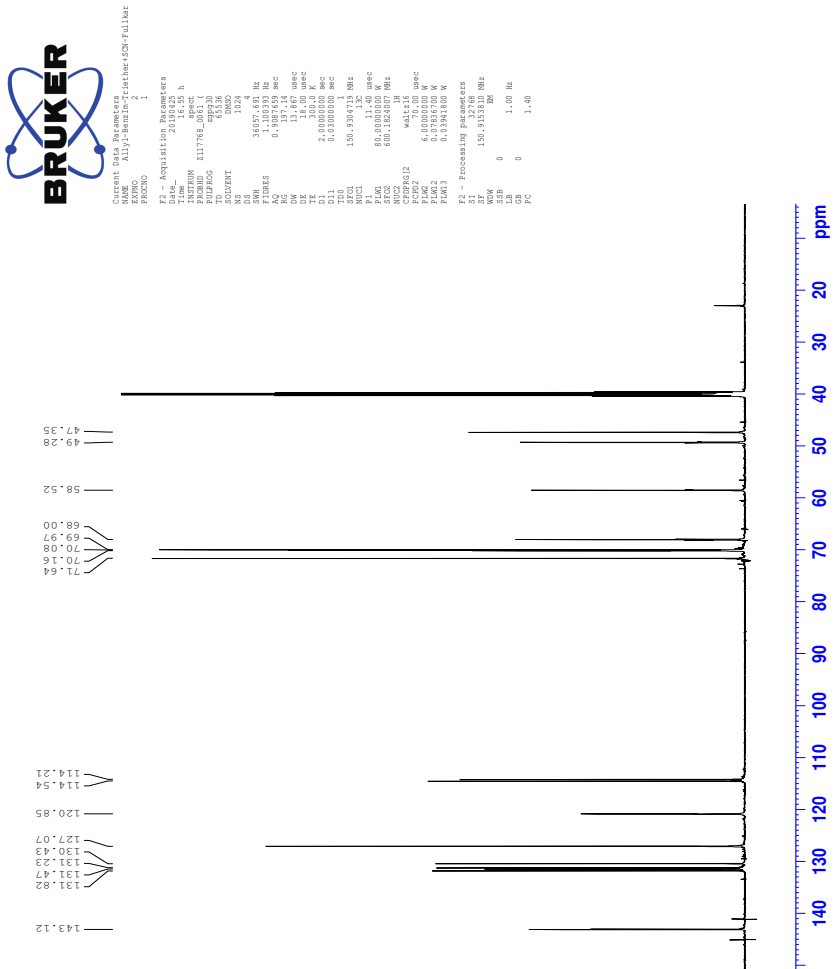
Mass	Calc. Mass	mDa	PPM	DBE	i-FIT	Norm	Conf (%)	Formula
66.0093	66.0092	0.1	1.5	4.5	2269.2	n/a	n/a	C2 N3

48 Spectra of IL 17d

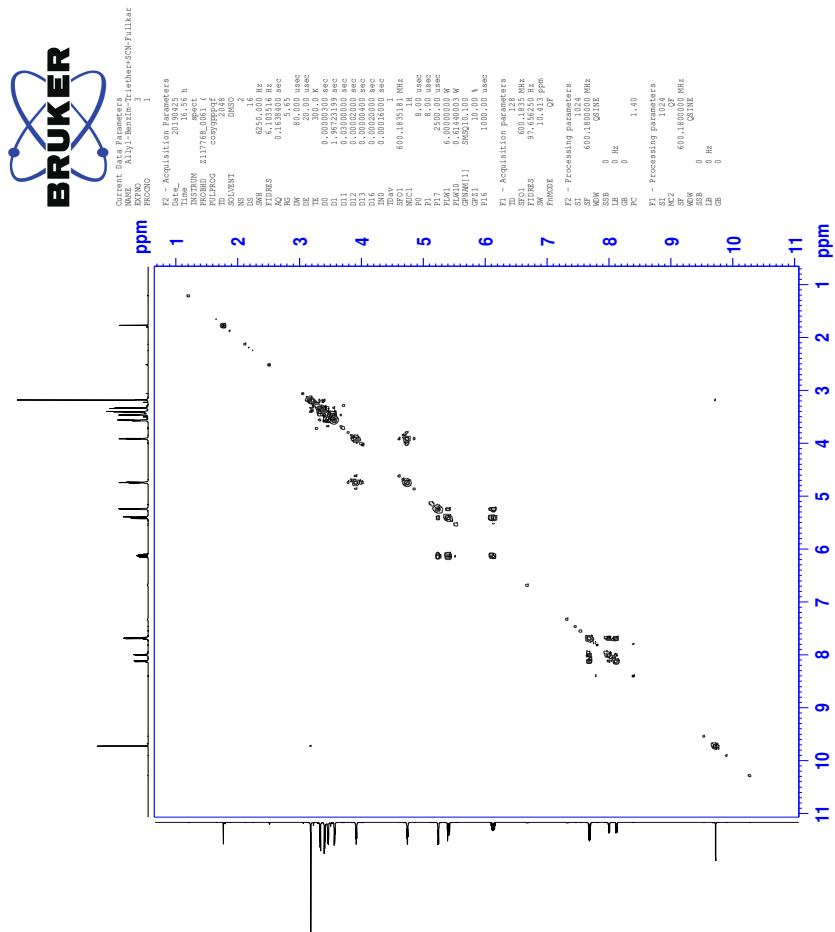
48.1 ^1H -NMR spectrum of IL 17d



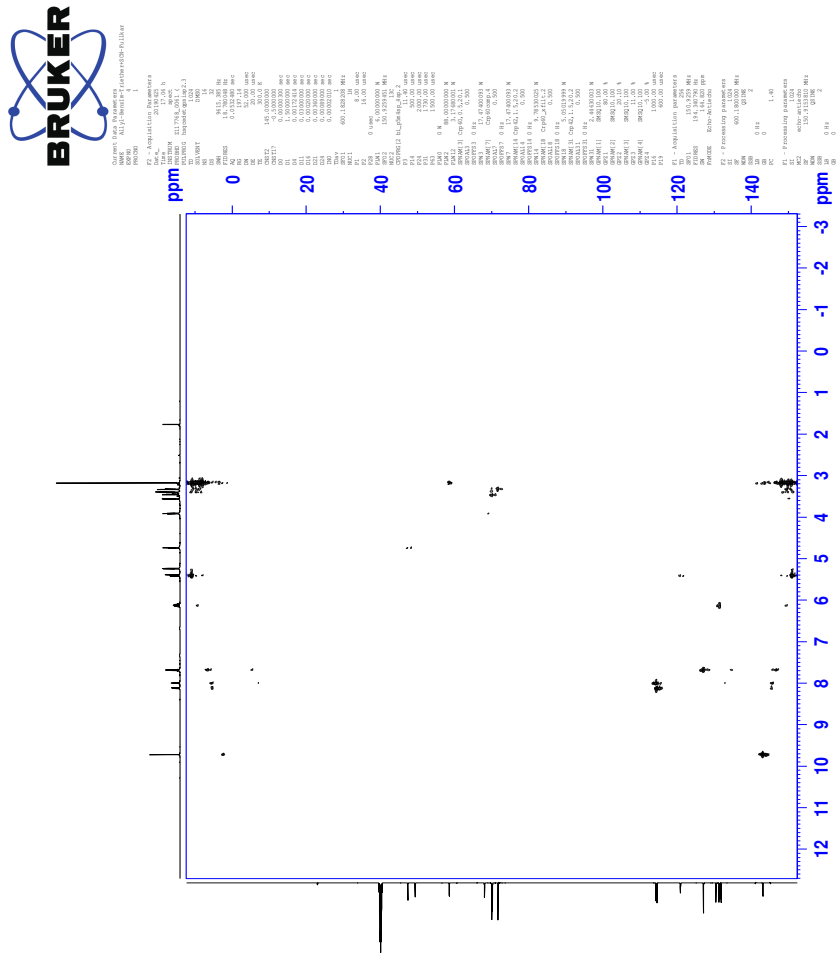
48.2 ^{13}C -NMR spectrum of IL 17d



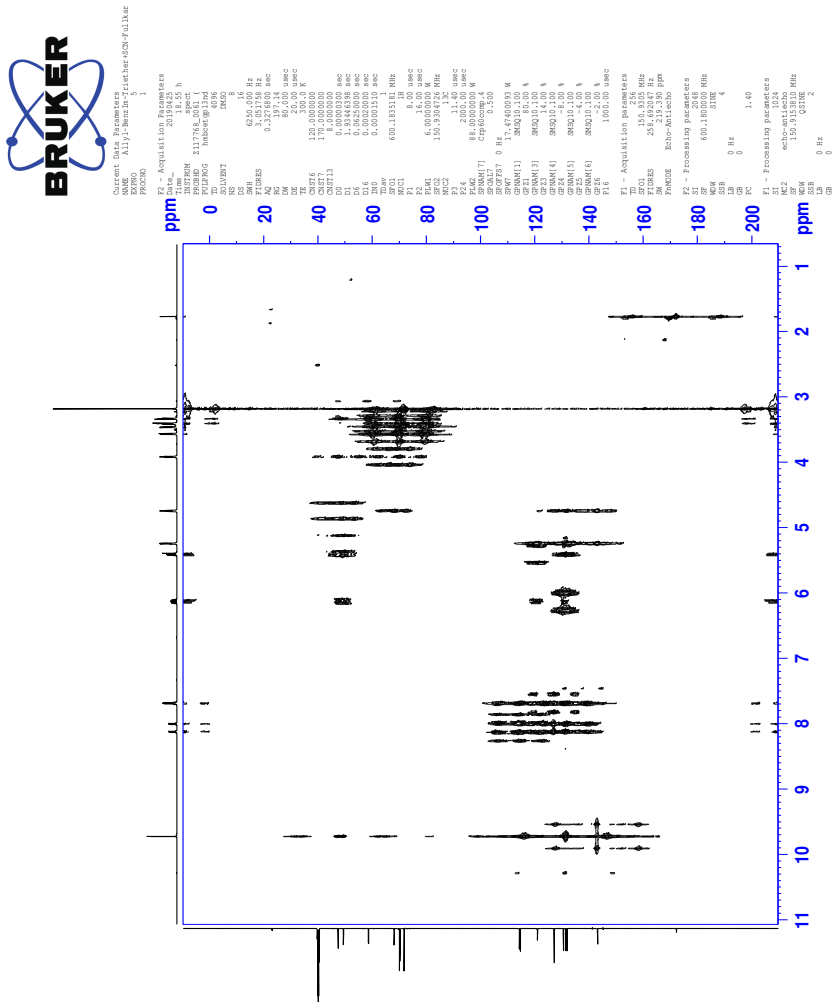
48.3 COSY-spectrum of IL 17d



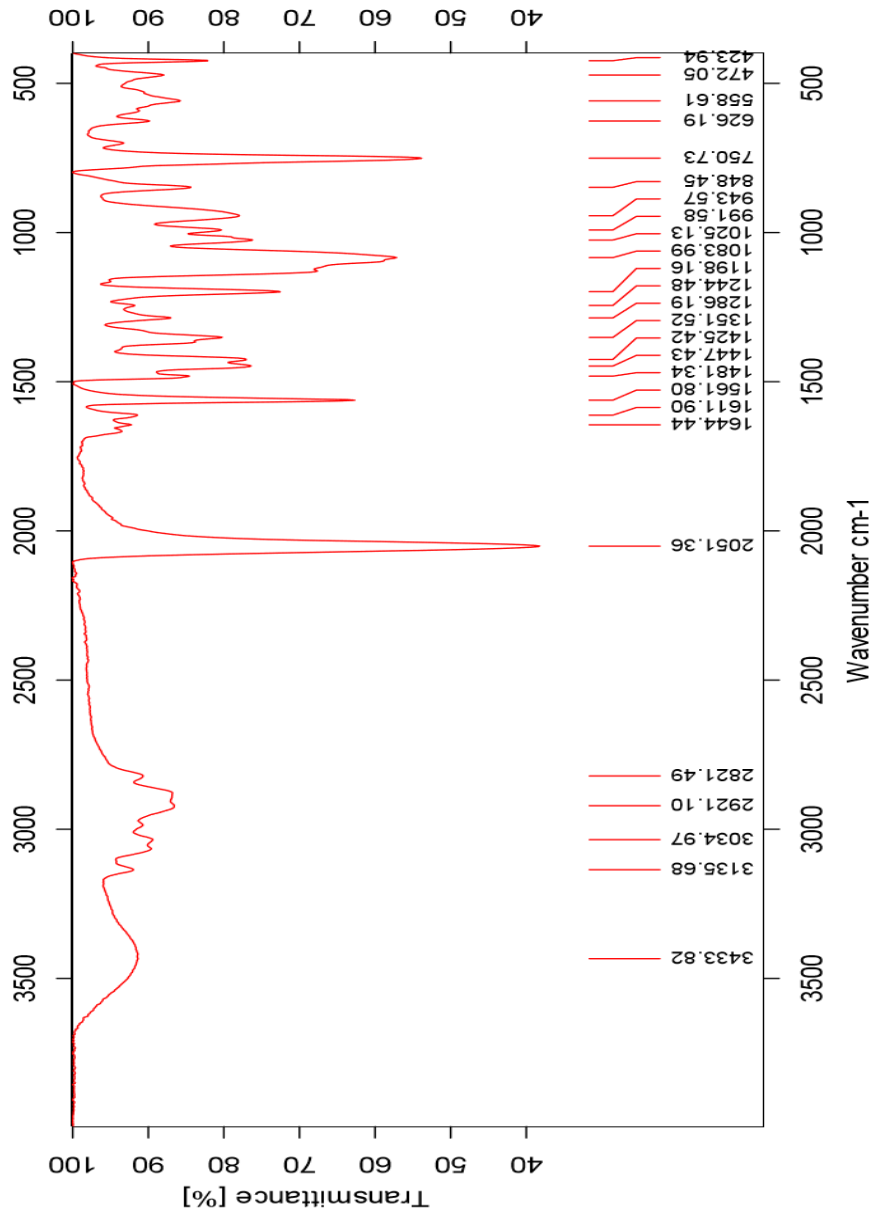
48.4 HSQC-spectrum of IL 17d



48.5 HMBC-spectrum of IL 17d



48.6 IR-spectrum of IL 17d



48.7 HR-MS positive mode spectrum of IL 17d

Elemental Composition Report

Page 1

Single Mass Analysis

Tolerance = 2.0 PPM / DBE: min = -50.0, max = 50.0

Element prediction: Off

Number of isotope peaks used for i-FIT = 3

Monoisotopic Mass, Even Electron Ions

4268 formula(e) evaluated with 3 results within limits (all results (up to 1000) for each mass)

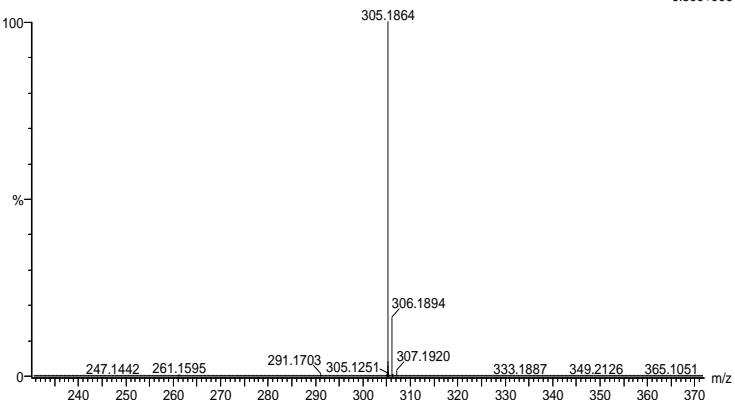
Elements Used:

C: 0-100 H: 0-150 11B: 0-1 N: 0-10 O: 0-10 Na: 0-1

2019-402 16 (0.305) AM2 (Ar,35000.0,0.00,0.00); Cm (12:16)

1: TOF MS ES+

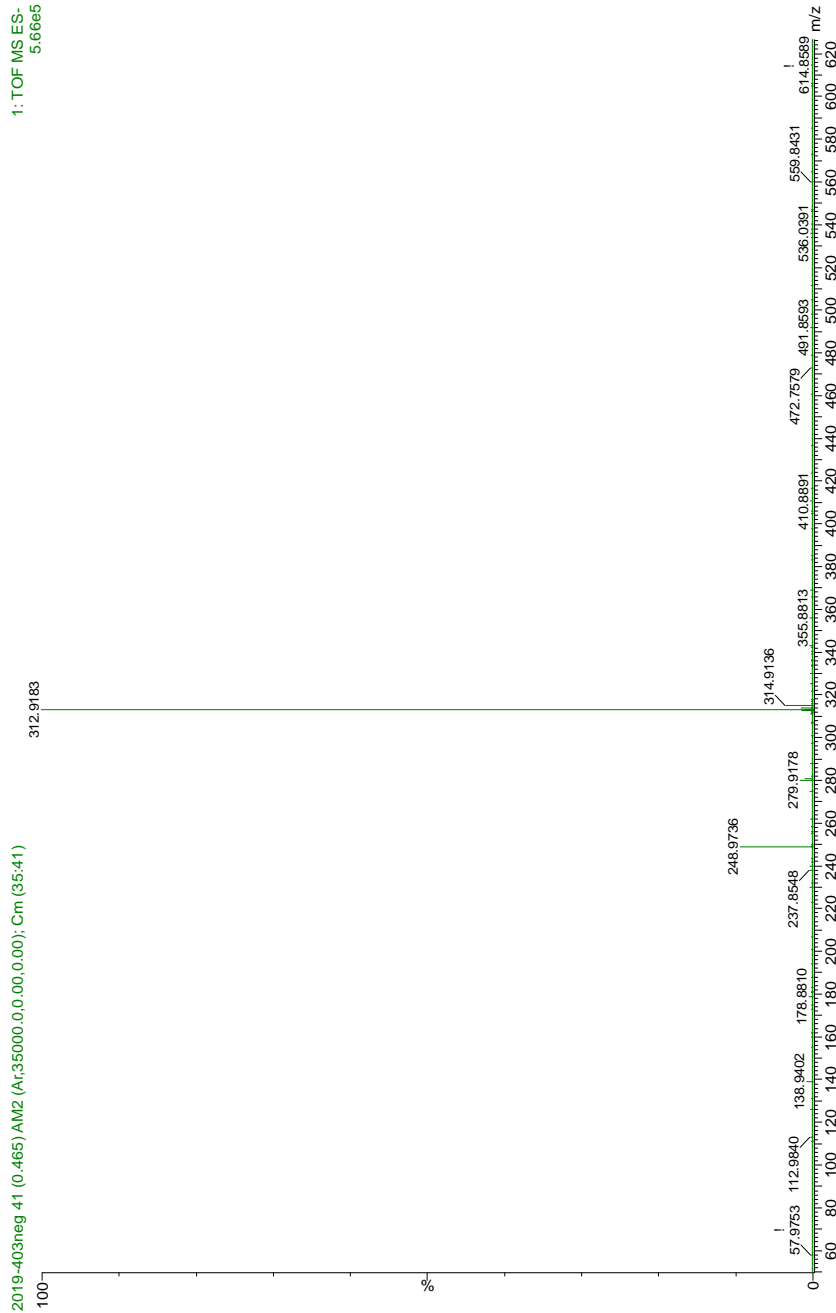
9.39e+006



Minimum: -50.0
Maximum: 5.0 2.0 50.0

Mass	Calc. Mass	mDa	PPM	DBE	i-FIT	Norm	Conf (%)	Formula
305.1864	305.1865	-0.1	-0.3	6.5	1502.0	0.065	93.74	C17 H25 N2 O3
	305.1860	0.4	1.3	-9.5	1510.7	8.786	0.02	C3 H30 N4 O10
	305.1860	0.4	1.3	-1.5	1504.7	2.774	6.24	C10 H27 11B N2 O6 Na

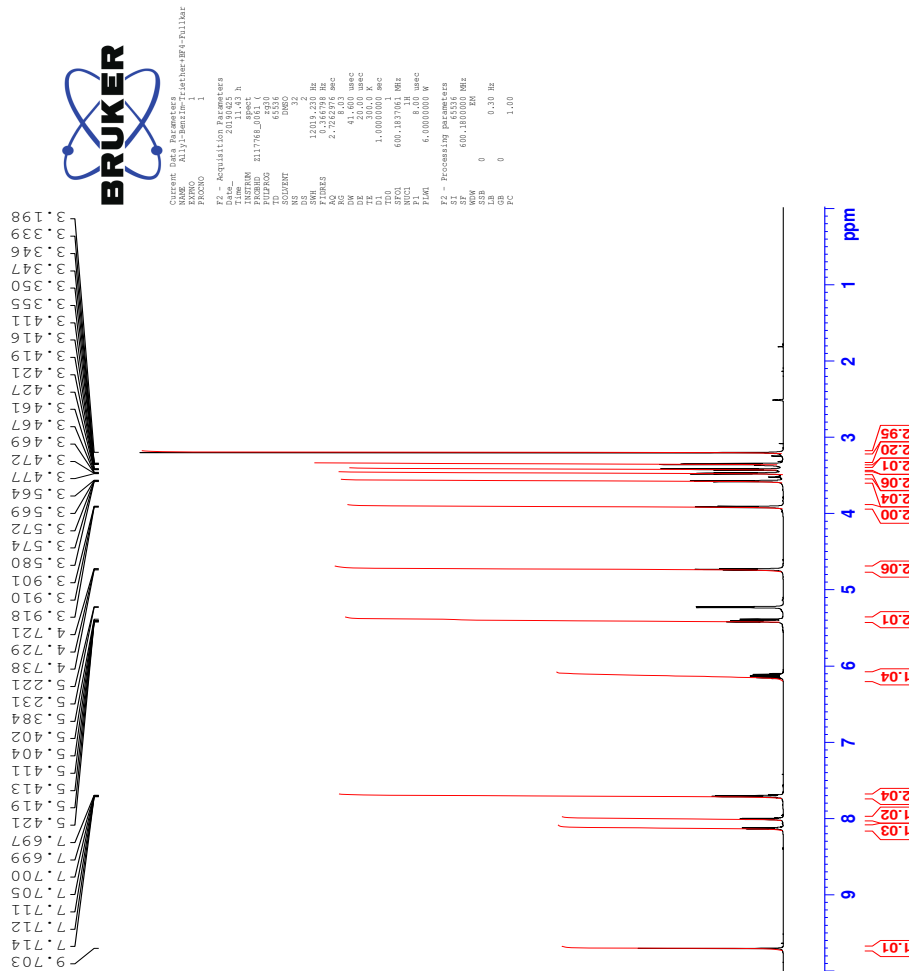
48.8 HR-MS negative mode spectrum of IL 17d



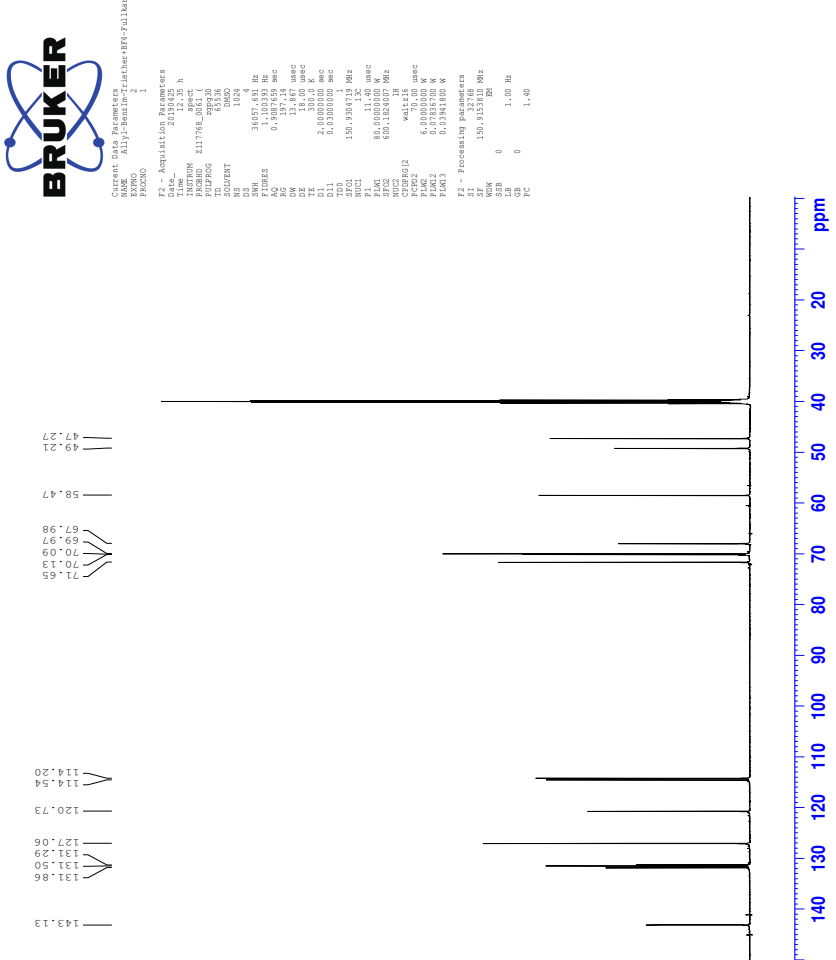
CCXC

49 Spectra of IL 17e

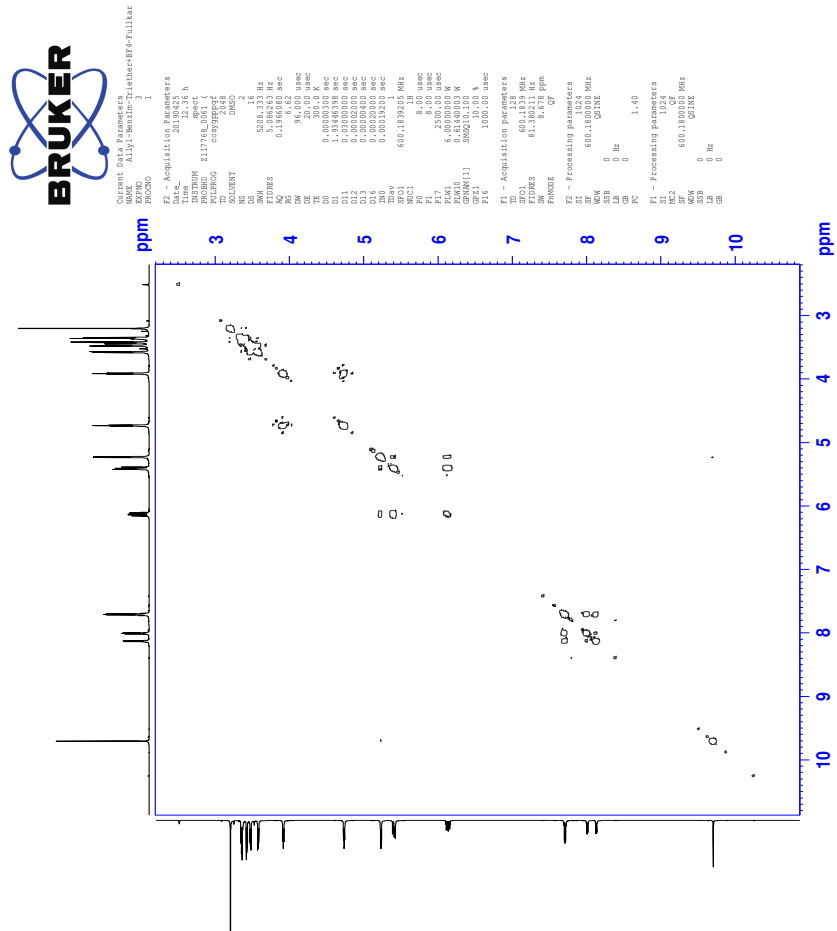
49.1 ^1H -NMR spectrum of IL 17e



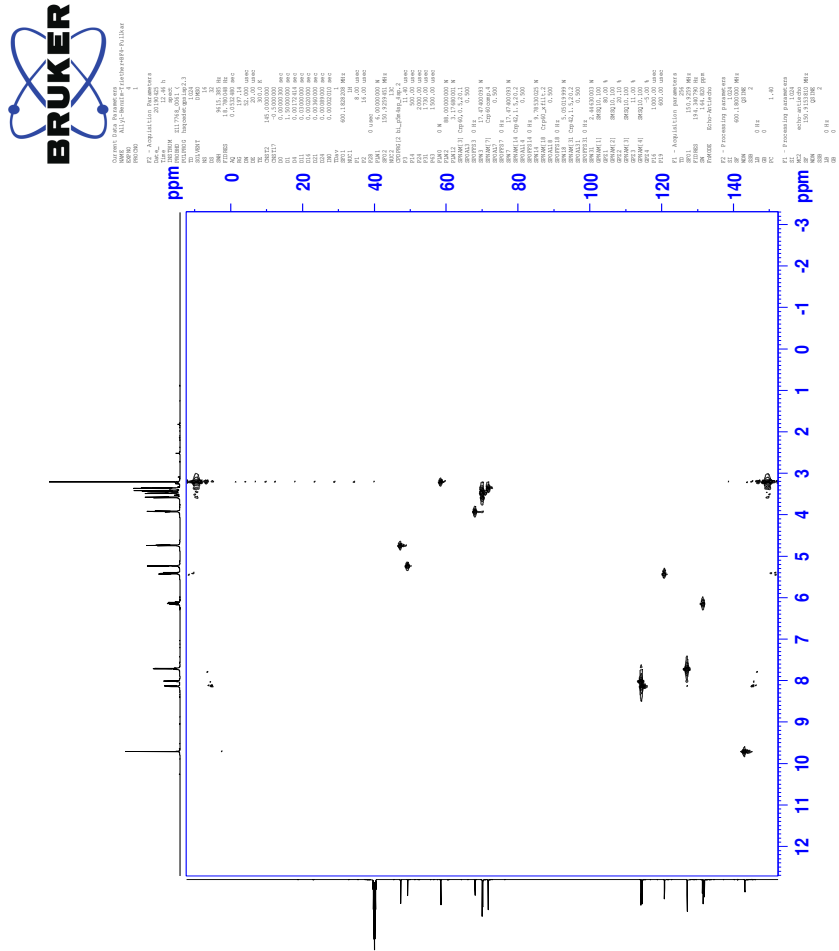
49.2 ^{13}C -NMR spectrum of IL 17e



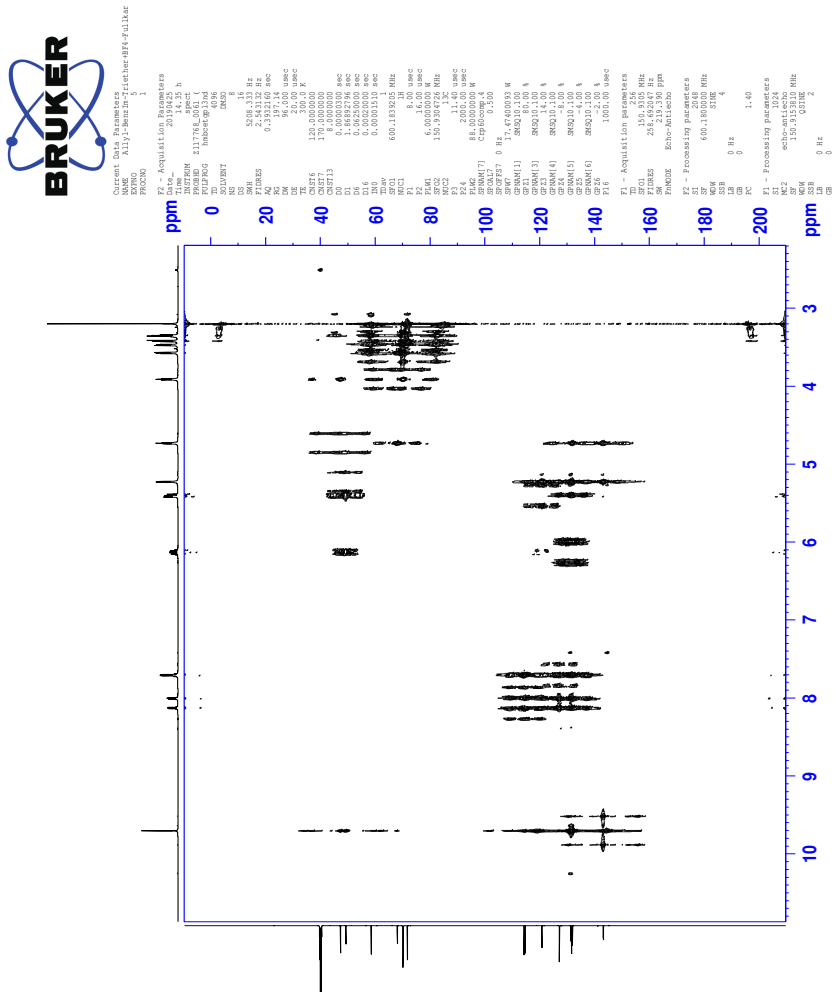
49.3 COSY-spectrum of IL 17e



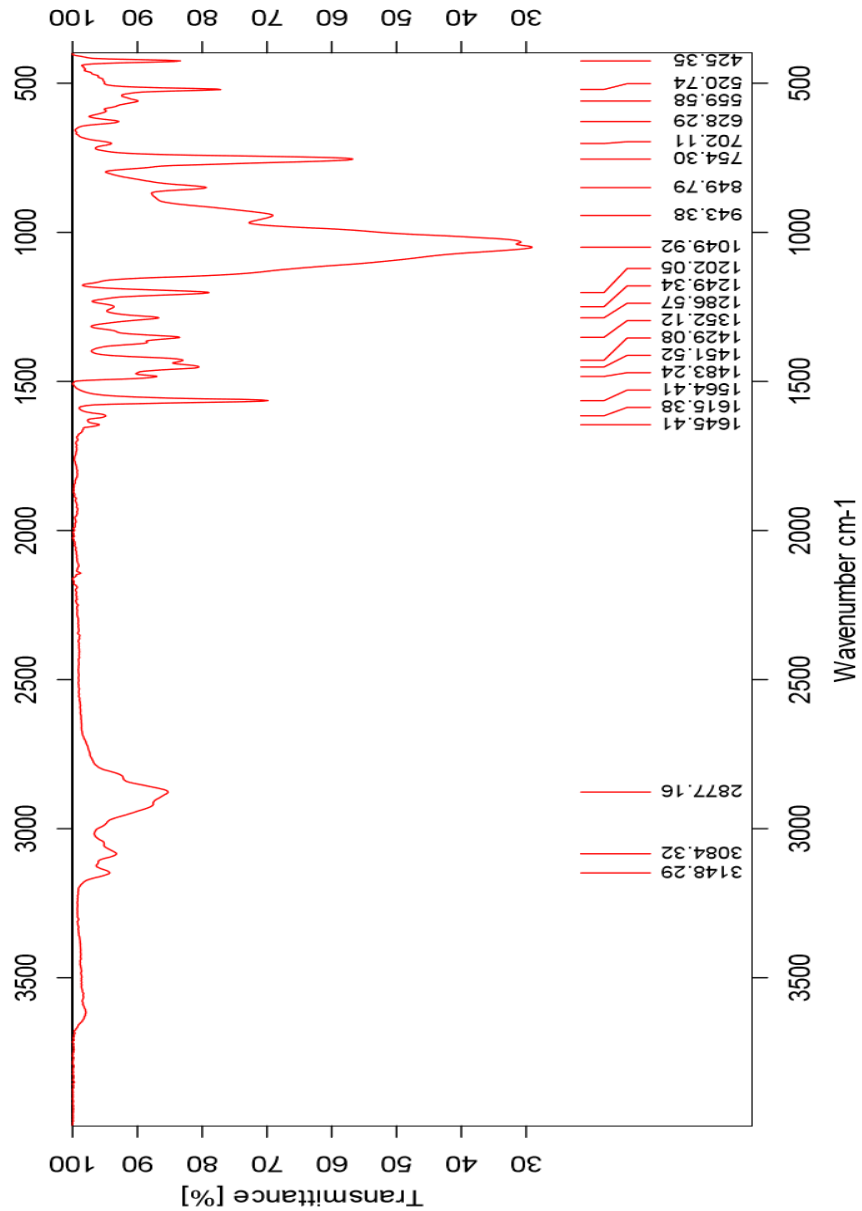
49.4 HSQC-spectrum of IL 17e



49.5 HMBC-spectrum of IL 17e



49.6 IR-spectrum of IL 17e



49.7 HR-MS positive mode spectrum of IL 17e

Elemental Composition Report

Page 1

Single Mass Analysis

Tolerance = 3.0 PPM / DBE: min = -50.0, max = 50.0

Element prediction: Off

Number of isotope peaks used for i-FIT = 3

Monoisotopic Mass, Even Electron Ions

2175 formula(e) evaluated with 3 results within limits (all results (up to 1000) for each mass)

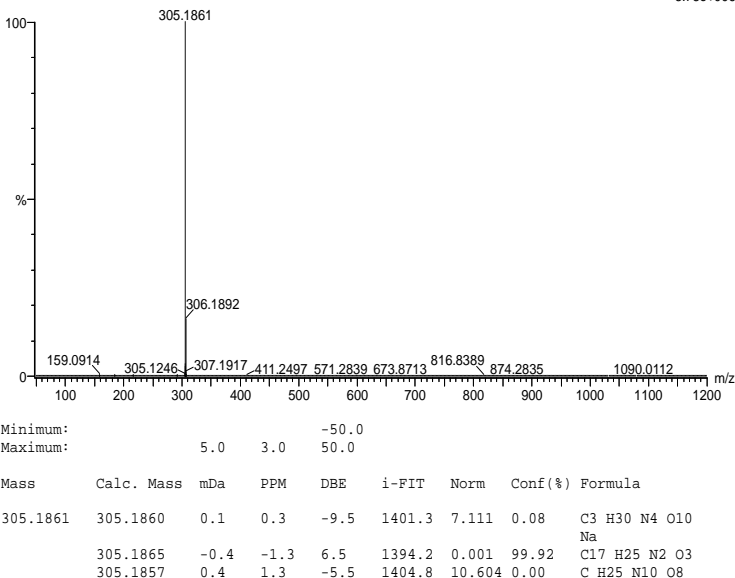
Elements Used:

C: 0-100 H: 0-150 N: 0-10 O: 0-10 Na: 0-1

2019-425 16 (0.305) AM2 (Ar,35000.0,0.00,0.00); Cm (15:16)

1: TOF MS ES+

3.73e+006



49.8 HR-MS negative mode spectrum of IL 17e

Elemental Composition Report

Page 1

Single Mass Analysis

Tolerance = 10.0 PPM / DBE: min = -50.0, max = 50.0

Element prediction: Off

Number of isotope peaks used for i-FIT = 3

Monoisotopic Mass, Even Electron Ions

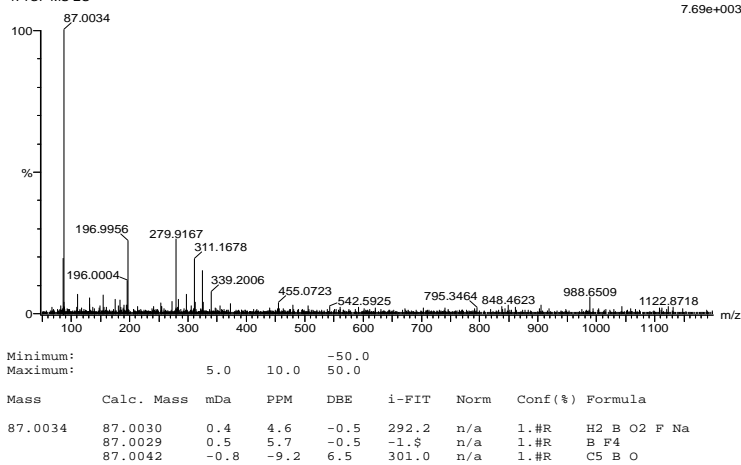
454 formula(e) evaluated with 3 results within limits (all results (up to 1000) for each mass)

Elements Used:

C: 0-100 H: 0-150 B: 0-2 N: 0-10 O: 0-10 F: 0-7 Na: 0-1

2019-405neg.30 (0.341) AM2 (Ar,35000.0,0.00,0.00); Cm (29:30)

1: TOF MS ES-



Minimum: 5.0 Maximum: 50.0

Mass	Calc. Mass	mDa	PPM	DBE	i-FIT	Norm	Conf (%)	Formula
87.0034	87.0030	0.4	4.6	-0.5	292.2	n/a	1.#R	H2 B O2 F Na
	87.0029	0.5	5.7	-0.5	-1.8	n/a	1.#R	B F4
	87.0042	-0.8	-9.2	6.5	301.0	n/a	1.#R	C5 B O

50 HPLC-data

50.1 HPLC-data for ILs 6-8

Average values of area under the peaks observed during HPLC-analysis of the oil phase after EDS are presented in Table 1 for ILs **6-8**.

Table 1: The average value of area under peaks obtained from HPLC during analysis of MO after EDS for ILs **6-8**.

IL	DBT	4,6-DMDBT
6b	40.2	61.0
6c	42.5	64.7
6d	46.0	66.4
6e	56	69.1
7b	39.1	54.4
7c	35.9	60.5
7d	45.8	65.8
7e	47.0	65.1
8b	38.5	55.8
8c	31.8	57.0
8d	42.9	64.8
8e	46.4	66.6

50.2 HPLC-data for optimization studies of IL 8c

In this section, the average value of the area under the peak observed during HPLC-analysis of the oil phase for the optimization studies for **IL 8c** are shown in Table 2-4.

Table 2: The average value of area under peaks obtained from HPLC during optimization of time for **IL 8c**.

Time [min]	DBT	4,6-DMDBT
15	22.8	56.5
30	22.8	54.6
45	22.5	54.1
60	22.7	53.5
120	32.2	57.6

Table 3: The average value of area under peaks obtained from HPLC during optimization of mass ratio IL:DBT for **IL 8c**.

Mass ratio IL:DBT	DBT	4,6-DMDBT
1:1	38.5	55.8
2:1	22.1	49.3
3:1	16.3	42.6
4:1	13.0	37.5
5:1	10.4	33.1

Table 4: The average value of area under peaks obtained from HPLC during optimization of temperature for IL **8c**.

Temperature [°C]	DBT	4,6-DMDBT
25	22.8	56.5
40	24.5	54.3
60	28.9	55.7
90	28.6	54.9

Recyclability study was performed for IL **8c** under the optimized conditions with MO containing DBT and 4,6-DMDBT in a total sulfur concentration of 500 ppm. The average value of the peaks obtained by HPLC are presented in Table 5.

Table 5: Recyclability test of IL **8c** with MO containing 500 ppm of DBT and 4,6-DMDBT.

Number of cycles	DBT	4,6-DMDBT
1	23.2	54.9
2	36.8	67.1
3	46.2	71.8
4	52.9	74.4
5	58.2	76.1
6	61.9	77.0
7	65.7	78.2
8	65.8	76.3
9	69.1	77.7

Recyclability study of IL **8c** with a MO containing DBT in a total concentration of 100 ppm was performed and the average value of the area under the peaks obtained by HPLC are presented in Table 6.

Table 6: Recyclability test of IL **8c** with MO containing 100 ppm DBT.

Number of cycles	DBT
1	15.2
2	22.2
3	27.1
4	29.4
5	31.6
6	32.5
7	33.6
8	34.5
9	35.0

50.3 HPLC-data for ILs 9-11

The average values of the area under the peaks obtained by HPLC-analysis of the oil phase after EDS with ILs **9-11** are presented in Table 7.

Table 7: The average value of area under peaks obtained from HPLC during analysis of MO after EDS for ILs **9-11**.

IL	DBT	4,6-DMDBT
9b	36.4	55.1
9c	36.4	57.5
9d	64.1	73.7
9e	43.6	62.2
10b	36.4	55.1
10c	36.4	57.5
10d	64.1	73.7
10e	43.6	62.2
11b	34	51.3
11c	31.6	55.4
11d	67.4	72.1
11e	38.7	58.6

50.4 HPLC-data for ILs 15-17

The average values of the area under the peaks obtained by HPLC-analysis of the oil phase after EDS with ILs **9-11** are presented in Table 7.

Table 8: The average value of area under peaks obtained from HPLC during analysis of MO after EDS for ILs **15-17**.

IL	DBT	4,6-DMDBT
15b	22.8	37.9
15c	-	-
15d	-	-
15e	-	-
16b	23.5	37.1
16c	29.1	47.2
16d	39.5	63.8
16e	31.2	53.1
17b	22.1	37.6
17c	22.0	45.7
17d	29.4	54.7
17e	29.0	52.8

